Benthic ecosystem response to polymetallic nodule extraction in the deep sea

UNIVERSITEIT GENT

Academic year 2018–2019
Publically defended on 1st October 2018

The research presented in this thesis received funding from the European Union Seventh Framework Programme (FP7/2007–2013) under the MIDAS (Managing Impacts of Deep-seA reSource exploitation) project, grant agreement n° 603418, by the JPI Oceans – Ecological Aspects of Deep Sea Mining project (Mining Impact) under NWO-ALW grant n° 856.14.002 and Bundesministerium für Bildung und Forschung (BMBF) grant n° 03F0707A-G.

Co-authors of one or more chapters: David Amptmeijer, Silvia Bianchelli, Peter van Breugel, Alastair Brown, Cinzia Corinaldesi, Marina R. Cunha, Roberto Danovaro, Antonio Dell'Anno, Patricia Esquete, Cristina Gambi, Andrey Gebruk, Katja Guilini, Matthias Haeckel, Freija Hauquier, Felix Janssen, Daniel O. B. Jones, Daniëlle de Jonge, Daniel Kersken, Kevin Köser, Lidia Lins, Yann Marcon, Lisa Mevenkamp, Massimiliano Molari, Leon Moodley, Dick van Oevelen, Autun Purser, Antonio Pusceddu, Ascensão Ravara, Clara F. Rodrigues, Erik Simon-Lledó, Karline Soetaert, Andrew K. Sweetman, Ann Vanreusel, Tobias R. Vonnahme, Ilja Voorsmit, Chih-Lin Wei, Frank Wenzhöfer, and Stig Westerlund.

Cover design: Ina Stratmann
Lay-out: Tanja Stratmann
Photos on the cover and between chapters: ROV Kiel 6000, Geomar (Germany), Ralph Schwarz.

ISBN: 9789082561159

Benthic ecosystem response to polymetallic nodule extraction in the deep sea

by Tanja Stratmann

Promotor: Prof. Dr. Karline Soetaert
Co-Promotor: Dr. Dick van Oevelen

Academic year 2018–2019

Thesis submitted in partial fulfillment of the requirements for the degree of Doctor in Science: Marine Sciences

GHENT UNIVERSITY
FACULTY OF SCIENCES

Members of the examination committee
Members of the reading committee*

Prof. Dr. Karline Soetaert, Promoter
NIOZ – Royal Netherlands Institute for Sea Research, Yerseke, The Netherlands
Ghent University, Ghent, Belgium

Dr. Dick van Oevelen, Co-Promotor
NIOZ – Royal Netherlands Institute for Sea Research, Yerseke, The Netherlands

Prof. Dr. Koen Sabbe, Chairman*
Ghent University, Ghent, Belgium

Prof. Dr. Ann Vanreusel, Secretary*
Ghent University, Ghent, Belgium

Prof. Dr. Tom Moens*
Ghent University, Ghent, Belgium

Prof. Dr. Andrew K. Sweetman*
Heriot-Watt University, Edinburgh, UK

Dr. Annemiek Vink*
Bundesanstalt für Geowissenschaften und Rohstoffe, Hannover, Germany

Dr. Lenaick Menot*
Institut Français de Recherche pour l'Exploitation de la Mer (Ifremer), Brest, France

Table of content

Acknowledgments

After more than 4 yr at the NIOZ – Royal Netherlands Institute for Sea Research in Yerseke, first at the Department of Ecosystem Studies and later at the Department of Estuarine and Delta Systems, it is time to say thanks.

Dick: First of all, thanks for employing me as your PhD student; this girl who came from a university in Denmark and did not know anything about food-web modeling, benthos work nor deep-sea mining. Instead, I had a background in Arctic marine research and dissolved organic matter. After 4 yr, I developed food-web models for different locations in the tropics and the Mediterranean Sea. I participated in two research cruises on board R/V *Sonne* and know to dismantle the CUBEs completely and set them together again. I learned to culture diatoms and conducted fancy *in situ* experiments in the deep sea that were not possible before. You are a great supervisor, always supporting me in any kind of weird idea, especially when I decided in 2016 to start an advanced Master in Statistical Data Analysis (MaStat) at Ghent University and I turned out to be more in Ghent than in Yerseke during some very busy weeks. You also gave extremely valuable comments to all my manuscripts and especially during the end of my PhD you turned them around really fast. Thanks for introducing me into the deep-sea community and get me in contact with a lot of great scientists.

Karline: Thanks for being my Promoter. I also apologize that I was very annoying during the last couple of weeks when I tried to organize all the administrative matters to submit my PhD thesis, while you were on research cruises and I contacted half of the cruise participants to get in contact with you.

Jury: Thanks to Prof. Dr. Koen Sabbe for being the chairman of my reading committee and thanks to Prof. Dr. Ann Vanreusel for being the secretary. Thank you to Prof. Dr. Tom Moens, Prof. Dr. Andrew K. Sweetman, Dr. Annemiek Vink, and Dr. Lenaick Menot for being members of my reading committee and spending the nice Belgian, German, Scottish or French summer and autumn reading more than 350 pages each time for the pre-defense and for the public defense.

Lab team: Dear **Pieter**, **Peter**, **Ivonne**, **Jan**, **Jan**, **Jurian** and **Anton**, you are the magicians from the ground floor. **Pieter**, you showed me everything that I learned during my PhD (except the modeling part), from culturing algae to extracting fatty acids and amino acids from sea cucumber tissue or sediment. **Peter**, you measured hundreds and hundreds of fatty acid, amino acid and bulk ^{13}C and ^{15}N samples for me and even realized that I did mistakes during my extractions by just looking at the chromatograms. I had never noticed that without you. In late winter/ early spring 2016 I was also supported by my two interns **Jana** and **Jonas** who spent two weeks in the lab freeze-drying, weighing and grinding sea cucumber tissue.

Office mates: When I started as a newbie at NIOZ, I shared my office with **Franscec** and **Sabine**. Later, they moved to NIOZ Texel or left NIOZ and I shared my office with **Sandra** and **Evert**. Thanks for all the fun discussions about life and football. Thanks in particular for discussions about data analysis, interpretation, cruise preparations, diatom culturing, and experimental design. Evert,

I want to thank you so much for translating my English summary into a Nederlands samenvatting.

My students: During my PhD I supervised one Bachelor student and three Master students who all helped me in becoming a (hopefully) better supervisor. Three of you even became co-authors on my papers, well done!

Members of YES and EDS: Thanks all for welcoming me so warmly at NIOZ-Yerseke when I arrived here in February 2014. Thanks **Camilla**, **Long**, **Claudia**, **Kiki**, **Koen**, **Aimee**, **Silvia**, **Laurine**, **Dorina**, **Sven**, **Loretta**, **Laura**, **Daan**, **Celine**, **Chiu**, **Alexander**, **Greg**, **Marieke**, **Tim**, **Rebecca**, **Anna**, **Sarah**, **Bas**, **Jaco**, **Natalie**, **Justin**, **Roeland**, **Jim**, **Justin**, **Zhenchang**, **Hélène**, **Lorenz**, **Haobing**, **Jildou**, **Clara**, and **Simeon** (and all that I forgot) for all the conversations we had during coffee breaks and lunch times. Thanks for the coffees on your terrace and for proofreading sections of my thesis, **Henriette**, thanks for the fun time we had on Texel while teaching during the NIOZ summer course last summer, **Tisja**. **Anna,** thanks for your translation of my English summary into my Nederlands samenvatting. **Emil**, thanks for correcting the Dutch translation of my English summary in my revised thesis.

Cruise participants of SO242-2 and SO254: I want to thank capitan **Oliver Meier**, his **crew**, and chief scientist **Prof Dr Antje Boetius** during SO242-2 and capitan **Lutz Mallon**, his **crew**, and chief Scientist **Prof Dr Meinhard Simon** during SO254 for these two very successful research cruises onboard R/V *Sonne*. A big thanks goes to **Dr Friedrich Abegg** and his ROV team (**Matthias**, **Patrick**, **Hannes**, **Torge**, **Arne**, **Martin**, **Inken**, and **Jan**) that are brilliant in deploying the CUBEs over any sea cucumber or hexactinellid sponge. I also want to acknowledge the researchers with whom I worked on board; most of these collaborations have ended or will end in publications. Thanks to **Andrew** (I guess I still need to clean your lander with a toothbrush), **Alastair**, **Lida**, **Lisa** (as you mentioned already in the acknowledgments of your PhD thesis, we are really a great team), **Autun**, and **Yann,** and the sponge team: **Peter**, **Sven**, **Tessa**, **Lars-Erik**, **Dennis**, **Klaus-Peter**, **Jackson**, **Katrin**, **Sadie**, and **Gert**.

Co-authors: As the list of co-authors that contributed to chapters in this thesis includes 38 names, I will not mention them all here, but just say thanks. In particular, developing food-web models was not possible without all your generous sharing of data.

Sport teams: When I arrived at the NIOZ' guest house "De Keete", "Insanity" was thé workout program at NIOZ. Hence, I joined the guys and girls and want to thank you all for this funny, but extremely exhausting way to achieve the perfect beach body. Later that spring, I joined **Lieke** and **Celine** running through Yerseke Moer; thanks girls for showing me the amazing nature that surrounds Yerseke. In autumn 2014 I eventually found my favorite sport in Yerseke when I joined **Heleen**'s Ashtanga Yoga classes, first at NIOZ and later at St. Ana's Kerke. Thanks for introducing me to Yoga in both, English and Dutch.

Friends in Ghent: When I started the MaStat at Ghent University, I made friends with a lot of Belgians and foreigners. Thanks for playing weird games until the bar tender closed the bar. Thanks for offering my a coffee at 2.00 h when no bar would serve coffee anymore and I still had to drive back to Zeeland.

Thanks for enjoying a party together where the singer was the worst musician I ever heard and thanks for having breakfast and lunches with me, though I always talked too much.

My family: Nachdem ich schon drei Seiten mit Danksagungen vollgeschrieben habe, möchte ich nun euch danken, **Annette** und **Siegfried**. Ihr seid wirklich großartige Eltern, die mich immer in allem unterstützt haben, seitdem eine kleine Neunjährige ankam und verkündete, sie wolle unbedingt Biologin werden. Zwanzig Jahre später ist es nun so weit, hier liegt meine Dissertation vor euch. **Mama**, danke dir für alle deine Mühe, mit er du irgendwelche seltsamen Referenzen aus Büchern für mich herausgesucht hast, für die du dich erst einmal eine halbe Stunde durch drei Bücherregale voller Bücher arbeiten musstest, weil ich mal wieder nicht wusste, wo das Buch eventuell stehen könnte. Papa, ich danke dir für alle deine Umzugshilfe und das Abholen vom Flughafen und Bahnhof während der letzten 10 Jahre, in denen ich von Stromberg nach Bremen, von Bremen nach Spanien und zurück nach Bremen, nach Aarhus in Dänemark und schließlich nach Krabbendijke in Zeeland gezogen bin. Meine Schwestern **Sara**, **Jana** und **Ina**: Auch wenn wir uns ständig überlegen, ob man als Einzelkind nicht besser dran sei, ich will keinen von euch missen. **Jana**, ich habe dir für deine Seegurkenpulverisierungsarbeit schon vorher gedankt, aber hier noch mal, vielen vielen Dank. Du sahst aber auch sehr süß aus in deinem weißen Laborkittel einschließlich Schutzbrille und Atemmaske. **Ina** vielen vielen Dank für das Excelmakro, dass du für Kapitel 2 programiert hast, für die technische Zeichnung in Kapitel 5 und für die vielen wissenschaftlichen Artikel, auf die ich über das NIOZ und die Universität Ghent keinen Zugriff hatte. **Ina** und **Moritz**, danke für eure kreativen Schneide- und Basteltätigkeiten und Fertigkeiten für einige Grafiken in Kapitel 1 und 2. **Sara**, vielen Dank für das Korrekturlesen meiner deutschen Zusammenfassung und dafür, dass ich deine Zugangsdaten zu Statista und Springer Professional nutzen konnte. Danke auch für deine künstlerischen Tätigkeiten für die Graphik in Kapitel 10.

Summaries

English summary

More than 70% of our planet is covered with oceans that have a mean depth of 3,800 m (Ramírez-Llodrà *et al.*, 2010). The deep sea, i.e., the ocean below 200 m water depth, is characterized by low water temperatures, high pressure, and darkness. Due to the absence of photosynthesis, the ecosystem depends on particulate organic carbon flux from the euphotic zone except at locations where chemosynthesis occurs. The largest ecosystem on Earth is the abyss, i.e., the seafloor between 3,000 and 6,000 m water depth, that extends over 54% of the Earth's surface (Gage and Tyler, 1991). The abyss includes abyssal mountains, hills, and plains that are comprised of soft sediment.

In some areas, the abyssal plains are covered with polymetallic nodules that lay on the sediment surface and/ or are buried within the upper 10 cm of sediment. These nodules are composed of concretions of iron oxide-hydroxide and manganese oxide and contain relatively high concentrations of nickel, cobalt, copper, and rare earth elements. Nodules form very slowly with growth rates between 1 to 10 mm Myr^{-1} (hydrogenetic growth) (Petersen *et al.*, 2016); though growth rates up to 250 mm Myr^{-1} were estimated for diagenetic growth (von Stackelberg, 2000). Because of their high metal content, polymetallic nodules are of economic interest. The Clarion-Clipperton Fracture Zone (CCZ) in the central Pacific, e.g., is estimated to contain more manganese, nickel, and cobalt in the form of polymetallic nodules than land-based reserves of these metals (International Seabed Authority, 2010; Hein and Koschinsky, 2014; Sverdrup, Ragnarsdottir and Koca, 2017; U.S. Geological Survey, 2018). However, a commercial extraction of nodules will have environmental impacts, such as noise pollution, potential release of toxic metals, the spreading of sediment plumes, habitat modification and destruction.

The objective of this PhD-thesis was to investigate the response of the benthic ecosystem to the extraction of polymetallic nodules in the deep sea. I focused in particular on the response of the ecosystem to habitat modification and destruction and studied the recovery from a small-scale sediment disturbance experiment in the Peru Basin, the so-called DISCOL experiment (acronym for "DISturbance and re-COLonization experiment in the South Pacific"; Thiel *et al.*, 1989).

Chapter 1 introduces the reader to the deep sea and to the specific deep-sea ecosystems fjord, submarine canyon, and abyss. Seafloor biota is described, and the different benthic size classes are defined. Furthermore, this chapter elaborates on trophic interactions among various feeding types in deep-sea food webs. The chapter describes polymetallic nodules, their formation, deep-sea mining, and the impact of nodule extraction in the deep sea. It also explains the DISCOL experiment and compares advantages and disadvantages of the different scientific methods used in this PhD thesis.

Assessing the benthic response to deep-sea mining requires a good understanding of the benthos itself. Therefore, **Chapter 2** describes the role of ben-

thos in the global carbon cycle. The “Random Forest” method was used to generate global seafloor maps of benthic biomass and benthic respiration based on data sets of meiofauna, macrofauna, and invertebrate megafauna biomass and sediment community oxygen consumption (SCOC). These maps were combined with a dataset on biomass-specific faunal respiration rates, assimilation efficiency, and production/biomass-ratios to derive global estimates of benthic faunal and prokaryotic respiration, benthic faunal secondary production, and benthic faunal ingestion. We also estimated global benthic biomass of meiofauna (9.94 Tg C), macrofauna (28.0 Tg C), and invertebrate megafauna (1.47 Tg C). Global benthic respiration was estimated to be 1.19 Pg C yr^{-1}, global benthic faunal secondary production was 0.28 Pg C yr^{-1}, and global benthic faunal ingestion was 1.55 Pg C yr^{-1}. Furthermore, our results showed that 47% of total benthic respiration, 50% of total benthic faunal secondary production, and 57% of total benthic faunal ingestion takes place at >2,000 m water depth.

In **Chapter 3**, we analyzed how important polymetallic nodules and their associated fauna were for food-web integrity in abyssal plains. We conducted an extensive literature research and combined the results with newly analyzed seafloor pictures from the Peru Basin and the CCZ. We developed interaction webs with 208 compartments for the Peru Basin and 478 compartments for the CCZ that included meiofauna, macrofauna, megafauna, fishes, food sources (suspended and sedimentary particulate organic matter, bacteria, dissolved organic carbon, carrion, and protists), and polymetallic nodules. These compartments were connected with 3,131 (Peru Basin) and 9,386 (CCZ) trophic and non-trophic links. We assessed how the number of network compartments, the number of connecting links, link density, and network connectance changed when polymetallic nodules were absent. Our results showed that nodule removal reduced the number of compartments by 26% in the Peru Basin and by 20% in the CCZ. In comparison, when the “highest impact taxon”, i.e., the taxon whose removal had the largest impact on food-web properties, was removed, only <5% of the faunal compartments were lost. Our analysis revealed that stalked sponges attached to nodules are key structural species in abyssal plains because they host a large commensal faunal community. Therefore, the absence of nodules in nodule-rich areas will lead to a local loss in biodiversity.

During the DISCOL experiment in 1989, 22% of a 10.8 km^2 circular area was ploughed with an 8 m wide plough harrow. As a result, nodules were ploughed into the sediment and surface sediment was turned upside down inside the plough tracks. Potential ecosystem recovery from this small-scale sediment disturbance was investigated in **Chapters 4**, **5**, **6**, and **7**.

In **Chapter 4**, we studied the long-term impact of the DISCOL experiment using holothurians as model organism for mobile deposit-feeding megafauna. During R/V *Sonne* cruise SO242-2 in September 2015, 3,760 pictures of the seafloor were taken with a towed “Ocean Floor Observation System” (OFOS) during four transects in the DEA. Additionally, 983 pictures were taken during four transects at reference sites approximately 4 km away from DEA. All holothurian specimens on these pictures were annotated, measured, and identified to

morphotypes. Our results showed that 26 yr after the DISCOL experiment, holothurian density did not differ between inside plough tracks/ disturbed sites (241±51 ind. ha^{-1}), outside plough tracks/ undisturbed sites (240±40 ind. ha^{-1}), and reference sites (241±33 ind. ha^{-1}). Also holothurian biomass and holothurian community respiration were not different between sites, indicating holothurian recovery from the small-scale benthic disturbance experiment within 26 yr.

Potential recovery of phytodetritus processing by the soft-sediment community at the DEA 26 yr after the DISCOL experiment was investigated in **Chapter 5**. We deployed large benthic incubation chambers (CUBEs; 50×50×50 cm) *in situ* at 4,100 m water depth inside plough tracks (with and without holothurians) and at reference sites (with holothurians). During these deployments, ^{13}C and ^{15}N-enriched diatoms (*Skeletonema costatum*) were injected into the CUBEs and water samples were taken in five time steps during the 3 d-incubations. At the end of the incubations, sediment and holothurians were sampled to measure the uptake of ^{13}C and ^{15}N into bacteria, nematodes, macrofauna, and holothurians. ^{13}C-DIC production over time was measured in the water samples. Total ^{13}C uptake by bacteria, nematodes, and holothurians was significantly lower inside plough tracks compared to reference sites; however, the number of replications was low. This implies that phytodetritus processing has not fully recovered 26 yr after the DISCOL experiment.

In **Chapter 6** we used data of macrofauna, megafauna, and fish diversity and density collected inside and outside plough tracks 0.1, 0.5, 3, 7, and 26 yr after the DISCOL experiment to develop food-web models for each time point using the linear inverse modeling approach. Total carbon stock was always higher outside plough tracks compared to inside plough tracks and 26 yr post-disturbance, the carbon stock inside plough tracks was 54% of the carbon stock outside plough tracks. Also the sum of all modeled carbon flows, i.e., the "total system throughput" *T*.., was always higher outside plough tracks compared to inside plough tracks. After 26 yr, this difference in *T*.. between outside and inside plough tracks was 56%, implying that carbon cycling had not recovered after 26 yr.

For **Chapter 7**, we extended the food-web models for 26 yr after the DISCOL experiment from **Chapter 6** to reference sites and additionally included bacteria, nematodes, other meiofaunal taxa, and three fish compartments. This resulted in the most highly resolved carbon-flux based food-web model developed for abyssal plains so far. It showed that *T*.. (mmol C m^{-2} d^{-1}) was not significantly different between reference sites (mean±std; 4.52±8.35×10^{-2}) and outside plough tracks (5.51±0.16), but it differed significantly between reference sites and inside plough tracks (4.52±8.35×10^{-2}), and between outside and inside plough tracks. The main contributor to differences in *T*.. was the microbial loop, which was depressed inside plough tracks compared to outside plough tracks or reference sites. This indicates that the microbial loop responds very sensitively to the small-scale sediment disturbance and has not recovered after 26 yr.

To study the response of bacteria, meiofauna, and macrofauna to deep-sea mining related re-settlement of sediment and sediment deposition, respectively, we studied two sediment deposition analogues: Deposition of mine tailings

in a Norwegian fjord ecosystem in **Chapter 8** and dense shelf water cascading (DSWC) in two Mediterranean submarine canyons in **Chapter 9**.

In **Chapter 8** we investigated how the benthic fjord ecosystem was affected by short-term exposure to iron ore tailings deposition and dead subsurface sediment deposition. Sediment cores were incubated with 0.1, 0.5, and 3 cm thick layers of inert iron ore tailings for 11 d and with 0.5 and 3 cm thick layers of dead subsurface sediment for 16 d. We measured bacterial, meiofaunal, and macrofaunal biomass, meiofaunal and macrofaunal diversity and community composition, and mortality of nematodes. Furthermore, we investigated SCOC, oxygen penetration depth, and uptake of ^{13}C from *Skeletonema costatum* by bacteria, nematodes, and macrofauna. Our results showed that burial under ≥0.1 cm of mine tailings reduced SCOC and ^{13}C uptake in all compartments, indicating decreased ability of the benthic community to process fresh phytodetritus. Additionally, a mine tailing deposition of 3 cm resulted in an increased nematode mortality, likely due to a lack of food. Three centimeter of dead subsurface sediment deposition also caused a rise in nematode mortality, however, in this case the increased mortality was the result of anoxic conditions inside the sediment. Hence, even a thin layer of mine tailing deposition (0.1 cm) has a short-term effect on the benthic ecosystem.

Submarine canyons are locations of enhanced carbon flux to the deep sea. To see spatial differences in carbon cycling among various sections of two deep-sea canyons at the Catalan margin and the Gulf of Lions (NW Mediterranean Sea), we developed carbon-based food-web models for the Cap de Creus canyon and the Lacaze-Duthiers canyon in **Chapter 9**. Our results indicate that carbon cycling in the upper Lacaze-Duthiers canyon and the middle section of the Cap de Creus canyon are dominated by active faunal carbon uptake by meiofauna. In comparison, carbon cycling in the upper and lower Cap de Creus canyon sections is dominated by carbon uptake by bacteria.

The continental shelf of the NW Mediterranean Sea has experienced dense shelf water cascading (DSWC) events almost every winter since 1993. These cascading events lead to sediment erosion and transport this sediment from the continental margin down the slope. To study the impact of these events on the benthic ecosystem, we extended our food webs for the upper and lower Cap de Creus canyon to a time series analyzing the situation directly after a very strong DSWC event in February/ March 2005. Further models were developed for the situation 0.5, 3, 3.5, 4, and 4.5 years after the major DSWC event. Our modelling results showed that the total carbon that was cycled in the food web was reduced in the upper canyon section directly after the DSWC event, but increased again within half a year. This indicates a fast recovery of the ecosystem, which was mainly related to increased nematode biomasses.

In **Chapter 10**, the results of this PhD thesis were integrated to assess the benthic ecosystem response to the removal of polymetallic nodules. Additionally, the benthic ecosystem response to sediment removal, suspension, and settlement were discussed. It was also presented how the benthic food web responds to sediment disturbance in the deep sea and it was evaluated how valid analogues are

to predict environmental impacts of deep-sea mining. Polymetallic nodule extraction was set in the global mining context and the environmental impacts of nickel, copper, and cobalt mining were compared with the environmental impacts of polymetallic nodule extraction. Finally, knowledge gaps about the ecosystem response to polymetallic nodule extraction in the deep sea were presented.

In conclusion, the research presented in this thesis shows that the benthic ecosystem will respond strongly to the extraction of polymetallic nodules in the deep sea. Deep-sea mining of these nodules will lead to a diversity loss due to the removal of hard substrate for sessile organisms, such as stalked sponges, and their associated fauna. Furthermore, results from a small-scale sediment disturbance indicate that carbon cycling might drop immediately after the mining operation and it might require more than 26 yr to return to background rates. Hence, benthic ecosystem recovery from industrial-scale mining will take decades to centuries. Sessile fauna, in fact, might never fully recover.

Nederlandse samenvatting

Meer dan 70% van onze planeet is bedekt met oceaanwater, met een gemiddelde diepte van 3.800 m (Ramírez-Llodrà *et al.*, 2010). Het deel van de oceaan, dieper dan 200 m waterdiepte, de diepzee, wordt gekenmerkt door lage watertemperaturen, hoge hydrostatische druk en duisternis. Omdat fotosynthese niet mogelijk is, zijn ecosysteem op deze diepten volledig afhankelijk van de aanvoer van, aan het oppervlakte geproduceerde, organische koolstofdeeltjes. Behalve op die plekken waar chemosynthese voorkomt. Het grootste ecosysteem op aarde is de “abyss”, het deel van de oceaan met een diepte van 3.000 tot 6.000 m. Het strekt zich uit over 54% van het aardoppervlak (Gage and Tyler, 1991). De “abyss” omvat abyssale bergen, heuvels en vlaktes die uit zacht sediment bestaan.

In sommige gebieden zijn de abyssale vlaktes bedekt met mangaanknollen, die op het sediment oppervlak liggen en/ of begraven zijn in de bovenste 10 cm van het sediment. Deze knollen bestaan uit verhardingen van ijzeroxide-hydroxide en mangaanoxide en bevatten verder nikkel, kobalt, koper en zeldzame aarde-elementen. Mangaanknollen worden heel langzaam gevormd, met groeisnelheden tussen de 1 en 10 mm per miljoen jaar, via hydrogenetische groei (Petersen *et al.*, 2016). En met groeisnelheden tot 250 mm per miljoen jaar via diagenetische groei (von Stackelberg, 2000). Vanwege hun hoge metaalgehalte, zijn mangaanknollen van economisch belang. Bijvoorbeeld de Clarion-Clipperton Fracture Zone (CCZ), gelegen in het centrale deel van de Grote Oceaan, bevat naar schatting meer mangaan, nikkel en kobalt, in de vorm van mangaanknollen, dan de op het landoppervlak aanwezige reserves van deze metalen (International Seabed Authority, 2010; Hein and Koschinsky, 2014; Sverdrup, Ragnarsdottir and Koca, 2017; U.S. Geological Survey, 2018). Het delven van deze knollen zal echter gevolgen hebben voor het milieu, zoals het vrijkomen van giftige metalen, sedimentpluimen, veranderen en vernietigen van habitat en geluidsvervuiling. Het doel van dit proefschrift was om de reactie van het benthisch ecosysteem in de diepzee op het delven van mangaanknollen te onderzoeken. Ik heb me met name gericht op de reactie op habitat-modificatie en -vernietiging. En het herstel bestudeerd van een kleinschalig sediment-verstoringsexperiment in Peru Basin, het zogenaamde DISCOL-experiment (“DISturbance and re-COLonization experiment in the South Pacific”; Thiel *et al.*, 1989).

Hoofdstuk 1 introduceert de lezer aan de diepzee en in de specifieke diepzee ecosystemen: fjord, onderzeese kloven, en de abyssale zone. Zeebodem biota wordt beschreven en de verschillende benthische grootteklassen worden gedefinieerd. Verder wordt in dit hoofdstuk ingegaan op trofische interacties tussen verschillende voedingswijzen in diepzee-voedselwebben. Het hoofdstuk beschrijft mangaanknollen, hun vorming, diepzeemijnbouw en de impact van knollenextractie in de diepzee. Het legt ook het DISCOL-experiment uit en vergelijkt voor- en nadelen van de verschillende wetenschappelijke benaderingen die in dit proefschrift worden gebruikt.

Voor het beoordelen van de benthische reactie op diepzee mijnbouw is een goed begrip nodig van het benthische systeem zelf. **Hoofdstuk 2** beschrijft

dus de rol van het benthische systeem in de globale koolstofcyclus. De “random forest”-methode is gebruikt om de zeebodem in kaart te brengen, met benthische biomassa en respiratie, gebaseerd op datasets van meiofauna, macrofauna en ongewervelde megafauna biomassa, en sediment zuurstof gebruik (Sediment Community Oxygen Consumption, SCOC). Deze kaarten zijn gecombineerd met een dataset van biomassa-specifieke dierlijke respiratie snelheden, assimilatie-efficiëntie en productie/biomassa ratio’s, om tot wereldwijde schattingen te komen van dierlijke en prokaryothische benthische respiratie, dierlijke secundaire productie en dierlijke inname. We hebben ook wereldwijde schattingen gemaakt van benthische meiofauna biomassa (9,94 Tg C), macrofauna (28,0 Tg C) en ongewervelde megafauna (1,55 Tg C). Wereldwijde benthische respiratie was geschat op 1,19 Pg C per jaar, wereldwijde benthische dierlijke secundaire productie was 0,28 Pg C per jaar en wereldwijde benthische dierlijke inname 1,40 Pg C per jaar. Verder laten onze resultaten zien dat 47% van de totale benthische respiratie, 50% van de totale benthische dierlijke secundaire productie en 57% van de totale benthische dierlijke inname plaats vond op >2000 m diepte.

In **Hoofdstuk 3** analyseerden we hoe belangrijk mangaanknollen en de geassocieerde dieren zijn voor de integriteit van het voedselweb van de abyssale vlakten. We combineerden een uitgebreide literatuurstudie met nieuw geanalyseerde zeebodem foto’s van Peru Basin en de CCZ. We maakten interactie netwerken met 208 componenten voor Peru Basin en 478 compartimenten voor de CCZ, met daarin meiofauna, macrofauna, megafauna, vissen, voedselbronnen (zwevende en in het sediment aanwezige organische deeltjes, bacteriën, opgelost organisch koolstof, aas en protisten) en mangaanknollen. Deze compartimenten werden verbonden met 3.131 (Peru Basin) en 9.386 (CCZ) trofische en non-trofische links. We onderzochten hoe het aantal netwerk-compartimenten, het aantal verbindingen, verbinding-dichtheid en netwerk-connectiviteit, veranderde wanneer de mangaanknollen afwezig waren. Onze analyse onthulde dat geteste sponzen die aan mangaanknollen zijn gehecht belangrijke structurele soorten zijn op abyssale vlakten omdat ze een grote commensale faunale gemeenschap huisvesten. Daarom zal de afwezigheid van mangaanknollen in knolrijke gebieden leiden tot een lokaal verlies aan biodiversiteit.

Tijdens het DISCOL-experiment in 1989, is 22% van een 10.8 km^2 cirkel geploegd met een verzwaarde, 8 m ploegeg. Daardoor werden mangaanknollen het sediment ingeploegd en werd oppervlakte-sediment omgekeerd in de ploegbanen. Potentieel ecosysteem herstel van deze kleinschalige sediment verstoring was onderzocht in **Hoofdstuk 4, 5, 6** en **7**.

In **Hoofdstuk 4** bestudeerden we de lange-termijn impact van het DISCOL-experiment met holothurians als model organismen voor mobiele op-depositie-voedende megafauna. Tijdens R/V *Sonne* cruise SO242-2 in september 2015, zijn 3.760 foto’s van de zeebodem genomen met een voortgetrokken “Ocean Floor Observation System” (OFOS), tijdens vier transecten op DEA (DISCOL experimenteel gebied). Daarbij zijn 983 foto’s genomen tijdens vier transecten op referentie-plekken, ongeveer 4 km van DEA. Alle holothurian specimen op deze foto’s werden genoteerd, gemeten en geïdentificeerd naar morfotype. Onze resultaten laten zien dat 26 jaar na het DISCOL-experiment,

holothurian dichtheid niet verschilt van binnen de ploegbanen/ verstoorde plekken (241±51 ind. ha^{-1}), buiten de ploegbanen/onverstoorde plekken (240±40 ind. ha^{-1}), en referentie-plekken (241±33 ind. ha^{-1}). Verder was holothurian biomassa en community respiratie niet verschillend tussen de plekken. Dit wijst op holothurian herstel van het kleinschalige benthische verstoringsexperiment, binnen 26 jaar.

Potentieel herstel van de fytodetritus verwerking door de zacht-sediment community op DEA, 26 jaar na het DISCOL-experiment, was onderzocht in **Hoofdstuk 5**. We hebben grote benthische incubatie kamers (CUBEs; 50×50×50 cm) *in situ* gebruikt op 4.100 m diepte, binnen de ploegbanen (met en zonder holothurians) en op de referentie-plekken (met holothurians). Tijdens het incuberen, werden met ^{13}C en ^{15}N verrijkte diatomeeën (*Skeletonema costatum*) geïnjecteerd in de CUBE's en watermonsters werden genomen op vijf tijdstappen tijdens de 3 dagen van incubatie. Aan het einde van de incubatie, werden sediment en holothurians gemonsterd om de inname van ^{13}C en ^{15}N door bacteriën, nematoden, macrofauna, en holothurians te meten. ^{13}C-DIC-productie over de tijd werd gemeten in de watermonsters. De totale ^{13}C inname door bacteriën, nematoden en holothurians was significant lager binnen de ploegbanen dan op de referentie plekken, maar het aantal replicaties was laag. Dit impliceert dat fytodetritus verwerking nog niet volledig was hersteld, 26 jaar na het DISCOL-experiment.

In **Hoofdstuk 6** hebben we de data voor macrofauna, megafauna en vis diversiteit en dichtheid gebruikt. Die is verzameld binnen en buiten de ploegbanen, 0.1, 0.5, 3, 7 en 26 jaar na het DISCOL-experiment. Om voedselweb-modellen te ontwikkelen voor elk tijds-punt, met behulp van de lineaire inverse modellering. De totale koolstof voorraad was altijd hoger buiten de ploegbanen dan daarbinnen en 26 jaar na de verstoring, was de koolstof voorraad binnen de ploegbanen 54% van de voorraad buiten de ploegbanen. De totale som van de gemodelleerde koolstof stromen, de "total system throughput" *T*.., was ook altijd lager buiten de ploegbanen dan daarbinnen. Na 26 jaar was dit verschil in *T*.. tussen buiten en binnen de ploegbanen 56%, dit impliceert dat de koolstof stroming nog niet was hersteld na 26 jaar.

Voor **Hoofdstuk 7** hebben we het voedselweb-model voor 26 jaar na het DISCOL-experiment van **Hoofdstuk 6** uitgebreid naar de referentieplekken en ook de bacteriën, nematoden, andere meiofaunale taxa en drie vis compartimenten meegenomen. Dit resulteerde in het meest uitgewerkte, op koolstof-stromingen gebaseerde voedselweb, ontwikkeld voor abyssale vlaktes tot nu toe. Het liet zien dat *T*.. (mmol C m^{-2} d^{-1}) niet significant verschilde tussen de referentieplekken (gemiddelde±standaardafwijking; 4,52±8,35×10^{-2}) en buiten de ploegbanen (5,51±0,16), maar het verschilde aanzienlijk tussen referentieplekken en binnen de ploegbanen (4,42±8,35×10^{-2}), en tussen buiten en binnen de ploegbanen. De belangrijkste oorzaak van verschillen in *T*.. was de microbiële lus die werd ingedrukt binnen de ploegbanen in vergelijking met buiten de ploegbanen of referentie plekken. Dit geeft aan dat de microbiële lus zeer gevoelig reageert op de kleinschalige sedimentverstoring en nog niet was hersteld na 26 jaar.

Om de reactie van bacteriën, meiofauna en macrofauna op diepzee mijnbouw gerelateerde sedimentresuspensie end sedimentdepositie te onderzoeken, hebben we twee sediment depositie analogen bestudeerd: depositie van mijnafval in een fjord ecosysteem in Noorwegen in **Hoofdstuk 8** en zwaar plaat-water cascades ("Dense Shelf Water Cascading", DSWC) in twee Mediterrane onderzee kloven in **Hoofdstuk 9**.

In **Hoofdstuk 8** hebben we onderzocht hoe het benthisch fjord ecosysteem was beïnvloed door korte-termijn expositie aan ijzererts afval depositie en depositie van dood sediment van onder het oppervlak. Sediment kernen werden geïncubeerd met een 0.1, 0.5 en 3 cm dikke laag inert ijzererts-afval voor 11 dagen en met een 0.5 en 3 cm dikke laag dood sediment van onder het oppervlak, voor 16 dagen. We hebben bacteriële, meiofaunale en macrofaunale biomassa, meiofaunale en macrofaunale diversiteit en gemeenschapssamenstelling en mortaliteit van nematoden gemeten. Verder hebben we SCOC, zuurstof penetratie-diepte en opname van ^{13}C van *Skeletonema costatum* door bacteriën, nematoden en macrofauna onderzocht. Onze resultaten laten zien dat begraven onder ≥0.1 cm mijnafval, SCOC en ^{13}C opname reduceerde in alle compartimenten. Dit wijst op een verminderd vermogen van de benthische gemeenschaptot het verwerken van verse fytodetritus. Mijnafval depositie van 3 cm resulteerde in een verhoogde nematoden mortaliteit, waarschijnlijk door een voedseltekort. 3 cm depositie van dood sediment van onder het oppervlakte veroorzaakte ook een verhoogde nematoden mortaliteit. Maar in dit geval was de mortaliteit het gevolg van zuurstofloze omstandigheden in het sediment. Dus, zelfs een dunne laag mijnafval depositie (0.1 cm) heeft een korte termijn effect op het benthische ecosysteem.

Onderzeese kloven zijn locaties van verhoogde koolstoftoevoer naar de diepzee. Om ruimtelijke verschillen in koolstofcyclering te zien tussen verschillende delen van twee diepzeekloven aan de Catalaanse rand en de Golf van Lions (NW Mediterrane Zee), ontwikkelden we koolstof-gebaseerde voedselwebmodellen voor de Cap de Creus kloof en de Lacaze-Duthiers kloof in **Hoofdstuk 9**. Onze resultaten geven aan dat koolstofcyclering in de bovenste Lacaze-Duthiers-kloof en de middelste sectie van de Cap de Creus kloof wordt gedomineerd door actieve faunale koolstofopname door meiofauna. Ter vergelijking, koolstofcyclering in de bovenste en onderste Cap de Creus kloof secties wordt gedomineerd door koolstofopname door bacteriën.

Op het continentaal plat van de NW-Middellandse Zee hebben zich sinds 1993 bijna elke winter DSWC gebeurtenissen voltrokken. Deze trapsgewijze gebeurtenissen leiden tot sedimenterosie en transporteren dit sediment van de continentale marge af de continentale helling. Om de impact van deze gebeurtenissen op het bentische ecosysteem te bestuderen, hebben we onze voedselwebben voor de bovenste en onderste Cap de Creus kloof uitgebreid naar een tijdreeks waarin de situatie meteen na een zeer sterk DSWC-evenement in februari / maart 2005 werd geanalyseerd. Er werden nog meer modellen ontwikkeld voor de situatie 0.5, 3, 3.5, 4 en 4.5 jaar na het grote DSWC-evenement. Onze modelleringsresultaten toonden aan dat de totale hoeveelheid koolstof die in het voedselweb was omgezet, meteen na het DSWC-evenement in

de bovenste kloofsectie was verminderd, maar binnen een half jaar opnieuw toenam. Dit duidt op een snel herstel van het ecosysteem, dat voornamelijk verband hield met verhoogde biomassa van nematoden.

In **Hoofdstuk 10** zijn de resultaten van dit proefschrift geïntegreerd om de benthische ecosysteemrespons op de verwijdering van mangaanknollen te beoordelen. Daarnaast is de reactie van het benthische ecosysteem op de verwijdering, resuspensie en depositie van sedimenten besproken. De respons van het bentisch voedselweb op sedimentverstoring in de diepzee werd geëvalueerd, alsook alsook de validiteit van analogen die gebruikt worden om milieueffecten van diepzeemijnbouw te voorspellen. Mangaanknollenextractie speelt zich af in de mijnbouwcontext, en de milieueffecten van terrestrische nikkel-, koper- en kobaltontginning werden vergeleken met de milieueffecten van mangaanknollenextractie. Ten slotte werden kennistekorten over de ecosysteemrespons op de extractie van mangaanknollen in de diepzee gepresenteerd.

Ter conclusie: het onderzoek in dit proefschrift laat zien dat het benthische ecosysteem sterk reageert op de extractie van mangaanknollen in de diepzee. Het delven van deze knollen zal leiden tot een verlies aan diversiteit door het verwijderen van hard substraat voor sessiele organismen, zoals gesteelde sponzen en hun geassocieerde fauna. Bovendien duiden de resultaten van een kleinschalige verstoring van het sediment erop dat koolstofcyclering onmiddellijk na de mijnbouw kan dalen en het kan meer dan 26 jaar duren om terug te keren naar achtergrondwaarden. Het herstel van bentische ecosystemen op de effecten van mijnbouw op industriële schaal zal daarom tientallen jaren tot eeuwen duren. De fauna van de diepzee zal mogelijks zelfs nooit helemaal herstellen.

Deutsche Zusammenfassung

Mehr als 70% unseres Planeten ist von Ozeanen bedeckt, die eine mittlere Tiefe von 3.800 m haben (Ramírez-Llodrà *et al.*, 2010). Die Tiefsee, so heißt der Ozean unterhalb von 200 m Wassertiefe, ist durch tiefe Wassertemperaturen, hohen Wasserdruck und Dunkelheit gekennzeichnet. Aufgrund des Fehlens von Fotosynthese hängt das Ökosystem außer in Gegenden, in denen Chemosynthese stattfindet, von herabsinkendem partikulären organischen Kohlenstoff aus der euphotischen Zone ab. Das größte Ökosystem der Erde ist das Abyss. Dies ist der Meeresboden zwischen 3.000 und 6.000 m Wassertiefe, welcher sich über 54% der Erdoberfläche erstreckt (Gage and Tyler, 1991). Das Abyss schließt abyssale Berge, Hügel und die Tiefsee-Ebenen ein, die aus feinem Sediment bestehen.

In einigen Gegenden sind die Tiefsee-Ebenen mit Manganknollen bedeckt, die auf der Sedimentoberfläche liegen und/ oder in den oberen 10 cm des Sediments begraben sind. Diese Knollen bestehen aus Ablagerungen aus Eisenoxidhydroxid und Manganoxid und enthalten zusätzlich Nickel, Kobalt, Kupfer und Seltene Erden. Manganknollen wachsen mit Wachstumsraten von 1 bis 10 mm pro Millionen Jahren (hydrogenetisches Wachstum) sehr langsam (Petersen *et al.*, 2016); allerdings wurden auch schon Wachstumsraten von bis zu 250 mm pro Millionen Jahre für diagenetisches Wachstum bestimmt (von Stackelberg, 2000). Wegen ihres hohen Metallgehaltes sind Manganknollen ökonomisch interessant. Schätzungen zur Clarion-Clipperton Fracture Zone (CCZ) im Mittelpazifik beispielsweise ergeben, dass diese Gegend mehr Mangan, Nickel und Kobalt in der Form von Manganknollen enthält als alle Landreserven für die jeweiligen Metalle (International Seabed Authority, 2010; Hein and Koschinsky, 2014; Sverdrup, Ragnarsdottir and Koca, 2017; U.S. Geological Survey, 2018). Allerdings hat der Abbau von Manganknollen Auswirkungen auf die Umwelt, wie zum Beispiel Licht- und Lärmverschmutzung, die Freisetzung von giftigen Metallen, Sedimentwolken, Habitatmodifizierung und -zerstörung. Das Ziel dieser Dissertation war das Untersuchen der Antwort des benthischen Ökosystems auf den Abbau von Manganknollen in der Tiefsee. Ich konzentrierte mich dabei vor allem auf die Antwort des Ökosystems auf Habitatmodifizierung und Zerstörung sowie untersuchte die Erholung von einem kleinskaligen Sedimentstörungsexperiment im Peru Becken, dem sogenannten DISCOL-Experiment (Akronym für „Störungs- und Rekolonisationsexperiment im Südpazifik“; Thiel *et al.*, 1989).

Kapitel 1 stellt dem Leser die Tiefsee im Allgemeinen und die spezifischen Tiefseeökosysteme Fjord, Canyon und das Abyss vor. Die Meeresbodenlebewesen werden beschrieben und die verschiedenen Größenklassen definiert. Desweiteren erläutert dieses Kapitel die trophischen Interaktionen ziwschen den verschiedenen Ernährungstypen in Tiefseenahrungsnetzen. Das Kapitel beschreibt Manganknollen, ihre Entstehung, Tiefseebergbau und die Auswirkung von Manganknollenabbau. Es erläutert auch das DISCOL-Experiment und vergleicht Vorteile und Nachteile der verschiedenen wissenschaftlichen Methoden, die in dieser Dissertation gebraucht wurden.

Um zu beurteilen, wie das benthische Ökosystem auf Tiefseebergbau reagiert, wird ein gutes Verständnis des Benthos vorausgesetzt. Deshalb beschreibt **Kapitel 2** die Rolle von Benthos im globalen Kohlenstoffkreislauf. Die „Random Forest"-Methode wurde genutzt, um weltweite Meereskarten zur benthischen Biomasse und Atmung zu erstellen, die auf Datensätzen zu Meiofauna-, Makrofauna und wirbellosen Megafaunabiomasse basieren sowie auf der Atmung der Sedimentlebewesen. Diese Karten wurden mit einem Datensatz zur biomassespezifischen Atmungsrate, zum Verhältnis von Produktion zu Biomasse und tierischen Nahrungsaufnahme kombiniert, um zu weltweiten Schätzungen von tierischer und prokaryotischer Atmung, tierischer Sekundärproduktion und tierischer Narhungsaufnahme zu gelangen. Wir schätzten außerdem die globale benthische Meiofauna- (9,94 Tg Kohlenstoff), Makrofauna- (28,0 Tg Kohlenstoff) und Megafaunabiomasse (1,47 Tg Kohlenstoff). Die globale benthische Atmungsrate wurde auf 1,19 Pg Kohlenstoff pro Jahr geschätzt, die globale benthische Sekundärproduktion der Tiere auf 0,28 Pg Kohlenstoff pro Jahr und die globale benthische Nahrungsaufnahme durch Tiere wurde auf 1,55 Pg Kohlenstoff pro Jahr geschätzt. Zudem zeigten unsere Ergebnisse, dass 47% der gesamten benthischen Atmung, 50% der benthischen Sekundärproduktion von Tieren und 57% der gesamten benthischen Nahrungsaufnahme durch Tiere unterhalb von 200 m Wassertiefe stattfand.

In **Kapitel 3** analysierten wir wie wichtig Manganknollen und ihre assoziierte Fauna für die Intaktheit des Nahrungsnetzes in Tiefsee-Ebenen sind. Wir führten eine ausgedehnte Literaturrecherche durch und kombinierten diese mit neu ausgewerteten Bildern des Meeresbodens vom Peru Becken und der CCZ. Wir entwickelten Interaktionsnetze mit 208 verschiedenen Nahrungsnetzgruppen im Fall des Peru Beckens und 478 Nahrungsnetzgruppen im Fall der CCZ, die Meiofauna, Makrofauna, Megafauna, Fische, verschiedene Nahrungsarten (frei schwebende organische Partikel, organisches Material im Sediment, Bakterien, gelöstes organisches Material, Aas und Protisten) und Manganknollen einschlossen. Diese Gruppen waren mit 3.131 (Peru Becken) bzw. 9.386 (CCZ) trophischen und nicht-trophischen Verbindungen verbunden. Wir untersuchten, wie sich die Anzahl an Nahrungsnetzgruppen, die Anzahl von Verbindungen, die Verbindungsdichte und Netzwerkkonnektanz veränderte, wenn Manganknollen nicht da waren. Unsere Ergebnisse zeigten, dass das Entfernen der Manganknolle die Netzwerkgruppenanzahl um 26% im Peru Becken und um 20% in der CCZ verringerte. Verglichen dazu führte das Entfernen des „Taxons mit den höchsten Auswirkungen", das heißt, das Taxon, dessen Entfernen die größte Auswirkung auf Nahrungsnetzeigenschaften hatte, zum Verlust von <5% der Nahrungsnetzgruppen. Außerdem enthüllte unsere Analyse, dass gestielte Schwämme, die auf Manganknollen wachsen, Schlüsselspezien der Tiefsee-Ebene sind, weil sie eine große Gruppe kommensaler Tiere beherbergen. Deshalb wird die Abwesenheit von Manganknollen in knollenreichen Gebieten zu einem lokalen Verlust von Biodiversität führen.

Während des DISCOL-Experiments 1989 wurden 22% eines 10,8 km^2-großen Kreises mit einer 8 m-breiten Pflugscharr gepflügt. Dies führte dazu, dass

die Manganknollen im Sediment begraben wurden und die Sedimentoberfläche in den Pflugspuren umgedreht wurde. Eine mögliche Erholung des Ökosystems von dieser kleinskaligen Sedimentstörung wurde in **Kapitel 4**, **5**, **6** und **7** untersucht.

In **Kapitel 4** untersuchten wir die Langzeitauswirkungen des DISCOL-Experiments anhand von Seegurken, die als Modelorganismen für die Detritus-fressende mobile Megafauna dienten. Während der Forschungsfahrt SO242-2 an Bord des Forschungsschiffes Sonne im September 2015 wurden 3.760 Bilder des Meeresbodens mit einem geschleppten „Ozeanbodenobservationssystem“ während vier Transsekte in der DISCOL-Experimentalfläche gemacht. Zusätzlich wurden 983 Bilder des Meeresbodens während vier Transsekte in der Referenzzone 4 km entfernt von der DISCOL-Experimentalfläche gemacht. Alle Seegurken auf diesen Bildern wurden gekennzeichnet, gemessen und einem bestimmten Seegurkentypen zugeordnet. Unsere Resultate zeigten, dass sich 26 Jahre nach dem DISCOL-Experiment die Seegurkendichte in der Pflugspur (241±51 Individuen pro Hektar) nicht von der Dichte außerhalb der Pflugspur (240±40 Individuen pro Hektar) oder der Referenzzone (241±33 Individuen pro Hektar) unterschied. Auch unterschied sich die Seegurkenbiomasse und die Atmung der Seegurkengemeinschaft nicht zwischen den einzelnen Orten, was bedeutet, dass sich die Seegurken von dem kleinskaligen benthischen Störungsexperiment innerhalb von 26 Jahren erholt hatten.

Die mögliche Erholung des Zersetzungsprozesses von Phytodetritus durch die Sedimentgemeinschaft in der DISCOL-Experimentalfläche wurde in **Kapitel 5** untersucht. Wir brachten große benthische Inkubationskammern (CUBEs; 50×50×50 cm) *in situ* in 4.100 m Wassertiefe in Pflugspuren (mit und ohne Seegurken) und im Referenzbereich (mit Seegurken) aus. Während dieser Inkubationen wurden mit ^{13}C und ^{15}N-angereicherte *Skeletonema costatum* in die CUBEs injiziert und Wasserproben zu fünf verschiedenen Zeitpunkten innerhalb des dreitägigen Experiments genommen. Am Ende der Inkubationszeit wurden Proben des Sediments und der Seegurken genommen, um die Aufnahme von ^{13}C und ^{15}N durch Bakterien, Nematoden, Makrofauna und Seegurken zu bestimmen. Die Gesamtaufnahme von ^{13}C durch Bakterien, Nematoden und Seegurken war in den Pflugspuren signifikant niedriger als im Referenzgebiet; allerdings war die Anzahl an Replikaten gering. Dies bedeutet, dass sich der Zersetzungsprozess von Phytodetritus nicht vollständig innerhalb von 26 Jahren erholt hat.

In **Kapitel 6** benutzten wir Daten zu Makrofauna-, Megafauna- und Fischdiversität und -dichte, die innerhalb und außerhalb der Pflugspuren 0,1 Jahre, 0,5 Jahre, 3 Jahre, 7 Jahre und 26 Jahre nach dem DISCOL-Experiment erhoben wurden, um für jeden dieser Zeitpunkte ein Nahrungsnetzmodell zu entwickeln, welches auf dem Linear-Inversen-Modellierungsansatz beruht. Der gesamte Kohlenstoffbestand war immer außerhalb der Pflugspuren höher als innerhalb und 26 Jahre nach dem DISCOL-Experiment betrug der Kohlenstoffbestand innerhalb der Pflugspuren 54% des Kohlenstoffbestandes verglichen mit außerhalb der Pflugspuren. Auch die Gesamtheit der modellierten Kohlenstoffflüsse, das heißt der „Gesamtsystemdurchfluss“ *T*.. war außerhalb der Pflugspuren stets größer als innerhalb der Pflugspuren. Nach 26 Jahren war die

Differenz des Gesamtsystemdurchflusses zwischen außerhalb und innerhalb der Pflugspuren 56%, was bedeutet, dass sich der Kohlenstoffkreislauf auch nach 26 Jahren nicht erholt hat.

In **Kapitel 7** erweiterten wir die Nahrungsnetzmodelle für den Zeitpunkt 26 Jahre nach dem DISCOL-Experiment um die Referenzzone und fügten zusätzlich Bakterien, Nematoden, andere Meiofaunagruppen und drei Fischgruppen hinzu. Dies führte zu dem am höchsten aufgelösten Kohlenstoff-basierten Nahrungsnetzmodell, welches bisher für Tiefsee-Ebenen entwickelt wurde. Es zeigte, dass sich *T*.. (mmol C m^{-2} d^{-1}) nicht signifikant zwischen der Referenzgegend (Mittelwert±Standardabweichung $4{,}52±8{,}35×10^{-2}$) und außerhalb der Pflugspur unterschied (5,51±0,16), aber signifikant unterschiedlich ziwschen der Referenzgegend und innerhalb der Pflugspur ($4{,}52±8{,}35×10^{-2}$) war und zwischen außerhalb und innerhalb der Pflugspur. Die Hauptursache für diesen Unterschied war die mikrobielle Schleife, welche niedriger innerhalb der Pflugspur verglichen mit außerhalb der Pflugspur oder Referenzgegend war. Es deutet daraufhin, dass die mikrobielle Schleife sehr sensibel auf das kleinskalige Sedimentstörungsexperiment reagiert und sich nach 26 Jahren noch nicht davon erholt hat.

Um die Antwort von Bakterien, Meiofauna und Makrofauna auf mit Tiefseebergbau verbundener Sedimentablagerung bzw. Sedimentausfällung zu erforschen, untersuchten wir zwei Sedimentablagerungsanalogien: die Ablagerung von Bergbaurückständen in einem norwegischen Fjordökosystem in **Kapitel 8** und in **Kapitel 9** wie schweres Schelfwasser zwei Mittelmeercanyons herunterfließt („Dense Shelf Water Cascading“).

In **Kapitel 8** untersuchten wir die Reaktion des benthischen Fjordökosystems, wenn es kurzzeitig Eisenerzrückständen und abgetötetem Sediment ausgesetzt ist. Sedimentbohrkerne wurden hierzu mit einer 0,1, 0,5 und 3 cm-dicken Schicht Eisenerzrückstände bedeckt und für 11 Tage inkubiert. Zusätzliche Sedimentbohrkerne wurden mit einer 0,5 und 3 cm-dicken Schicht abgetötetem Sediment bedeckt und für 16 Tage inkubiert. Wir maßen Bakterien-, Meiofauna- und Makrofaunabiomasse, Meiofauna- und Makrofaunadiversität, die Zusammensetzung der Meiofauna- und Makrofaunagemeinschaft und die Mortalität der Nematoden. Zusätzlich untersuchten wir die Atmungsrate der Sedimentlebewesen, die Tiefe bis zu der Sauerstoff ins Sediment eindringt und die Aufnahme von ^{13}C aus *Skeletonema costatum* durch Bakterien, Nematoden und Makrofauna. Unsere Ergebnisse zeigten, dass das Begraben unter ≥0,1 cm Eisenerzrückstände die Atmungsrate der Sedimentlebewesen und die Aufnahme von ^{13}C durch alle Lebewesen reduzierte. Dies bedeutet, dass die Fähigkeit der benthischen Gemeinschaft, frisches Phytodetritus zu zersetzen, verringert war. Des Weiteren führte das Bedecken mit einer 3 cm dicken Schicht Eisenerzrückstände zu einer erhöhten Nematodenmortalität. Auch das Bedecken mit 3 cm abgetötetem Sediment führte zu einer höheren Mortalität unter Nematoden, aber dieses Mal wurde es durch anoxische Bedingungen im Sediment verursacht. Folglich hat bereits das Begraben unter einer dünnen Schicht Eisenerzrückstände (0,1 cm) kurzzeitige Auswirkungen auf das benthische Ökosystem.

Tiefseecanyons sind Orte mit verstärktem Kohlenstoffeintrag in die Tiefsee. Um räumliche Unterschiede im Kohlenstoffkreislauf zwischen verschiedenen Abschnitten zweier Tiefseecanyons am katalanischen Kontinentalrand und im Golf von Lyon (nordwestliches Mittelmeer) zu untersuchen, entwickelten wir in **Kapitel 9** auf Kohlenstoff basierende Nahrungsnetzmodelle für den Cap de Creus-Canyon und den Lacaze-Duthiers-Canyon. Unsere Ergebnisse weisen daraufhin, dass der Kohlenstoffkreislauf im oberen Abschnitt des Lacaze-Duthiers-Canyons und im mittleren Abschnitt des Cap de Creus-Canyons von aktiver tierischer Kohlenstoffaufnahme dominiert werden. Im Vergleich dazu wird der Kohlenstoffkreislauf im oberen und unteren Cap de Creus-Canyon von der Kohlenstoffaufnahme durch Bakterien dominiert.

Der Festlandsockel des nordwestlichen Mittelmeeres ist seit 1993 fast jeden Winter schweren „Dense Shelf Water Cascading"-Ereignissen ausgesetzt. Diese „Cascading"-Ereignisse führen zu Sedimenterosion und transportieren dieses Sediment vom Festlandsockel den Abhang hinunter. Um den Einfluss dieser Ereignisse auf das benthische Ökossystem zu untersuchen, erweiterten wir die Nahrungsnetzmodelle für den oberen und unteren Abschnitt des Cap de Creus-Canyons um eine Zeitserie und analysierten die Lage direkt nach einem starken „Dense Shelf Water Cascading"-Ereignis im Februar/ März 2005. Weitere Modelle wurden für die Situation nach 0,5, 3, 3,5, 4 und 4,5 Jahren nach dem starken „Cascading"-Ereignis erstellt. Unsere Ergebnisse zeigten, dass der gesamte Kohlenstoff, der innerhalb des Nahrungsnetzes zirkulierte, direkt nach dem „Cascading"-Ereignis im oberen Abschnitt des Cap de Creus-Canyon reduziert war, sich aber innerhalb eines halben Jahres wieder erholt hatte. Das deutet auf eine schnelle Erholung des Ökosystems hin, was vor allem an einer erhöhten Nematodenbiomasse liegt.

In **Kapitel 10** integriere ich meine Ergebnisse zur Antwort des benthischen Ökosystems auf den Abbau von Manganknollen in der Tiefsee. Zusätzlich wurden die Antwort des benthischen Ökosystems auf das Entfernen von Sediment, Sedimentsuspension und Wiederablagerung erläutert. Es wurde auch aufgezeigt, wie das benthische Ökosystem auf eine Störung des Sediments in der Tiefsee reagiert und es wurde evaluiert, wie zulässig Analogien sind, um Umweltauswirkungen durch Tiefseebergbau zu untersuchen. Manganknollenabbau wurde in den globalen Bergbaukontext gebracht und die Umweltauswirkungen von Nickel, Kupfer und Kobaltabbau wurden den Auswirkungen von Tiefseebergbau gegenübergestellt. Abschließend wurden Wissenslücken zur Antwort des Ökosystems auf den Manganknollenabbau in der Tiefsee aufgezeigt.

Zusammenfassend zeigen die Ergebnisse dieser Dissertation, dass das benthische Ökosystem stark auf den Abbau von Manganknollen in der Tiefsee reagiert. Der Abbau dieser Knollen wird zu einem Diversitätsverlust führen, weil das Hartsubstrat sessiler Organismen, wie zum Beispiel gestielter Schwämme, und der mit ihnen assoziierten Fauna, entfernt wird. Außerdem zeigen die Ergebnisse eines kleinskaligen Störungexperiments, dass der Kohlenstoffkreislauf vermutlich nach der Bergbauoperation stark abfällt und es somit mehr als 26 Jahre dauern könnte, bis sich die Ursprungsraten wieder

eingestellt haben. Folglich wird sich das benthische Ökosytem nach industriellem Manganknollenabbau erst nach Jahrzehnten bis Jahrhunderten erholen. Sessile Fauna wird sich eventuell nie vollständig vom Manganknollenabbau erholen.

Chapter 1 : General introduction

1. General introduction

1.1 The deep sea

The deep sea begins at the continental shelf at 200 m water depth (Thistle, 2003) and contains 73% of the water in the oceans (Ramirez-Llodra *et al.*, 2010). Its seafloor covers more than 62% of the Earth's surface (Gage and Tyler, 1991) and is divided into the three depth zones: "bathyal"[1] between 200 and 3,000 m water depth (Zezina, 1997), "abyssal"[2] between 3,000 and 6,000 m water depth (Zezina, 1997) and "hadal" at >6,000 m water depth (Gage and Tyler, 1991).

The deep sea environment is characterized by low water temperature (except in the Mediterranean Sea [14°C] and the Red Sea [21°C]; Ramírez-Llodrà *et al.*, 2010) and high pressure that ranges from 20×10^5 Pa at the continental shelf to $>1{,}000\times10^5$ Pa in the deepest trenches (Thistle, 2003). Below 250 m depth, the photosynthetically active radiation (PAR) is generally insufficient to support photosynthesis (Thistle, 2003), though crustose corraline algae have been observed at 268 m depth at the Bahamas (Littler *et al.*, 1985). Hence, the deep sea – except at hydrothermal vents and cold-seeps – is a "detritus based ecosystem" (Ramírez-Llodrà *et al.*, 2010) that relies on external input of particulate organic matter (POM) from the euphotic zone, such as marine snow (De La Rocha and Passow, 2007) and fecal pellets (Iseki, 1981; Pfannkuche and Lochte, 1993; Michels *et al.*, 2008). It is estimated that only 15% of the global net primary production leaves the euphotic zone (Woodward, 2007) and only 0.7% of the organic carbon in the surface water, i.e., 0.31±0.30 Pg org. C, reaches the seafloor at >2,000 m depth per year (Dunne, Sarmiento and Gnanadesikan, 2007). In particular, the abyssal plains are therefore considered to be „food-limited" (Smith *et al.*, 2008).

Particulate organic carbon (POC) often reaches the deep-sea seafloor in seasonal pulses. At the Porcupine Seabight in the temperate NE Atlantic, for instance, a patchy layer of phytodetritus was observed at the seafloor between 1,370 (bathyal) and 4,100 m (abyssal) water depth from April to July 1979 (Billett, Lampitt and Rice, 1983). The detrital layer consisted of diatoms, fecal pellets, and gelatinous aggregations of coccolithophores, dinoflagellates, eggs of crustaceans, smaller fecal pellets, and other amorphous organic matter (Billett, Lampitt and Rice, 1983). At Station M in the NE Pacific, aggregates of phytodetritus were also observed (Smith, Kaufmann and Baldwin, 1994). These aggregates reached the abyssal seafloor at 4,100 m depth in pulses from July to December 1990, approximately 1.5 months after the initial peaks in particulate organic matter flux had been detected in sediment traps 600 and 50 m above the seafloor (Smith, Kaufmann and Baldwin, 1994).

---

[1] For Gage and Tyler (1991), the bathyal ranged from 200 m to 2000 m water depth.

[2] Edward Forbes called the ocean at >100 fathoms water depth (100 fathoms = 183 m) abyss and described it as an area "where life is either extinguished, or exhibits but a few sparks to mark its lingering presence" (Forbes, 1854, p. 26). Later on, Wyville Thomson (1880, p. 35) reported that "the abyssal fauna would seem […] to attain its fullest development in a zone of depth between 600, and 1,000 and 1,200 fathoms" and would still be simlar from "1,200 or 1,500 fathoms downwards". This depth range corresponds to today's bathyal depth.

Box 1.1: Benthic-pelagic coupling

Benthic-pelagic coupling or bentho-pelagic coupling describes "those processes which connect the bottom substrate and the water column habitats through the exchange of mass, energy and nutrients" (Griffiths *et al.*, 2017). It includes "the deposition on the sea-bed of organic-rich particles originating in the upper water column" (Gooday, 2002) and the efflux of dissolved organic carbon (DOC) and nutrients from the sediment to the water column (Raffaelli *et al.*, 2003).

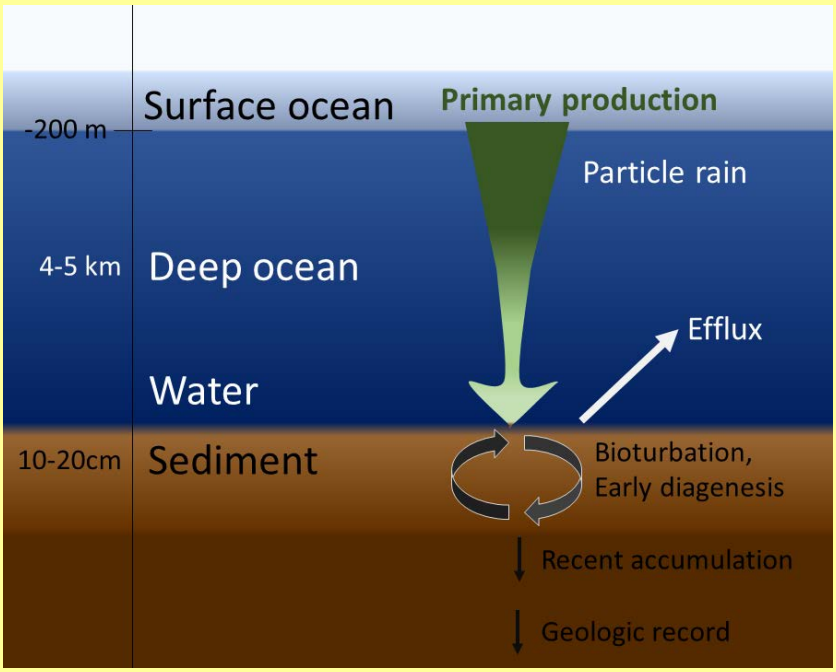

Figure 1-1. Schematic representation of benthic-pelagic coupling (modified from Smith *et al.*, 1997). The green arrow symbolizes the benthic-pelagic coupling, i.e., the rain of particles, i.e., particulate organic carbon (POC), from the primary producers in the surface waters to the seafloor. At the seafloor, parts of the POC are bioturbated, i.e., they are reworked into the sediment by fauna, and mineralized during early diagenesis. POC that is mineralized to e.g., dissolved organic carbon (DOC) or dissolved inorganic carbon (DIC), leaves the sediment via efflux to the water column. In contrast, POC that escapes early diagenesis accumulates first and over geological timescales it is buried in the sediment.

1.1.1 Fjords

Fjords are semi-enclosed marine basins that are formed by glacial overdeepening[3] (Howe *et al.*, 2010). They often have an entrance sill which separates the deep waters inside the fjord from coastal waters outside the fjord and in this

[3] Overdeepening: "The erosive process by which a glacial deepens and widens an inherited preglacial valley to below the level of the subglacial surface." (Licker, 2008)

way restrict the water circulation and oxygen renewal (Howe *et al.*, 2010). Fjords occur in polar, subpolar, and temperate climate zones (Howe *et al.*, 2010): Polar fjords in E and N Greenland, the Canadian Arctic, and Antarctica are permanently covered by sea ice or are connected to a resident glacier (Howe *et al.*, 2010). They are supplied with sediment from subglacial rivers, the glacial bed, and icebergs (Howe *et al.*, 2010). Subpolar fjords exist in areas with mean summer air temperatures >0°C, like on Svalbard, in W Greenland, the Canadian Arctic or in Antarctica (Howe *et al.*, 2010). They are covered by seasonal sea ice in winter and are not necessarily connected to glaciers; sediment is supplied from subglacial meltwater runoff, terrestrial rivers, and icebergs (Howe *et al.*, 2010). Temperate fjords are located in Iceland, Alaska, Chile, Scotland, New Zealand, and Norway (Howe *et al.*, 2010). Norwegian fjords are vulnerable to hydroelectric power plants (Kaartvedt and Svendsen, 1990; Manzetti and Stenersen, 2010), tunnel-construction projects that dump rock into the fjords (Manzetti and Stenersen, 2010), effluent discharges (Johansen *et al.*, 2018), and submarine mine tailings placement (STP) (Ramirez-Llodra *et al.*, 2015). The longest and deepest Norwegian fjord is the Sognefjord with a length of 205 km and a maximum depth of 1,304 m (Manzetti and Stenersen, 2010).

1.1.2 Submarine canyons

Submarine canyons are cut into continental shelves as well as slopes and occur globally (5,854 canyons worldwide; Harris and Whiteway, 2011). They are formed by erosion during slumping, submarine landslides or turbidity currents (Harris and Whiteway, 2011) and channel sediment and organic matter to the deep sea (Sanchez-Vidal *et al.*, 2008; Martín *et al.*, 2013). Canyons are hotspot of marine biodiversity (De Leo *et al.*, 2010), and can have increased benthic faunal biomasses, such as holothurians (De Leo *et al.*, 2010; van Oevelen, Soetaert, *et al.*, 2011).

Mediterranean canyons are different from other canyon in the world: They are more closely spaced, have a more dendritic shape with 12.9 limps per 100,000 km^2, have a mean length of 26.5 km, are very steep (mean slope: 6.5°), and have a smaller depth ranges (1,613 m) compared to other canyons (Harris and Whiteway, 2011). Since 1993, canyons at the Catalan Margin and the Gulf of Lions (NW Mediterranean Sea) have experienced dense shelf water cascading events nearly every winter.

Box 1.2: Dense shelf water cascading

Dense shelf water cascading (DSWC) refers to a case of buoyancy driven current (Shapiro, Huthnance and Ivanov, 2003): The density of surface water increases because of cooling, evaporation, freezing or salinization on the continental shelf until this denser water overflows the shelf edge. It flows along the continental slope until it reaches water with ambient density. DSWC have been detected at mid-latitudes (e.g., Rockall Bank, Celtic Sea, Malin shelf, Skagerrak), in the tropics and subtropics (e.g., Catalan Margin, Adriatic Sea, North American south-eastern shelf, Northern Gulf of California), and in polar areas (e.g., Antarctica, Beaufort Sea shelf) (Shapiro, Huthnance and Ivanov, 2003; Durrieu de Madron *et al.*, 2005). Since 1993, the Catalan Margin and Gulf of Lions (NW Mediterranean Sea) have experienced DSWC events nearly every winter. These events lead to an irreversible exchange of shelf water and it has been estimated that during the major DSWC event in 2005, 66% of the shelf water from the Gulf of Lions was transported down the continental slope (Canals *et al.*, 2006).

1.1.3 The abyss

The abyss is the largest ecosystem on Earth (306,595,900 km^2 area, Harris *et al.*, 2014 or 54% of Earth's surface, Gage and Tyler, 1991) and covers 85% of the ocean floor (Harris *et al.*, 2014) (Figure 1-2). It consists of abyssal plains (32.9% of the abyss) that have a seabed relief[4] of 0 to 300 m and can be very flat with slopes of <0.05° (Cormier and Sloan, 2018), the abyssal hills with a relief of 300 to 1,000 m (48.7% of the abyss) and abyssal mountains (18.4% of the abyss; relief: >1,000 m) (Harris *et al.*, 2014).

The abyssal plains are subdivided by deep sea trenches, island arcs, and mid-ocean ridges, such as the Mid-Atlantic Ridge or the East-Pacific Rise, and punctuated with abyssal hills and abyssal mountains (Smith *et al.*, 2008). Over geological time scales, these plains were formed by turbidity currents, i.e., a slurry of seawater and sediments, that were triggered by earthquakes, tsunamis or storms at the continental margins (Cormier and Sloan, 2018). In the Atlantic Ocean or the Antarctic Ocean with their passive margins[5], no obstacles stopped the flow of these turbidity currents towards the oceanic basins, resulting in very smooth abyssal plains (Cormier and Sloan, 2018) with sediment thicknesses of 50 to 5,000 m in the N Atlantic (Whittaker *et al.*, 2013). In contrast, in the Pacific Ocean with its deep trenches in subduction zones, the turbidity currents were trapped inside the trenches and the currents never reached the oceanic basins (Cormier and Sloan, 2018). Therefore, the abyssal plains were formed through slow pelagic sedimentation (Cormier and Sloan, 2018), resulting in a sediment thickness between 0 and 1,000 m in the SE Pacific (Whittaker *et al.*, 2013).

[4] Relief: "The vertical difference in elevation between the hilltops […] and the […] valleys of a given region." (Neuendorf, James and Jackson, 2005).

[5] Passive margin: A passive margin is a continental margin that is not a plate margin (Allaby, 2008b).

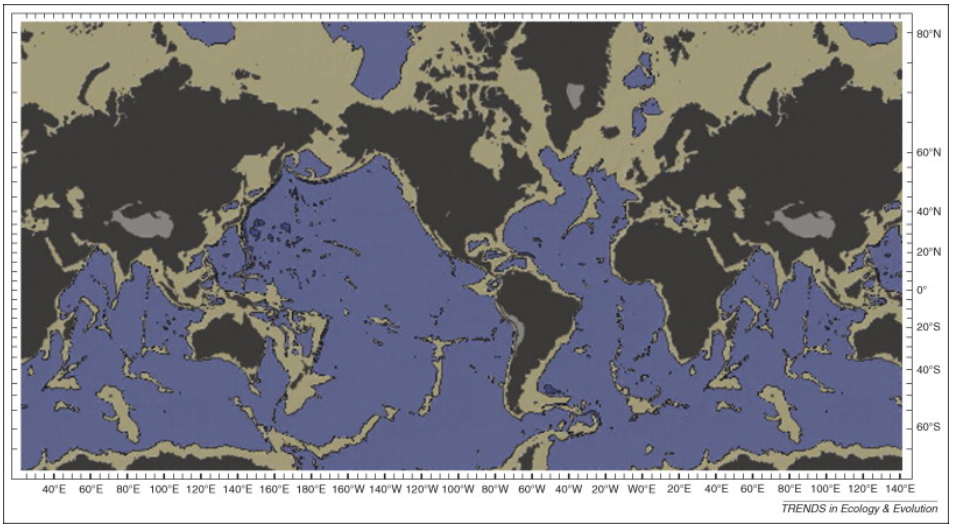

Figure 1-2. Global map of the abyssal seafloor (blue) between 3,000 and 6,000 m water depth. The sublittoral (0 to 200 m water depth; Gage and Tyler, 1991) and bathyal seafloor (200 to 3,000 m water depth; Smith *et al.*, 2008) are shown in light brownish-gray, the hadal seafloor (>6,000 m water depth; Gage and Tyler, 1991) is shown in dark blue and landmasses are shown in dark brownish-gray. Source: Smith *et al.* (2008).

1.2 Seafloor biota

The seafloor biota consists of prokaryotes and benthos. **Prokaryotes**, i.e., Bacteria and Archaea, are the most abundant seafloor biota with densities of 4.60×10^{7} cells cm^{-3} (= 1.70×10^{28} prokaryotic cells globally) in the upper 10 cm of sediment (Whitman, Coleman and Wiebe, 1998). Benthos refers to protozoan and metazoan faunal organisms living in, on, or near the seafloor. They have important roles in the marine ecosystem: By bioturbation, i.e., the reworking of sediments by fauna (Meysman, Middelburg and Heip, 2006), benthos change the texture of the sediment (Meadows and Tait, 1989) and reduce slope failure (Shaikh, Meadows and Meadows, 1998). Bio-irrigation, i.e., the increased exchange of solutes between pore water and the overlaying water column due to flushing of faunal burrows (Meysman, Middelburg and Heip, 2006) affects nutrient cycling (Davenport, Shull and Devol, 2012) and increases oxygenation of sediment (Braeckman *et al.*, 2010). Ecosystem engineers, i.e., organisms that alter the physical environment and in this way directly or indirectly change how resources are available to other organisms (Jones, Lawton and Shachak, 1994), can change hydrodynamics. Furthermore, benthic organisms, such as scleractinian corals or sponges, can form biological structures that provide new habitats for associated fauna (Beaulieu, 2001; Buhl-Mortensen *et al.*, 2010).

Benthos are classified in size classes depending on a taxonomic definition (= meiofauna, macrofauna, megafauna; Mare, 1942) or depending on a statistical entity (= meiobenthos, macrobenthos, megabenthos; McIntyre, 1969). Generally, **meiobenthos** include organisms of the sizes 32 µm to 250 µm (research programs of the European Union)/ 300 µm (American research programs) (Rex and Etter,

2010); however, often no upper size limit is used. **Macrobenthos** include all organism that are retained on a 250 µm/ 300 µm sieve and **megabenthos** are roughly defined as organisms that are visible on photographs (>1 or >3 cm) (Rex and Etter, 2010).

Using the taxonomic definition of **meiofauna**, the deep-sea meiofaunal community consist of protozoan meiofauna, i.e., foraminifera (61-76% of all meiofauna at PAP, Madeira Abyssal Plain, and Cape Verde Abyssal Plain; Gooday, 1996), and metazoan meiofauna which is dominated by nematodes (80 to 99% of all metazoan meiofauna in the NE Atlantic; Vincx *et al.*, 1994). The second most abundant metazoan meiofauna taxon in the NE Atlantic is copepods (Vincx *et al.*, 1994) and other metazoan meiofauna taxa include turbellarians and ostracods (Rex *et al.*, 2006; Giere, 2009). Nematodes are mainly bacterivores, followed by omnivores and predators, whereas epistrate feeders only contribute a few percent to the nematode community (Giere, 2009).

The deep-sea metazoan **macrofaunal** community consists mainly of polychaetes (Rex *et al.*, 2006) that contribute 60 to 83% to the total macrofauna at PAP, but only 33% in the central Indian Ocean (Ingole and Koslow, 2005) and 26% near the Kuril-Kamchatka Trench (NW Pacific) (Brandt *et al.*, 2015). Other dominating macrofauna taxa are peracarid crustaceans (e.g., 18% tanaids and 6% isopods in the central N Pacific; Hessler and Jumars, 1974) and molluscs (e.g., 7% bivalves in the central N Pacific; Hessler and Jumars, 1974). The five most abundant polychaete families at Station M are Paraonidae, Spionidae, Capitellidae, Pilargidae, and Cirratulidae, whereas the five most abundant polychaete families at PAP are Opheliidae, Cirratulidae, Spionidae, Paraonidae, and Sabellidae (Laguionie-Marchais *et al.*, 2013). Hence, the dominating feeding types of polychaetes at these specific locations are surface/ subsurface deposit feeder and suspension feeder (Jumars, Dorgan and Lindsay, 2015).

The **megafauna** community composition differs depending on the trophic state of the abyssal plain. In the eutrophic Pacific abyssal plain of the equatorial upwelling zone (5°S to 5°N), where the POC flux is on average 3.6 mg C_{org} m^{-2} d^{-1} (Honjo *et al.*, 1995), the metazoan megafauna consist mainly of burrowing echinoids, filter-feeding hexactinellid poriferans, epibenthic holothurians and endobenthic echiurans (Smith and Demopoulos, 2003). In the mesotrophic equatorial Pacific abyssal plain (9 to 10°N) with an average POC flux of 1.3 mg C_{org} m^{-2} d^{-1} (Honjo *et al.*, 1995), the dominant megafauna include poriferans, and holothurians (Smith and Demopoulos, 2003). The megafauna of the oligotrophic central N Pacific abyssal plain (28 to 31°N, 155 to 159°W, Smith and Demopoulos, 2003; mean POC flux of 0.8 mg C_{org} m^{-2} d^{-1}, Smith, 1992) consist of holothurians, cnidarians, and very mobile scavengers (Smith and Demopoulos, 2003), such as lysianassid amphipods (Barnard and Ingram, 1986).

Demersal fish lives on or associated with the seafloor and includes benthic and benthopelagic fish (Drazen and Sutton, 2017). Common fish species in the abyss are the tripod fish (family Chlorophthalmidae), the rattail (*Coryphaenoides* sp.), *Ipnops* sp., *Bathysaurus* sp., and Ophidiidae (Gage and Tyler, 1991; Priede *et al.*, 1991; Linley, 2014).

The biomass and abundance of deep-sea biota decreases exponentially with depth, whereupon the density of larger fauna declines more rapidly than the density of smaller fauna (Rex *et al.*, 2006) confirming Thiel's (1975) size structure hypothesis.

Box 1.3: Size structure hypothesis

The size structure of deep-sea benthos was analyzed by Thiel (1975) and he hypothesized that "with increasing depth small organisms gain importance in the total metabolism of benthic deep-sea associations". He generalized even further: "Associations governed by constantly limited food availability are composed of small individuals on the average."

1.3 Benthic ecosystem dynamics

Certain benthic taxa are able to respond rapidly to the deposition of phytodetritus. Within 1.5 d, bacteria together with foraminifera processed 50% of the total amount of ^{13}C-enriched phytodetritus that was either ingested or respired by the benthic community in an *in situ* experiment at 2,170 m depth in the NE Atlantic (Moodley *et al.*, 2002).

Living benthic meiofaunal foraminifera also colonized the phytodetritus on the seafloor between 3,800 and 4,600 m depth in the NE Atlantic likely within 1 to 2 months either by migration from the sediment into the phytodetritus, by reproduction inside the phytodetritus or by a combination of both processes (Gooday, 1988). Meiofaunal nematodes incorporated ^{13}C-enriched phytodetritus within 3 d in an *in situ* experiment in the Peru Basin (SE Pacific) (Stratmann, Mevenkamp, *et al.*, 2018/ **Chapter 5**). However, a study at the Porcupine Abyssal Plain (PAP) showed that most of the ^{13}C-uptake by nematodes in the 0 to 2 cm layer occurred between 8 and 23 d (Witte, Aberle, *et al.*, 2003).

In the same experiment, macrofauna dominated the incorporation of ^{13}C-enriched phytodetritus over the first 2.5 d (Witte, Aberle, *et al.*, 2003), whereas in an *in situ* experiment in the abyssal plains of the Clarion-Clipperton Fracture Zone (CCZ) in the mesotrophic E Pacific, bacteria, not macrofauna were responsible for most of the turnover of the added ^{13}C-enriched phytodetritus within the initial <1.5 d (Sweetman, Smith, *et al.*, 2016).

The megafauna deposit feeder *Oneirophanta mutabilis* had a seasonally varying concentration of phytopigment in its gut that mirrored exactly the seasonal deposition of phytodetritus in at PAP (Witbaard *et al.*, 2001). However, this seasonal difference in concentrations also implies that this holothurian species did not selectively feed at local hotspots of increased phytodetritus concentrations (Witbaard *et al.*, 2001).

The seafloor community as a whole can react to pulses of fresh phytodetritus by increased sediment community oxygen consumption (SCOC). At Station M, the highest SCOC were measured in June/ July, when the POC flux at 50 m and 600 m above the seafloor was likewise at a maximum, and lowest in February

(Drazen, Baldwin and Smith, 1998). In contrast, SCOC measurements at PAP showed no seasonal differences (Witbaard *et al.*, 2001).

Besides intra-annual variations in phytrodetritus input, the abyssal plains also experience inter-annual variability. Synchronous to the El Niño/ La Niña event between 1997 and 1999, the community structure of the dominant mobile epibenthic megafauna, i.e., mobile epibenthic fauna ≥1 cm in size, changed at 4,100 m depth at Station M (Ruhl and Smith, 2004). The holothurians *Elpidia minutissima* and *Peniagone vitrea* increased in densities from 1989 to 1996, but dropped between 1999 and 2000 and were absent afterwards (*E. minutissima*) or dropped between 2001 and 2002 (*P. vitrea*) (Ruhl and Smith, 2004). In contrast, the holothurian species *Peniagone diaphana*, *Abyssocucumis abyssorum*, *Scotoplanes globosa*, *Psychropotes longicauda*, the echinoids *Echinocrepis* spp., and the ophiuroids *Ophiura* spp. were low in densities since 1989, except for *P. diaphna*, that was also high in densities in 1995, but rose steeply between 2001 and 2002 (Ruhl and Smith, 2004). At about the same time, between 1989 to 1999 also the invertebrate megafauna at PAP changed radically with a significant rise in densities of actiniarians, annelids, pycnogonids, tunicates, ophiuroids, and the holothurians *Amperima rosea* and *Ellipinion molle*, though the wet weight biomass did not change significantly (Billett *et al.*, 2001). Since the densities of *A. rosea* increased by more than 3 orders of magnitude between 1996 and 1999 and also in 2002, this event became known as "Amperima event" (Billett *et al.*, 2010).

1.4 Deep-sea food webs

The abyssal plain food web (Figure 1-3) is detritus-based, i.e., it receives its organic carbon in the form of phytodetritus from the euphotic zone higher in the water column. This phytodetritus sinks to the seafloor where it is filtered out of the water column by filter and suspension feeder, such as alcyonaceans, cnidarians or poriferans (Fox, Barnes and Ruppert, 2003). Phytodetritus that settles on the seafloor contributes to the sedimentary detritus pool which is ingested by deposit feeders, such as holothurians (Box 1-4) (Roberts *et al.*, 2000). Filter and suspension feeders as well as deposit feeders are the prey of predators, such as asteroids or crustaceans (Fox, Barnes and Ruppert, 2003), and fish[6] (Drazen and Sutton, 2017). Some species have no specific feeding preferences and are omnivores, such as echinoids (Smith and Stockley, 2005). When organisms die, they contribute to the carrion pool on which scavengers, such as scavenging amphipods (Iken *et al.*, 2001) or specific fish species (Drazen and Sutton, 2017) feed. Prokaryotes, however, dominate carbon flows in the deep sea via the microbial loop (van Oevelen, Bergmann, *et al.*, 2011; Dunlop *et al.*, 2016; Durden *et al.*, 2017). They take up dissolved organic carbon (DOC) which is released from the seafloor as a result of hydrolysis of the detritus pool and in return, they are grazed upon by bacterivorous nematodes. However, they can also be ingested by deposit feeders when these ingest sediment. Phytodetritus and in particular refractory detritus that is not mineralized is buried in the sediment.

[6] Fish is often kept as a separate food-web compartment due to differences in metabolic activity between marine invertebrates and marine fish (Seibel and Drazen, 2007).

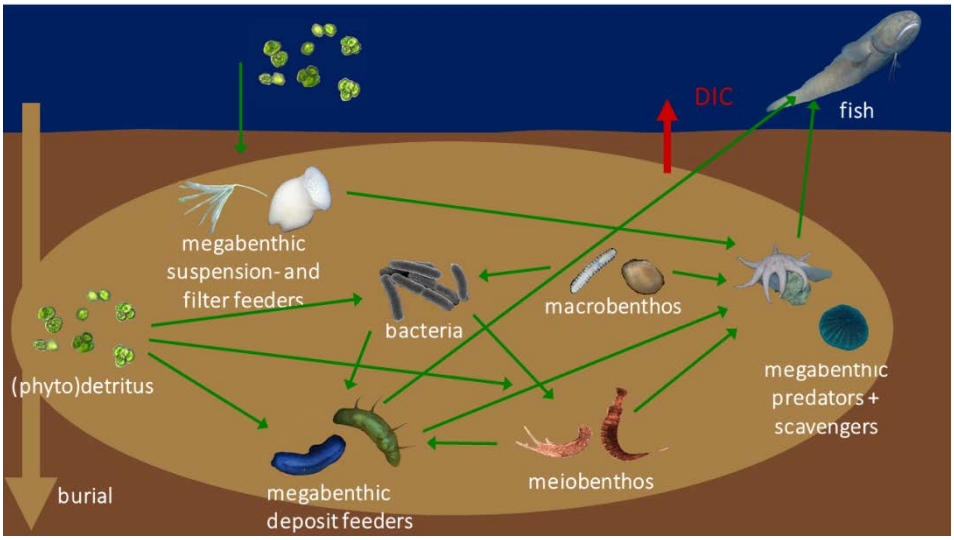

Figure 1-3. Scheme of a simplied deep-sea food web. The green arrows show the flow of phytodetritus through the food web, the red arrow indicates the respiration of dissolved inorganic carbon (DIC) and the brown arrow indicate the burial of detritus.

Box 1.4: Holothurians

Holothurians are one of the most abundant epifauna in the deep sea (Ruhl, 2007; Billett *et al.*, 2010; Alt *et al.*, 2013). On soft sediment, deposit feeding holothurians either dig into the sediment as funnel-feeders or conveyor belt-feeders or rake the surface sediment as rake feeders (Massin, 1982) in order to take up particulate organic matter that is deposited on the sediment or buried in the sediment (Roberts *et al.*, 2000). Depending on the species, holothurians feed more or less selectively. The analysis of gut contents from holothurians collected at the Porcupine Abyssal Plain (PAP, NE Atlantic) showed that *Amperima rosea*, *Peniagone diaphana*, and *Oneirophanta mutabilis* feed selectively on fresh phytodetritus. However, when this is scarce, *O. mutabilis* feeds on more refractory detritus material (FitzGeorge-Balfour *et al.*, 2010). Holothurians with a less selective feeding behavior are *Psychropotes longicauda*, *Pseudostichopus villosus*, and *Molpadia blakei* (FitzGeorge-Balfour *et al.*, 2010).

The presence of holothurians has an impact on the food availability for other benthic fauna. In the Nazaré canyon (NE Atlantic), e.g., the whole population of *Molpadia musculus* was estimated to remove approximately 0.43±0.13 g biopolymeric C and 0.13±0.03 g N m^{-2} d^{-1} from the sediment (Amaro *et al.*, 2010) and at PAP *A. rosea* and *Ellipinion molle* together with other fauna were estimated to remove the phytosterols from freshly deposited phytodetritus in less than four months (Ginger *et al.*, 2001).

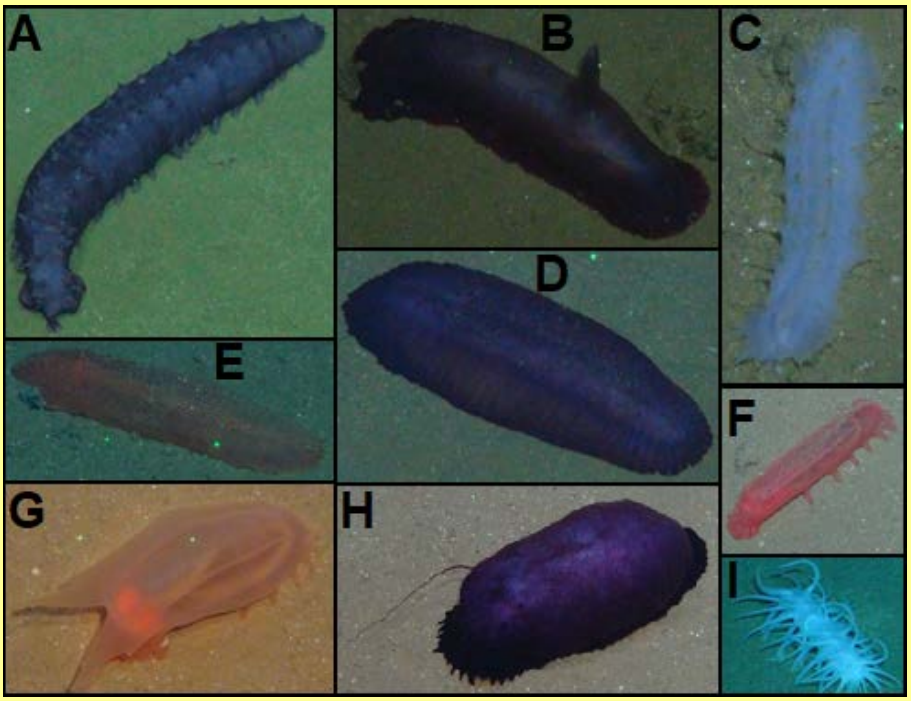

Figure 1-4. Examples of holothurians from the Peru Basin. Photos: ROV KIEL 6000 (Geomar, Kiel, Germany). A) *Psychronaetes hanseni*, B) *Psychropotes semperima*, C) *Synallactes profundi*, D) *Benthodytes typica*, E) *Bathyplotes* sp., F) *Peniagone elongata*, G) *Amperima* sp., H) *Benthothuria* sp., I) *Oneirophanta mutabilis*. Photos: ROV KIEL 6000 (Geomar, Kiel, Germany).

Whereas holothurians alter the chemical composition of detritus in the sediment, this detritus composition also affects the species composition of holothurians (Wigham *et al.*, 2003; FitzGeorge-Balfour *et al.*, 2010). At PAP, especially *A. rosea*, *P. diaphana* and *O. mutabilis* had a high concentration of carotenoids in their ovaries (FitzGeorge-Balfour *et al.*, 2010) which are important for the reproductive success of the species (Tsushima, 2007; Svensson and Wong, 2011). Therefore, Wigham *et al.* (2003) suggested that higher concentrations of carotenoids in the gonads of *A. rosea* as compared to other holothurians might give this species a reproductive advantage which could explain the "Amperima event". During this event the density of *A. rosea* increased by three orders of magnitude due to large-scale recruitment events that followed changes in the organic carbon flux to the abyssal plain, while the total megafauna biomass did not change significantly (Billett *et al.*, 2010).

1.5 Polymetallic nodules

Polymetallic nodules, also called manganese nodules, are concretions of Fe oxide-hydroxide and Mn oxide (Hein and Koschinsky, 2014) in various shapes, such as in the shape of cauliflowers or potatoes (Kuhn *et al.*, 2017). Their average size ranges from 2 to 8 cm (Kuhn *et al.*, 2017) and in the CCZ the largest nodules are 14 cm long (Morgan and Cronan, 2000), whereas in the Peru Basin (SE Pacific) the largest nodules are 20 cm long (von Stackelberg, 2000).

Box 1.5: Discovery of polymetallic nodules

Figure 1-5. Picture of the first ever discovered fragment of a polymetallic nodule from 2,800 m water depth in the Atlantic Ocean that was collected on February 18th 1873 during the Challenger expedition. This polymetallic nodule fragment is part of the Challenger collection of the Natural History Museum, London. Photo: T. Stratmann.

The first fragment of a polymetallic nodule was dredged on February 18th 1873 during the Challenger expedition[7] at 25°45'N, 20°14'W in the Atlantic (Figure 1-5) and the first whole polymetallic nodules were retrieved from a dredge tow on March 7th 1873 at 20°39'N, 50°33'W (Murray and Renard, 1891):

> *"In the mud there were also some sharks' teeth of at least two genera, and a number of very peculiar black oval bodies about an inch long, with the surface irregularly reticulated, and within; the reticulates closely and symmetrically granulated the whole appearance singularly like that of the phosphatic concretions which are so abundant in*

[7] Glasby (1977) reported that the first polymetallic nodule was collected in the Kara Sea by a Swedish expedition in 1868. However, the Swedish expedition of 1868 sailed under the scientific direction of Adolf Erik Nordenskiöld aboard the vessel *Sofia* to Spitsbergen and around the Svalbard archipelago, but they never sailed into the Kara Sea (Nordenskiöld, 1868; Leslie, 1879; Jones, 2008). In contrast, first in 1875 Nordenskiöld explored the Kara Sea (Youmans, 1875; Leslie, 1879; Jones, 2008) and in Nordenskiöld 1881's popular account about the voyage of the Vega along the Northeast Passage from 1878 to 1880 (Jones, 2008) a drawing of "manganiferous iron-ore formations" (Nordenskiöld, 1881) sampled in the Kara Sea was printed.

the greensand and trias. My first impression was that both the teeth and the concretions were drifted fossils, but on handing over a portion of one of the latter to Mr. Buchanan for examination, he found that it consisted of almost pure peroxide of manganese.
The character both of the exterior and interior of the nodule strongly recalled the black base of the coral which we dredged in 1,530 fathoms[8] *on the 18th of February; and ongoing into the matter, Mr. Buchanan found not only that the base of the coral retaining its external organic form had the composition of a lump of pyrolusite, but that the glossy black film covering the stem and branches of the coral gave also the reaction of manganese*." (Wyville Thomson, 1873)

During the expedition from 1872 to 1876, polymetallic nodules (Figure 1-6) were found between 2,791 and 5,719 m water depth at 26 different stations in the Atlantic, Indian, and Pacific Ocean (Murray and Renard, 1891; Figure 1-7).

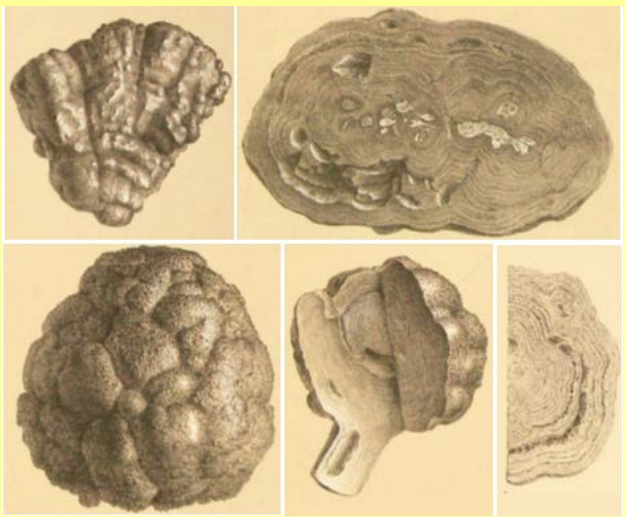

Figure 1-6. Drawings of polymetallic nodules collected during the Challenger expedition from 1872 to 1876 in the Atlantic, Southern, and Pacific Ocean. Source: Murray and Renard (1891).

[8] 100 fathoms = 183 m (Murray and Renard, 1891).

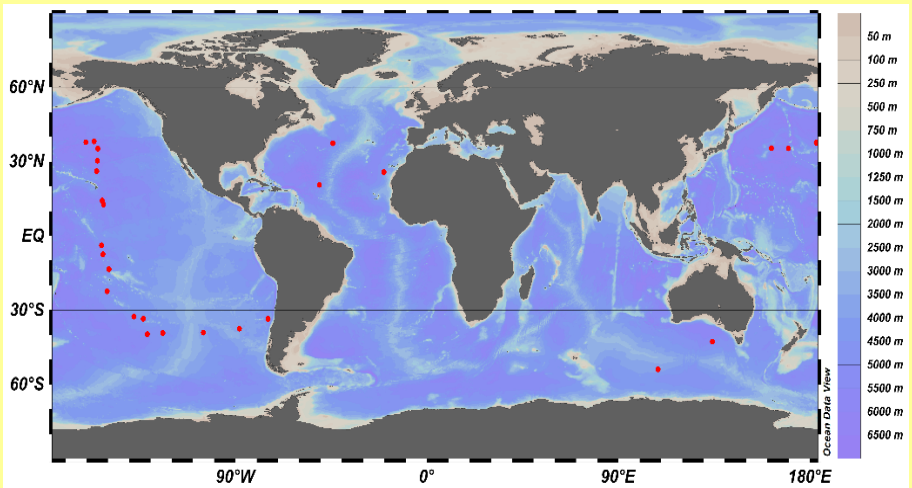

Figure 1-7. Map of the sampling stations (red dots) where the Challenger expedition found fragments of polymetallic nodules or complete polymetallic nodules (Murray and Renard 1891).

1.5.1 Occurrence of polymetallic nodules

Figure 1-8. Polymetallic nodules half-buried in the surface sediment of the Peru Basin. Source: ROV KIEL 6000 (Geomar, Kiel, Germany).

Polymetallic nodules occur globally on the sediment surface (Figure 1-8) or buried within the upper 10 cm of sediment between 3,500 and 6,500 m water depth (Hein *et al.*, 2013). They have also been found in the Baltic Sea with 15–40 kg ferromanganese concretions m^{-2} in the Bothnian Bay, 18–24 kg m^{-2} in the Gulf of Finland, up to 17 kg m^{-2} in the Gulf of Riga and 10–16 kg m^{-2} in the Baltic Proper (Glasby *et al.*, 1997), but the content of economically valuable metals is lower than in deep-sea nodules (Kuhn *et al.*, 2017).

Nodules are present in high densities in areas with well oxygenated bottom waters, sedimentation rates of less than 20 mm ky^{-1}, and a high abundance of potential nuclei (Hein *et al.*, 2013; Petersen *et al.*, 2016). Prerequisite for the formation of high-grade nodules[9] is the depth of the calcite compensation depth[10] (CCD) relative to the seafloor (Verlaan, Cronan and Morgan, 2004). When the seafloor is above the CCD, the carbonate does not dissolve in areas with high primary production, but instead dilutes the organic carbon flux (Verlaan, Cronan and Morgan, 2004). However, when the seafloor is far below the CCD, the supply of organic carbon to the seafloor can be insufficient for diagenetic enrichment in manganese, copper, and nickel (Verlaan, Cronan and Morgan, 2004). Therefore, nodules of the highest grade are formed near the CCD where the conditions for diagenesis in sediments are optimal (Verlaan, Cronan and Morgan, 2004).

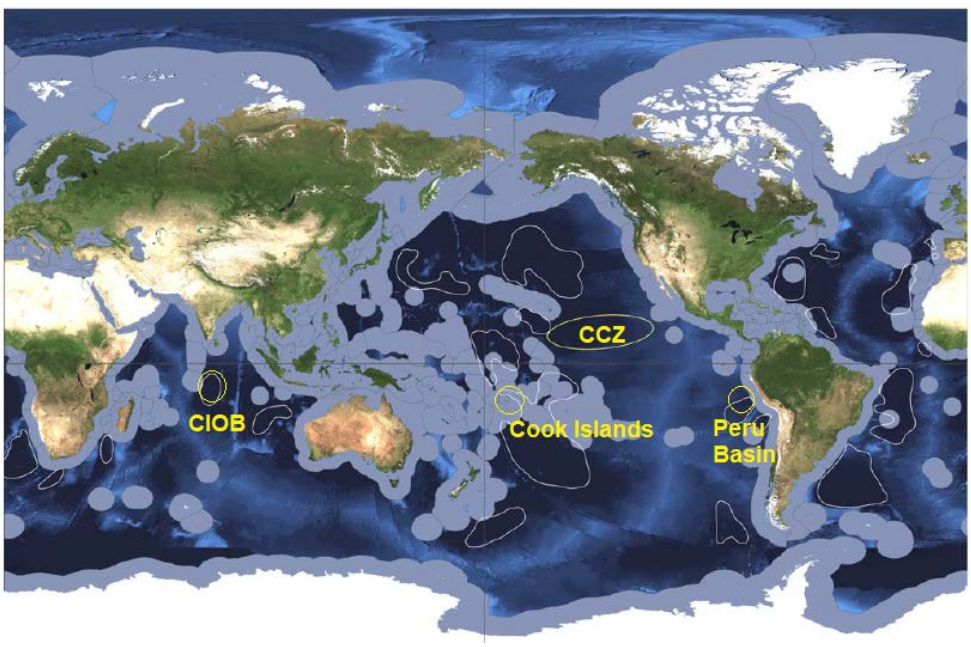

Figure 1-9. Map of the global distribution of polymetallic nodule areas that are of economic interest, i.e., the Clarion Clipperton Fracture Zone (CCZ), around the Cook Islands, in the Peru Basin, and in the Central Indian Ocean Basin (CIOB).
The gray-colored areas represent the exclusive economic zones (EEZ). Map modified from Hein *et al.* (2013).

Polymetallic nodule areas of economic interest are the CCZ, the Central Indian Ocean Basin (CIOB), the Peru Basin, and the Cook Islands area (Figure 1-9; Kuhn *et al.*, 2017). The nodule density in the CCZ ranges from 0 to 30 kg nodule wet weight m^{-2} and the average density is 15 kg m^{-2} (Kuhn *et al.*, 2017).

[9] High-grade nodules: "Nodules in which the sum percentages of nickel, copper, and cobalt (Ni + Cu + Co) is higher than 2.5%." (International Seabed Authority, 2010).
[10] Calcite compensation depth: "The depth in the ocean (about 5,000 m) below which solution of calcium carbonate occurs at a faster rate than its deposition." (Geller, 2003).

However, fields with polymetallic nodules are not distributed equally in the CCZ, but are present in patches which can extend over several 1,000s km^2 (Kuhn *et al.*, 2017). In comparison, the average density of nodules in the Peru Basin is 10 kg m^{-2}, with highest abundances (max. 66.8 kg m^{-2}) found at 4,235 m depth near the CCD (von Stackelberg, 2000). The nodule densities are between 19 and 45 kg m^{-2} (max. 58 kg m^{-2}) around the Cook Islands and on average 4.5 kg m^{-2} in the CIOB (Kuhn *et al.*, 2017).

1.5.2 Formation of polymetallic nodules

Polymetallic nodules form either via hydrogenetic growth, i.e., minerals from the ambient seawater precipitate around a nucleus, such as fragments of old polymetallic nodules or rock, shark teeth or shells of plankton, or via diagenetic growth, i.e., minerals from the sediment pore water precipitate around a nucleus (Figure 1-10; Hein and Koschinsky, 2014; Petersen *et al.*, 2016).

During hydrogenetic growth, metals dissolved in seawater are absorbed by very fine iron and manganese oxide particles, i.e., "nanoparticles" or "colloids" (Petersen *et al.*, 2016). As manganese oxide particles are negatively charged at the surface, they scavenge positively charged ions that occur in trace concentrations in seawater, such as cobalt, nickel, and copper ions (Petersen *et al.*, 2016). In contrast, iron oxide particles are slightly positively charged at the surface and therefore scavenge negatively charged ions, such as molybdenum, vanadium, arsenic, and rare earth element oxyanions (Petersen *et al.*, 2016). These nanoparticles and their scavenged trace metals accrete in concentric manganese and iron oxide layers around the nucleus with growth rates of 1 to 10 mm Myr^{-1} (Petersen *et al.*, 2016).

During diagenetic growth, organic carbon is degraded in the presence of dissolved oxygen during aerobic respiration (Kuhn *et al.*, 2017). After the depletion of dissolved oxygen, the degradation of organic carbon occurs during suboxic diagenesis with nitrate, manganese dioxide, iron(III) oxide, or sulfate as secondary oxidants (Kuhn *et al.*, 2017). When manganese oxides oxidize the organic carbon, manganous ions are released to the interstitial water and diffuse into oxidized sediment layers where they oxidize again to manganese dioxide (Kuhn *et al.*, 2017). If this process occurs close to the sediment surface (Kuhn *et al.*, 2017), diagenetic growth can occur with rates of up to 250 mm Myr^{-1} (von Stackelberg, 2000).

"Mixed-type diagenetic-hydrogenetic" polymetallic nodules (Bau *et al.*, 2014), i.e., nodules of combined diagenetic and hydrogenetic origin, grow with intermediate rates of 10s mm Myr^{-1} (Hein, 2016).

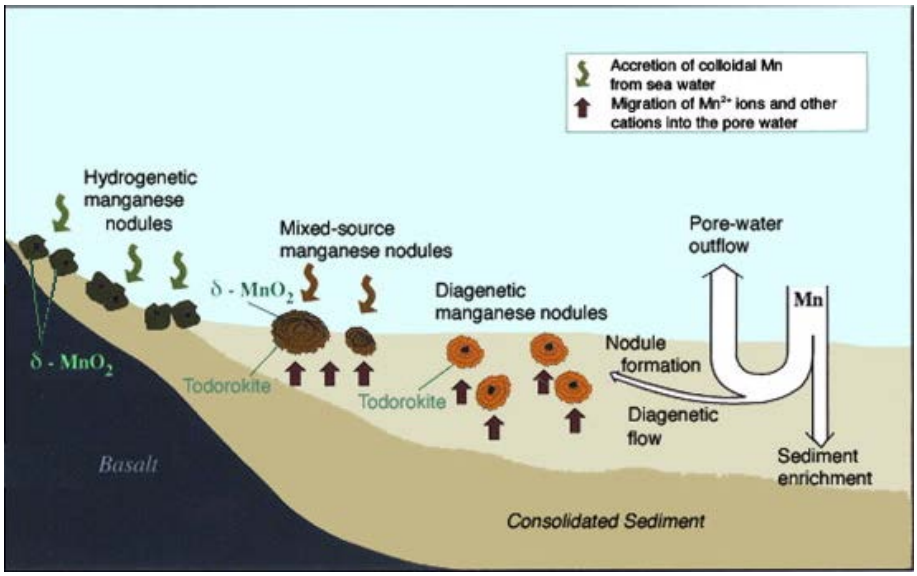

Figure 1-10. Schematic representation of the formation of hydrogenetic, diagenetic, and "mixed-type diagenetic-hydrogenetic" (Bau *et al.*, 2014) polymetallic nodules. Figure modified from Hein *et al.* (2013).

1.5.3 Chemical composition of polymetallic nodules

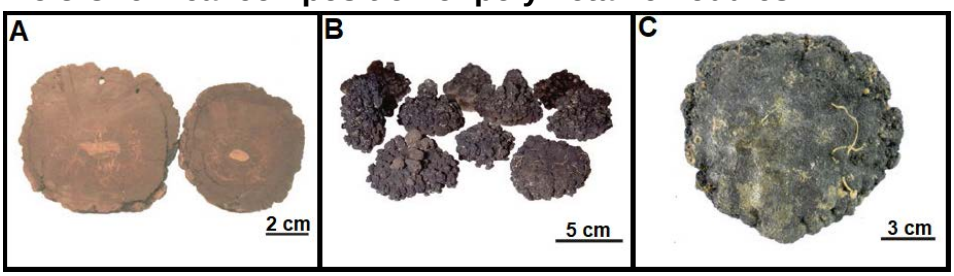

Figure 1-11. A) Hydrogenetic nodules from Manihiki Plateau, Cook Islands (central S Pacific), B) diagenetic nodules from the Peru Basin (SE Pacific), C) "mixed-type diagenetic-hydrogenetic" nodules from the Clarion Clipperton Fracture Zone (central N Pacific). Source: Kuhn *et al.* (2017).

The chemical composition of polymetallic nodules (Table 1-1) depends on geographic location, water depth, growth rate, and type of formation (hydrogenetic vs. diagenetic) (Kuhn *et al.*, 2017). Hydrogenetic nodules (Figure 1-11A), such as the nodules from the Penrhyn and Samoa Basin abyssal plains in the exclusive economic zone (EEZ) of the Cook Islands, have Mn/Fe ratios of ≤5, high contents of cobalt (0.41%), nickel (0.38%), titanium (1.20%), and total rare earth elements (REE) plus yttrium (0.17%) (Hein *et al.*, 2015; Kuhn *et al.*, 2017). In contrast, diagenetic nodules (Figure 1-11B), such as the nodules from the Peru Basin, have Mn/Fe ratios of >5 and are enriched in nickel (1.30%), copper (0.60%), barium (0.32%), zinc (0.18%), molybdenum (0.055%), lithium (0.031%), and gallium (0.0032%) (Kuhn *et al.*, 2017). "Mixed-type" nodules (Figure 1-11C) occur, e.g., in the CCZ (Wegorzewski and Kuhn, 2014). Their

chemical elements range in content between those of hydrogenetic and diagenetic nodules, except for copper (1.07% in CCZ nodules), barium (0.0035% in CCZ nodules), and molybdenum (0.00059% in CCZ nodules) (Kuhn *et al.*, 2017).

Table 1-1. The mean content of certain economically interesting chemical elements in polymetallic nodules collected at the Clarion-Clipperton Fracture Zone (CCZ, central N Pacific), the Central Indian Ocean Basin (CIOB, Indian Ocean), Peru Basin (SE Pacific), and around the Cook Islands (central S Pacific). Data are taken from Petersen *et al.* (2016).
Abbreviations: Mn = manganese, Ni = nickel, Cu = copper, Co = cobalt, Ti = titanium, Mo = molybdenum, Li = lithium, REE = rare earth elements, Y = yttrium.

Element	**CCZ**	**CIOB**	**Peru Basin**	**Cook Islands**
Mn (wt%)	28.4	24.4	34.2	16.1
Ni (wt%)	1.3	1.1	1.3	0.4
Cu (wt%)	1.1	1.0	0.6	0.2
Co (wt%)	0.21	0.11	0.05	0.41
Ti (wt%)	0.28	0.40	0.16	1.20
Mo (ppm[11])	590	600	547	295
Li (ppm)	131	110	311	-
REE + Y (ppm)	813	1039	403	1665
Type of formation	Mixed-type diagenetic-hydrogenetic	Mixed-type diagenetic-hydrogenetic	Diagenetic	Hydrogenetic

1.6 Deep-sea mining

Polymetallic nodules are considered potential sources of nickel, copper, cobalt, manganese, molybdenum, lithium, rare earth elements, and several rare metals (hafnium, lithium, niobium, platinum, tantalum, tellurium, tungsten, zirconium) (Hein *et al.*, 2013; Hein and Koschinsky, 2014). Especially the rare earth elements and rare metals are important components of several high and green technology application, such as photovoltaic solar cells, computer chips, hybrid and electric car batteries (Hein *et al.*, 2013). However, in the future, their supplies from land-based mines that are often limited to a few producer states (e.g., China contributes 95% to the global rare earth element production; Hein *et al.*, 2013) might not cover the rising demands from fast-expanding economies such as China, India, Brazil, or Indonesia (Hein *et al.*, 2013). Therefore, an additional source of these elements could be deep-sea minerals.

Estimates for the CCZ suggest that it contains 21,100 Mt dry weight nodules and therefore 5,950 Mt manganese, 270 Mt nickel, 234 Mt copper, and 46 Mt cobalt (International Seabed Authority, 2010). This is 9 times higher than the land-based reserves of manganese, 3.6 times higher than the reserves for nickel, 37% of the land-based reserves of copper, and 4.5 times higher than the land-based reserves for cobalt (International Seabed Authority, 2010; Hein and

[11] 1,000 ppm = 0.1% (Hein, 2016).

Koschinsky, 2014; Sverdrup, Ragnarsdottir and Koca, 2017; U.S. Geological Survey, 2018; Table 1-2). Furthermore, nodules in the CCZ have higher metal tonnages of molybdenum, arsenic, yttrium, tellurium, and thallium than global land-based reserves (Hein *et al.*, 2013; Hein and Koschinsky, 2014; Table 1-2).

An exemplary CCZ contractor area of 75,000 km^2 with a nodule abundance of 5 kg m^{-2} is estimated to contain 375 Mt wet weight nodules which is equivalent to 281 Mt dry weight nodules or 67 Mt metals assuming a metal content of 22% for manganese, 1% for nickel, 0.78% for copper, and 0.1% for cobalt (Sharma, 2017). If, in the future, 30 to 60 Mt of the metals are being mined with a rate of 1.5 Mt nodules yr^{-1} (Legal and Technical Commission, 2008) and an extraction efficiency of 79 to 89% (Sharma, 2017) over 20 yr, the annual metal production will be 0.36 Mt yr^{-1} (Sharma, 2017). Using the metal prices from 2011, this annual metal production has a value of US-$937 million and the total yield for one mining site in 20 yr is $19 billion (Sharma, 2017). In comparison, this single deep-sea mining operation is estimated to cost $12 billion, leaving a revenue of $7 billion (Sharma, 2017).

For the CIOB, the nodule-rich area, the so-called Indian Ocean Nodule Field (IONF), is estimated to contain 1,400 Mt polymetallic nodules with a nickel, copper, and cobalt content of 2.48 to 2.53% (Kuhn *et al.*, 2017). This amounts to 22 Mt nickel, copper, and cobalt combined (Kuhn *et al.*, 2017). The exploration license area of India alone (150,000 km^2) is estimated to provide ~700 Mt polymetallic nodules holding 14 Mt copper and nickel combined (Banakar, 2010). In comparison, India's land-based reserves are estimated to contain ~2.7 Mt of copper (Bhavan, 2018) which will last for an additional 10 yr when assuming that the copper consumption (~0.26 Mt yr^{-1}) will be the same as during 2007 and 2008 (Banakar, 2010). Nickel ore, however, is not mined in land-based nickel mines in India (state 2010; Banakar, 2010).

Six ~20,000 km^2 areas with varying combinations of metal abundances in the EEZ of the Cook Islands contain between 151 and 357 Mt dry weight nodules each (Hein *et al.*, 2015). This is equivalent to 21 to 61 Mt manganese, 2 to 4 Mt titanium, 0.5 to 2 Mt cobalt, 0.3 to 1.2 Mt nickel and 0.2 to 0.8 Mt copper per area (Hein *et al.*, 2015). Hence, if these areas are mined with a rate of 2.6 Mt dry weight polymetallic nodules yr^{-1}, each area will contribute between 13 and 22% to the 2013 global production of titanium and between 8 and 12% to the 2013 global production of copper (Hein *et al.*, 2015). Their contribution to the 2013 global rare earth element production will range from 3 to 6% (Hein *et al.*, 2015).

Table 1-2. Comparison of metal tonnages ($\times 10^6$ t) in polymetallic nodules from the Clarion Clipperton Fracture Zone (CCZ), in the global land-based reserve base[12] and global land-based reserves[13]. Metals presented in bold are those metals that have higher metal tonnages in the CCZ nodules than in the global land-based reserve base or global land-based reserves.
Data from [a]International Seabed Authority (2010), [b]Hein and Koschinsky (2014), [c]Hein *et al.* (2013), [d]U.S. Geological Survey (2018), [e]Sverdrup, Ragnarsdottir and Koca (2017).

	CCZ polymetallic nodules	**Global land-based reserve base**	**Global land-based reserves**
Manganese	**5,950**[a]	5,200[b]	630[b]
Copper	234[a]	1,300[b]	630[b]
Titanium	59[b]	900[b]	414[b]
Total rare earth elements as oxides	17[b]	150[b]	110[b]
Nickel	**270**[a]	150[b]	74[d]
Vanadium	9.4[c]	38[c]	14[c]
Molybdenum	**12**[b]	19[b]	9.8[b]
Lithium	2.7[b]	14[b]	13[b]
Cobalt	**46**[a]	13[b]	10.3[e]
Tungsten	1.3[b]	6.3[b]	2.9[b]
Niobium	0.40[b]	3.0[b]	2.9[b]
Arsenic	**1.4**[c]	1.6[c]	1.0[c]
Thorium	0.32[c]	1.2[c]	1.2[c]
Bismuth	0.18[c]	0.7[c]	0.3[c]
Yttrium	**1.9**[b]	0.48[b]	0.42[b]
Total Platinum-Group Metals[14]	0.003[c]	0.08[c]	0.07[c]
Tellurium	**0.07**[b]	0.05[b]	0.022[b]
Thallium	**4.2**[c]	0.0007[c]	0.0004[c]

[12] Reserve base: "That part of an identified resource that meets specified minimum physical and chemical criteria related to current mining and production practices, including those for grade, quality, thickness, and depth. The reserve base is the in-place demonstrated (measured plus indicated) resource from which reserves are estimated." (U.S. Geological Survey, 2001).
[13] Reserves: "Resources that are currently economically extractable." (Hein and Koschinsky, 2014).
[14] Platinum-group metals: platinum, palladium, iridium, rhodium, osmium, ruthenium (Hein *et al.*, 2013).

Box 1.6: The legal framework of deep-sea mining

About 80% of the seafloor with favorable conditions for the development of polymetallic nodules lies beyond limits of national jurisdiction (Petersen *et al.*, 2016), that is referred to as "the Area" in the first article of the United Nations Convention on the Law of the Sea (UNCLOS; UN General Assembly, 1982). This "Area" and all its resources, i.e., "all solid, liquid or gaseous mineral resources […] at or beneath the seabed, including polymetallic nodules" (UNCLOS, Part XI, Article 133), are "the common heritage of mankind" (UNCLOS, Part XI, Article 136). The International Seabed Authority (ISA) in Kingston (Jamaica) acts on behalf of mankind (UNCLOS, Part XI, Article 137.2) and administers the resources in "the Area".

Therefore, the ISA oversees the exploration of polymetallic nodules in the CIOB and in the CCZ (0°N, 160°W to 23.5°N, 115°W; International Seabed Authority, 2011). Until March 2018, the ISA has granted 16 15-yr contracts to 15 contractors (max. initial contractor area: 150,000 km^2, max. contractor area after 8 yr: 75,000 km^2; International Seabed Authority, 2013) for the exploration of polymetallic nodules in the CCZ (Figure 1-12) and one 15-yr contract for exploration of polymetallic nodules in the CIOB (Figure 1-13) (www.isa.org; accessed: March 24th 2018). The ISA also established nine "Areas of Particulate Environmental Interest" (APEI) with an individual size of ~160,000 km in the CCZ (Legal and Technical Commission, 2011). Each APEI consists of a 200 km×200 km core area that is enclosed in a 100 km buffer zone (Legal and Technical Commission, 2011) and it should "protect biodiversity and ecosystem structure and function" (Legal and Technical Commission, 2011) and it should furthermore "include a wide range of the habitat present in the Clarion-Clipperton Zone within the areas of particular environmental interest (e.g., seamount and fracture zone structures)" (Legal and Technical Commission, 2011). All APEIs together cover 1,440,000 km^2, i.e., ~25% of the CCZ area that is managed by the ISA (Figure 1-12; Lodge *et al.*, 2014).

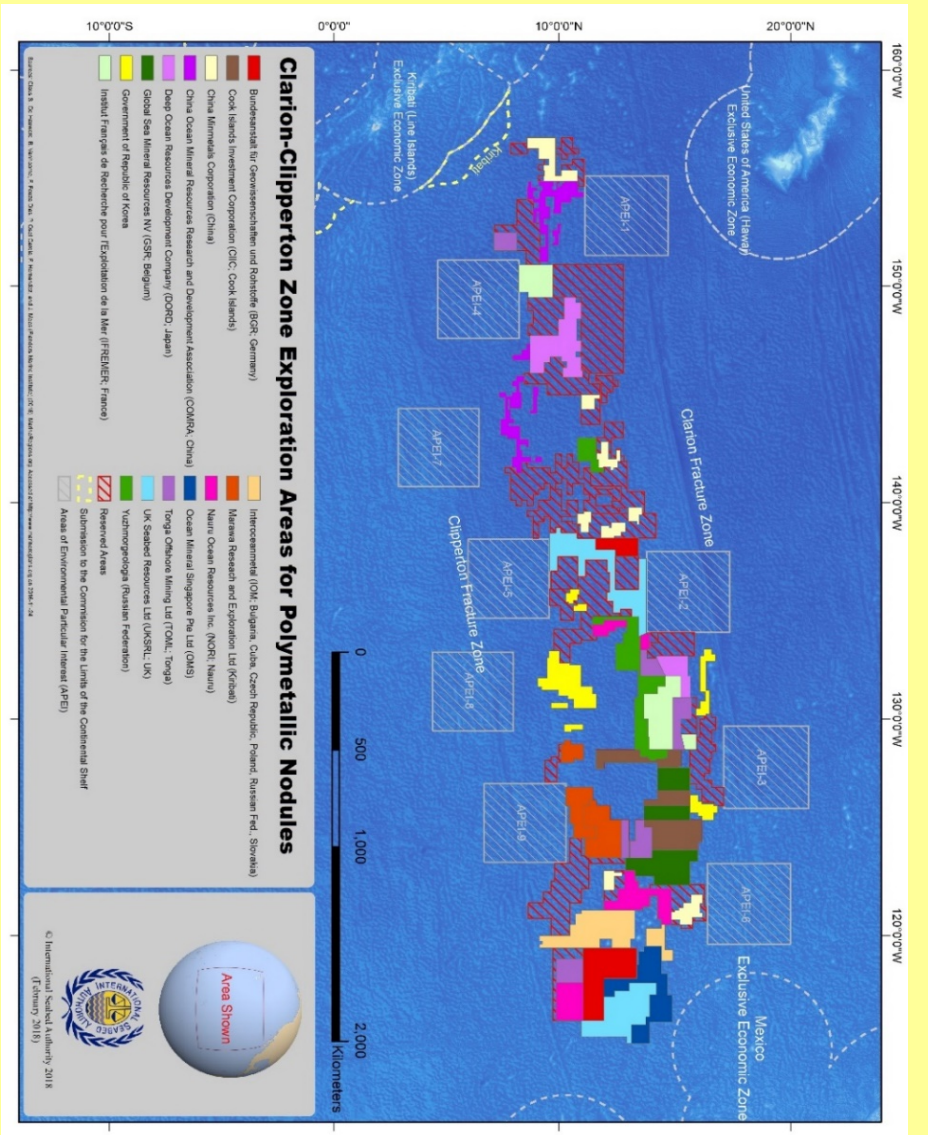

Figure 1-12. Map of the contract areas for polymetallic nodules exploration in the Clarion-Clipperton Fracture Zone. Source: International Seabed Authority (https://www.isa.org.jm/maps; accessed: March 24th 2018).

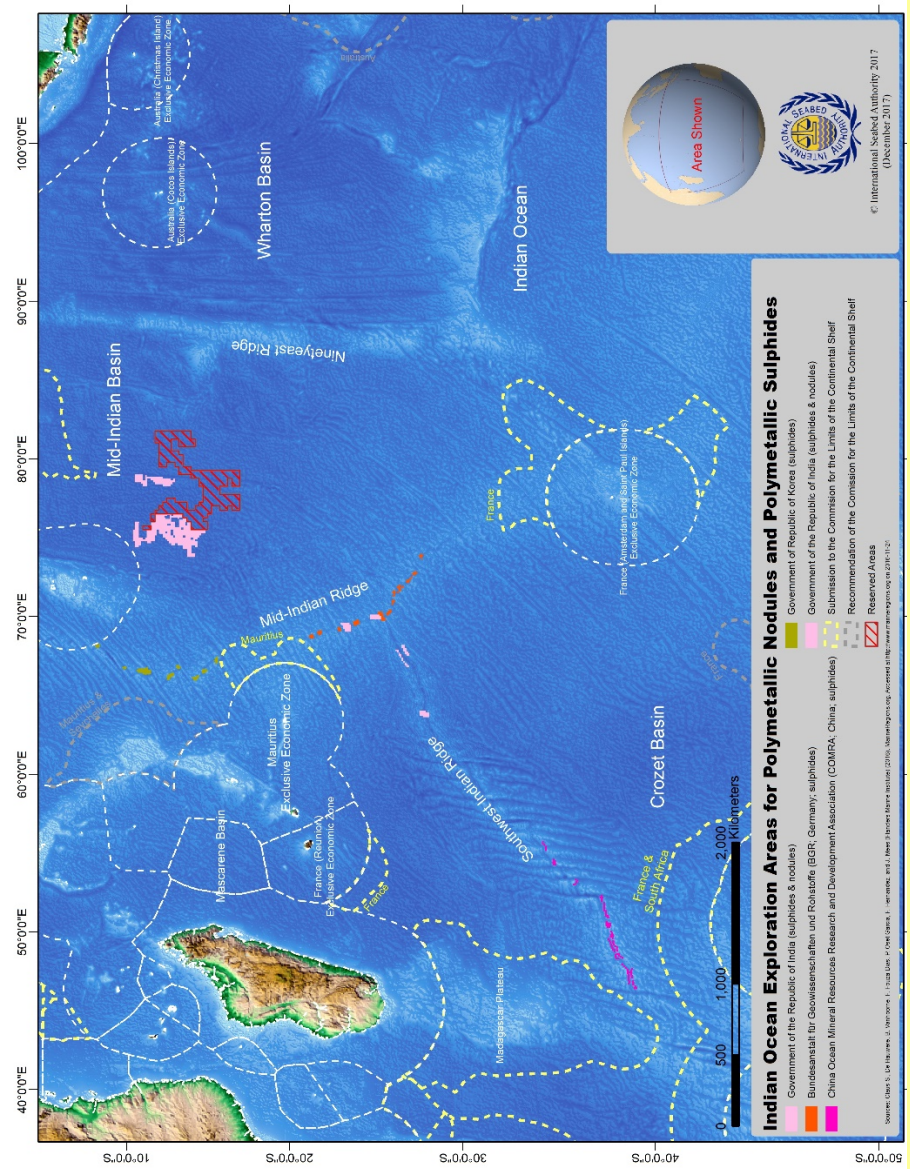

Figure 1-13. Map of the contract area for polymetallic nodule exploration in the Central Indian Ocean Basin. Source: International Seabed Authority (https://www.isa.org.jm/maps; accessed: March 28th 2018).

1.6.1 Environmental impacts of deep-sea mining

Environmental impacts of deep-sea mining are noise pollution, potential release of toxic metals, sediment and nodule removal, and sediment plume creation:

Underwater noise pollution might extend 600 km away from the mining operation and cause masking effects in marine mammals in a radius of 15 km around the mining operation as projected for the planned Solwara 1 seabed mining project off Papua New Guinea (SW Pacific) (Steiner, 2009). At this site, Nautilus Minerals Ltd. holds a license granted by the Government of Papua New Guinea in 2011 to explore marine mineral deposits at 1,600 m depth that consist predominantly of copper, but also contain gold (Gwyther and Wright, 2008; Filer and Gabriel, 2017). This noise pollution will again stop when the mining operations end.

If the oxic 10 cm of surface sediment with an average pore water manganous ion (Mn^{2+}) concentration of 15 μmol L^{-1} in the Peru Basin (Haeckel *et al.*, 2001) are suspended up to 1 m above the bottom, the concentration of Mn^{2+} in this 1 m bottom water will be 1.2 μmol L^{-1} (Koschinsky, Borowski and Halbach, 2003). This is ten times more than the average Mn^{2+} concentration in the seawater (0.1 μmol L^{-1}) (Koschinsky, Borowski and Halbach, 2003). In comparison, if also suboxic sediment is suspended up to 1 m into the water column, the concentration of Mn^{2+} in the bottom water will be 165 μmol L^{-1} (Koschinsky, Borowski and Halbach, 2003). However, the concentration of dissolved heavy metals in the bottom water might return to pre-mining values within hours. A mesocosm disturbance experiment with sediment cores from the Peru Basin showed that the dissolved heavy metal concentrations in the overlaying water in the sediment cores returned to pre-disturbance values after 30 min (Koschinsky *et al.*, 2001).

The extraction of polymetallic nodules by a hydraulic collector is expected to remove the upper 15 cm of surface sediment in the mining track (K. Murphy *et al.*, 2016). About 90% of this extracted sediment are likely to be discharged via the seabed mining tool exhaust at the seafloor (K. Murphy *et al.*, 2016). The remaining 10% of extracted sediment will be released as dewatering discharge ~1,000 m above the seafloor (K. Murphy *et al.*, 2016). In a mining scenario with a mining speed of 0.3 m s^{-1}, this results in an discharge of 465 t sediment h^{-1} at the seafloor and 52 t sediment h^{-1} at 1,000 m above the seafloor (K. Murphy *et al.*, 2016). The sediment plume at the seafloor that is created by the discharged sediment was modeled for a mining operation in which the seabed mining tool (width: 15 m) extracts the nodules in a "lawn mowing" pattern (area size: 144 km^2) with a speed of 0.53 m s^{-1} (K. Murphy *et al.*, 2016). When the mining operation runs for 1 yr, the mined 144 km^2 of seafloor will be covered with more than 10 cm of re-settled sediment and 519 km^2 of seafloor outside the directly mined area will be covered with 0.1 to 1 cm of re-settled sediment (K. Murphy *et al.*, 2016). Additional 5,374 km^2 of seafloor outside the mined area will be covered with 0.1 to 1 mm of re-settled sediment (K. Murphy *et al.*, 2016; Aleynik *et al.*, 2017). After the resettlement of the sediment particles, it might take more than 20 yr of sediment consolidation until the sediment fabric resem-

bles the pre-mining sediment fabric (Becker *et al.*, 2001). Another model simulated a mining scenario in which 4,000 t sediment were released as dewatering discharge 500 m below the sea surface in the Peru Basin (Rolinski, Segschneider and Sündermann, 2001). The model shows that the finer particles remain suspended in the water column between 5 months and 7 yr, whereas 66% of the coarser material has a particle residence time of less than one month (Rolinski, Segschneider and Sündermann, 2001).

Besides clinkers and glacial drop stones, polymetallic nodules are the only hard substrate in abyssal plains (Ramírez-Llodrà *et al.*, 2011) and their extraction will destroy the habitat inside the mining tracks. Furthermore, the removal will cause a restructuring of the sediment profile, a compaction of the seafloor inside the mining tracks, and a change in carbon content in the surface sediments (Khripounoff *et al.*, 2006; Miljutin *et al.*, 2011; K. Murphy *et al.*, 2016). Based on ISA indications about the target polymetallic nodule density (average abundance area: 10 kg m^{-2}, high abundance area: 20 kg m^{-2}; Murphy *et al.*, 2016) and commercially desirable annual production (annual production: 1.5–4 Mt polymetallic nodules; Murphy *et al.*, 2016), between 75 and 400 km^2 of seafloor will be directly impacted annually by the extraction of the nodules (K. Murphy *et al.*, 2016). After 30 yr of deep-sea mining activity in a 75,000 km^2 large claim area (nodule density: 10 kg m^{-2}, annual production: 4 Mt yr^{-1}), 16% of the total claim area will be affected either directly by the extraction of the polymetallic nodules or indirectly by the plume (K. Murphy *et al.*, 2016). In comparison, if the nodule density is 15 kg m^{-2} and the annual production is 2.5 Mt yr^{-1}, 6.7% of the 75,000 km^2 large claim area will be impacted directly or indirectly (K. Murphy *et al.*, 2016).

1.6.2 Recovery from deep-sea mining

To study the potential recovery of the abyssal ecosystem from deep-sea mining, extensive research has been conducted in the past decades: In the central Pacific, first mining tests were performed by the Ocean Mining Associates consortium (OMA) in 1976 and by Ocean Management Inc. (OMI) within the “Deep Ocean Mining Environmental Study” (DOMES) in 1978 (Jones *et al.*, 2017). In 1978/ 1979 the Ocean Minerals Company consortium (OMCO) performed a test in the central CCZ whose site was revisited in 1998 and 2004 (Jones *et al.*, 2017). In 1991 and 1993, the “Benthic Impact Experiment” I and II (BIE) were performed to study the effect of a sediment plume and in 1994 the “Japan Deep-Sea Impact Experiment” (JET) was conducted to likewise test the impact of sediment resuspension and resettlement (Jones *et al.*, 2017). In 1995, the benthic impact experiment (IOM BIE) was performed in the eastern CCZ and this site was revisited in 1997, 2000, and 2015 (Jones *et al.*, 2017). The “Indian Deep-Sea Environment Experiment” (INDEX) was conducted in 1997 in the Central Indian Ocean Basin and monitored before, during and after the experiment (Ingole *et al.*, 2000, 2001; Rodrigues, Sharma and Nagender Nath, 2001; Ingole, Pavithran and Ansari, 2005; Jones *et al.*, 2017). The best monitored deep-sea experiment, however, was the DISCOL experiment in the Peru Basin (Bluhm, 1994; Bluhm, Schriever and Thiel, 1995; Bussau, Schriever and Thiel, 1995; Borowski and

Thiel, 1998; Gollner *et al.*, 2017; Jones *et al.*, 2017) which provides a unique opportunity to study the recovery from a small-scale sediment disturbance over three decades.

Box 1.7: The DISCOL experiment

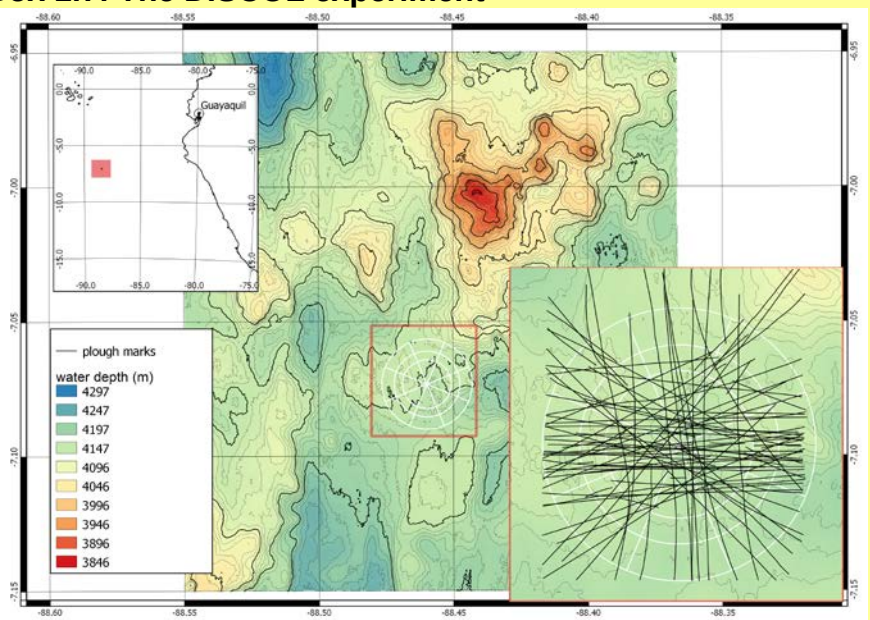

Figure 1-14. Location of the DISCOL experimental area (DEA; red square on the map) in the Peru Basin (SE Pacific). The white circle represents the DEA with its subdivision into eight pie slices and three rings and the black lines show the plough marks. Source: Stratmann, Lins, *et al.* (2018)/ **Chapter 6**.

Initially planned as a test of a new seafloor mining tool collector system (Thiel, 1991), the Ministry of Science and Technology of the Federal Republic of Germany (Bundesministerium für Forschung und Technologie, BMFT) approved a research proposal for the time period between 1988 to 1990 to conduct an independent research project called "DISturbance and reCOLonization experiment in the South Pacific" (acronym: DISCOL) (Thiel *et al.*, 1989). This project aimed "to conduct a large scale experiment involving disturbing an extended bottom area to observe its recolonization over several years, possibly for a decade or even longer" (Thiel *et al.*, 1989). In 1989, during R/V *Sonne* cruise SO61, an experimental area was selected that was supposed to be relatively flat, have no outcrops and have a low polymetallic nodule density (~5 kg m^{-2}) to prevent seafloor mining tool failure (Thiel *et al.*, 1989). The so-called "DISCOL Experimental Area" (DEA) is a circular 10.8 km^2 large area (diameter: 3,754 m) at 07°04.4'S, 88°27.6'W (central position) 1,037.12 km off Guayaquil in the Peru Basin (SE Pacific) (Thiel *et al.*, 1989; Greinert, 2015) (Figure 1-14).The water depth ranges from 3,800 to 4,300 m (Greinert, 2015).

Figure 1-15. Picture of the plough-harrow with double-sided plow shares that was used to disturb the sediment of the DEA. Source: https://www.discol.de (accessed: April 1st 2018).

For the disturbance experiment, the DEA was divided into eight equal-sized pie-shaped sections and furthermore into three concentric rings (Thiel *et al.*, 1989; Figure 1-14). The first ring ("central circular area") had a radius of 1,000 m, the second ring ("inner ring") had a width of 350 m and the third ring ("outer ring") had a width of 500 m (Thiel *et al.*, 1989).

After a pre-impact sampling campaign (February 11th to 20th, 1989) inside (box corer and multi-corer) and outside (baited traps and trawls) of DEA, the surface sediment of ~22% of the circular area was disturbed by crossing it 78 times with a plough-harrow during the impact phase from February 20th to March 18th 1989 (Thiel *et al.*, 1989; Figure 1-14). This plough-harrow (Figure 1-15) weighed 2.2 t, was 8 m wide and consisted of two subunits with double-sided plow shares known from potato harvesters (Thiel *et al.*, 1989). However, in contrast to an industrial-scale deep-sea mining event, the plow-harrow did not extract the polymetallic nodules from the sediment, but plowed them into the sediment.

Undisturbed areas: Areas inside the DEA, but outside the experimental area, that are covered with varying densities of polymetallic nodules (Bluhm, Schriever and Thiel, 1995; Figure 1-16A).

Apparently undisturbed areas: Areas inside the DEA that were not directly impacted by the plow-harrow, but that are covered by different levels of re-settled sediment visible as sediment blanketing of the nodules (Bluhm, Schriever and Thiel, 1995; Figure 1-16B).

Partially disturbed areas: Areas that directly border on disturbed areas. They are characterized by lateral heaps of surface sediment and a thick blanket of nodules (Bluhm, Schriever and Thiel, 1995; Figure 1-16C).

Disturbed areas: Areas that are directly impacted by the plow-harrow. They show a disrupted sediment surface that can be covered by re-settled sediment and almost all nodules are buried in the sediment (Bluhm, Schriever and Thiel, 1995; Figure 1-16D).

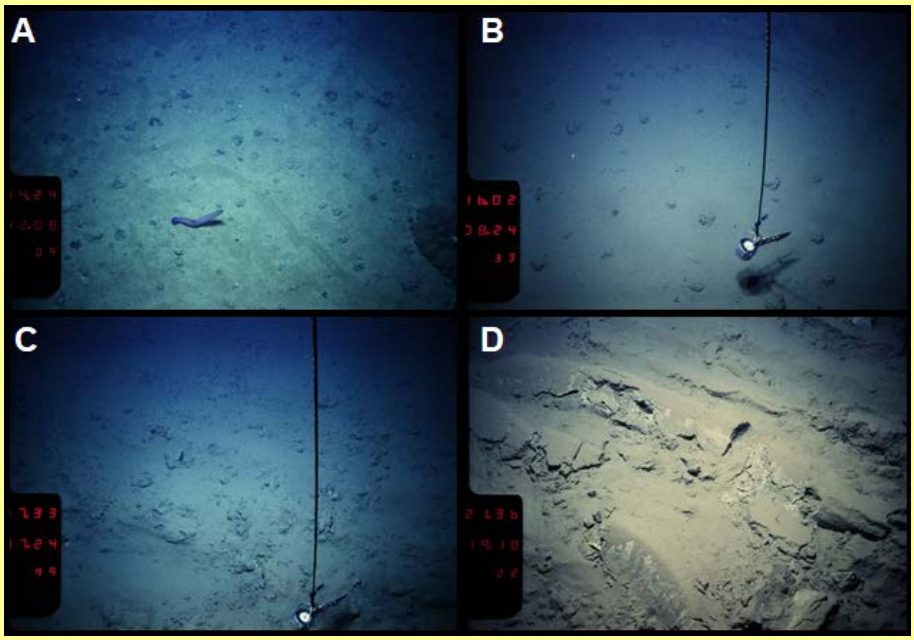

Figure 1-16. Pictures of the four different disturbance levels A) “undisturbed”, B) “apparently undisturbed”, C) “partially undisturbed” and D) “disturbed” that were created during the impact phase. Source: https://www.discol.de (accessed: April 1st 2018).

Further recolonization studies were conducted

- 0.5 yr after the experiment in September 1989: *DISCOL 2 cruise* (Schriever, 1990),
- after 3 yr in January 1992: *DISCOL 3 cruise* (Schriever and Thiel, 1992),
- after 7 yr in February 1996: *ATESEPP cruise* (Schriever, Koschinsky and Bluhm, 1996), and
- after 26 yr in September 2015: *DISCOL revisited cruise* (Boetius, 2015).

Box 1.8: Conceptual recovery model by Jumars

Before the DISCOL experiment was conducted, Jumars (1981) hypothesized in a conceptual paper how the different food-web compartments might recover from deep-sea mining and he summarized the outcome of his conceptual recovery model in the following figure:

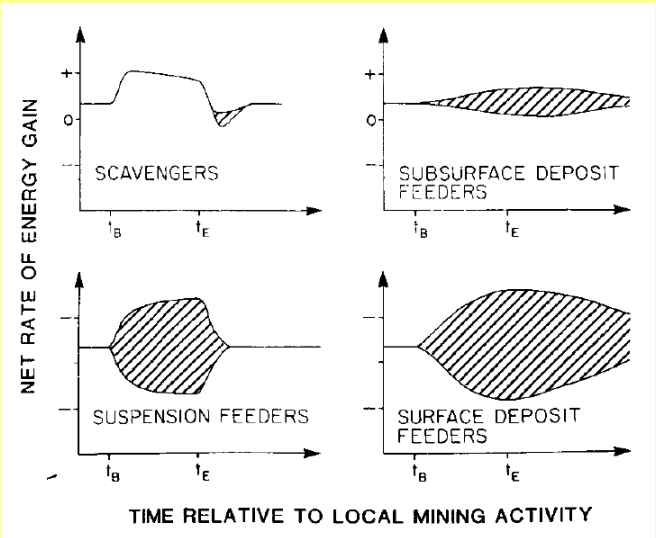

Figure 10-17. Predictions of net rate of energy gain over time for the different feeding guilds that were not immediately suffering from mining-induced mortality (i.e., fauna outside plough tracks).
Abbreviations are: t_B = start of local mining, tE = end of local mining, shaded area = major prediction uncertainty. Source: Jumars (1981)

1.7 Research approach

In this PhD thesis, experiments were combined with modeling approaches to assess how the benthic ecosystem responds to polymetallic nodule extraction in the deep sea.

1.7.1 Experimental approaches

In **Chapter 5** and **Chapter 8**, *pulse-chase* experiments were performed in which a food source (i.e., the diatom *Skeletonema costatum*) was enriched in the stable isotopes ^{15}N and ^{13}N and fed to the benthic community. Subsequently, this substrate was traced through the different food-web compartments. Pulse-chase experiments using stable isotopes have a long tradition in ecology (Middelburg, 2014) and allow to assess the short-term uptake of fresh phytodetritus. Deep-sea ecosystems at 4,000 m water depth, however, rarely encounter fresh phytodetritus. Therefore, the selection of the substrate is essential, as the aim in each experiment should be to mimic the reality as much as possible. Additionally, Jeffreys *et al.* (2013) showed that the abyssal plain macrofaunal community has preferences for specific phytodetritus types. Hence, if the substrate is

inadequate, lower than natural uptake rates could be measured, and the investigator would erroneously assume impaired ecosystem functioning. Furthermore, a comparison of results from Stratmann, Mevenkamp, *et al.* (2018) for the Peru Basin and Witte, Wenzhöfer, *et al.* (2003) for the Porcupine Abyssal Plain indicate that the food-web compartment that dominates the phytodetritus mineralization might change over time. Hence, also the length of the incubations could determine the experimental output.

The experiment presented in **Chapter 8** was furthermore conducted in meso-scale core incubations that impeded that nematodes migrated horizontally to avoid anoxic conditions or to find food sources. Additionally, no lateral flow of oxygenated water could re-oxygenate the anoxic sediment. This lateral flow of water might re-oxygenate coarse sediment from coastal areas, deep-sea sediment however is so fine, that no water would flow laterally, independent of the presence or absence of core walls. It is anyway very unlikely that 3 cm of sediment deposition in the CCZ leads to anoxic conditions, as the oxygen penetration depth is between 1 and 4.5 m (Volz *et al.*, 2018).

1.7.2 Modeling approach

Chapters 2, **3**, **6**, **7**, and **9** used various modeling approaches to assess the benthic ecosystem response to polymetallic nodule extraction in the deep sea: Modeling is a very useful approach when datasets are limited or underlying concepts in nature are investigated. However, a model never resembles reality, but is always a simplification of nature. Therefore, models depend heavily on high quality data as the same model can give very opposing results when two different datasets are used.

In **Chapter 2**, "Random Forest" was used to project biomass estimates on a global scale. Random Forest is a supervised learning algorithm and a member of the Regression Tree Analysis (Breiman, 2001). It uses decision trees on a training dataset that was generated by bootstrapping. In each split, one random sample from the predictor is selected from the whole set of predictors as split candidate. This gives weaker predictors the same chance to be selected, and the average of trees will be less variable and lead to better predictions (James, 2013).

In **Chapters 6**, **7**, **9** the "Linear Inverse Modeling" approach was applied to develop carbon-based food-web models (van Oevelen *et al.*, 2010). This approach is based on the concept of mass balance (Vézina and Platt, 1988) and quantifies carbon flows among food-web compartments in a pre-defined topological food web. For this purpose, the model combines two matrix equations,
the equality equation $E \times x = f$ [Equation 1-1]
and the inequality equation $Gx \geq h$, [Equation 1-2]
where x corresponds to the unknown flows and f and h are empirical data (van Oevelen *et al.*, 2010), such as physiological constraints like assimilation efficiency, net growth efficiency, growth rate, mortality rate, or respiration rate. When all data types are integrated, the linear inverse model equations look like these:
$E_{(m+d)\times n} \times x_{n\times 1} = f_{(m+d)\times 1}$ [Equation 1-3]

$G_{c\times n} \times x_{n\times 1} \geq h_{c\times 1}$, [Equation 1-4]

with n = number of flows, m = number of mass balances, d = number of equalities, and c = number of inequalities (van Oevelen *et al.*, 2010).

When the number of independent equations equals the number of unknown flows, the model is of full rank and there exists exactly one solution. However, a food web is generally underdetermined, i.e., there are fewer independent equations than unknown flows. In this case, an infinite amount of solutions exists, and the likelihood approach is applied to sample the solution space (van Oevelen *et al.*, 2010).

Linear inverse modeling is limited by the type of data required. To quantify carbon flows among the food-web compartments, abundance data have to be converted to carbon stocks and therefore the quality of conversion factors determines whether these carbon stocks reflect the reality or not. The best option is certainly to sample biomasses instead of abundances, but this is rarely done. Furthermore, physiological constraints are not known for all food-web compartment, so that literature data are implemented as inequalities. When site specific flux constraints are unknown for specific parameters, fluxes measured in different ecosystems might have to be implemented. Hence, the largest disadvantage of linear inverse modeling is the dependence on high quality data; however, this method also allows to construct food webs in highly under-sampled areas, such as the deep sea .

1.8 The international framework

This PhD thesis was conducted in the framework of MIDAS ("Managing Impacts of Deep Sea Resource Exploitation") and the Joint Program Initiative Ocean (JPIO) – Ecological Impacts of Deep Sea Mining. MIDAS was funded by the European Union's Seventh Framework Program and ran for 3 years from November 1st 2013 to October 31th 2016. It included 32 partners across Europe and investigated the environmental impacts of mineral and energy resource extraction in the deep sea. The minerals included polymetallic sulfides, polymetallic nodules, cobalt-rich ferromanganese crusts, rare earth elements, and furthermore the energy resource methane hydrate.

The research was interdisciplinary organized in work packages ranging from geological impacts, plume dynamics, ecotoxicology, species connectivity, ecosystem services and functioning, to which the author of this PhD thesis contributed, ecosystem resilience and recovery, management practice, protocol and standard development, legal instruments, and new monitoring technologies.

The JPI-Oceans project ran from January 2015 to December 2017 and involved partners from 11 different European countries. The focus of this project was the three research campaigns on board RV *Sonne* to the CCZ (SO239) and to the Peru Basin (SO242-1 and SO242) in 2015.

1.9 Outline of the thesis

Using experimental, observational, and modeling approaches, this PhD thesis aimed to gain further knowledge of environmental impacts that are related to the extraction of polymetallic nodules in the deep sea (Figure 1-18).

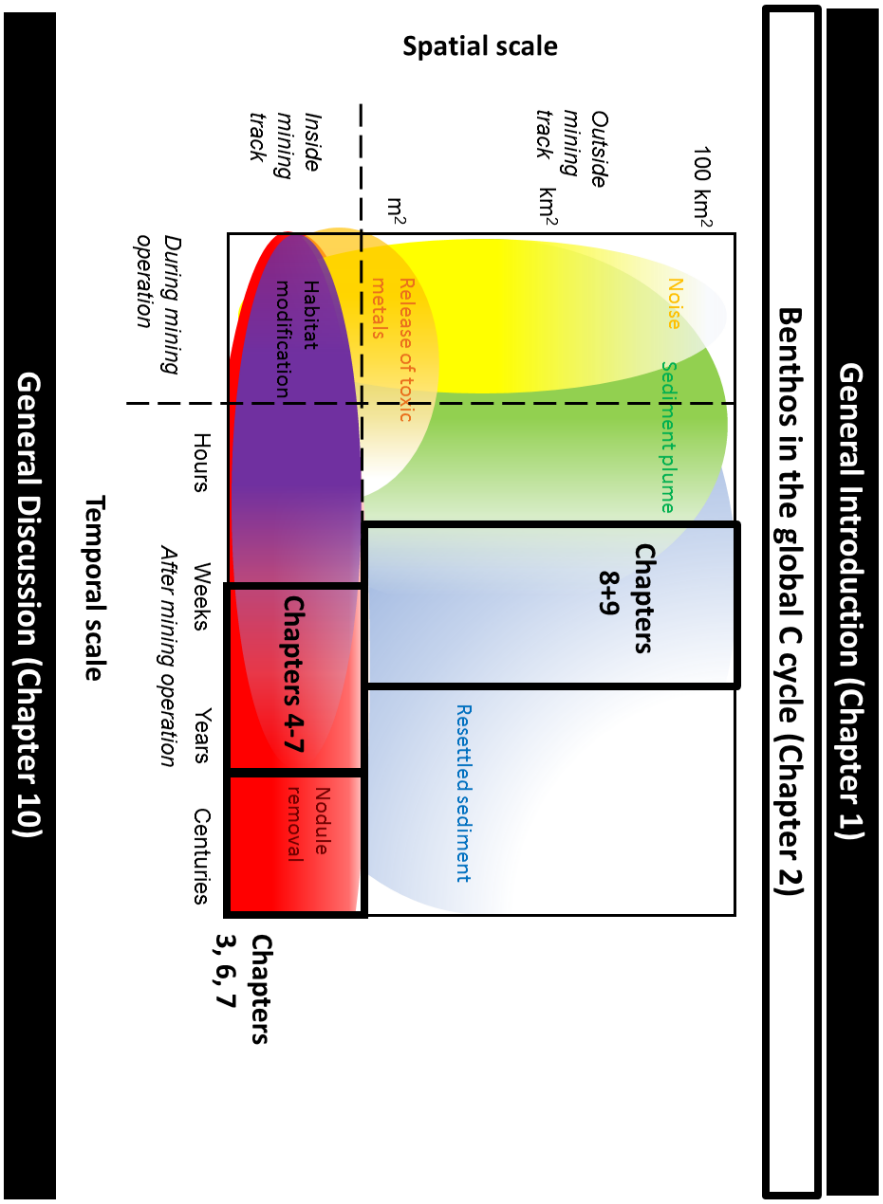

Figure 1-18. Schematic representation of the content of this PhD thesis. The figure between the black bars symbolizes the environmental impacts on a spatial and temporal scale. Each colored cloud corresponds to another environmental impact and the black frames with “Chapter XX” indicate which chapter addresses the specific environmental impact.

After investigating the importance of abyssal plains in the global marine carbon cycle and the role of benthos for this cycle, this PhD thesis investigates these environmental impacts and responds to the following research questions:

Nodule removal

- *Would the extraction of polymetallic nodules impact trophic and/ or non-trophic interactions among species?* (Chapter 3)
- *How would the number of network compartments, number of links, link density, and web connectance be affected?* (Chapter 3)
- *Do faunal biomass […] of the food webs vary and/ or has the difference between the two sites converged over time?* (Chapter 6)
- *How do the model outcomes [for nodule-dependent fauna] compare with conceptual model predictions on benthic community recovery from polymetallic nodule mining published by Jumars (1981)?* (Chapter 6)

Sediment removal

- *Do Holothuroidea assemblages differ inside plough tracks, outside plough tracks, and in reference areas?* (Chapter 4)
- *Have Holothuroidea population densities recovered after 26 yr?* (Chapter 4)
- *Do Holothuroidea respiration rates differ between sites?* (Chapter 4)
- *Has ecosystem functioning in the form of carbon uptake and partitioning recovered 26 yr after a disturbance event?* (Chapter 5)
- *Do faunal biomass and trophic composition of the food webs vary and/ or has the difference between the two sites converged over time?* (Chapter 6)
- *How do the model outcomes compare with conceptual model predictions on benthic community recovery from polymetallic nodule mining published by Jumars (1981)?* (Chapter 6)
- *Is total carbon cycling different between reference sites, outside plough tracks, and inside plough tracks?* (Chapter 7)

Sediment suspension and settlement

- *Does the exposure to burial with mine tailings alter the benthic community structure on the short term due to mortality and changes in vertical community distribution?* (Chapter 8)
- *Do changes in benthic community structure due to tailings disposal cause a reduced processing of organic matter as assessed from O_2 consumption, ^{13}C-labeled phytodetritus uptake and production of dissolved inorganic carbon?* (Chapter 8)
- *Is the response of benthic organisms to tailings different than to a deposition event with natural subsurface sediment?* (Chapter 8)
- *How does the food web in the Cap de Creus canyon react to the major DSWC event in winter 2005?* (Chapter 9)

Chapter 2 : The role of benthos in the global marine carbon cycle

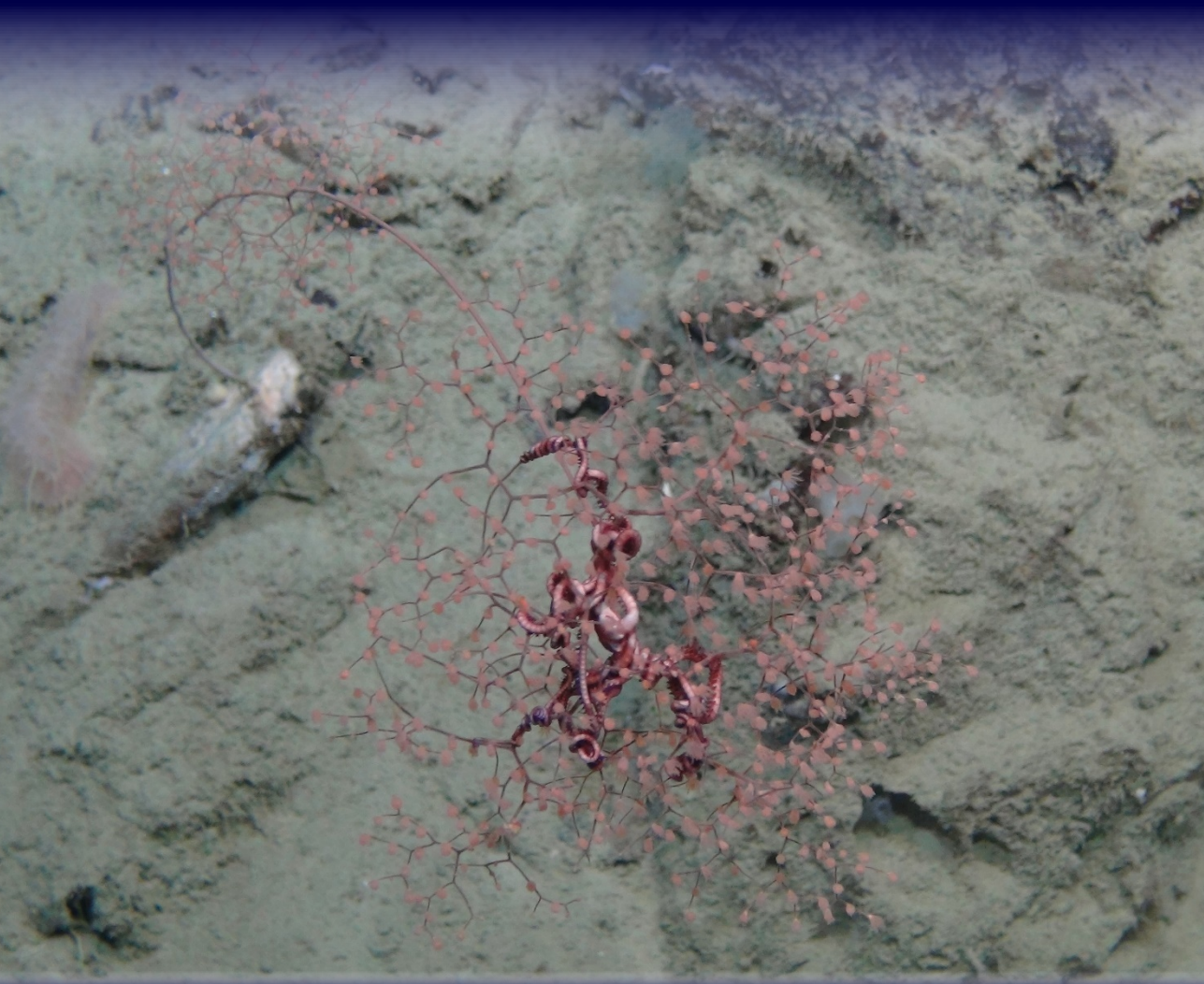

2. The role of benthos in the global marine carbon cycle

Tanja Stratmann, Karline Soetaert, Chih-Lin Wei, and Dick van Oevelen;
In preparation.

2.1 Abstract

We present estimates of the contribution of benthos, i.e., prokaryotes, meiofauna, macrofauna, and invertebrate megafauna, to the global stocks and cycling of marine organic carbon. Benthic biomass and sediment community oxygen consumption data were used to generate global seafloor maps using the random forest method. These maps were combined with a novel dataset of biomass-specific faunal respiration, production/biomass-ratios, and assimilation efficiency to arrive at global projections of benthic respiration (prokaryotes and fauna), faunal secondary production, and faunal ingestion. Global benthic biomass was estimated to be 9.94 Tg carbon (C), 28.0 Tg C, and 1.47 Tg C for meiofauna, macrofauna, and invertebrate megafauna, respectively. Their summed biomass was between 1 and 4% of the global marine heterotrophic consumer biomass. Global benthic respiration was estimated to be 1.19 Pg C yr^{-1}, global faunal benthic secondary production 0.28 Pg C yr^{-1}, and global faunal benthic ingestion 1.40 Pg C yr^{-1}. Faunal respiration showed a latitudinal trend with meiofaunal respiration dominating deep-sea faunal benthic respiration in the subtropics and tropics, whereas macrofaunal respiration governed deep-sea benthic respiration in polar regions. A seafloor partitioning into four depth regimes showed that 47% of total benthic respiration (prokaryotic + faunal), 50% of total benthic secondary production, and 57% of total benthic ingestion occured in abyssal plains and continental rises. Benthic invertebrates contributed 1% to total marine herbivory and they ingested up to 76% of total net export production. In the future, the contribution of benthos to the global marine organic carbon cycle will likely change because the global particulate organic carbon export flux to the seafloor on which large parts of the benthos depend is projected to decrease.

2.2 Introduction

The seafloor covers 71% of the Earth's surface (Gage and Tyler, 1991) and supports diverse ecosystems (Roberts *et al.*, 2002; Roberts, Wheeler and Freiwald, 2006; Short *et al.*, 2007; Ramírez-Llodrà *et al.*, 2010; Giri *et al.*, 2011; Duarte, 2017) that play a pivotal role in the global carbon (C) cycle and the climate system (Sarmiento *et al.*, 1998; Thurber *et al.*, 2014). Most of the seafloor is devoid of direct sunlight and biota therefore rely on external inputs for their energy supply. About 15% of the global marine net primary production (65 Pg C yr^{-1}; Woodward, 2007) is exported from the photic zone in particulate form (9.6 Pg C yr^{-1}; Dunne, Sarmiento and Gnanadesikan, 2007) as marine snow (De La Rocha and Passow, 2007) or fecal pellets (Iseki, 1981; Pfannkuche, 1993; Michels *et al.*, 2008) and ultimately settles on the seafloor. The depositional flux of this organic matter is inversely related to water depth (Andersson *et al.*, 2004) as organic matter degrades during the downward transit (Ploug, 2001; Marsay *et al.*, 2015; Belcher *et al.*, 2016). In addition to spatial variation in surface productivity (Woodward, 2007), this inverse relationship creates an energy limitation gradient moving from the coast (0–50 m), along the continental shelf (50–200 m) and slope (200–2,000 m) down to the deep abyssal plains (>4,000 m). The energy gradient is a key driver of benthic biodiversity (Woolley *et al.*, 2016) and biomass (Rex *et al.*, 2006; Wei *et al.*, 2010) patterns of the seafloor. It remains however unclear how C cycling within the benthic ecosystem responds to this energy gradient.

Benthos, i.e., organisms living in, on or near the seafloor, include benthic prokaryotes, meiofauna, macrofauna, and megafauna. Prokaryotes, i.e., Bacteria and Archaea, in the upper 10 cm of sediment have densities of 4.60×10^{7} cells cm^{-3} (= 1.70×10^{28} prokaryotic cells globally) (Whitman, Coleman and Wiebe, 1998) and are therefore the most abundant benthic organisms. They play a key role in short-term C cycling in the deep sea (Sweetman *et al.*, 2018) and C-based food-web models for deep-sea stations in the NE Atlantic and the NE Pacific estimated that they contribute >70% to the sediment community oxygen consumption (SCOC) at these specific sites (van Oevelen, Soetaert and Heip, 2012; Dunlop *et al.*, 2016; Durden *et al.*, 2017). Benthic meio-fauna, i.e., protozoan and metazoan fauna between 32 µm (deep-sea meiofauna)/ 63 µm (shallower water depth) and 250–300 µm (deep-sea meiofauna; Rex and Etter, 2010)/ 500 µm size (shallower water depth; Giere, 2009), can actively rework sediment particles and build microscale burrows in the sediment (Schratzberger and Ingels, 2018). It has even been shown in ancient sediment that meiofauna bioturbated oxygen depleted, unconsolidated sediment enriched in organic matter that was avoided by macrofauna due to the lack of oxygen (Löhr and Kennedy, 2015). Additionally, meiofauna is a food source for juvenile and small adult fish (Schückel *et al.*, 2013; Carpentier *et al.*, 2014). It also contributes to organic matter mineralization and nutrient regeneration by stimulating the microbial community (Coull, 1999). The next larger benthic size class, the macrofauna (250/ 300/ 500 µm–1 cm size), also bioturbates, i.e., reworks the sediment (bioturbation *sensu* Meysman, Middelburg and Heip, 2006), and in this way changes the texture of the sediment (Meadows and Tait, 1989) and reduces slope failure (Shaikh,

Meadows and Meadows, 1998). Macrofauna can also be an ecosystem engineer, i.e., an organism that alters the physical environment and in this way changes directly or indirectly the availability of resources to other organisms (Jones, Lawton and Shachak, 1994), and modifies hydrodynamics. The polychaete *Laniche conchilega*, for instance, protrudes from the sediment and increase or decrease flow velocities depending on the tube density and length (Borsje *et al.*, 2014). Further invertebrate megafaunal ecosystem engineers are scleractinian corals and sponges that form biological structures which provide new habitats for associated fauna (Beaulieu, 2001; Buhl-Mortensen *et al.*, 2010). Especially cold-water coral reefs and deep-sea sponge grounds are deep-sea hotspots of the benthic C cycle: Respiration rates in these reefs can be 9–20 higher than in adjacent sediment communities (Cathalot *et al.*, 2015).

Hence, the role of the various benthic size classes in C cycling can differ very locally: In the middle section of the submarine Nazaré canyon (Portuguese Margin, NE Atlantic), for instance, megafaunal sea cucumbers were estimated to contribute >50% to the total respiration, whereas in deeper sections of that canyon, sea cucumbers were predicted to add <1% to the total respiration (van Oevelen, Soetaert, *et al.*, 2011). A good understanding of spatial differences in the marine C cycle are, however, essential to project realistic responses of the marine realm to climate change (Jones *et al.*, 2014; Sweetman *et al.*, 2017; Snelgrove *et al.*, 2018) and to identify potential areas of C sequestration.

To identify potential spatial and/ or bathymetric patterns in benthic respiration, benthic invertebrate secondary production, and ingestion, global seafloor estimates were generated. Furthermore, global benthic C stocks were compared with all other marine C pools and the quantitative contribution of benthos to the global marine C cycle was assessed. We addressed the following research questions: (1) Do the different size classes show different spatial and/ or bathymetric patterns? (2) How much of the global net primary production is processed by benthos globally? (3) How will C processing change in the future due to climate change?

2.3 Material and methods

We generated global maps of meiofauna, macrofauna, and invertebrate megafauna biomasses and sediment community oxygen consumption (SCOC) based on globally distributed datasets on benthic biomass (Wei *et al.*, 2010) and SCOC (Snelgrove *et al.*, 2018) using random forest. These maps were combined with a database for physiological data such as marine invertebrate assimilation efficiency (*AE*), biomass-specific faunal respiration (*r*), and production/biomass-ratio (*P/B-ratio*) to estimate faunal and prokaryotic benthic respiration, faunal secondary production, and faunal ingestion rates. Subsequently, we summarized the data for four different depth regimes (Figure 2-1).

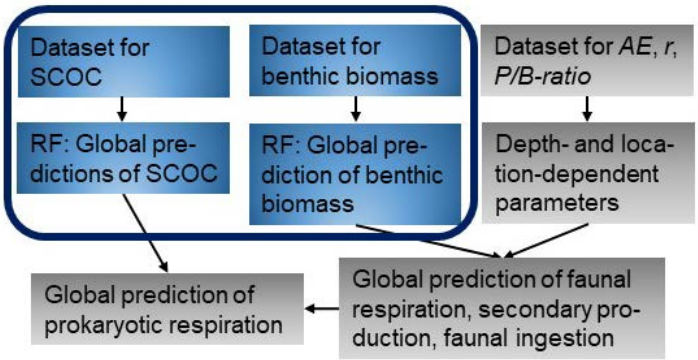

Figure 2-1. Schematic representation of all steps of analysis. The blue boxes represent steps that have been published previously (Wei *et al.*, 2010; Snelgrove *et al.*, 2018) and were repeated here, whereas the gray boxes show steps that were performed exclusively for this analysis.
Abbreviations are: *AE* = assimilation efficiency, *r* = biomass-specific faunal respiration, *P/B-ratio* = production/biomass-ratio, SCOC = sediment community oxygen consumption, RF = random forest algorithm.

2.3.1 Datasets of sediment community oxygen consumption and benthic biomasses, random forest, and global predictions

Snelgrove *et al.* (2018) compiled a global dataset of 1,075 SCOC data based on ship-board measurements of sediment cores and *in situ* sediment incubations. Subsequently, the authors converted the oxygen consumption rates (mmol O_2 m^{-2} d^{-1}) into C respiration rates (mmol C m^{-2} d^{-1}) using a respiratory coefficient (RQ) of 1 mol C / mol O_2. A dataset for benthic biomass of meiofauna, macrofauna, and invertebrate megafauna by Wei *et al.* (2010) included 629 entries for benthic meiofauna biomass, 1,483 entries for benthic macrofauna biomass, and 133 entries for benthic invertebrate megafauna biomass that were converted to mmol C m^{-2}. A map of sampling locations is presented in Figure 1 of Wei *et al.* (2010).

The machine-learning algorithm random forest (RF) is based on binary decision trees (Breiman, 2001). It used 21 environmental parameters (Supplementary list 2-1) to project SCOC and 24 environmental parameters (Supplementary list 2-1) to project benthic biomasses (meiofauna, macrofauna, invertebrate megafauna) for the global seafloor (1°×1° grid cells, equivalent to ~111 km×111 km). The RF modeling was performed in the R package *randomForest* (Breiman *et al.*, 2017) and detailed descriptions can be found in Snelgrove *et al.* (2018) (SCOC) and Wei *et al.* (2010) (benthic biomass).

The predicted values of SCOC and benthic biomass for each 1°×1° grid cell per size class were subsequently classified into four depth regimes according to the average water depth for each grid cell (see details below).

2.3.2 Database for assimilation efficiency, biomass-specific faunal respiration, and production/biomass-ratio

An extensive literature search was performed to gather published data on biomass-specific faunal respiration *r* (d^{-1}), production/biomass-ratio *P/B-ratio* (d^{-1}), and assimilation efficiency *AE* which were compiled in a database. For each data entry, additional information about the geographical location, sampling depth (in m), sampling date (when available), species name for which the specific parameter was measured, and the measurement method/ approach were extracted from the publications. Whenever information about the size of the organism was reported, this data was used to classify the species as benthic meiofauna, macrofauna, or megafauna. When no information was available, the "World Register of Marine Species" (Horton *et al.*, 2018) was consulted to classify the species in a size class.

The full dataset of *r* included 64 studies with 1,903 data entries that reported oxygen consumption rates in 23 different units, of which 13 could be converted into biomass-specific faunal respiration *r* (d^{-1}) by multiplication of the oxygen consumption rates with specific conversion factors assuming a respiratory coefficient of 1 (Glud, 2008). If necessary, taxon-specific conversion factors as presented in Rowe (1983), Soetaert and Heip (1995), and Wieser (1960) were used to convert wet weight or dry weight to C content (mmol C). After exclusion of all data entries for which a conversion to *r* was not possible, the reduced dataset contained 516 data entries from 44 different studies (references are given in Supplementary list 2-2).

The full *P/B-ratio* dataset included 595 data entries from 91 publications (references are given in Supplementary list 2-3).

AE was defined as:

$$AE = \frac{(I-F)}{I} \qquad \text{[Equation 2-1]}$$

(modified from Conover, 1966), where *I* is the ingested food and *F* is the feces production (Crisp, 1971). The dataset included 26 studies with a total of 143 data entries (references are given in Supplementary list 2-4).

2.3.3 Depth- and location-dependent parameters

We classified the global seafloor into the following four depth regimes (Dunne, Sarmiento and Gnanadesikan, 2007): 1) the nearshore <50 m water depth, 2) the continental shelf between 50 and 200 m water depth, 3) the continental slope between 200 and 2,000 m, and 4) the continental rise/ abyssal plains >2,000 m deep.

Physiological data (*r*, *P/B-ratio*, and *AE*) were categorized according to size class (benthic meiofauna, macrofauna, megafauna) and depth regime (nearshore, continental shelf, continental slope, continental rise/ abyssal plains). Data from the Mediterranean Sea (>200 m water depth) were treated separately because the water temperature of the Mediterranean Deep Water is considerably higher (12.7 to 13.6°C; UNEP/MAP, 2012) than the average abyssal water temperature (2°C; Ramírez-Llodrà *et al.*, 2010). A summary of the data is presented in Table 2-1.

Table 2-1. Descriptive statistics for biomass-specific faunal respiration *r* (d^{-1}), production/biomass *(P/B)-ratio* (d^{-1}), and assimilation efficiency *AE* for benthic meiofauna (MEI), macrofauna (MAC), and megafauna (MEG) for near-shore areas (NS; <50 m water depth), continental shelves (CSh; 50–200 m water depth), and continental slopes (CSl; 200–2,000 m water depth). *n* corresponds to the number of data points extracted from the literature specified in Supplementary list 2-2 to 2-4.

Fauna	Depth	*n*	Min	Lower quantile	Median	Upper quantile	Max
r							
MEI	NS	137	2.27×10^{-6}	1.00×10^{-3}	1.00×10^{-2}	4.98×10^{-2}	0.12
MEI	CSl	39	6.30×10^{-6}	2.03×10^{-2}	3.80×10^{-2}	6.96×10^{-2}	0.13
MAC	NS	39	1.44×10^{-6}	2.53×10^{-4}	2.73×10^{-3}	1.83×10^{-2}	3.70×10^{-2}
MAC	CSl	10	6.30×10^{-5}	7.12×10^{-5}	7.05×10^{-3}	2.28×10^{-2}	3.84×10^{-2}
MEG	NS	196	2.19×10^{-7}	4.80×10^{-6}	3.40×10^{-5}	2.77×10^{-3}	6.82×10^{-3}
MEG	CSh	10	5.11×10^{-7}	8.64×10^{-7}	3.63×10^{-6}	4.73×10^{-5}	5.64×10^{-5}
MEG	CSl	48	7.49×10^{-8}	1.45×10^{-6}	2.03×10^{-5}	4.21×10^{-3}	8.58×10^{-3}
(P/B)-ratio							
MEI	NS	10	7.40×10^{-3}	4.50×10^{-2}	6.58×10^{-2}	0.13	0.17
MAC	NS	361	1.41×10^{-7}	3.21×10^{-3}	6.03×10^{-3}	1.21×10^{-2}	2.48×10^{-2}
MAC	CSh	62	3.29×10^{-4}	3.84×10^{-3}	7.12×10^{-3}	1.21×10^{-2}	2.42×10^{-2}
MAC	CSl (Med. Sea)	55	1.34×10^{-3}	1.37×10^{-2}	1.84×10^{-2}	2.21×10^{-2}	3.46×10^{-2}
MAC	CSl (except Med. Sea)	8	2.74×10^{-4}	8.49×10^{-4}	1.56×10^{-3}	4.77×10^{-3}	6.85×10^{-3}
MEG	NS	80	1.37×10^{-5}	2.11×10^{-3}	9.45×10^{-3}	3.99×10^{-2}	9.59×10^{-2}
MEG	CSl (Med. Sea)	10	1.11×10^{-2}	1.22×10^{-2}	1.83×10^{-2}	2.23×10^{-2}	2.36×10^{-2}
MEG	CSl (except Med. Sea)	9	1.37×10^{-4}	2.74×10^{-4}	1.48×10^{-3}	1.42×10^{-2}	2.17×10^{-2}
AE							
MEI	NS	5	0.18	0.26	0.27	0.41	0.60
MAC		12	0.48	0.62	0.72	0.87	0.93
MEG		126	0.13	0.48	0.65	0.80	1.00

Due to a lack of sufficient data in the literature, statistically significant data are missing for several size classes and/ or depth ranges. There were <5 data points available for *r* for benthic meiofauna and macrofauna at continental shelves and continental rises/ abyssal plains. Hence, in subsequent analyses the near-shore values for benthic meiofauna had to be used for the <200 m depth regime and continental slope data were used for the >200 m depth regime. Near-shore benthic meiofauna *P/B-ratio* was used for all water depths for benthic meiofauna, whereas the continental slope benthic macrofauna and megafauna *P/B-ratios* were used for all depths >2,000 m. Insufficient data for *AE* for >50 m depth required the use of near-shore data for all water depths in the following analysis.

2.3.4 Global predictions of respiration, secondary production, and ingestion

Predictions of benthic invertebrate respiration, production, and ingestion for the global seafloor (1°×1° grid cells) were based on the average water depth (m) for each grid cell because the biomass-specific metabolic rate can decline with depth (Brown *et al.*, 2018).

Benthic faunal respiration of each size class for every grid cell $R_{x,y,i,j}$ (mmol C m^{-2} d^{-1}) was calculated as:

$$R_{x,y,i,j} = r_{i,j} \times B_{x,y,i}, \quad \text{[Equation 2-2]}$$

where $B_{x,y,i}$ (mmol C m^{-2}) is the faunal biomass prediction for each size class *i* for every grid cell *x,y* from section 2.3.1 (above) and $r_{i,j}$ is the corresponding median value of biomass-specific faunal respiration from Table 2-1 for the specific size class *i* and depth regime *j*.

The benthic prokaryotic respiration $R_{x,y,Prokaryotes}$ (mmol C m^{-2} d^{-1}) for every 1°×1° grid cell was calculated as:

$$R_{x,y,Prokaryotes} = SCOC_{x,y} - \sum R_{x,y,Fauna}, \quad \text{[Equation 2-3]}$$

using the SCOC predictions from section 2.3.1 (above).

The global benthic faunal production $P_{x,y,i,j}$ (mmol C m^{-2} d^{-1}) was calculated for benthic meiofauna, macrofauna, and megafauna per 1°×1° grid cell as:

$$P_{x,y,i,j} = \frac{P}{B} ratio_{i,j} \times B_{x,y,i}, \quad \text{[Equation 2-4]}$$

where $B_{x,y,i}$ is the biomass prediction for meiofauna, macrofauna, and megafauna from section 2.3.1 (above) and $P/B\text{-}ratio_{i,j}$ is the median production/biomass-ratio for size class *i* and depth regime *j* from Table 2-1.

The faunal ingestion $I_{x,y,i,j}$ for each 1°×1° grid cell and size class was calculated based on the benthic faunal production $P_{x,y,i,j}$ and benthic faunal respiration $R_{x,y,i,j}$ estimates as:

$$I_{x,y,i,j} = \frac{\left(R_{x,y,i,j} + P_{x,y,i,j}\right)}{AE_{i,j}}, \quad \text{[Equation 2-5]}$$

where $AE_{i,j}$ is the median assimilation efficiency value for size class *i* and depth regime *j* from Table 2-1.

The predicted values of benthic respiration, faunal secondary production, and ingestion for each 1°×1° grid cell per size class were subsequently classified into the four depth regimes according to the average water depth for each grid cell.

2.3.5 Data analysis

The area-integrated total benthic invertebrate biomass *total* $B_{i,j}$ per depth regime *j* was calculated as:

$$total\ B_{i,j} = area_j \times \widetilde{B_{i,j}}, \quad \text{[Equation 2-6]}$$

where $area_j$ is the surface area that each specific depth regime *j* covers on the globe and $\widetilde{B_{i,j}}$ is the median biomass per faunal size class *i* and depth regime *j*.

The area-integrated total C flow, i.e., respiration, secondary production, or ingestion, per depth regime *j*, *total C flow*$_{i,j,k}$ was calculated as:

$$total\ C\ flow_{i,j,k} = area_j \times C\ \widetilde{flow}_{i,j,k}, \quad \text{[Equation 2-7]}$$

where $area_j$ is the global surface area of each specific depth regime and $C\ \widetilde{flow}_{i,j,k}$ is the median C flow *k* (respiration, secondary production, or ingestion) per size class *i* and depth regime *j*.

Biomass data are expressed as mmol C m^{-2} (surface-specific) and Pg C (area-integrated) and flux data are expressed as mmol C m^{-2} d^{-1} and Pg C yr^{-1} (area-integrated) to be consistent with the units used in other papers dealing with global C cycling.

2.4 Results

2.4.1 Carbon stocks in the marine realm

The marine realm contains C in its inorganic form, i.e., dissolved carbon dioxide, HCO_3^- and CO_3^{2-} (3.50×10^4 Pg C; Alexandrov, 2008), and in its organic form (1.71×10^3 to 1.72×10^3 Pg C; Table 2-2). This organic C pool includes particulate organic carbon (POC), dissolved organic carbon (DOC) of which about 80% is truly dissolved (<1 nm) and 20% has colloidal size (1–1,000 nm) (Verdugo, 2012), recent sedimentary C, and biomass.

The biomass consists of autotrophic primary producers, heterotrophic consumers, mixotrophs, such as Rhizaria, prokaryotes, and viruses. Autotrophic primary producers are composed of phytoplankton that contributes 7% to the total primary producer biomass (Table 2-2), saltmarshes, mangroves, seagrass, microphytobenthos, and macroalgae. Eukaryotic heterotrophic consumers comprise zooplankton, fish, pinnipeds, i.e., seals, cetaceans, i.e., whales, dolphins, and porpoises, and benthos. All eukaryotic heterotrophic consumers combined have a total biomass of 0.99 to 3.22 Pg C of which between 88 and 91% are fish (Table 2-2). Benthic meiofauna, macrofauna, and invertebrate megafauna have a total biomass of 9.98×10^{-3} Pg C in near-shore areas, 7.73×10^{-3} Pg C at continental shelves, 7.95×10^{-3} Pg C at continental slopes, and 1.37×10^{-2} Pg C at continental rises/ abyssal plains (Table 2-3). Hence, they contribute between 1 to 4% to the global eukaryotic heterotrophic consumer biomass and thereby have a biomass comparable to pinnipeds or cetaceans. Prokaryotes have the largest biomass in the marine realm (6.68 Pg C; Arístegui *et al.*, 2009; Kallmeyer *et al.*, 2012) of which 61% is sedimentary prokaryotic C (Kallmeyer *et al.*, 2012).

Table 2-2. Integrated C pools (Pg C; 1 Pg = 10^{15} g) of the world oceans.

C pool	Pg C	References
Primary producers		
Phytoplankton	0.25	Kostadinov *et al.* (2016)
Macroalgae	0.54	Woodwell *et al.* (1978)
Mangroves[1]	1.92	Doughty *et al.* (2015); Giri *et al.* (2011)
Microphytobenthos	(no data available)	
Saltmarshes[2]	0.18	Doughty *et al.* (2015); Mcowen *et al.* (2017)
Seagrass	0.76–1.5	Fourquean *et al.* (2012)
Consumers		
Benthic meiofauna	9.94×10^{-3}	this study
Benthic macrofauna	2.80×10^{-2}	this study
Benthic megafauna	1.47×10^{-3}	this study
Fish	0.90–2.84	Jennings *et al.* (2008); Watson, Stock and Sarmiento (2015)
Meso- and macrozooplankton (epipelagic zone)	0.02–0.31	Moriarty *et al.* (2013); Biard *et al.* (2016)
Pinniped	5.10×10^{-3}	Christensen (2006)
Cetacean	2.50×10^{-2}	Christensen (2006)
Rhizaria (upper 500 m)	0.20	Biard *et al.* (2016)
Virus	0.20	Suttle (2005)
Pelagic prokaryotes[3]		
Epipelagic prokaryotes	1.19	Arístegui *et al.* (2009)
Mesopelagic prokaryotes	0.47	Arístegui *et al.* (2009)
Bathypelagic prokaryotes	0.92	Arístegui *et al.* (2009)
Sedimentary prokaryotes	4.10	Kallmeyer *et al.* (2012)

[1]The integrated mangrove biomass was calculated by multiplying the mean above + below ground biomass (139 Mg C ha^{-1}; Doughty *et al.*, 2015) with the total area that mangrove forests cover on Earth (1.38×10^{7} ha; Giri *et al.*, 2011).

[2]The integrated saltmarsh biomass was determined by multiplying the mean above + below ground biomass (33 Mg C ha^{-1}; Doughty *et al.*, 2015) with the total area that saltmarshes cover on Earth (5.50×10^{6} ha; Mcowen *et al.*, 2017).

[3]The integrated (epi-, meso-, bathy-) pelagic prokaryotic biomasses were calculated by multiplying the layer-specific prokaryote biomasses (0.94, 0.24, and 0.7 mmol C m^{-3}, respectively; Arístegui *et al.*, 2009) with the volume of the corresponding pelagic zones (1.03×10^{17}, 1.64×10^{17}, and 1.10×10^{18} m^3, respectively; Sayre *et al.*, 2017).

Table 2-3. Benthic biomass of meiofauna, macrofauna, and invertebrate megafauna for near shore (<50 m), continental shelf (50–200 m), continental slope (200–2,000 m), and continental rise/ abyssal plain (>2,000 m). Area data are from Dunne, Sarmiento and Gnanadesikan (2007).
Data are presented as: mean±SD (median); area integrated biomass is calculated as described in section 2.3.5 (above).

Meiofauna		**Macrofauna**		**Megafauna**	
(mmol C m^{-2})	**($\times 10^{-3}$ Pg C)**	**(mmol C m^{-2})**	**($\times 10^{-3}$ Pg C)**	**(mmol C m^{-2})**	**($\times 10^{-3}$ Pg C)**
Near shore (area: 0.71×10^{13} m^2)					
18.1±0.39 (15.1)	1.29	108±3.40 (9.92)	8.45	3.32±0.09 (2.80)	0.24
Continental shelf (area: 0.95×10^{13} m^2)					
15.5±0.26 (13.9)	1.58	72.6±1.94 (53.0)	6.04	1.59±0.04 (0.97)	0.11
Continental slope (area: 2.24×10^{13} m^2)					
6.75±0.10 (5.05)	1.36	32.4±0.56 (23.7)	6.37	1.42±0.02 (0.83)	0.22
Continental rise/ abyssal plain (area: 31.1×10^{13} m^2)					
2.37±0.02 (1.53)	5.71	6.79±0.06 (1.90)	7.09	0.35±0.02 (0.24)	0.90
Global					
	9.94		28.0		1.47

2.4.2 Partitioning of sediment respiration within benthos

Global SCOC was estimated to be 1.19 Pg C yr^{-1} distributed over near-shore areas (0.21 Pg C yr^{-1}), continental shelves (0.21 Pg C yr^{-1}), continental slopes (0.21 Pg C yr^{-1}), and continental rises/ abyssal plains (0.56 Pg C yr^{-1}). The lowest SCOC values were estimated for the N and S Pacific Gyre, the Indian Ocean Gyre as well as the N and S Atlantic Gyre (Figure 2-2). In contrast, the Argentinian Sea (SW Atlantic), the eastern Bay of Biscay, North Sea as well as Baltic Sea in the NE Atlantic, and the Yellow Sea, Java Sea as well as Arafura Sea in the W Pacific were estimated to have the highest SCOC values (Figure 2-2).

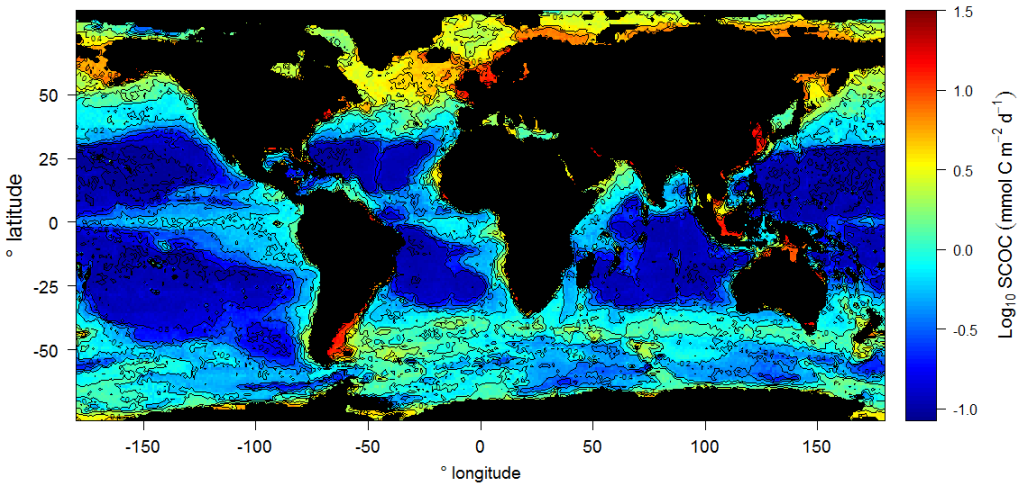

Figure 2-2. Global log_{10} sediment community oxygen consumption (SCOC; mmol C m^{-2} d^{-1}).

Prokaryotic respiration (Figure 2-3a, Table 2-4) averaged at 1.04 mmol C m^{-2} d^{-1} and was lowest in the abyssal plains and continental rises (0.51 mmol C m^{-2} d^{-1}) and highest in the coastal areas <50 m water depth (7.90 mmol C m^{-2} d^{-1}). Benthic meiofaunal respiration (average respiration rate: 0.11 mmol C m^{-2} d^{-1}; Figure 2-3b) was highest on the continental slope (0.26 mmol C m^{-2} d^{-1}) and lowest at continental rises and in abyssal plains where the respiration rate was only one third of the slope rate (8.84×10^{-2} mmol C m^{-2} d^{-1}) (Table 2-4). The depth regime with the highest benthic macrofaunal respiration (average respiration rate: 7.67×10^{-2} mmol C m^{-2} d^{-1}; Figure 2-3c) was the near-shore area, where the respiration rate amounted to 0.31 mmol C m^{-2} d^{-1} (Table 2-4). The lowest respiration rates (mmol C m^{-2} d^{-1}) were predicted for benthic invertebrate megafauna (average respiration rate: 4.29×10^{-6}; Figure 2-3d) with values ranging from 9.31×10^{-5} mmol C m^{-2} d^{-1} in near-shore areas to 1.17×10^{-7} mmol C m^{-2} d^{-1} on the continental rise and in abyssal plains (Table 2-4).

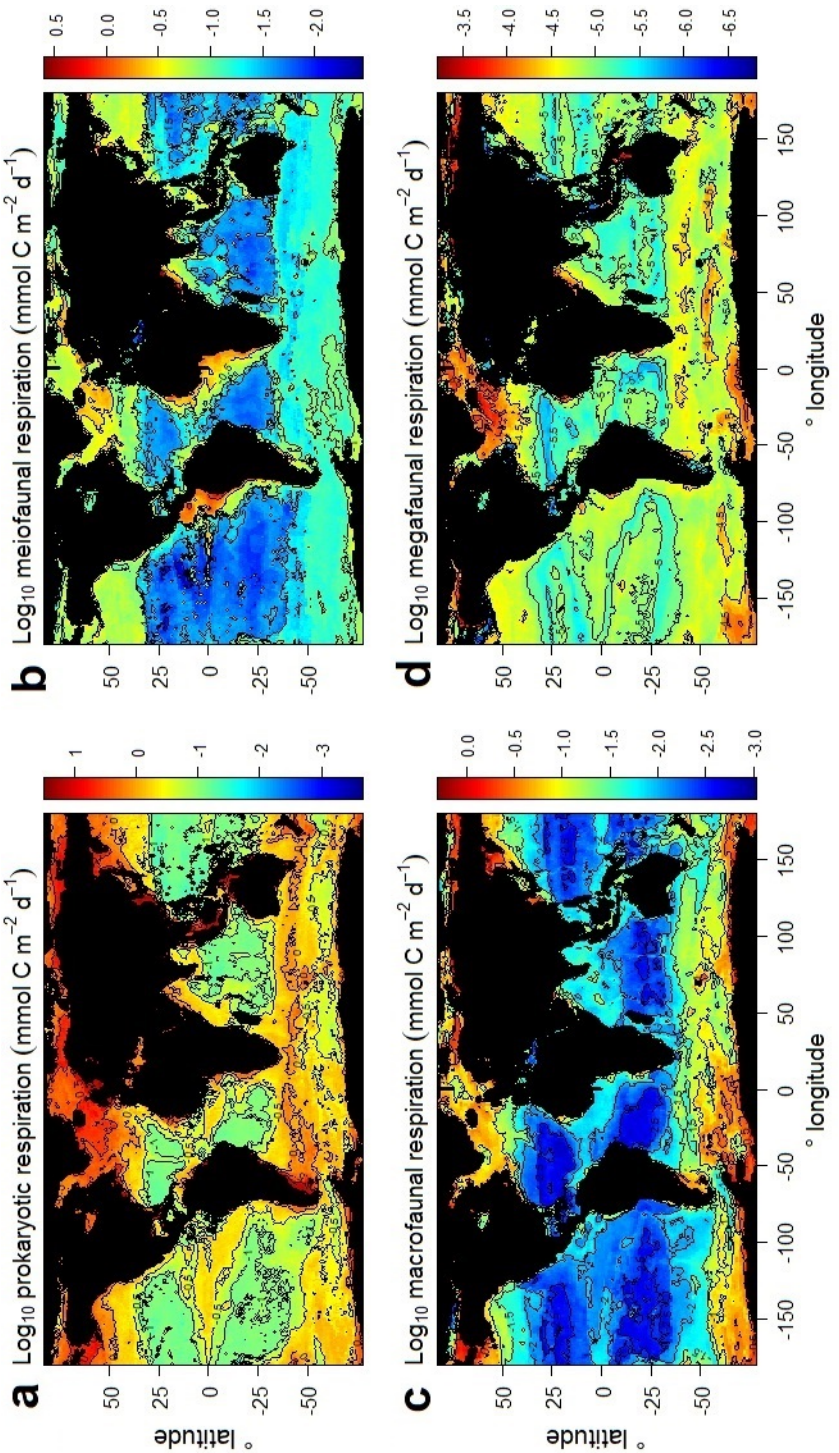

Figure 2-3. Global $\log_{10}$ benthic respiration (mmol C m^{-2} d^{-1}) of (a) prokaryotes, (b) meiofauna, (c) macrofauna, and (d) invertebrate megafauna. Note the differences in scales among panels.

Table 2-4. Respiration rates classified into size class and depth regime. Data are presented as: mean±SE (median); area integrated C flows are calculated as described in section 2.3.5. Area data are from Dunne, Sarmiento and Gnanadesikan (2007).

Benthos type	**(mmol C m^{-2} d^{-1})**	**(Pg C yr^{-1})**
Near shore (Area: 0.71×10^{13} m^2)		
Prokaryotes	7.90±0.17 (6.40)	0.20
Meiofauna	$0.18\pm3.91\times10^{-3}$ (0.15)	4.66×10^{-3}
Macrofauna	$0.31\pm9.20\times10^{-3}$ (0.28)	8.68×10^{-3}
Megafauna	$9.31\times10^{-5}\pm5.57\times10^{-6}$ (6.62×10^{-5})	2.06×10^{-6}
Total benthos		0.21
Continental shelf (Area: 0.95×10^{13} m^2)		
Prokaryotes	6.04±0.11 (4.77)	0.20
Meiofauna	$0.16\pm2.58\times10^{-3}$ (0.14)	5.83×10^{-3}
Macrofauna	$0.19\pm4.78\times10^{-3}$ (0.15)	6.20×10^{-3}
Megafauna	$5.67\times10^{-6}\pm2.20\times10^{-7}$ (3.59×10^{-6})	1.49×10^{-7}
Total benthic fauna		0.21
Continental slope (Area: 2.24×10^{13} m^2)		
Prokaryotes	$2.26\pm3.05\times10^{-2}$ (1.78)	0.17
Meiofauna	$0.26\pm4.05\times10^{-3}$ (0.19)	1.89×10^{-2}
Macrofauna	$0.23\pm3.57\times10^{-3}$ (0.17)	1.66×10^{-2}
Megafauna	$3.70\times10^{-5}\pm7.18\times10^{-7}$ (2.90×10^{-5})	2.84×10^{-6}
Total benthic fauna		0.21
Continental rise/ abyssal plain (Area: 31.1×10^{13} m^2)		
Prokaryotes	$0.51\pm3.29\times10^{-3}$ (0.34)	0.46
Meiofauna	$8.84\times10^{-2}\pm6.81\times10^{-4}$ (5.79×10^{-2})	7.88×10^{-2}
Macrofauna	$4.79\times10^{-2}\pm4.20\times10^{-4}$ (1.34×10^{-2})	1.82×10^{-2}
Megafauna	$1.17\times10^{-7}\pm3.52\times10^{-9}$ (7.43×10^{-8})	1.01×10^{-7}
Total benthic fauna		0.56

Prokaryotes dominated respiration in all depth regimes, whereas benthic invertebtrate megafauna always contributed the least to SCOC (Figure 2-4). The proportional contribution of benthic meiofauna and macrofauna changed with latitude, especially at water depth >200 m. The benthic meiofauna contribution to SCOC at the continental slope and continental rise/ abyssal plain was highest at the equator, whereas the contribution of benthic macrofauna was highest near the poles, especially in the southern hemisphere (50°–69°S).

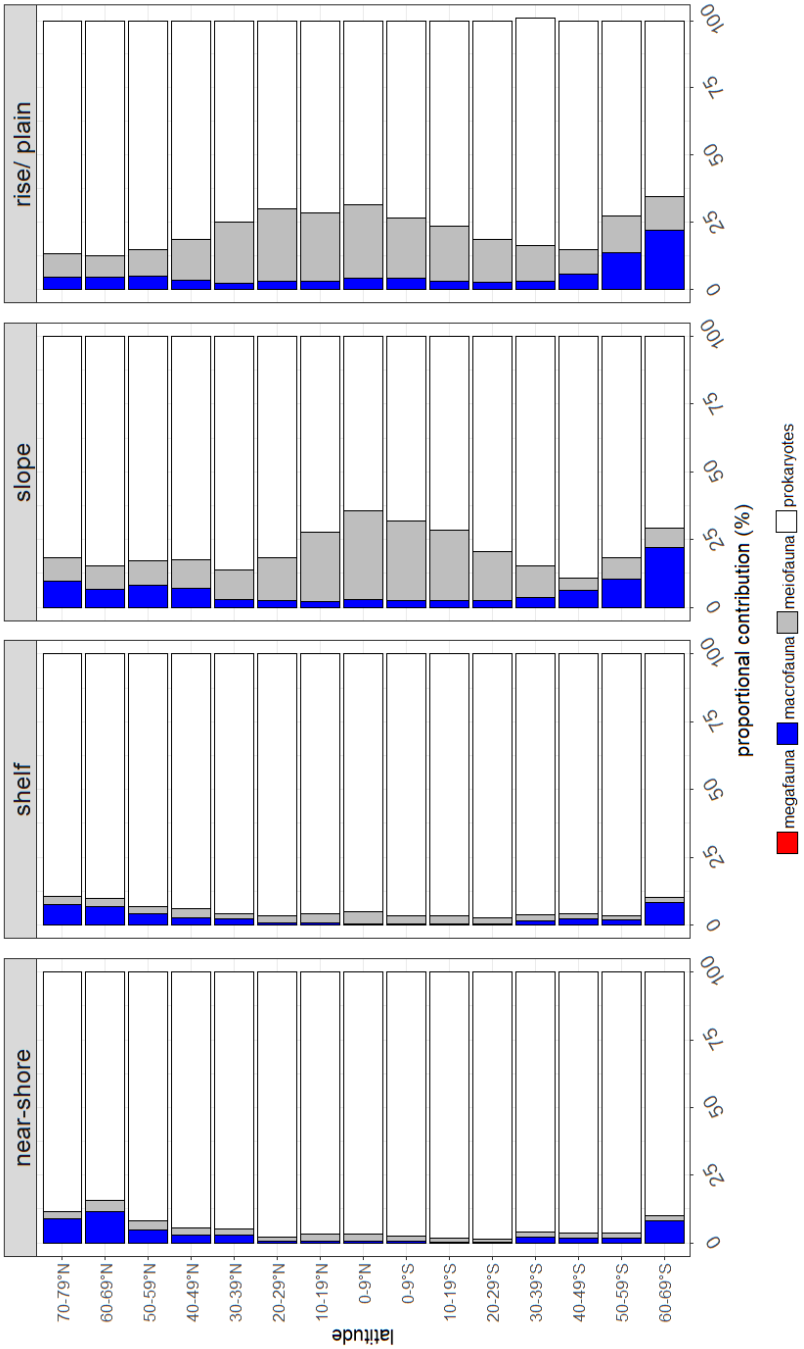

Figure 2-4. Proportional contribution (%) of benthic invertebrate megafauna, macrofauna, meiofauna, and prokaryotes to total sediment community oxygen consumption (SCOC) in near-shore areas (<50 m depth), at continental shelves (50–200 m depth), continental slopes (200–2,000 m depth), and continental rises/ abyssal plains (>2,000 m depth) along a latitudinal gradient. Benthic megafauna is not discernable in the figure because its proportional contribution is <1%.

2.4.3 Global secondary production of marine benthic invertebrates

Global benthic meiofaunal production was estimated to be 0.24 Pg C yr^{-1} (Table 2-5), which was 6.5 times higher than the global benthic macrofaunal production and 125 times higher than the global benthic megafaunal production. This meiofaunal production (mmol C m^{-2} d^{-1}) was depth-dependent (Figure 2-5), with the near-shore meiofaunal production ranging from 0.25 (70°–79°S latitude) to 2.17 (30°–39°N latitude), whereas the continental rise/ abyssal plain production of the same size class ranged from 6.62×10^{-2} (20°–29°S latitude) to 0.42 (60°–69°N latitude). In contrast, benthic macrofaunal production (Figure 2-5) changed mainly with latitude, i.e., the average production between 30°N and 30°S (ranges of low production for continental shelves: 29°N–19°S; ranges of low production for continental rises/ plains: 39°N–39°S) accounted for only 14–26% of the average production between 30° and 80°N and 30° and 80°S. Hence, benthic macrofauna appeared to be more productive in the temperate and polar areas than in the tropics and parts of the subtropics. Benthic invertebrate megafaunal production (mmol C m^{-2} d^{-1}; Figure 2-5) also decreased with depth, therefore megabenthos production in the deep sea (≥200 m) was estimated to be about one order of magnitude lower (1.09×10^{-3}) than the production in shallower waters <200 m (2.78×10^{-2}).

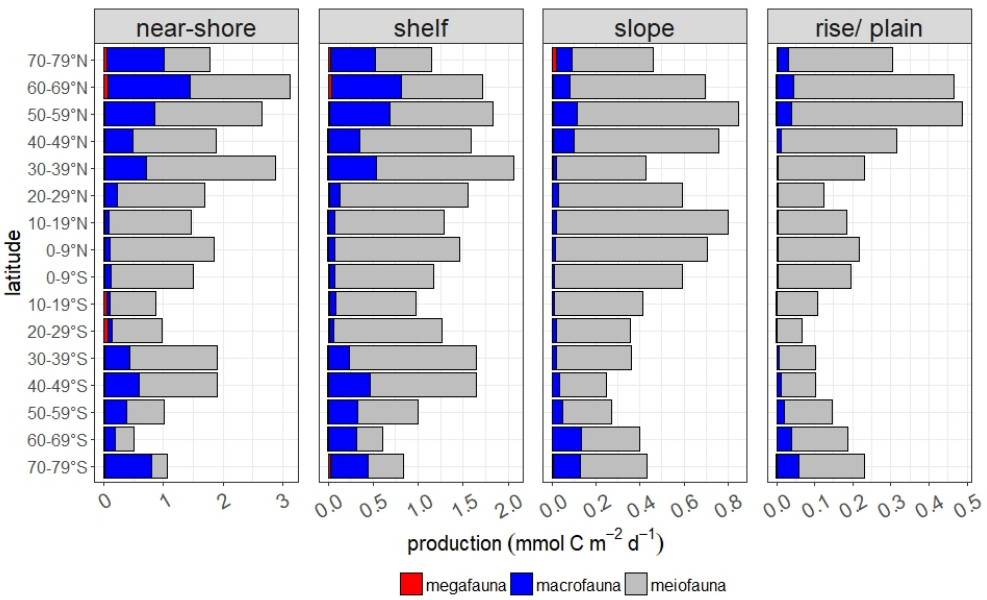

Figure 2-5. Production (mmol C m^{-2} d^{-1}) of benthic invertebrate megafauna, macrofauna, and meiofauna in near-shore areas (<50 m depth), at continental shelves (50–200 m depth), continental slopes (200–2,000 m depth), and continental rises/ abyssal plain (>2,000 m depth) along a latitudinal gradient. Note different x-axis scales.

Table 2-5. Production rates classified into size class and depth regime. Data are presented as: mean±SE (median); area integrated C flows are calculated as described in section 2.3.5. Area data are from Dunne, Sarmiento and Gnanadesikan (2007).

Benthos type	**(mmol C m^{-2} d^{-1})**	**(Pg C yr^{-1})**
Near shore (Area: 0.71×10^{13} m^2)		
Meiofauna	$1.20\pm2.49\times10^{-2}$ (1.03)	3.20×10^{-2}
Macrofauna	$0.62\pm1.96\times10^{-2}$ (0.54)	1.69×10^{-2}
Megafauna	$3.83\times10^{-2}\pm4.95\times10^{-3}$ (2.73×10^{-2})	8.49×10^{-4}
Total benthic fauna		4.97×10^{-2}
Continental shelf (Area: 0.95×10^{13} m^2)		
Meiofauna	$0.99\pm1.52\times10^{-2}$ (0.88)	3.65×10^{-2}
Macrofauna	$0.45\pm1.27\times10^{-2}$ (0.30)	1.23×10^{-2}
Megafauna	$2.18\times10^{-2}\pm3.80\times10^{-3}$ (1.08×10^{-2})	4.49×10^{-4}
Total benthic fauna		4.92×10^{-2}
Continental slope (Area: 2.24×10^{13} m^2)		
Meiofauna	$0.46\pm6.59\times10^{-3}$ (0.35)	3.45×10^{-2}
Macrofauna	$7.29\times10^{-2}\pm4.80\times10^{-3}$ (4.00×10^{-2})	3.92×10^{-3}
Megafauna	$5.23\times10^{-3}\pm1.53\times10^{-4}$ (1.60×10^{-3})	1.57×10^{-4}
Total benthic fauna		3.86×10^{-2}
Continental rise/ abyssal plain (Area: 31.1×10^{13} m^2)		
Meiofauna	$0.16\pm1.24\times10^{-3}$ (0.10)	0.14
Macrofauna	$1.18\times10^{-2}\pm1.71\times10^{-4}$ (3.03×10^{-3})	4.12×10^{-3}
Megafauna	$5.88\times10^{-4}\pm7.75\times10^{-6}$ (3.59×10^{-4})	4.89×10^{-4}
Total benthic fauna		0.14

2.4.4 Global ingestion by marine benthic invertebrates

Total C ingestion (Pg C yr^{-1}) of benthic meiofauna, macrofauna, and invertebrate megafauna was calculated to be 1.43, 0.11, and 2.63×10^{-3}, respectively (Table 2-6). On average, 1.31 mmol C m^{-2} d^{-1} was ingested by meiofauna, 0.16 mmol C m^{-2} d^{-1} was ingested by macrofauna, and 2.31×10^{-3} mmol C m^{-2} d^{-1} was ingested by megafauna. When broken down into depth regimes, the near-shore areas contributed 0.23 Pg C yr^{-1}, continental shelfs 0.20 Pg C yr^{-1}, continental slopes 0.24 Pg C yr^{-1}, and the continental rises/ abyssal plains 0.88 Pg C yr^{-1} to the total global ingestion rate (Table 2-6).

Table 2-6. Ingestion rates classified into size class and depth regime. Data are presented as: mean±SE (median); area integrated C flows are calculated as described in section 2.3.5. Area data are from Dunne, Sarmiento and Gnanadesikan (2007).

Benthos type	(mmol C m^{-2} d^{-1})	(Pg C yr^{-1})
Near-shore (Area: 0.71×10^{13} m^2)		
Meiofauna	6.55±0.20 (6.65)	0.21
Macrofauna	$1.05\pm6.10\times10^{-2}$ (0.60)	1.87×10^{-2}
Megafauna	$4.00\times10^{-2}\pm2.32\times10^{-3}$ (2.87×10^{-2})	8.91×10^{-4}
Total benthic fauna		0.23
Continental shelf (Area: 0.95×10^{13} m^2)		
Meiofauna	$4.39\pm9.28\times10^{-2}$ (4.12)	0.17
Macrofauna	$0.89\pm3.19\times10^{-2}$ (0.58)	2.42×10^{-2}
Megafauna	$2.30\times10^{-2}\pm8.85\times10^{-4}$ (1.47×10^{-2})	6.11×10^{-4}
Total benthic fauna		0.20
Continental slope (Area: 2.24×10^{13} m^2)		
Meiofauna	$2.87\pm5.51\times10^{-2}$ (2.08)	0.20
Macrofauna	$0.45\pm8.95\times10^{-3}$ (0.37)	3.65×10^{-2}
Megafauna	$4.63\times10^{-3}\pm9.20\times10^{-5}$ (3.56×10^{-3})	3.49×10^{-4}
Total benthic fauna		0.24
Continental rise/ abyssal plain (Area: 31.1×10^{13} m^2)		
Meiofauna	$0.98\pm9.20\times10^{-3}$ (0.62)	0.85
Macrofauna	$8.42\times10^{-2}\pm9.57\times10^{-4}$ (1.96×10^{-2})	2.67×10^{-2}
Megafauna	$8.96\times10^{-4}\pm8.04\times10^{-6}$ (5.74×10^{-4})	7.81×10^{-4}
Total benthic fauna		0.88

2.5 Discussion

To understand how changes in benthic faunal biomass will affect the global marine organic C cycle in the future, we need to improve our understanding of the role of benthos in the cycle under current climatic conditions. In the discussion, we evaluate spatial patterns in benthic respiration and secondary production. Afterwards we assess the role of benthos in the global organic C cycle and estimate differences in benthic faunal respiration and secondary production for the time period 2091 to 2100 compared to 2006 to 2015.

2.5.1 Model limitations

Despite the large datasets on which this study is based, there are several model limitations: The benthic biomass and abundance records used in the Random Forest model to calculate benthic C stocks were mainly collected along the coasts of industrialized countries (Wei *et al.*, 2010). In comparison, the dataset for the southern hemisphere, the tropics, and the open ocean was very limited. Hence, for large parts of the oceans, benthic biomasses were projected without adequate data to calibrate the model. Furthermore, the sediment community oxy-

gen consumption (SCOC) dataset used to project global benthic respiration included both, shipboard estimates and *in situ* measurements (Snelgrove *et al.*, 2018). A comparison between *in situ* chamber measurements and shipboard chemostatic systems with box cored or diver collected sediment from 20 m water depth on the Louisiana continental shelf (Gulf of Mexico) revealed significant differences in SCOC rates between the two approaches (Miller-Way *et al.*, 1994): Shipboard measurements overestimated SCOC rates five-times compared to *in situ* lander systems. A comparison of SCOC measured with a benthic flux chamber landers (total oxygen uptake, TOU), measured by oxygen microprofiling with a profiling lander (diffusive oxygen uptake, DOU), and shipboard measurements in the SE Atlantic between 399 to 4,986 m showed again significant differences in SCOC rates between shipboard and *in situ* measurements (Nøhr Glud *et al.*, 1994): Depth-integrated oxygen consumption rates based on *ex situ* DOU measurements were higher than those calculated for *in situ* DOU measurements and the ratio between *ex situ* DOU and *in situ* DOU measurements increased with increasing water depth (Nøhr Glud *et al.*, 1994). Hence, global SCOC projections are likely overestimates.

The database for P/B-ratios, assimilation efficiency, and biomass-specific faunal respiration rates lacked data for several depth ranges (for details see Table 2-1), so that data from shallower water depths were used. Biomass-specific faunal respiration rates are temperature dependent (e.g., Salomon and Buchholz, 2000) and correcting near-shore values with Q_{10} values might be a possibility to take depth-related temperature differences into account. However, this requires detailed knowledge about taxon-specific Q_{10} values, as e.g., two different isopod species have Q_{10} values that range from 3.2 to 4.2. Therefore, using biomass-specific faunal respiration rates from the continental slope for abyssal plains/ the continental rise might overestimate oxygen consumption rates of fauna in low latitudes and mid-latitudes, where the temperature decreases gradually below the permanent thermocline. Hence, the contribution of meiofauna to total benthic respiration around the equator might be an artifact, but the data for the polar regions should be less biased due to reduced temperature differences with depth. The effect of using the same assimilation efficiency values for all depth ranges cannot be assessed due to a lack of data. The secondary production, however, was likely overestimated at lager depth when values from shallower depth were used, as Table 2-1 indicates a decreasing trend in P/B-ratio with increasing water depth.

The overall model performance of the random forest model is reported in Wei *et al.* (2010) and Snelgrove *et al.* (2018). Briefly, the random forest models for biomasses had R^2-values between 0.78 and 0.81 for biomasses of bacteria, meiofauna, and macrofauna, and R^2-values of 0.63 to 0.68 for invertebrate megafauna biomass (Wei *et al.*, 2010). The random forest model for SCOC had an R^2-value of 0.80 (Snelgrove *et al.*, 2018).

2.5.2 Latitudinal trends in benthic respiration and secondary production

We observed a latitudinal trend in faunal respiration: Benthic meiofauna respiration governed deep-sea benthic faunal respiration in the subtropics and

tropics, whereas macrofauna respiration dominated deep-sea benthic faunal respiration in polar regions. Benthic secondary production and ingestion also showed a latitudinal pattern, with absolute and relative higher macrofauna production and ingestion at higher latitudes, although this trend was weaker.

The dominance of macrofauna in benthic faunal respiration at higher latitudes could be related to strong benthic-pelagic coupling (Smith, Mincks and Demaster, 2006), short food chains (Kędra *et al.*, 2015; E. J. Murphy *et al.*, 2016), and weaker microbial loops in the overlying waters at high latitudes (Kirchman, Morán and Ducklow, 2009). Especially around the West Antarctic Peninsula, rapid sinking of particulate organic matter and temperature-related reduced microbial remineralization leads to the development of "food banks" of labile phytodetritus in the sediment (Mincks, Smith and Demaster, 2005). Since larger size classes can exploit labile phytodetritus more efficiently than smaller size classes (Stratmann, Mevenkamp, *et al.*, 2018/ **Chapter 5**), macrofauna might outcompete meiofauna at the poles.

In contrast, at lower latitudes the "transfer efficiency" of organic matter to the deep sea is lower (Weber *et al.*, 2016) and more refractory detritus reaches the seafloor: In fact, decomposition experiments with particulate organic matter from deep Atlantic water showed that below 200 m, the POC could not be degraded (Menzel and Goering, 1966). Hence, if meiofauna can digest this refractory detritus and additionally exploit available food sources under oligotrophic conditions more efficiently than macrofauna (Albertelli *et al.*, 1999), meiofauna can outcompete macrofauna at lower latitude. However, to test this hypothesis, further pulse-chase experiments with very refractory material are required.

2.5.3 Role of faunal benthos in the marine carbon cycle

Organic C in the marine realm has an allochthonous and an autochtonous origin. Allochtonous material is produced in terrestrial ecosystems and exported to the oceans via rivers (0.45 Pg C yr^{-1}; del Giorgio and Duarte, 2002; Cole *et al.*, 2007) and via atmospheric deposition (0.48 to 3.00 Pg C yr^{-1}; del Giorgio and Duarte, 2002). Autochtonous material, in contrast, is produced by phototrophic, chemotrophic, and mixotrophic primary producers in the oceans. Autotrophic primary producers have a net primary production (NPP) of 48.2 to 53.3 Pg C yr^{-1} (Duarte and Cebrian, 1996; Duarte, 2017). Chemoautotrophs produce 0.77 Pg C yr^{-1} (38% in the euphotic zone, 14% in the water masses below the euphotic zone, and 45% in the sediment) (Middelburg, 2011), and mixotrophic Rhizaria produce additionally 7.81×10^{-3} Pg C yr^{-1} (Biard *et al.*, 2016).

Herbivores graze on 26.6 to 27.9 Pg C yr^{-1} of living primary producers (Duarte and Cebrian, 1996; Duarte, 2017) and are comprised mainly of herbivorous fish (Thayer *et al.*, 1984; Floeter *et al.*, 2005), birds (Nienhuis and Groenendijk, 1986; Nacken and Reise, 2000), benthic invertebrates such as sea urchins (Thayer *et al.*, 1984; Harrold and Reed, 1985), and zooplankton (Calbert and Landry, 2004). Between 16.9 and 19.0 Pg C yr^{-1} of NPP is degraded by decomposers that take up detrital dissolved and particulate C (Duarte and Cebrian, 1996; Duarte, 2017). Additionally, 0.29 to 2.03 Pg C yr^{-1} of NPP is ex-

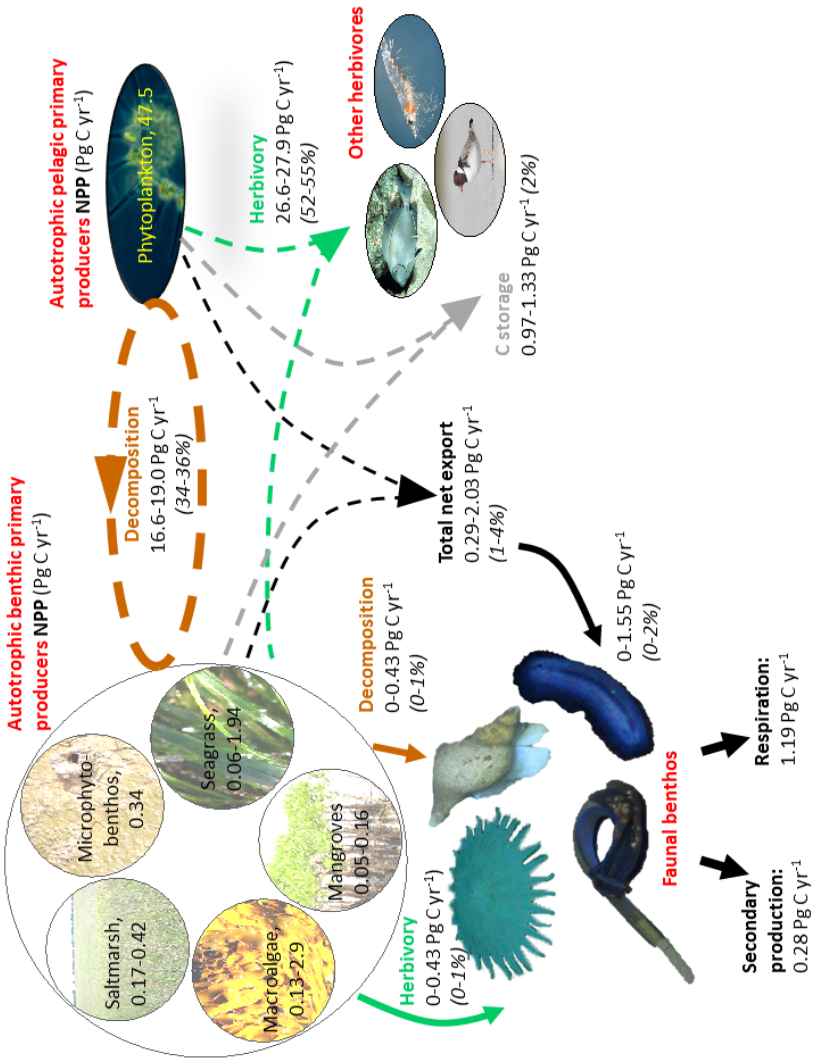

Figure 2-6. Benthos mediated C flows (Pg C yr^{-1}) in marine food webs. Values in parentheses show the percentage of net primary production (NPP) that is lost due to decomposition, net export (total net export includes the exported part of NPP, i.e., net export, that is consumed by faunal benthos), C storage, and herbivory. The numbers in the autotrophic primary producer compartments show the producer-specific net primary production. Note that the figure does not show all C flows (e.g., no fecal pellet production by other herbivores, no carrion).

ported beyond the euphotic zone and 0.97 to 1.33 Pg C yr^{-1} of NPP accumulates as nondecomposed detritus on the sediment surface and represents the stored C (Duarte and Cebrian, 1996; Duarte, 2017). Based on our depth-integrated faunal ingestion rates, a maximum of 0.43 Pg C yr^{-1} (0.23 Pg C yr^{-1} in the near shore-area and 0.20 Pg C yr^{-1} on the continental shelf) of the decomposed benthic net primary production can be ingested by benthic fauna (Figure 2-6). This implies that benthic fauna contribute up to 17% to the total C decomposition of benthic

autotrophic primary producers. Additionally, benthic fauna ingest 52% of the net export production (1.06 Pg C yr^{-1}) (Duarte and Cebrian, 1996; Duarte, 2017) and they account for 5% of the total marine herbivory that is dominated by zooplankton grazing on phytoplankton (95.0% of total marine herbivory) (Duarte and Cebrian, 1996; Duarte, 2017).

2.5.4 Carbon processing and climate change

The global export flux of POC to the seafloor is projected to decrease because of climate change (Jones *et al.*, 2014). Benthic faunal biomass that depends on this detritus flux as food source is therefore expected to be 5.2% lower in 2091 to 2100 compared to 2006 to 2015 (Jones *et al.*, 2014). As our respiration and secondary production estimates are based on biomass data, we can translate these biomass reductions to changes in process rates using median global biomass estimates for meiofauna (1.78 mmol C m^{-2}), macrofauna (2.50 mmol C m^{-2}), and megafauna (0.27 mmol C m^{-2}), and *r* and *P/B-ratios* data for continental slopes. A predicted reduction of meiofauna biomass by 5.87% (Jones *et al.*, 2014) will lead to 1.45 mmol C m^{-2} yr^{-1} less meiofaunal respiration and 2.51 mmol C m^{-2} yr^{-1} less meiofaunal secondary production. Reductions of 5.39×10^{-3} mmol C m^{-2} yr^{-1} in respiration and 1.19×10^{-1} mmol C m^{-2} yr^{-1} in secondary production will occur when macrofauna biomass is reduced by 8.38% (Jones *et al.*, 2014). A drop in megafauna biomass by 5.15% (Jones *et al.*, 2014) will result in 1.03×10^{-4} mmol C m^{-2} yr^{-1} less respiration and 7.51×10^{-2} mmol C m^{-2} yr^{-1} less secondary production. However, Jones *et al.* (2014) also discussed that the reduction in POC will cause a size-shift towards smaller organisms that have a higher respiration rate, which was not taken into account here. Hence, the actual reduction in benthic respiration might be smaller if the density of meiofauna increases while macrofauna densities decrease.

2.6 Supplement

Supplementary list 2-1. List of environmental predictors used to project benthic biomasses and sediment community oxygen consumption (SCOC). Details can be found in Snelgrove *et al.* (2018) and Wei *et al.* (2010).

Environmental predictors	Variable
Benthic biomass	
Primary production	Chlorophyll-a concentration, sea surface temperature, photosynthetically available radiation, particulate backscatter, mixed layer depth, phytoplankton growth rate, C concentration, Chlorophyll based net primary production.
Water colum	Integrated C to 500 m above seafloor, integrated N to 500 m above seafloor, integrated detrtical C to 500 m above seafloor, integrated detrital N to 500 m above seafloor, integrated phytoplankton to 500 m above seafloor, integrated zooplankton to 500 m above seafllor, detritical C flux at 500 m above seafloor, detrital N flux at 500 m above seafloor.
Bottom water	Temperature, salinity, oxygen concentration, nitrate concentration, phosphate concentration, silicate concentration.
Water depth	Water depth.
SCOC	
Terrain	Slope of terrain, terrain roughness.
Bottom water	Temperature, salinity, oxygen concentration, silicate concentration, phosphate concentration, nitrate concentration.
POC export	Chlorophyll-a concentration, Chlorophyll based net primary production, export depth, euphotic depth.
Seafloor Abundances and biomasses	Prokaryotic abundance, prokaryotic biomass, meiofauna abundance, meiofauna biomass, macrofauna abundance, macrofauna biomass, megafauna abundance, megafauna biomass.
Sediment community oxygen consumption	Sediment community oxygen consumption.

Supplementary list 2-2. List of publications from which *biomass-specific faunal respiration* r were extracted for '2.3.3 Depth- and location-dependent parameters'.
Abbreviations used: CSh = continental shelf (50–200 m), CSl = continental slope (200–2,000 m), NS = near-shore (0–50 m), CR/ AP = continental rise/ abyssal plain (>2,000 m).

Depth	Reference
Meiobenthos	
NS	*NE Atlantic:* Geslin *et al.* (2011), Hannah, Rogerson and Laybourn-Parry (1994), Lasker, Wells and McIntyre (1970); *NE Atlantic/ Dutch Delta and Schelde area:* Braeckman *et al.* (2013), Moens, Verbeeck and Vincx (1999), Moodley *et al.* (2008); *NW Atlantic:* Teal and Wieser (1966), Warwick and Price (1979), Wieser and Kanwisher (1960), Wieser and Kanwisher (1961), Wieser *et al.* (1974).
CSl	*NE Atlantic:* Geslin *et al.* (2011); *NW Pacific:* Nomaki *et al.* (2007); Shirayama (1992).
Macrobenthos	
NS	*NE Atlantic:* Lasserre (1970); *NE Atlantic/ North Sea:* Asmus (1984); *NW Atlantic:* Coull and Vernberg (1970); *Baltic Sea:* Clausen and Riisgård (1996), Nielsen *et al.* (1995); *Central Pacific:* Wilson *et al.* (2013).
CSl	*NE Atlantic:* van Oevelen *et al.* (2009); *Indian Ocean/ Arabian Sea:* Treude *et al.* (2002); *NW Pacific:* Nomaki *et al.* (2007); *SW Pacific:* Sommer *et al.* (2010).
Megabenthos	
NS	*NE Atlantic:* Ansell (1973), Astall and Jones (1991); *NE Atlantic/ North Sea:* Asmus (1984), Fox (1936); *NE Atlantic/ Dutch Delta and Schelde area:* Koopmans, Martens and Wijffels (2010); *NW Atlantic:* Brown and Shick (1979); *W Atlantic:* Warnock and Liddell (1985); *Baltic Sea:* Fox (1936), Nielsen *et al.* (1995), Petersen, Schou and Thor (1995); *Central Pacific:* Wilson *et al.* (2013); *NE Pacific:* Webster (1975); *NW Pacific:* Childress *et al.* (1990), Takemae, Nakaya and Motokawa (2009), Yu, Qi, *et al.* (2013); *SW Pacific:* Johnson (1973), Maxwell, Gardner and Heath (2009), Pentreath (1971); *Southern Ocean:* Belman and Giese (1974), Magniez and Féral (1988).
CSh	*NE Atlantic/ North Sea:* Fox (1936); *Baltic Sea:* Fox (1936); *NE Pacific:* Johnson (1976), Webster (1975).

CSl	*NE Atlantic:* van Oevelen *et al.* (2009); *W Atlantic:* Baumiller and Labarbera (1989); *Central Pacific:* Wilson *et al.* (2013); *NE Pacific:* Smith (1983); *NW Pacific:* Childress *et al.* (1990).
CR/ AP	*NE Atlantic:* Hughes (2010), Hughes *et al.* (2011); *Indian Ocean/ Arabian Sea:* Treude *et al.* (2002); *SE Pacific:* Brown *et al.* (2018).

Supplementary list 2-3. List of publications from which production/biomass (*P/B*)-*ratio* were extracted for '2.3.3 Depth- and location-dependent parameters'.
Abbreviations used: CSh = continental shelf (50–200 m), CSl = continental slope (200–2,000 m), NS = near-shore (0–50 m).

Depth	Reference
Meiobenthos	
NS	*NE Atlantic/ North Sea:* Fleeger and Palmer (1982), Herman, Heip and Vranken (1983), Vranken and Heip (1986); *Mediterranean Sea:* Ceccherelli and Rossi (1984).
Macrobenthos	
NS	*NE Atlantic:* Bachelet (1982), Bachelet and Yacine-Kassab (1987), Norderhaug and Christie (2011), Oyenekan (1986), Oyenekan (1987), Oyenekan (1988), Pérez, Marquiegui and Belzunce (2007), Warwick, George and Davies (1978), Warwick and Price (1975), Wildish and Peer (1981); *NE Atlantic/ Dutch Delta and Schelde area:* Mees, Abdulkerim and Hamerlynck (1994), Wolff and de Wolf (1977); *NE Atlantic/ North Sea:* Asmus (1987), Cunha, Moreira and Sorbe (2000), George and Warwick (1985), Gillet and Torresani (2003), Klein, Rachor and Gerlach (1975), Rachor *et al.* (1982), Rees (1983), Sheader (1977); *NW Atlantic:* Burke and Mann (2003), Feller (1982), Fredette *et al.* (1990), Howe, Maurer and Leathem (1988), Otegui, Blankensteyn and Pagliosa (2012), Price and Warwick (1980), San Vincente and Sorbe (1995), Sarda, Valiela and Foreman (1995), Sprung (1993), Subida, Cunha and Moreira (2005); *SW Atlantic:* Caetano *et al.* (2006), Caetano, Veloso and Cardoso (2003), Cardoso and Veloso (1996), Cardoso and Veloso (2003), de Souza and Borzone (2007), Petracco *et al.* (2012), Petracco *et al.* (2014), Petracco, Veloso and Cardoso (2003), Veloso, Cardoso and Petracco (2003); *W Atlantic:* Franz and Tanacredi (1992); *Baltic Sea:* Birklund (1977), Kristensen (1984), Loo and Rosenberg (1996), Möller and Rosenberg (1982), Sarvala and Uitto (1991); *Indian Ocean:* Ali and Salman (1987), Laudien, Brey and Arntz (2003), Melake (1993); *Mediterranean Sea:* Ambrogi (1990), Cartes *et al.* (2009), Martín and Grémare (1997), Daas *et al.* (2011), Fraschetti *et al.* (1997), Giangrande and Fraschetti (1993); *N Pacific:* Highsmith and Coyle (1990); *NE Pacific:* Arntz *et al.* (1987), Vetter (1996); *NW Pacific:* Sudo and Azeta (1996), Yu and Suh (2002); *SW Pacific:* Fenton (1996); *W Pacific:* Berry and bin Othman (1983); *Southern Ocean:* Brey and Clarke (1993), Kalejta (1992), van Senus and McLachlan (1986).

CSh	*NE Atlantic:* San Vincente and Sorbe (1995); *NE Atlantic/ North Sea:* Buchanan and Warwick (1974); *NW Atlantic:* Wildish (1984), Collie (1985); *Baltic Sea:* Josefson (1982); *Mediterranean Sea:* Cartes *et al.* (2009), Cartes and Sorbe (1999), Cartes, Mamouridis and Fanelli (2011), Ligas *et al.* (2009).
CSl	*Mediterranean Sea:* Cartes, Elizalde and Sorbe (2000), Josefson (1982); *Southern Ocean:* Brey and Clarke (1993).
Megabenthos	
NS	*NE Atlantic:* Gillet and Torresani (2003), Norderhaug and Christie (2011), Sprung (1993), Warwick, George and Davies (1978); *NE Atlantic/ North Sea:* Chambers and Milne (1975), Heip and Herman (1979), Kristensen (1984); *NW Atlantic:* Fredette *et al.* (1990), Howe, Maurer and Leathem (1988); *SW Atlantic:* Koch and Wolff (2002), Lizarralde and Cazzaniga (2009), Turra *et al.* (2015); *Baltic Sea:* Loo and Rosenberg (1996); *Mediterranean Sea:* Mistri and Ceccherelli (1994); *N Pacific:* Highsmith and Coyle (1990); *SE Pacific:* Clasing *et al.* (1994); *Southern Ocean:* Brey and Clarke (1993), Brey, Pearse, *et al.* (1995), Mclachlan (1979).
CSl	*Mediterranean Sea:* Cartes, Mamouridis and Fanelli (2011), Cartes, Elizalde and Sorbe (2001), Cartes and Sorbe (1999); *SE Pacific:* Baumgarten *et al.* (2014); *Southern Ocean:* Brey and Clarke (1993), Brey, Pearse, *et al.* (1995); Brey *et al.* (1998), Gorny *et al.* (1993).

Supplementary list 2-4. List of publications from which assimilation efficiency (*AE*) data were extracted for '2.3.3 Depth- and location-dependent parameters'.
Abbreviation used: NS = near-shore (0–50 m).

Depth	Reference
Meiobenthos	
NS	*NW Atlantic:* Navarro and Thompson (1996); *Lab experiment:* Herman and Vranken (1988).
Macrobenthos	
NS	*NE Atlantic/ Dutch Delta and Schelde area:* Smaal and Vonck (1997); *NE Atlantic/ North Sea:* Grahame (1973), Jordana *et al.* (2001); *NE Pacific:* Johnson (1976); *SE Pacific:* Velasco and Navarro (2003).
Megabenthos	
NS	*NE Atlantic:* Labarta, Fernández-Reiríz and Babarro (1997), Pérez Camacho, Labarta and Navarro (2000); *NW Atlantic:* Navarro and Thompson (1996), Nelson, MacDonald and Robinson (2012), Sejr *et al.* (2004); *W Atlantic:* Kreeger and Newell (2001); *NE Pacific:* Arifin and Bendell-Young (1997); *NW Pacific:* Han, Lee and Wang (2008), Yu, Hu, *et al.* (2013), Zhou *et al.* (2006); *W Pacific:* Enríquez-Ocaña *et al.* (2012), Nieves-Soto *et al.* (2013), Peña-Messina *et al.* (2009); *SE Pacific:* Velasco and Navarro (2003); *SW Pacific:* Lee (1997), Yukihira, Lucas and Klumpp (2000), Ren, Ross and Hayden (2006).

Chapter 3 : Polymetallic nodules are essential for the food-web integrity of Pacific abyssal plains

3. Polymetallic nodules are essential for the food-web integrity of Pacific abyssal plains

Tanja Stratmann, David Amptmeijer, Daniel Kersken, Karline Soetaert, and Dick van Oevelen;
To be submitted.

3.1 Abstract

The abyssal seafloor is often covered with polymetallic nodules that provide hard substrate for sessile organisms. Possible future extraction of these mineral-rich nodules will likely modify the trophic and non-trophic interactions within the abyssal food web, but the importance of nodules and their associated sessile fauna in supporting this food web remains unclear. Here, we present highly-resolved interaction webs with 208 (Peru Basin, PB, SE Pacific) and 478 (Clarion-Clipperton Fracture Zone, CCZ, central Pacific) network compartments based on an extensive literature research. Compartments were connected with 3,131 and 9,386 (CCZ) trophic and non-trophic (e.g., substrate-providing nodules) links. The webs were used to assess how nodule absence could modify the number of network compartments, number of links, link density, and web connectance. We show that nodule absence in the Peru Basin would reduce the number of food-web compartments and links by 26% and 37%, respectively. Absence of nodules in the CCZ would result in a loss of 20% of the compartments and 20% of the network links. Subsequent analysis identified stalked sponges, living attached to the nodules, as key structural species that support a high diversity of commensal fauna. We conclude that nodules are critical for food-web integrity and that their absence will likely lead to a loss in local benthic biodiversity.

3.2 Introduction

In his famous book "On the Origin of Species", Charles Darwin described "how plants and animals […] are bound together by a web of complex relations" (Darwin, 1859). He speculated that, as bumblebees were important pollinators of common red clover (*Trifolium pretense*) and heartsease (*Viola tricolor*), the extinction of bumblebees would result in the disappearance of these flowers. Moreover, the density of bumblebees was controlled by field-mice, which destroy bee nests and combs, while density of mice was dependent on the presence of cats (Darwin, 1859). Through his conclusion that it is quite credible that the presence of large numbers of cats might determine, through intervention of mice and of bees, the frequency of certain flowers in a district, Darwin realized how non-trophic interactions, i.e., the pollination activity of bumblebees and the destructive activity of mice, and trophic interactions are intimately intertwined in real-life food webs. Non-trophic, indirect, and facilitative interactions can even contribute more links to the food web than trophic interactions themselves (Ohgushi, 2008).

The high diversity of non-trophic interactions, including mutualism, commensalism, antagonism, neutralism, amensalism, and competition (Kéfi *et al.*, 2012), and their importance for food webs is increasingly being recognized in the terrestrial and marine realm (e.g., Kéfi *et al.*, 2012; Baiser, Whitaker and Ellison, 2013; Sanders *et al.*, 2014; van der Zee *et al.*, 2016). In temperate fringing saltmarshes and tropical seagrass meadows, non-trophic effects via the habitat-modifiers cordgrass or seagrass affected 11% of all species (van der Zee *et al.*, 2016), whereas an additional 24% of all species in the saltmarsh and 64% of all species in the seagrass meadows were dependent on the joint impacts of primary and secondary habitat modifiers, i.e., mussels and crabs (van der Zee *et al.*, 2016).

Studies of abyssal food webs at ocean depths between 3,000 and 6,000 m so far tend to focus on trophic interactions (e.g., Iken *et al.*, 2001; Aberle and Witte, 2003; Sweetman and Witte, 2008; van Oevelen, Soetaert and Heip, 2012; Dunlop *et al.*, 2016), because abyssal plains are strongly food-limited (Smith *et al.*, 2008). In addition, abyssal plains lack extensive reef formation by ecosystem engineers, such as cold-water corals (Roberts, Wheeler and Freiwald, 2006). The upper centimeters to decimeters of sediment are also well-oxygenated, reducing the importance of habitat modification by sediment ventilating or bioturbating fauna (Meysman, Middelburg and Heip, 2006).

Some parts of the abyssal seafloor are, however, covered by polymetallic nodules, i.e., slowly growing (10s mm My^{-1}; Hein, 2016) precipitates of predominantly manganese oxides and iron oxy-hydroxides that contain metals such as nickel, cobalt, and copper (Hein and Koschinsky, 2014). Nodules lay partially buried on the sediment surface with mean abundances (based on nodule wet weight) of 4.5 kg m^{-2} (central Indian Ocean Basin) to 15 kg m^{-2} (Clarion-Clipperton Fracture Zone, CCZ, NE Pacific) (Kuhn *et al.*, 2017) and provide the rare commodity of hard substrate in the abyss that is used by both sessile fauna, e.g., Porifera, Antipatharia, Alcyonacea, or Ascidiacea, and mobile fauna, e.g., Cephalopoda (Amon *et al.*, 2016; Purser *et al.*, 2016; Vanreusel *et al.*, 2016). In this

way, nodules add an extra network of non-trophic interactions among sessile organisms and their associated fauna to the food web.

Abyssal plains have so far been relatively untouched by anthropogenic impacts due to their extreme depths and distance from continents (Ramírez-Llodrà *et al.*, 2011), but this may change in the near future. Deep-sea mining is a potential future commercial activity that targets the nodules for their metal content (Hein and Koschinsky, 2014). Deep-sea mining will remove nodules from the seafloor and thereby modify the supporting role of nodules and associated fauna for the abyssal food web. It is therefore of imminent importance to understand how nodules support trophic and non-trophic interactions in the abyss.

Here, we develop high-resolution trophic and non-trophic interaction webs for two nodule-rich areas in the Pacific Ocean, i.e., the Peru Basin (PB) in the SE Pacific and the CCZ, based on an extensive literature research, supplemented with the analysis of high-resolution seafloor images. An important element of these webs is that they include both dependencies between taxa and between taxa *and* polymetallic nodules. Potential deep-sea mining impacts are subsequently assessed by knock-down effects through the food web following the removal of non-trophic links among nodules and fauna.

3.3 Material and methods

3.3.1 Study sites

The PB is located in the southern Pacific (5°S to 24°S) and extends from the Atacama Trench west of Peru westwards (to 110°W) into the Pacific (Klein, 1993; Bharatdwaj, 2006). The water depth ranges from 3,900 to 4,300 m (Glasby, 2006) and sedimentation rates vary between 0.4 and 2.0 cm kyr^{-1} (Haeckel *et al.*, 2001). Surface sediments consist of silty clays or clayey silts[1] (Grupe, Becker and Oebius, 2001) and have an organic carbon (C) content of 0.5 to 1.0 wt%. The oxygen concentration decreases from 132 µmol L^{-1} at the sediment-water interphase to zero at 6 to 15 cm sediment depth (Haeckel *et al.*, 2001). Mean nodule abundance in the PB is >10 kg m^{-2} (Glasby, 2006) and the mean nodule diameter is 7.8 cm (Schoening, Jones and Greinert, 2017). Industrial polymetallic nodule extraction, however, is not anticipated in this area.

The CCZ (0°N, 160°W to 23.5°N, 115°W; International Seabed Authority, 2011) is bound by the Clarion Fracture Zone in the North and the Clipperton Fracture Zone in the South. Water depth ranges from 3,900 m in the East (Amon *et al.*, 2016) to 5,300 m in the West (Jung *et al.*, 1998) with a mean water depth of 4,794 m (Wedding *et al.*, 2013). The CCZ is part of the "mesotrophic" abyss[2] (Hannides and Smith, 2003) and experiences a gradient in particulate organic carbon (POC) input from north (1.3 mg C_{org} m^{-2} d^{-1}) to south (1.8 mg C_{org} m^{-2} d^{-1}) and west (1.6 mg C_{org} m^{-2} d^{-1}) to east (1.8 mg C_{org} m^{-2} d^{-1})

[1] Particle size according to Udden-Wentworth scale: 4–62.5 µm, silt; <4 µm, clay (Allaby, 2008a).

[2] The "mesotrophic abyss" is characterized by a particulate organic carbon flux between 0.5 and 1.6 g C m^{-2} yr^{-1} and ranges from 5°N to 15°N (Hannides and Smith, 2003).

(Vanreusel *et al.*, 2016). The sediment is largely composed of siliceous, silty clay (International Seabed Authority, 2010). Nodules occur with a mean abundance of 15 kg m^{-2} (Kuhn *et al.*, 2017) and a mean diameter of 3.6 cm (Schoening, Jones and Greinert, 2017). Because of this high nodule density and high metal contents, the CCZ is an important area for future mining operations and (until March 2018) the International Seabed Authority (ISA) has granted 16 15-yr contracts for the exploration of polymetallic nodules in the CCZ.

3.3.2 Data compilation

Detailed food webs were developed including the size classes meio-, macro-, and megabenthos at the highest taxonomic resolution possible and explicitly taking into account whether each compartment lives in the sediment, associated with other fauna, or on polymetallic nodules. For this purpose, a systematic literature review was conducted to identify all fauna/ higher taxa (if possible on genus level) of the study areas following the PRISMA guidelines for systematic reviews and meta-analyses (Moher *et al.*, 2009). The key words "polymetallic nodule", "manganese nodule fauna*", "manganese nodule", and "Clarion-Clipperton Fracture Zone" identified 598 articles in the database "Web of Science". Additional 106 records were identified through other sources, including DISCOL publications (http://www.drbluhm.de/indexe.html) and the database "Google Scholar". After duplicates were removed, title and abstract of 685 records were screened for relevancy, after which 487 records were excluded. Full text was unavailable for another three records that were therefore also left out. Hence, a total of 195 full-text records were assessed for eligibility. Another 134 full-text records were subsequently excluded as they lacked information about the substrate on which the organisms were found. Full-text records were also omitted when taxonomic resolution was too low or if they provided duplicate data. In the end, 61 publications were used to develop the trophic interaction matrix. All references can be found in Supplementary table 3-1 (PB) and Supplementary table 3-2 (CCZ).

The extensive literature survey was supplemented by novel data obtained from high-resolution seafloor images. We scanned 1,544 seafloor images that were taken with the remotely operated vehicle "ROV KIEL 6000" (Geomar, Kiel, Germany) in the DISCOL experimental area (PB) during R/V *Sonne* cruise SO242-2 (Boetius, 2015) and during R/V *Sonne* cruise SO239 to the CCZ (Martínez Arbizu and Haeckel, 2015) and identified Porifera and commensal fauna on 253 pictures.

The lowest recorded taxonomic ranks of all metazoans and protozoans that were identified in the qualitative synthesis and picture analysis were compiled in a database. We also noted whether organisms were reported or observed attached to a polymetallic nodule, sitting on or living in sediment, or were associated with an organism attached to a nodule. The latter case was interpreted as a commensal relation, when only one of two interacting species benefitted and the other remained unaffected. For each taxon, the taxonomic ranks phylum, class, order, family, and genus were determined using the database "World Register of

Marine Species: WoRMS" (Horton *et al.*, 2018). Recorded specimens were furthermore classified as meiobenthos (>32 µm; Ahnert and Schriever, 2001; Radziejewska, 2002), macrobenthos (>250 µm/ >500 µm; Borowski and Thiel, 1998; Borowski, 2001), and megabenthos (>1 cm) based on information from original publications or based on information published in WoRMS (Horton *et al.*, 2018).

As findings in published literature were reported in different taxonomic resolution, we selected the lowest common taxonomic resolution of each phyla as food-web compartment. For instance, all data entries of meiobenthos contained information about the phylum, class, order, and family. Hence, family was chosen as lowest taxonomic rank for meiobenthos. Depending on geographical location and size class, taxonomic resolution differed and a list with the taxonomic resolution of each specific taxon is reported in Supplementary tables 3-1 and 3-2.

3.3.3 Trophic interaction matrix

Feeding preferences/ prey types of each specimen in the dataset were identified by inquiries of published literature and the databases "WoRMS" (Horton *et al.*, 2018) and "FishBase" (Froese and Pauly, 2017) (Supplementary table 3-3). One binary trophic interaction matrix per location was developed by connecting all food-web compartments via all reported trophic links to its prey/ food source. Hence, when a specific fish species preferably feeds on crustaceans, this specific fish species compartment was connected via trophic links to all compartments in the food web that include crustaceans. However, it was assumed that predatory megabenthos would not feed on meiobenthos unless they are known to catch their prey by digging into the seafloor.

Particulate organic matter (POM) suspended in the water column (wPOM), sedimentary POM (sPOM), bacteria, dissolved organic carbon (DOC), carrion, and protists were reported in literature as food sources for abyssal food webs and were consequently included.

3.3.4 Non-trophic interaction matrix

The binary non-trophic interaction matrix contained all non-trophic links between food-web compartments and the additional compartment "polymetallic nodules". Commensal relations among faunal compartments that were reported in the database (section '3.3.2 Data compilation') were implemented in the matrix as present (= 1) or absent (= 0). All faunal compartments, for which the literature or the image analysis indicated that they would use nodules as substrate, were linked to the nodule compartment. Whenever the taxon of a faunal compartment was observed both attached to a nodule and living on/ in the sediment or associated with more than one faunal compartment, the present (= 1) non-trophic relation was defined as "facultative". In contrast, when the taxon occurred exclusively attached to nodules or only in association with a specific faunal compartment, the present (= 1) non-trophic relation was defined as "obligatory".

3.3.5 Food-web indices

The trophic interaction matrix was used to calculate the well-established food-web indices: "number of network compartments" S, "number of network links" L, "link density" D ($D = \frac{L}{S}$), and "connectance" C ($C = \frac{L}{S^2}$), i.e., the fraction of realized links compared to all possible links (Pimm, Lawton and Cohen, 1991).

3.3.6 Assessment of the absence of nodules and absence of specific faunal compartments

The effect of polymetallic nodules on the food-web structure was investigated by removing the nodule compartment from the non-trophic interaction matrix and assessing the resulting knock-down on other compartments (i.e., the secondary extinction of other compartments because of the loss of the nodule compartment). Hence, all compartments directly depending on the nodules were removed first. In a subsequent iteration, all compartments depending on a removed compartment through a non-trophic or exclusively trophic (i.e., when preying only on the removed compartment) interaction were removed, and so on. After all lost compartments were identified, the previously collected information about the type of non-trophic interaction (facultative vs. obligatory) was used to identify whether the loss was a result of facultative or obligatory dependence.

To compare the loss of non-trophic links through nodule absence against the removal of trophic links, a comparable knock-down analysis of the "most connected taxa" and the "taxa with most non-trophic interactions" was also carried out. The most connected taxon is defined as the food-web compartment with most trophic links, *sensu* van der Zee *et al.* (2016). The "highest impact taxon", i.e., the faunal compartment whose removal has the largest impact on food-web properties, was identified by removing each faunal compartment individually and calculating the food-web properties. The compartment whose individual removal resulted in the largest absolute difference in food-web properties between the default food-web and the modified food-web was defined as the "highest impact taxon". When more than one food-web compartment was identified as most connected taxon, the food-web indices were summarized as mean±SD.

3.4 Results

3.4.1 Peru Basin

The PB interaction web contained trophic interactions between 202 faunal compartments (+ 5 food source compartments, + 1 nodule compartment), of which 52% belonged to meiobenthos, 17% to macrobenthos, and 31% to megabenthos (Figure 3-1). Most faunal compartments were detritivores (45%), filter feeders (19%), and predators (13%) (Figure 3-2). The non-trophic interaction web contained 116 interactions among compartments in the food web. The most connected taxon was the meiobenthic predator *Chromaspirina* sp. (Nematoda) with 106 trophic links and the taxon with most non-trophic interactions was the megabenthic compartment Isopoda with 9 non-trophic links.

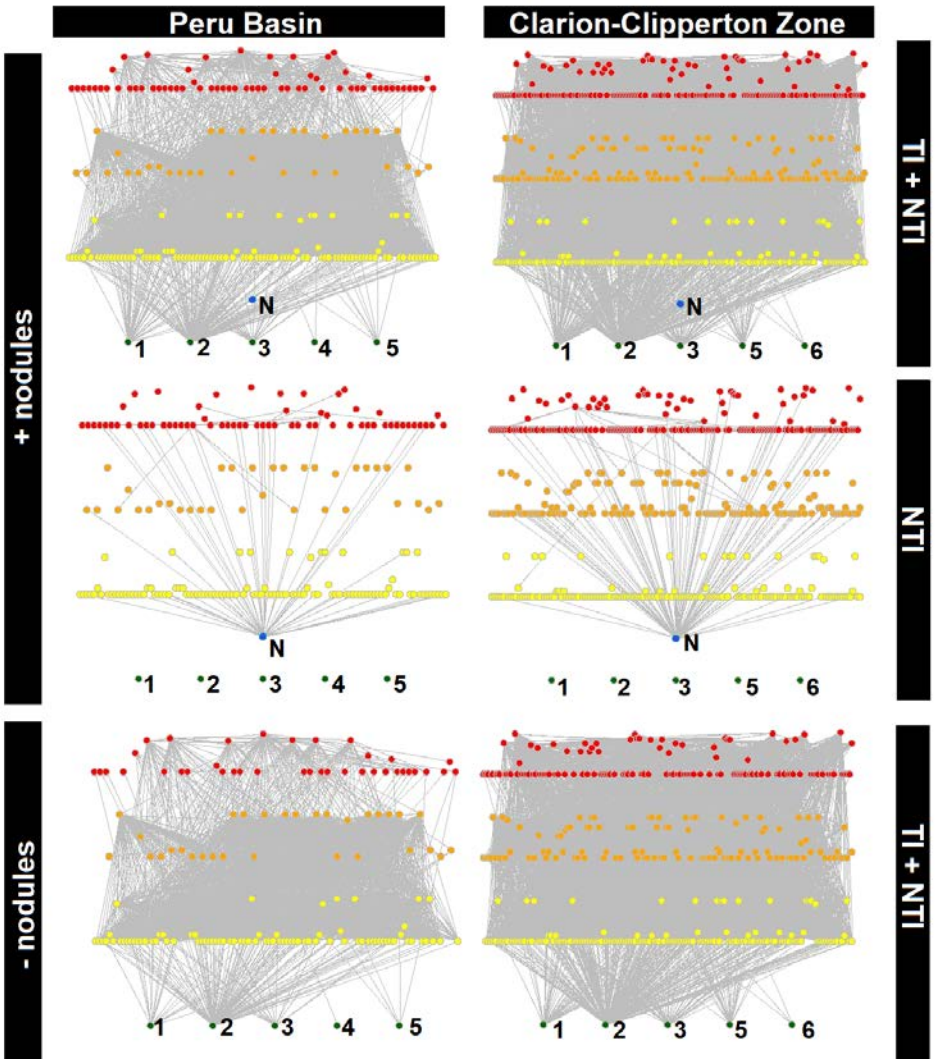

Figure 3-1. Interaction webs with trophic and non-trophic interactions for the Peru Basin (left panels) and the Clarion-Clipperton Fracture Zone (right panel) in the presence (+ nodules) and absence of polymetallic nodules (- nodules).
Each node represents one food-web compartment in the food webs and the color of nodes corresponds to the size class (yellow = meiobenthos, orange = macrobenthos, red = megabenthos) and to an external food source (green) or polymetallic nodule (blue; label "N"). The higher the position of a specific node is in comparison to other nodes of the same color, i.e., size class, the higher is the trophic level of this specific compartment. The food sources are 1) suspended particulate organic matter, 2) sedimentary POM, 3) bacteria, 4) dissolved organic carbon (DOC), 5) carrion, and 6) protists.
Abbreviations used: TI = trophic interactions, NTI = non-trophic interactions.

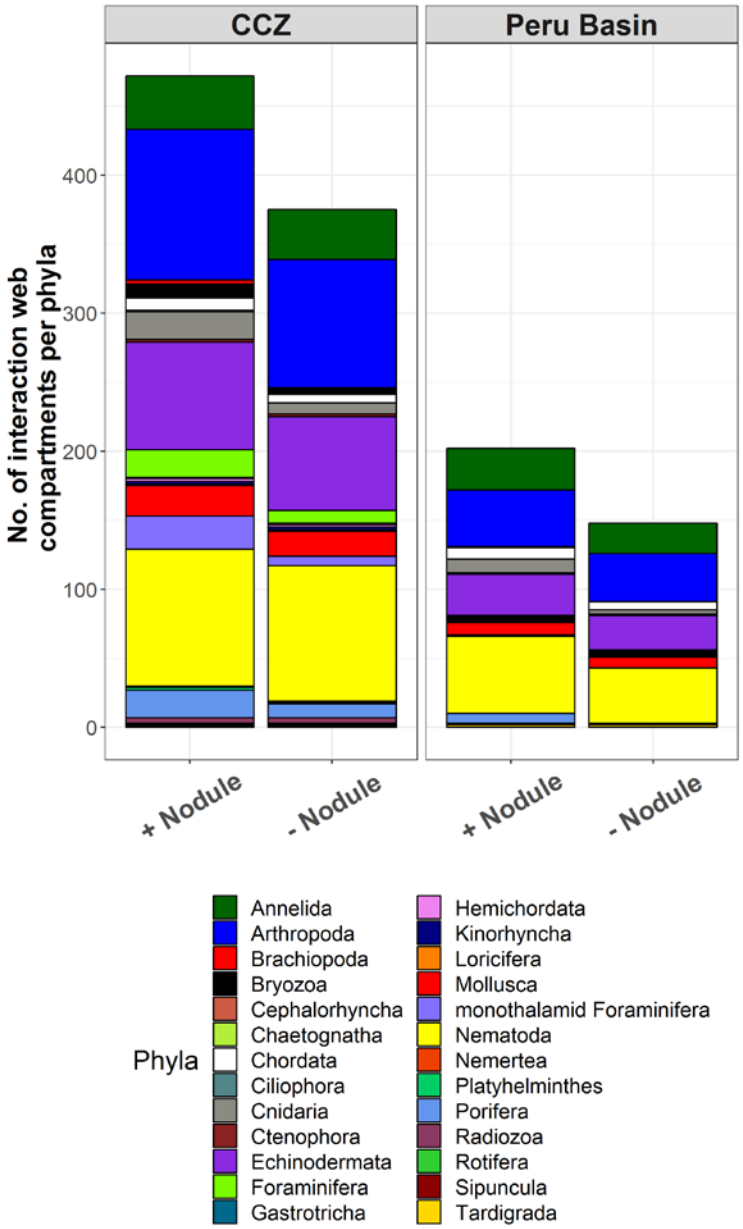

Figure 3-2. Number of interaction web compartments per feeding type that were part of the non-trophic and trophic interaction matrices for the Peru Basin and the Clarion-Clipperton Fracture Zone (CCZ) site.

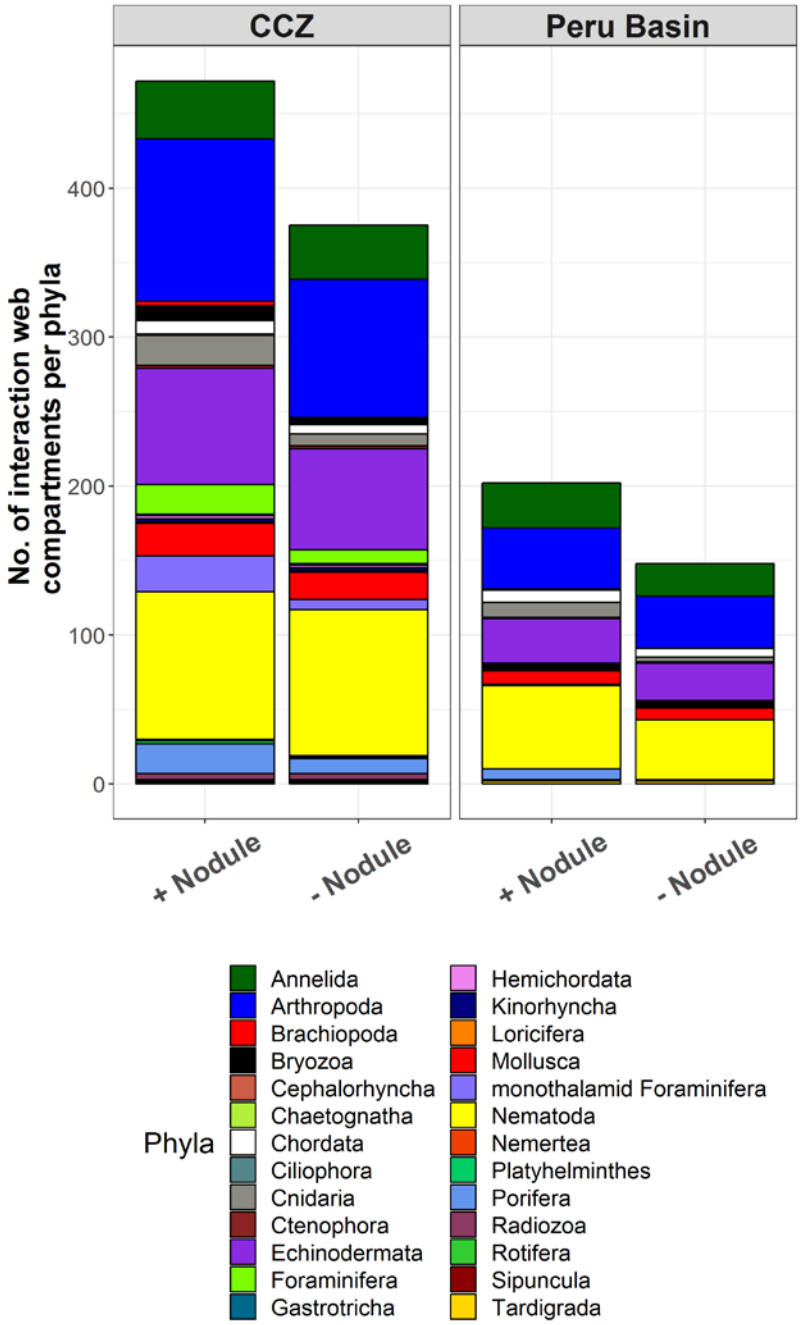

Figure 3-3. Number of interaction web compartments per phyla that were part of the non-trophic and trophic interaction matrices for the Peru Basin and the Clarion-Clipperton Fracture Zone (CCZ) site.

The absence of polymetallic nodules resulted in the loss of 26% of all faunal compartments (Figure 3-1), of which 45% belonged to meiobenthos, 7% to macrobenthos, and 48% to megabenthos. When polymetallic nodules were missing, all parasites, 64% of the exclusively filter feeding, 55% of the exclusively bacterivory, and 50% of the exclusively scavenging interaction web compartments were lost (Figure 3-2).

Highest losses occurred in Bryozoa, monothalamid Foraminifera[3], Porifera (all 100% loss), and Cnidaria (70% loss) (Figure 3-3). Only one of the faunal compartments was removed from the interaction web due to a cascade through trophic interactions, i.e., due to the loss of its single food source. All other interaction web compartments were removed due to a disappearance of non-trophic interactions. Of these, 40% were removed as they obligatorily depended on polymetallic nodules as substrate and 41% due to their facultative dependence on the nodule (i.e., the compartment was not always found attached to nodules). The remaining 19% were removed because of their commensal relationships with the Porifera *Caulophacus* sp., *Hyalonema* sp., *Staurocalyptus* sp., and *Bathyxiphus* sp. They comprised the macrobenthic compartments Amphipoda, Isopoda, and Mysidacea and the megabenthic compartments Alcyonacea, *Antedon* sp., Brisingida, Cephalopoda, Isopoda, Munidopsis, and Ophiuroidea.

The highest-impact taxon was the megabenthic Porifera *Hyalonema* sp. whose removal resulted in the loss of 9 compartments (Table 3-1) which is 4% of all faunal compartments. In contrast, the removal of the most connected taxa did not result in any knock-down loss of other interaction web compartments.

3.4.2 CCZ

A total of 472 faunal compartments (+ 5 food source compartments, + 1 nodule compartment) were identified for the CCZ trophic interaction web (Figure 3-1) that included 33% meiobenthos, 33% macrobenthos, and 34% megabenthos. Seventy-eight percent of all faunal compartments were exclusively detritivores, filter feeders, and predators (Figure 3-2). The non-trophic interaction web contained 234 links. The most connected taxa were the megabenthic Rhabditophora and Turbellaria (180 trophic links each) and megabenthic Actiniaria was the taxon with most non-trophic interactions.

Nodule absence resulted in the loss of 21% of all faunal compartments (Table 3-1), divided into meiobenthos (6%), macrobenthos (45%), and megabenthos (49%). The nodule absence led to a complete loss (100%) of the combined feeding type “filter feeder/ predator” (Figure 3-2). Furthermore, filter feeding interaction web compartments were reduced by 63% and 25% less “detritivores/ bacterivores” were present (Figure 3-2). The most affected phyla were Ciliophora (100% loss), Bryozoa (75% loss), monothalamid Foraminifera (71%

[3] According to a new supraordinal classification system by Pawlowski, Holzmann and Tyszka (2013), Foraminifera consist of single-chambered “monothalamid Foraminifera” including Xenophyophyores (in the network analysis called “monothalamid Foraminifera”) and two multi-chambered orders “Tubothalamea” and “Globothalamea” (in the network analysis called “Foraminifera”).

loss), Brachiopoda (67% loss), and Cnidaria (60% loss) (Figure 3-3). All these compartments were removed due to non-trophic interactions, i.e., obligatory dependence on polymetallic nodules as substrate (44%), facultative dependence on nodules (44%), and the dependence on other faunal compartments (12%). The latter association between faunal compartments included the commensal relationship of Actiniaria with Pennatulacea, i.e., Actiniaria colonized Pennatulacea. Further commensal relationships existed between meio- and macrobenthic Amphipoda, macrobenthic Hesionidae, megabenthic Actiniaria, Alcyonacea, Cirripedia, Comatulida, *Freyella* sp., *Munidopsis* sp., *Ophiura* sp., Phlebobranchia (all megabenthos), *and* Porifera (*Caulophacus* sp., *Chondrocladia* sp., *Corbitella* sp., *Hyalonema* sp., *Hyalostylus* sp.).

Table 3-1. The network properties "number of network compartments" (S), "number of network links" (L), "link density" (D), and "connectance" (C), calculated for the trophic interaction web of the Peru Basin and the trophic interaction web of the Clarion-Clipperton Fracture Zone when polymetallic nodules are present and absent, and without the most connected taxon, without the taxon with most non-trophic links and without the highest impact taxa. When there was more than one most connected taxon, taxon with most non-trophic links or highest impact taxon per site (Peru Basin or Clarion-Clipperton Fracture Zone), data are presented as mean±SD. The change in percent with respect to the default web is shown in brackets; when mean±SD are reported, it is the change in percentage of the mean value with respect to the corresponding value of the default web.

	S	***L***	***D***	***C***
Peru Basin				
With polymetallic nodules	208*	3,131	15	0.072
Without polymetallic nodules	154 (-26.0%)	1,962 (-37.3%)	13 (-13.3%)	0.083 (+15.3%)
Without most connected taxon	207 (-0.48%)	3,001 (-4.15%)	14 (-6.67%)	0.070 (-2.78%)
Without taxon with most non-trophic links	207 (-0.48%)	3,119 (-0.38%)	15 (-0%)	0.073 (+1.39%)
Without highest impact taxon	199 (-4.33%)	2,993 (-4.41%)	15 (-0%)	0.076 (+5.56)
Clarion-Clipperton Fracture Zone				
With polymetallic nodules	478⁑	9,386	20	0.041
Without polymetallic nodules	383 (-19.9%)	7,480 (-20.3%)	20 (-0%)	0.051 (+24.4%)
Without most connected taxon	477±0 (-0.21%)	9,206±0 (-1.92%)	19±0 (-5.00%)	0.040±0 (-2.44%)

Without taxon with most non-trophic links	477 (-0.21%)	9,379 (-0.07%)	20 (-0%)	0.041 (-0%)
Without highest impact taxon	468 (-2.09%)	9,293±40 (-0.99%)	20 (-0%)	0.04±0.00 (-2.44%)

*206 network compartments = 202 faunal compartments + 5 food source compartments. + 1 polymetallic nodule compartment.
‡478 network compartments = 472 faunal compartments + 5 food source compartments. + 1 polymetallic nodule compartment.

The highest impact taxa were the megabenthic Porifera *Hyalonema* sp. and *Caulophacus* sp., whose removal resulted in the loss of 10 interaction web compartments each (Table 3-1). In comparison, the removal of the most connected taxa did not lead to any knock-down of other faunal compartments.

3.4.3 Changes in food-web properties

Absence of polymetallic nodules as hard substrate resulted in a substantial reduction in the number of food-web links (37% in the PB and 20% in the CCZ, Table 3-1). Link density, i.e., average number of links per compartment, was the food-web property that was least affected by nodule absence (no change in the CCZ and decrease by 13% in the PB). Food-web connectance, i.e., the fraction of realized links (Hall and Raffaelli, 1993), increased by 15% in the PB and by 24% in the CCZ.

Removal of the most connected taxon and the taxon with most non-trophic links decreased the number of food-web links by 4% in the PB and by 2% in the CCZ. In comparison, when the taxon with most non-trophic interactions was removed, the number of food-web links was 0.4% (PB) and 0.1% (CCZ) lower than the number of links in the corresponding default food webs. Link density was not affected by the removal of the "taxon with most non-trophic links", but removing the most connected taxon caused a loss in link density of 7% in the PB and of 5% in the CCZ. The connectance decreased when the most connected taxon was removed, but it was unaffected when the taxon with most non-trophic interactions in the CCZ was removed. Removing the highest impact taxon resulted in an increase in connectance (6%) in the PB, but in a small loss in connectance (2%) in the CCZ (Table 3-1).

3.5 Discussion

Our results consistently show that for two nodule-rich abyssal areas, PB and CCZ, which are ~6,000 km apart (*Google Earth*, 2018) and have separate data sets, the absence of polymetallic nodules will lead to a strong modification of the food-web structure due to losses of web links and compartments. The loss of compartments was almost exclusively the result of existing non-trophic interactions between nodules as hard substrate and sessile organisms or sessile organisms attached to nodules and their associated fauna. Here, we compare our results of food-web properties with food webs. We also discuss the role polymetallic nodules and of stalked Porifera in polymetallic nodule areas.

3.5.1 Model limitations

As the highly resolved binary food webs for the Peru Basin and the CCZ are based on systematic meta-analyses, the studies have some limitations: The literature that was gathered in this study used different lower and upper limits to identify meiobenthos and macrobenthos. Furthermore, only few studies reported the use of an upper size limit for meiobenthos (e.g., Mahatma, 2009), whereas the majority of the studies did not report any upper size limit and likely included all infauna that was retained on sieves with the lower size limit. Hence, smaller macrobenthos might be classified as meiobenthos and therefore were erroneously implemented as meiobenthos in the interaction web models. In return, many authors used the term "meiobenthos" synonymously to "meiofauna" (e.g., Giere, 2009) instead of distinguishing between the statistical entity "meiobenthos" based on body size and the taxonomic category "meiofauna" (McIntyre, 1969). As a result, larger meiofaunal organisms, such as nematodes or harpacticoids, might be excluded from macrobenthos, though e.g., nematodes dominated the macrobenthic community in the CCZ (De Smet *et al.*, 2017). Therefore, when authors (e.g., Borowski, 2001) stated that specific taxa were excluded from the analysis of a specific size range because the authors used taxonomic categories, they were included in the correct size class based on body size. Despite these attempts to achieve comparability, the interaction web models likely lacked specific meio- and macrobenthic taxa. Hence, phyla rather than size classes should be considered when assessing the importance of polymetallic nodules for the food web.

Additionally, especially the interaction web developed for the Peru Basin missed specific phyla, such as meiobenthic Foraminifera (see Supplementary table 3-1), due to a lack of publications about these phyla. However, this lack of literature was likely caused by a limit in specific taxonomic expertise during previous research cruises to the Peru Basin rather than caused by a deliberate omission of specific phyla. In contrast, the CCZ interaction web was based on a more balanced dataset for the different taxa due to the extensive baseline studies that were conducted in the CCZ during the last five years.

Authors reported some faunal groups only in a very coarse taxonomic resolution (see Supplementary table 3-1 and 3-2) which made it difficult to specify diets or feeding preferences. Hence, compartments with artificially high numbers of trophic links were implemented in the models. However, an increasing number of trophic links decreases the probability that a compartment is lost due to a lack of food. Therefore, this study likely underestimated the importance of polymetallic nodules for food-web integrity, in particular for compartments of coarse taxonomic resolution or for compartments for which information about diet is poor.

The non-trophic interaction matrix only included commensalism and no other types of non-trophic interactions, such as competition (Kéfi *et al.*, 2012). Interspecific competition for food resources might be one reason for sympatric speciation in abyssal detrivorous holothurians: They have a high morphological diversity of tentacles that enabled the sympatric species to develop different feeding strategies and in this way overcome competition for food (Roberts and Moore, 1997). Hence, on evolutionary time scales, including competition in the food web

would likely result in an increase in diversity and therefore an increase in compartments and food-web links. In contrast, on the short term, competition would probably have no effect on the food-web structure and the non-trophic interactions that have been implemented in the model account for most of the secondary extinctions and shifts in food-web structure that can be expected from the absence of polymetallic nodules.

3.5.2 Properties of abyssal plain food webs

Theoretical food-web studies indicate that the removal of highly connected species can lead to a cascade of secondary extinctions (Sole and Montoya, 2001; Dunne, Williams and Martinez, 2002). However, in highly connected webs, such as the Skipwidth Pond food web for an English freshwater pond (Warren, 1989), removing the most connected species had no effect (Dunne, Williams and Martinez, 2002). This specific food web included 36 omnivorous invertebrate food-web compartments and was detritus based (Warren, 1989). Therefore, the removal of its basal node, the detritus, resulted in an immediate food web collapse (Dunne, Williams and Martinez, 2002). In comparison, >50% species had to be removed randomly to have the same effect (Dunne, Williams and Martinez, 2002). Coastal ecosystems, such as salt marshes or seagrass beds, are also detritus based and contain many invertebrates. van der Zee *et al.* (2016) showed that removing the most connected species had very little relative effect on the number of species and connectance in established seagrass meadows and established fringing marshes. In contrast, facilitation by primary (cordgrass/ seagrass) and secondary (mussels/ crabs) habitat modifiers had a four times higher relative effect on the number of species in established fringing salt marshes and a 20-times higher relative effect on connectance (van der Zee *et al.*, 2016).

The deep-sea food webs for the abyssal plains of the CCZ and the Peru Basin are likewise detritus-based and dominated by invertebrates. The most connected species were generalist feeding invertebrate predators (*Chromaspirina* sp., Rhabditophora, and Turbellaria) whose removal had no effect on any other food-web compartment. However, similar to the coastal ecosystem food-webs described by van der Zee *et al.* (2016), removing the primary habitat modifier, in this case the polymetallic nodule, had the highest impact: It resulted in an increase in connectance by 15% (Peru Basin) to 24% (CCZ). This increase in connectance is comparable to the increase in connectance after removal of the secondary modifier in fringing salt marshes (21%) (van der Zee *et al.*, 2016) and stresses the importance of non-trophic interactions, whereas most connected species seem not to be important when they are generalist invertebrates.

The effect of biodiversity loss seems to depend stronger on the type of food web (e.g., source webs, like detritus-based webs; Dunne, Williams and Martinez, 2002) than on connectance. The Skipwith Pond food web had the highest connectance (0.315) in a collection of 16 different food webs, but behaved similarly to our deep-sea food webs with a connectance that is comparable to the connectance of the Chesapeake Bay food web (Dunne, Williams and Martinez,

2002). The latter food web was a bentho-pelagic food-web model including several fish species (Baird and Ulanowicz, 1989) and experienced increased secondary extinctions when 20 – 30% of the primary species are removed.

3.5.3 Role of stalked Porifera and potential consequences of future deep-sea mining

This study shows that the removal of stalked Porifera compartments had the largest impact on network properties (so called "highest impact taxa"), because they host commensal faunal communities, such as filter and suspension feeders (e.g., Alcyonacea, Antedon, Brisingida), scavengers (e.g., Amphipoda), and predators (e.g., Isopoda, Cephalopoda, Ophiuroidea). In fact, sponge stalks were identified previously as "habitat islands" for deep-sea fauna (Ilan, Ben-Eliahu and Galil, 1994) as they allow suspension feeders to settle higher up in the benthic boundary layer, where the laminar flow has a higher velocity (Buhl-Mortensen *et al.*, 2010). In this way, stalked Porifera provide physical structure for other organisms extending the two-dimensional environment into a three-dimensional environment. Therefore, they can be considered "structural species" (*sensu* Huston, 1994). An analysis of photograph transects at Station M in the NE Pacific, for example, showed that 87% of the observed stalks that emerged from the soft sediment of the abyssal plain seafloor consisted of the hexactinellid *Hyalonema* spp., of which only 14% were alive (Beaulieu, 2001). These stalks hosted a diverse epifaunal community of suspension feeders: the examination of 35 stalk communities showed that they harbored 8,580 individuals that could be classified into 139 taxa belonging to 13 different phyla (Beaulieu, 2001).

Our comprehensive analysis evidently and quantitatively shows the importance of polymetallic nodules and attached stalked Porifera for the abyssal food web. It is therefore clear that the absence of polymetallic nodules due to deep-sea mining would lead to a significant depreciation of biodiversity. It is not clear, however, whether this would be only a local effect in the affected areas or would result in regional or even global loss of biodiversity (Van Dover *et al.*, 2017; Niner *et al.*, 2018). The deep sea is still poorly studied (Ramírez-Llodrà *et al.*, 2010), new species are discovered regularly in abyssal plains (e.g., Amon *et al.*, 2016) and we often lack information about species ranges.

3.6 Conclusion

Previous modelling studies about the impact of deep-sea mining on the benthic ecosystem focused on C flows (Stratmann, Lins, *et al.*, 2018/ **Chapter 6**; **Chapter 7)**. These food-web models, however, group individual taxa in feeding types (Soetaert and van Oevelen, 2009; van Oevelen *et al.*, 2010) which can mask biodiversity loss. Furthermore, the models concentrated on trophic interactions, though it was shown for coastal ecosystems that non-trophic interactions structure food webs (van der Zee *et al.*, 2016). Therefore, we developed binary interaction webs including both, trophic and non-trophic interactions. These webs show that non-trophic interactions are important for food-web integrity: The absence of polymetallic nodules will result in a reduced food-web complexity and a loss in

biodiversity. Additionally, we identified stalked Porifera as “structural species” that host a high diversity of commensal fauna.

Acknowledgments

We thank the chief scientists Pedro Martínez Arbizu (SO239) and Antje Boetius (SO242-2) as well as captain and crew of RV Sonne for their excellent support during the SO239 ‘EcoResponse’ cruise and the SO242-2 ‘DISCOL revisited’ cruise. We further thank the ‘ROV Kiel 6000’ team from Geomar, Kiel (Germany).

3.7 Supplement

Supplementary table 3-1. Specification of the lowest taxonomic level to which the network compartments for the Peru Basin interaction webs were resolved for the size classes meiobenthos, macrobenthos, and megabenthos.

Phylum	Class	Order	Lowest taxonomic level	References
Meiobenthos				
Annelida	Polychaeta		Family	Thiel *et al.* (1993)
Arthropoda	Hexanauplia	Calanoida	Order	Ahnert and Schriever (2001)
Arthropoda	Hexanauplia	Cyclopoida	Order	Ahnert and Schriever (2001)
Arthropoda	Hexanauplia	Harpacticoida	Family	Ahnert and Schriever (2001); Bussau, Schriever and Thiel (1995)
Arthropoda	Hexanauplia	Misophrioida	Order	Ahnert and Schriever (2001)
Arthropoda	Malacostraca	Amphipoda	Order	Ahnert and Schriever (2001)
Arthropoda	Malacostraca	Cumacea	Order	Ahnert and Schriever (2001)
Arthropoda	Malacostraca	Isopoda	Order	Ahnert and Schriever (2001)
Arthropoda	Malacostraca	Tanaidacea	Order	Ahnert and Schriever (2001); Borowski (2001); Borowski and Thiel (1998)
Arthropoda	Ostracoda		Class	Ahnert and Schriever (2001); Bussau, Schriever and Thiel (1995)
Chordata	Ascidiacea		Class	Ahnert and Schriever (2001)
Gastrotricha			Phylum	Ahnert and Schriever (2001); Bussau, Schriever and Thiel (1995)
Kinorhyncha			Phylum	Ahnert and Schriever (2001); Bussau, Schriever and Thiel (1995)
Loricifera			Phylum	Ahnert and Schriever (2001); Bussau, Schriever and Thiel (1995)
Mollusca	Aplacophora		Class	Ahnert and Schriever (2001)
Mollusca	Bivalvia		Class	Ahnert and Schriever (2001)
Mollusca	Gastropoda		Class	Ahnert and Schriever (2001)
Mollusca	Scaphopoda		Class	Ahnert and Schriever (2001); Borowski (2001)

Nematoda			Genus	Borowski (2001); Bussau, Schriever and Thiel (1995); Singh *et al.* (2016); Thiel *et al.* (1993); Vopel and Thiel (2001)
Rotifera			Phylum	Ahnert and Schriever (2001)
Tardigrada			Genus	Bussau, Schriever and Thiel (1995)
Macrobenthos				
Annelida	Polychaeta		Family	Borowski (2001); Borowski and Thiel (1998); Thiel *et al.* (1993)
Arthropoda	Hexanauplia	Harpacticoida	Order	Borowski (2001); Borowski and Thiel (1998)
Arthropoda	Malacostraca	Amphipoda	Order	Ahnert and Schriever (2001)
Arthropoda	Malacostraca	Cumacea	Order	Borowski (2001); Borowski and Thiel (1998)
Arthropoda	Malacostraca	Isopoda	Order	Borowski (2001); Borowski and Thiel (1998)
Arthropoda	Malacostraca	Mysidacea	Order	Photo analysis by Porifera taxonomist (Daniel Kersken)
Echinodermata	Asteroidea		Class	Borowski and Thiel (1998)
Echinodermata	Echinoidea		Class	Borowski (2001)
Echinodermata	Ophiuroidea		Class	Borowski (2001)
Foraminifera			Phylum	Borowski and Thiel (1998)
Mollusca	Bivalvia		Class	Borowski (2001); Borowski and Thiel (1998)
Mollusca	Gastropoda		Class	Borowski (2001)
Megabenthos				
Arthropoda	Hexanauplia	Scalpelliformes	Order	Bluhm (1994)
Arthropoda	Malacostraca	Decapoda	Genus	Bluhm (1994)
Arthropoda	Malacostraca	Isopoda	Order	Bluhm (1994)
Bryozoa			Phylum	Bluhm (1993); Bluhm (1994); Bluhm, Schriever and Thiel (1995)
Chordata			Family	Bluhm (1993); Bluhm (1994); Bluhm (2001)

Cnidaria	Scyphozoa	Order	Bluhm (1994)
Cnidaria	Hydrozoa	Order	Bluhm (1994)
Ctenophora		Phylum	Bluhm (1994)
Echinodermata	Asteroidea	Order	Bluhm (1994)
Echinodermata	Crinoidea	Genus	Bluhm (1994)
Echinodermata	Echinoidea	Genus	Bluhm (1994)
Echinodermata	Holothuroidea	Genus	Stratmann, Voorsmit, *et al*. (2018)/ **Chapter 4**; Bluhm and Gebruk (1999); Bluhm (1994)
Echinodermata	Ophiuroidea	Class	Bluhm (1993); Bluhm (2001)
Foraminifera		Phylum	Bluhm (1994)
Hemichordata		Class	Bluhm (1993); Bluhm (1994)
Mollusca		Class	Bluhm (1993); Bluhm (1994); Bluhm (2001); Purser *et al.* (2016)
Porifera		Genus	Bluhm (1994); Photo analysis by Porifera taxonomist (Daniel Kersken)

Supplementary table 3-2. Specification of the lowest taxonomic level to which the network compartments for the Clarion-Clipperton Fracture Zone interaction webs were resolved for the size classes meiobenthos, macrobenthos, and megabenthos.

Phylum	Class	Order	Lowest taxonomic level	References
Meiobenthos				
Arthropoda	Hexanauplia	Calanoida	Family	Markhaseva, Mohrbeck and Renz (2017)
Arthropoda	Hexanauplia	Cyclopoida	Family	Mahatma (2009)
Arthropoda	Hexanauplia	Harpacticoida	Family	Mahatma (2009); Mullineaux (1987)
Arthropoda	Hexanauplia	Poecilostomatoida	Family	Mahatma (2009)
Arthropoda	Malacostraca	Amphipoda	Order	Radziejewska (2002)
Arthropoda	Malacostraca	Isopoda	Order	Amon *et al*. (2016); Mahatma (2009); Martínez Arbizu and Haeckel (2015); Radziejewska (2002)
Arthropoda	Malacostraca	Tanaidacea	Order	Mahatma (2009); Mullineaux (1987)
Arthropoda	Maxillopoda		Class	Mahatma (2009)
Arthropoda	Ostracoda		Class	Mahatma (2009); Radziejewska (2002)
Foraminifera			Family	Goineau and Gooday (2015); Gooday, Goineau and Voltski (2015); Nozawa *et al.* (2006); Veillette (2006)
Gastrotricha			Phylum	Mahatma (2009); Radziejewska (2002)
Kinorhyncha			Phylum	Mahatma (2009); Radziejewska (2002)
Loricifera			Phylum	Mahatma (2009); Radziejewska (2002)
Mollusca	Bivalvia		Phylum	Amon *et al*. (2016); Amon, Ziegler, Drazen *et al.* (2017); Goineau and Gooday (2015); Kamenskaya, Melnik and Gooday (2013); Mahatma (2009); Mullineaux (1987)

Nematoda			Genus	Miljutin and Miljutina (2009a); Miljutin and Miljutina (2009b); Miljutina *et al*. (2010); Miljutin *et al.* (2011); Miljutina and Miljutin (2012); Miljutin, Miljutina and Messié (2015); Pape *et al.* (2017)
Radiozoa			Genus	Goineau and Voltski (2015)
Rotifera			Phylum	Mahatma (2009)
Tardigrada			Phylum	Mahatma (2009); Radziejewska (2002)
Macrobenthos				
Annelida	Polychaeta		Family	Borowski (1994); De Smet *et al.* (2017); Janssen *et al*. (2015); Martínez Arbizu and Haeckel (2015)
Arthropoda	Arachnida		Subclass	De Smet *et al.* (2017)
Arthropoda	Hexanauplia		Order	De Smet *et al.* (2017)
Arthropoda	Malacostraca	Amphipoda	Family	Amon, Ziegler, Drazen *et al.* (2017); Wilson (1987)
Arthropoda	Malacostraca	Cumacea	Order	Martínez Arbizu and Haeckel (2015)
Arthropoda	Malacostraca	Euphausiacea	Order	Martínez Arbizu and Haeckel (2015)
Arthropoda	Malacostraca	Isopoda	Family	De Smet *et al.* (2017); Janssen *et al.* (2015); Janssen *et al.* (2015); Martínez Arbizu and Haeckel (2015); Wilson (1987); Wilson (2017)
Arthropoda	Malacostraca	Leptostraca	Order	Martínez Arbizu and Haeckel (2015)
Arthropoda	Malacostraca	Mysidacea	Order	De Smet *et al.* (2017); Martínez Arbizu and Haeckel (2015)
Arthropoda	Malacostraca	Tanaidacea	Family	Martínez Arbizu and Haeckel (2015); Wilson (1987); Wilson (2017)
Brachiopoda			Genus	Mullineaux (1987); Veillette (2006)
Bryozoa			Genus	Mullineaux (1987); Veillette (2006)
Chaetognatha				De Smet *et al.* (2017)
Ciliophora			Class	Mullineaux (1987)

Cnidaria	Hydrozoa		Order	Dahlgren *et al.* (2016)
Cnidaria	Scyphozoa		Genus	Dahlgren *et al.* (2016); Veillette (2006)
Echinodermata	Ophiuroidea		Genus	Glover *et al*. (2016)
Foraminifera			Family	Gooday, Goineau and Voltski (2015); Goineau and Voltski (2015); Goineau and Gooday (2017); Kamenskaya *et al*. (2012); Kamenskaya *et al.* (2015); Kamenskaya *et al.* (2017); Mullineaux (1987); Mullineaux (1988); Veillette (2006)
Mollusca	Bivalvia		Family	Foell and Pawson (1986); Martínez Arbizu and Haeckel (2015); Mullineaux (1987); Veillette (2006); Wiklund *et al.* (2017)
Mollusca	Gastropoda		Class	Martínez Arbizu and Haeckel (2015)
Mollusca	Monoplacophora		Class	Mullineaux (1987); Wiklund *et al.* (2017)
Mollusca	Polyplacophora		Class	Martínez Arbizu and Haeckel (2015); Wiklund *et al.* (2017)
Mollusca	Scaphopoda		Genus	Wiklund *et al.* (2017)
Mollusca	Solenogastres		Class	Wiklund *et al.* (2017)
Megabenthos				
Annelida	Polychaeta		Family	Amon *et al.* (2016); Amon, Ziegler, Drazen *et al*. (2017); Janssen *et al*. (2015); Martínez Arbizu and Haeckel (2015); Tilot (2006)
Arthropoda	Hexanauplia	Scalpelliformes	Genus	Amon, Ziegler, Drazen *et al.* (2017); Foell and Pawson (1986)
Arthropoda	Malacostraca	Amphipoda	Genus	Amon *et al.* (2016); Amon, Ziegler, Drazen *et al*. (2017); Foell and Pawson (1986); Leitner *et al.* (2017); Photo analysis by Porifera taxonomist (Daniel Kersken); Tilot (2006)
Arthropoda	Malacostraca	Decapoda	Genus	Amon *et al.* (2016); Amon, Ziegler, Drazen *et al*. (2017); Foell and Pawson (1986); Leitner *et al.* (2017); Tilot (2006)

Arthropoda	Malacostraca	Mysida	Order	Photo analysis by Porifera taxonomist (Daniel Kersken)
Arthropoda	Maxillopoda (Infraclass: Cirripedia)		Infraclass	Mahatma (2009); Martínez Arbizu and Haeckel (2015)
Arthropoda	Pycnogonida		Class	Amon *et al.* (2016)
Brachiopoda			Phylum	Kamenskaya, Melnik and Gooday (2013); Mullineaux (1987); Veillette (2006)
Bryozoa			Order	Amon *et al.* (2016); Foell and Pawson (1986); Mullineaux (1987); Veillette (2006)
Chordata			Family	Amon *et al.* (2016); Amon, Ziegler, Drazen *et al.* (2017); Foell and Pawson (1986); Leitner *et al.* (2017); Tilot (2006); Veillette (2006)
Cnidaria	Anthozoa		Order	Amon *et al.* (2016); Cairns (2016); Dahlgren *et al.* (2016); Foell and Pawson (1986); Kamenskaya, Melnik and Gooday (2013); Martínez Arbizu and Haeckel (2015); Molodtsova and Opresko (2017); Rodrigues, Sharma and Nagender Nath (2001); Tilot (2006); Vanreusel *et al.* (2016)
Cnidaria	Scyphozoa		Family	Amon *et al.* (2016); Dahlgren *et al.* (2016); Foell and Pawson (1986); Tilot (2006); Veillette (2006)
Cnidaria	Hydrozoa		Class	Dahlgren *et al.* (2016); Foell and Pawson (1986); Martínez Arbizu and Haeckel (2015); Mullineaux (1987); Radziejewska (2002); Tilot (2006); Vanreusel *et al.* (2016)
Ctenophora			Order	Amon, Ziegler, Drazen *et al.* (2017)

Echinodermata	Asteroidea	Genus	Amon *et al.* (2016); Amon, Ziegler, Kremenetskaia, *et al.* (2017); Glover *et al.* (2016); Martínez Arbizu and Haeckel (2015); Tilot (1992); Tilot (2006)
Echinodermata	Crinoidea	Order	Amon *et al.* (2016); Amon, Ziegler, Kremenetskaia, *et al.* (2017); Tilot (1992); Tilot (2006)
Echinodermata	Echinoidea	Family	Amon *et al.* (2016); Amon, Ziegler, Kremenetskaia, *et al.* (2017); Leitner *et al.* (2017); Tilot (1992); Tilot (2006)
Echinodermata	Holothuroidea	Genus	Amon *et al.* (2016); Amon, Ziegler, Kremenetskaia, *et al.* (2017); Glover *et al.* (2016); Mahatma, Martínez Arbizu and Ivanenko (2008); Rodrigues, Sharma and Nagender Nath (2001); Tilot (1992); Tilot (2006)
Echinodermata	Ophiuroidea	Genus	Amon *et al.* (2016); Amon, Ziegler, Kremenetskaia, *et al.* (2017); Glover *et al.* (2016); Kersken, Janussen and Martínez Arbizu (2017a); Leitner *et al.* (2017); Martínez Arbizu and Haeckel (2015); Tilot (1992); Tilot (2006)
Foraminifera		Family	Gooday, Goineau and Voltski (2015); Goineau and Gooday (2015); Gooday, Goineau and Voltski (2015); Gooday *et al.* (2017); Goineau and Gooday (2017); Kamenskaya *et al.* (2012); Kamenskaya, Melnik and Gooday (2013); Kamenskaya *et al.* (2015); Kamenskaya *et al.* (2017); Mullineaux (1987); Mullineaux (1988); Nozawa *et al.* (2006); Veillette (2006); Veillette (2006)

Hemichordata	Class	Foell and Pawson (1986); Tilot (2006)
Mollusca	Class	Amon *et al.* (2016); Amon, Ziegler, Drazen *et al.* (2017); Foell and Pawson (1986); Goineau and Gooday (2015); Kamenskaya, Melnik and Gooday (2013); Mahatma (2009); Martínez Arbizu and Haeckel (2015); Mullineaux (1987); Radziejewska (2002); Tilot (2006); Veillette (2006); Wiklund *et al*. (2017)
Platyhelminthes	Class	Veillette (2006)
Porifera	Genus	Amon *et al.* (2016); Photo analysis by Porifera taxonomist (Daniel Kersken); Foell and Pawson (1986); Kersken, Janussen and Martínez Arbizu (2017b); Lim *et al*. (2017); Rodrigues, Sharma and Nagender Nath (2001); Tilot (1992); Tilot (2006);

Supplementary table 3-3. Publications used to identify feeding preferences/ food sources of all taxa implemented in the interaction webs.

Phylum	References
Annelida	Horton *et al.* (2018); Jumars, Dorgan and Lindsay (2015)
Arthropoda	Allen, Tyler and Varney (2000); Bradford-Grieve (2004); Chertoprud *et al.* (2007); Fox, Barnes and Ruppert (2003); Gage and Tyler (1991); Gardiner (1975); Giere (2009); Horton *et al.* (2018); Humes (1974); Kapiris (2012); Svavarsson, Gudmundsson and Brattegard (1993); Watling, (1990); Wicksten and Packard (2005); Wicksten *et al.* (2017); Wolff (1962)
Brachiopoda	http://www.uvm.edu/perkins/PGMWeb/Glossary/Brachio-pods.htm (Accessed: 18 October 2017)
Bryozoa	Fox, Barnes and Ruppert (2003)
Cephalorhyncha	Peel (2017)
Chaetognatha	Horton *et al.* (2018)
Chordata	Bergstad *et al.* (2012); Horton *et al.* (2018); Linley *et al.* (2016); Naranjo-Elizondo *et al.* (2016); Priede (2017)
Ciliophora	Epstein, Burkovsky and Shiaris (1992)
Cnidaria	Horton *et al.* (2018); Larson (1979); Matsumoto, Baxter and Chen (1997)
Ctenophora	https://faculty.washington.edu/cemills/Ctenophores.html (Accessed: 18 October 2017)
Echinodermata	Baumiller (2008); Byrne and O'Hara (2017); Carey (1972); Courtene-Jones *et al.* (2017); Gage and Tyler (1991); Gale, Hamel and Mercier (2013); Gooday *et al.* (2014); Horton *et al.* (2018); Howell *et al.* (2004); Huffard *et al.* (2016); Jangoux (1982); Massin (1982); Michel *et al.* (2016); Pearson and Gage (1984); Roberts and Moore (1997); Warner (1982)
Foraminifera	Beldean and Filipescu (2008); Enge *et al.* (2016); Hoffmann (2009); Kamenskaya (2005); Kuhnt and Collins (1995); Levin (1994); Loeblich and Tappan (1960); Lynn (2008); Margulis and Chapman (2009); Murray (2014); Nobes and Uthicke (2008)
Gastrotricha	Giere (2009)
Hemichordata	Knight-Jones (1952)
Kinorhyncha	Giere (2009)
Loricifera	Giere (2009)
Mollusca	Allen and Morgan (1981); Fox, Barnes and Ruppert (2003); Horton *et al.* (2018); Junqueira De Souza Dantas, Laut and Caetano (2017); Krylova *et al.* (2015); Le Pennec *et al.* (2003); Tyler *et al.* (1992); Valls, Rueda and Quetglas (2017)
Nematoda	Barnes and Ferrero (2009); Bussau and Vopel (1999); Bussau (1993); Decraemer (1996); Holovachov *et al.*

	(2011); Horton *et al.* (2018); Miljutin and Miljutina (2009b); Nanajkar and Ingole (2010); Soetaert and Heip (1995); Vanhove, Arntz and Vincx (1999); Zhinan (1983); Zograf *et al.* (2017)
Nemertea	McDermott and Roe (1985)
Platyhelminthes	Fox, Barnes and Ruppert (2003)
Porifera	Horton *et al.* (2018); Vacelet, Kelly and Schlacher-Hoenlinger (2009)
Radiozoa	Giere (2009)
Rotifera	Giere (2009)
Sipuncula	Fox, Barnes and Ruppert (2003)
Tardigrada	Giere (2009)

RECOVERY FROM A DEEP-SEA DISTURBANCE EXPERIMENT

Chapter 4 : Recovery of Holothuroidea population density, community composition, and respiration activity after a deep-sea disturbance experiment

4. Recovery of Holothuroidea population density, community composition, and respiration activity after a deep-sea disturbance experiment

Tanja Stratmann, Ilja Voorsmit, Andrey Gebruk, Alastair Brown, Autun Purser, Yann Marcon, Andrew K. Sweetman, Daniel O. B. Jones, and Dick van Oevelen;
Modified from *Limnology and Oceanography*, 2018: 00: 00–00. doi: 10.1002/lno.10929.

4.1 Abstract

Mining polymetallic nodules on abyssal plains will have adverse impacts on deep-sea ecosystems, but it is largely unknown whether the impacted ecosystem will recover, and if so, at what rate. In 1989 the "DISturbance and reCOLonization" (DISCOL) experiment was conducted in the Peru Basin, where the seafloor was disturbed with a plough harrow construction to explore the effect of small-scale sediment disturbance as an analogue to deep-sea mining. Densities of Holothuroidea in the region were last investigated 7 yr post-disturbance until 19 yr later, the DISCOL experimental site was revisited in 2015. An "Ocean Floor Observatory System" was used to photograph the seabed across ploughed and unploughed seafloor and at reference sites. The images were analyzed to determine the Holothuroidea population density and community composition, which were combined with *in situ* respiration measurements of individual Holothuroidea to generate a respiration budget of the study area. For the first time since the experimental disturbance, similar Holothuroidea densities were observed at the DISCOLexperimental site and at reference sites. The Holothuroidea assemblage was dominated by *Amperima* sp., *Mesothuria* sp., and *Benthodytes typica*, together contributing 46% to the Holothuroidea population density. Biomass and respiration were similar among sites, with a Holothuroidea community respiration of $5.84\times10^{-4}\pm8.74\times10^{-5}$ mmol C m^{-2} d^{-1} at reference sites. Although these results indicate recovery of Holothuroidea, extrapolations regarding recovery from deep-sea mining activities must be made with caution: results presented here are based on a relatively small-scale disturbance experiment as compared to industrial-scale nodule mining, and also only represent one taxonomic class of the megafauna.

4.2 Introduction

Interest in mining polymetallic nodules from abyssal plains has increased substantially since the 1960s (Glasby, 2000; Jones *et al.*, 2017). Polymetallic nodules contain valuable metals such as copper, cobalt, nickel, and rare earth elements (Wang and Müller, 2009) and are therefore considered economically interesting resources. However, deep-sea mining activities will have negative impacts on these vulnerable deep-sea ecosystems through the removal of hard substratum (i.e., polymetallic nodules) essential for sessile (e.g., Amon *et al.*, 2016; Vanreusel *et al.*, 2016) and mobile (Purser *et al.*, 2016; Leitner *et al.*, 2017) fauna. Further negative impacts may result from the disturbance and/ or removal of the upper sediment layer (Thiel and Forschungsverbund Tiefsee-Umweltschutz, 2001), i.e., the habitat that contains the majority of organisms and their food sources (Danovaro, Fabiano and Della Croce, 1993; Danovaro *et al.*, 1995; Haeckel *et al.*, 2001). Sessile fauna and infauna will be removed in the mining tracks (Borowski and Thiel, 1998; Bluhm, 2001; Borowski, 2001), and fauna in and on adjacent sediments may be blanketed by mechanically displaced sediment (Thiel and Forschungsverbund Tiefsee-Umweltschutz, 2001). Re-suspended sediment and sediment plumes may smother both sessile and mobile fauna over extended areas, or potentially adversely impact filter feeding organisms (Jankowski and Zielke, 2001; Thiel and Forschungsverbund Tiefsee-Umweltschutz, 2001; Brooke, Holmes and Young, 2009).

Ecological concerns about deep-sea mining have resulted in several deep-sea experiments studying ecosystem recovery following disturbance (Jones *et al.*, 2017). To investigate the recovery from small-scale disturbance experiments employing isolated individual disturbance tracks, Vanreusel *et al.* (2016) used ROV video surveys to compare sessile and mobile metazoan epifauna densities at disturbed and undisturbed sites with high and low "polymetallic nodule" coverage in the Clarion-Clipperton Fracture Zone (CCZ, central Pacific). The mobile metazoan epifauna in a 20 yr-old experimental mining track at a nodule-free site comprised mainly Holothuroidea and Ophiuroidea (1,500 ind. ha^{-1}), whereas the density at the reference site was substantially higher (3,000 ind. ha^{-1}). In contrast, the same study showed that mobile metazoan epifauna at a nodule-rich site in another, 37 yr-old mining track in the CCZ consisted exclusively of Echinoidea (1,000 ind. ha^{-1}) and had a 70% lower mobile epifauna density than the reference site, where Holothuroidea and Ophiuroidea were also present.

The most extensively studied and largest-scale disturbance experiment conducted to date is the "DISturbance and reCOLonization experiment" (DISCOL) in the Peru Basin. This experiment was conducted in a 10.8 km^2 circular area, DISCOL Experimental Area or "DEA" in short, which was ploughed 78 times on diametric courses in 1989 to mimic a small-scale deep-sea mining disturbance event (Foell, Thiel and Schriever, 1990, 1992; Bluhm, 2001). The DEA can be considered "small-scale" in comparison to commercial mining as the 10.8 km^2 represent between 1.4% and 3.6% of the area projected to be disturbed by one individual mining operation per year (Smith *et al.*, 2009). The imposed disturbance occurred on two levels: (1) direct impacts inside "plough tracks" where polymetallic nodules were ploughed into the sediment (~22% of DEA) and

(2) indirect impacts from plume exposure associated with the ploughing outside plough tracks (~70-75% of the DEA; Thiel *et al.*, 1989; Bluhm and Thiel, 1996). Four sites, each approximately 4 km away from the DEA served as reference areas as they were considered to be outside the area of plume influence.

Biological investigations were conducted inside the disturbance tracks, outside the tracks, and at the reference sites prior to the DISCOL disturbance (reference sites; DISCOL 1/1 cruise), immediately following DISCOL disturbance (inside and outside tracks; DISCOL 1/2 cruise) and 0.5 yr (DISCOL 2 cruise), three (DISCOL 3 cruise), and 7 yr (ECOBENT cruise) post DISCOL disturbance (Bluhm, 2001) to assess ecosystem recovery over time. The disturbance experiment impacted the meiofaunal, macrofaunal, and megafaunal size classes of the benthic community, but the magnitude of disturbance differed markedly among size classes and functional groups. For example, the abundance of meiofaunal harpacticoids was approximately 20% lower inside plough tracks compared to outside plough tracks immediately following the DISCOL disturbance, a difference that persisted up to 7 yr after the DISCOL disturbance (Ahnert and Schriever, 2001). In contrast, total macrofauna abundance inside plough tracks was 66% lower than outside plough tracks immediately following the DISCOL disturbance, but was similar between inside and outside plough tracks 3 yr after the DISCOL disturbance (Borowski, 2001). Sessile megafauna, such as Cnidaria, Crinoidea, and Ascidiacea, was virtually absent from inside plough tracks following ploughing, and did not recover to pre-disturbance densities during the subsequent 7 yr (Bluhm, 2001). Their slow recovery is likely a result of the removal of hard substratum from the seafloor (Vanreusel *et al.*, 2016). Total megafaunal densities were significantly lower inside plough tracks directly after the DISCOL disturbance, 0.5 yr after, and 7 yr after the DISCOL disturbance, but not significantly different 3 yr after the DISCOL disturbance (Bluhm, 2001). Holothuroidea, the dominant taxa of mobile megafauna, remained reduced at inside plough tracks (75±50 ind. ha^{-1}) when compared with densities observed outside plough tracks (169±79 ind. ha^{-1}) 7 yr after the DISCOL disturbance (Bluhm, 2001), though the difference was not statistically significant because of the large variability within the data.

These deposit-feeding Holothuroidea are a key component of abyssal benthic communities as they engage in key ecosystem functions of the deep sea, such as modifying the quality of the organic matter of the sediment (Smallwood *et al.*, 1999), processing of fresh phytodetritus (Bett *et al.*, 2001; FitzGeorge-Balfour *et al.*, 2010), and mineralization through nutrient regeneration or respiration (Thurber *et al.*, 2014). Holothurians make a contribution to mineralization as they were estimated to respire between 1% and 6% of the particulate organic carbon (POC) flux per year on Pacific and Atlantic abyssal plains (Ruhl *et al.*, 2014). Many holothurian species are large in comparison to other abyssal benthic invertebrates and can therefore be counted and identified from images with comparative ease (Durden, Schoening, *et al.*, 2016). Holothuroidea are also mobile, with some species moving >100 cm h^{-1} over the seafloor (Jamieson *et al.*, 2011) and some species having the capacity to swim (Miller and Pawson, 1990; Rogacheva,

Gebruk and Alt, 2012). Holothuroidea can respond to fresh phytodetritus deposition events with large-scale recruitment within 1 yr (Billett *et al.*, 2010). One would therefore expect that Holothuroidea may recover in regions of disturbed seafloor comparatively quickly.

In this study, we assessed Holothuroidea population density and community composition 26 yr after the initial disturbance at the DISCOL area, by determining abundances from high-resolution photos taken of the seafloor both within and outside plough tracks, and at reference sites south and southeast of the DEA. The results of this abundance estimation were then combined with *in situ* respiration rate measurements to identify any differences in respiratory activity of Holothuroidea at the various sites. These data were compared with earlier Holothuroidea population density data to investigate (1) whether the Holothuroidea assemblages differed between inside plough tracks, outside plough tracks, and reference areas, (2) whether Holothuroidea population densities had recovered after 26 yr, and (3) whether Holothuroidea respiration rates differed between sites. The mechanisms underlying the observed recovery dynamics are discussed and considered in the context of future mining operations.

4.3 Methods

4.3.1 Study site

The seafloor in the Peru Basin in the tropical Southeast Pacific Ocean is typically between 4,000 and 4,400 m deep (Wiedicke and Weber, 1996), has a bottom water temperature of 2.9°C, salinity of 34.6 PSU, and oxygen concentration of 145.3±1.3 (mean±SD) µmol L^{-1} (Boetius, 2015). Bottom water currents alternate between periods of comparatively strong (>5 cm s^{-1}) unidirectional currents and periods of slower (<1–3 cm s^{-1}) current flow without prevalent direction (Klein, Rachor and Gerlach, 1975). The DEA itself is centered on 07°04.4’S, 88°27.6’W and is between 4,140 and 4,160 m deep (Bluhm, Schriever and Thiel, 1995). Sediment in the DEA typically consists of a 5–15 cm thick surface layer of semi-liquid, dark brown sediment (0.55±0.11% organic C) and a sublayer of consolidated grayish clay (0.70±0.08% organic C) (Grupe, Becker and Oebius, 2001; Marchig *et al.*, 2001; Oebius *et al.*, 2001). Surface sediments in the DEA have 18.1±11.3 kg m^{-2} of polymetallic nodules (Marchig *et al.*, 2001). The DEA plough tracks are still clearly visible (Figure 4-1) and consequently we identified three disturbance categories for the study: inside and outside plough tracks in the DEA, and reference sites south and southeast of the DEA (hereafter referred to as reference site) (Figure 4-1).

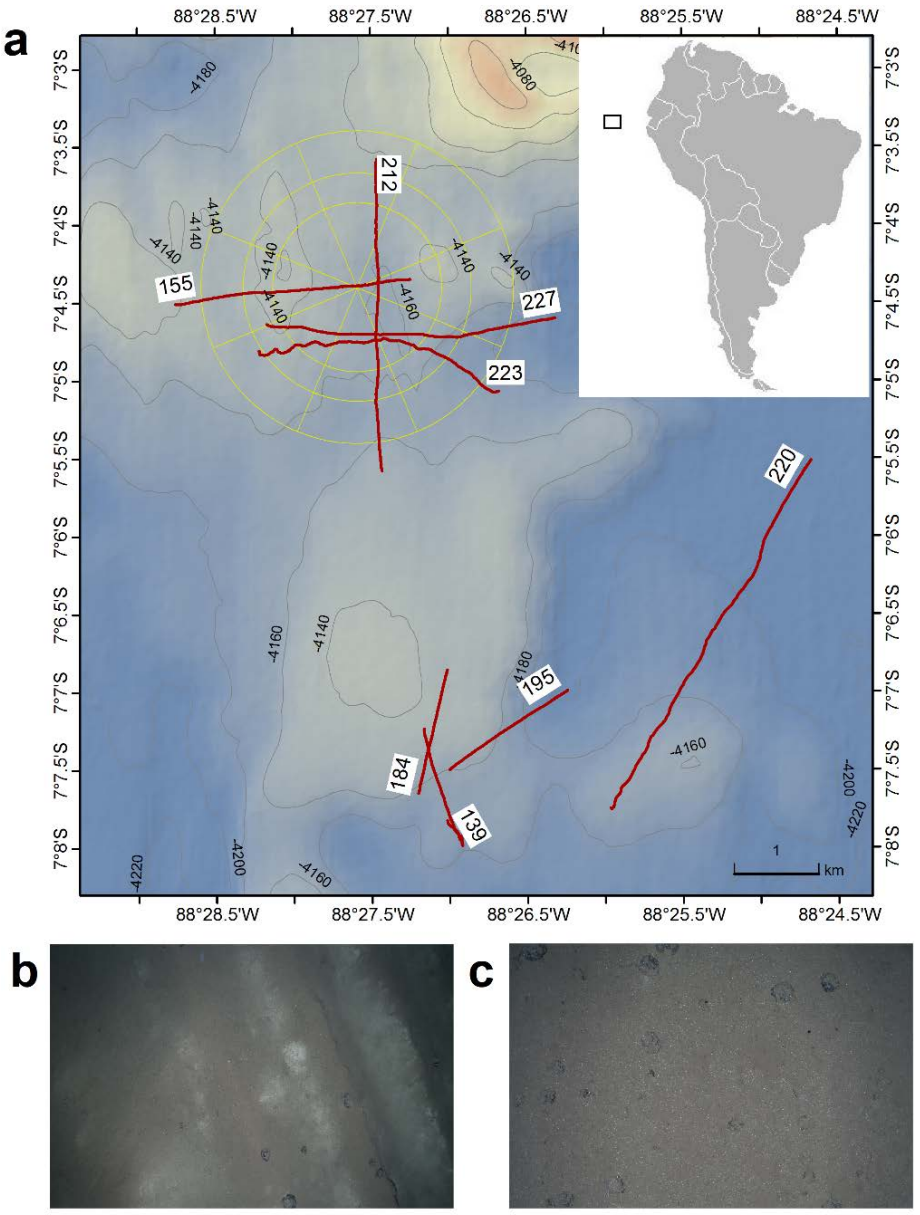

Figure 4-1. (a) Map of the Peru Basin with bottom transects of all ocean floor observation system (OFOS) deployments inside the DISCOL experimental area (DEA, yellow circles) and at the southern and southeastern reference site. The numbers on white background correspond to the site numbers in Table 4-1. The black rectangle in the inserted map shows the exact location of DEA but is unscaled. (b) Photograph of plough marks in the sediment at the DISCOL experimental area. (c) Photograph of the seafloor at the reference site. Photographs (b, c) were taken by ROV Kiel 6000, Geomar.

4.3.2 Assessment of Holothuroidea assemblage

A high-resolution digital camera (CANON EOS 5D Mark III, modified for underwater applications by iSiTEC) on the towed "Ocean Floor Observation System" (OFOS) was used to photograph the seafloor. The OFOS was deployed from the R/V *Sonne* during cruise SO242-2 (chief scientist: Prof. Dr. Antje Boetius) and towed 1.5 m above the seafloor at a speed of approximately 0.5 knots, photographing the seafloor every 20 s (~5.5 m^2 seafloor per image) (Purser *et al.*, 2016). In contrast, during previous DISCOL cruises (from directly following to 7 yr after the DISCOL disturbance), the OFOS was equipped with analog still-photo cameras (DISCOL 1/1, DISCOL 1/2, and DISCOL 2 cruises: Benthos 377 camera; DISCOL 3 and ECOBENT cruises: Photosea 5,000 camera; Bluhm, Schriever and Thiel, 1995; Schriever, Koschinsky and Bluhm, 1996). For these deployments, the system was towed approximately 3 m above the seafloor and the photographs were taken selectively by scientists (Bluhm and Gebruk, 1999; Jones *et al.*, 2017).

For this study, the OFOS was deployed four times (= four transects) at the DEA (Figure 4-1; Table 4-1), where a total of 3,760 usable (neither under- nor overexposed, correct altitude, and without suspended sediment obscuration) pictures were taken. Images were classified as "inside plough tracks" when plough tracks were visible (1,838 photos) and otherwise classified as "outside plough tracks" (1,922 photos; Table 4-1). The OFOS was also deployed four times (= four transects) for this study at reference sites outside the DEA (Figure 4-1; Table 4-1), where a total of 983 usable pictures were taken. Each photo transect was treated as a replicate resulting in four replicates for each level of disturbance (i.e., inside plough tracks, outside plough tracks, and reference site).

Photographs were loaded into the open-source software "Program for Annotation of Photographs and Rapid Analysis (of Zillions and Zillions) of Images" (PAPARA(ZZ)I) (Marcon and Purser, 2017). All Holothuroidea in non-overlapping pictures were first annotated by morphotype. Subsequently, morphotypes were identified to family, genus, or species level by an expert deep-sea Holothuroidea taxonomist (A. Gebruk). Reference was made to Bluhm and Gebruk (1999) and the "Atlas of Abyssal Megafauna Morphotypes of the Clipperton-Clarion Fracture Zone" (ccfzatlas.com). In PAPARA(ZZ)I body length and body width were measured for all Holothuroidea which lay straight using as reference for scaling a set of three laser points on the seafloor that formed an equilateral triangle of 0.5 m.

4.3.3 Assessment of total sediment community oxygen consumption and Holothuroidea community respiration

The sediment community oxygen consumption (SCOC) was measured *in situ* at the DISCOL reference site by deploying a benthic chamber lander (KUM GmbH, Germany) that was equipment with HydroFlash^{TM} O_2 (Kongsberg Maritime Contros GmbH, Germany) optodes. After deployment of the lander, incubation chambers (20×20×20 cm) were slowly pushed into the sediment after which the oxygen concentration inside the chambers was continuously recorded

over a period of 3 d (Boetius, 2015). From the linear decrease in oxygen concentration, the oxygen consumption rate was estimated.

Table 4-1. "Ocean floor observation system" (OFOS) transects. For each disturbance level (outside plough tracks, inside plough tracks, and reference) photos of four OFOS transects were analyzed (Ref S = reference south; Ref SE = reference southeast; inPT = inside plough tracks within DEA; outPT = outside plough tracks within DEA). As both inside and outside plough tracks within DEA photo sets originate from the same bottom tracks, the only difference between the photos was the presence of visible plough marks in the images.

OFOS transect	Start of bottom transect	End of bottom transect	Usable photos	Seafloor area imaged (m^2)	Disturbance level
139	7°07.71'S, 8°826.92'W	7°07.24'S, 8°827.16'W	87	418.0	Ref S
184	7°07.65'S, 8°827.20'W	7°06.86'S, 8°827.01'W	408	2,069.0	Ref S
195	7°07.49'S, 8°827.00'W	7°06.98'S, 8°826.22'W	494	3,015.7	Ref S
220	7°07.75'S, 8°825.96'W	7°05.76'S, 8°824.83'W	983	5,434.7	Ref SE
155	7°04.50'S, 8°828.74'W	7°04.35'S, 8°827.36'W	498	2,901.5	inPT
212	7°05.57'S, 8°827.42'W	7°03.57'S, 8°827.46'W	792	390.4	inPT
223	7°04.81'S, 8°828.21'W	7°05.06'S, 8°826.67'W	156	797.4	inPT
227	7°04.65'S, 8°827.99'W	7°04.60'S, 8°826.36'W	392	1,957.7	inPT
155	7°04.50'S, 8°828.74'W	7°04.35'S, 8°827.25'W	338	2,062.5	outPT
212	7°05.57'S, 8°827.42'W	7°03.58'S, 8°827.45'W	473	2,439.5	outPT
223	7°04.80'S, 8°828.21'W	7°05.07'S, 8°826.71'W	676	3,610.7	outPT
227	7°04.63'S, 8°828.16'W	7°04.60'S, 8°826.33'W	435	2,508.0	outPT

Holothuroidea community respiration was calculated based on abundance (see above) and *in situ* respiration rates of 13 individual Holothuroidea sampled during R/V *Sonne* cruise 242-2 (Brown *et al.*, 2018). Briefly, the "benthic incubation chamber system 3" (BICS3) (Hughes *et al.*, 2011) was attached to the GEOMAR Ocean elevator (Linke, 2011) and lowered to the seafloor. Holothuroidea were collected individually with the ROV Kiel 6000 and placed individually in three respiration chambers. The forth respiration chamber was kept empty as a control. After a Holothuroidea was placed in a chamber, the lid was

closed immediately, and oxygen consumption was measured over a period of at least 70 h (84.8±14.3 h), with the empty chamber being used to assess the oxygen consumption rate of bottom seawater. Afterwards, the elevator platform with the BICS3 was brought to the surface, the Holothuroidea were collected, and body length and width of each specimen were measured.

For the conversion of body length and width of individual Holothuroidea annotated on the OFOS photos into individual respiration rates, the body volume of the 13 Holothuroidea specimens (*Amperima* sp., *Benthodytes* sp., *Benthodytes typica*, *Mesothuria* sp., *Peniagone* sp. 2 (benthopelagic), Synallactidae gen. sp. 2) collected inside DEA was related to background-corrected respiration rates (measured originally in mmol O^2 ind^{-1} d^{-1}, Brown *et al.*, 2018; but converted to mmol C ind^{-1} d^{-1} assuming a respiratory quotient of 1). The body volume of the 13 Holothuroidea specimens was calculated as the body length×body width^2. This formed the basis of the linear regression analysis of body volume vs. background-corrected respiration rates for all individual organisms ($respiration\ rate = 9.00 \times 10^{-5} \times body\ length \times body\ width^2$; $n = 13$, $r^2 = 0.41$, $p = <0.001$). Subsequently, body length and width measurements of Holothuroidea from the OFOS pictures were converted into respiration rates following the equation given above whenever the organisms laid straight. When the length could not be measured, e.g., when the specimen was in a curved position, an average size for that specific morphotype was taken. The respiration per unit area was calculated as the sum of individual respiration rates divided by the area for which Holothuroidea abundance was determined.

4.3.4 Data analysis

For the Holothuroidea dataset after 26 yr, Hill numbers or effective number of species (N_0[1], N_1[2], and N_2[3]; Hill, 1973) were asymptotically estimated by rarefaction and extrapolation (Supplementary figure 4-1) following Chao *et al.* (2014) using the *iNext* package (Hsieh, Ma and Chao, 2016) in the open-source software R (R-Core Team, 2017). Analysis of similarities in assemblage composition of Holothuroidea was based on square-root transformed faunal density data using the ANOSIM routine in PRIMER6 (Clarke and Gorley, 2006). The contribution of individual morphotypes to the similarity or dissimilarity between sites was calculated with the SIMPER routine in PRIMER6.

Differences in Hill numbers, Holothuroidea densities, and $\log_{10}$-transformed respiration rates among disturbance levels (inside plough tracks, outside plough tracks, reference site) were tested with One-Way ANOVA after assumptions of normality and homogeneity of variances were confirmed by Shapiro–Wilk test and Brown–Forsythe test.

---

[1] Hill number N_0 = species richness/ total number of species that are present (Hill, 1973; Chao *et al.*, 2014).

[2] Hill number $N_1 = e^{H'}$, where *H'* is the Shannon index ($H' = -\sum p_i \times \ln p_i$, with p_i = proportion of individuals in the *i*th species; Magurran, 2004).

[3] Hill number $N_2 = \frac{1}{D}$, where *D* is the Simpson's index ($D = \sum p_i^2$, with p_i = proportion of individuals in the *i*th species; Magurran, 2004).

The Holothuroidea population densities were also analyzed over time (i.e., pre-disturbance -0.1, 0.1, 0.5, 3, 7, and 26 yr post-DISCOL disturbance) inside plough tracks, outside plough tracks, and at reference sites. The raw Holothuroidea density data from the earlier cruises were taken from Annex 2.08 in Bluhm (2001) and combined with the Holothuroidea density data of the present study. This resulted in an $n = 6$ for DISCOL 1/1 (reference site), $n = 4$ and $n = 5$ for DISCOL 1/2 (inside plough tracks and outside plough tracks, respectively), $n = 3$, $n = 4$, and $n = 2$ for DISCOL 2 (inside plough tracks, outside plough tracks, and reference site, respectively), $n = 4$, $n = 4$, and $n = 3$ for DISCOL 3, $n = 4$, $n = 4$, and $n = 5$ for ECOBENT, and $n = 4$, $n = 4$, and $n = 4$ for DISCOL revisited. To meet the assumptions of normality and homogeneity of variances, the Holothuroidea density data were $\log_{10}$-transformed, before an unweighted One-Way ANOVA was applied to compare differences in Holothuroidea densities from inside plough tracks, outside plough tracks, and reference sites of the same year. Results are expressed as mean±SD if not stated otherwise.

4.4 Results

4.4.1 Holothuroidea population density and community composition

A total of 23 different Holothuroidea morphotypes were identified from the full image set (Figure 4-2). Where image quality was insufficient to identify morphotype, Holothuroidea were classified as “unknown Holothuroidea”. A total of 22 morphotypes were found inside plough tracks, including single records of *Abyssocucumis abyssorum* and *Galatheaturia* sp., 20 morphotypes outside plough tracks, including a single record of *Benthodytes gosarsi*, and 17 morphotypes at the reference sites (Figure 4-3). The most abundant species were *Amperima* sp., *Benthodytes typical*, and *Mesothuria* sp. (Figure 4-3, Table 4-2), which together contributed 46±6% to the total density. However, their ranking in species abundance varied among sites (Figure 4-3).

The density of Holothuroidea did not differ among sites (ANOVA: $F_{2,9} = 0.042$, $p = 0.96$) with mean densities (ind. ha^{-1}) of 241±51 inside plough tracks, 240±40 outside plough tracks, and 241±33 at reference sites. There were no differences in mean density of each morphotype among sites (ANOSIM: $R = 0.019$, $p = 0.39$), either. Similarity in species composition among sites was driven by *Benthodytes typica* (contribution to similarity between disturbed and undisturbed sites: 10.46% to 16.28%), *Amperima* sp. (10.49%), and the group of unknown Holothuroidea (10.28% and 10.54%). Hill numbers N_0, N_1, and N_2 did not differ significantly among sites, either (ANOVA for N_0: $F_{2,9} = 0.005$, $p = 1.00$; ANOVA for N_1: $F_{2,9} = 1.246$, $p = 0.33$; ANOVA for N_2: $F_{2,9} = 0.021$, $p = 0.98$; Table 4-3).

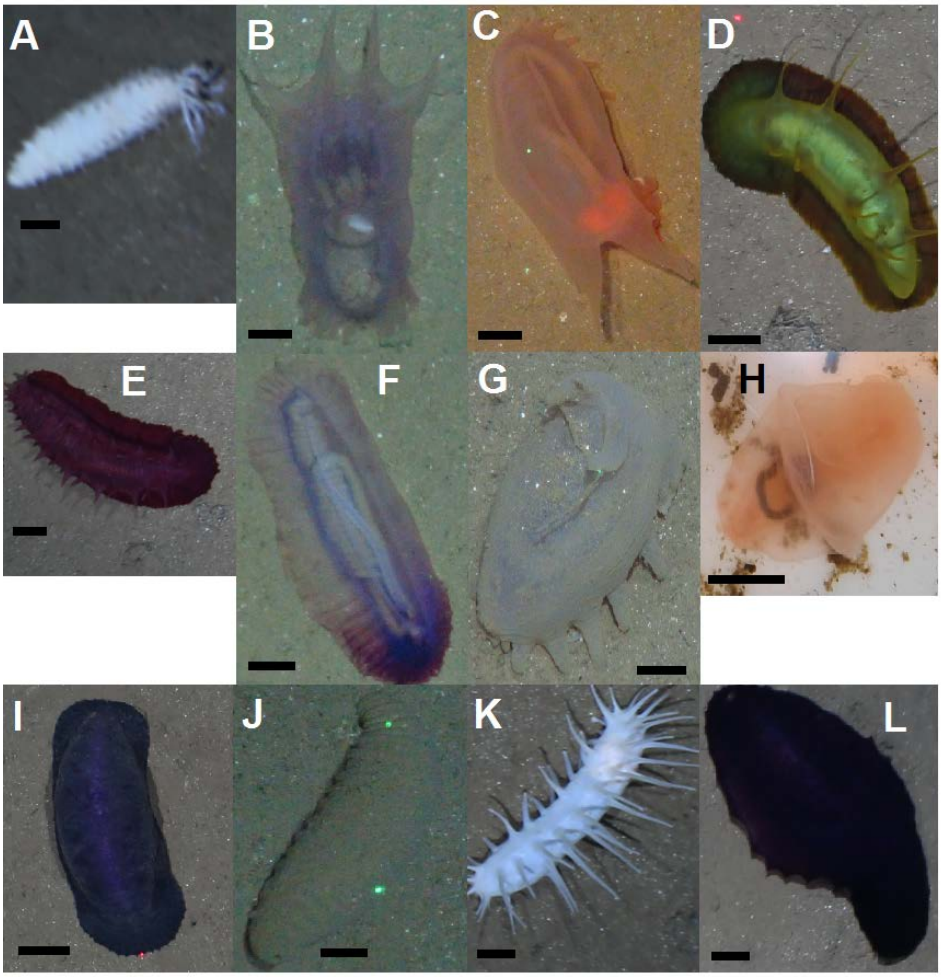

Figure 4-2. Images of Holothuroidea morphotypes used in the present study: (A) *Abyssocucumis abyssorum*, (B) Elpidiidae gen. sp. 1 (= *Achlyoinice* sp. in Bluhm and Gebruk, 1999), (C) *Amperima* sp., (D) *Benthodytes gosarsi*, (E) *Benthodytes* sp., (F) *Benthodytes typica*, (G) Elpidiidae gen. sp. 2 ("double velum" morphotype in ccfzatlas.com), (H) Elpidiidae gen. sp. 3, (I) *Benthothuria* sp., (J) *Mesothuria* sp., (K) *Oneirophanta* sp., (L) *Galatheathuria* sp., (M) *Peniagone* sp. (= morphotype "palmata" in ccfzatlas.com), (N) *Peniagone* sp. 1, (O) *Peniagone* sp. 2 (benthopelagic), (P) *Psychronaetes hanseni*, (Q) *Psychropotes depressa*, (R) *Psychropotes longicauda*, (S) *Bathyplotes* sp., (T) Synallactidae gen. sp. 1, (U) Synallactidae gen. sp. 2, (V) *Synallactes profundi*, (W) *Synallactes* sp. (morphotype "pink" in ccfzatlas.com).
The black bar represents 1 cm length. Photographs (A, C- F, I, K- M, P-W) from AWI; (B, G, J, N) from ROV Kiel 6000, Geomar; (H, O) from T. Stratmann. (Continued on the next page)

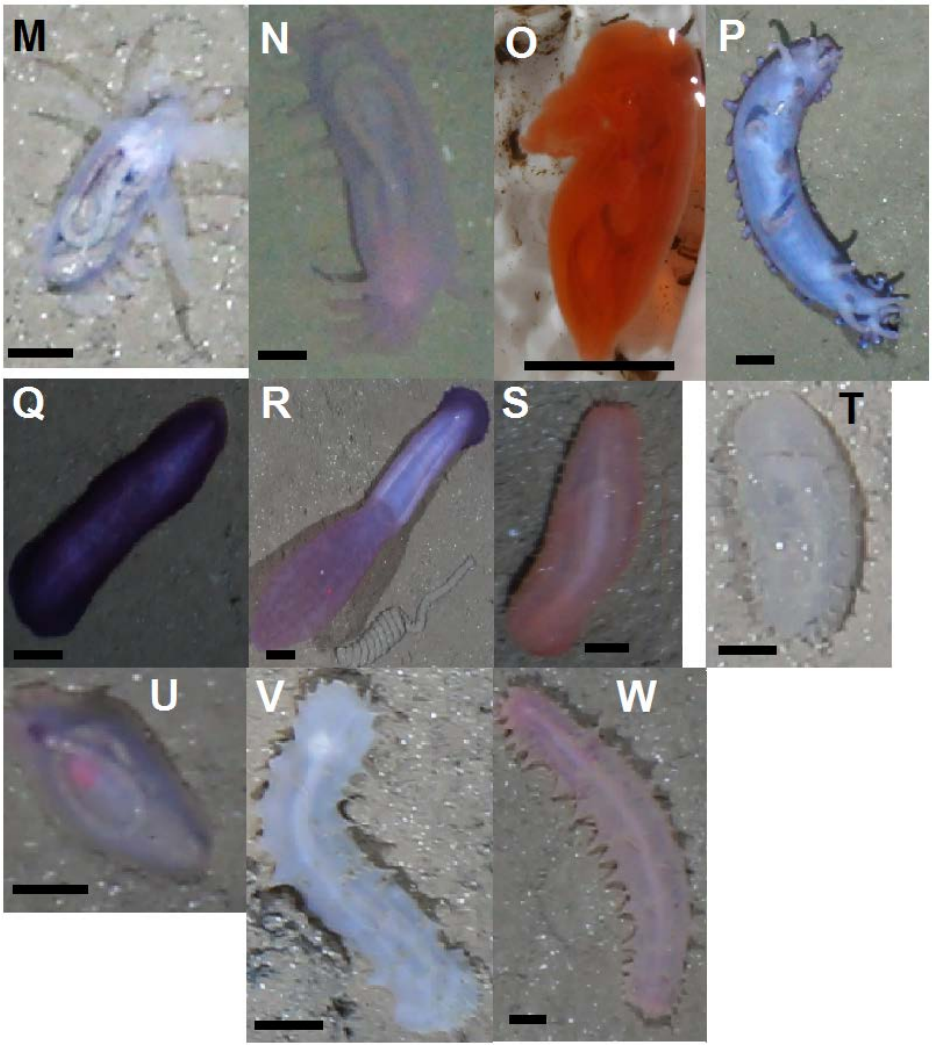

Figure 4-2 continued.

Table 4-2. Density (ind. ha^{-1}) and respiration ($\times 10^{-3}$ mmol C m^{-2} d^{-1}) of the three most abundant Holothuroidea taxa for each location (Ref S = reference south; Ref SE = reference southeast; inPT = inside plough tracks within DEA; outPT = outside plough tracks within DEA).

OFOS transect	Disturbance level	*Benthodytes typica*		*Amperima* sp.		*Mesothuria* sp.	
		Density	Respiration	Density	Respiration	Density	Respiration
139	Ref S	Not seen		52	0.22	52	0.06
184	Ref S	34	0.14	25	0.07	49	0.05
195	Ref S	47	0.27	41	0.12	41	0.05
220	Ref SE	38	0.29	15	0.06	22	0.04
155	inPT	28	0.20	25	0.08	35	0.02
212	inPT	62	0.43	28	0.11	26	0.03
223	inPT	25	0.16	50	0.22	25	0.46
227	inPT	97	0.63	26	0.11	31	0.06
155	outPT	20	0.09	66	0.32	25	0.05
212	outPT	70	0.33	50	0.29	41	0.07
223	outPT	36	0.26	25	0.13	25	0.07
227	outPT	53	0.43	18	0.10	26	0.06

4.4.2 Holothuroidea density changes over time

The holothurian mean density of 142±37 ind. ha^{-1} of the pre-disturbance study in February 1989 dropped by 87% (18±10 ind. ha^{-1}) inside plough tracks and by 39% (86±31 ind. ha^{-1}) outside plough tracks immediately after the disturbance (Figure 4-4; Bluhm, 2001). This difference in mean Holothuroidea densities between inside and outside plough tracks 0.1 yr post-DISCOL disturbance was statistical significant (ANOVA: $F_{1,7} = 26.23$, $p = 0.001$) and persisted until 0.5 yr after the DISCOL disturbance (ANOVA: $F_{2,6} = 16.46$, $p = 0.004$) (Bluhm, 2001). Three years after the DISCOL disturbance, Holothuroidea mean densities inside plough tracks (99±54 ind. ha^{-1}) were 37% of the mean densities outside plough tracks (266±200 ind. ha^{-1}; Bluhm, 2001), but the difference between disturbance levels was not significant anymore due to a large variability among the OFOS tracks (ANOVA: $F_{2,8} = 4.18$, $p = 0.06$).

4.4.3 Holothuroidea community respiration

Holothuroidea community respiration ($\times 10^{-3}$ mmol C m^{-2} d^{-1}) was not significantly different among the reference sites (0.58±0.09), outside plough tracks (0.77±0.10), and inside plough tracks (0.80±0.30) (ANOVA: $F_{2,9} = 1.468$, $p = 0.281$).

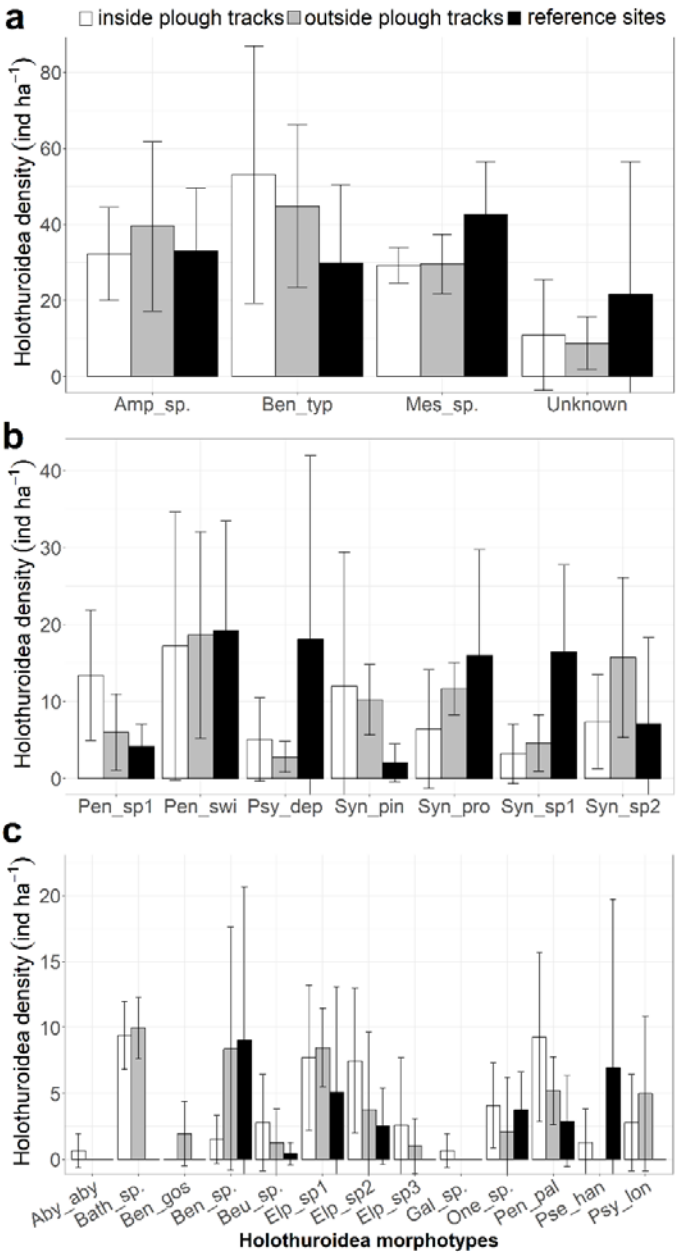

Figure 4-3. Holothuroidea morphotype densities >60 ind. ha^{-1} (a), >40 ind. ha^{-1} (b), and >10 ind. ha^{-1} (c) in the three areas inside plough tracks, outside plough tracks, and reference, shown as mean values with standard deviations.
Abbreviations: Aby_aby = *Abyssocucumis abyssorum*, Amp_sp. = *Amperima* sp., Bath_sp. = *Bathyplotes* sp., Ben_gos = *Benthodytes gosarsi*, Ben_sp. = *Benthodytes* sp., Ben_typ = *Benthodytes typica*, Beu_sp. = *Benthothuria* sp., Elp_sp1 = Elpidiidae gen. sp. 1 (= *Achlyoinice* sp. in Bluhm and Gebruk, 1999), Elp_sp2 = Elpidiidae gen. sp. 2 ("double velum" morphotype in ccfzatlas.com), Elp_sp3 = Elpidiidae gen. sp. 3, Gal_sp. = *Galatheathuria* sp., Mes_sp. = *Mesothuria* sp., One_sp. = *Oneirophanta* sp.,

Pen_pal = *Peniagone* sp. (= morphotype "palmate" in ccfzatlas.com), Pen_sp1 = *Peniagone* sp. 1, Pen_swi = *Peniagone* sp. 2 (benthopelagic), Pse_han = *Psychronaetes hanseni*, Psy_dep = *Psychropotes depressa*, Psy_lon = *Psychropotes longicauda*, Syn_pin = *Synallactes* sp. (morphotype "pink" in ccfzatlas.com), Syn_pro = *Synallactes profundi*, Syn_sp1 = Synallactidae gen. sp. 1, Syn_sp2 = Synallactidae gen. sp. 2, Unknown = Unknown Holothurian.

Table 4-3. Holothuroidea density (ind. ha^{-1}), respiration ($\times 10^{-3}$ mmol C m^{-2} d^{-1}), and abundance based diversity metrics (asymptotic estimate±SE; N_0: Hill number 0, N_1: Hill number 1, N_2: Hill number 2) for each location (Ref S = reference south; Ref SE = reference southeast; inPT = inside plough tracks within DEA; outPT = outside plough tracks within DEA).

OFOS transect	**Disturbance level**	**Density**	**Respiration**	N_0	N_1	N_2
139	Ref S	261	0.60	9.40±3.18	11.0±3.21	15.0±3.15
184	Ref S	230	0.46	38.0±30.5	14.0±3.05	9.65±1.48
195	Ref S	274	0.66	14.5±1.02	11.2±0.96	9.42±0.96
220	Ref SE	200	0.62	11.2±0.53	6.40±0.61	4.45±0.51
Mean± SD	Ref	241± 33	0.58± 0.09			
155	inPT	183	0.45	17.9±5.20	12.9±1.67	10.7±1.57
212	inPT	293	1.04	26.0±5.25	16.6±1.43	11.4±1.39
223	inPT	214	0.66	11.5±3.30	11.4±2.97	11.3±2.80
227	inPT	272	1.06	19.4±4.72	10.9±1.74	6.32±1.55
Mean± SD	inPT	241± 51	0.80± 0.30			
155	outPT	233	0.71	14.6±1.10	11.8±1.61	8.48±1.68
212	outPT	297	0.92	22.4±4.74	13.6±1.73	9.16±1.62
223	outPT	226	0.74	20.7±1.30	14.8±0.95	11.1±1.10
227	outPT	203	0.73	14.7±1.24	12.3±1.39	9.32±1.70
Mean± SD	outPT	240± 40	0.77± 0.10			

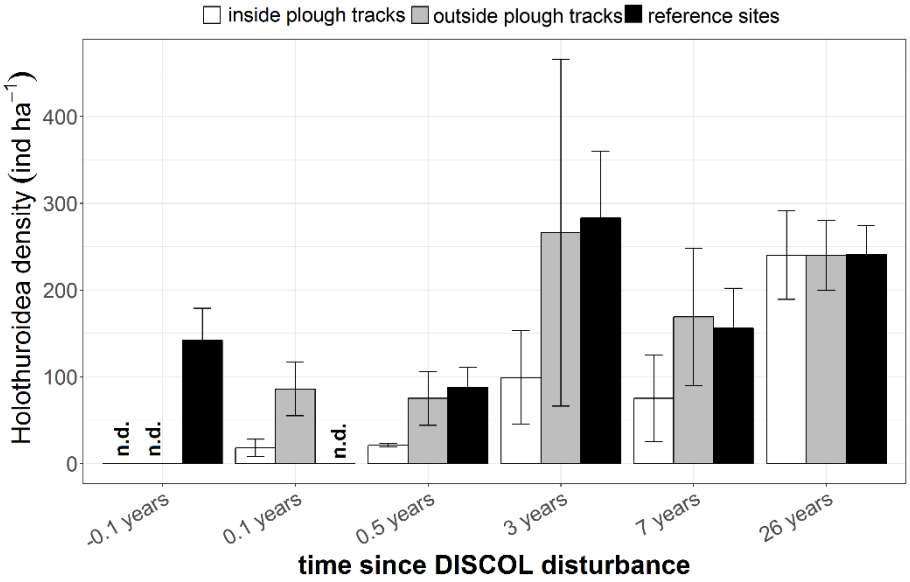

Figure 4-4. Holothuroidea densities measured during all previous post-disturbance DISCOL cruises inside as well as outside plough tracks, and, pre- and post-impact in the reference areas (no data were available for the cruise 0.1 yr after ploughing). Data from pre-disturbance (-0.1 yr), 0.1 yr, 0.5 yr, 3 yr, and 7 yr after the DISCOL experiment were taken from Bluhm (2001) annex 2.08. "n. d." means that no data were available for this specific disturbance and year (inside and outside plough tracks at -0.1 yr; reference at 0.1 yr).

4.5 Discussion

Deep-sea mining for polymetallic nodules will impact the benthic ecosystem in various ways (Jones *et al.*, 2017) and it is therefore vital to estimate how long it may take for ecosystems to recover from the resultant seafloor disturbances (Gollner *et al.*, 2017). Data presented here demonstrate that Holothuroidea population density, community composition, and respiration have recovered 26 yr after a sediment disturbance event in the Peru Basin. We here discuss the mechanisms involved in the recovery of Holothuroidea composition and functioning following the experimental disturbance and consider these in the context of future deep-sea mining activities.

4.5.1 Holothuroidea assemblage and densities

Holothuroidea assemblages in abyssal plains are often dominated by a few species, such as *Amperima rosea*, *Oneirophanta mutabilis*, *Psychropotes longicauda*, and *Pseudostichopus villosus* at the Porcupine Abyssal Plain (PAP, Northeast Atlantic; Billett *et al.*, 2001, 2010) or *Abyssocucumis abyssorum*, *Peniagone vitrea*, and *Elpidia minutissima* at Station M in the Northeast Pacific (Smith, Kaufmann and Wakefield, 1993). The Holothuroidea assemblage in the Peru Basin therefore resembles a typical deep-sea community, where

Amperima sp., *Benthodytes typica*, and *Mesothuria* sp. comprise almost 50% of the total Holothuroidea.

A key finding of this study is that Holothuroidea density and community composition recovered from a disturbance after 26 yr. These results are in contrast with a study on megafaunal recovery from the CCZ, where isolated individual disturbance tracks still showed reduced Holothuroidea densities up to 37 yr after the disturbance (Vanreusel *et al.*, 2016). This discrepancy may be a result of various factors, including temporal variability in Holothuroidea abundance, different disturbance methods and scales, and/ or differences in the food supply to the CCZ compared to the DISCOL area.

The abundance of particular mobile abyssal megafauna taxa can fluctuate inter-annually by one to three orders of magnitude (Ruhl, 2007). For example, the density of the Holothuroidea *Amperima rosea* increased by more than two orders of magnitude at the Porcupine Abyssal Plain (PAP, Northeast Atlantic) during the famous "Amperima event" (Billett *et al.*, 2001, 2010), likely in response to increased food supply to the seafloor. Hence, photo transects performed at a particular time only represent a snapshot of the megafaunal assemblage and do not show potential temporal variability. Holothuroidea abundance in a comparatively narrow and short mining track (Vanreusel *et al.*, 2016), where the number of individual specimen observed is likely very low, is especially prone to such spatial and temporal sampling bias.

Another key difference between the CCZ and DISCOL studies is the imposed disturbance method. During the DISCOL experiment the upper sediment layer was mixed in a ~2.4 km^2 area (22% of 10.8 km^2 DEA; Thiel *et al.*, 1989) leaving a mosaic of dark-brown sediment and grayish clay (Figure 4-1B). In contrast, the disturbance at the CCZ involved complete removal of the upper 5 cm of sediment in individual 2.5 m wide tracks (Khripounoff *et al.*, 2006). Surface sediments in the CCZ contain about 0.48% organic C (per dry sediment), whereas the carCbon content in sediments below 5 cm in the CCZ is only 0.35% (Khripounoff *et al.*, 2006). Hence, food availability in the CCZ tracks were reduced which may have contributed to the lower abundances. Other potential causes could be changes in water content with sediment depth (Grupe, Becker and Oebius, 2001), differences in sediment compactness, sediment grain size, terrain, or texture of the surface sediment in the tracks. Finally, the investigated site at the northwestern CCZ is more oligotrophic as compared to the DISCOL site, with a POC flux estimated to be 1.5 mg C_{org} m^{-2} d^{-1} (Vanreusel *et al.*, 2016). The flux of POC in the Peru Basin is higher, with model estimates of 3.86 mg C_{org} m^{-2} d^{-1} (Haeckel *et al.*, 2001). Consequently, re-establishing food availability in tracks following disturbance will likely differ between the CCZ and the Peru Basin, because of differences in disturbance method and trophic status.

4.5.2 Holothuroidea respiration

The total Holothuroidea respiration at the reference site (5.84×10^{-4} mmol C m^{-2} d^{-1}) was comparable to, but at the lower end of the echinoderm respiration calculated for PAP (respiration range: 3.13×10^{-4} to 1.25×10^{-3} mmol C m^{-2} d^{-1}; Ruhl *et al.*, 2014) and one order of magnitude lower than the

absolute echinoderm respiration calculated for Station M (respiration range: 4.69×10^{-3}–2.03×10^{-2} mmol C m^{-2} d^{-1}; Ruhl *et al.*, 2014). The latter difference can be attributed to the dominance of non-Holothuroidea echinoderms to the total echinoderm respiration at Station M. When only the total respiration rate of the dominant species Ophiuroidea, *Elpidia* spp. and *Echinocrepis rostrata* (Ruhl *et al.*, 2014) were considered, the Holothuroidea respiration at Station M was in the same order of magnitude as the Peru Basin taking into account the overall higher Holothuroidea densities in the Northeast Pacific than in the Southeast Pacific (Ruhl, 2007; Ruhl *et al.*, 2014).

The relative contribution of Holothuroidea to the total benthic respiration depends on the supply of POC to the system (Ruhl *et al.*, 2014). In food-limited abyssal plains such as at Station M, model estimates indicated that Holothuroidea contribute between 1.44% and 2.42% to the total community respiration (Dunlop *et al.*, 2016). In the present study, the Holothuroidea contributed even less to the total benthic respiration with an estimated 0.19% of the community respiration of $0.32\pm3.53\times10^{-2}$ mmol O_2 m^{-2} d^{-1}.

4.5.3 Holothuroidea recovery over time

Most Holothuroidea are mobile and move over the sediment or engage in swimming behavior (Miller and Pawson, 1990; Kaufmann and Smith, 1997; Jamieson *et al.*, 2011; Rogacheva, Gebruk and Alt, 2012). Assuming a unidirectional movement of 10 and 65 cm h^{-1} (Kaufmann and Smith, 1997), Holothuroidea would need approximately 8 months to cross the entire DEA, of which only 22% was directly denuded of Holothuroidea (Thiel *et al.*, 1989). Even though Holothuroidea species alternate between unidirectional movement, a run-and-mill strategy and loops (Kaufmann and Smith, 1997), recolonization based on movement alone can be expected within 1 yr. Hence, the recovery period reported in this study (3 yr for a partial recovery and >20 yr for full recovery) are comparatively long, which warrants further consideration.

Deposit-feeding Holothuroidea depend on organic compounds from the sediment (Amaro *et al.*, 2010) and some species feed selectively on fresh organic detritus (FitzGeorge-Balfour *et al.*, 2010) and pigment-rich organic matter (Hudson *et al.*, 2005). Additionally, movement activity of Holothuroidea has been linked to their search for patchily-distributed high-quality organic resources, including fresh phytodetritus (Smith, Matthiopoulos and Priede, 1997). Food conditions in the disturbance tracks are thought to be unfavorable due to a dilution of high-quality organic matter by the ploughing disturbance (e.g., protein concentrations 0.5 yr post-disturbance at undisturbed sites: 6.86 ± 3.59 g protein m^{-2} and at disturbed sites: 3.59 ± 1.53 g protein m^{-2}; Forschungsverbund Tiefsee-Umweltschutz, unpubl.). Hence, one would expect that Holothuroidea would respond to these poorer food conditions by active emigration out of the disturbance tracks, leaving their densities in the disturbance tracks reduced compared to the surrounding sediments (i.e., outside plough tracks and reference sites). So, even though Holothuroidea have the capacity to recolonize the disturbed area in due time, recolonization may lag behind due to unfavorable food conditions. We speculate that this may explain the relatively long recovery periods found in our study.

However, holothurians are also selective for the finer sediment particle fraction (Khripounoff and Sibuet, 1980) and therefore a change in the sediment particle size and composition in disturbance tracks could reduce the recolonization speed as well.

4.6 Outlook to deep-sea mining impacts

We found that Holothuroidea abundance, community composition, and respiration activity recovered from a small-scale disturbance event in the Peru Basin on an annual to decadal scale. However, the results of this study cannot be directly extrapolated to mining scenarios, as they describe the recovery of one mobile conspicuous taxon only and other taxonomic groups, especially those of sessile organisms, will have very different recovery rates. Recovery also occurred in a relatively lightly disturbed area of only 10.8 km^2, whereas a single mining operation will likely remove polymetallic nodules from an area between 300 km^2 and 800 km^2 per year (Smith *et al.*, 2009). The type of disturbance examined here (sediment and nodules ploughing with little removal of the upper sediment) is also not representative of an actual mining activity, which will be associated with nodule and surface sediment removal (Thiel and Forschungsverbund Tiefsee-Umweltschutz, 2001). Furthermore, the CCZ is a key target area for deep-sea mining and spans across a range of trophic settings, which may delay recovery, and potentially cumulative effects, such as overlapping mining plumes from nearby mining operations or climate change-related shifts in POC export fluxes (Levin *et al.*, 2016; Sweetman *et al.*, 2017; Yool *et al.*, 2017) were not considered in this current study. Ultimately, to gain more knowledge about potential recovery rates of fauna after industrial-scale mining, a scientifically supported industrial test-mining operation in the CCZ is required, and all species of megafauna as well as size classes of fauna should be monitored for several decades after resource extraction.

Acknowledgments

The authors thank PI Antje Boetius, Felix Janssen, the scientific party, the captain and crew of R/V *Sonne* as well as the ROV Kiel 6000 team from Geomar (Kiel) for their excellent support during cruise SO242-2. We thank the editor and two anonymous reviewers for their comments that helped to improve a previous version of this manuscript.

4.7 Supplement

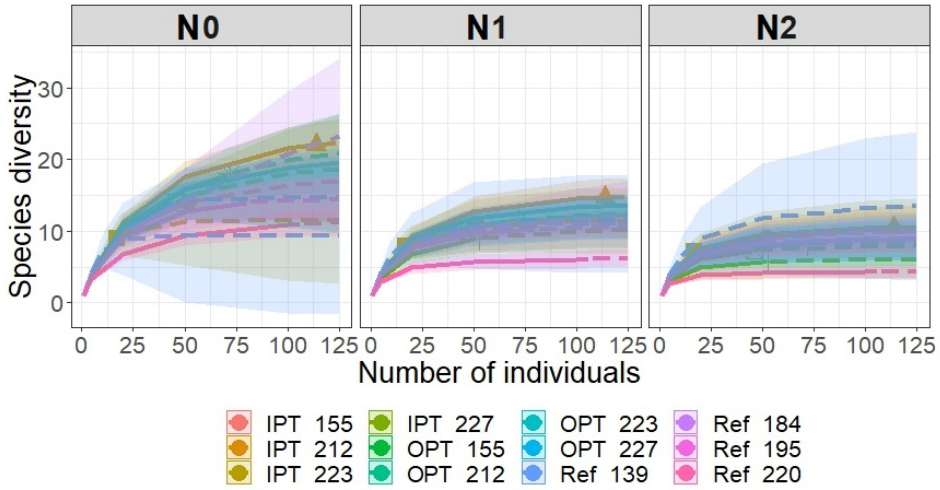

Supplementary figure 4-1. Individual-based rarefaction (solid lines) and extrapolation (dashed lines) curves for the Hill numbers N_0 (left panel), N_1 (middle panel), and N_2 (right panel). Shaded areas show the 95% confidence intervals for each sample (the sample numbers correspond to the OFOS transects in table 4-2).
Abbreviations are: IPT = inside plough tracks within DEA, OPT = outside plough tracks within DEA, Ref = reference sites.

Chapter 5 : Has phytodetritus processing by an abyssal soft-sediment community recovered 26 yr after an experimental disturbance?

5. Has phytodetritus processing by an abyssal soft-sediment community recovered 26 yr after an experimental disturbance?

Tanja Stratmann[1], Lisa Mevenkamp[1], Andrew K. Sweetman, Ann Vanreusel, and Dick van Oevelen;
Modified from *Frontiers in Marine Sciences*, 2018: 5:59. doi: 10.3389/fmars.2018.00059.

5.1 Abstract

The potential harvest of polymetallic nodules will heavily impact the abyssal, soft sediment ecosystem by removing sediment, hard substrate, and associated fauna inside mined areas. It is therefore important to know whether the ecosystem can recover from this disturbance and if so, at which rate. The first objective of this study was to measure recovery of phytodetritus processing by the benthic food web from a sediment disturbance experiment that was carried out in 1989. The second objective was to determine the role of holothurians in the uptake of fresh phytodetritus by the benthic food web. To meet both objectives, large benthic incubation chambers (CUBEs; 50×50×50 cm) were deployed inside plough tracks (with and without holothurian presence) and at a reference site (holothurian presence, only) at 4,100 m water depth. Shortly after deployment, ^{13}C- and ^{15}N-labelled phytodetritus was injected in the incubation chambers and during the subsequent 3 d incubation period, water samples were taken five times to measure the production of ^{13}C-dissolved inorganic C over time. At the end of the incubation, holothurians and sediment samples were taken to determine biomass, densities, and incorporation of ^{13}C and ^{15}N into bacteria, nematodes, macrofauna, and holothurians. For the first objective, the results showed that biomass of bacteria, nematodes, and macrofauna did not differ between reference sites and plough track sites when holothurians were present. Additionally, meiofauna and macrofauna coarse taxonomic composition was not significantly different between the sites. In contrast, total ^{13}C uptake by bacteria, nematodes, and holothurians was significantly lower at plough track sites compared to reference sites, though the number of replicates was low. This result suggests that important ecosystem functions such as organic matter processing have not fully recovered from the disturbance that occurred 26 yr prior to our study. For the second objective, the analysis indicated that holothurians incorporated 2.16×10^{-3} mmol labile phytodetritus C m^{-2} d^{-1} into their biomass, which is one order of magnitude less as compared to bacteria, but 1.3 times higher than macrofauna and one order of magnitude higher than nematodes. Additionally, holothurians incorporated more phytodetritus carbon per unit biomass than macrofauna and meiofauna, suggesting a size-dependence in phytodetritus carbon uptake.

[1] These authors have contributed equally to this work.

5.2 Introduction

Abyssal plains, i.e., the ocean floor between 3,000 and 6,000 m water depth, cover more than 50% of the Earth's surface and form the largest ecosystem on Earth (Smith *et al.*, 2008). Although the remote abyssal plains seem to be far away from anthropogenic influences, they experience increased pressure from oil and gas extraction activities and disposal of litter and waste (Ramírez-Llodrà *et al.*, 2011). In the near future, they may also be affected by climate change (Sweetman *et al.*, 2017), as well as by potential deep-sea mineral extraction of polymetallic nodules (Ramírez-Llodrà *et al.*, 2011; Petersen *et al.*, 2016). Polymetallic nodules are potato-like deposits that grow extremely slowly at a rate of millimeters per million years (Guichard, Reyss and Yokoyama, 1978). They are typically found at the sediment surface at an average abundance of 15 kg m^{-2} in the Clarion-Clipperton Fracture Zone (CCZ, NE Pacific), 10 kg m^{-2} in the Peru Basin (SE Pacific) and 4.5 kg m^{-2} in the central Indian Ocean Basin (Kuhn *et al.*, 2017). Nodules provide hard substrate that is essential for some sessile epifauna and associated megafauna (Purser *et al.*, 2016; Vanreusel *et al.*, 2016). The extraction of polymetallic nodules will not only eliminate this hard substrate, but will also disturb and resuspend the surface sediment (Thiel and Forschungsverbund Tiefsee-Umweltschutz, 2001), which is critical for detritus feeding mobile epifauna and the biota that inhabit the sediment (Borowski and Thiel, 1998; Bluhm, 2001; Borowski, 2001).

We presently lack sufficient knowledge to assess if, and at what rate, the ecosystem will recover from these disturbances (Mengerink *et al.*, 2014). The first insights on ecosystem recovery and resilience were provided by small-scale disturbance experiments that have been carried out at several sites in the Pacific and Indian Ocean (Jones *et al.*, 2017). These studies focused on recovery of density and diversity of meiofauna, macrofauna, and megafauna (Ingole *et al.*, 2000; Ahnert and Schriever, 2001; Bluhm, 2001; Borowski, 2001; Ingole, Pavithran and Ansari, 2005). For the DISCOL ("DISturbance and reCOLonization experiment"; Bluhm, 2001) area in the Peru Basin (tropical SE Pacific), in particular, it was found that recovery of megafauna densities after 26 yr was between 11% (Anthozoa) and 167% (Holothuroidea) (Gollner *et al.*, 2017). Macrofauna recovered to 85% within 7 yr (Borowski, 2001) and meiofauna densities after 26 yr had recovered to 90% (Gollner *et al.*, 2017). However, the recovery of key ecosystem functions, such as nutrient cycling, organic matter processing, and secondary production (Thurber *et al.*, 2014) has not been assessed in detail yet.

Pulse-chase experiments using stable isotopically labeled substrates have been used to study ecosystem functioning and food-web dynamics in the deep sea (Middelburg, 2014). These studies are performed either *in situ* with benthic landers (Moodley *et al.*, 2002; Sweetman and Witte, 2008) or *ex situ* with sediment cores onboard research vessels (Guilini *et al.*, 2010). In both approaches phytodetritus, e.g., diatoms or coccolithophores (Jeffreys *et al.*, 2013), or zooplankton fecal pellets (Mayor *et al.*, 2012) that have been enriched in ^{13}C and/ or ^{15}N are added to the benthic ecosystem (*pulse*) to track the uptake and processing of this material by microorganisms, meiofauna, metazoan macrofauna, and

foraminifera (*chase*). Despite the high importance of deep-sea megafauna, dominated by holothurians, as e.g., grazers of labile phytodetritus (Miller *et al.*, 2000; Gallucci, Fonseca and Soltwedel, 2008; Amaro *et al.*, 2010), logistic challenges of deep-sea research have so far hampered the inclusion of megafauna in these stable isotope studies. This represents a major gap in our understanding of abyssal food webs (van Oevelen, Soetaert and Heip, 2012). Due to slow recovery rates and high vulnerability of deep-sea megafauna to mechanical disturbance (Bluhm, 2001; Vanreusel *et al.*, 2016; Stratmann, Voorsmit, *et al.*, 2018/ **Chapter 4**), insight on the contribution of megafauna to important ecosystem functions is particularly relevant in the context of deep-sea mining impact assessments.

In this study, we conducted pulse-chase experiments at the DISCOL experimental area (DEA) to quantify ecosystem recovery of an abyssal ecosystem following a sediment disturbance event that occurred 26 yr prior to our study. The DEA is a 10.8 km^2 large circular area (Bluhm, 2001) that was ploughed diametrically 78 times in 1989 (Foell, Thiel and Schriever, 1990, 1992) to induce a disturbance that would mimic small-scale mining of polymetallic nodules. We deployed newly designed benthic incubation chambers that enabled us to include larger megafauna in pulse-chase studies. A recent visit to the DEA allowed us to assess (1) the recovery of ecosystem functioning in the form of carbon (C) uptake and partitioning 26 yr after a disturbance event and (2) the contribution of holothurians to the total uptake of fresh phytodetritus.

5.3 Material and methods

5.3.1 Design of the benthic incubation chambers

Benthic incubation chambers (henceforth called CUBEs in reference to their cubical design) were designed by the Royal Netherlands Institute for Sea Research with a large Poly(methyl methacrylate) (PMMA) chamber (50×50×50 cm, Figure 5-1A, Supplementary figure 5-1). The CUBEs have an open bottom to enclose a megafaunal specimen on the seafloor. Each CUBE is further equipped with a stirring plate to ensure homogenously mixed water and an injection port with a 30 mL syringe to add a tracer (e.g., phytodetritus or bromide) at a preset time. A rosette with six 35 mL sampling syringes is fitted on the CUBE for repeated water sampling and a 6,000 m-rated oxygen optode (Contros HydroFlash® O_2; Kongsberg Maritime Contros GmbH, Germany) is inserted in the chamber top for continuous oxygen measurements. A titanium housing holds the battery pack, controller board and temperature sensor. The chamber has a PMMA door (22×42 cm) on one side that can be opened and closed by the ROV to allow sampling of enclosed specimens. We also noticed that a deployment with "the door open" significantly minimized sediment disturbance. Four ventilation valves in the top of the CUBE ensure that all air escapes during the descent, but that the CUBE remains sealed at the seafloor. All edges and corners are fortified with a stainless steel 316 frame that ends in a stainless-steel grip bar (total CUBE height: 100 cm). The stirring plate has a diameter of 20 cm, is adjustable in height and has an adjustable stirring capacity from 0 to 100% (0–18 rpm). Stirring tests using uranine as passive tracer for seven different stirring capacities (10%, 20%,

30%, 40%, 50%, 75%, 100%) showed that the uranine concentration reached an equilibrium in the CUBE between 1.5 min (100% stirring capacity) and 6.3 min (10% stirring capacity). This mixing speed is fast enough to consider the water column inside to be homogenously mixed during the incubation. The battery pack consists of 12 D-sized alkaline batteries connected in series (~18 V power if new batteries are used) and supplies power to the motors of the sampling rosette, stirring plate, injection device and O_2 optode. The CUBEs run fully autonomously following a script that is saved on a micro SD or SDHC card and the program is activated when the ROV triggers a start flap, i.e., a flexible plastic flap at the side of the CUBE (Figure 5-1A).

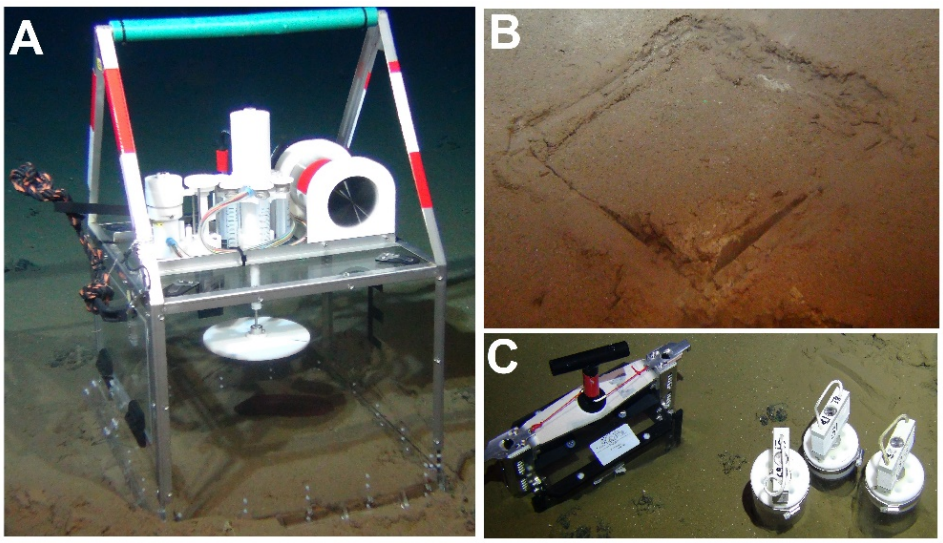

Figure 5-1. *In situ* pulse-chase tracer experiment with holothurian at 4,100 m depth in the Peru Basin. (A) Deployment of the benthic incubator (CUBE) over *Benthodytes* sp. in a plough track in the DEA west. (B) Imprint of CUBE in the sediment after its removal by ROV at the end of the incubation. (C) Sampling of sediment inside the CUBE imprint for macrofauna (bladecorer), meiofauna, bacteria, and sediment characteristics (push cores). Photos by ROV Kiel 6000 (GEOMAR, Kiel, Germany).

5.3.2 Experimental set-up and sampling procedures

The study was conducted during R/V *Sonne* cruise SO242-2 to the DEA (-88.45°E, -7.07°N; Figure 5-2A) in September 2015 and included three different treatments. Two CUBE incubations were performed at the southern reference station (Figure 5-2A, C) with an enclosed holothurian (one identified later as *Benthodytes* sp. and one as *Amperima* sp.) and are henceforth referred to as "Ref+hol". Three incubations were conducted inside the 8-m wide plough tracks (Figure 5-2A, B) each enclosing a holothurian (identified later as twice *Amperima* sp. and *Peniagone* sp. and will be referred to as "PT+hol") and two incubations inside the plough tracks without a holothurian, referred to as "PT-hol". We note that this (unbalanced) experimental design was a compromise following from practical and logistical limitations, while allowing us to focus on ecosystem

recovery (“Ref+hol” vs. “PT+hol”) and the impact of holothurians (“PT+hol” vs. “PT-hol”).

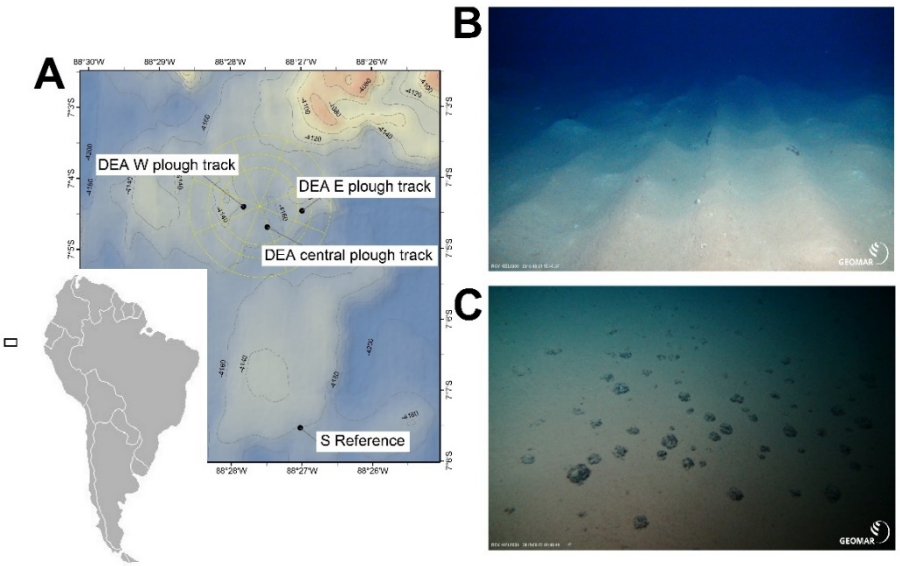

Figure 5-2. Map of the study area in the Peru Basin/ SE Pacific (A) with photos of the seafloor at ~4,100 m water depth. (B) Plough tracks at DISCOL experimental area (DEA) west are still visible after 26 yr. (C) Undisturbed seafloor in the southern reference site outside DEA. Photos were taken by ROV Kiel 6000 (GEOMAR, Kiel, Germany). The black square in (A) indicates the location of the sampling area in the Pacific but is un-scaled.

The CUBEs were deployed on a dedicated lander (i.e., the elevator; Linke, 2011) that was placed at a specific location (reference site, disturbed site within a plough track) using a video-guided release system. The ROV KIEL 6000 lifted a CUBE from the elevator and placed it gently over a holothurian to trap it (Figure 5-1A, treatments “PT+hol” and “Ref+hol”) or directly on the seafloor (treatment “PT-hol”). The incubation was subsequently started by moving the start flap. Each CUBE deployment lasted 3 d. The first water sample was taken after 45 min, followed by the injection of 0.5 g dry weight (DW) (equivalent to 40 mmol C m^{-2} and 5 mmol N m^{-2}) freeze-dried *Skeletonema costatum* (29 at% ^{13}C and 37 at% ^{15}N). Stirring capacity was increased from 50% to 100% for 10 min and then stopped for 45 min to allow for a homogeneous settling of the freeze-dried diatoms. Afterwards, stirring was set to 25% and subsequently water samples were taken at 0.07, 1, 2, and 3 d after the start of the incubation. Unfortunately, oxygen concentrations could not be measured due to the sensor malfunctioning. At the end of the experiment, the side door of the CUBE was opened, and the holothurian was carefully sampled with the suction sampler into the suction container of the ROV. The CUBE was lifted and put aside to leave a

clear imprint in the sediment (Figure 5-1B). A bladecorer (20.5×9×30 cm; designed by Max Planck Institute for Marine Microbiology, Germany) for macrofauna sampling was pressed into the sediment at a random place within the imprint square and released. The bladecorer was left in place until three push cores were taken from within the experimental area to minimize sediment disturbance (Figure 5-1C).

Aboard R/V *Sonne*, the water samples were filtered through a 0.2 µm syringe filter in 20 mL headspace vials for DIC and ^{13}C-DIC concentration analysis and preserved by the addition of 20 µL 0.24 mol L^{-1} $HgCl_2$. The overlying water from the push cores was carefully siphoned off and sieved (32 µm). Subsequently, the cores were sliced in 0–2 and 2–5 cm intervals in a climate room at *in situ* temperature (2.9°C) and meiofauna from the overlying water was added to the 0–2 cm layer. The different sediment layers of the three push cores from a single CUBE deployment were pooled and homogenized to reduce spatial variability and ensure sufficient amounts of sediment for the planned analyses. Subsequently, two 35 mL subsamples were taken and stored frozen at -21°C for bacterial specific phospholipid-derived fatty acid (PLFA) analysis, sediment porosity, bulk N/^{15}N and organic C/^{13}C determination. The remaining sediment was fixed in 4% borax-buffered formaldehyde for meiofauna analysis (abundance and isotope enrichment). The upper 5 cm of the sediment in the bladecorer was sieved over a 500 µm sieve with filtered seawater (0.7 µm) at *in situ* temperature. All macrofauna were fixed in 4% borax-buffered formaldehyde.

5.3.3 Sediment analysis

Sediment porosity was determined by the weight difference between wet sediment and freeze-dried sediment assuming a sediment density of 2.55 g cm^{-3} (Haeckel *et al.*, 2001) The organic C/^{13}C and N/^{15}N of ~20 mg freeze-dried, acidified sediment was measured with at Thermo Flash EA 1112 elemental analyzer (EA; Thermo Fisher Scientific, USA) coupled to a DELTA V Advantage Isotope Ratio Mass Spectrometer (IRMS; Thermo Fisher Scientific, USA).

5.3.4 Bacteria analysis

Bacterial biomass and incorporation of phytodetritus ^{13}C into bacteria were determined through the analysis of bacterial-specific PLFAs. Lipids were extracted from ~2.5 g freeze-dried, finely ground sediment with a modified Bligh and Dyer extraction method (Boschker, de Brouwer and Cappenberg, 1999; Moodley *et al.*, 2002). The lipid extract was fractioned into different lipid classes on a silicic-acid column by sequentially eluting with chloroform (neutral lipids), acetone (glycolipids), and methanol (polar lipids). The polar lipid fraction was derivatized to fatty acid methyl esters (FAME) and measured on a HP 61530 gas chromatograph (Hewlet Packard/ Agilent, USA) coupled with a DELTA-Plus Isotope Ratio Mass Spectrometer (Thermo Fisher Scientific, USA) with a polar analytical column (ZB5-5MS; 60 m length, 0.32 mm diameter, 0.25 µm film thickness; Phenomenex, USA).

The bacterial biomass was calculated based on the concentration of the bacterial specific PLFAs i14:0, i15:0, a15:0, i16:0, and 18:1ω7c, assuming that

these represent 28% of the C in all bacterial PLFA and that PLFAs represent 6% of the total C in bacterial cells (Middelburg *et al.*, 2000).

5.3.5 Meiofauna analysis

Meiofauna was extracted from sediment by washing the samples over a 32 µm sieve and subsequent density centrifugation of the fraction retained on the 32 µm sieve with Ludox HS40 (Dupont) at 3,000 rpm (specific density of 1.18; Heip, Vincx and Vranken, 1985). The centrifugation was repeated three times, the supernatant was sieved (32 µm) and fixed again in 4% borax-buffered formaldehyde. Meiofauna organisms were counted for density estimates and identified to higher taxon level with a stereomicroscope (50× magnification).

Due to the small body-size of meiofauna, several hundreds of organisms needed to be pooled to have sufficient biomass for the analysis of organic C, ^{13}C, N, and ^{15}N. Therefore, only the most abundant taxon, i.e., nematodes, was analyzed. A total of 500 nematodes were randomly handpicked per sample (or less when not enough nematodes were present in a sample) and transferred to a few drops of Milli-Q water in 8×5 mm silver capsules (pre-combusted for 4 h at 450°C). The samples were dried overnight at 60°C, acidified with 20 µL 2% HCl and dried again at 60°C on a hot plate. Capsules were closed, and organic C and N content was analyzed following the procedure described above for sediment.

5.3.6 Macrofauna analysis

Macrofauna was counted for density estimates and identified to lowest taxonomic level and when possible to family level in case of polychaetes using a stereomicroscope. For the analysis of organic C, ^{13}C, N, and ^{15}N, dried, whole organisms were packed in pre-combusted 8×5 mm silver capsules, measured following the procedure for meiofauna. Unfortunately, 39% of the macrofauna samples were compromised during sample preparation for the elemental analyzer after density determination and had to be discarded.

5.3.7 Megafauna analysis

Individual holothurian specimens were retrieved from the ROV suction containers, measured for length, height, and width and dissected to separate gut and gut contents from the other somatic tissue. All tissue samples were shock frozen in liquid nitrogen and stored at -21°C. After freeze-drying the somatic tissue excluding the gut tissue was manually ground to fine powder and organic C, ^{13}C, N, and ^{15}N were measured in ~2 mg holothurian powder as described above for macrofauna.

For the holothurian biomass determination, wet weight (WW) of each specimen was calculated based on the length (L) of the organism using the length-wet weight relationship $WW = 0.859 \times L^{1.813}$ (n = 13, R^2 = 0.68) identified for intact holothurians from Brown *et al.* (2018). Holothurian WW was converted to DW using a conversion determined for the holothurians in the Peru Basin in Brown *et al.* (2018) ($DW = 0.04 \times WW + 0.13$; n = 13, R^2 = 0.98) and then converted into organic C using the organic C content measured for dried tissue

sample of each individual (C content in holothurians ranged from 1.96% to 9.69%).

5.3.8 DIC analysis

For the analysis of DIC and ^{13}C-DIC, He-gas was injected through the septum into the head-space vials to create a head-space of ~1.5 mL. The sample was acidified with 10 µL concentrated H_3PO_4 per 1 mL water to transform all inorganic C into gaseous CO_2 in the headspace. From the headspace, a 500 µL sample was taken and injected into a Flash 1112 Series elemental analyzer (EA) coupled via a Conflo III to a Thermo Delta V continuous flow isotope ratio mass spectrometer (IRMS) for the analysis of DIC concentration and isotopic composition (Gillikin and Bouillon, 2007).

5.3.9 Calculations

The incorporation (I) of phytodetritus C and N into particulate organic carbon (POC) and particulate nitrogen (PN), i.e., phytodetritus C and N recovered from the sediment, and bacteria, meiofauna, several macrofauna specimen, and megafauna was calculated as follows. The R_{sample} is the ratio of $^{13}C/^{12}C$ or $^{15}N/^{14}N$ in the samples and is calculated based on the $^{13}C/^{15}N$ output of the IRMS:

$$R_{sample} = \left(\frac{\delta^{13}C}{1000+1}\right) \times R_{standard} \text{ or}$$

$$R_{sample} = \left(\frac{\delta^{15}N}{1000+1}\right) \times R_{standard}, \qquad \text{[Equation 5-1]}$$

where $R_{standard}$ for C is 0.0111802 and for N it is 0.0036782. The fraction (F) of the heavy isotopes ^{13}C and ^{15}N in the sample (F_{sample}) and background ($F_{background}$) material is calculated as:

$$F = \frac{^{13}C}{\left(^{13}C + ^{12}C\right)} = \frac{R}{(R+1)}. \qquad \text{[Equation 5-2]}$$

The incorporation of phytodetrital C and N (I) is:

$$I = \left(F_{sample} - F_{background}\right) \times \frac{total\ C\ or\ N\ pool}{phytodetritus\ enrichment}. \qquad \text{[Equation 5-3]}$$

Macrofauna incorporation rates could not be estimated for all incubations due to unfortunate sample loss (see above). Therefore, the total phytodetritus C and N incorporation rate is defined as the sum of bacteria and nematode phytodetritus C and N incorporation in the top (0–2 cm) and bottom sediment layer (2–5 cm) plus the phytodetritus C and N incorporation into holothurians.

The bulk carbon:nitrogen-ratio (C_{bulk}:N_{bulk}-ratio) of organisms (meiofauna and macrofauna) or somatic tissue (holothurians) and phytodetritus was calculated as the molar ratio. The C_{uptake}:N_{uptake}-ratio was calculated as incorporation of phytodetritus C in the organism divided by the incorporation of phytodetritus N in the organism.

The total biomass of nematodes was calculated as the biomass of an individual nematode (C content of individual nematode = C content of number of measured nematodes divided by number of measured nematodes) times the density of nematodes in the sediment that was determined during counting of meio-

fauna. The biomass of macrofauna was calculated as the taxon-specific (polychaetes, arthropods, nematodes) macrofauna density times the average taxon-specific individual biomass.

5.3.10 Statistical analysis

Due to the low number of replicates (n = 2 for Ref+hol, n = 3 for PT+hol, n = 2 for PT-hol), differences in density, biomass and ecosystem functioning, i.e., phytodetritus C and N uptake and phytodetritus C-DIC production, between treatments were assessed by comparing the 83.4% confidence intervals (CI). These 83.4% CI were calculated by bootstrapping 10,000 boots-trap replicates using the *boot* package in R (Canty and Ripley, 2017) and represent a type 1 error probability (α) of 0.05 (Knol, Pestman and Grobbee, 2011). This means that the difference in means between treatments is statistically not significant for $\alpha = 0.05$ when the 83.4% CI overlap. Data are presented as mean with lower 83.4% CI–upper 83.4% CI, except for contributions to total density or uptake which are presented as mean±SD. The C_{uptake}:N_{uptake}-ratios and C_{uptake}:N_{uptake}-ratio were presented as median with 1st quantile and 3rd quantile.

For the analysis of differences in benthic community composition between treatments, the density data of meiofauna and macrofauna of the upper 5 cm were combined and square-root transformed before applying the "Analysis of Similarities" (ANOSIM) routine for Bray-Curtis similarity in PRIMER 6 (Clarke and Gorley, 2006).

A one-sample Wilcoxon signed-rank test on $\log_{10}$-transformed data was conducted to determine whether the difference between the median C_{uptake}:N_{uptake}-ratio of nematodes, macrofauna or holothurians combined for all sites and the C_{uptake}:N_{uptake}-ratio of the added phytodetritus were significant.

5.4 Results

5.4.1 Visual inspection of the sites

Plough marks from the 26 yr-old disturbance were clearly visible as several centimeter-high ripples and valleys (Figure 5-2B). The sediment surface inside the plough tracks was a mosaic of original brownish surface sediment and white patches originating from sediment that was turned upside down during ploughing. The ploughing effectively buried the polymetallic nodules into the sediment leaving the plough tracks cleared of the typical hard substrate-providing surface nodules. In contrast, the reference site (Figure 5-2C) had a very smooth brown sediment surface with a homogenous distribution of surface polymetallic nodules.

5.4.2 Benthic biomass, density, and community composition

Based on the 83.4% CIs, mean biomass of bacteria and macrofauna (Table 5-1) in the upper 5 cm of sediment did not differ between reference site, plough track site, or presence of holothurians. In contrast, the mean nematode biomass in the lower (2–5 cm) sediment layer differed significantly between treatments PT-hol [0.22 (0.21–0.22) mmol C m^{-2}] and Ref+hol [0.19 (0.19–

0.20) mmol C m^{-2}], but not between PT+hol and PT-hol or Ref+hol in the same sediment layer. Also, the mean nematode biomass in the upper sediment layer (0–2 cm) was not different between the reference sites, plough track site or presence of holothurians.

Table 5-1. Mean biomass and (lower 84.3% CI–upper 84.3% CI) (mmol C m^{-2}) of bacteria, nematodes, and macrofauna in the three different treatments Ref+hol (incubation at reference station outside DEA including holothurians), PT+hol (incubation inside plough tracks inside DEA including holothurians), and PT-hol (incubation inside plough tracks inside DEA without holothurians).

		Bacteria biomass	**Nematodes biomass**	**Macrofauna biomass**
PT+hol	0–2 cm	13.81 (8.21–19.45)	0.27 (0.19–0.34)	
	2–5 cm	10.90 (2.47–19.20)	0.24 (0.15–0.33)	
	0–5 cm			0.94 (0.58–1.29)
PT-hol	0–2 cm	13.98 (11.44–16.52)	0.31 (0.15–0.46)	
	2–5 cm	17.82 (8.67–26.89)	0.22 (0.21–0.22)	
	0–5 cm			1.08 (0.37–1.79)
Ref+hol	0–2 cm	11.77 (11.73–11.81)	0.20 (0.16–0.24)	
	2–5 cm	12.73 (9.32–16.12)	0.19 (0.19–0.20)	
	0–5 cm			1.90 (0.94–2.85)

Total mean meiofauna density was not significantly different between the treatments based on the 83.4% CI (Table 5-2). Nematodes contributed most to the total meiofauna density in the upper 5 cm of sediment (Ref+hol: 88.43±0.19%, PT+hol: 90.62±1.36%, PT-hol: 88.33±0.52%), followed by harpacticoid copepods (Ref+hol: 5.74±0.70%, PT+hol: 5.01±1.09%, PT-hol: 6.98±0.11%), and nauplii (Ref+hol: 4.01±0.77%, PT+hol: 2.92±0.67%, PT-hol: 3.13±0.58%).

Based on the 83.4% CI the total macrofauna densities of the different treatments were significantly different from each other (Table 5-2). About 25% of the macrofauna consisted of polychaetes at Ref+hol (26.14±1.61%) and PT+hol (25.40±9.91%). At PT-hol, polychaetes contributed only 8.33±0.00% to the total macrofauna density and the macrofauna assemblage was dominated by harpacticoids (33.33±0.00%), followed by isopods, tanaids, and nematodes that contributed each 12.50±5.89% to the total macrofauna density. Large nematodes were the second largest contributor to macrofauna density in the Ref+hol treatment (21.59±4.82%), whereas this role was taken by ostracods in the PT+hol

treatment (15.08±14.35%). When the combined meiofauna and macrofauna species composition in the upper 5 cm was compared, no significant difference was detected between the three treatments (ANOSIM: p = 0.87).

Table 5-2. Total mean density and (lower 84.3% CI–upper 84.3% CI) of meiofauna (ind. 10 cm^{-2}) and macrofauna (ind. m^{-2}) in the three different treatments Ref+hol (incubation at reference station outside DEA including holothurians), PT+hol (incubation inside plough tracks inside DEA including holothurians), and PT-hol (incubation inside plough tracks inside DEA without holothurians).

		Meiofauna density	Macrofauna density
PT+hol	0–2 cm	122 (108–136)	
	2–5 cm	81 (52–111)	
	0–5 cm		363 (343–383)
PT-hol	0–2 cm	118 (82–155)	
	2–5 cm	52 (43–61)	
	0–5 cm		654 (654–654)
Ref+hol	0–2 cm	108 (101–114)	
	2–5 cm	62 (56–69)	
	0–5 cm		518 (439–599)

5.4.3 Phytodetritus processing

The total mean amount of phytodetritus C (mmol C m^{-2}) that was incorporated into bacteria, nematodes, and holothurians (if present) was 0.39 (0.56–1.42) in the PT-hol treatment, 0.99 (0.57–1.43) in the PT+hol treatment, and 2.36 (1.80–2.91) in the Ref+hol treatment (Figure 5-3A-C). Based on the 83.4% CI, phytodetritus C uptake by bacteria (mmol C m^{-2}) in the upper sediment layer was significantly different between Ref+hol (0.27–0.45) and PT-hol (0.13–0.27). In the lower sediment layer phytodetritus C uptake by bacteria (mmol C m^{-2}) differed significantly between Ref+hol (0.46–0.51) and PT+hol (0.01–0.04) and between Ref+hol (0.27–0.45) and PT-hol (0.04–0.34). Nematodes in the 0–2 cm sediment layer from the PT-hol treatment (1.10×10^{-3}–1.90×10^{-3} mmol C m^{-2}) incorporated significantly more phytodetritus C than nematodes from the same sediment layer of the Ref+hol treatment (6.00×10^{-4}–9.00×10^{-4} mmol C m^{-2}). In the 2–5 cm sediment layer, the uptake of phytodetritus C (mmol C m^{-2}) by nematodes was in the same range at Ref+hol [4.50×10^{-4} (3.00×10^{-4}–6.00×10^{-4})] and PT+hol [4.33×10^{-4} (3.00×10^{-4}–6.00×10^{-4})], but less than at PT-hol [8.50×10^{-4} (6.00×10^{-4}–1.10×10^{-3})].

Holothurians incorporated (not significantly) more phytodetritus C in treatment Ref+hol [1.52 (1.03–2.00) mmol C m^{-2}] than in treatment PT+hol [0.71 (0.29–1.11) mmol C m^{-2}], but they had also a smaller biomass (mmol C ind^{-1}) in the latter [Ref+hol: 122 (115–129); PT+hol: 36.8 (28.6–44.9)]. Most of the phytodetritus C (mmol C m^{-2}) that was added to the CUBEs was recovered in the sediment (POC) [Ref+hol: 5.02 (5.01–5.03), PT+hol: 7.29 (2.76–11.80), PT-hol: 6.47 (4.91–8.01); Figure 5-3D] and in the gut content of holothurians [Ref+hol: 0.84 (0.02–1.64), PT+hol: 0.43 (0.03–0.82)]. Respiration of phytodetritus C-DIC (mmol C m^{-2}) occurred linearly over time (Figure 5-4) and after 3 d of incubation

it was 3.19 (2.97–3.42) at PT-hol, 2.22 (1.59–2.86) at PT+hol and 3.07 (2.65–3.49) at Ref+hol (Figure 5-3E). Hence, based on the 83.4% CI, phytodetritus C-DIC respiration was significantly lower in treatment PT+hol compared to treatment PT-hol.

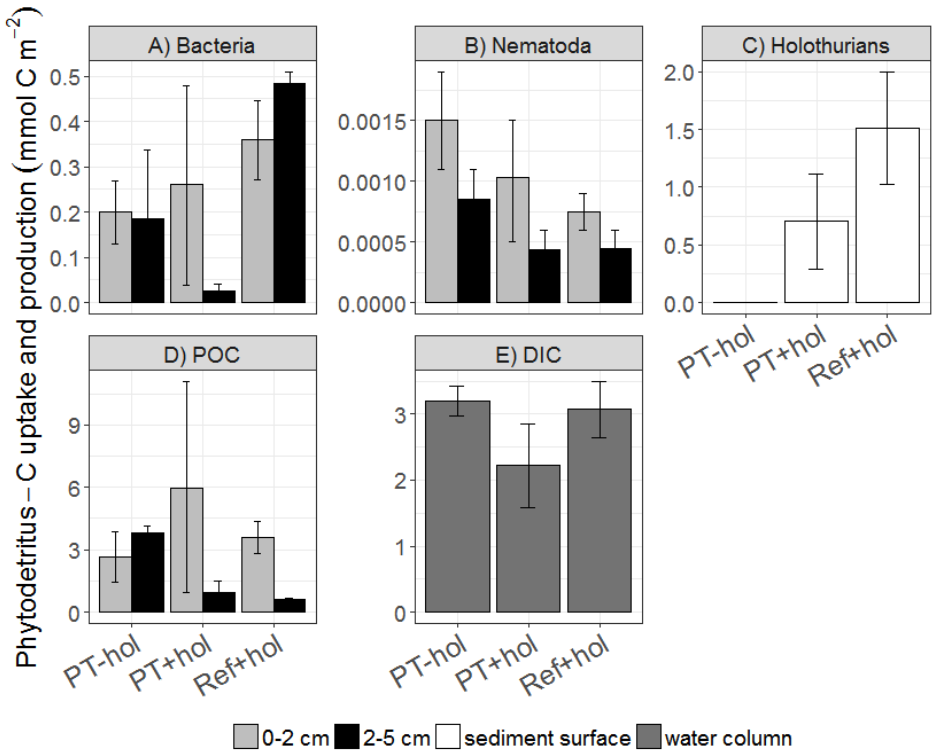

Figure 5-3. Uptake and production of phytodetritus C (in mmol C m^{-2}) (A) bacteria, (B) Nematoda, (C) holothurians, (D) POC, i.e., phytodetritus C recovered from the sediment, and (E) DIC per sediment depth interval (in cm) and treatment. Error bars show the 83.4% confidence intervals. PT-hol, incubation inside plough tracks inside DEA without holothurian; PT+hol, incubation inside plough tracks inside DEA including holothurians; Ref+hol, incubation at the reference station outside DEA including holothurians.

Nematodes incorporated between 8.52×10^{-7} (5.83×10^{-7}–1.12×10^{-6}) mmol N m^{-2} phytodetritus N (PT+hol) and 1.51×10^{-6} (1.23×10^{-6}–1.78×10^{-6}) mmol N m^{-2} phytodetritus N (PT-hol; Figure 5-5) and therefore significantly less phytodetritus N at PT+hol than at PT-hol. Holothurians took up 0.15 (0.04–0.26) mmol N m^{-2} phytodetritus N in treatment PT+hol and 0.31 (0.20–0.41) mmol N m^{-2} phytodetritus N in treatment Ref+hol (Figure 5-5). Between 0.88 (0.36–1.40) mmol N m^{-2} phytodetritus N (PT+hol) and 1.06 (0.73–1.38) mmol N m^{-2} phytodetritus N (Ref+hol) was traced back in the sediment (PN; Figure 5-5).

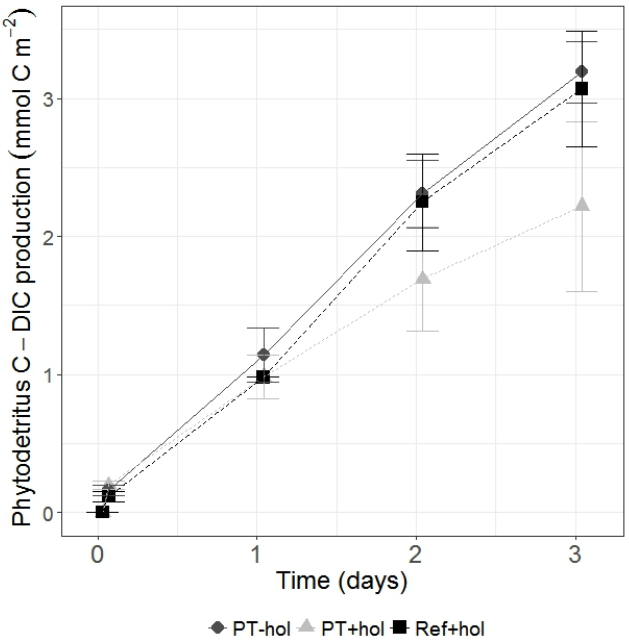

Figure 5-4. Production of phytodetritus C-DIC (in mmol C m^{-2}) over time (in days) for all treatments. Error bars show the 83.4% confidence intervals. PT-hol, incubation inside plough tracks inside DEA without holothurians; PT+hol, incubation inside plough tracks inside DEA including holothurians; Ref+hol, incubation at the reference station outside DEA including holothurians.

5.4.4 C:N-ratio

The phytodetritus that was added in the pulse-chase experiment had a C_{uptake}:N_{uptake}-ratio of 6.54 and C_{bulk}:N_{bulk}-ratio of 7.73. The (median) C_{uptake}:N_{uptake}-ratio of nematodes from both sediment layers combined (n = 7), macrofauna (n = 20), and holothurians (n = 5) was 16.56 (1st quantile: 14.34, 3rd quantile: 7.75), 11.44 (1st quantile: 9.38, 3rd quantile: 18.74), and 4.88 (1st quantile: 4.88, 3rd quantile: 5.06), respectively (Figure 5-6). The C_{bulk}:N_{bulk}-ratios were 7.12 (1st quantile: 6.57, 3rd quantile: 7.68), 5.57 (1st quantile: 3.62, 3rd quantile: 6.27) and 4.48 (1st quantile: 4.46, 3rd quantile: 4.63) for nematodes, macrofauna, and holothurians, respectively. The difference between the median of the $\log_{10}$-transformed C_{uptake}:N_{uptake}-ratios of nematodes, macrofauna, somatic tissue of holothurians, and the $\log_{10}$-transformed C_{uptake}:N_{uptake}-ratio of the added phytodetritus (0.82) was significant for nematodes ($Z = 2.48$, $p = 0.01$) and macrofauna ($Z = 3.92$, $p \leq 0.001$), but not for holothurians ($Z = -0.67$, $p = 0.63$).

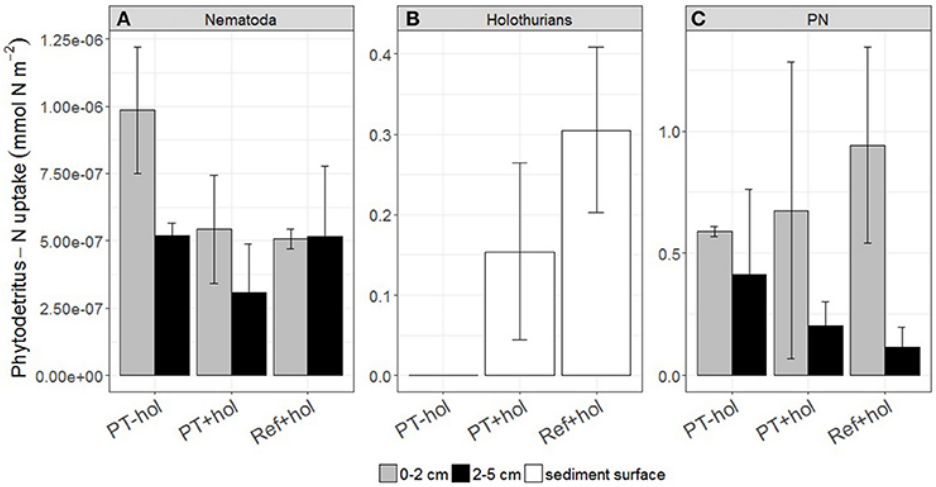

Figure 5-5. Uptake of phytodetritus nitrogen (in mmol N m^{-2}) by (A) Nematoda, (B) holothurians, and (C) particulate nitrogen (PN), i.e., phytodetritus N recovered from the sediment, per sediment depth interval (in cm) and treatment. Error bars show the 83.4% confidence intervals. PT-hol, incubation inside plough tracks inside DEA without holothurians; PT+hol, incubation inside plough tracks inside DEA including holothurians; Ref+hol, incubation at the reference station outside DEA including holothurians.

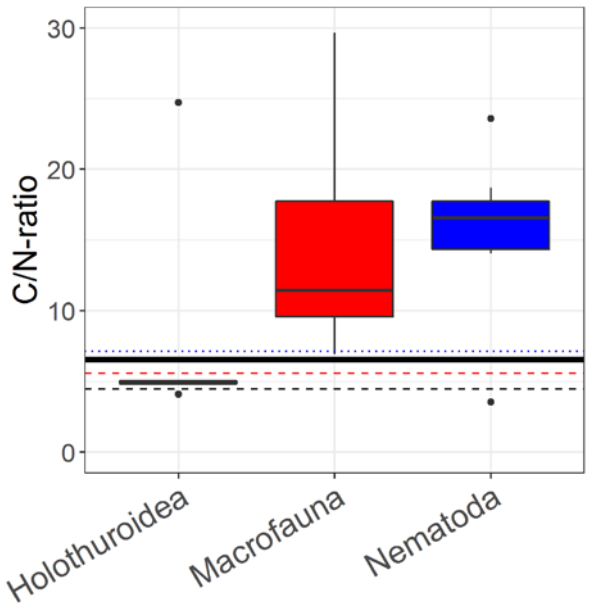

Figure 5-6. Boxplots of the C_{uptake}:N_{uptake}-ratio, i.e., the incorporation of phytodetritus C in the organism divided by the incorporation of phytodetritus N in the organism, of holothurians (n = 5), macrofauna (n = 20) and nematodes (n = 14). The black solid line represents the C:N-ratio of the added phytodetritus (*Skeletonema costatum*), the black dashed line shows the median C:N-ratio, i.e., the molecular C:N-ratio, of somatic tissue of holothurians, the red dashed line shows the median C:N-ratio of macrofauna, and the blue dotted line the median C:N-ratio of nematodes.

5.5 Discussion

This study shows that the ecosystem function of a previously disturbed seafloor had not completely recovered 26 yr post-disturbance. Here we relate these results to other studies on small-scale deep-sea disturbances. We also compare the processing of labile phytodetritus by the benthos with similar pulse-chase studies and discuss the role of holothurians in deep-sea ecosystem functioning.

5.5.1 Recovery of ecosystem functioning from deep-sea mining

As ecosystem functions in the deep sea are often interrelated to ecosystem services, such as nutrient regeneration and fisheries (Thurber *et al.*, 2014), it is of major concern to decipher which processes of ecosystem functioning are able to recover from deep-sea mining and over what timescales. However, only few studies on ecosystem functions in deep-sea disturbance experiments have been conducted so far, hence a direct comparison between studies is cumbersome.

Our study showed that the bacteria in the 2–5 cm sediment layer did not incorporate phytodetritus C in equal amounts at reference sites compared to plough track sites. This is intriguing, because bacteria can incorporate up to 32% of the total processed label at the Pakistan margin (Woulds *et al.*, 2009) and contribute 74% to total sediment community oxygen consumption at the lower continental slope and in abyssal plains (Heip *et al.*, 2001). Reasons for this difference could be a varying level of sediment reworking by the holothurians inside the CUBEs that made more or less phytodetritus accessible to the subsurface bacteria or a different bacteria composition in the 2–5 cm sediment layer. During the ploughing of the seafloor in 1989 parts of the surface sediment were removed and sediment was relocated inside the plough tracks. Hence, the sediment of the 2–5 cm layer in the reference area may be different from the 2–5 cm layer inside the plough tracks. This sediment difference may also cause a concurrent difference in the bacterial composition.

When comparing the total amount of phytodetritus C incorporated in bacteria and nematodes in the upper 5 cm of sediment and taken up by holothurians, the uptake was significantly lower at plough track sites compared to reference sites. This difference might be caused by lower, though not significantly, uptake of phytodetritus C by holothurians at the plough track site compared to the reference site. However, it might also indicate that ecosystem function in the form of phytodetritus C processing takes more than 26 yr in the DEA to recover from the small-scale disturbance experiment in 1989. In contrast, ecosystem function in the form of respiration of large megafauna, i.e., holothurians, in the DISCOL area recovers faster. Stratmann, Voorsmit, *et al.* (2018)/ **Chapter 4** compared the respiration rates of holothurians in plough tracks inside DEA ("disturbed") with the respiration rates of holothurians outside plough tracks inside DEA ("undisturbed") and with rates from holothurians at reference sites ("reference") ~4 km away from DEA. Measured rates of oxygen consumption were not significantly different at the disturbed, undisturbed, and reference sites, indicating holothurian community respiration recovery within 26 yr.

While future deep-sea mining is unlikely in the Peru Basin, exploration licenses have been issued in the CCZ. Here, ecosystem functioning in the form of nutrient cycling and sediment community oxygen consumption was reported for the French claim of the CCZ (Khripounoff *et al.*, 2006). The authors deployed a benthic lander at a reference station and inside a 2.5 m-wide mining track, which was created in 1978 by dredging away the upper 4.5 cm of the sediment during a small-scale deep-sea mining experiment (Khripounoff *et al.*, 2006). Sediment community oxygen consumption and nutrient fluxes of silicate, nitrate, and phosphate were not different between the reference and disturbed location 26 yr after the disturbance (Khripounoff *et al.*, 2006), leading the authors to conclude that ecosystem functioning in terms of nutrient cycling had recovered.

Although these studies indicate that ecosystem function recovery takes at least 26 yr, time scales for recovery from industrial-scale deep-sea mining scenarios will likely be much longer. The DISCOL experiment was conducted in a relatively lightly disturbed area of 10.8 km^2, of which only about 22% were ploughed within a month (Thiel *et al.*, 1989). In contrast, a single mining operation will likely remove polymetallic nodules over an area of 300 to 800 km^2 per year (Smith *et al.*, 2009) and last for 15–30 yr (Levin *et al.*, 2016). Moreover, we did not take cumulative effects of deep-sea mining into account, such as the overlap of sediment plumes from close-by mining operations, changes in POC export fluxes due to climate change or biodiversity loss due to deep-sea mining (Levin *et al.*, 2016; Sweetman *et al.*, 2017; Van Dover *et al.*, 2017; Yool *et al.*, 2017).

5.5.2 Role of holothurians in labile phytodetritus processing

Another main objective of our study was to quantify the role of holothurians in phytodetritus processing. Due to an unfortunate loss of macrofauna samples, we have insufficient data to determine the total phytodetritus uptake by macrofauna except for one deployment. In this deployment (PT+hol), the macrofauna incorporated a total of 1.66×10^{-3} mmol phytodetritus C m^{-2} d^{-1} (0.4% of total uptake), suggesting that macrofauna play a comparatively limited role in the phytodetritus uptake in the Peru Basin. This is also supported by a comparison with *in situ* studies on short-term phytodetritus processing by Woulds *et al.* (2009). At sites between 1,200 and 1,850 m at the Pakistan margin metazoan macrofauna took up between (mean±SD) 1±0.5 and 4±1% of the processed label (Woulds *et al.*, 2009). Therefore, the role of holothurians in the processing of phytodetritus at the DISCOL site can be estimated by neglecting the missing macrofauna contribution. However, this will overestimate the importance of holothurians, because the megafauna density in the CUBEs (1 holothurian specimen 0.25 m^{-2}, extrapolated to 4 holothurian specimen 1 m^{-2}) is two orders of magnitudes higher than under natural conditions (0.02 holothurian specimen m^{-2}; Stratmann, Voorsmit, *et al.*, 2018/ **Chapter 4**). To correct for the scale-effect of the incubation chamber and allow translation of the results to natural conditions, we multiplied the average holothurian uptake (0.09 mmol phytodetritus C $ind.^{-1}$ d^{-1}) with the holothurian density in the Peru Basin (240 ind. ha^{-1}; Stratmann, Voorsmit, *et al.*, 2018/ **Chapter 4**) to find a daily uptake of phytodetritus C by holothurians of 2.16×10^{-3} mmol phytodetritus C m^{-2} d^{-1}. Hence, based on data

from the PT+hol treatment, the contribution of holothurian incorporation of labile phytodetritus to the total uptake of this C pool in the Peru Basin is one order of magnitude lower than the contribution of bacteria (7.30×10^{-2} mmol phytodetritus C m^{-2} d^{-1}), but one order of magnitude higher than the contribution of nematodes (4.80×10^{-4} mmol phytodetritus C m^{-2} d^{-1}). It is also 1.3 times larger than the contribution of macrofauna (1.66×10^{-3} mmol phytodetritus C m^{-2} d^{-1}) assuming that the uptake measured for this specific incubation is representative for the whole experiment. Even though bacterial uptake is one order of magnitude higher than the megafauna uptake, the uptake of megafauna is the highest of the metazoans suggesting that their activity should be considered in the structure of deep benthic food webs.

5.5.3 Size-class dependent uptake of phytodetritus

Because half of the labile detritus that reached the seafloor on the Porcupine Abyssal Plain (PAP) in the NE Atlantic was modeled to be available for deposit feeders (Durden *et al.*, 2017), it is interesting to investigate which size class of metazoan deposit-feeding benthos will most likely benefit from it. Levin *et al.* (1999) hypothesized that larger macrofauna organisms have better access to freshly deposited organic matter than smaller macrofauna organisms and therefore would be first in taking it up. These authors tested this hypothesis in one of the first *in situ* tracer studies at the North Carolina slope (NE Atlantic). The regression of dry weight of macrofauna against diatom tracer uptake across taxa showed no relation with macrofaunal body size (Levin *et al.*, 1999). However, the tested size was limited to macrofauna (>300 µm), whereas in the present study, we studied a substantially broader size spectrum ranging from nematodes/meiofauna (32 µm to 1 mm; 10^{-6} to 10^{-5} mmol C ind^{-1}), macrofauna (>500 µm; 10^{-4} to 10^{-2} mmol C ind^{-1}) to holothurians (>1 cm; 10^{0} to 10^{2} mmol C ind^{-1}) (Figure 5-7). A non-linear regression analysis of these data shows a highly significant positive relationship between individual size B and biomass-specific phytodetritus C uptake I ($I = 0.09B^{0.4}$; $n = 43$, $R^2 = 0.78$; $F_{(1, 42)} = 145.9$, $p \leq 0.0001$). Hence, our results suggest that larger organisms in the deep sea may be more important in exploiting labile phytodetritus than smaller ones and therefore the link between surface productivity and organism productivity might be stronger for larger fauna as opposed to smaller size classes. However, the holothurians we included are selective feeding species, i.e., *Peniagone* sp. and *Amperima* sp. (Wigham *et al.*, 2003; FitzGeorge-Balfour *et al.*, 2010). It will be interesting to find out how strong the correlation between size class and fresh phytodetritus uptake is when other feeding types, such as the fermenters *Psychropotes longicauda* and *Pseudostichopus villosus* (Roberts *et al.*, 2001), conveyor belt feeders or funnel feeders (Massin, 1982), are included.

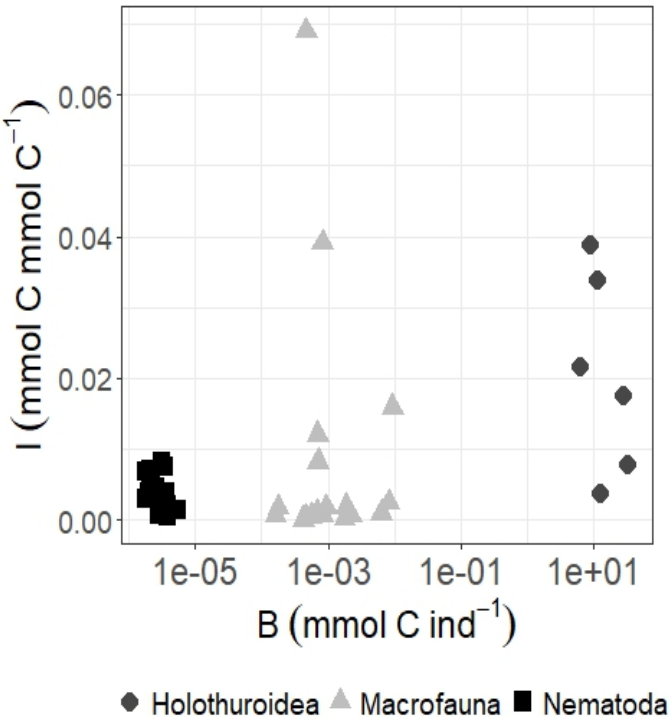

Figure 5-7. Biomass-specific phytodetritus C incorporation *I* (in mmol phytodetritus C mmol C^{-1}) per individual biomass *B* (mmol C ind^{-1}) of holothurians, macrofauna, and Nematoda.

5.5.4 C:N stoichiometry

The results of the faunal uptake data were also explored for a potential size-dependent difference in uptake of phytodetritus C compared to nitrogen. A comparison of C_{uptake}:N_{uptake}-ratio showed that nematodes and macrofauna took up more phytodetritus C relative to phytodetritus nitrogen, whereas holothurians incorporated slightly more phytodetritus nitrogen relative to phytodetritus C when comparing it to the food source *Skeletonema costatum* (Figure 5-6). The C_{uptake}:N_{uptake}-ratio of the incorporated phytodetritus by nematodes and macrofauna was also higher than the bulk chemical composition of their body tissue, suggesting that they retained preferentially more C as compared to nitrogen. Such a dissimilar incorporation has been used to infer C vs. N limitation of benthic organisms. For example, a higher assimilation efficiency or proteinaceous N (mean±SD: 24.6±10.5%) was found for the shallow-water mussel *Mytilus edulis* as compared to carbohydrates (16.7±7.1%) or proteinaceous C (9.5±3.1%) (Kreeger, Hawkins and Bayne, 1996). This led the authors to conclude that *M. edulis* was more nitrogen limited than energy or protein limited, and the higher assimilation efficiency of nitrogen would be a strategy to compensate for the low nitrogen content in their food. Although based on a comparatively short incubation time, the higher C retention as compared to nitrogen by nematodes and

macrofauna may indicate that the nematodes and macrofauna at this specific site are more C or energy limited as opposed to nitrogen limited.

5.6 Conclusion

This is one of the few studies that investigate ecosystem function in an abyssal plain that was previously disturbed by a mimicked deep-sea mining experiment. Despite the low number of replications, the results indicate that the processing of fresh phytodetritus has not fully recovered after 26 yr as the uptake of fresh phytodetritus by bacteria, nematodes, and holothurians is significantly lower in plough tracks compared to reference sites.

Furthermore, the deployment of large (0.25 m^2) benthic incubation chambers allowed to determine the role of holothurians in the uptake of phytodetritus and showed that their uptake is highest compared to the other metazoans (meiofauna, macrofauna). The analysis of size-class dependent uptake of the phytodetritus resulted in a higher biomass-specific uptake of phytodetritus for holothurians than for nematodes implying that for the metabolism of holothurians phytodetritus is relatively more important than for the metabolism of smaller size classes. Additionally, the elevated C:N-ratios of incorporated phytodetritus in nematodes and macrofauna relative to their tissue C:N ratio let us speculate that these benthic organisms are likely more C than N limited at this particular study site.

Acknowledgments

We thank the captain and crew of RV Sonne as well as the ROV Kiel 6000 team from Geomar, Kiel for their excellent support during cruise SO242-2. We are grateful for the technical assistance by Pieter van Rijswijk and Peter van Breugel (NIOZ) and we thank Ina Stratmann (University of Paderborn) for preparing the technical drawing of the CUBE. Yann Marcon (Marum) is thanked for preparing the map of the study site.

5.7 Supplement

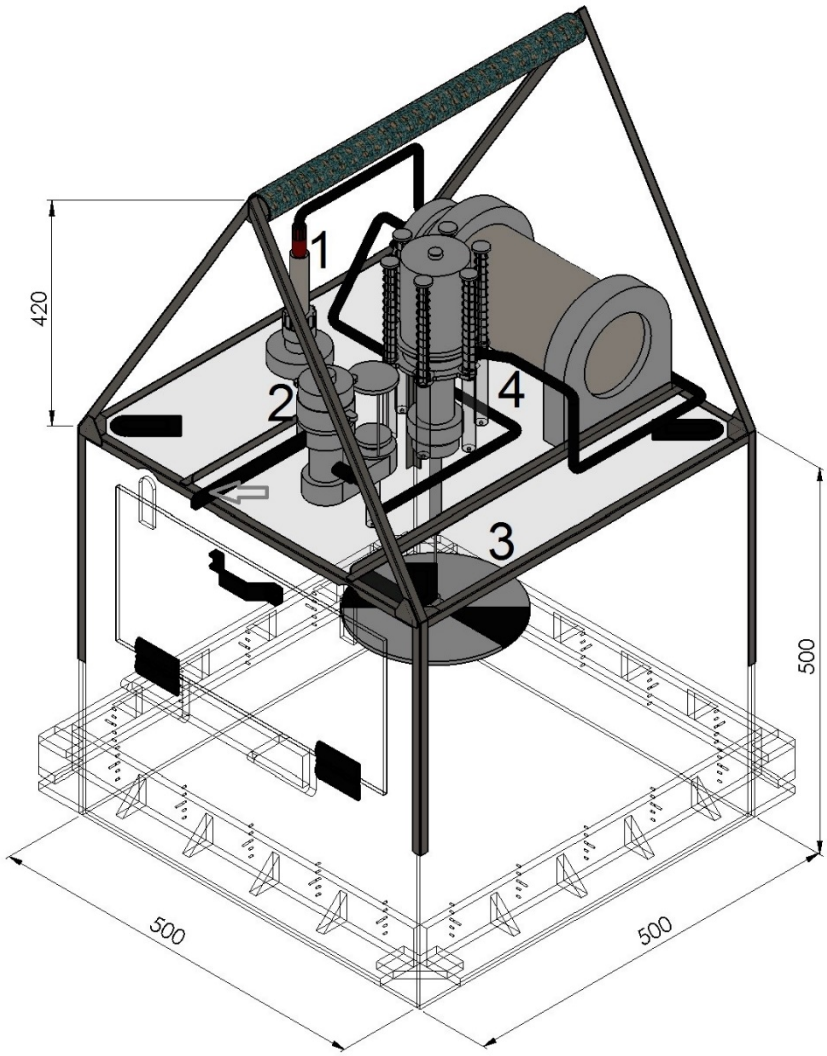

Supplementary figure 5-1. Technical drawing of the benthic incubation chamber CUBE with indicated dimensions given in mm. (1) oxygen optode, (2) injection device with the start flap, (3) stirring plate, (4) sampling rosette six 35 mL sampling syringes. The arrow points towards the start flap.

Chapter 6 : Abyssal plain faunal carbon flows remain depressed 26 yr after a simulated deep-sea mining disturbance

6. Abyssal plain faunal carbon flows remain depressed 26 yr after a simulated deep-sea mining disturbance

Tanja Stratmann, Lidia Lins, Autun Purser, Yann Marcon, Clara F. Rodrigues, Ascensão Ravara, Marina R. Cunha, Erik Simon-Lledó, Daniel O. B. Jones, Andrew K. Sweetman, Kevin Köser, and Dick van Oevelen;
Modified from *Biogeosciences*, 2018: 15: 4131–4145. doi: 10.5194/bg-15-4131-2018.

6.1 Abstract

Future deep-sea mining for polymetallic nodules in abyssal plains will negatively impact the benthic ecosystem, but it is largely unclear whether this ecosystem will be able to recover from mining disturbance and if so, to what extent and at what timescale. During the "DISturbance and recolonization" (DISCOL) experiment, a total of 22% of the seafloor within a 10.8 km^2 circular area of the nodule-rich seafloor in the Peru Basin (SE Pacific) was ploughed in 1989 to bury nodules and mix the surface sediment. This area was revisited 0.1, 0.5, 3, 7, and 26 yr after the disturbance to assess macrofauna, invertebrate megafauna and fish density and diversity. We used this unique abyssal faunal time series to develop carbon-based food-web models for each point in the time series using the linear inverse modeling approach for sediments subjected to two disturbance levels: 1) outside the plough tracks, not directly disturbed by plough, but probably affected by additional sedimentation; and 2) into the plough tracks. Total faunal carbon stock was always higher outside plough tracks compared to in the plough tracks. After 26 yr, the carbon stock in the plough tracks was 54% of the carbon stock outside plough tracks. Deposit feeders were least affected by the disturbance, with modeled respiration, external predation, and excretion rates being reduced by only 2.6% in the plough tracks compared with outside plough tracks after 26 yr. In contrast, the respiration rate of filter and suspension feeders was 79.5% lower in the plough tracks after 26 yr. The "total system throughput" (*T*..), i.e., the total sum of modeled carbon flows in the food web, was higher throughout the time series outside plough tracks compared to the corresponding plough tracks area and was lowest in the plough tracks directly after the disturbance ($8.63\times10^{-3}\pm1.58\times10^{-5}$ mmol C m^{-2} d^{-1}). Even 26 yr after the DISCOL disturbance, the discrepancy of *T*.. between outside and inside plough tracks was still 56%. Hence, C cycling within the faunal compartments of an abyssal plain ecosystem remains reduced 26 yr after physical disturbance, and a longer period is required for the system to recover from such a small-scale sediment disturbance experiment.

6.2 Introduction

Abyssal plains cover approximately 50% of the world's surface and 75% of the seafloor (Ramírez-Llodrà *et al.*, 2010). The abyssal seafloor is primarily composed of soft sediments consisting of fine-grained erosional detritus and biogenic particles (Smith *et al.*, 2008). Occasionally, hard substrate occurs in the form of clinker from steam ships, glacial drop stones, outcrops of basaltic rock, whale carcasses, and marine litter (Kidd and Huggett, 1981; Ruhl, Ellena and Smith, 2008; Ramírez-Llodrà *et al.*, 2011; Radziejewska, 2014; Amon, Hilário, *et al.*, 2017). In some soft-sediment regions, islands of hard substrate are provided by polymetallic nodules, authigenically formed deposits of metals, that grow at approximately of 2 to 20 mm per million years (Guichard, Reyss and Yokoyama, 1978; Kuhn *et al.*, 2017). These nodules have shapes and sizes of cauliflower florets, cannon balls, or potatoes, and are found on the sediment surface and in the sediment at water depths between 4,000 and 6,000 m in areas of the Pacific, Atlantic, and Indian Ocean (Kuhn *et al.*, 2017; Devey *et al.*, 2018).

Polymetallic nodules are rich in metals, such as nickel, copper, cobalt, molybdenum, zirconium, lithium, and rare-earth elements (Hein *et al.*, 2013), and occur in sufficient densities for potential exploitation by commercial mining in the Clarion-Clipperton Fracture Zone (CCZ; equatorial Pacific), around the Cook Islands (equatorial Pacific), in the Peru Basin (E Pacific), and in the central Indian Ocean basin (Kuhn *et al.*, 2017). Extracting these polymetallic nodules during deep-sea mining operations will have severe impacts on the benthic ecosystem, such as the removal of hard substrate (i.e., nodules) and the relatively food-rich surface sediments from the seafloor, physically causing the mortality of organisms within the mining tracks and resettlement of resuspended particles (Thiel and Forschungsverbund Tiefsee-Umweltschutz, 2001; Levin *et al.*, 2016). Choosing appropriate regulations on deep-sea mining requires knowledge on ecosystem recovery from these activities, but to date information on these rates is not extensive, especially on the recovery of ecosystem functions, such as food-web structure and carbon (C) cycling (Vanreusel *et al.*, 2016; Gollner *et al.*, 2017; Jones *et al.*, 2017; Stratmann, Mevenkamp, *et al.*, 2018/ **Chapter 5**; Stratmann, Voorsmit, *et al.*, 2018/ **Chapter 4**).

In the Peru Basin (SE Pacific), a small-scale sediment disturbance experiment was conducted during the "DISturbance and reCOLonization" experiment (DISCOL) in 1989, which was aimed at mimicking deep-sea mining. A 10.8 km^2 circular area (Figure 6-1) was ploughed diametrically 78 times with an 8 m wide plough-harrow; a treatment which did not remove nodules, but disturbed the surface sediment, buried nodules into the sediment and created a sediment plume (Thiel *et al.*, 1989). This experimental disturbance resulted in a heavily disturbed center and a less affected periphery of the DISCOL area (Foell, Thiel and Schriever, 1990, 1992; Bluhm, 2001). Over 26 yr, the region was revisited five times to assess the post-disturbance (PD) situation: directly after the disturbance event, March 1989: hereafter referred to as "$PD_{0.1}$"; 0.5 yr later, September 1989: "$PD_{0.5}$"; 3 yr later, January 1992: "PD_3"; 7 yr later, February 1996: "PD_7"; 26 yr later, September 2015: "PD_{26}". During subsequent visits, densities of macrofauna and invertebrate megafauna were assessed, but data on meiofaunal and microbial

communities were collected only sparsely. Therefore, the food-web models presented in this work cover post-disturbance 1989 (no adequate pre-disturbance sampling took place in 1989) to 2015, and contain only macrofauna, invertebrate megafauna, and fish data.

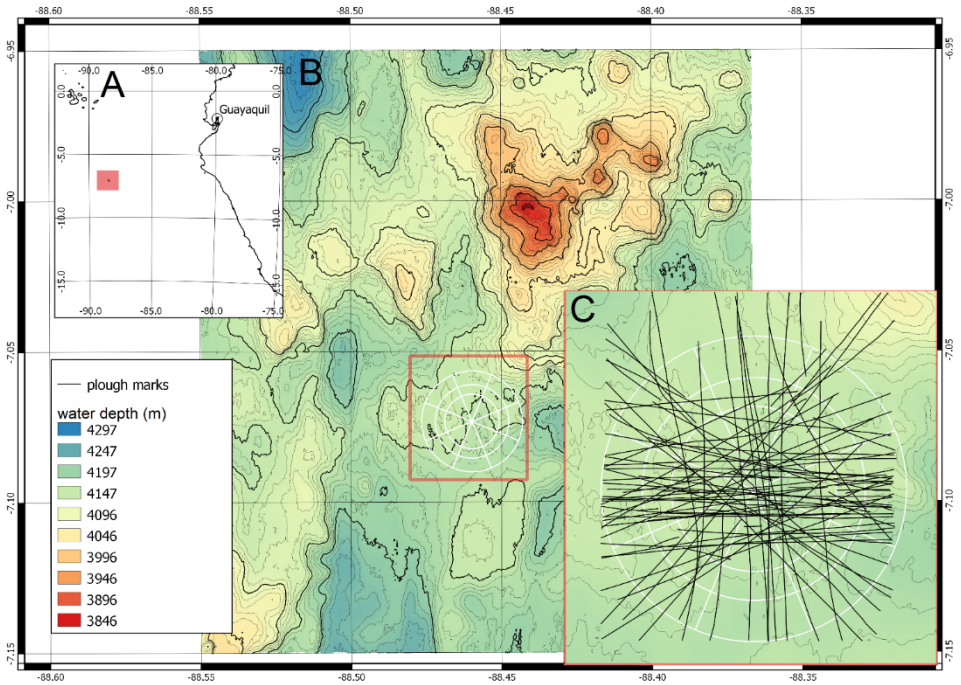

Figure 6-1. (A) Location of the DISCOL experimental area (DEA) in the Peru Basin (SE Pacific; red square), (B) detailed map of the DEA indicated by the white circle, (C) location of all plough tracks (black lines) that were observed by the "AUV Abyss" (Geomar Kiel) after 26 yr during R/V *Sonne* cruise SO242-1 (Greinert, 2015).

Linear inverse modeling is an approach that has been developed to disentangle C flows between food-web compartments for data-sparse systems (Klepper and Van De Kamer, 1987; Vézina and Platt, 1988). It has been applied to assess differences in C and nitrogen (N) cycling in various ecosystems, including the abyssal-plain food web at Station M (NE Pacific) under various particulate organic carbon (POC) flux regimes (Dunlop *et al.*, 2016), and a comparison of food-web flows between abyssal hills and plains at the Porcupine Abyssal Plain (PAP) in the NE Atlantic (Durden *et al.*, 2017).

The aim of this study was (1) to assess whether faunal C stock and trophic composition of the food webs varied and/ or converged over the time series outside and in the plough tracks at DISCOL; (2) to compare our model outcomes with the conceptual and qualitative predictions on benthic community recovery from polymetallic nodule mining published by Jumars (1981), and (3) to infer the recovery rate of C cycling following from a deep-sea sediment disturbance experiment using the network index "total system throughput" $\Delta T..$, i.e., the sum of all C flows in the food web (Kones *et al.*, 2009), developed over time.

6.3 Methods

6.3.1 Linear inverse model

Linear inverse modeling is based on the principle of mass balance and various data sources (Vézina and Platt, 1988), i.e., faunal C stock and physiological constraints, that are implemented in the model, either as equalities or inequalities, and they are solved simultaneously. A food-web model with all compartments present in the food web, e.g., the PD_{26} food-web model outside plough tracks, consisted of 147 C flows with 14 mass balances, i.e., food-web compartments, and 76 data inequalities leading to a mathematically under-determined model (14 equalities vs. 147 unknown flows). Therefore, the linear inverse models (LIMs) were solved with the R package *LIM* (van Oevelen *et al.*, 2010) in R (R-Core Team, 2017) following the likelihood approach (van Oevelen *et al.*, 2010) to quantify means and standard deviations of each of the C flows from a set of 100,000 solutions. This set was sufficient to guarantee convergence of means and standard deviations within a 2.5% deviation.

Food-web models from different sites and/ or points in time were compared quantitatively by calculating *T*.. with the R package *NetIndices* (Kones *et al.*, 2009) for each of the 100,000 model solutions and subsequently summarized as mean±SD. A decrease in the difference of *T*.. between the food webs from outside and in the plough tracks (ΔT..) over time was taken as a sign of ecosystem recovery following disturbance.

6.3.2 Data availability

Macrofauna, invertebrate megafauna, and fish density data (mean±SD; ind. m^{-2}) for the first four cruises ($PD_{0.1}$ to PD_7) were extracted from the original papers (Borowski and Thiel, 1998; Bluhm, 2001 annex 2.8; Borowski, 2001), and methodological details can be found in those papers. In brief, macrofaunal samples (> 500 µm size fraction) were collected with a 0.25 m^{-2} box corer (number of samples is reported in Table 6-1), and densities of invertebrate megafauna and fish were assessed on still photos and videos taken with a towed "Ocean Floor Observation System" (OFOS) underwater camera system (extent of total surveyed area is reported in Table 6-1). During the PD_{26} cruise (R/V *Sonne* cruise SO242-2; Boetius, 2015), macrofauna were collected with a square 50×50×60 cm box corer (outside plough tracks: $n = 7$; inside plough tracks: $n = 3$), and the upper 5 cm of sediment were sieved on a 500 µm sieve (Greinert, 2015). All organisms retained on the sieve were preserved in 96% un-denaturated ethanol on board (Greinert, 2015) and were sorted and identified ashore under a stereomicroscope to the same taxonomic level as the previous cruises. Invertebrate megafauna and fish density during the PD_{26} cruise were acquired by deploying the OFOS (Boetius, 2015). Every 20 s, the OFOS automatically took a picture from approximately 1.5 m above the seafloor (Boetius, 2015; Stratmann, Voorsmit, *et al.*, 2018/ **Chapter 4**) resulting in 1,740 images of plough marks (inside plough tracks) and 6,624 images from outside plough tracks (Boetius, 2015). A subset of 300 pictures from inside plough tracks (surface area: 1,441 m^2) and 300 pictures from the outside plough tracks (surface area: 1,420 m^2) were randomly selected from the original set of pictures and annotated using the open-

source annotation software PAPARA(ZZ)I (Marcon and Purser, 2017). Invertebrate megafauna were identified to the same taxonomic levels as for the previous megafauna studies conducted within the DISCOL experimental area (DEA) (Bluhm, 2001), whereas fishes were identified to genus level using the CCZ species atlas (www.ccfzatlas.com; last access: February 14th 2018).

Table 6-1. Number of box cores ($n_{box\ cores}$) taken for macrofauna sampling outside plough tracks (outPT) and inside plough tracks (inPT) directly after the disturbance event in March 1989 ($PD_{0.1}$), 0.5-yr post disturbance (September 1989, $PD_{0.5}$), 3-yr post disturbance (January 1992, PD_3), 7-yr post disturbance (February 1996, PD_7), and 26-yr post disturbance events (September 2015, PD_{26}). Number of "OFOS" tracks ("Ocean Floor Observatory System"; $n_{OFOS\ tracks}$) analyzed to estimate invertebrate megafauna and fish density and total area of seafloor (m^2) that was surveyed during each sampling event outside and inside plough tracks.
References: [1]Borowski and Thiel (1998), [2]Borowski (2001), [3]this study, [4]Bluhm (2001).

	Macrofauna			**Invertebrate megafauna and fish**				
	$n_{box\ cores}$		**Ref.**	**$n_{OFOS\ tracks}$**		**Total area surveyed (m^2)**		**Ref.**
	outPT	**inPT**		**outPT**	**inPT**	**outPT**	**inPT**	
$PD_{0.1}$	21	7	[1, 2]	4	5	76,120	15,639	[4]
$PD_{0.5}$	22	8	[1, 2]	4	3	53,542	11,708	[4]
PD_3	20	9	[1, 2]	4	4	32,457	6,673	[4]
PD_7	8	8	[2]	4	4	64,536	16,013	[4]
PD_{26}*	7	3	[3]			1,420	1,441	[3]

*During PD_{26}, the densities of invertebrate megafauna and fish were estimated on 300 pictures from outside plough tracks and 300 pictures from inside plough tracks that were randomly selected from a 21 OFOS tracks (Boetius, 2015).

The above-mentioned density data collected for macrofauna, invertebrate megafauna, and fish were used to build food-web models to resolve C fluxes; hence, all faunal density data required conversion into C units before they could be used in the food-web model. Converting density data to C stocks was challenging in the current study, as few to no conversion factors for deep-sea fauna are available in the literature. Below, we describe the approach that we used to tackle this problem for macrofauna, invertebrate megafauna, and fish.

Measuring the C content of a macrofaunal specimen requires its complete combustion, which means that the specimen cannot be kept as a voucher. Macrofaunal samples collected for this study are part of the Biological Research Collection of Marine Invertebrates (Department of Biology & Centre for Environmental and Marine Studies, University of Aveiro, Portugal) and were therefore not sacrificed. Instead, we used C conversion factors of macrofaunal specimens previously collected within the framework of a pulse-chase experiment in the Clarion-Clipperton Fracture Zone (CCZ, NE Pacific), in which a deep-sea benthic lander (3 incubation chambers, 20×20×20 cm each) was deployed at water depths between 4,050 and 4,200 m (Sweetman *et al.*, 2018). The upper 5 cm of the sediment of the incubation chambers were sieved on a 500 µm sieve and preserved in 4% buffered formaldehyde. Ashore, samples were sorted and identified

under a dissecting microscope, and C content of individual freeze-dried, acidified specimens was determined with a Thermo Flash EA 1112 elemental analyzer (EA; Thermo Fisher Scientific, USA) to give the individual biomass in mmol C ind^{-1}. Macrofaunal density data (ind. m^{-2}) from all cruises were converted to macrofaunal C stocks (mmol C m^{-2}) by multiplying each taxon-specific density (ind. m^{-2}) with the mean, taxon-specific, individual biomass value for macrofauna (mmol C ind^{-1}; Table 6-2). Subsequently, C stock data of all taxa with the same feeding type (Table 6-2) were summed to calculate the C stock of each macrofaunal compartment (mmol C m^{-2}; Supplementary table 6-1, Figure 6-2).

The invertebrate megafaunal density data (ind. m^{-2}) of the time series was converted to C stocks (mmol C m^{-2}) by multiplying taxon-specific density with a taxon-specific mean biomass per invertebrate megafaunal specimen (mmol C ind^{-1}; Table 6-2). To determine this taxon-specific biomass per invertebrate megafaunal specimen, size measurements were used as follows. The "AUV Abyss" (Geomar Kiel) equipped with a Canon EOS 6D camera system with 8–15 mm f4 fisheye zoom lens and 24 LED arrays for lightning (Kwasnitschka *et al.*, 2016) flew approximately 4.5 m above the seafloor at a speed of 1.5 m s^{-1} and took one picture every second (Greinert, 2015). Machine-vision processing was used to generate a photomosaic (Kwasnitschka *et al.*, 2016). A subsample covering an area of 16,206 m^2 of the mosaic was annotated using the web-based annotation software "BIIGLE 2.0" (Langenkämper *et al.*, 2017). Lengths of all invertebrate megafaunal taxa for which data were available from previous cruises were measured using the approach presented in Durden *et al.* (2016). Briefly, depending on the taxon, either body length, diameter of the disk, or length of an arm was measured on the photomosaic and converted into biomass per individual (g ind^{-1}) using the relationship between measured body dimensions (mm) and preserved wet weight (g ind^{-1}) (Durden, Bett, *et al.*, 2016). Subsequently, the preserved wet weight (g ind^{-1}) was converted to fresh wet weight (g ind^{-1}) using conversion factors from Durden *et al.* (2016) and to organic C (g C ind^{-1} and mmol C ind^{-1}) using the taxon-specific conversion factors presented in Rowe (1983) (a detailed list with all conversion factors is presented in Supplementary table 6-2). For the taxa Cnidaria and Porifera no conversion factors were available. Therefore, taxon-specific individual biomass values were extracted from a study from the CCZ (Tilot, 1992). The individual biomass of Hemichordata was calculated as the average biomass of an individual deep-sea invertebrate megafaunal organism (B, mmol C ind^{-1}) at 4,100 m depth following from the ratio of the regression for total biomass and abundance by Rex *et al.* (2006):

$$B = \frac{10^{(-0.734-0.00039\times depth)}}{10^{(-0.245-0.00037\times depth)}}. \qquad \text{[Equation 6-1]}$$

Following the approach applied to the macrofauna dataset, individual C stocks of taxa with similar feeding types (Table 6-2) were summed to determine C stocks of invertebrate megafauna food-web compartments (mmol C m^{-2}; Supplementary table 6-1, Figure 6-2).

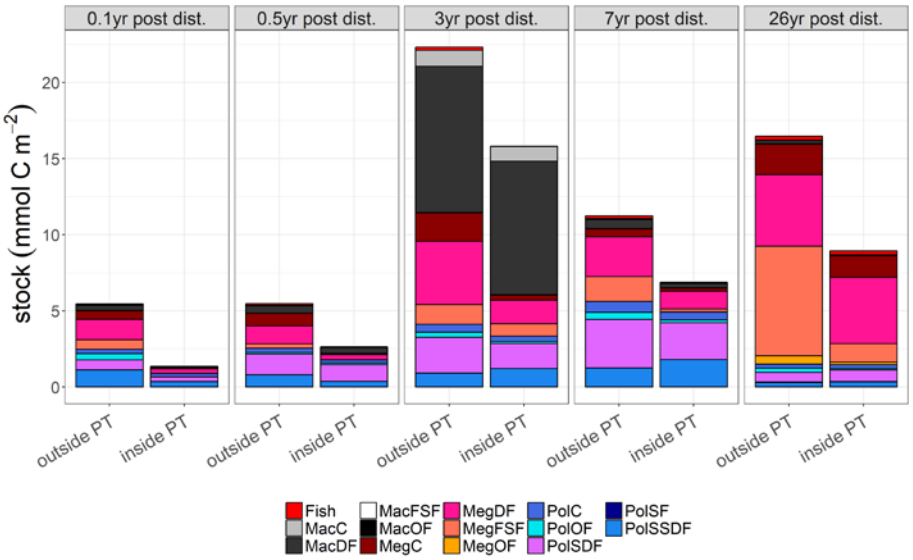

Figure 6-2. Mean C stocks (mmol C m^{-2}) of the food-web compartments for outside (outside PT) and inside (inside PT) plough tracks at the DISCOL experimental area (Peru Basin, SE Pacific) 0.1 yr post disturbance ($PD_{0.1}$), for 0.5 yr post disturbance ($PD_{0.5}$), for 3 yr post disturbance (PD_3), for 7 yr post disturbance (PD_7), and for 26 yr post disturbance (PD_{26}). For visibility reasons, no error bars are plotted, but mean±SD of each food-web compartment are presented in Supplementary table 6-1.
The abbreviation are: MacC = macrofauna carnivores, MacDF = macrofauna deposit feeders, MacFSF = macrofauna filter/ suspension feeders, MacO = macrofauna omnivores, MegC = invertebrate megafauna carnivores, MegDF = invertebrate megafauna deposit feeders, MegFSF = invertebrate megafauna filter/ suspension feeders, MegOF = invertebrate megafauna omnivores, PolC = polychaete carnivores, PolOF = polychaete omnivores, PolSDF = polychaete surface deposit feeders, PolSF = polychaete suspension feeders, PolSSDF = polychaete subsurface deposit feeders.

Individual biomass of fish was calculated using the allometric relationship for *Ipnops agassizii*:

$$wet\ weight = a \times length^b, \qquad \text{[Equation 6-2]}$$

where a = 0.0049 and b = 3.03 (Froese, Thorson and Reyes, 2014; Froese and Pauly, 2017), as *Ipnops* sp. was the most abundant fish observed at the DEA (60% of total fish density outside plough tracks and 40% of total fish density inside plough tracks). The length (mm) of all *Ipnops* sp. specimens was measured on the annotated 600 pictures (300 pictures from outside plough tracks, 300 pictures from inside plough tracks) in PAPARA(ZZ)I (Marcon and Purser, 2017) using three laser points captured in each image (distance between laser points: 0.5 m; Boetius, 2015). The wet weight (g) was converted to dry weight and subsequently to C content (mmol C ind^{-1}) using the taxon-specific conversion factors presented in Brey *et al.* (2010).

Table 6-2. Taxon-specific biomass per individual (mmol C ind^{-1}) for macrofauna and invertebrate megafauna including the specific feeding types. Macrofaunal biomass data are based on macrofaunal specimens collected in the abyssal plains of the Clarion-Clipperton Fracture Zone (NE Pacific) (Sweetman *et al.*, 2018). In contrast, invertebrate megafaunal biomass was estimated by converting size-measurements of specific body parts of organisms from DEA that were acquired using photo-annotation into preserved wet weight per organism using the relationships presented in Durden *et al.* (2016). Subsequently, the preserved wet weight was converted into fresh wet weight and biomass following the conversions presented in Durden *et al.* (2016) and Rowe (1983). Whenever no conversion factors for a specific taxon were reported in Durden *et al.* (2016) mean taxon-specific biomass data per individual were extracted from Tilot (1992) for the CCZ. *n* refers to the number of individuals used to estimate taxon-specific biomasses. A detailed list with exact conversion factors for invertebrate megafauna is presented in Supplementary table 6-2.

The abbreviations are: C = carnivores, DF = deposit feeders, FSF = filter/ suspension feeders, O = omnivores, PolC = carnivorous polychaetes, PolOF = omnivorous polychaetes, PolSF = suspension-feeding polychaetes, PolSDF = surface deposit-feeding polychaetes, PolSSDF = subsurface deposit-feeding polychaetes, S = scavengers.

References: [1]Fox, Barnes and Ruppert (2003), [2]Menzies (1962), [3]McClain, Johnson and Rex (2004), [4]Smith and Stockley (2005), [5]Gage and Tyler (1991), [7]Jumars, Dorgan and Lindsay (2015), [8]Bluhm (2001), [9]Drazen and Sutton (2017).

Taxon	Feeding type	n	Biomass (mmol C ind^{-1}) (Mean±SE)
Macrofauna			
Bivalvia[a]	FSF[1]	7	$1.4\times10^{-3}\pm3.1\times10^{-4}$
Cumacea[a]	DF[1]	2	$3.1\times10^{-3}\pm4.4\times10^{-4}$
Echinoidea[b]	85% O, 15% DF[4]	64	$9.7\times10^{-3}\pm3.6\times10^{-3}$
Gastropoda[a]	90% DF, 10% C[3]	2	$8.6\times10^{-2}\pm2.8\times10^{-2}$
Isopoda[a]	93% DF, 7% C[2]	4	$1.3\times10^{-3}\pm5.3\times10^{-4}$
Ophiuroidea[b]	C[1]	64	$9.7\times10^{-3}\pm3.6\times10^{-3}$
Polychaeta[a]	PolSF, PolSDF, PolSSDF, PolC, PolOF[7]	26	$1.3\times10^{-2}\pm7.2\times10^{-3}$
Scaphopoda[b]	C[1]	64	$9.7\times10^{-3}\pm3.6\times10^{-3}$
Tanaidacea[a]	DF[1]	5	$5.5\times10^{-3}\pm4.7\times10^{-3}$
Megafauna			
Actiniaria	FSF[1]	301	$3.0\times10^{-1}\pm5.0\times10^{-2}$
Alcyonacea[d]	FSF[1]		2.2×10^{1}
Antipatharia	FSF[1]	3	$1.8\times10^{2}\pm3.9\times10^{1}$
Ascidiacea[d]	FSF[1]		8.3×10^{-1}
Asteroidea	C[1]	53	$1.4\times10^{2}\pm6.0$
Cephalopoda	C[1]	7	$4.7\times10^{1}\pm1.1\times10^{1}$
Ceriantharia[d]	FSF[1]		1.9×10^{3}
Cnidaria[c]	FSF[1]		2.4×10^{-1}
Crinoidea[d]	FSF[1]		5.3
Crustacea	C[1, 8]	541	$2.6\pm4.3\times10^{-1}$
Echinoidea[d]	15% DF, 85% OF[4]		5.9×10^{1}
Hemichordata[g]	DF[5, 8]		2.2×10^{1}
Holothuroidea[e]	DF[1]	450	$1.5\times10^{1}\pm1.6\times10^{1}$

Ophiuroidea	C[1]	527	$1.6\times10^{1}\pm4.4\times10^{-1}$
Pennatularia[d]	FSF[1]		2.2×10^{1}
Polychaeta	PolSF, PolSDF, PolSSDF, PolC, PolOF[7]	62	$5.3\times10^{-1}\pm1.5\times10^{-3}$
Porifera[c]	FSF[1]		6.7
Fish			
Osteichthyes[f]	S, C[9]	10	$7.3\times10^{1}\pm1.3\times10^{1}$

[a]Taxon-specific individual biomass; [b]Individual biomass calculated based on all other macrofauna data; [c]Median taxon-specific individual biomass for individuals from the Porcupine Abyssal Plain where Durden *et al.* (2016) did not have reliable dimension measurements; [d]Mean taxon-specific biomass data per individual were extracted from Tilot (1992) for the CCZ; [e]Individual biomass of *Benthodytes* sp., one of the most abundant holothurian morphotype at the DISCOL site (Stratmann, Voorsmit, *et al.*, 2018/ **Chapter 4**); [f]Individual biomass of *Ipnops* sp., the most abundant deep-sea fish at the PD_{26} outside plough tracks; [g]Individual biomass calculated for mean benthic invertebrate megafauna at 4,100 m depth based on the biomass-bathymetry and abundance-bathymetry relationships presented in Rex *et al.* (2006).

6.3.3 Food-web structure

Faunal C stocks were further divided into feeding guilds in order to define food-web compartments of the model. Fish (Osteichthyes) were classified as scavenger/ predator, and macrofauna and invertebrate megafauna were divided into filter/ suspension feeders (FSF), deposit feeders (DF), carnivores (C), and omnivores (OF) (Figure 6-3; Table 6-2). Since feeding types are well described for polychaetes (Jumars, Dorgan and Lindsay, 2015), we made a further detailed classification of the macrofaunal polychaetes into suspension feeders (PolSF), surface deposit feeders (PolSDF), subsurface deposit feeders (PolSSDF), carnivores (PolC), and omnivores (PolOF).

External C sources that were considered in the model included suspended detritus in the water column (Det_w), labile (lDet_s), and semi-labile detritus (sDet_s) in the sediment. Suspended detritus was considered a food source for polychaete, macrofaunal, and invertebrate megafaunal suspension feeders. Labile and semi-labile sedimentary detritus was a source for deposit-feeding and omnivorous polychaetes, macrofauna, and invertebrate megafauna. Omnivores and carnivores of each size class preyed upon organisms of the same and smaller size classes, i.e., MegC and MegOF preyed upon MegDF, MegFSF, MacFSF, MacDF, MacC, MacOF, PolSDF, PolSSDF, PolSF, PolOF, and PolC. Furthermore, MacC, PolC, MacOF, and PolOF preyed upon MacFSF, MacDF, PolSDF, PolSSDF, and PolSF. Fish preyed upon all fauna and the carcass pool. This carcass pool consisted of all fauna (macrofauna, invertebrate megafauna, and fish) that died in the food web and was also a food source of omnivores.

C losses from the food web were respiration to dissolved inorganic carbon (DIC), predation on macrofauna, invertebrate megafauna, and fish by pelagic/ benthopelagic fishes, scavenging on carcasses by pelagic/ benthopelagic scavengers, and feces production by all faunal compartments.

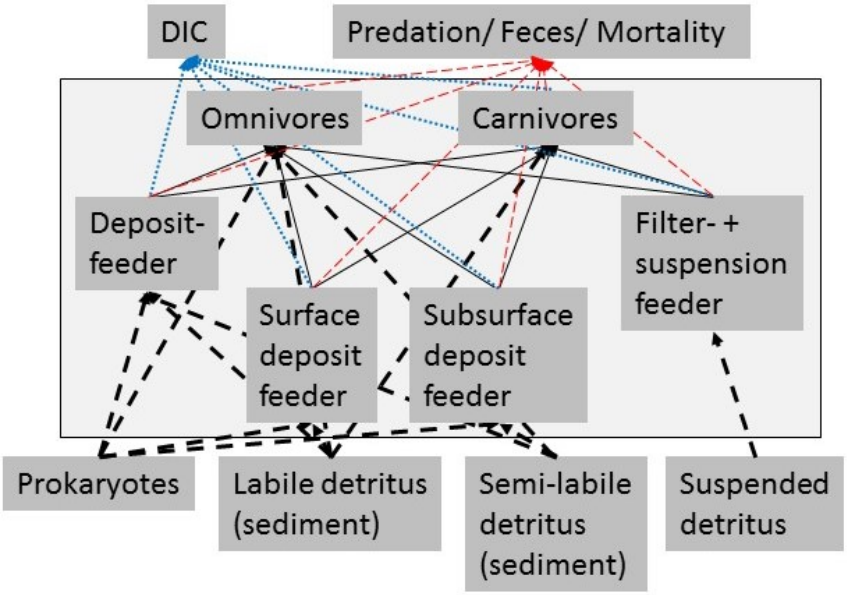

Figure 6-3. Simplified schematic representation of the food-web structure that forms the basis of the linear inverse model (LIM). All compartments inside the box were part of the food-web model, whereas compartments outside the black box were only considered as C influx or efflux, but they were not directly modeled. To simplify the graph, for macrofauna, polychaetes, and invertebrate megafauna, only feeding types were presented and no size classes. Solid black arrows represent the C flux between food-web compartments and black dashed arrows represent the influx of C to the model. Blue-dotted arrows show the loss of C from the food web via respiration to DIC. The red dashed arrows indicate the loss of C from the food web as feces and as predation by pelagic/ benthopelagic fish.

6.3.4 Literature constraints

C flows between faunal compartments are constrained in all models by various minimum and maximum process rates and conversion efficiencies.
Assimilation efficiency (*AE*) is calculated as:

$$AE = \frac{(I-F)}{I}, \qquad \text{[Equation 6-3]}$$

where *I* is the ingested food and *F* is the feces (Crisp, 1971). The min–max range was set from 0.62 to 0.87 for macrofauna, including polychaetes (**Chapter 2**), from 0.48 to 0.80 for megafauna (**Chapter 2**) and from 0.84 to 0.87 for fish (Drazen, Reisenbichler and Robison, 2007).

Net growth efficiency (*NGE*) is defined as:

$$NGE = \frac{P}{(P+R)}, \qquad \text{[Equation 6-4]}$$

with *P* being secondary production and *R* being respiration (Clausen and Riisgård, 1996). The min–max ranges are set to 0.60 to 0.72 for macrofauna, including polychaetes (Navarro *et al.*, 1994; Nielsen *et al.*, 1995; Clausen and Riisgård, 1996), from 0.48 to 0.60 for megafauna (Nielsen *et al.*, 1995; Mondal, 2006;

Koopmans, Martens and Wijffels, 2010), and from 0.37 to 0.71 for fish (Childress *et al.*, 1980).

The secondary production P (mmol C m^{-2}) is calculated as:

$$P=\frac{P}{B}\text{-}ratio\times C\ stock, \quad \text{[Equation 6-5]}$$

with $\frac{P}{B}$-*ratios* of macrofauna, including polychaetes (8.49×10^{-4} to 4.77×10^{-3} d^{-1}; **Chapter 2**), invertebrate megafauna (2.74×10^{-4} to 1.42×10^{-2} d^{-1}; **Chapter 2**) and fish (6.30×10^{-4} d^{-1}; Randall, 2002; Collins *et al.*, 2005).

The respiration rate R (mmol C m^{-2}) was calculated as:

$$R=bsFR\times C\ stock, \quad \text{[Equation 6-6]}$$

where *bsFR* is the biomass-specific faunal respiration rate (d^{-1}), and ranges were fixed between 7.12×10^{-5} to 2.28×10^{-2} d^{-1} for macrofauna, including polychaetes (**Chapter 2**), 2.74×10^{-4} to 1.42×10^{-2} d^{-1} for invertebrate megafauna (**Chapter 2**), and 2.3×10^{-4} and 3.6×10^{-4} d for fishes (Smith and Hessler, 1974; Mahaut, Sibuet and Shirayama, 1995).

6.3.5 Statistical analysis

Statistical differences between individual compartment C stocks from outside vs. inside plough tracks for the same sampling event ($PD_{0.1}$, $PD_{0.5}$, PD_3, and PD_7; PD_{26} were omitted because of a lack of invertebrate megafaunal replicates) were assessed by calculating Hedges' d (Hedges and Olkin, 1985a), which is especially suitable for small sample sizes (Koricheva, Gurevitch and Mengersen, 2013):

$$d = \frac{\overline{Y_E}-\overline{Y_C}}{\sqrt{\frac{(n_E-1)s_E^2+(n_C-1)s_C^2}{n_E+n_C-2}}}J \quad \text{[Equation 6-7]}$$

with $$J = 1-\frac{3}{4(n_E+n_C-2)-1} \quad \text{[Equation 6-8]}$$

where $\bar{Y}_E$ is the mean of the experimental group (i.e., C stock from inside plough tracks of a particular year), $\bar{Y}_C$ is the mean of the control group (i.e., C stock from inside plough tracks of the respective year), s_E and s_C are the standard deviations with corresponding groups, n_E and n_C are the sample sizes of the corresponding groups. The variance of Hedges' d σ_d^2 (Koricheva, Gurevitch and Mengersen, 2013) is estimated as:

$$\sigma_d{}^2 = \frac{n_E+n_C}{n_E n_C}+\frac{d^2}{2(n_E+n_C)}. \quad \text{[Equation 6-9]}$$

The weighted Hedges' d and estimated variances (Hedges and Olkin, 1985b) of the sum of all C stocks of the same sampling event were calculated as:

$$d_+ = \frac{\Sigma\frac{d_i}{\sigma_{d_i}{}^2}}{\Sigma\frac{1}{\sigma_{d_i}{}^2}}, \quad \text{[Equation 6-10]}$$

with $$\sigma_{d_+}{}^2 = \frac{1}{\Sigma\frac{1}{\sigma_{d_i}{}^2}}. \quad \text{[Equation 6-11]}$$

Following Cohen's (1988) rule of thumb for effect sizes, Hedges' $d = |0.2|$ signifies a small experimental effect, implying that C stocks of the food-web compartments are similar between outside and inside plough tracks. When Hedges' $d = |0.5|$, the effect size is medium, hence there is moderate difference, and when Hedges' $d = |0.8|$, the effect size is large, i.e., there is a large difference between C stocks of compartments from outside and inside plough tracks.

The network index *T*.. was compared between the outside and inside plough tracks of the same sampling event by assessing the fraction of the *T*.. values of the 100,000 model solutions of the outside plough track food web that were larger than the *T*.. values of the 100,000 model solutions of the outside plough track food web. When this fraction is > 0.95, the difference in "total system throughput" between the two food webs from the same sampling event is considered significantly different (van Oevelen, Soetaert, *et al.*, 2011), indicating that C flows in the food web from that specific sampling event have not recovered from the experimental disturbance.

6.4 Results

6.4.1 Food-web structure and trophic composition

Total faunal C stocks were always higher outside plough tracks as compared to inside plough tracks during the same sampling year (Figure 6-2, Supplementary table 6-1), and ranged from a minimum of 5.5±1.3 mmol C m^{-2} ($PD_{0.1}$) to a maximum 22.3±3.4 mmol C m^{-2} (PD_3) outside plough tracks and from a minimum of 1.4±1.2 mmol C m^{-2} ($PD_{0.1}$) to a maximum 15.8±2.0 mmol C m^{-2} (PD_3) inside plough tracks. During $PD_{0.1}$, the total faunal C stock inside plough tracks was only 25% of the total faunal C stock outside plough tracks, whereas during PD_3 the total faunal C stock inside plough tracks was 71% of the total faunal C stock outside plough tracks. During PD_{26}, the faunal C stock inside plough tracks was 54% of the C stock outside plough tracks. Absolute weighted Hedges' d $|d_+|$ of all faunal compartment C stocks for $PD_{0.1}$ to PD_7 ranged from 0.53±0.02 during $PD_{0.5}$ to 0.75±0.02 during PD_3 (Supplementary table 6-3), indicating a moderate experimental effect and therefore that C stocks of all faunal compartments failed to recover over the period analyzed ($PD_{0.1}$ to PD_7).

Faunal C stocks outside and inside plough tracks from $PD_{0.1}$ to PD_7 were dominated by deposit feeders (from 63% outside plough tracks to 83% inside plough tracks during $PD_{0.5}$ and inside plough tracks during PD_3) (Figure 6-4). In contrast, outside plough tracks during PD_{26}, filter- and suspension feeders had the largest contribution to total faunal C stock (44%), whereas deposit feeders only contributed 35%. Inside plough tracks during PD_{26}, deposit feeders had the highest C stock (61%), followed by carnivores (19%) and filter and suspension feeders (14%).

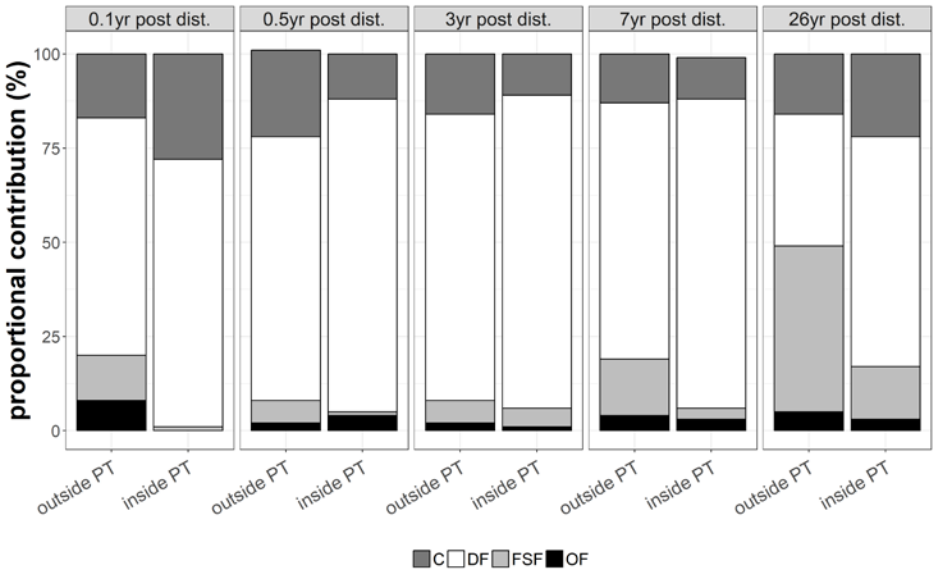

Figure 6-4. Proportional contribution (in %) of the feeding types C = carnivores, DF = deposit feeders, FSF = filter and suspension feeders, OF = omnivores to the total C stocks outside and inside plough tracks in the DISCOL experimental area (Peru Basin, SE Pacific) 0.1 yr post disturbance ($PD_{0.1}$), for 0.5 yr post disturbance ($PD_{0.5}$), for 3 yr post disturbance (PD_3), for 7 yr post disturbance (PD_7), and for 26 yr post disturbance (PD_{26}).

6.4.2 Carbon flows

Total faunal C ingestion (mmol C m^{-2} d^{-1}) ranged from $8.6\times10^{-3}\pm1.6\times10^{-5}$ inside plough tracks during $PD_{0.1}$ to $1.5\times10^{-1}\pm8.6\times10^{-4}$ outside plough tracks during PD_3 and was always lower inside plough tracks compared to outside plough tracks (Figure 6-5A). Ingestion consisted mainly of sedimentary detritus (labile and semi-labile) that contributed between 57% (outside plough tracks, PD_{26}) and 100% (inside plough tracks, $PD_{0.1}$) to the total C ingestion.

Faunal respiration (mmol C m^{-2} d^{-1}) ranged from $6.0\times10^{-3}\pm6.8\times10^{-5}$ (inside plough tracks, $PD_{0.5}$) to $3.9\times10^{-2}\pm3.7\times10^{-4}$ (outside plough tracks, PD_3) (Table 6-3). During the 26 yr after the DISCOL experiment, modeled faunal respiration was always higher outside plough tracks than inside plough tracks (Table 6-3, Figure 6-5B). Over time, non-polychaete macrofauna contributed least to total faunal respiration, except inside plough tracks during $PD_{0.5}$ and at both sites during PD_3. During this PD_3 sampling campaign, macrofauna contributed 50% outside plough tracks and 58% inside plough tracks to total faunal respiration. Polychaetes respired between 19% of the total fauna respiration outside plough tracks during PD_{26} and 78% of total faunal respiration inside plough tracks during $PD_{0.5}$. Invertebrate megafaunal contribution to respiration was highest during PD_{26}, when they respired 65% of the total faunal respiration inside plough tracks and 79% of the total faunal respiration outside plough tracks. The contribution of fish to total faunal respiration was always <2%. Besides respiration,

feces production contributed between 20% inside plough tracks during PD_3 and 35% outside plough tracks during $PD_{0.1}$ to total C outflow from the food web (Figure 6-5). The contribution of the combined outflow of predation by external predators and scavengers on carcasses to the total C loss from the food web ranged from 50% inside plough tracks during PD_7 to 65% inside plough tracks during $PD_{0.1}$.

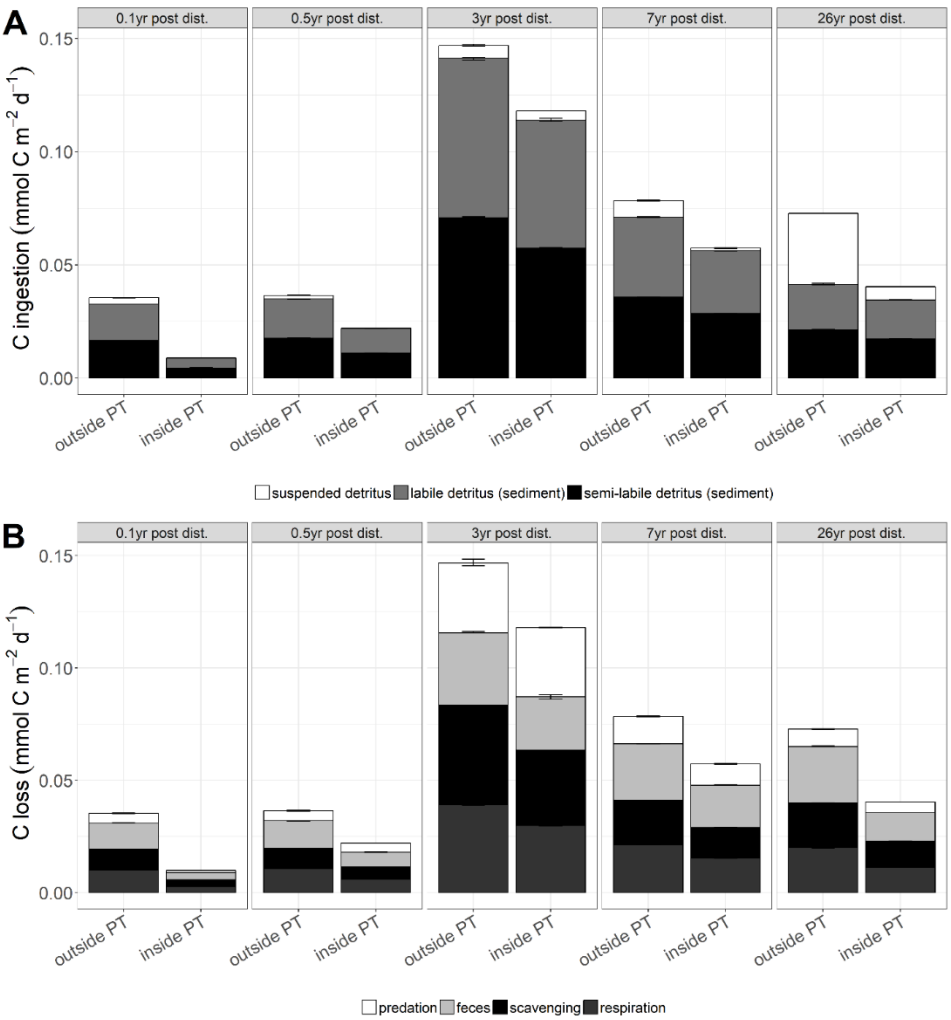

Figure 6-5. (A) Mean faunal C ingestion (mmol C m^{-2} d^{-1}) as suspended detritus, sedimentary labile and sedimentary semi-labile detritus outside and inside plough tracks 0.1 yr post-disturbance ($PD_{0.1}$), 0.5 yr post disturbance ($PD_{0.5}$), 3 yr post disturbance (PD_3), 7 yr post disturbance (PD_7), and 26 yr post disturbance (PD_{26}). (B) Mean C losses (mmol C m^{-2} d^{-1}) from the food webs as predation, feces, scavenging on the carcass, and faunal respiration outside and inside plough tracks during $PD_{0.1}$, $PD_{0.5}$, PD_3, PD_7, and PD_{26}. In both figures, the error bars represent 1 standard deviation.

Table 6-3. Faunal respiration rate ($\times 10^{-2}$ mmol C m^{-2} d^{-1}) and contribution (%) of the size classes macrofauna (Mac), polychaetes (Pol), invertebrate megafauna (Inv. Meg), and fish to the respiration outside plough tracks (outPT) and inside plough tracks (inPT) directly after the disturbance event in March 1989 ($PD_{0.1}$), 0.5 yr post-disturbance (September 1989, $PD_{0.5}$), 3 yr post-disturbance (January 1992, PD_3), 7 yr post-disturbance (February 1996, PD_7), and 26 yr post-disturbance (September 2015, PD_{26}).

	$PD_{0.1}$, outPT	**$PD_{0.1}$, inPT**	**$PD_{0.5}$, outPT**	**$PD_{0.5}$, inPT**	**PD_3, outPT**	**PD_3, inPT**
Faunal respiration	1.02± 1.17× 10^{-2}	0.27± 5.23× 10^{-4}	1.07± 5.73× 10^{-3}	0.60± 6.75× 10^{-3}	3.92± 3.68× 10^{-2}	2.99± 2.33× 10^{-2}
Mac	8.63	7.34	9.73	14.4	50.0	58.3
Pol	61.6	77.8	62.7	77.6	27.1	30.0
Inv. Meg	29.5	14.9	27.1	8.04	22.3	11.5
Fish	0.30	0.00	0.53	0.00	0.64	7.75 $\times 10^{-2}$

Table 6-3 continued.

	PD7, outPT	**PD7, inPT**	**PD26, outPT**	**PD26, inPT**
Faunal respiration	2.14± 2.5.$\times 10^{-2}$	1.54± 1.49$\times 10^{-2}$	2.00± 1.50$\times 10^{-2}$	1.13± 1.04$\times 10^{-2}$
Mac	6.50	4.51	2.64	1.19
Pol	67.1	83.5	18.5	32.4
Inv. Meg	25.8	11.6	78.7	64.9
Fish	0.66	0.35	0.17	1.44

The fraction of *T*.. values that were larger for the food webs outside plough tracks than inside plough tracks during the same sampling event was 1.0 at $PD_{0.1}$, $PD_{0.5}$, PD_3, PD_7, and PD_{26}. No decreasing trend in ΔT.. over time was visible (Figure 6-6), in fact, the largest Δ *T*.. were calculated for PD_3 (7.9×10^{-2} $\pm 2.0\times 10^{-3}$ mmol C m^{-2} d^{-1}) and PD_{26} ($7.7\times 10^{-2}\pm 9.41\times 10^{-4}$ mmol C m^{-2} d^{-1}).

6.5 Discussion

This study assessed the change over time of food-web structure and the ecosystem function “faunal C cycling” in an abyssal, nodule-rich, soft-sediment ecosystem after an experimental sediment disturbance. From the 26-year time series, we show that total faunal C stock inside plough tracks was still only about half of total faunal C stock outside plough tracks. Furthermore, the role of the various feeding types in the C cycling differed. In all, the “total system throughput” *T*.., i.e., the sum of all C flows in the food web, was also significantly lower inside plough tracks as compared to outside plough tracks 26 yr after the experimental mining disturbance.

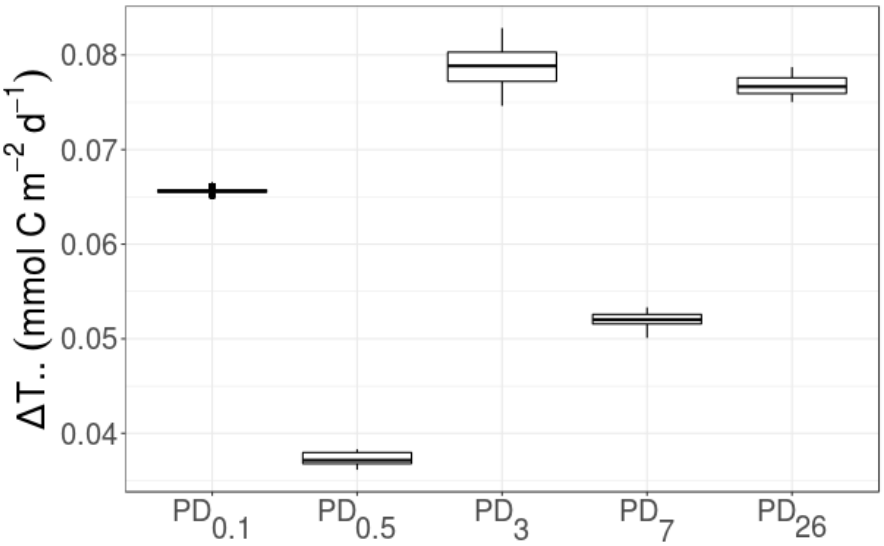

Figure 6-6. Development of Δ*T*.. (mmol C m^{-2} d^{-1}), i.e., the difference in "total system throughput" *T*.. outside plough tracks compared to inside plough tracks, over time. $PD_{0.1}$ corresponds to 0.1 yr post-disturbance, $PD_{0.5}$ is 0.5 yr post-disturbance, PD_3 is 3 yr post-disturbance, PD_7 is 7 yr post-disturbance, and PD_{26} is 26 yr post-disturbance.

6.5.1 Model limitations

Our results are unique, as they allowed us, for the first time, to assess recovery of C cycling in benthic deep-sea food webs from a small-scale sediment disturbance in polymetallic nodule-rich areas. However, the models proposed here come with limitations. Pre-disturbance samples and samples from reference sites were not collected for all food-web compartments. A notable omission is the lack of data for microbes and meiofauna throughout the times series, hence our C cycling models only resolve C cycling by macro- and megafaunal compartments. Another omission is the lack of a baseline to which the "outside plough track" food web at $PD_{0.1}$ could be compared to assess the impact that the disturbance effect had on sites outside the plough tracks. Hence, we cannot determine whether the high biomass and C flows at PD_3 were due to the onset of the positive (La Niña) phase of the El Niño Southern Oscillation (Trenberth, 1997), a phenomenon which is known to lead to a comparatively high POC export flux in the Pacific Ocean (e.g., Station M; Ruhl, Ellena and Smith, 2008).

Standard procedures to assess invertebrate megafaunal and fish densities have evolved during the 26 yr of post-disturbance monitoring. The OFOS system used 26 yr after the initial DISCOL experiment took pictures automatically every 20 s from a distance of 1.5 m above the seafloor (Boetius, 2015; Stratmann, Voorsmit, *et al.*, 2018/ **Chapter 4**). By contrast, the OFOS system used in former cruises was towed approximately 3 m above the seafloor, and pictures were taken selectively by the operating scientists (Bluhm and Gebruk, 1999). Therefore, the procedure used in the former cruises very likely overestimated rare and charismatic invertebrate megafauna, and probably underestimated dominant fauna and organisms of small size (<3 cm) for $PD_{0.1}$ to $PD_{7,}$ as compared to PD_{26}.

Previous cruises to the DEA focused on monitoring changes in faunal density and diversity, but not on changes in C stock. Hence, a major task in this study was to find appropriate conversion factors to convert density into C stocks. However, no individual biomass data for macrofaunal taxa were available for the Peru Basin, so we used data from sampling stations of similar water depths in the eastern CCZ (Sweetman *et al.*, 2018). As organisms in deep-sea regions with higher organic C input are larger than their counterparts from areas with lower organic C input (McClain *et al.*, 2012), using individual biomass data from the CCZ, a more oligotrophic region than the Peru Basin (Haeckel *et al.*, 2001; Vanreusel *et al.*, 2016), might have underestimated C stocks for macrofauna. However, this potential bias has likely limited impact on the interpretation of the comparative results within the time series, because the same methodology was applied throughout. Moreover, the determination of invertebrate megafaunal C stocks was also difficult, as no size measurements were taken from invertebrate megafaunal individuals during the $PD_{0.1}$ to PD_7 cruises. Consequently, it was not possible to detect differences in size classes between inside and outside plough tracks or recruitment events in, e.g., echinoderms (Ruhl, 2007) following the DISCOL experiment. Instead, we used fixed conversion factors for the different taxa for the entire time series.

6.5.2 Feeding-type specific differences in recovery

Eight years before the experimental disturbance experiment was conducted at the DISCOL area, Jumars (1981) qualitatively predicted the response of different feeding types in the benthic community to polymetallic nodule removal. Although several seabed test mining or mining simulations were performed since then (Jones *et al.*, 2017), no study compared or verified these conceptual predictions on feeding-type specific differences in recovery from deep-sea mining. As few comparative studies are available, we compare here our food-web model results with those of the conceptual model predictions for scavengers, surface and subsurface deposit feeders, and suspension feeders by Jumars (1981).

Jumars (1981) predicted that organisms inside the mining tracks would be killed either by the fluid shear of the dredge/ plough or by abrasion and increased temperatures inside the rising pipe with a mortality rate of > 95%. In contrast, the impact on mobile and sessile organisms in the vicinity of the tracks would depend on their feeding type (Jumars, 1981).

The author also predicted that the density of mobile scavengers, such as fish and lysianassid amphipods would rise shortly after the disturbance in response to the increased abundance of dying or dead organisms within the mining tracks. In fact, experiments with baits at PAP and the Porcupine Seabight (NE Atlantic) showed that the scavenging deep-sea fish *Coryphaenoides armatus* intercept bait within 30 min (Collins, Priede and Bagley, 1999) and stayed at the food fall for 114±55 min (Collins *et al.*, 1998). Therefore, the absence of fish inside plough tracks during $PD_{0.1}$ and $PD_{0.5}$ could be related to a lack of prey in a potential predator-prey relationship (Bailey, Ruhl and Smith, 2006). However, because of the relatively small area of plough tracks (only 22% of the 10.8 km^2 of sediment were ploughed; Thiel *et al.*, 1989), the low density of deep-sea fish

(e.g., between 7.5 and 32 ind. ha^{-1} of the dominant fish genus *Coryphaenoides* sp. at Station M; Bailey, Ruhl and Smith, 2006) and high motility of fish, this observation is likely coincidental.

Jumars (1981) predicted that, on a short term, subsurface deposit feeders outside the mining tracks would be the least impacted feeding type, because of their relative isolation from the re-settled sediment, and their relative independence of organic matter on the sediment surface, whereas subsurface deposit feeders inside the mining tracks would experience high mortality. For the long-term recovery, the author pointed to the dependence of subsurface deposit feeders on bacterial production in the sediment covered with re-settled sediment. Moreover, this newly settling sediment would alter both sediment composition and food concentration in the sediment. As the total rate of sediment deposition would increase both inside and beyond mining tracks, Jumars (1981) anticipated that surface deposit feeders would endure stronger impacts from deep-sea mining activities compared with subsurface deposit feeders.

In our food-web model, subsurface and surface deposit feeders were grouped into the deposit feeder category, except for polychaetes, for which we kept the surface-subsurface distinction. The C stock of PolSSDF fluctuated by one order of magnitude over the 26 yr time series and had high C stock values outside plough tracks during $PD_{0.1}$, inside plough tracks during PD_3 and inside and outside plough tracks during PD_7. Hence, predictions by Jumars (1981) for subsurface deposit feeders are difficult to test, but Hedges' *d* for PolSSDF was |1.47| at $PD_{0.1}$ and decreased steadily to |0.66| at PD_7 (Supplementary table 6-3), indicating a very strong experimental effect after the disturbance event and a logarithmic recovery over time. In comparison, the recovery of surface deposit feeders might be delayed, owing to potential unfavorable food conditions as Stratmann, Voorsmit, *et al.* (2018)/ **Chapter 4** hypothesized in a study about holothurian densities at the DISCOL experimental area.

Jumars (1981) expected that the suspension feeders outside the mining tracks would be negatively affected during the presence of the sediment plumes and/ or as long as their filtration apparatus was clogged by sediment. This "clogging" hypothesis could not be tested here, because the models did not resolve these unknown changes in faunal physiology, so we could only assess C cycling differences associated with differences in C stocks. Furthermore, Jumars (1981) anticipated that the recovery of nodule-associated organisms, such as filter and suspension feeding Porifera, Antipatharia, or Ascidiacea (Vanreusel *et al.*, 2016) would require more than 10,000 yr, owing to the slow growth rate of polymetallic nodules (Guichard, Reyss and Yokoyama, 1978; Kuhn *et al.*, 2017) and the removal and/ or burial of the nodules. This hypothesis could not be tested directly, because nodules were not removed in this experiment, but only ploughed into the sediment. However, the disappearance of nodules from the sediment surface will likely have the same effect on sessile epifauna that depend on nodules as hard substrate independently of the method by which the nodules disappeared. Immediately after the initial DISCOL disturbance event, the respiration rate of filter and suspension feeders inside plough tracks was only 1% of the respiration rate of this feeding type outside plough tracks. After 26 yr, total respiration rate of

filter- and suspension feeders inside plough tracks was still 80% lower than in the outside plough tracks. Part of this difference at PD_{26} resulted from the presence of a single specimen of Alcyonacea with a biomass of 4.71 mmol C m^{-2} outside plough tracks. Even if we ignore this Alcyonacea specimen in the model, the respiration of suspension and filter feeding inside plough tracks would still be 71% lower compared to outside plough tracks, indicating a slow recovery of this feeding group.

6.6 Conclusion

Deep-sea mining will negatively impact abyssal benthic ecosystems. It is therefore important to be able to estimate how long recovery of the ecosystem after a deep-sea mining operation will take. This study used the linear inverse modeling technique to compare C flows between different food-web compartments outside and inside plough tracks at the DISCOL experimental area in the Peru Basin over a period of 26 yr. Even after 26 yr, total faunal C stock and total food-web activity (i.e., summed C cycling) inside plough tracks was only approximately half (54% and 56% respectively) of total faunal C stock and food-web activity outside plough tracks. Deposit feeders were the least impacted by the sediment disturbance, with less than 3% relative difference in total C loss (i.e., respiration, external predation, and feces production) between outside and inside plough tracks after 26 yr. In contrast, filter and suspension feeders recovered less and the relative difference in respiration rates between inside and outside plough tracks was 79%. Overall, ecosystem function (as measured by total C cycling) within the macrofauna, invertebrate megafauna, and fish has not fully recovered 26 yr after the experimental disturbance.

Acknowledgments

We thank the chief scientists Jens Greinert (SO242-1) and Antje Boetius (SO242-2) as well as the captain and crew of R/V *Sonne* for their excellent support during both legs of cruise SO242. We also thank the “AUV Abyss” team from Geomar, Kiel (Germany), Daniëlle de Jonge (Groningen University, the Netherlands) for identifying the fish species and Sebastian Rieger (Geomar, Kiel, Germany) for preparing the map of Figure 1.

6.7 Supplement

Supplementary table 6-1. C stock of food-web compartments ($\times 10^{-2}$ mmol C m^{-2}) for outside (outPT) and inside plough tracks (inPT) directly after the disturbance event in March 1989 ($PD_{0.1}$), 0.5 yr post disturbance (September 1989, $PD_{0.5}$), 3 yr post disturbance (January 1992, PD_3), 7 yr post disturbance (February 1996, PD_7) and 26 yr post disturbance (September 2015, PD_{26}). n.d. = not detected.

Data are presented as mean±SD, except for megafauna and fish at the PD_{26} disturbed and PD_{26} undisturbed sites, where no replicate photo tracks were analyzed (for details see Material and Methods).

Abbreviations are: MacFSF = filter and suspension feeding macrofauna, MacDF = deposit feeding macrofauna, MacC = carnivory macrofauna, MacOF = omnivorous feeding macrofauna, PolSF = suspension feeding polychaetes, PolSDF = surface deposit feeding polychaetes, PolSSDF = subsurface deposit feeding polychaetes, PolC = carnivory polychaetes, PolOF = omnivorous feeding polychaetes, MegFSF = filter and suspension feeding megafauna, MegDF = deposit feeding megafauna, MegC =carnivory megafauna, MegOF = omnivorous feeding megafauna.

References: [1]this study, [2]Borowski and Thiel (1998), [3]Borowski (2001), [4]Bluhm (2001) and corresponding annex 2.08.

Compartment	**$PD_{0.1}$, outPT**	**$PD_{0.1}$, inPT**	**$PD_{0.5}$, outPT**	**$PD_{0.5}$, inPT**	**PD_3, outPT**	**PD_3, inPT**	**Ref.**
MacFSF	3.42± 2.10	0.26± 0.64	2.61± 1.46	1.46± 0.39	3.60± 1.16	2.40± 1.33	1-3
MacDF	33.6± 62.2	2.29± 1.87	47.2± 29.4	38.5± 29.5	960± 39.3	877± 29.8	1-3
MacC	6.06± 20.6	7.04± 0.79	4.75± 9.80	4.50± 9.78	106± 13.0	97.3± 9.81	1-3
MacOF	0.19± 0.17	0.46± 0.55	0.21± 0.34	0.25± 0.34	0.32± 0.34	0.27± 0.38	1-3
PolSF	n.d.	n.d.	n.d.	n.d.	n.d.	n.d.	1-3
PolSDF	65.6± 51.1	29.9± 71.2	135± 42.9	110± 73.7	235± 60.1	164± 53.6	1-3
PolSSDF	112± 39.0	35.5± 77.6	80.0± 33.1	37.1± 42.9	90.8± 37.4	122± 46.3	1-3
PolC	29.3± 26.1	23.1± 62.7	26.9± 19.2	21.1± 32.3	52.6± 28.5	34.6± 24.6	1-3
PolOF	40.4± 30.6	n.d.	11.2± 12.4	8.99± 21.1	33.3± 22.7	13.0± 15.1	1-3
Total Mac+Pol	**291± 100**	**98.5± 123**	**308± 66.5**	**222± 98.6**	**1,482± 89.8**	**1,311± 82.7**	**1-3**
MegFSF	61.8± 58.5	0.44± 0.38	28.5± 9.09	1.87± 0.90	128± 81.6	81.4± 159	1, 4
MegDF	134± 48.5	28.9± 16.1	118± 47.6	32.1± 3.47	416± 309	155± 82.7	1, 4
MegC	56.3± 19.9	8.41± 4.91	82.9± 33.5	6.83± 3.20	186± 74.7	33.1± 19.5	1, 4
MegOF	0.39± 0.93	n.d.	0.49± 1.05	n.d.	0.64± 1.39	n.d.	1, 4
Total Meg	**252± 78.6**	**37.8± 16.9**	**230± 58.9**	**40.8± 4.80**	**731± 328**	**269± 181**	**1, 4**

Osteich-thyes	2.47± 1.89	n.d.	9.00± 6.53	n.d.	20.4± 10.5	1.74± 3.48	[1, 4]

Supplementary table 6-1 continued.

Compart-ment	**PD_7, outPT**	**PD_7, inPT**	**PD_{26}, outPT**	**PD_{26}, inPT**	**Ref.**
MacFSF	3.15±0.56	1.58±0.56	2.93	2.00	[1-3]
MacDF	59.1±32.9	29.4±32.8	20.6	2.37	[1-3]
MacC	6.09±10.9	2.58±10.9	2.87	0.54	[1-3]
MacOF	0.29±0.59	0.32±0.29	0.22	0.26	[1-3]
PolSF	n.d.	n.d.	2.82	2.20	[1-3]
PolSDF	320±56.8	241±118	63.9	77.0	[1-3]
PolSSDF	124±35.3	180±102	29.1	33.0	[1-3]
PolC	71.7±26.9	50.9±54.2	27.7	26.4	[1-3]
PolOF	45.3±21.4	19.2±33.2	26.3	8.80	[1-3]
Total Mac+Pol	**630±82.8**	**525±172**	**176**	**153**	**[1-3]**
MegFSF	162±125	18.1±33.9	720	121	[1, 4]
MegDF	262±123	117±77.7	471	436	[1, 4]
MegC	51.6±15.7	20.3±7.61	200	143	[1, 4]
MegOF	1.04±1.30	2.57±3.38	54.1	15.1	[1, 4]
Total Meg	**477±176**	**158±85.2**	**1,445**	**715**	**[1, 4]**
Osteich-thyes	17.9±7.61	5.17±6.39	25.8	25.5	[1, 4]

Supplementary table 6-2. Conversion factors used to calculate taxon-specific biomass per individual.

Abbreviations: *D* = measured dimension, *DW* = dry weight, *fWW* = fresh wet weight, *pWW* = preserved wet weight, *tsiB* = taxon-specific individual biomass.

References: [1]Durden, Bett, *et al.* (2016), [2]Rowe (1983), [3]Tilot (1992), [4]Froese, Thorson and Reyes (2014), [5]Froese and Pauly (2017), [6]Brey et al. (2010).

Taxon	*D*	Conversion factors			Ref.
		***D* (mm) → *fWW* (g)**	***D* (mm) → *pWW* (g)**	***pWW* (g) → *fWW* (g)**	
Actiniaria	Column D		$pWW = 26 \times 10^{-4} \times D^{2.36}$	$fWW = \frac{pWW}{0.887}$	1, 2
Alcyonacea					3
Antipatharia	Column D		$pWW = 12 \times 10^{-4} \times D^{2.578}$	$fWW = \frac{pWW}{0.664}$	1, 2
Ascidiacea					3
Asteroidea	Radius from center of disk to end of arm		$pWW = 26 \times 10^{-4} \times D^{2.133}$	$fWW = \frac{pWW}{0.873}$	1, 2
Cephalopoda	Arm length		$pWW = 3 \times 10^{-4} \times D^{2.438}$	$fWW = \frac{pWW}{0.415}$	1, 2
Ceriantharia					3
Cnidaria				$fWW = \frac{pWW}{0.71}$	1, 2
Crinoidea					3
Crustacea	Body length		$pWW = 6 \times 10^{-4} \times D^{2.747}$	$fWW = \frac{pWW}{0.78}$	1, 2
Echinoidea					3
Ophiuroidea	Radius from center of disk to end of arm		$pWW = 21 \times 10^{-4} \times D^{1.764}$	$fWW = \frac{pWW}{0.835}$	1, 2
Polychaeta	Body length		$pWW = 2 \times 10^{-4} \times D^{2.307}$	$fWW = \frac{pWW}{0.812}$	1, 2
Porifera[c]				$fWW = \frac{pWW}{0.791}$	1, 2
Osteichthyes[f]	Body length	$fWW = 0.0049 \times D^{3.03}$			4, 5, 6

Supplementary table 6-2 continued.

Taxon	D	Conversion factors			Ref.
		D (mm) → fWW (g)	D (mm) → pWW (g)	pWW (g) → fWW (g)	
Polychaeta	Body length		$pWW = 2 \times 10^{-4} \times D^{2.307}$	$fWW = \frac{pWW}{0.812}$	1, 2
Porifera[c]				$fWW = \frac{pWW}{0.791}$	1, 2
Osteichthyes[f]	Body length	$fWW = 0.0049 \times D^{3.03}$			4, 5, 6

Supplementary table 6-3. Calculation of "Hedges' *d*", standard deviation σ_d^2, "weighted Hedges' *d*", and standard deviation σ_{d+}^2 for each compartment biomass of the same sampling event ($PD_{0.1}$, $PD_{0.5}$, PD_3, and PD_7).
Abbreviations of the compartment names are: MacC = macrofauna carnivores, MacDF = macrofauna deposit feeders, MacFSF = macrofauna filter/ suspension feeders, MacO = macrofauna omnivores, MegC = megafauna carnivores, MegDF = megafauna deposit feeders, MegFSF = megafauna filter/ suspension feeders, MegOF = megafauna omnivores, PolC = polychaete carnivores, PolOF = polychaete omnivores, PolSDF = polychaete surface deposit feeders, PolSF = polychaete suspension feeders, PolSSDF = polychaete subsurface deposit feeders.

Table part A: $PD_{0.1}$

Compartment name	$n_{dist.\ sediment}$	$n_{undist.\ sediment}$	$\lvert d \rvert$	σ_d^2	$\lvert d_+ \rvert$	σ_{d+}^2	$1/\sigma_d^2$	d/σ_d^2	d^2/σ_d^2
Fish	4	5	1.54	0.58			1.72	-2.64	4.06
MacC	7	21	0.05	0.19			5.25	0.28	0.01
MacDF	7	21	0.56	0.20			5.10	-2.84	1.58
MacFSF	7	21	1.64	0.24			4.19	-6.89	11.33
MacOF	7	21	0.87	0.20			4.90	4.25	3.69
MegC	4	5	2.77	0.88			1.14	-3.16	8.75
MegDF	4	5	2.45	0.78			1.28	-3.13	7.66
MegFSF	4	5	1.23	0.53			1.87	-2.31	2.85
MegOF	4	5	0.49	0.46			2.16	-1.05	0.51
PolC	7	21	0.16	0.19			5.24	-0.83	0.13
PolOF	7	21	1.46	0.23			4.37	-6.39	9.34
PolSDF	7	21	0.61	0.20			5.07	-3.12	1.92
PolSF	7	21	n.d.	n.d.			n.d.	n.d.	n.d.
PolSSDF	7	21	1.47	0.23			4.37	-6.41	9.41
					0.73	**0.02**	**46.7**	**-34.3**	**61.2**

Table part B: $PD_{0.5}$

Compartment name	$n_{dist.\ sediment}$	$n_{un-dist.\ sediment}$	$\lvert d \rvert$	σ_d^2	$\lvert d_+ \rvert$	σ_{d+}^2	$1/\sigma_d^2$	d/σ_d^2	d^2/σ_d^2
Fish	3	4	1.50	0.74			1.34	-2.01	3.02
MacC	8	22	0.02	0.17			5.87	-0.15	0.00
MacDF	8	22	0.29	0.17			5.82	-1.67	0.48
MacFSF	8	22	0.87	0.18			5.46	-4.78	4.18
MacOF	8	22	0.14	0.17			5.86	0.80	0.11
MegC	3	4	2.46	1.02			0.98	-2.42	5.96
MegDF	3	4	1.96	0.86			1.17	-2.28	4.47
MegFSF	3	4	3.17	1.30			0.77	-2.44	7.73
MegOF	8	4	0.78	0.40			2.50	-1.95	1.52
PolC	8	22	0.24	0.17			5.83	-1.42	0.35
PolOF	8	22	0.14	0.17			5.85	-0.84	0.12
PolSDF	8	22	0.46	0.17			5.75	-2.67	1.24
PolSF	8	22	n.d.	n.d.			n.d.	n.d.	n.d.
PolSSDF	8	22	1.17	0.19			5.18	-6.04	7.04
					0.53	**0.02**	**52.4**	**-27.9**	**36.2**

Table part C: PD_3

Compartment name	$n_{dist.\ sediment}$	$n_{un-dist.\ sediment}$	$\lvert d \rvert$	σ_d^2	$\lvert d_+ \rvert$	σ_{d+}^2	$1/\sigma_d^2$	d/σ_d^2	d^2/σ_d^2
Fish	4	4	2.07	0.77			1.30	-2.70	5.60
MacC	9	20	0.70	0.17			5.90	-4.11	2.86
MacDF	9	20	2.20	0.24			4.09	-8.99	19.74
MacFSF	9	20	0.96	0.18			5.65	-5.43	5.22
MacOF	9	20	0.13	0.16			6.20	-0.81	0.11
MegC	4	4	2.44	0.87			1.15	-2.80	6.81
MegDF	4	4	1.00	0.56			1.78	-1.78	1.79
MegFSF	4	4	0.32	0.51			1.97	-0.63	0.20
MegOF	4	4	0.57	0.52			1.92	-1.09	0.62
PolC	9	20	0.64	0.17			5.95	-3.80	2.42
PolOF	9	20	0.95	0.18			5.66	-5.38	5.12
PolSDF	9	20	1.18	0.19			5.40	-6.39	7.57
PolSF	9	20	n.d.	n.d.			n.d.	n.d.	n.d.
PolSSDF	9	20	0.75	0.17			5.85	4.41	3.32
					0.75	**0.02**	**52.8**	**-39.5**	**61.4**

Table part D: PD_7

Compartment name	$n_{dist.\ sediment}$	$n_{un-dist.\ sediment}$	$\|d\|$	σ_d^2	$\|d_+\|$	σ_{d+}^2	$1/\sigma_d^2$	d/σ_d^2	d^2/σ_d^2
Fish	4	4	1.58	0.66			1.53	-2.40	3.79
MacC	8	8	0.30	0.25			3.95	-1.20	0.37
MacDF	8	8	0.85	0.27			3.67	-3.13	2.68
MacFSF	8	8	2.67	0.47			2.12	-5.65	15.08
MacOF	8	8	0.05	0.25			4.00	0.19	0.01
MegC	4	4	2.21	0.80			1.24	-2.74	6.05
MegDF	4	4	1.23	0.59			1.68	-2.06	2.53
MegFSF	4	4	1.37	0.62			1.62	-2.22	3.03
MegOF	4	4	0.52	0.52			1.93	1.01	0.52
PolC	5	5	0.44	0.41			2.44	-1.07	0.47
PolOF	5	5	0.84	0.44			2.30	-1.94	1.64
PolSDF	5	5	0.77	0.43			2.33	-1.79	1.38
PolSF	5	5	n.d.	n.d.			n.d.	n.d.	n.d.
PolSSDF	5	5	0.66	0.42			2.37	1.57	1.04
					0.69	**0.03**	**31.2**	**-21.5**	**38.6**

Chapter 7 : Benthic microbial loop has not recovered from a small-scale seabed disturbance after 26 years

7. Benthic microbial loop has not recovered from a small-scale seabed disturbance after 26 years

Tanja Stratmann[1], Daniëlle de Jonge[1], Freija Hauquier, Lidia Lins, Lisa Mevenkamp, Ann Vanreusel, Erik Simon-Lledó, Daniel O. B. Jones, Autun Purser, Yann Marcon, Clara F. Rodrigues, Ascensão Ravara, Patricia Esquete, Marina R. Cunha, Tobias R. Vonnahme, Massimilano Molari, Frank Wenzhöfer, Felix Janssen, Peter van Breugel, Matthias Haeckel, Andrew K. Sweetman, Karline Soetaert, and Dick van Oevelen;
In preparation.

7.1 Abstract

Future extraction of polymetallic nodules in abyssal plains will severely impact the benthic ecosystem. Here, we developed highly resolved quantitative carbon-flux food-web models based on an extensive and novel set of data from the Peru Basin (SE Pacific). In 1989, a small-scale sediment disturbance experiment, the so-called "DISCOL experiment", was conducted in the Peru Basin that buried nodules and disturbed the sediment to mimic deep-sea mining. Separate models for inside plough tracks, outside plough tracks, and reference sites further away were developed which included 41 food-web compartments. These compartments comprised detritus, prokaryotes, nematodes, other meiofaunal taxa, macrofaunal polychaete, and other macrofauna taxa, holothurians, other megafauna, and three fish taxa. We show that 26 yr after the disturbance, total carbon throughput *T*.., i.e., the sum of all carbon flows, is still significantly depressed inside plough tracks ($4.52 \pm 8.35 \times 10^{-2}$ mmol C m^{-2} d^{-1}) compared to outside plough tracks (5.51 ± 0.16 mmol C m^{-2} d^{-1}) and at reference sites ($4.52 \pm 8.35 \times 10^{-2}$ mmol C m^{-2} d^{-1}). The difference in *T*.. between reference sites and outside plough tracks was not significant. The largest contributor to *T*.. and the main reason for the difference in *T*.. between sites was the microbial loop. It contributed between 57% outside plough tracks and 62% at reference sites to *T*.… Hence, particularly the microbial loop seems to be very sensitive to the impact of deep-sea mining and therefore could be used as ecosystem indicator to assess the stage of recovery from polymetallic nodule extraction. The scavenging pathway only accounted for 0.17% (reference sites) to 0.39% (inside plough tracks) of *T*.… Total amount of carbon ingested by the three fish taxa was 4.68×10^{-3}% (reference sites) to 0.15% (inside plough tracks) of *T*.…

[1] These authors have contributed equally to this work.

7.2 Introduction

Deep-sea mining refers to the extraction of mineral resources in the deep sea, such as polymetallic nodules, polymetallic sulfides, and ferromanganese crusts. Polymetallic nodules are Fe oxide-hydroxide-Mn oxide concretions (Hein and Koschinsky, 2014) that lay on the sediment surface of abyssal plains between 3,500 and 6,500 m water depth (Hein *et al.*, 2013). They grow extremely slowly, either hydrogenetically at rates of 1 to 10 mm Myr^{-1} (Petersen *et al.*, 2016) or diagenetically at rates of up to 250 mm Myr^{-1} (von Stackelberg, 2000). High nickel, cobalt, and copper content of polymetallic nodules (Petersen *et al.*, 2016) awoke interest from the industry as estimates for the Clarion-Clipperton Fracture Zone (CCZ; central Pacific) show that the nodules in this area contain 9 times more manganese, 4 times more nickel and 5 times more cobalt than land-based reserves (Hein and Koschinsky, 2014; Sverdrup, Ragnarsdottir and Koca, 2017; U.S. Geological Survey, 2018). However, nodules also provide an important hard substrate in abyssal plains (Smith *et al.*, 2008): Vanreusel *et al.* (2016), e.g., showed that sessile and mobile megafauna densities are enhanced in areas with nodule coverage in comparison to area without nodules. Nodules are furthermore essential for food-web integrity in Pacific abyssal plains (**Chapter 3**).

The extraction of polymetallic nodules will have various environmental impacts, such as removal of hard substrate, habitat modification and destruction (Oebius *et al.*, 2001), potential release of toxic metals (Koschinsky, Borowski and Halbach, 2003), creation of sediment plumes and resettlement of sediment (Oebius *et al.*, 2001; K. Murphy *et al.*, 2016) as well as noise and light pollution (Miller *et al.*, 2018). To investigate how the deep-sea ecosystem responds to these impacts, the 'DISturbance and reCOLonization' (DISCOL) experiment was conducted in the northern Peru Basin in 1989. During this experiment, a 10.8 km^2 circular area called "DISCOL experimental area" (DEA) was ploughed diametrically 78 times with an 8 m-wide plough-harrow to create a small-scale sediment disturbance (Thiel *et al.*, 1989). As a result, 22% of the DEA (Thiel *et al.*, 1989) was disturbed by reshuffling of sediment and by ploughing polymetallic nodules into the surface sediment. During five follow-up cruises between March 1989 and September 2015 (Thiel *et al.*, 1989; Schriever, 1990; Schriever and Thiel, 1992; Schriever, Koschinsky and Bluhm, 1996; Boetius, 2015; Greinert, 2015), it was investigated whether macrofauna and megafauna species composition, density, and diversity recovered (Bluhm and Gebruk, 1999; Bluhm, 2001; Borowski, 2001; Stratmann, Voorsmit, *et al.*, 2018/ **Chapter 4**). Additionally, meiofauna, biogeochemistry, and ecosystem functioning were investigated in 2015 (Boetius, 2015; Vonnahme, 2016; Paul *et al.*, 2018; Stratmann, Mevenkamp, *et al.*, 2018/ **Chapter 5**).

Despite all these research efforts, the results remain inconclusive: Meiofauna densities inside plough tracks, e.g., recovered to 90% of the densities at the reference sites after 26 yr, but the variability in densities inside plough tracks is high (Gollner *et al.*, 2017). In comparison, nematodes in the surface sediment (0–2 cm) incorporate significantly more phytodetritus inside plough tracks in the absence of large holothurians than at reference sites in the presence of holothurians (Stratmann, Mevenkamp, *et al.*, 2018/ **Chapter 5**). Holothurian densities between

inside and outside plough tracks were not significantly different anymore 3 yr after the DISCOL experiment (Stratmann, Voorsmit, *et al.*, 2018/ **Chapter 4**), but the combined macrofauna and megafauna carbon (C) stock was still 46% lower inside the tracks compared to outside the tracks after 26 yr (Stratmann, Lins, *et al.*, 2018/ **Chapter 6**).

We integrated these results and combined them with unpublished data collected by state-of-the-art sampling, such as guided boxcoring, seafloor imaging using HR-photographs from towed frames and AUV, best conversion factors, and a large physiological database (**Chapter 2**) to develop the most highly resolved food-web model that exists for the deep sea so far. The food-web model uses the linear inverse modeling approach that estimates C flows among food-web compartments in pre-defined topological food webs (Vézina and Platt, 1988). For this purpose, linear inverse modeling combines data on C stocks, physiological constraints, such as mortality or respiration rates, and site specific fluxes, such as detritus deposition or community respiration (Vézina and Platt, 1988; van Oevelen *et al.*, 2010).

We investigated in particular the microbial loop, scavenging and the role of fish. Scavenging on carrion was neglected in previous deep-sea food webs (e.g., van Oevelen, Soetaert and Heip, 2012; Dunlop *et al.*, 2016; Durden *et al.*, 2017), though a meta-study on 23 food webs across all ecosystems showed that including scavenging resulted in 22% more links per species and a 26% higher food-web connectance (Wilson and Wolkovich, 2011). The authors concluded that facultative scavenging has a large effect on food webs because up to 45% of the food-web links could be related to scavenging. Fishes have also been included only sporadically (e.g., Stratmann, Lins, *et al.*, 2018), though their role in abyssal food webs is interesting, because they can bypass the conventional phytodetritus-based food web by scavenging on epipelagic nekton falls (Drazen *et al.*, 2008).

The aim of this study was (1) to assess whether total C cycling was different between reference sites, outside plough tracks, and inside plough tracks, (2) to assess the role of the microbial loop, and (3) to analyze the role of scavenging and fish in the food web.

7.3 Material and methods

7.3.1 Study site

The Peru Basin in the SE Pacific extends from the East Pacific Rise at 110°W to the Atacama Trench west of the coast of Peru (Klein, 1993; Bharatdwaj, 2006). In the North, the Peru Basin borders on the Carnegie Ridge at 5°S and in the South, it borders on the Sala-y-Gomez Ridge and the Nazca Ridge at 24°S (Klein, 1993; Bharatdwaj, 2006). The Peru Basin has a water depth between 4,000 and 4,400 m (Wiedicke and Weber, 1996) and a bottom water temperature of 2.9°C (Boetius, 2015). The DEA is located in the northern part of the Peru Basin at 07°04.4’S, 88°27.6’W (Thiel *et al.*, 1989), where the water depth ranges from 3,800 to 4,300 m (Greinert, 2015). The effect of the DISCOL disturbance was assessed inside plough tracks, outside plough tracks, i.e., areas next to plough-

tracks where re-suspended sediment settled, and at reference sites 4 km away from DEA that were unaffected by the disturbance experiment.

7.3.2 Food-web structure

Compartments defined in the food web are detritus, dissolved organic carbon (DOC), prokaryotes, meiofaunal nematodes, other metazoan meiofauna, macrofaunal polychaetes, other metazoan macrofauna, holothurians, other invertebrate megafauna, fishes, and carrion.

Detritus was divided into different lability classes, namely labile detritus (lDet), semi-labile detritus (sDet), and refractory detritus (rDet) (*sensu* van Oevelen, Soetaert and Heip, 2012).

Metazoan meiofauna consisted of Nematoda, Harpacticoida and their nauplii, Polychaeta, Ostracoda, Tardigrada, Bivalvia, Kinorhyncha, Gastrotricha, Tanaidacea, Cyclopoida, Gastropoda, Loricifera, Oligochaeta, Rotifera, and Isopoda. Based on the four most abundant nematode families in the abyssal CCZ (Miljutin *et al.*, 2011), Nematoda were divided into the feeding types non-selective deposit feeder (NemNSDF), epistrate feeder (NemEF), and omnivores/ predators (NemOP) (Supplementary table 7-1). Meiofaunal polychaetes were divided into feeding types following the feeding type classification for macrofauna. Polychaetes for which site-specific information was available. The remaining metazoan meiofauna were classified as filter and suspension feeders (MeiFSF), bacterivores (MeiB), deposit feeders (MeiDF), predators (MeiP), and omnivores (MeiOF) (Supplementary table 7-1).

Metazoan macrofauna taxa included Polychaeta, Copepoda, Amphipoda, Tanaidacea, Isopoda, Cumacea, Nematoda, Bivalvia, Gastropoda, Scaphopoda, Echinoidea, Ostracoda, and Ophiuroidea. As polychaetes were identified to family level, Jumars, Dorgan and Lindsay's (2015) review paper was used to classify the polychaetes into suspension feeders (PolSF), surface deposit feeders (PolSDF), subsurface deposit feeders (PolSSDF), predators (PolP), and omnivores (PolOF) (Supplementary table 7-2). Differences in polychaete family composition among the three sites further allowed a site-specific feeding-type differentiation. All other macrofauna taxa were classified as filter and suspension feeder (MacFSF), deposit feeder (MacDF), predators (MacP), and omnivores (MacOF) (Supplementary table 7-2).

Megafaunal taxa of the phyla Annelida, Arthropoda, Chordata (except fish), Cnidaria, Echinodermata (except Holothuria), Hemichordata, Mollusca, and Porifera were combined in the feeding types deposit feeders (MegDF), suspension and filter feeders (MegFSF), surface deposit feeders (MegSDF), subsurface deposit feeders (MegSSDF), predators (MegP), omnivores (MegOF), and scavengers (MegS) (Supplementary table 7-3). Furthermore, the five holothurian morphotypes *Amperima* sp., *Benthodytes typica*, *Mesothuria* sp., *Peniagone* sp. (including *Peniagone* sp. morphotype "palmata", *Peniagone* sp. 1, *Peniagone* sp. 2 benthopelagic), and *Psychropotes depressa* that contributed together between 80% (outside plough tracks) and 83% (reference sites) to the total holothurian biomass (Stratmann, Voorsmit, *et al.*, 2018/ **Chapter 4**) were kept as separate

food-web compartments (Supplementary table 7-3). All other holothurian morphotypes were summed as filter and suspension feeding holothurians (HolFSF) and surface-deposit feeding holothurians (HolSDF).

Fish were divided into *Bathysaurus* sp., *Ipnops* sp., and Ophidiidae. *Bathysaurus* sp. predates on *Ipnops* sp., Ophidiidae, Amphipoda, Cirripedia, Isopoda, Munidopsidae, *Probeebei* sp., Pycnogonida, and other crustaceans and it scavenges carrion (Sulak *et al.*, 1985; Crabtree, Carter and Musick, 1991; Drazen and Sutton, 2017). *Ipnops* sp. predates upon Polychaeta, Amphipoda, Isopoda, other crustaceans, and Mollusca (Crabtree, Carter and Musick, 1991; Drazen and Sutton, 2017). Ophidiidae predates on Polychaeta, Amphipoda, Isopoda, other crustaceans, Mollusca and it scavenges carrion (Crabtree, Carter and Musick, 1991; Drazen and Sutton, 2017; Gerringer *et al.*, 2017). Based on the contribution of carrion to the Ophidiidae diet by weight (0–0.2%; Gerringer *et al.*, 2017; Crabtree, Carter and Musick, 1991), 0 to 0.2% of the diet of *Bathysaurus* sp. and Ophidiidae consists of carrion. The contribution of the different megafaunal compartments to the fish diet (Supplementary table 7.4) was calculated based on the contribution of each prey taxon to the feeding-type specific C stock.

7.3.3 Food-web links

C transfer links in the food web were defined as follows: Sedimentary and suspended detritus pools in the model, i.e., suspended and sedimentary labile detritus, suspended and sedimentary semi-labile detritus, and sedimentary refractory detritus, received C input from an external phytodetritus and an external semi-labile detritus pool. Suspended labile and semi-labile detritus were C sources for all filter- and suspension feeders (MeiFSF, MacFSF, PolSF, MegFSF, and HolFF). Sedimentary labile detritus and prokaryotes were linked to epistrate feeders (NemEF), non-selective deposit feeders (NemNSDF), surface deposit feeders (PolSDF and HolSDF), subsurface deposit feeders (PolSSDF), other deposit feeders (MeiDF, MacDF, and MegDF), deposit-feeding holothurians (*Amperima* sp., *Benthodytes* sp., *Mesothuria* sp., *Peniagone* sp., and *Psychropotes* sp.), and omnivores (NemOP, MeiOF, PolOF, MacOF, and MegOF). Sedimentary semi-labile detritus was taken up by non-selective deposit feeders, surface and subsurface deposit feeders, other deposit feeders, omnivores, and the holothurians *Benthodytes* sp., *Mesothuria* sp., and *Psychropotes* sp.. Predators and omnivores preyed upon all faunal organisms from the same and smaller size classes, e.g., MacP preyed upon other macrofauna and all meiofauna. Meiofaunal (NemOP, MeiP) and macrofaunal predators (PolP, MacP) could also predate on members of its own compartment. Additionally, omnivores and scavengers (MegS, *Bathysaurus mollis*, and Ophidiidae) scavenged from the carrion compartment. *Ipnops* sp. predated upon MegFSF, MegDF, MegP, and MegS (Supplementary table 7-4). *Bathysaurus mollis* predated upon MegFSF, MegDF, MegP, MegS, *Ipnops* sp., and Ophidiidae (Supplementary table 7-4) and Ophidiidae predated upon MegFSF, MegDF, MegP, and MegS (Supplementary table 7-4).

All faunal compartments produced feces that contributed to the semi-labile and refractory detritus pool. Furthermore, dead nematodes and other meta-

zoan meiofauna formed part of the semi-labile detritus pool, whereas dead polychaetes, other metazoan macrofauna, holothurians, other megafauna, and fishes contributed to carrion. Sedimentary labile, semi-labile, and refractory detritus hydrolyzed to DOC that was taken up by prokaryotes. Prokaryotes respired C as dissolved inorganic carbon (DIC) and contributed to the DOC pool by virus-induced prokaryotic lysis. The DOC pool further increased by influx of external DOC to the system. Other C fluxes out of the model included the burial of refractory detritus, respiration by all faunal compartments and prokaryotes, the efflux of DOC, external scavengers scavenging carrion, and predation on polychaetes, other macrofauna, holothurians, other megafauna, and fishes by external predators. A schematic representation of all C flows within the food web is shown in Figure 7-1.

7.3.4 Data availability

Data on detritus stocks, prokaryotic abundance and C stock, meiofaunal density, community composition, and C stocks, and megafaunal density, community composition, and C stocks are unpublished and were specifically collected during R/V *Sonne* cruise SO242-1 (Greinert, 2015) and R/V *Sonne* cruise SO242-2 (Boetius, 2015) to develop these food-web models.

7.3.4.1 Carbon stocks of food-web compartments

To quantify the labile, semi-labile, and refractory detritus and prokaryote pools in the upper 5 cm of sediment, sediment samples were taken with ROV-deployed push corers, multi-corer, benthic lander, and bladecorer at reference sites, outside plough tracks, and inside plough tracks. The number of replicates per sample parameter at the three different sites is presented in Table 7.1.

Table 7-1. Number of samples taken to determine sediment porosity, labile, semi-labile, and refractory detritus stocks, prokaryote stocks, meiofauna stocks, and macrofauna stocks at reference sites (Ref.), outside plough tracks (OPT), and inside plough tracks (ITP).

Sample parameter	Ref	OPT	ITP
Sediment porosity*	3	4	5
Labile detritus	9	9	18
Semi-labile detritus	3	2	2
Refractory detritus*	9	9	18
Prokaryotes*	9	9	18
Meiofauna	2	6	18
Macrofauna	10	7	3

*For the analysis of sediment porosity, labile detritus, refractory detritus, and prokaryotes, sediment samples were taken of the microhabitats “plough track valley” and “plough track ripple”.

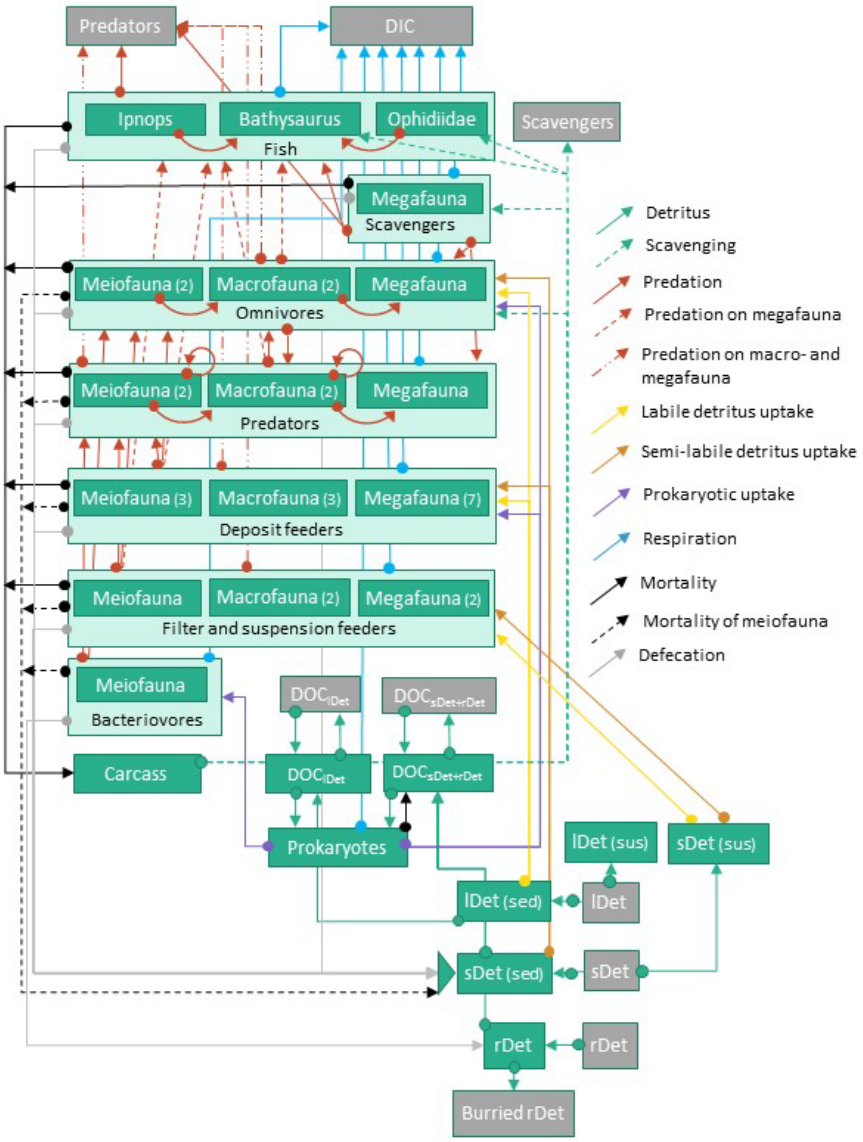

Figure 7-1. Schematic representation of the topological food web used for the linear inverse models. Green boxes show all food-web compartments inside the model, whereas gray boxes show external compartments that were not explicitly modeled. Light green boxes show the feeding types bacterivores, filter and suspension feeders, deposit feeders, predators, omnivores, and fish. Dark green represents the size classes meiofauna, macrofauna, megafauna, and the specific fish taxa *Ipnops* sp., *Bathysaurus mollis*, and Ophidiidae. The numbers in brackets behind the size classes specify the number of food-web compartments of that specific size class and feeding type. The arrows symbolize C flows leading from the C source (arrow ending with a big dot) to C sink (arrowhead). Abbreviations are: DOC = dissolved organic matter, lDet (sus) = suspended labile detritus, sDet (sus) = suspended semi-labile detritus, lDet (sed) = labile detritus in the sediment, sDet (sed) = semi-labile detritus in the sediments, rDet = refractory detritus.

The labile detritus pool is defined as the average chlorophyll-a (chl-a) content in the surface sediment (*sensu* van Oevelen, Bergmann, *et al.*, 2011) that was extracted in 90% acetone. Subsequently, the chl-a concentration was measured photometrically following Jeffrey's and Humphrey (1975) approach for mixed phytoplankton populations and converted to C units with a C to chl-a-ratio of 40 (de Jonge, 1980). The semi-labile detritus pool is defined as the sum of proteins, carbohydrates, and lipids, i.e., the so-called biopolymeric C (Fabiano, Danovaro and Fraschetti, 1995). The concentration of total hydrolysable amino acids (THAA) in the surface sediment was measured following Veuger *et al.* (2005). As neither lipid nor carbohydrate concentrations in the sediment were measured, a ratio of 0.12 : 1 : 1.32 for lipids : THAAs : carbohydrates (Laubier and Monniot, 1985) was used to calculate the total biopolymeric C pool. The refractory detritus pool refers to the particulate organic carbon (POC) stock in the surface sediment that was measured after acidification by flash combustion (Verardo, Froelich and McIntyre, 1990) using a CNS-analyzer and from which the labile and semi-labile detritus pools were subtracted.

Prokaryotic abundance in the surface sediment (0–1cm) was determined using the Acridine Orange Direct Count (AODC) method and converted into prokaryotic C stock (mmol C m^{-2}) by multiplying the abundance with a factor of 12.5 fg C $cell^{-1}$, i.e., C content of prokaryotic cells in waters from the southern subtropical Pacific (15°S) (Fukuda *et al.*, 1998). The 0–1 cm prokaryotic C stock was extrapolated to the 0–5 cm prokaryotic C stock as:

$$C\ stock_{0-5cm} = \sum C\ stock_{0-1cm} \times e^{-0.1\times(x+1)} \qquad \text{[Equation 7-1]}$$

based on previous C stock measurements in the Peru Basin (Forschungsverbund Tiefsee-Umweltschutz, unpubl.). $C\ stock_{0-1cm}$ corresponds to the C stock in the surface sediment (0–1 cm) and $(x + 1)$ is the sediment interval (i.e., x = 1 for the sediment interval 1–2 cm).

Metazoan meiofaunal C stock was determined from ROV-deployed push corers (Table 7-1) of which the upper 5 cm of sediment was preserved in 4% borax-buffered formaldehyde. Ashore, sediment samples were washed over a 32 µm sieve and meiofauna was extracted by density centrifugation with Ludox HS40 (Dupont) at 3,000 rpm (Burgess, 2001). Meiofauna were identified to higher taxon level and counted with a stereomicroscope (50× magnification) to determine taxon-specific densities. Stocks of all meiofauna taxa were calculated by multiplying the taxon-specific densities with the conversion factors from Supplementary table 7-1. Subsequently, stocks of the different taxa were grouped according to feeding type (see section 7.3.2).

Metazoan macrofauna were collected with a 50×50×60 cm box corer at reference sites, outside plough tracks, and inside plough tracks (Table 7-1). The sediment of the upper 5 cm was sieved on a 500 µm sieve and all organisms that were retained on this sieve were preserved in 96% un-denaturated ethanol. Ashore, all macrofauna were sorted under a stereomicroscope and identified to higher taxon level and to family level, respectively, in case of Polychaeta. Macrofauna and macrofaunal polychaete stocks were calculated by multiplying the macrofauna and macrofaunal polychaete densities from the box corers with

taxon-specific individual biomass data from Supplementary table 7-2. Subsequently, the different C stocks were combined in feeding types as described in section 7.3.2.

Densities and subsequently biomass of holothurians at reference sites, outside plough tracks, and inside plough tracks were measured from >4,500 seafloor photographs as described by Stratmann, Voorsmit, *et al.* (2018)/ **Chapter 4**. C stocks of the holothurian morphotypes were calculated as the product of the morphotype-specific densities (Stratmann, Voorsmit, *et al.*, 2018/ **Chapter 4**) and the median morphotype specific individual biomasses (Supplementary table 7-3) and grouped into individual holothurian food-web compartments as described in section 7.3.2. Density of other metazoan megafaunal taxa (ind. m^{-2}) was determined on seafloor images that were taken with the towed "Ocean Floor Observation System" (OFOS). For each disturbance level (reference sites, outside plough tracks, inside plough tracks), 300 pictures were randomly selected and annotated with the open-source annotation software PAPARA(ZZ)I (Marcon and Purser, 2017). Densities of all metazoan megafauna were converted to C stocks (mmol C m^{-2}) by appropriate conversion factors (Supplementary table 7-3).

Fishes seen on OFOS pictures were identified to family and when possible to genus level using the "Atlas of Abyssal Megafauna Morphotypes of the Clipperton-Clarion Fracture Zone: Osteichthyes" identification guide (Linley, 2014). Subsequently, fish densities were converted to C stocks (mmol C m^{-2}) using fish-taxon dependent conversion factors (Supplementary table 7-4).

The resulting stock of each food-web compartment is presented in Table 7-2.

Table 7-2. C stocks (mmol C m^{-2}) of the food-web compartments at reference sites (Ref), outside plough tracks (OPT), and inside plough tracks (IPT).

Compartment	**Ref.**	**OPT**	**IPT**
Detritus			
Labile detritus (lDet)	6.37	5.70	5.25
Semi-labile detritus (sDet)	406	538	367
Refractory detritus (rDet)	6955	7168	7808
Prokaryotes			
Prokaryotes (Pro)	8.52	8.48	8.17
Meiofaunal Nematoda			
Non-selective deposit feeding nematodes (NemNSDF)	0.22	0.42	0.33
Epistrate feeding nematodes (NemEF)	0.11	0.21	0.17
Omnivory/ predatory nematodes (NemOP)	0.11	0.21	0.17
Meiofauna (except Nematoda)			
Meiofauna filter and suspension feeders (MeiFSF)	3.87×10^{-2}	6.70×10^{-2}	4.34×10^{-2}
Meiofauna bacterivores (MeiBF)	4.66×10^{-4}	8.09×10^{-4}	1.07×10^{-3}
Meiofauna deposit feeders (MeiDF)	1.33	2.09	1.82

Meiofauna predators (MeiP)	6.61×10^{-2}	6.85×10^{-2}	3.51×10^{-2}
Meiofauna omnivores (MeiO)	0.18	0.37	0.48
Macrofaunal Polychaeta			
Polychaete suspension feeders (PolSF)	0.14	0.21	0.24
Polychaete surface deposit feeders (PolSDF)	0.40	0.46	0.52
Polychaete subsurface deposit feeders (PolSSDF)	0.17	0.16	0.20
Polychaete predators (PolP)	0.24	0.22	0.21
Polychaete omnivores (PolO)	0.11	0.18	0.07
Macrofauna (except Polychaeta)			
Macrofauna filter feeders (MacFSF)	3.61×10^{-2}	3.87×10^{-2}	2.63×10^{-2}
Macrofauna deposit feeders (MacDF)	1.35	0.38	0.11
Macrofauna predators (MacP)	0.18	8.48×10^{-2}	5.09×10^{-2}
Macrofauna omnivore (MacO)	4.05×10^{-2}	4.24×10^{-2}	5.04×10^{-2}
Holothuroidea			
Amperima sp.	6.01×10^{-2}	7.17×10^{-2}	5.85×10^{-2}
Benthodytes typica	6.76×10^{-2}	0.10	0.12
Mesothuria sp.	1.84×10^{-2}	1.27×10^{-2}	1.26×10^{-2}
Peniagone sp.	2.12×10^{-2}	1.68×10^{-2}	1.89×10^{-2}
Psychropotes depressa	5.11×10^{-2}	7.97×10^{-3}	1.43×10^{-2}
Filter and suspension feeding holothurians (HolFSF)	0.00	0.00	4.56×10^{-3}
Surface-deposit feeding holothurians (HolSDF)	4.35×10^{-2}	5.23×10^{-2}	4.41×10^{-2}
Megafauna (except Holothuroidea)			
Megafauna filter and suspension feeders (MegFSF)	9.15	7.35	4.10
Megafauna deposit feeders (MegDF)	2.56	2.42	3.53
Megafauna predators (MegP)	3.63	2.66	6.58
Megafauna scavengers (MegS)	1.43×10^{-2}	1.51×10^{-2}	6.19×10^{-2}
Megafauna omnivores (MegO)	0.82	1.06	2.01
Fishes			
Bathysaurus sp.	0.00	4.73	14.7
Ipnops sp.	0.21	0.23	0.12
Ophidiidae	0.00	0.11	1.00

7.3.4.2 Site-specific flux constraints

C flows between food-web compartments were constrained using site-specific flux and physiological constraints that were implemented in the linear inverse model either as equalities or inequalities, i.e., minimum and maximum

flux rates. A description of how fluxes were measured and the corresponding references is given in the text below and the data are presented in Table 7-3.

Table 7-3. Data on C fluxes (mmol C m^{-2} d^{-1}) that were fed into the model as inequalities [minimum, maximum] or equalities (single value).
Abbreviations are: Ref. = reference sites, OPT = outside plough tracks, IPT = inside plough tracks.

C flux	Value
Labile+semi-labile detritus deposition	[0.18, 0.33]
Refractory detritus deposition‡	[4.11×10^{-3}, ∞]
Labile+semi-labile detritus degradation rate‡	[2.19×10^{-5}, ∞]×C stock
Refractory detritus degradation rate‡	[2.74×10^{-9}, ∞]×C stock
Burial flux of refractory detritus	Ref.: 8.95×10^{-2}, OPT: 8.95×10^{-2}, IPT: 9.92×10^{-2}
Diffusive flux of DOC from the sediment	Ref.: -2.69×10^{-3}, OPT: 7.37×10^{-5}, IPT: -8.71×10^{-5}
Total C mineralization*	Ref. (n = 25): [0.69, 0.90], OPT (n = 28): [0.53, 0.70], IPT (n = 19): [0.51, 0.68]
Prokaryotic C production*	Ref. (n = 6): [0.34, 0.68] , OPT (n = 8): [0.40, 1.00], IPT (n = 14): [0.11, 0.37]

*Minimum and maximum values correspond to the 1st and 3rd quartile of the dataset.
‡Constraints were adjusted in the fitting step.

Labile+semi-labile detritus deposition refers to the sum of labile and semi-labile detritus deposition to the system, whereas refractory detritus deposition describes the deposition of refractory detritus to the system. Correspondingly, labile+semi-labile degradation rate relates to the total loss of labile and semi-labile detritus via dissolution of detritus to DOC and uptake by fauna. Refractory detritus degradation is the dissolution of refractory detritus to DOC. These four fluxes were estimated by Haeckel *et al.* (2001) in a numerical diagenetic model for the Peru Basin based on pore water profiles of oxygen, nitrate, nitrite, ammonia, phosphate, manganese, sulfate, silicate, and pH.

Burial of refractory detritus (*BFc*) was calculated following Ståhl *et al.* (2004) as:

$$BF_c = \omega \times DBD \times sedOC, \qquad \text{[Equation 7-2]}$$

where ω is the sediment accumulation rate (2 cm ky^{-1}; Haeckel *et al.*, 2001), *DBD* is the dry bulk density (2.65 g cm^{-3}; Buchanan, 1984), and *sedOC* is the sediment organic C content of the 14–16 cm sediment layer (reference sites: 0.74± 5.45×10^{-2} wt%, n = 6; outside plough tracks: 0.74±4.77×10^{-2} wt%, n = 9; inside plough tracks: 0.82±5.43×10^{-2} wt%, n = 18).

Diffusive DOC flux out of the sediment J_0 was inferred from the DOC concentration difference in the overlaying water and the pore water in the surface sediment (0–2 cm). It was calculated with Fick's First Law:

$$J_0 = -\varphi^m \times D_{sw} \times \frac{dC}{dz_0}, \quad \text{[Equation 7-3]}$$

where φ^m is the porosity of the surface sediment, D_{sw} is the molecular diffusion coefficient of DOC, dC is the DOC concentration gradient between porewater and bottom water, and dz_0 is the distance over which the concentration gradient was measured (Lahajnar *et al.*, 2005). Porosity of surface sediment was measured at reference sites (0.93±0.01), outside plough tracks (0.93±0.01), and inside plough tracks (0.92±0.01) by weight loss due to freeze-drying. The difference in DOC concentration between porewater at the midpoint of the sampling interval, i.e., 1 cm for a 0–2 cm sediment slice, and bottom water was 11.32 µmol DOC L^{-1} at the reference sites, -0.31±0.95 µmol DOC L^{-1} outside plough tracks, and 0.37±0.71 µmol DOC L^{-1} inside plough tracks (Paul *et al.*, 2018). The molecular diffusion coefficient of DOC for deep-sea regions is 2.96×10^{-7} cm^2 s^{-1} (Lahajnar *et al.*, 2005).

Total C respiration was measured as diffusive oxygen uptake (DOU) rates by microprofiling with the ROV deployed ROV-Profiler (MPI, Bremen) and by microprofiling with a benthic flux lander system (MPI, Bremen).

Prokaryotic C production was measured as ^{13}H-leucin incorporation by prokaryotes and converted to prokaryotic production following Danovaro (2010b):

$$PCP = LI \times (\%Leu) \times M \times 0.86, \quad \text{[Equation 7-4]}$$

where PCP is the prokaryotic C production (in mmol C m^{-2} d^{-1}). LI is the leucine incorporation rate (nmol Leu g dry sediment d^{-1}), $\%Leu$ is the leucine fraction in the total prokaryotic amino acid pool (0.073), M is the molar weight of leucine (131.2 g mol^{-1}) and 0.86 is the conversion factor of prokaryotic protein production to prokaryotic C production.

7.3.4.3 Physiological constraints

Physiological constraints from the literature are summarized in Table 7-4 and have been used extensively in various published C-flux food-web models. Details about how individual process rates were calculated are described in the text below.

Prokaryotic growth efficiency (*PGE*) in deep-sea sediments was estimated in a pulse-chase experiment with ^{13}C labelled substrate as:

$$PGE = \frac{I_P}{(I_P + R_P)}, \quad \text{[Equation 7-5]}$$

where I_P was the amount of added C that was incorporated by prokaryotes and R_P was the amount of C that was mineralized by prokaryotes (Mayor *et al.*, 2012).

The minimum and maximum values of virus-induced prokaryotic mortality (*VIPM*) corresponded to the $mean_{VIPM} - SD_{VIPM}$ and the $mean_{VIPM} + SD_{VIPM}$ values for sediments below 1,000 m water depth (Danovaro, Dell'Anno, *et al.*, 2008).

Assimilation efficiency *AE* was defined as:

$$AE = \frac{(I-F)}{I}, \quad \text{[Equation 7-6]}$$

with *I* being the ingested food and *F* being the feces (Crisp, 1971). The minimum and maximum values were the lower and upper quartile values of *AE* for invertebrate meiofauna, macrofauna, and megafauna published in **Chapter 2**. The minimum and maximum *AE* values for fish corresponded to the range of *AE* measured in shallow and deep-water fishes (Drazen, Reisenbichler and Robison, 2007).

Net growth efficiency *NGE* was:

$$NGE = \frac{G}{(G+R)}, \quad \text{[Equation 7-7]}$$

where *G* was the growth and *R* was the respiration (Clausen and Riisgård, 1996).

The minimum and maximum invertebrate production rates *P* (mmol C m^{-2} d^{-1}) were calculated as:

$$P = \frac{P}{B}\text{-}ratio \times C\ stock, \quad \text{[Equation 7-8]}$$

where $\frac{P}{B}$-*ratio* was the production/biomass-ratio (d^{-1}) for invertebrate meiofauna, macrofauna, and megafauna from **Chapter 2**. The maximum secondary production *P* (mmol C m^{-2} d^{-1}) for fish was calculated using the allometric relationship between annual *P/B-ratio* (yr^{-1}) and fish weight *W* (g):

$$log_{10}\frac{P}{B}\text{-}ratio = 0.42 - 0.35 \times 5.86 \times log_{10}(W) \quad \text{[Equation 7-9]}$$

(Randall, 2002) for an individual biomass of scavenging benthic deep-sea fish calculated as:

$$log_{10}W = 0.62 + 5.86 \times 10^{-41} \times depth \quad \text{[Equation 7-10]}$$

(Collins *et al.*, 2005) for a water *depth* of 4,100 m.

The mortality *M* (mmol C m^{-2} d^{-1}) always ranged from 0 to the maximum production *P*.

Similar to *P*, the respiration *R* (mmol C m^{-2} d^{-1}) was calculated as:

$$R = r \times C\ stock, \quad \text{[Equation 7-11]}$$

where *r* was the biomass-specific faunal respiration (d^{-1}) for invertebrate meiofauna, macrofauna, and megafauna from **Chapter 2**. *R* calculations for the food-web compartments *Amperima* sp., *Benthodytes typica*, *Mesothuria* sp., and *Peniagone* sp. were based on average *in situ r* measurements of *Amperima* sp. (*n* = 3), *Benthodytes* sp. (*n* = 7), *Mesothuria* sp. (*n* = 1), and *Peniagone* sp. (*n* = 1) specimens, respectively, in the Peru Basin (Brown *et al.*, 2018). Biomass-specific faunal respiration of the food-web compartments *Psychropotes depressa*, HolFSF, and HolSDF was based on a dataset of 5 different holothurian genera (*n* = 13; Brown *et al.*, 2018). *R* of fish was calculated as described in Equation 7-11: Ophidiidae *r* was based on a measurement for Ophidiidae (Drazen and Seibel, 2007) and *r* of the food-web compartments *Bathysaurus* sp. and *Ipnops* sp. was based on a dataset of 7 demersal fish species (*Antimora microlepis*, *Pachycara gymninium*, *Sebastolobus altivelis*, *Coryphaenoides acrolepis*, *Cyclothone acclinidens*, *Corphaenoides armatus*, *Synaphobranchus kaupi*; *n* = 26; Smith and Hessler, 1974; Smith, 1978; Smith and Laver, 1981; Smith and Brown, 1983; Drazen and Seibel, 2007; Drazen and Yeh, 2012).

Feeding selectivity described the proportionally higher uptake of labile C pools, i.e., labile detritus, semi-labile detritus, and prokaryotes, than present in the detritus stock (van Oevelen, Soetaert and Heip, 2012). Feeding preference of mixed omnivores and predators signified the contribution of predation to their

diet and was pre-defined to range from 0.75 to 1.00 (*sensu* van Oevelen, Soetaert and Heip, 2012).

Table 7-4. Equality (single value) and inequality constraints [minimum, maximum] of physiological processes that were implemented in the food-web models. See Table 7-2 for full compartment names.
References: [1]Mayor *et al.* (2012), [2]Danovaro, Dell'Anno, *et al.* (2008), [3]**Chapter 2** and references therein, [4]Clausen and Riisgård (1996), [5]Navarro *et al.* (1994), [6]Nielsen *et al.* (1995), [7]Koopmans, Martens and Wijffels (2010), [8]Mondal (2006), [9]Brown *et al.* (2018), [10]Drazen, Reisenbichler and Robison (2007), [11]Childress *et al.* (1980), [12]Collins *et al.* (2005), [13]Randall (2002), [14]Drazen and Seibel (2007), [15]Drazen and Yeh (2012), [16]Smith and Hessler (1974), [17]Smith and Brown (1983), [18]Smith and Laver, (1981), [19]Smith (1978), [20]this study, [21]van Oevelen, Soetaert and Heip (2012).

Processes	**Size classes/ compartments**	**Value**	**Ref.**
Prokaryotic growth efficiency (-)	Prokaryotes	[0.28, 0.73]	1
Virus-induced prokaryotic mortality (-)	Prokaryotes	[0.87, 0.91]	2
Assimilation efficiency (-)	Meiofauna*	[0.26, 0.41]	3
	Macrofauna*	[0.62, 0.87]	3
	Megafauna*	[0.48, 0.80]	3
	Fish	[0.84, 0.87]	10
Net growth efficiency (-)	Meiofauna⁂	[0.69, 0.95]	3
	Macrofauna	[0.60, 0.72]	4, 5, 6
	Megafauna	[0.48, 0.60]	6, 7, 8
	Fish	[0.37, 0.71]	11
Secondary production (mmol C m^{-2} d^{-1})	Meiofauna*	[4.50×10^{-2}, 0.13]×C stock	3
	Macrofauna‡	[8.49×10^{-4}, 4.77×10^{-3}]× C stock	3
	Megafauna‡	[2.74×10^{-4}, 1.42×10^{-2}]× C stock	3
	Fish	[0, 6.30×10^{-4}]×C stock	12, 13
Mortality (mmol C m^{-2} d^{-1})	Meiofauna	[0, 0.13]×C stock	
	Macrofauna	[0, 4.77×10^{-3}]×C stock	
	Megafauna	[0, 1.42×10^{-2}]×C stock	
	Fish	[0, 6.30×10^{-4}]×C stock	
Respiration (mmol C m^{-2} d^{-1})	Meiofauna‡	[2.03×10^{-2}, 6.96×10^{-2}] ×C stock	3
	Macrofauna‡	[7.12×10^{-5}, 2.28×10^{-2}] × C stock	3
	Megafauna‡ (except Holothuroidea)	[1.23×10^{-6}, 1.42×10^{-3}] × C stock	3
	Holothuroidea (except *Amperima* sp.,	[9.95×10^{-3}, 3.37×10^{-2}] × C stock	9

	Benthodytes typica, *Mesothuria* sp., *Peniagone* sp.)		
	Amperima sp.	[0, 3.36×10^{-2}]×C stock	9
	Benthodytes typica	[0, 1.94×10^{-2}]×C stock	9
	Mesothuria sp.	[0, 5.47×10^{-2}]×C stock	9
	Peniagone sp.	[0, 1.89×10^{-2}]×C stock	9
	Ophidiidae	5.91×10^{-4}×C stock	14
	Bathysaurus sp., *Ipnops* sp.	[1.79×10^{-4}, 8.54×10^{-4}]× C stock	14-19
Feeding selectivity (-)	NemNSDF, MeiDF, MacDF, MegDF, PolSSDF, *Mesothuria* sp.	[1, 15]	20, 21
	PolSDF, HolSDF, *Benthodytes typica*, *Psychropotes depressa*	[50, 1000]	21
Feeding preference (-)	NemOP	[0.75, 1.0]	21

*Due to a lack of data for abyssal plains, the data from near-shore areas were applied.
⁑As only insufficient data were found for the continental rise/ abyssal plain depth regime, data from the continental slope are presented here.
⁂Net growth efficiency for meiofauna was calculated as described in Equation 7-6 using production and respiration rates from **Chapter 2**.

7.3.5 Incorporation of isotope tracer data in the linear inverse model

Stratmann, Mevenkamp, *et al.* (2018)/ **Chapter 5** investigated site-specific differences (reference sites vs. inside plough tracks) in the incorporation of fresh phytodetritus C by prokaryotes, meiofauna, macrofauna, and holothurians (Table 7-5) by conducting *in situ* pulse-chase experiments with ^{13}C labelled *Skeletonema costatum*. These phytodetritus C incorporation rates *I* were integrated in the linear inverse model to further constrain C flows (van Oevelen, Soetaert, *et al.*, 2006; van Oevelen, Soetaert and Heip, 2012).

The secondary production based on phytodetritus C incorporation P_P was implemented as:

$$P_P = I \times B, \quad \text{[Equation 7-12]}$$

and as:

$$P_P = U_P \times AE \times NGE, \quad \text{[Equation 7-13]}$$

where U_P is the uptake of phytodetritus C (mmol C m^{-2} d^{-1}).

Table 7-5. Phytodetritus C incorporation rates *I* (mmol phytodetritus C mmol C^{-1} d^{-1}) in prokaryotes, several Nematoda, macrofauna, and holothurians based on pulse-chase experiments by Stratmann, Mevenkamp, *et al.* (2018)/ **Chapter 5**. The data are presented as inequalities [minimum, maximum] or equalities (single values). See Table 7-2 for full compartment names, sites are abbreviated as: Ref. = reference sites, OPT = outside plough tracks, IPT = inside plough tracks.

Size class	Food-web compartments	Phytodetritus C incorporation
Prokaryotes		Ref. + OPT: [4.62×10^{-3}, 1.46×10^{-2}] IPT: [2.49×10^{-3}, 1.02×10^{-2}]
Nematoda	NemNSDF, NemEF	Ref. + OPT: [1.53×10^{-3}, 2.95×10^{-3}] IPT: [1.23×10^{-3}, 3.23×10^{-3}]
Polychaeta	PolSDF	[3.79×10^{-3}, 4.62×10^{-3}]
Macrofauna	MacDF	[9.40×10^{-5}, 1.20×10^{-3}]
	MacFSF	[2.49×10^{-4}, 1.25×10^{-3}]
Holothurians	*Amperima* sp.	[1.24×10^{-3}, 1.13×10^{-2}]
	Benthodytes typica	5.86×10^{-3}
	Mesothuria sp., *Psychropotes depressa*, HolSDF	[1.24×10^{-3}, 1.29×10^{-2}]
	Peniagone	1.29×10^{-2}

7.3.6 Linear inverse model and network indices

Linear inverse models were developed for steady state conditions. When all compartments are present in the food web, it contains 428 C flows with 49 mass balances, i.e., 41 food-web compartments plus 8 data equalities, and 238 data inequalities. This implies that the model was mathematically under-determined (49 equalities vs. 428 unknown flows). Hence, the models were solved in the R package *LIM* (van Oevelen *et al.*, 2010) in R (R-Core Team, 2017) on the Peregrine HPC cluster of the University of Groningen (The Netherlands). Following the likelihood approach (van Oevelen *et al.*, 2010), 100,000 solutions were sampled in 25 parallel sessions, i.e., 4,000 solutions per session. For each flow, means and standard deviations of the 100,000 solutions were calculated which showed a convergence of standard deviations to a ±2% error margin.

Network indices "Total system throughput" (*T..*), i.e., the sum of all C flows in the food web, "Finn's cycling index", i.e., the portion of *T..* that is cycled (Finn, 1980), "number of links" (*L*), "link density" (*LD*), and "connectance" (C) were calculated with the R package *NetIndices* (Kones *et al.*, 2009) for each of the 100,000 model solutions and summarized as mean±SD.

Furthermore, the trophic level of each faunal compartment was calculated for each of the 100,000 model solutions with the R package *NetIndices* (Kones *et al.*, 2009) and summarized as mean±SD. The trophic level of the carcass pool $TL_{carcass}$ was calculated for each model solution as the weighted average of inflow source compartments as:

$$TL_{carcass} = 1 + \sum_{j=1}^{n} \frac{T^{*}_{carcass,j}}{T_{carcass}} \times TL_{j}, \qquad \text{[Equation 7-14]}$$

where *n* is the number of internal food-web compartments, *j* are food-web compartments, $T^*_{carcass,j}$ is the flow matrix excluding external flows, and $T_{carcass}$ is the total inflow to the carcass compartment excluding external sources.

7.3.7 Statistical analysis of differences in carbon flows

Statistical differences between disturbance levels for individual C flows, C flow pathways or network indices were determined using the approach presented in van Oevelen, Soetaert, *et al.* (2011). Briefly, the fraction of flow values of one randomized flow set that was larger than the fraction of flow values of another randomized flow set was calculated and used to define significance. When the fraction was >90% or <10%, the difference between the flows was considered to be significant; when the fraction was >95% or <5%, the difference was considered to be highly significant.

7.4 Results

7.4.1 Food-web structure

The food webs at reference sites, outside plough tracks, and inside plough tracks contained 38, 40, and 41 compartments, respectively (Figure 7-2, Table 7-6). Filter-feeding holothurians were absent outside plough tracks and at reference sites. Additionally, the fish compartments *Bathysaurus mollis* und Ophidiidae were missing at reference sites.

Table 7-6. Network indices calculated for the food webs at reference sites (Ref.), outside plough tracks (OPT), and inside plough tracks (IPT).

Site	Number of food-web compartments *n*	Total number of links *L*	Link density *LD*	Connectance *C*
Ref.	38	358	9.42	0.21
OPT	40	380	9.50	0.20
IPT	41	389	9.49	0.20

Food-web compartments were connected with 358 (reference sites) to 389 (inside plough tracks) links and had a link density between 9.42 (reference sites) and 9.49 (outside plough tracks) (Table 7-6).

Maximum trophic levels at the three sites were calculated to be 3.80±0.19, 3.97±0.19, and 3.76±0.17 for reference sites, outside plough tracks, and inside plough tracks, respectively. Mean trophic levels of the carrion compartment were calculated to be 2.64±0.17, 2.46±8.28×10^{-2}, and 2.52±8.70×10^{-2} and mean trophic levels of carnivores were 3.33±0.35, 3.36±0.42, and 3.18±0.42. Mean trophic levels of deposit feeders were calculated to be 2.31±0.32, 2.31±0.32, and 2.22±0.32. For both feeding types (carnivores and deposit feeders), the difference between sites was not significant (Table 7-7).

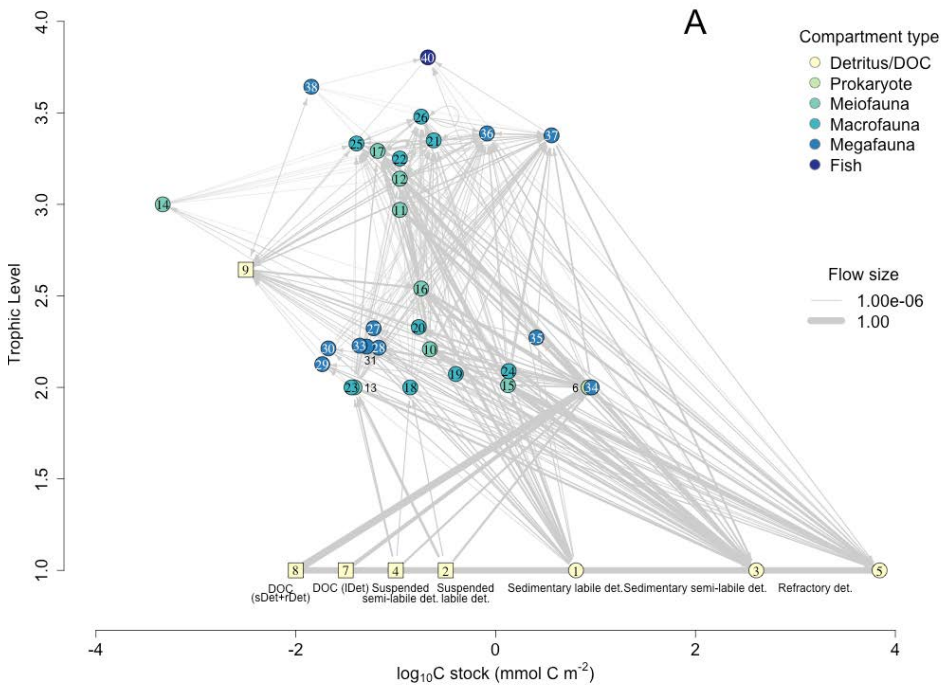

Figure 7-2. Food-web structure of the (A) reference sites, (B) outside plough tracks, and (C) inside plough tracks. Square nodes represent compartments for which C stock values were assigned for plotting purposes. The thickness of a link denotes the flow magnitude (in mmol C m^{-2} d^{-1}).

Numbers inside every node correspond to the compartments as follows: 1 = sedimentary labile detritus, 2 = suspended labile detritus, 3 = sedimentary semi-labile detritus, 4 = suspended semi-labile detritus, 5 = sedimentary refractory detritus, 6 = prokaryotes, 7 = labile detritus-based DOC in the sediment, 8 = semi-labile and refractory detritus-based DOC in the sediment, 9 = carrion, 10 = non-selective deposit feeding nematodes, 11 = epistrate feeding nematodes, 12 = omnivory predatory nematodes, 13 = meiofauna filter and suspension feeder, 14 = meiofauna bacterivore, 15 = meiofauna deposit feeder, 16 = meiofauna predator, 17 = meiofauna omnivore, 18 = polychaete suspension feeder, 19 = polychaete surface deposit feeder, 20 = polychaete subsurface deposit feeder, 21 = polychaete predator, 22 = polychaete omnivore, 23 = macrofauna filter feeder, 24 = macrofauna deposit feeder, 25 = macrofauna omnivore, 26 = macrofauna predator, 27 = *Amperima* sp., 28 = *Benthodytes typica*, 29 = *Mesothuria* sp., 30 = *Peniagone* sp., 31 = *Psychropotes depressa*, 32 = filter and suspension feeding holothurians, 33 = surface-deposit feeding holothurians, 34 = megafauna filter and suspension feeder, 35 = megafauna deposit feeder, 36 = megafauna omnivore, 37 = megafauna predator, 38 = megafauna scavengers, 39 = *Bathysaurus mollis*, 40 = *Ipnops* sp., and 41 = Ophidiidae.

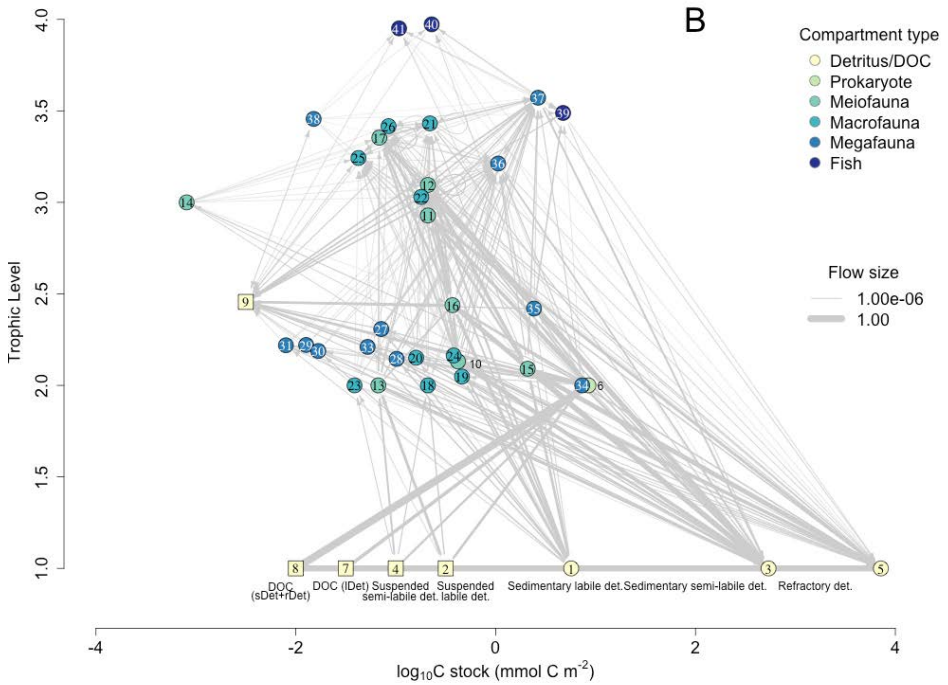

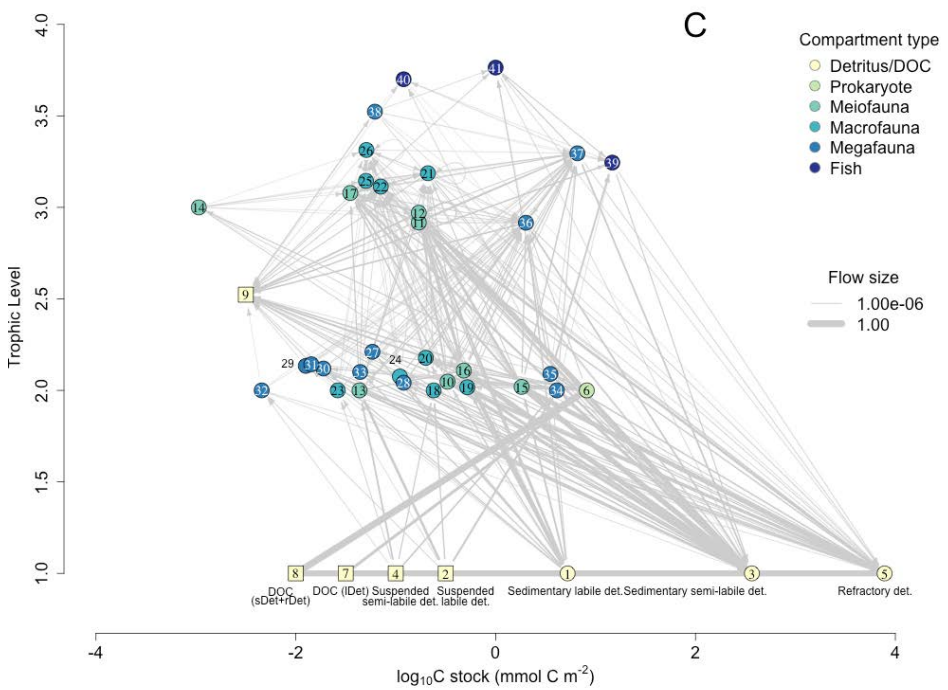

Figure 7-2 continued.

Table 7-7. Pairwise comparisons of trophic levels, network indices, and specific C pathways between reference sites and outside plough tracks (Ref. vs. OPT), reference sites and inside plough tracks (IPT), and outside and inside plough tracks (OPT vs. IPT). The numbers indicate the fraction of flow values of one randomized flow set that was larger than the fraction of flow values of another randomized flow set. Significant differences are presented in *italic* and highly significant differences in **bold**.

	Ref. vs. OPT	**Ref. vs. IPT**	**OPT vs. IPT**
Trophic level			
Carrion	0.85	0.74	0.29
Carnivores	0.41	0.53	0.37
Deposit feeders	0.50	0.64	0.36
Network index			
Total C throughput *T*..	0.20	**1.00**	**0.00**
Finn's cycling index *FCI*	**0.00**	0.43	**0.00**
Specific C pathway			
Microbial loop	0.89	**1.00**	**1.00**
Scavenging pathway	**0.02**	0.27	**0.97**

It was estimated that the trophic level of 35 of the 41 food-web compartments changed from the reference site, to outside plough tracks, to inside plough tracks, whereas the trophic levels of prokaryotes, meiofauna bacterivores, and filter and suspension feeders remained constant (Figure 7-3).

7.4.2 Carbon flows

Modelled total C input (mmol C m^{-2} d^{-1}), i.e., deposition and filter/ suspension feeding, was $0.69\pm2.99\times10^{-2}$ inside plough tracks, $0.70\pm3.89\times10^{-2}$ outside plough tracks, and $0.90\pm2.31\times10^{-2}$ at reference sites (Figure 7-4A). It was dominated by refractory detritus deposition that contributed between 52% (outside plough tracks) and 64% (reference sites) to total C input. The contribution of labile detritus deposition and filter/ suspension feeding on this detritus type to total C input was between 23% (reference sites) and 28% (inside plough tracks) and semi-labile detritus accounted for 14% (reference sites) to 20% (inside plough tracks). DOC influx (mmol C m^{-2} d^{-1}) was $2.69\times10^{-3}\pm1.09\times10^{-3}$ (0.30% of total C input) at reference sites and $8.71\times10^{-5}\pm3.57\times10^{-5}$ (0.38% of total C input) inside plough tracks.

Most C was lost via respiration (85% inside plough tracks to 89% at reference sites), followed by C burial whose contribution was 10% at reference sites, 13% outside plough tracks, and 14% inside plough tracks (Figure 7-4B). DOC efflux resulted in a loss of $7.37\times10^{-5}\pm3.01\times10^{-5}$ mmol C m^{-2} d^{-1} outside plough tracks; no DOC efflux was measured (and therefore modeled) at reference sites and inside plough tracks (Table 7-3; Figure 7-4B).

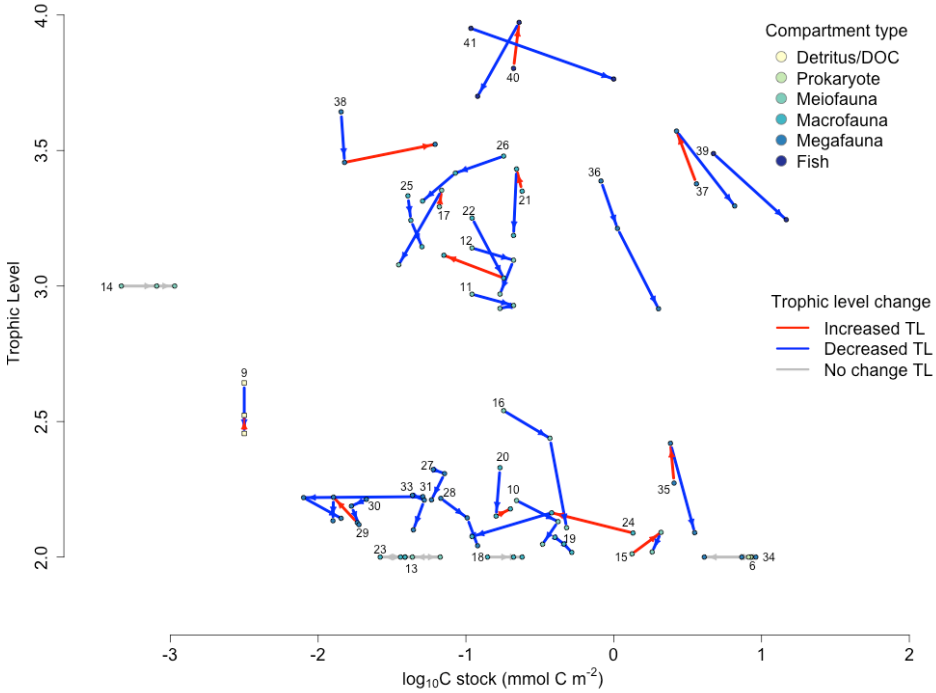

Figure 7-3. Change in trophic level of each food-web compartment from the reference site situation to the outside plough track situation, to the inside plough track situation. Detritus compartments were omitted except for the carcass compartment. Filter and suspension feeding holothurians were omitted as they only occurred inside plough tracks. *Bathysaurus mollis* and Ophidiidae did not occur at the reference sites, hence only the change from outside to inside plough tracks is shown.
Red arrows denote an increase in trophic level, blue arrows denote a decrease in trophic level, gray arrows denote only a change in biomass. Numbers inside every node correspond to individual food-web compartments as presented in Figure 7-2.

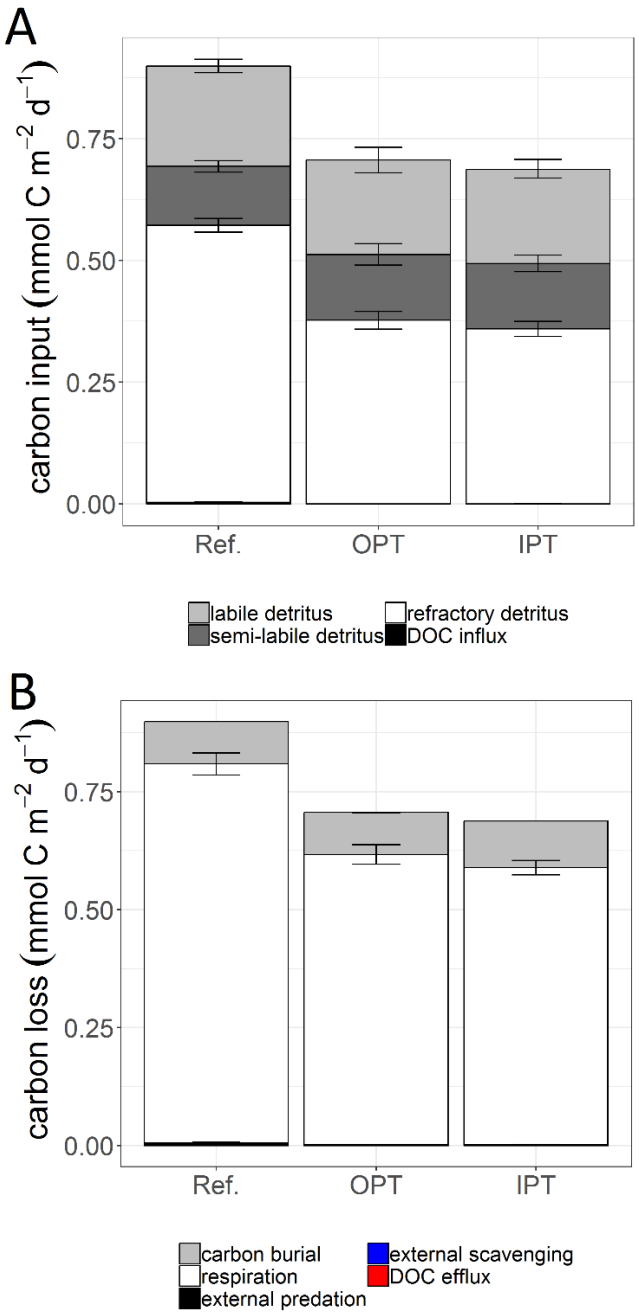

Figure 7-4. (A) C input (mmol C m^{-2} d^{-1}) as labile detritus, semi-labile detritus, and refractory detritus deposition and DOC influx to the reference sites (Ref.), outside plough tracks (OPT), and inside plough tracks (IPT). (B) C loss (mmol C m^{-2} d^{-1}) as C burial, respiration, external predation, external scavenging, and DOC efflux at reference sites, outside plough tracks, and inside plough tracks. Error side bars represent 1 standard deviation; C loss by burial was fixed in the model and therefore the standard deviation is 0.

Table 7-8. Modelled respiration (mmol C m^{-2} d^{-1}) of the different size classes at reference sites (Ref.), outside plough tracks (OPT), and inside plough tracks (IPT). Data are presented as mean±SD; contribution (in %) of size class-specific speciation to total respiration.

	Ref.	**OPT**	**IPT**
Total respiration	$0.80\pm2.3\times10^{-2}$	$0.61\pm2.08\times10^{-2}$	$0.59\pm1.53\times10^{-2}$
Prokaryotes	$0.74\pm2.30\times10^{-2}$; 91.5	$0.51\pm1.95\times10^{-2}$; 83.8	$0.50\pm1.43\times10^{-2}$; 85.4
Meiofauna	$4.01\times10^{-2}\pm4.45\times10^{-3}$; 4.98	$5.99\times10^{-2}\pm6.73\times10^{-3}$; 9.75	$5.18\times10^{-2}\pm4.94\times10^{-3}$; 8.83
Nematoda	$1.08\times10^{-2}\pm1.23\times10^{-3}$; 1.34	$1.78\times10^{-2}\pm2.09\times10^{-3}$; 2.90	$1.48\times10^{-2}\pm2.13\times10^{-3}$; 2.52
Macrofauna (except polychaetes)	$2.13\times10^{-3}\pm4.17\times10^{-4}$; 0.26	$1.11\times10^{-3}\pm1.67\times10^{-4}$; 0.18	$5.99\times10^{-4}\pm6.15\times10^{-5}$; 0.10
Macrofaunal polychaetes	$2.57\times10^{-3}\pm4.01\times10^{-4}$; 0.32	$2.95\times10^{-3}\pm4.88\times10^{-2}$; 0.48	$2.90\times10^{-3}\pm3.50\times10^{-4}$; 0.49
Holothurians	$2.76\times10^{-3}\pm4.26\times10^{-4}$; 0.34	$2.47\times10^{-3}\pm4.05\times10^{-4}$; 0.40	$2.35\times10^{-3}\pm3.13\times10^{-4}$; 0.40
Megafauna (except holothurians)	$9.61\times10^{-3}\pm1.86\times10^{-3}$; 1.20	$1.40\times10^{-2}\pm1.98\times10^{-3}$; 2.28	$9.61\times10^{-3}\pm1.34\times10^{-3}$; 1.64
Fish	$1.09\times10^{-4}\pm3.39\times10^{-5}$; 0.01	$1.04\times10^{-3}\pm6.92\times10^{-5}$; 0.17	$3.38\times10^{-3}\pm1.13\times10^{-4}$; 0.58

Modelled respiration (mmol C m^{-2} d^{-1}) ranged from $0.59\pm1.53\times10^{-2}$ (inside plough tracks) to $0.80\pm2.36\times10^{-2}$ (reference sites) (Table 7-8) and was significantly different between reference sites and inside plough tracks (fraction of respiration values that were higher at one site compared to another side: 1.00) reference sites and outside plough tracks (fraction of respiration values that were higher at one site compared to another side: 1.00), but not between outside and inside plough tracks (fraction of respiration values that were higher at one site compared to another side: 0.87). It was dominated by prokaryotic respiration that contributed between 84% (outside plough tracks) and 92% (reference sites) to total respiration.

7.4.3 Network indices

Modelled total C throughput *T*.. was 5.36±0.10 mmol C m^{-2} d^{-1}, 5.51±0.16 mmol C m^{-2} d^{-1}, and $4.52\pm8.35\times10^{-2}$ mmol C m^{-2} d^{-1} at reference sites, outside plough tracks, and inside plough tracks, respectively. The difference in *T*.. between inside plough tracks and the other two sites was highly significant, but not the difference in *T*.. between reference sites and outside plough tracks (Table 7-7).

Modelled Finn's cycling index *FCI* was $0.23\pm1.26\times10^{-2}$, $0.35\pm2.30\times10^{-2}$, and $0.23\pm9.56\times10^{-3}$ at reference sites, outside plough tracks, and inside plough tracks, respectively, and differed highly significantly between reference sites and outside plough track, and between outside plough track and inside plough track (Table 7-7).

7.4.4 Specific carbon pathways

The microbial loop, i.e., detritus dissolution, DOC uptake by prokaryotes, viral-induced prokaryotic lysis, prokaryotic respiration, and faunal grazing on prokaryotes, had an estimated C flow of $3.34\pm6.84\times10^{-2}$ mmol C m^{-2} d^{-1} at the reference site, which was 62% of *T*... Outside plough tracks, the microbial loop was estimated to account for $3.16\pm8.40\times10^{-2}$ mmol C m^{-2} d^{-1} (57% of *T*..) and was significantly higher than inside plough tracks ($2.19\pm4.47\times10^{-2}$ mmol C m^{-2} d^{-1}; 48% of *T*..; Table 7-7). In comparison, the estimated C flow through the microbial loop inside plough tracks was 66% of the estimated C flow through the microbial loop at the reference site.

An estimated C flow of $8.85\times10^{-2}\pm3.40\times10^{-3}$ mmol C m^{-2} d^{-1} was channeled through the scavenging pathway, i.e., scavengers feeding on carrion, at the reference site, which was only 0.17% of *T*... Outside plough tracks, the estimated C flow through the scavenging pathway was $2.17\times10^{-2}\pm1.08\times10^{-2}$ mmol C $^{-2}$ d^{-1}, which was 0.39% of *T*.. and inside plough tracks $1.07\times10^{-2}\pm4.37\times10^{-3}$ mmol C $^{-2}$ d^{-1} was estimated to flow through the scavenging pathway (0.24% of *T*..). The estimated amount of C that was channeled through the scavenging pathway differed between reference sites and outside plough tracks, and between outside and inside plough tracks (Table 7-7).

It was estimated that *Bathysaurus mollis* ingested <0.01% (outside plough tracks) to 0.11% (inside plough tracks) of *T*.. (Figure 7-5). In comparison,

Ipnops sp. was estimated to ingest <0.01% of *T.*. (all sites) and fish of the family Ophidiidae were estimated to ingest between <0.01% (outside plough tracks) and 0.03% (inside plough tracks) of *T.*. (Figure 7-5).

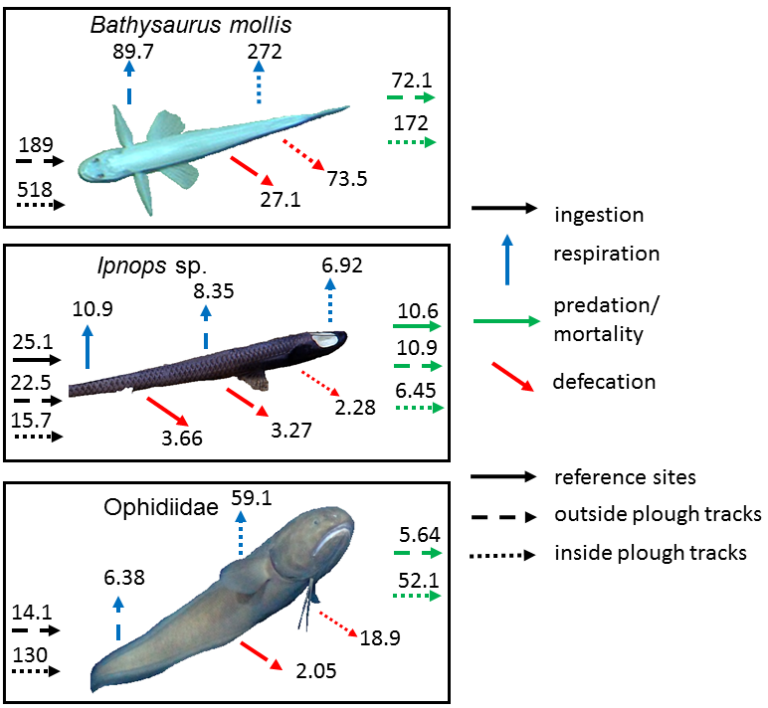

Figure 7-5. Role of fishes in benthic food webs at reference sites, outside plough tracks, and inside plough tracks. The arrows symbolize the C flows (ingestion, respiration, predation/ natural mortality, defecation) and the numbers correspond to the mean C flux in $\times 10^{-5}$ mmol C m^{-2} d^{-1}. Photo courtesy: Atlas of Abyssal Megafauna Morphotype of the Clipperton-Clarion Fracture Zone; NOAA Okeanos Explorer Program, Gulf of Mexico 2012 Expedition; ROV KIEL 6000, Geomar, Kiel.

7.5 Discussion

We investigated differences in C flows between reference sites, outside plough tracks, and inside plough tracks 26 yr after the DISCOL experiment to assess whether the ecosystem has recovered from the small-scale sediment disturbance. Our results show that total C throughput *T.*., i.e., the sum of all C flows, inside plough tracks has in fact not recovered to reference values after 26 years. Here, we discuss the implication of these results and identify the main possible ecological effects. Furthermore, we assess the role of fish and scavenging in marine deep-sea food webs.

7.5.1 Model limitation

Though these food-web models are very detailed, they have some limitations: Refractory detritus deposition modelled by Haeckel *et al.* (2001)

(4.11×10^{-3} to 1.10×10^{-2} mmol C m^{-2} d^{-1}) was too narrowly constrained and incompatible with our model. After removing the maximum refractory detritus deposition constraint, the linear inverse model estimated a refractory detritus deposition (mmol C m^{-2} d^{-1}) of $0.57\pm1.43\times10^{-2}$, $0.38\pm1.82\times10^{-2}$, and $0.36\pm1.55\times10^{-2}$ at reference sites, outside plough tracks, and inside plough tracks, which was about 50 times larger than the predicted maximum constraint. This discrepancy could be related to differences in the definition of labile and non-labile, i.e., refractory detritus. Whereas Haeckel *et al.* (2001) based the distinction between labile and non-labile detritus on degradation rates, we based the division into labile and non-labile detritus on detritus type, hence, labile detritus included all phytodetritus and biopolymeric C, whereas refractory detritus was composed of the "rest". However, our estimated refractory detritus deposition of $0.57\pm1.43\times10^{-2}$ mmol C m^{-2} d^{-1} at the reference site is comparable to the refractory detritus deposition of 0.54 mmol C m^{-2} d^{-1} that Dunlop *et al.* (2016) estimated in a food-web model for the abyssal plains of Station M (NE Pacific). For this model the authors implemented Haeckel's *et al.* (2001) maximum refractory detritus deposition as minimum constraint.

We did not include external (pelagic) prey in our model, although demersal fish can actively prey on midwater fauna: in the Porcupine Seabight, e.g., only 13% of demersal fish exclusively prey on benthos, 35% prey only on pelagic prey, whereas 52% have a mixed diet (Haedrich and Merrett, 1991).

Foraminifera and especially Xenophyophores are very diverse in nodule-rich abyssal plains, such as in the Clarion-Clipperton Zone (Kamenskaya, Melnik and Gooday, 2013; Gooday, Goineau and Voltski, 2015). There, they have densities of 1,600 ind. ha^{-1}, in contrast to the second most abundant taxon Actiniaria that occurs with densities of 170 ind. ha^{-1} (Kamenskaya, Melnik and Gooday, 2013). In the Peru Basin, Xenophyophores have densities of 4,880 ind. ha^{-1} (reference site), 3,957 ind. ha^{-1} (outside plough tracks), and 5,612 ind. ha^{-1} (inside plough tracks). However, it is not possible to assess on pictures whether the tests of Xenophyophores contain a living cell (Andrew Gooday, personal communication). Therefore, we were not able to determine their biomass and excluded this taxon from the food-web model.

7.5.2 Impaired microbial loop after mimicked deep-sea mining

Differences in *T.*. between reference sites and inside plough tracks, and among outside and inside plough tracks were mainly the result of significant differences in the amount of C that was channeled through the microbial loop. In fact, both prokaryotic biomass and prokaryotic C production inside plough tracks were reduced compared to reference sites. Deming (1985) found in box corer samples from 1,850 m water depth a decrease in total number of bacteria from 9.41×10^{8} bacterial cells g^{-1} dry weight sediment 1 cm below the sediment surface to 4.24×10^{8} bacterial cells g^{-1} dry weight sediment at 5 cm sediment depth and 2.50×10^{7} bacterial cells g^{-1} dry weight sediment 15 cm inside the sediment. Hence, reshuffling of sediment and turning the sediment surface upside down during the DISCOL experiment brought sediment to the surface that likely contained less prokaryotes than the original surface sediment. These prokaryotes

might even have a different community composition than the prokaryotic community composition in the original surface sediment, as Shulse *et al.* (2017) found vertical differences in the microbial assemblages of sediments from the CCZ. If prokaryotes from lower sediment layers also had a lower prokaryotic C production rate (Luna *et al.*, 2013) as an adaptation to the reduced C availability compared to the surface sediment, then the prokaryotic C production in the newly exposed surface sediment would be even further reduced.

Based on our results from the small-scale sediment disturbance experiment in the Peru Basin we can assume that also industrial-scale polymetallic nodule extraction will impair the microbial loop. In this way deep-sea mining might affect not only the benthic, but also the pelagic ecosystem. Virus-induced prokaryotic mortality which is part of the microbial loop was estimated to release between 0.37 and 0.63 Gt C as labile organic detritus per year to the world oceans (Danovaro, Dell'Anno, *et al.*, 2008). Though the microbial loop in deep-sea sediments was found to be rather inefficient (Pozzato *et al.*, 2013; Middelburg, 2018), i.e., there was no significant transfer of C derived from bacteria to metazoan consumers in sediments of the Arabian Sea (Pozzato *et al.*, 2013), dissolved organic matter (DOM) produced via the viral shunt can be released from the sediment into the overlaying water where it could fuel the mesopelagic microbial loop (Tanaka, 2009). Hence, if deep-sea mining leads to a reduction of benthic prokaryotic biomass and subsequently to a decrease in DOM release to the water column that is produced via viral-induced lysis of prokaryotes, the microbial loop in the mesopelagic will have a reduced supply with DOM. Consequently, less C could be transferred to higher trophic levels. However, further research is required to verify this hypothesis.

7.5.3 Role of fish and scavenging in deep-sea food webs

Long-term changes in benthopelagic fish abundance have been observed in the abyss: At Station M (SE Pacific), e.g., the annual mean abundance of the abundant grenadier fish (*Coryphaenoides* spp.) was positively correlated with total numbers of mobile epibenthic megafauna and increased from 8 ind. ha^{-1} in 1989 to 28 ind. ha^{-1} in 2004 (Bailey, Ruhl and Smith, 2006). The second most abundant fish species *Bathysaurus mollis* had an average abundance of 1 ind. ha^{-1} (Bailey, Ruhl and Smith, 2006). In comparison, we observed an overall fish abundance of 34 ind. ha^{-1} in the Peru Basin that ingested at most 0.15% of the total system throughput. Hence, to fulfill their metabolic C demand, demersal fish are not dependent on allochthonous input of carrion. Bypassing the phytodetrital pathway as observed by Drazen *et al.* (2008) in macrourid fishes at Station M therefore has likely other reasons which require further research.

Besides large whale falls that support a specialized faunal community (Smith and Baco, 2003), gelatinous zooplankton food-falls, such as salp-falls (Henschke *et al.*, 2013; Smith *et al.*, 2014), thaliacean-falls (Lebrato and Jones, 2009), or jellyfish-falls (Yamamoto *et al.*, 2007; Sweetman and Chapman, 2011; Sweetman, Smith, *et al.*, 2014), and fish-falls (Soltwedel *et al.*, 2003; Yamamoto *et al.*, 2009) contribute to the carrion pool in the deep sea. There, especially smaller carcasses can have a very short residence time: For example, a 36 cm long

fish carcass at the deep-sea observatory "Hausgarten" (Fram Strait) was estimated to be consumed by scavengers within 7 h (Soltwedel *et al.*, 2003). Also at 1,250 m water depth in the Norwegian Sognejord *Scomber scombrus* (mackerel) baits were removed within (mean±SE) 7.0±1.7 h (Sweetman, Smith, *et al.*, 2014). This residence time translates to removal rates of 245% d^{-1} for mackerel (*Scomber scombrus*) baits (Sweetman, Smith, *et al.*, 2014). Removal rates for fresh jellyfish baits are even higher (383% d^{-1}; Sweetman *et al.*, 2014). It is difficult to convert removal rates (in % d^{-1}) to scavenging rates (in mmol C m^{-2} d^{-1}) because knowledge of the deep-sea carrion pool is very limited. However, when we combine the removal rates for jellyfish baits with the C stock of jellyfish falls at the seafloor of another Norwegian fjord (Sweetman and Chapman, 2015), scavenging rates on jellyfish-based carrion range from 0.37 to 1.19 mmol C m^{-2} d^{-1}.

In comparison, our scavenging rate estimate is about four times lower (8.85×10^{-2} mmol C m^{-2} d^{-1} at reference sites) than the minimum scavenging rate calculated for the jellyfish falls. However, the jellyfish deposition in the Norwegian fjord was rather high (0 to 6.07 mmol C m^{-2} d^{-1}; Sweetman and Chapman, 2015) in comparison to the Gulf of California, where the annual squid carcass deposition ranged from 4.17×10^{-3} to 1.01 mmol C d^{-1} (Hoving *et al.*, 2017). Hence, further research on scavenging rates of carrion that originates from natural mortality is necessary to verify our estimates for the Peru Basin.

7.6 Conclusion

Using the most detailed linear inverse model that has been developed for the deep sea so far, this study shows that 26 yr after a small-scale sediment disturbance, total C cycling is still 16% lower inside plough tracks compared to reference sites and 18% lower inside plough tracks compared to outside plough tracks. This indicates that the ecosystem has not recovered from this small-scale sediment disturbance and especially the microbial loop is still impaired. We further show that the role of scavenging and demersal fish in the deep-sea C cycle is limited because their contributions to total C cycling are <1% in both cases.

Acknowledgments

We thank the chief scientists Jens Greinert (SO242-1) and Antje Boetius (SO242-2) as well as captain and crew of RV Sonne for their excellent support during both legs of cruise SO242. We further thank the 'ROV Kiel 6000' team and the 'AUV Abyss' team from Geomar, Kiel (Germany).

7.7 Supplement

Supplementary table 7-1. Feeding types and taxon-specific biomasses (mmol C ind^{-1}) of all metazoan meiofauna included in the food-web models.
Abbreviations are: MeiB = meiofauna bacterivores, MeiDF = meiofauna deposit feeders, MeiFSF = meiofauna filter and suspension feeders, MeiP = meiofauna predators, MeiOF = meiofauna omnivores, NemNSDF = nematode non-selective deposit feeders, NemEF = nematode epistratum feeders, NemOP = nematode omnivores and predators; IPT = inside plough tracks, OPT = outside plough tracks, Ref. = reference sites.
References for biomasses: [a]Stratmann, Mevenkamp, *et al.* (2018)/ **Chapter 5**, [b]Galéron *et al.* (2000), [c]Zeng *et al.* (2018), [d](Bianchelli *et al.*, 2010), [e](Rex *et al.*, 2006).
References for feeding types: [1]Giere (2009), [2]Fox, Barnes and Ruppert (2003), [3]Enríquez-García, Nandini and Sarma, (2013), [4]McClain, Johnson and Rex (2004), [5]Menzies (1962), [6]Heiner, Vinther Sørensen and Møbjerg Kristensen (2018), [7]Miljutin *et al.* (2011), [8]Giere (2006), [9]Stratmann, Lins, *et al.* (2018)/ **Chapter 6**.

Taxon	Feeding type	Biomass	Ref.
Bivalvia*	MeiFSF	3.48×10^{-5}	1, 2, d
Cyclopoida	50% MeiOF, 50% MeiP	5.97×10^{-7}	1, 3, b
Gastropoda⁂	90% MeiDF, 10% MeiP	1.59×10^{-5}	4, d
Gastrotricha‡	MeiB	5.96×10^{-7}	1, d
Harpacticoida	MeiDF	7.01×10^{-5}	1, 2, b
Isopoda*	93% MeiDF, 7% MeiP	1.24×10^{-4}	5, d
Kinorhyncha*	50% MeiB, 50% MeiDF	4.22×10^{-6}	1, 2, d
Loricifera⁂	MeiB	1.59×10^{-5}	6, e
Nematoda	50% NemNSDF, 25% NemEF, 25% NemOP	2.97×10^{-6}	7, a
Oligochaeta*	MeiDF	9.43×10^{-5}	8, d
Ostracoda	MeiOF	4.98×10^{-4}	1, c
Polychaeta	Ref.: 54% MeiDF, 13% MeiFSF, 23% MeiP, 10% MeiOF; OPT: 50% MeiDF, 17% MeiFSF, 18% MeiP, 15% MeiOF; IPT: 58% MeiDF, 19% MeiFSF, 17% MeiP, 6% MeiOF	1.48×10^{-4}	9, c
Rotifera⁂	MeiDF	1.59×10^{-5}	1, e
Tanaidacea‡	MeiOF	1.18×10^{-5}	1, d
Tardigrada‡	MeiB	1.05×10^{-7}	1, d

*Taxon-specific individual biomasses for abyssal plains (B_{4000}; mmol C ind^{-1}) were calculated as $B_{4000} = 10^{log_{10}(B_{1887})-\beta_{meiofauna}\times\Delta depth}$, where B_{1887} corresponds to the taxon-specific individual biomass (mmol C ind^{-1}) from the southern open slope of the Catalan Margin (1,887 m depth; NW Mediterranean Sea) (Bianchelli *et al.*, 2010). $\beta_{meiofauna}$ (=1.70×10^{-4}) corresponds to β in the regression analysis for meiofauna biomass in Rex *et al.* (2006) and $\Delta depth$ is the depth difference between the abyssal plains (~4,000 m depth for the DISCOL experimental site) and the slope station (1,887 m depth).
‡Taxon-specific individual biomasses for abyssal plains (B_{4000}; mmol C ind^{-1}) were calculated as $B_{4000} = 10^{log_{10}(B_{985})-\beta_{meiofauna}\times\Delta depth}$, where B_{985} corresponds to the taxon-specific individual biomass (mmol C ind^{-1}) from the southern open slope of the Catalan

Margin (985 m depth; NW Mediterranean Sea) (Bianchelli *et al.*, 2010) and $\Delta depth$ is the depth difference between the abyssal plains (~4,000 m depth for the DISCOL experimental site) and the slope station (985 m depth).

⁂The individual biomass corresponds to the mean biomass of an individual deep-sea meiofaunal organisms at 4,100 m depth (Rex *et al.*, 2006).

Supplementary table 7-2. Feeding types of all metazoan macrofauna included in the food-web models. The taxon-specific individual biomass data (mmol C ind^{-1}) were taken from Stratmann, Lins, *et al.* (2018)/ **Chapter 6**, Stratmann, Mevenkamp, *et al.* (2018)/ **Chapter 5** and Sweetman *et al.* (in review).
Abbreviations are: MacDF = macrofauna deposit feeders, MacFSF = macrofauna filter and suspension feeders, MacOF = macrofauna omnivores, MacP = macrofauna predators, PolSDF = polychaete surface deposit feeders, PolSF = polychaete suspension feeders, PolSSDF = polychaete subsurface deposit feeders, PolP = polychaete predators, PolOF = polychaete omnivores;
IPT = inside plough tracks, OPT = outside plough tracks, Ref. = reference sites.
References for feeding types: [1]Gage and Tyler (1991), [2]Horton *et al.* (2018), [3]Fox, Barnes and Ruppert (2003), [4]Smith and Stockley (2005), [5]McClain, Johnson and Rex (2004), [6]Menzies (1962), [7]Iken *et al.* (2001), [8]Jumars, Dorgan and Lindsay (2015), [9]Vannier, Abe and Ikuta (1998), [10]Gowing and Wishner (1986).

Taxon	Feeding type	Biomass	Ref.
Amphipoda	50% MacOF, 50% MacP	3.68×10^{-3}	1, 2
Bivalvia	MacFSF	1.41×10^{-3}	3
Copepoda	MacDF	5.39×10^{-4}	10
Cumacea	MacDF	3.09×10^{-3}	3
Echinoidea	85% MacOF, 15% MacDF	9.66×10^{-3}	4
Gastropoda	90% MacDF, 10% MacP	8.56×10^{-2}	5
Isopoda	93% MacDF, 7% MacP	1.33×10^{-3}	6
Nematoda*	75% MacDF, 25% MacP	3.26×10^{-4}	9
Ophiuroidea	MacDF	9.66×10^{-3}	7
Ostracoda	MacOF	2.27×10^{-3}	3
Polychaeta	Ref.: 13% PolSF, 38% PolSDF, 16% PolSSDF, 23% PolP, 10% PolOF; OPT: 17% PolSF, 37% PolSDF, 13% PolSSDF, 18% PolP, 15% PolOF; IPT: 19% PolSF, 42% PolSDF, 16% PolSSDF, 17% PolP, 6% PolOF	1.33×10^{-2}	8
Scaphopoda	MacP	9.66×10^{-3}	3
Tanaidacea	MacDF	5.48×10^{-3}	3

*Macrofaunal nematodes were divided into feeding types following the feeding type classification for meiofaunal nematodes.

Supplementary table 7-3. Feeding types for megafaunal specimens photographed with an "Ocean Floor Observatory System" in the Peru Basin (SE Pacific). Median taxon-specific individual biomass (mmol C ind^{-1}) was calculated as described in Stratmann, Lins, *et al.* (2018)/ **Chapter 6** based on length measurements of individual organisms in the Peru Basin. "*n*" refers to the number of individuals used to estimate taxon-specific biomasses. Abbreviations are: MegDF = megafauna deposit feeders, MegFSF = megafauna filter and suspension feeders, MegSDF = megafauna surface deposit feeders, MegSSDF = megafauna subsurface deposit feeders, MegP = megafauna predators, MegOF = megafauna omnivores, MegS = megafauna scavengers;
IPT = inside plough tracks, OPT = outside plough tracks, Ref. = reference sites.
References for biomasses: [1]Stratmann, Voorsmit, *et al.* (2018)/ **Chapter 4**, [2]Tilot (1992), [3]Stratmann, Lins, *et al.* (2018)/ **Chapter 6**, [4]Durden, Bett, *et al.* (2016), [5]Rex *et al.* (2006), [6]this study.
References for feeding types: [7]Fox, Barnes and Ruppert (2003), [8]Gage and Tyler (1991), [9]Horton *et al.* (2018), [10]Menzies (1962), [11]Escobar-Briones *et al.* (2002), [12]MacAvoy *et al.* (2008), [13]Nakamura, Chen and Mitarai (2015), [14]Smith and Stockley (2005), [15]McClain, Johnson and Rex (2004), [16]Bluhm (2001), [17]Fratt and Dearborn (1984), [18]Wigham *et al.* (2003), [20]Roberts *et al.* (2000), [21]Iken *et al.* (2001), [22]Billett *et al.* (2001), [23]Hudson *et al.* (2004).

Phylum	**Taxa**	**Feeding type**	***n***	**Bio-mass**	**Ref.**
Annelida	Polychaeta[a]	Ref.: 54% MegDF, 13% MegSF, 23% MegP, 10% MegOF; OPT: 50% MegDF, 17% MegSF, 18% MegP, 15% MegOF; IPT: 58% MegDF, 19% MegSF, 17% MegP, 6% MegOF	62	0.12	3
Arthropoda	Amphipoda	50% MegP/ 50%MegS[21]	8	3.58	6
	Cirripedia	MegFSF[7]	2	176	6
	Isopoda	93% MegDF, 7% MegP[10]	19	8.13	6
	Munidopsidae	MegDF[21]	41	267	6
	Probeebei sp.	MegDF[8]	421	68.3	6
	Pycnogonida	50% MegP, 50% DF[8, 21]	41	3.73	6
	Other crustaceans[b]	MegP[8]	41	267	6
Chordata	Ascidiacea[c]	MegFSF[7]		0.83	2
Cnidaria	Actiniaria	MegFSF[7]	301	0.12	3
	Antipatharia	MegFSF[7]	3	166	3
	Ceriantharia[c]	MegFSF[7]		1923	2
	Gorgonaria	MegFSF[7]		21.7	2
	Other Cnidaria[d]	MegFSF[7]		0.24	3

Echinoder-mata	Asteroidea	50% MegDF, 50% MegP[21]	53	224	[3]
	Crinoidea[c]	MegFSF[7]		5.33	[2]
	Echinoidea[c]	15% MegDF, 85% MegOF[14]		59.2	[2]
	Ophiuroidea	MegOF[8]	527	14.4	[3]
	Holothurian morphotypes				
	Abyssocucumis abyssorum	MegFSF[7, 20]	1	4.98	[1]
	Amperima sp.	MegSDF[7, 18, 21]	73	18.1	[1]
	Bathyplotes sp.[d]	MegSDF[23]	552	7.48	[1]
	Benthodytes gosarsi	MegSDF[7, 21]	2	61.1	[1]
	Benthodytes sp.	MegSDF[7, 21]	12	3.00	[1]
	Benthodytes typica	MegSDF[7, 21]	123	22.7	[1]
	Benthothuria sp.[d]	MegSDF[23]	552	7.48	[1]
	Elpidiidae gen. sp.1	MegSDF[22]	24	2.84	[1]
	Elpidiidae gen. sp. 2	MegSDF[22]	15	11.0	[1]
	Elpidiidae gen. sp. 3	MegSDF[22]	5	2.06	[1]
	Galatheathuria sp.	MegFSF[22]	6	66.0	[1]
	Mesothuria sp.	MegSSDF[7, 21]	94	4.32	[1]
	Oneirophanta sp.	MegSDF[7, 21]	11	9.99	[1]
	Peniagone sp. (morphotype “palmata”)	MegSDF[7, 21]	21	1.71	[1]
	Peniagone sp. 1	MegSDF[7, 19, 21]	21	3.27	[1]
	Peniagone sp. 2 (benthopelagic)[d]	MegSDF[7, 19, 21]	552	7.48	[1]
	Psychronaetes hanseni[d]	MegSDF[20]	552	7.48	[1]
	Psychropotes depressa	MegSDF[7, 21]	13	28.2	[1]
	Psychropotes longicauda	MegSDF[7, 21]	9	4.44	[1]

	Synallactidae gen. sp. 1[e]	MegSDF	26	2.41	[1]
	Synallactidae gen. sp. 2[e]	MegSDF	46	2.10	[1]
	Synallactes profundi[e]	MegSDF	17	2.46	[1]
	Synallactes sp. (morphotype "pink")[d]	MegSDF	11	4.36	[1]
	Unknown holothurians[d]	MegSDF	552	7.48	[1]
Hemichordata	Hemichordata[f]	MegDF[8]		22.4	[5]
Mollusca	Gastropoda[f]	90% MegDF, 10% MegP[15]		22.4	[3]
Porifera	Porifera[c]	MegFSF[7]		6.74	[2]

[a]Megafaunal polychaete feeding type composition was based on the macrofaunal polychaete feeding type composition.

[b]As no conversion factors were available for "other crustaceans", the taxon-specific biomass data for Munidopsidae were used.

[c]Mean taxon-specific biomass data per individual were extracted from Tilot (1992) for the CCZ.

[d]The taxon-specific individual biomass of this holothurian morphotype is the mean biomass of all holothurians.

[e]As the gut content of a specimen of Synallactidae collected in the Peru Basin (Stratmann, unpublished data) showed an 18 times enrichment in org. C compared to surrounding sediment, all Synallactidae, *Synallactes profundi*, and *Synallactes* sp. were classified as surface deposit feeder.

[f]Individual biomass calculated for mean benthos megafauna at 4,100 m depth based on the biomass-bathymetry and abundance-bathymetry relationships presented in Rex *et al.* (2006).

Supplementary table 7-4. Diet, fish taxon-dependent conversion factors, and taxon-specific individual biomass (mean±SD, median) of all fish specimens that were observed on pictures taken with the "Ocean Floor Observatory System" in the Peru Basin. "*n*" refers to the number of individuals used to estimate taxon-specific biomasses.
Abbreviations are: DW = dry weight, WW = wet weight;
IPT = inside plough tracks, OPT = outside plough tracks, Ref. = reference sites.
References for feeding types: [a]Crabtree, Carter and Musick (1991), [b]Drazen and Sutton (2017), [c]Sulak *et al.* (1985), [d]Gerringer *et al.* (2017).

Diet	**Conversion factors***				***n***	**Biomass (mmol C ind^{-1})**
	a ($\times 10^{-3}$)	***b***	**DW/ WW**	**C/ DW**		
Bathysaurus mollis						
0–1.6% MegFSF, 11.2–12.5% MegDF, 0.2–2.4% MegP, 0.01–0.02% MegS, 43–100% *Ipnops* sp., 43–100% Ophidiidae, 0.2% carrion[a, b, c]	3.24	3.16	0.24	0.42	2	OPT: 6,715; IPT: 21,114
***Ipnops* sp.**						
3–6% MegFSF, 28.8–79.8% MegDF, 13.1–64.7% MegP, 3.5–6.6% MegS[a, b]	4.90	3.03	0.24	0.42	10	Ref.: 64.1; OPT: 108; IPT: 7.4±0.29, 87.4
Ophidiidae						
0.3–0.6% MegFSF, 28.7–79.6% MegDF, 13–64.6% MegP, 3.5–6.6% MegS, 0.2% carrion[a, b, d]	1.02	3.06	0.17	0.38	3	OPT: 154; IPT: 720±675, 720

*Length *L* (cm) of each specimen was measured in PAPARA(ZZ)I (Marcon and Purser, 2017) using a unilateral triangle of laser points as reference (see also Stratmann, Voorsmit, *et al.*, 2018/ **Chapter 4**). This length measurement was converted to wet-weight *WW* (g WW ind^{-1}) following Froese, Thorson and Reyes (2014): $WW = a \times L^b$, where *a* and *b* are taxon-dependent conversion factors, and subsequently to individual biomass (mmol C ind^{-1}) using conversion factors from Brey *et al.* (2010).

ANALOGUES OF SEDIMENT DISTURBANCE

Chapter 8 : Impaired short-term functioning of a benthic community from a deep Norwegian fjord following deposition of mine tailings and sediments

8. Impaired short-term functioning of a benthic community from a deep Norwegian fjord following deposition of mine tailings and sediments

Lisa Mevenkamp[1], **Tanja Stratmann**[1], Katja Guilini, Leon Moodley, Dick van Oevelen, Ann Vanreusel, Stig Westerlund, and Andrew K. Sweetman;
Modified from *Frontiers in Marine Sciences*, 2017: 4:169. doi: 10.3389/fmars.2017.00169.

8.1 Abstract

The extraction of minerals from land-based mines necessitates the disposal of large amounts of mine tailings. Dumping and storage of tailings into the marine environment, such as fjords, is currently being performed without knowing the potential ecological consequences. This study investigated the effect of short-term exposure to different deposition depths of inert iron ore tailings (0.1, 0.5, and 3 cm) and dead subsurface sediment (0.5 and 3 cm) on a deep water (200 m) fjord benthic assemblage in a microcosm experiment. Biotic and abiotic variables were measured to determine structural and functional changes of the benthic community following an 11 and 16 d exposure with tailings and dead sediment, respectively. Structural changes of macrofauna, meiofauna, and bacteria were measured in terms of biomass, density, community composition, and mortality while measures of oxygen penetration depth, sediment community oxygen consumption, and ^{13}C-uptake and processing by biota revealed changes in the functioning of the system. Burial with mine tailings and natural sediments modified the structure and functioning of the benthic community albeit in a different way. Mine tailings deposition of 0.1 cm and more resulted in a reduced capacity of the benthic community to remineralize fresh ^{13}C-labeled algal material, as evidenced by the reduced sediment community oxygen consumption and uptake rates in all biological compartments. At 3 cm of tailings deposition, it was evident that nematode mortality was higher inside the tailings layer, likely caused by reduced food availability. In contrast, dead sediment addition led to an increase in oxygen consumption and bacterial carbon uptake comparable to control conditions, thereby leaving deeper sediment layers anoxic and in turn causing nematode mortality at 3 cm deposition. This study clearly shows that even small levels (0.1 cm) of instantaneous burial by mine tailings may significantly reduce benthic ecosystem functioning on the short term. Furthermore, it reveals the importance of substrate characteristics and origin when studying the effects of substrate addition on marine benthic fauna. Our findings should alert decision makers when considering approval of new deep-sea tailings placement sites as this technique will have major negative impacts on benthic ecosystem functioning over large areas.

[1] These authors have contributed equally to this work.

8.2 Introduction

The extraction of mineral resources on land produces large amounts of fine waste material known as mine tailings (Jamieson, 2011). About 60% (iron) to 99.99% (gold) of the ore processed in mines is discarded as non-economic by-product resulting in an annual waste production of 14 billion tons of fine tailings worldwide (Jones and Boger, 2012; Vogt, 2013). While many solutions for the recycling of tailings have been proposed (Bian *et al.*, 2012; Adiansyah *et al.*, 2015), the vast majority is discarded in landfills, lakes, riverine systems, and the marine environment. The environmental and socio-economic consequences of tailings disposal can be devastating so that a proper management and sustainable use of mine tailings requires more attention (Franks *et al.*, 2011; Bian *et al.*, 2012; Adiansyah *et al.*, 2015). For reasons of risk reduction on land as well as economic and esthetical considerations (Kvassnes and Iversen, 2013) the disposal of inert tailings material into streams and the marine environment known as riverine tailings disposal (RTD), submarine tailings placement (STP), and deep-sea tailings placement (DSTP) have been proposed and implemented (Vogt, 2013). But, due to the irreversible environmental impacts resulting from direct tailings discharge into riverine systems the use of this approach has seized and RTD is no longer implemented (Vogt, 2013). Submarine tailings placement, however, is allowed and applied at 14 mining sites worldwide (status in 2013) while new sites are still being targeted (Vogt, 2013). Currently, 0.6% of all industrial-sized mines discharge their tailings into the marine environment with Norway as main contributor (Vogt, 2013). In 2013, Norway, the country with most STP sites worldwide, had 7 operational STP sites, and 2 sites in a planning stage (Kvassnes and Iversen, 2013).

STP occurs mainly at continental margins at depths between 30 and 1,000 m or more including highly productive ecosystems such as fjords and canyons (De Leo *et al.*, 2010; Vogt, 2013; Thurber *et al.*, 2014). Continental margins are significant contributors to biodiversity and productivity and fulfil an important role for the provision of ecosystem services (Walsh, 1991). These include a wide range of regulatory services, such as nutrient cycling, natural carbon (C) sequestration, and primary and secondary production, but also direct provisioning services, such as fisheries and mineral or genetic resources (Armstrong *et al.*, 2012; Thurber *et al.*, 2014). Despite this key role, only few studies have assessed the impacts of mine tailings disposal on the functioning of bathyal benthic communities. The environmental impacts of STP can be manifold, including hypersedimentation, changes in grain size, smothering of benthic fauna, and toxicity by the release of heavy metals or chemicals (Ramirez-Llodra *et al.*, 2015). To prevent irreversible impacts on the environment it is of particular interest to get an understanding of the risks of STP and the magnitude of its impact on marine biota and ecosystem functioning. A large amount of scientific data is available in the “gray literature” from monitoring programs accompanying STP operations (Ramirez-Llodra *et al.*, 2015). However, many of these monitoring studies only report impacts on one or few aspects of the ecosystem and often good baseline studies are lacking (Ramirez-Llodra *et al.*, 2015). Furthermore, to be able to give recommendations for future environmental management with regard to land-

based mining but also regarding possible future marine mining scenarios, it is crucial to investigate threshold values for tailings deposition. And although monitoring studies have incorporated the impact of tailings disposal at various distances from the outfall (Olsgard and Hasle, 1993) it is difficult to infer threshold values for the directly impacted communities as benthic fauna might naturally vary with depth and distance from the outfall due to changes in grain size or food availability. Especially the composition of meiofauna taxa and nematode species in particular and their vertical distribution in the sediment are strongly determined by abiotic factors such as grain size and sediment oxygenation (Jansson, 1967; Higgins and Thiel, 1988; Coull, 1999; Moodley, Chen, *et al.*, 2000) making this group particularly vulnerable to sediment burial and disturbance.

Some important ecosystem functions, e.g., organic matter remineralization or primary and secondary production, are strongly driven by biotic factors, such as biomass, diversity, or bioturbation (Lohrer, Thrush and Gibbs, 2004; Danovaro, Gambi, *et al.*, 2008; Braeckman *et al.*, 2010). Moreover, different trophic levels and functional groups can exhibit tight interactions, and changes in the structure of one taxon can have strong repercussions on others which in turn influences ecosystem functioning (Gilbertson, Solan and Prosser, 2012; Piot, Nozais and Archambault, 2014). Therefore, to fully understand the complexity of the processes shaping the structure and functioning of benthic ecosystems under various stressors, well-designed, controlled experiments resembling natural conditions as close as possible, including multiple trophic levels, and community-based approaches, are needed (Hale *et al.*, 2011; Wernberg, Smale and Thomsen, 2012). Oxygen consumption is a good proxy for the depth-integrated overall remineralization of organic matter by benthic communities through aerobic and anaerobic processes (Moodley, Heip and Middelburg, 1998; Middelburg, Duarte and Gattuso, 2005) and has been proven a very useful indicator in various impact studies (Vanaverbeke *et al.*, 2008; Sweetman *et al.*, 2010; Sweetman, Norling, *et al.*, 2014). Furthermore, the processing of organic matter can be traced through different trophic levels by introducing labile organic material with isotopically enriched C signatures (Middelburg *et al.*, 2000; Boschker and Middelburg, 2002; van Oevelen, Soetaert, *et al.*, 2006). In combination with estimates of biomass and density it is also possible to assess the relative contribution of each biotic component to the observed functional changes (van Oevelen, Soetaert, *et al.*, 2006).

To understand the potential environmental impacts of DSTP on the structure and functioning of soft-sediment communities and to assess threshold levels for tailings deposition, we conducted a microcosm experiment with soft-bottom fauna from a deep Norwegian fjord. For this purpose, natural, undisturbed sediments were incubated in the laboratory under *in situ* conditions and subjected to three different levels of deposition with mine tailings. Structural changes of the macrofaunal, meiofaunal, and bacterial communities were assessed using measures of biomass, densities, and diversity. Furthermore, mortality was assessed in macrofauna by “life-checking” and in meiobenthic nematodes by using a staining technique with Trypan Blue. Next to these structural impacts we investigated ecosystem functioning responses such as oxygen consumption dynamics

and phytodetritus processing by the different biotic compartments making use of stable isotope tracing techniques. To isolate the effect of the tailings from deposition with natural sediment an additional experimental treatment (i.e., the deposition of dead sediment) was included in the experimental setup.

We hypothesized that (1) exposure to burial with mine tailings will alter the benthic community structure on the short term due to mortality and changes in vertical community distribution; (2) changes in benthic community structure due to tailings disposal will cause a reduced processing of organic matter as assessed from O_2 consumption, ^{13}C-labeled phytodetritus uptake, and production of dissolved inorganic carbon (DIC) and (3) the response of benthic organisms to tailings is different than to a deposition event with natural subsurface sediment.

8.3 Materials and methods

8.3.1 Study site and sediment collection

Sediments were collected from 207 m depth in the Norwegian Hadangerfjord (59°43.48′N, 5°24.18′E, SW Norway) on board MS Solvik (October 28, 2014). Three sediment cores (~14 cm) were subsampled from 14 boxcore deployments with a total of 42 subsampled sediment cores. The cores were transported to the laboratory at the International Research Institute of Stavanger (IRIS, Norway) and maintained in the dark at *in situ* temperature (8°C) for acclimatization. The cores were continuously supplied with fresh, cooled, and sand-filtered seawater (salinity: 33.02) from a nearby fjord by a flow-through system via gravity feed. Twelve cores were randomly assigned to the following treatments (n = 4): 0.1, 0.5, and 3 cm of mine tailing (MT) addition. Six cores were assigned to the following treatments (n = 3): 0.5 and 3 cm dead sediment (DS) addition. Inert, ground up tailings from a Norwegian iron ore mine were used for the MT treatments. For the DS treatment, subsurface sediment (<20 cm) was taken from the boxcores, temporarily frozen (-80°C for more than 3 d) to kill fauna and thawed prior to application. Four cores served as controls, i.e., no tailings or sediment was added. The remaining cores were used to measure granulometry of the natural sediment, for nematode staining tests and to determine the necessary amount of substrate required to build up to the target deposition thickness. The latter was experimentally determined as follows: Slurries of tailings and sediment were made from a known amount of material with the estimate to build 1 cm and were added to two separate spare cores. After 24 h of settlement, the actual sediment height was measured and more tailings/sediment was added until a total build-up of 10 cm. From this information the required amount of tailings/sediment was calculated.

8.3.2 Experiment set-up and incubation procedure

To start the experiment, the respective amounts of substrate were added to the cores and were left for 24 h to allow settlement of particles. The different treatment thicknesses of the tailings addition could be easily distinguished from the Control (Figure 8-1A) with visual inspection as the mine tailings formed a dense, gray-reddish layer with a separation of fine, light particles on top and

coarser, darker particles below (Figure 8-1B–D). This distinction was less clear for the dead sediment addition treatments (Figure 8-1E–F).

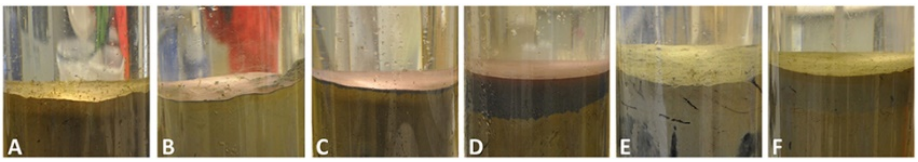

Figure 8-1. Surface layers of the incubation cores 24 h after deposition. (A) Control, (B) 0.1 cm mine tailings, (C) 0.5 cm mine tailings, (D) 3 cm mine tailings, (E) 0.5 cm dead sediment, (F) 3 cm dead sediment.

The incubation procedure involved a series of manipulations, measurements, and samples obtained at the various time points throughout the incubation duration of 11 and 16 d for the MT and DS treatments, respectively (Figure 8-2).

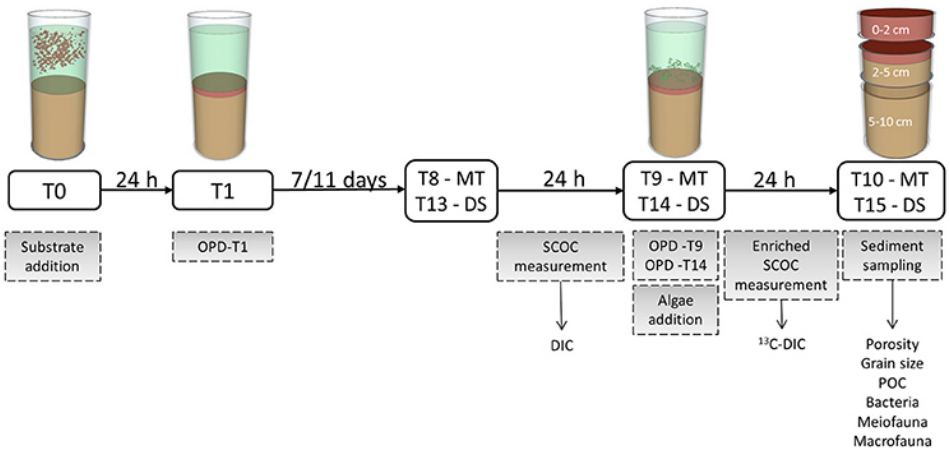

Figure 8-2. Scheme of manipulations and samplings during the experiment. Treatments included the addition of mine tailings (MT) with 0.1, 0.5, and 3 cm thickness and the addition of dead sediment (DS) with 0.5 and 3 cm thickness. "T" indicates the days of incubation after substrate addition. Actions and measurements are shown in gray boxes whereas arrows indicate from which measurements the different variables were obtained. Abbreviations: OPD = oxygen penetration depth, SCOC = sediment community oxygen consumption, DIC = dissolved inorganic carbon, POC = particulate organic carbon.

After substrate addition at T0, particles were allowed to settle for 24 h. One day after tailing addition (T1) the overlying water in the cores was clear indicating that full settlement of particles had taken place and oxygen penetration depth (OPD) in the sediment was determined. At day 8 (T8) and day 13 (T13) for MT and DS, respectively, rates of sediment community oxygen consumption (SCOC) were determined followed by a second OPD measurement. Subsequently, at day 9 (T9) for the MT and day 14 (T14) for the DS treatments, 31 mg (equivalent to 47 mmol C m^{-2}) dried *Skeletonema costatum*, that was enriched in ^{13}C (28% enrichment), was pipetted homogenously on the sediment surface in the

cores and SCOC was measured once again. The isotopically enriched algae provided a tool to trace ^{13}C-C throughout the benthic assemblage and enabled quantification of fresh organic C processing. At day 10 (T10) for the MT treatments and day 15 (T15) for the DS treatments the experiment was terminated by sampling the sediment for faunal and sediment analyses. The different incubation durations for the two treatments are the result of logistic difficulties.

The Control followed the same time frame and sampling procedures as the MT treatments, thus, with an incubation time of 11 d.

After the experiment, sediments were sampled by inserting a smaller meiofauna core (~5 cm) into the experimental core and the overlying water in the experimental cores was carefully siphoned off. The sediment surrounding the meiofauna core was sliced in three intervals (0–2, 2–5, and 5–10 cm) measured from the surface of the added substrate. Each layer was homogenized in a bucket and subsamples were taken with 30 mL syringes and immediately stored frozen at -21°C for analysis of sediment characteristics (porosity, total organic carbon TOC, POC) and bacterial specific phospholipid-derived fatty acids (PLFA). Sediment porosity was determined for each treatment and sediment layer by weight loss after freeze-drying. The sediment granulometry of two separate control cores, each sliced in 0.5 cm intervals and of one mine tailings sample were measured by laser diffraction with a Malvern Mastersize 2000 particle analyzer (Malvern Instruments, UK). Grain size classes were determined according to the Wentworth scale (Wentworth, 1922). After acidification, TOC content was quantified with a Thermo Flash EA 1112 elemental analyzer (Thermo Fisher Scientific, USA).

8.3.3 Analyses determining structural changes of the benthic community

The remaining sediment from the experimental core was sieved over a 500 and 38 µm sieve. The macrofauna fraction (>500 µm) was qualitatively screened under a stereomicroscope ("life check", see Moodley *et al.*, 1997) before fixation in 4% formaldehyde to avoid abundance overestimates which could result from the lack of decomposition of dead organisms under low temperature conditions in a short-term experiment. In all samples, all encountered macrofauna specimens were found to be alive. The preserved samples were later identified to the lowest taxonomic level.

After siphoning off the overlying water of the meiofauna core, the sediment was sliced in intervals of 0.5 cm starting from the surface of the added substrate down to 2 cm depth of the natural sediment and in 1 cm intervals down to 5 cm depth. After slicing of the meiofauna cores, 5 or 10 mL of 4% Trypan blue solution (see "8.3.4 Nematode staining test") were added to the 0.5 and 1 cm sediment slices, respectively, and samples were shaken vigorously before incubation for 2 h in sampling vials to ensure sufficient exposure with the stain. Subsequently, the samples were washed with filtered (10 µm) seawater on a 32 µm sieve until most of the stain was washed out and fixed on 4% buffered formaldehyde. Meiofauna was extracted from the sediment by washing the samples over two stacked sieves of 1 mm and 32 µm. The 32 µm fraction was subjected to density centrifugation with Ludox HS40 (Dupont) at 3,000 rpm (specific density of

1.18; Heip, Vincx and Vranken, 1985). Centrifugation was done three times and the supernatant was sieved (32 μm) and fixed in 4% buffered formaldehyde. Meiofauna was identified to higher taxon level with a stereomicroscope (50×magnification) and nematodes were categorized in "stained" and "unstained". Copepods and their nauplii were removed from the analysis because those taxa were found after sieving (32 μm) the seawater from the flow through system for 30 min. This may point toward the ability of copepods and nauplii to penetrate or inhabit the sand filter. No other meiofauna taxa or larger organisms were found after sieving the water. No meiofauna was found when checking a 30 mL subsample of mine tailings.

Biomass of the three biotic size classes (macrofauna, meiofauna, bacteria) is expressed as organic C content per area (mg C m^{-2}) and was directly calculated from the ratio mass spectrometer output (see '8.3.5 Analyses determining functional changes of the benthic community').

8.3.4 Nematode staining test

Trypan blue is a dye commonly used in cell viability assessments (Louis and Siegel, 2011) that has already been successfully applied to assess soil nematode mortality (Womersley and Ching, 1989). To assess nematode mortality, a new staining protocol with Trypan blue was developed and tested prior to the experiment. To test the protocol, the upper 1.5 cm of two spare cores were sliced in 0.5 cm intervals and three sample vials containing slices of one core were submerged in hot water (±80°C) for 10 min to kill the meiofauna. After 2 h, all samples (dead and live) were stained with 3 mL of 4% Trypan blue solution (prepared with distilled water) and left to incubate for 2 h. In the live samples 16.4±6.84% of nematodes were stained while in the dead samples this percentage was 77.8±7.97%. However, a proportion of 7.05±1.13% and 13.3±4.77% of the nematodes in live and dead samples, respectively, were left "uncategorized" due to an incomplete staining of the bodies.

8.3.5 Analyses determining functional changes of the benthic community

Oxygen penetration depth (OPD) was determined by means of a microprofiler equipped with oxygen microsensors (50 μm tip; Unisense A.S., Denmark). After 2-point sensor calibration (0% calibration: Na_2SO_3; 100% calibration: air-bubbled seawater), oxygen concentration in each core (1 profile per core) was measured by penetrating in 100 μm steps into the sediment until oxygen concentration was below detection limit (0.3 μM).

SCOC was measured over a 24 h period in the dark in cores that were sealed off with lids that were fitted with a stirrer and an oxygen optode (PreSens, Germany). During this period the cores were disconnected from the water flow through system. Water samples of 10 mL (filtered through a 0.2 μm filter and conserved by the addition of 10 μL $HgCl_2$) were taken in headspace vials at the beginning and at the end of the incubation for later analysis of the dissolved in-

organic carbon (DIC) flux and ^{13}C-DIC measurements. For these analyses a headspace of ~1.5 ml was created by injecting Helium gas through a septum. The samples were subsequently acidified with 20 µL concentrated H_3PO_4 to transform DIC into gaseous CO_2. A 500 µL sample of the CO_2 was then injected into a HP 61530 gas chromatograph (Hewlett-Packard/Agilent, USA) connected to a DELTA-Plus Isotope Ratio Mass Spectrometer (Thermo Fisher Scientific, USA) to determine DIC concentrations and ^{13}C composition as described by Moodley, Boschker, *et al.* (2000). The ^{13}C composition in the freeze-dried, grinded sediment subsamples was quantified with a Thermo Flash EA 1112 elemental analyzer (Thermo Fisher Scientific, USA) coupled with a DELTA V Advantage Isotope Ratio Mass Spectrometer (Thermo Fisher Scientific, USA).

The >500 µm macrofaunal fraction was grouped in the following taxonomic groups: Echinodermata, Mollusca, Polychaeta, Sipunculida. Within each sample, each taxonomic group was individually freeze-dried to determine total dry weight. After homogenization, a weighted subsample was taken for isotope and biomass analysis (as described above for sediment, e.g., Moodley *et al.* 2005). In two samples, one individual or pieces of a sea pen (Pennatulacea) were found which were removed from the stable isotope analysis. The meiofauna fraction (>38 µm) of the experimental core sediment was fixed on 4% buffered formaldehyde for stable isotope analysis of nematodes. For this purpose 130 randomly hand-picked nematodes per sample were transferred to a few drops of Milli-Q water in silver capsules (8×5 mm) that had been pre-combusted for 4 h at 450°C. The nematode samples were dried overnight at 60°C, acidified with 20 µl 2% HCl and dried on a hot plate at 60°C. After acidification the samples were closed and bulk C and N content as well as δ^{13}C and δ^{15}N were measured as described for the sediment.

Bacterial tracer uptake and biomass was based on concentrations of bacteria specific PLFA (i14:0, i15:0, a15:0, i16:0, and 18:1ω7c; Middelburg *et al.*, 2000). These PLFAs were extracted from freeze-dried, grinded sediment using the Bligh and Dyer method (Bligh and Dyer, 1959) according to the protocol by Boschker (2004). Subsequently the extracted PLFAs were derivatized to fatty acid methyl esters (FAME) that were analyzed by GC/C-IRMS (HP 61530 gas chromatographer, Hewlett-Packard/ Agilent, USA; DELTA-Plus Isotope Ratio Mass Spectrometer, Thermo Fisher Scientific, USA) with a polar analytical column (ZB5-5MS; 60 m length, 0.32 mm diameter, 0.25 µm film thickness; Phenomenex, USA).

The incorporation of ^{13}C into macrofaunal, nematode, and bacterial biomass was calculated as described by different papers (Middelburg *et al.*, 2000; Moodley *et al.*, 2002; van Oevelen, Middelburg, *et al.*, 2006; Guilini *et al.*, 2011). Total algal tracer uptake is expressed as the quotient of total ^{13}C uptake (I) and the ^{13}C content in *S. costatum* (28%) (see Moodley *et al.*, 2002).

8.3.6 Statistical analyses

To include the depth dependency of samples, all data sets containing depth information were analyzed using a Permanova analysis with a nested design allowing statistical comparison between treatments and within depth layers

(Primer software version 6.1.11 with the Permanova+ add-on, Clarke, 1993; Anderson, Gorley and Clarke, 2008). Table 8-1 shows the Permanova designs for the various variables. When the main test yielded significant differences pairwise tests were performed and, if the number of possible permutations was lower than 100, Monte Carlo tests were applied to estimate p-values [p(MC)] with increased accuracy. Graphs were computed using Prism 6 (GraphPad Software, Inc.). Throughout the manuscript, data is reported as mean and standard error, unless mentioned otherwise.

Table 8-1. Permanova designs for the analysis of various parameters.

Parameter	**Factor**	**Nested in**	**Fixed/ random**
Porosity, TOC	Treatment		Fixed
Faunal densities, diversity and community structure	Depth		Fixed
Biomass of macrofauna, meiofauna and bacteria Uptake of macrofauna, nematodes and bacteria	Core ID	Treatment	Random
OPD; SCOC	Treatment		Fixed
	Time		Fixed
	Core ID	Treatment	Random

As grain size was measured in one spare core it was not analyzed statistically. Porosity and TOC were tested with Permanova for differences between treatments and the control within each layer. Standardized densities in individuals per m^2 and individuals per 10 cm^2 were used for macro- and meiofauna analysis, respectively. Total (whole core) meiofauna and macrofauna densities were analyzed using ANOVA in R (R-Core Team, 2017) to assess differences between treatments after the assumptions of normality and homogeneity of variances were assured. Pairwise comparisons were conducted by means of the TukeyHSD test. For reasons of better comparison, statistical analyses were done on data from the sediment intervals of 0–2, 2–5, and 5–10 cm starting at the added substrate surface for macrofauna and bacteria and on 0–2 and 2–5 cm intervals for meiofauna. Nematode distribution and mortality on a high depth interval resolution was analyzed graphically and descriptively. The contribution of specific macro- and meiofauna taxa to differences in their community composition was determined by a similarity of percentages (SIMPER) analysis. Shannon and Simpson diversity indices and Pielou's evenness index were calculated for meio- and macrofauna densities and tested in terms of whole core diversity (ANOVA) and per depth layer (Permanova).

Due to the repeated measures character of OPD and SCOC data a Permanova analysis was used to test for differences between the factors Treatment and Time (Permanova design, Table 8-1). Univariate data of DIC was analyzed using ANOVA to assess differences between treatments after the assumptions of normality and homogeneity of variances were assured. Total (whole core) tracer

uptake of the different biotic compartments was analyzed with Permanova as assumptions for normality and homogeneity of variances were not met. Depth layer information was included with Permanova as described above.

8.4 Results

8.4.1 Effect of substrate addition on abiotic variables

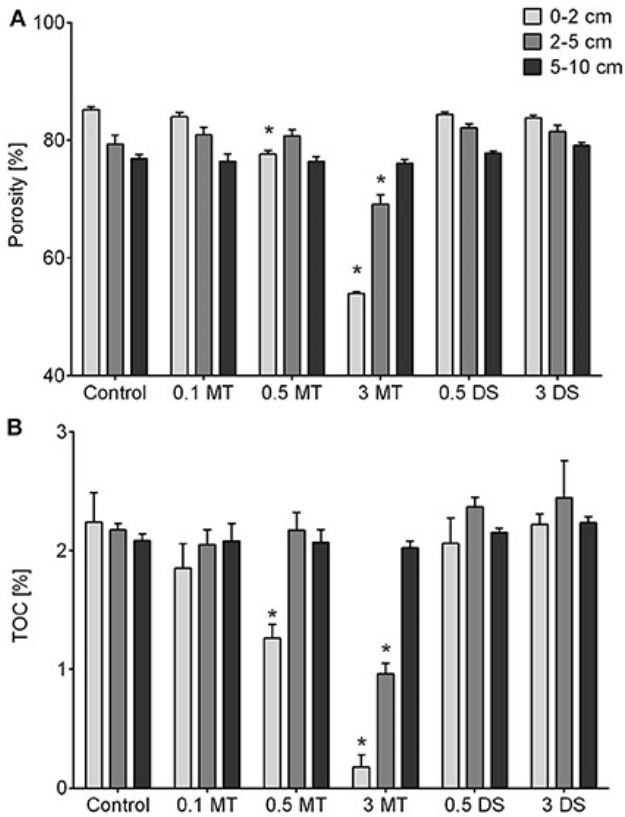

Figure 8-3. (A) Porosity and (B) total organic carbon (TOC) content of all depth layers per treatment. Error bars denote standard error and an asterisk indicates significant ($p < 0.05$) differences with the control.
Abbreviations: 0.1 MT = 0.1 cm mine tailing addition, 0.5 MT = 0.5 cm mine tailing addition, 3 MT = 3 cm mine tailing addition, 0.5 DS = 0.5 cm dead sediment addition, 3 DS = 3 cm dead sediment addition.

The natural sediment was composed of fine silt characterized by a median grain size of 11.94±0.34 µm in the 0–2 cm layer, 12.26±0.13 µm in the 2–5 cm layer and 12.59±0.56 µm in the 5–10 cm layer. In contrast, the mine tailings were composed of very fine sand with a median grain size of 101.31 µm. The difference in median grain size between the mine tailings and the natural sediment was also reflected in the lower porosity of the added layers of tailings compared to the natural sediment [Permanova, $p(MC) \leq 0.003$, Figure 8-3A]. Additionally, TOC

was lower in the layers with added tailings compared to control cores [Permanova, p(MC) ≤ 0.013, Figure 8-3B].

8.4.2 Structural changes of the benthic community

Total macrofauna densities ranged from 12,971±3,573 ind. m^{-2} in the 3 DS treatment to 20,040±2,780 ind. m^{-2} in the 0.1 MT treatment. Though total densities did not significantly differ between treatments, a decreasing trend with sediment depth was observed. Within each sediment depth layer community composition was similar between treatments and control. Within each mine tailings treatment and the control, the community composition in the 0–2 cm layer was different from the deeper layers [Permanova, p(MC) ≤ 0.0400]. Main contributors to the dissimilarities between the 0–2 and 2–5 cm and between the 0–2 and 5–10 cm layers were *Kelliella militaris* (bivalve, 6.5%, 7.23%), *Macrochaeta* sp. (polychaete, 4.11%, 4.45%), *Ophelina modesta* (polychaete, 3.39%, 3.84%), *Mendicula pygmaea* (bivalve, 3.27%, 3.54%), *Sipuncula* sp. (2.14%, 4.05%), and *Nucula nitidosa* (bivalve, 2.83%, 3.46%) with much higher densities in the top (0–2 cm) layer and *Paramphinome jeffreysii* (polychaete, 4.26%, 3.67%) and *Levinsenia gracilis* (polychaete, 2.27%, 3.67%) showing the opposite trend. This depth effect in community composition was not observed in the DS treatments, thus, all organisms were distributed similarly throughout those cores.

Total meiofauna densities (including stained and unstained nematodes) were significantly lower (712±252 ind. 10 cm^{-2}) in the 3 DS treatment compared to the control (2,080 ±93 ind. 10 cm^{-2}, TukeyHSD, p = 0.0115). This difference was attributed to a reduction in nematode densities (TukeyHSD, p = 0.0105) which was the most abundant taxon (94.91±0.34% of meiofauna community). Nematodes were found in high densities in all surface layers, indicating that the animals were able to move into the added MT and DS substrate (Figure 8-4). Interestingly, mortality in the MT treatment was substantially higher as compared to the controls (Figure 8-4), with mortality exceeding 80% in the 0.5 MT and 3 MT treatment. Furthermore, mortality in the 3 DS treatment was high throughout the whole core and not only in the added substrate layer (17.74–63.56%). The addition of mine tailings had no effect on the whole-core meiofauna community composition (faunal mortality not taken into account). In both DS treatments, however, it differed from the control [Permanova, p(perm) ≤ 0.0073] due to reduced densities of nematodes, oligochaetes, and polychaetes (SIMPER). When taking depth layers into account we observed that all taxa were equally successful in migrating into the mine tailings since community composition remained similar in the Control and MT treatments within the upper 2 cm. Also within the deeper layer (2–5 cm) meiofauna community composition remained similar in all treatments when compared to the Control [Permanova, p(perm) ≤ 0.0162]. Interestingly, within each treatment, meiofauna community composition differed between depth layers (0–2 and 2–5 cm) for all treatments except the 3 MT and 3 DS treatments [Permanova, p(MC) ≤ 0.049]. Differences

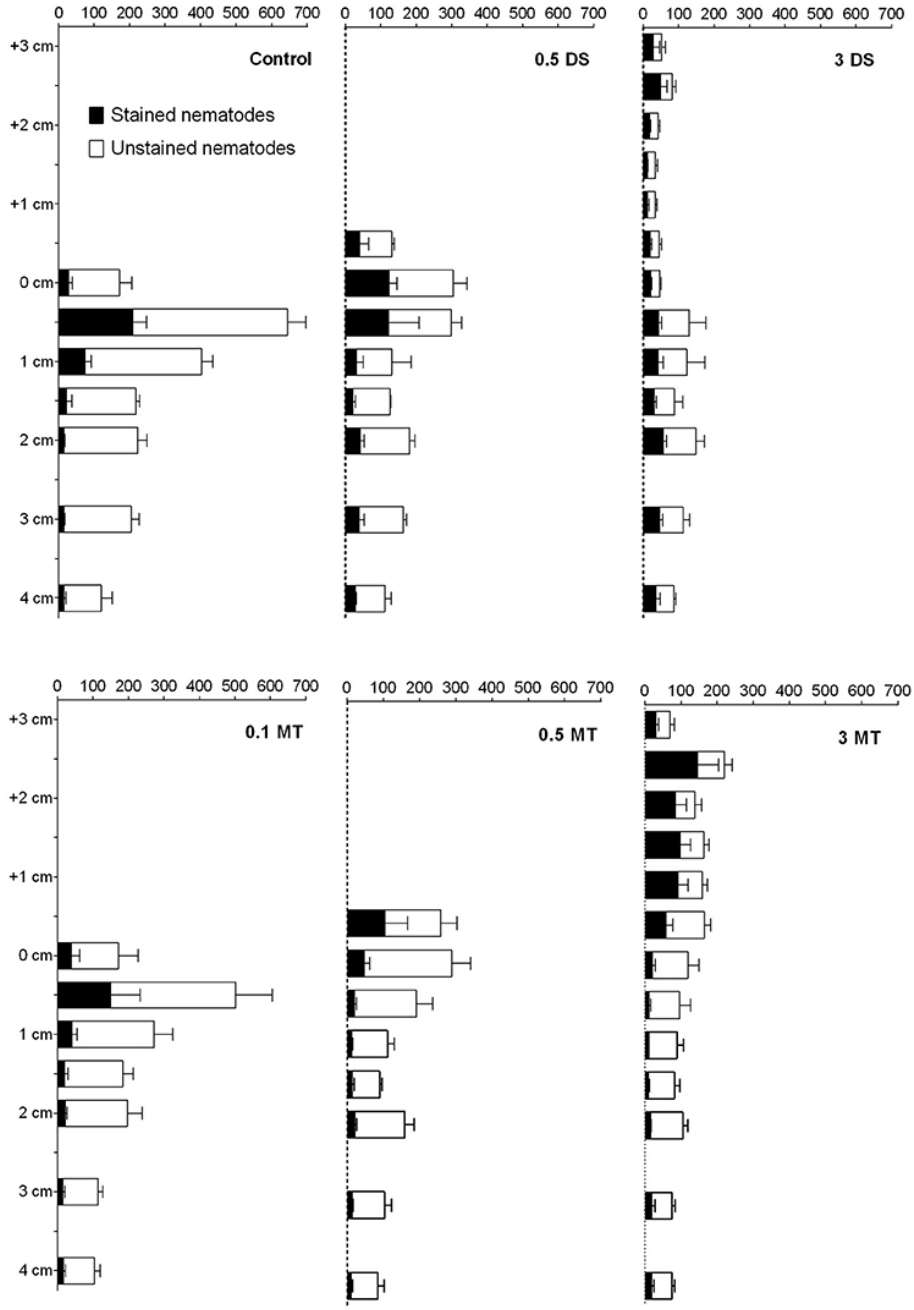

Figure 8-4. Mean abundances (x-axis) of stained (dead) and unstained (alive) nematodes in the different substrate addition treatments. Error bars indicate standard error.
Abbreviations: 0.1 MT = 0.1 cm mine tailing addition, 0.5 MT = 0.5 cm mine tailing addition, 3 MT = 3 cm mine tailing addition, 0.5 DS = 0.5 cm dead sediment addition, 3 DS = 3 cm dead sediment addition.

could be attributed to lower abundances of Kinorhyncha, Ostracoda, Nematoda, and Polychaeta in the 2–5 cm layer (SIMPER). Overall, meiofauna higher taxon diversity and evenness were low and did not differ between treatments with the

exception that evenness was significantly higher in the upper layer of the 3 DS treatment compared to the control due to reduced nematode densities and, thus, reduced dominance of this taxon. Diversity and evenness did not differ between treatments.

In the control situation, total biomass was highest for bacteria (9,824.93±1,503.20 mg C m^{-2}) followed by macrofauna (716.47± 109.45mg C m^{-2}) and nematodes (413.67±90.01 mg C m^{-2}; Figure 8-5). The high variability in macrofaunal biomass did not reveal any differences between treatments or depth. For bacteria and nematodes, however, the addition of 3 cm of mine tailings resulted in a reduced biomass in the 0–2 cm layer compared to the control [Permanova, p(MC) ≤ 0.0341]. Furthermore, nematode biomass was reduced in the upper layer of the 3 DS treatment and the 2–5 cm layer of the 0.5 MT treatment [Permanova, p(MC) ≤ 0.0197].

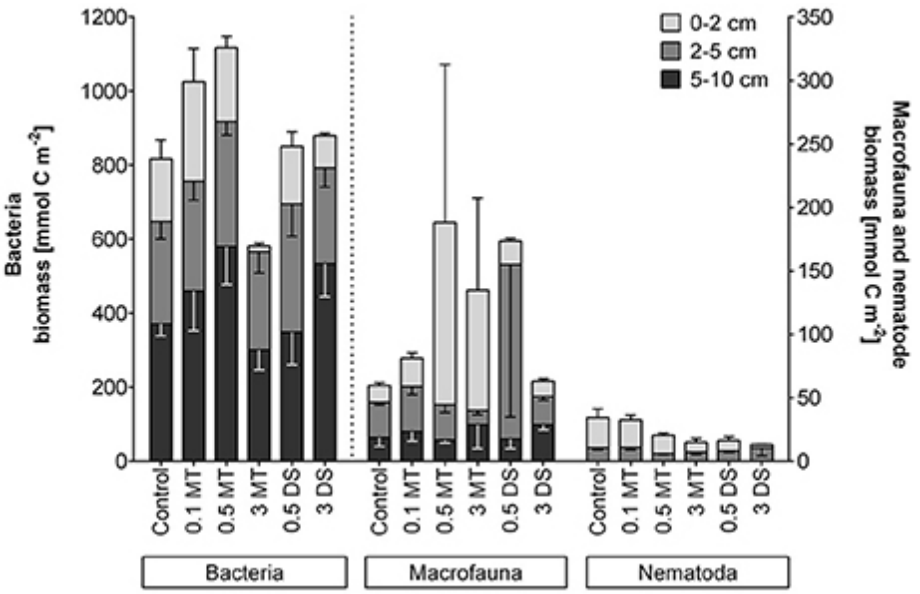

Figure 8-5. Biomass per depth and treatment in the three biological compartments measured: Bacteria (left y-axis), macrofauna, and Nematoda (right y-axis). Error bars depict standard errors and point downwards for the 2–5 cm and 5–10 cm data for better visualization.

Abbreviations: 0.1 MT = 0.1 cm mine tailing addition, 0.5 MT = 0.5 cm mine tailing addition, 3 MT = 3 cm mine tailing addition, 0.5 DS = 0.5 cm dead sediment addition, 3 DS = 3 cm dead sediment addition.

8.4.3 Functional changes of the benthic community

Under control conditions oxygen penetrated 1.17±0.11 cm deep into the sediment at the start of the experiment and remained stable throughout the experiment (Figure 8-6). The OPD of the 3 cm mine tailings treatment was 2.98±0.54 cm, which means that oxygen did not reach beyond the tailings, leaving the natural sediment anoxic. Moreover, the OPD decreased to 1.49±0.18 cm

at the end of the experiment [Permanova, p(perm) = 0.0098]. The deposition of dead sediment resulted in a shallower OPD compared to the Control (0.61±0.05 cm and 0.57±0.06 cm for 0.5 DS and 3 DS, respectively) after the deposition event [Permanova, p(MC) ≤ 0.036], but gradually deepened and approached control conditions at the end of the experiment.

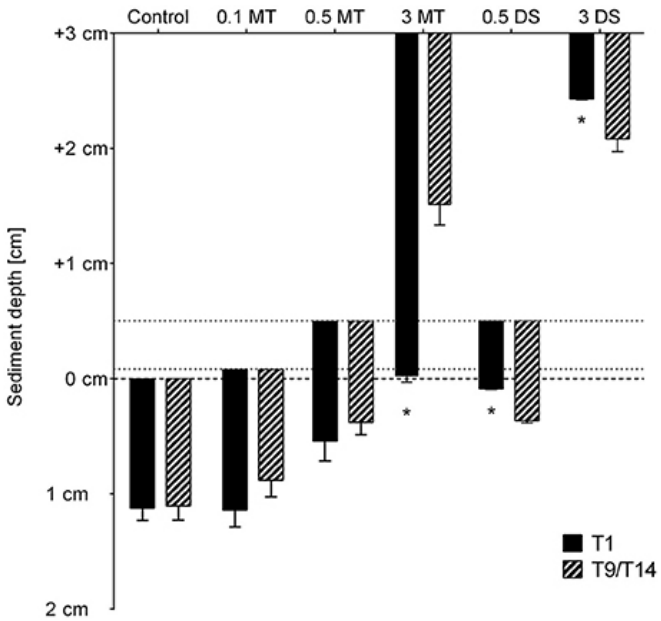

Figure 8-6. Oxygen penetration depth (OPD) in the sediments of the different treatments 1 d after settlement of the substrate (T1) and at the end of the experiment (T9/ T14). Error bars denote standard error and an asterisk indicates significant ($p < 0.05$) differences with the control.
Abbreviations: 0.1 MT = 0.1 cm mine tailing addition, 0.5 MT = 0.5 cm mine tailing addition, 3 MT = 3 cm mine tailing addition, 0.5 DS = 0.5 cm dead sediment addition, 3 DS = 3 cm dead sediment addition. The dashed line at y = 0 represents the natural sediment surface while above this layer the added substrate surface is indicated.

After 8 d (MT) and 13 d (DS) of incubation, the sediment community oxygen consumption (SCOC) was reduced in the 0.5 and 3 MT treatments compared to the Control [Permanova, p(perm) ≤ 0.0236] while in the 3 DS treatment SCOC increased [Permanova, p(perm) = 0.0342, Figure 8-7]. The SCOC increased in all treatments after addition of the algal tracer [Permanova, p(perm) =0.0001, Figure 8-7].

A large fraction of 85.21±1.40% of the added algal C was not processed and remained in the form of POC in the sediment, especially in the 0–2 cm layer (Figure 8-8A). Of the added algal C 9.70±1.01% was respired into DIC (Figure 8-8B). No significant differences in total ^{13}C-POC or algal ^{13}C-DIC were found between treatments.

Total tracer-C uptake was reduced in the 3 MT treatment for nematodes and macrofauna (Permanova, p ≤ 0.0038) and for bacteria (Permanova, p =

0.0523, borderline significant, Figure 8-8C–E). Additionally, uptake by nematodes was lower for the 0.5 MT, 0.5 DS, and 3 DS treatment [Permanova, p(MC) ≤ 0.0365]. When taking depth into account, a significant decrease in tracer uptake by nematodes was observed in the top layer (0–2 cm) of the MT and DS treatments. In general, uptake was highest in the upper 2 cm for bacteria and nematodes while macrofaunal uptake was high in the upper 5 cm with significantly lower values in the 5–10 cm layer (p(MC) < 0.01).

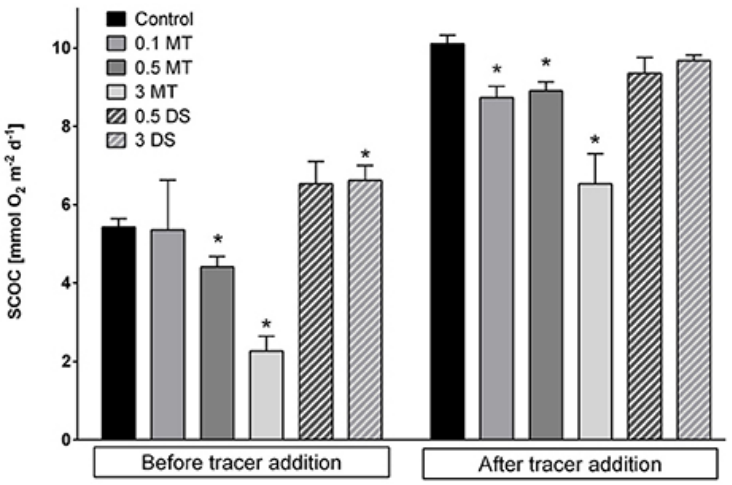

Figure 8-7. Mean sediment community oxygen consumption (SCOC) in mmol O_2 m^{-2} d^{-1} before and after tracer addition for the different substrate addition treatments. Error bars denote standard error and an asterisk indicates significant ($p < 0.05$) differences with the control.
Abbreviations: 0.1 MT = 0.1 cm mine tailing addition, 0.5 MT = 0.5 cm mine tailing addition, 3 MT = 3 cm mine tailing addition, 0.5 DS = 0.5 cm dead sediment addition, 3 DS = 3 cm dead sediment addition.

8.5 Discussion

With the continuing STP and prospect of new STP sites from land based mining facilities in many locations, but also with the perspective of deep-sea mineral extraction (e.g., massive sulfides and polymetallic nodules) and associated disposal of waste sediment, there is an urgent need for quantitative assessments of the environmental impact of tailings deposits in marine environments (Mengerink *et al.*, 2014; Ramirez-Llodra *et al.*, 2015; Levin *et al.*, 2016). Due to the slow growth and long life spans of many deep-sea taxa (Young, 2003) they are particularly vulnerable to the impacts associated with tailings placement such as hyper sedimentation, changes in grain size, or toxicity effects (Kvassnes and Iversen, 2013). To our knowledge, this experimental study is the first of its kind to investigate the impacts of different levels of inert mine tailings and sediment deposition on both, structure and functioning, of upper bathyal soft-bottom communities.

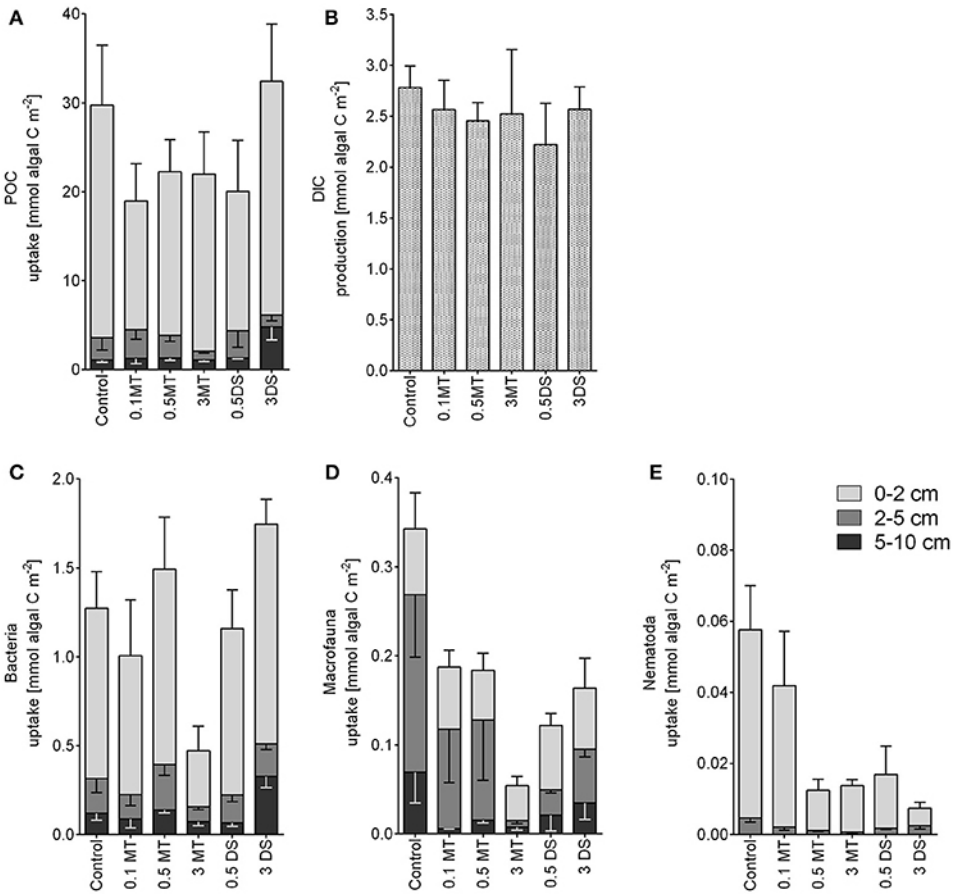

Figure 8-8. Particulate organic carbon (POC, A) per treatment and depth; (B) dissolved inorganic carbon (DIC, B) per treatment; and uptake of algal ^{13}C per depth and treatment of (C) Bacteria, (D) Macrofauna, and (E) Nematoda. Error bars depict standard errors and point downwards for the 2–5 cm and 5–10 cm data for better visualization.
Abbreviations: 0.1 MT = 0.1 cm mine tailing addition, 0.5 MT = 0.5 cm mine tailing addition, 3 MT = 3 cm mine tailing addition, 0.5 DS = 0.5 cm dead sediment addition, 3 DS = 3 cm dead sediment addition.

8.5.1 Substrate addition induces structural changes of the benthic community

Sediment characteristics substantially determine the composition of benthic assemblages and whereas meiofauna communities are strongly influenced by sediment grain size (Jansson, 1967; Coull, 1999), macrofauna community structure is most likely governed by factors of e.g., food availability, sediment oxygenation, and biotic interactions rather than grain size (Snelgrove and Butman, 1994; Seiderer and Newell, 1999). In our experiment, the physical modifications from substrate addition were visible in the different properties of the new, added substrates with much coarser grain size, lower porosity, and a low TOC in the mine tailings and relatively high TOC in the dead sediment. These results confirm

the successful addition of both substrates and physical modification of the upper sediment layers.

Furthermore, the addition of each of the two substrates immediately changed oxygen conditions in the natural sediment. The two most extreme treatments (3 MT and 3 DS) resulted in anoxic conditions of the natural sediment throughout the entire experiment duration. The first hypoxia related response of benthic invertebrates is migration to more suitable areas in the sediment, although successful migration strongly depends on the mobility of the individual taxa or species and the properties of the added substrate (e.g., grain size, porosity; Jansson, 1967; Maurer *et al.*, 1986; Hendelberg and Jensen, 1993; Diaz and Rosenberg, 1995; Wetzel, Fleeger and Powers, 2001). Accordingly, we observed migration into the added substrate of most metazoan taxa and an upward shift in meio- and macrofauna community composition in all treatments. Successful migration of benthic organisms into added, non-native substrates is well-known (Maurer *et al.*, 1986; Schratzberger, Rees and Boyd, 2000; Bolam, 2011), however, the upward shift in our experiment was accompanied by a high nematode mortality in both substrate additions. Without the applied nematode staining technique this observation would have been missed and the impacts of substrate addition on nematodes would have been underestimated.

In the mine tailings, nematode mortality was possibly linked to a strongly reduced food availability. Compared to other taxa, nematodes are often reported to be able to survive situations of severe stress, such as temporary hypoxia or seawater acidification (Josefson and Widbom, 1988; Widdicombe *et al.*, 2009; Schade *et al.*, 2016) and the capability to change feeding modes to some extent may be advantageous in those situations (Moens and Vincx, 1997). Bacterial growth strongly depends on the availability of organic matter (Danovaro, 1996; Kirchman and Rich, 1997; Eiler *et al.*, 2003); so despite the fact, that the tailings were well oxygenated, the low organic C content did not support strong bacterial growth resulting in very low food availability for meio- and macrofauna inside the added layer. The survival of nematodes in low food conditions is very species dependent, but generally an incubation time of 10 or more days, as applied here, is sufficient to set the worms at their limit (Ott, 1972; Ott and Schiemer, 1973; Wieser *et al.*, 1974).

In contrast, the mechanism behind the nematode mortality and reduced densities in the DS treatment is likely different from that of the MT treatment. High bacterial biomass and TOC in the added dead sediment, compared to conditions in the control, should have led to higher concentrations of food for the nematodes. Nevertheless, we observed a strong reduction in nematode densities and high proportions of dead nematodes in all layers throughout the core. Here, the cause is likely linked to the anoxic conditions in the sediment produced by the high bacterial activity in terms of C uptake and resulting increased oxygen demand. In a laboratory experiment with an intertidal meiofauna community, Steyaert *et al.* (2007) found that suboxic and anoxic conditions for 14 d led to a decrease by about a third in nematode densities with species-specific survival. Similarly, other studies report hypoxia associated mortality of nematode fauna and shifts in meiofauna community composition toward hypoxia adapted species

(Hendelberg and Jensen, 1993; Moodley *et al.*, 1997; Wetzel, Fleeger and Powers, 2001; Van Colen *et al.*, 2009). Low nematode densities in the 3 DS treatment possibly result from a combination of the high mortality and decomposition of dead nematodes, potentially also facilitated by the longer incubation time in the dead sediment treatments.

Macrofaunal responses were less obvious and organisms showed no signs of mortality. Nevertheless, whereas tailings addition resulted in an upward shift of the entire macrofauna community, dead sediment addition resulted in a less clear distinction between surface and subsurface community composition compared to the control situation. The stress response of macrofauna is species-specific and depends on their mobility, oxygen requirements, and feeding type (Chou, Yu and Loh, 2004; Hinchey *et al.*, 2006; Smit *et al.*, 2008). In a meta-analysis, Smit *et al.* (2008) predicted from marine species sensitivity distributions that instantaneous burial with 5.4 cm of natural sediment would negatively affect about half of the 32 analyzed macrofauna species. Furthermore, burial with 0.63 cm already affected 5% of the tested macrofauna species. Substrate addition and especially tailings addition may lead to emigration or death of certain macrofaunal organisms on a longer term if requirements of oxygen and food availability are not met. While several studies on shallow water ecosystems report on the effects of burial with sediment following dredging (Bonvicini Pagliai *et al.*, 1985; De Grave and Whitaker, 1999; Thrush and Dayton, 2002; Bolam, 2011) or strong hydrodynamic disturbances (Miller, Muir and Hauser, 2002 and citation therein; e.g., Dernie, Kaiser and Warwick, 2003), we need to be cautious in comparing these results with tailings burial. Indeed, as observed in this study, the specific characteristics of tailings in terms of grain size, organic matter content, and porosity (disregarding any toxicological properties) compared to the natural sediment led to differing structural responses and community functioning (see "8.5.2 Community functioning changes as a result of structural changes induced by substrate deposition").

The differential response of meiofauna and macrofauna to low oxygen concentrations and starvation contradicts the general perception that the meiofauna are more resistant to different stressors than macrofauna. Many authors studying the effect of hypoxia on benthic communities report a more negative effect of long hypoxic events on macrofauna, including mortality, whereas meiofauna is generally less affected and can withstand long hypoxic events (Weigelt and Rumohr, 1986; Josefson and Widbom, 1988; Diaz and Rosenberg, 1995; Van Colen *et al.*, 2009). However, these studies focused on hypoxia in the water column which was not the case in our experiment where the overlying water was always well oxygenated. Here, the greater capacity of macrofauna to move vertically in the sediment could have enabled organisms to reach oxygenated layers as well as food-rich surface layers ensuring their survival. The loss of distinction between the macrofaunal community composition in different depth layers in the dead sediment treatments could be a first indication to support this hypothesis. Thus, while meiofauna could not compensate the very rapid occurrence of anoxic conditions in the sediment by vertical migration, macrofauna may have been more successful in doing so.

Despite a comparatively low standing stock, the high activity and life cycle turnover rates of meiobenthic organisms make them a particularly important part of the benthic environment when it comes to biomass production and food consumption (Gerlach, 1971; Coull, 1999). Furthermore, they can exert a strong impact on other benthic organisms by enhancing bacterial productivity (Gerlach, 1978) and influencing macrobenthic species interactions which can result in modified ecosystem properties (Piot, Nozais and Archambault, 2014). Therefore, the high nematode mortality induced by substrate burial may lead to strong repercussions on other benthic organisms on a longer term.

8.5.2 Community functioning changes as a result of structural changes induced by substrate deposition

In this study we observed strong, negative effects of substrate addition on the benthic community structure in terms of biomass and composition. These changes led to adverse effects of benthic functioning in terms of respiration rates and organic matter processing. Oxygen is a key element in the aerobic respiration and metabolism of organisms and, thus, tightly linked to the mineralization of organic C and the activity of benthic organisms. Therefore, OPD and SCOC can provide a reliable indication of organic matter remineralization rates (Moodley, Heip and Middelburg, 1998) and, combined with stable isotope C uptake data of the biota, has proven to be a good tool to assess ecosystem functioning and responses of the benthos to environmental disturbances (Bratton, Colman and Seal, 2003; Sweetman *et al.*, 2010; Sweetman, Norling, *et al.*, 2014; Sweetman, Chelsky, *et al.*, 2016).

Immediately after settlement of the added substrates, a shift in OPD occurred in most treatments. OPD did not decrease at 0.1 and 0.5 cm tailings addition but shifted upwards leaving previously oxygenated deeper sediment layers anoxic. Furthermore, despite an increase in OPD at 3 cm of tailings addition compared to the control, the underlying, previously oxygenated sediment became anoxic because oxygen did not penetrate through the mine tailings layer to the natural sediment anymore. Similarly, Cummings, Vopel and Thrush (2009) observed an upward shift of the OPD when marine sediments were exposed to very thin layers of terrestrial sediments. In this study OPD (measured throughout 3 d) penetrated ±0.7 mm in the control situation, while after the addition of ±1.1 mm of terrestrial sediment oxygen only penetrated ±0.3 mm into the underlying sediments. Thus, comparable to our study, organisms inhabiting the surface sediment will become exposed to a deterioration of biogeochemical conditions after the addition of a non-native substrate. In our experiment, however, OPD in the tailings treatments became shallower toward the end of the experiment possibly by a higher biogenic activity inside the tailings due to faunal migration. Sediment deposition resulted in a decreased OPD at the start of the experiment that might be linked to strong microbial respiration due to high organic matter contents of the added sediment. Also in this case, underlying sediment layers were exposed to biogeochemical changes negatively affecting structure and functioning of biota. Toward the end of the experiment OPD deepened to values comparable to

the control indicating a possible stabilization of the biogeochemical conditions in the dead sediment treatments to a pre-disturbance state.

Values of SCOC in our control incubations were comparable to those reported in other studies with Norwegian fjord fauna (Ishida *et al.*, 2013; Sweetman, Norling, *et al.*, 2014; Sweetman, Chelsky, *et al.*, 2016). The SCOC measurements after 8 and 13 d of incubation (MT and DS, respectively) informed about the effect of substrate addition on the SCOC, while the second measurement informed about the response of the sediment community to input of algal detritus. Mine tailings burial reduced oxygen consumption in the 0.5 and 3 cm treatments, but SCOC increased in the dead sediment treatments when compared to the control. Low organic matter content associated with low bacterial biomass and faunal mortality may explain the reduced SCOC measurements in the mine tailings treatments. On the contrary, high organic matter content and an increase in SCOC in the dead sediments may point toward increased bacterial activity as they play a key role in the C turnover in marine sediments (Rowe and Deming, 1985; Deming and Baross, 1993). However, in the dead sediment treatments, addition of fresh organic matter in the form of labeled algae did not lead to a pronounced increase in oxygen consumption as it did in the mine tailings treatments and the control. This is possibly due to the already high rate of organic matter processing and strong bacterial respiration resulting from the organic matter input originating from the dead sediment itself. It is important to note that SCOC increased in all treatments after algae addition but, at the same time, the negative effect of tailings addition on the processing of a new food source became more pronounced when compared to the control situation. This way even a deposition of 0.1 cm sufficed to induce a significant reduction in SCOC, illustrating that the benthic community was hampered to process fresh organic matter by as little as 0.1 cm of tailings.

Bacteria dominate deep-sea ecosystems in terms of abundance and biomass and are the main contributors to organic matter remineralization (Wei *et al.*, 2010; Danovaro, Snelgrove and Tyler, 2014). Similarly, in our experiment we observed that bacteria had a higher biomass and took up considerably more added algal C compared to macro- and meiofauna. Interestingly, at 0.1 cm tailings addition, bacterial tracer uptake and biomass remained close to control conditions while a decreasing trend of tracer uptake was already visible for macro- and meiofauna. Here, the tailings layer may have posed a physical barrier for those organisms to reach the new source of organic matter present on the sediment surface. At 3 cm tailings addition, low bacterial biomass and possibly reduced faunal activity in terms of bioturbation lead to a lower fraction of the added algae being transported to deeper layers and an overall reduced tracer uptake. Bioturbation by infauna strongly influences ecosystem functioning, especially in sediments where disturbances are low, as it provides structure to the sediments and is responsible for irrigation, transport of nutrients, and organic matter to deeper layers and providing various microhabitats for meiofauna and bacterial communities (Mermillod-Blondin *et al.*, 2004; Meysman, Middelburg and Heip, 2006; Braeckman *et al.*, 2010).

Continental margins are responsible of 10–15% of the global ocean primary production and fulfil an important role in the sequestration of atmospheric C and transport to the deep-ocean (Muller-Karger *et al.*, 2005; Fennel, 2010). Furthermore, with high denitrification rates these regions adjacent to land boundaries act as a barrier for nitrogen input from land and atmosphere into the open ocean (Fennel, 2010). This disproportional contribution to the total ocean nutrient cycling is the result of tight biological interactions, biogeochemical transformations facilitated by microorganisms and characteristic hydrodynamics (Renaud *et al.*, 2007; Hofmann *et al.*, 2011). Therefore, disturbing these ecosystems by activities such as mine tailings placement, can have implications on a much larger scale.

8.5.3 The origin of the added substrate results in differential responses

This study clearly illustrated how both substrates used in this experiment resulted in differential responses. Mine tailings addition mainly induced food-limitation for all benthic compartments in the added layers, whereas the high bacterial respiration in the dead sediment layer initially led to oxygen limitation in deeper layers. In the sediment addition treatments, oxygen conditions seemed to return to conditions similar to the control indicating a possible biochemical recovery of the sediments to normal conditions after the 15 d period. With bacterial and macrofaunal biomass and uptake being similar to control conditions, it is possible that those taxa might recover relatively fast. Meiofauna, however, suffered most in this scenario with strongly reduced densities, low C uptake, and increased mortality. The interconnectedness of the three benthic compartments is widely acknowledged and changes in one taxon can have strong repercussions on the other (Gerlach, 1971, 1978; Alongi and Tenore, 1985; Evrard *et al.*, 2010; Leduc and Pilditch, 2013; Piot, Nozais and Archambault, 2014), thus we cannot exclude the possibility of adverse effects on the long term. As a naturally occurring phenomenon, marine organisms are to some extent adapted to sedimentation and resuspension, and ecosystems may show increased resilience to sediment disturbance, particularly if they are subjected to a high intensity of natural disturbance (Schratzberger and Warwick, 1998; Leduc and Pilditch, 2013). However, man-made sedimentation events may exceed natural variability in sediment load and frequency and may induce permanent changes in the ecosystem. In the mine tailings treatments, no signs of recovery of the benthic community to control conditions were observed within the experiment duration of 11 d. In fact, monitoring studies for STP have shown that after cessation of extensive tailings discharge (up to 4–5 cm tailings addition per year during >20 y) it may take 1–4 yr before the tailings are fully recolonized while differences in community compositions still prevail (Olsgard and Hasle, 1993; Burd, 2002). However, it remains uncertain if, accompanied with faunal recovery, also ecosystem function will return to normal values. Unfortunately, controlled experiments to determine threshold levels for sediment overburden and tolerated frequencies are largely missing (Miller, Muir and Hauser, 2002).

Our study contributes to reducing this knowledge gap since comparing different deposition depths and substrates allows us to gain some information on threshold values and differentiate the effects of substrate characteristics on benthic community structure and functioning. When applying the precautionary principle in a STP scenario, instantaneous depositions with as little as 0.1 cm of tailings over large areas have to be avoided to maintain ecosystem functioning in terms of organic matter remineralization at normal levels. Structural changes of biota with reduced biomass and shifts in vertical distribution become apparent at 0.5 cm burial with tailings and intensify at 3 cm tailings deposition. It remains unclear how fast biological communities can recover from the short-term effects and how repeated burial with tailings will affect species survival on a longer term. Furthermore, macrofauna is often used to assess and monitor environmental impacts, but it was actually the most tolerant group in our experiment while the response of meiofauna was much more pronounced. Therefore, monitoring studies should make use of a more integrated approach covering multiple size groups representing different functional traits and trophic levels.

8.6 Conclusion

Our research clearly shows that burial with both, mine tailing or dead sediment, has strong negative effects on the biota and the functioning of benthic communities. However, the processes behind the impacts were different between the two substrate additions.

The most severe effects were observed at 3 cm of tailings deposition with a reduction of bacterial and meiofaunal biomass by more than half, reduced algal C uptake of all biological compartments and reduced sediment community oxygen consumption. However, already at 0.1 cm tailings deposition, the ability of the benthic community to process organic matter was significantly reduced while the structure of the community remained largely unaffected at this level. This emphasizes the importance of using multiple trophic levels and an ecosystem-based approach in laboratory experiments including measures of ecosystem functioning. The addition of dead sediment, on the other hand, resulted in an increase in bacterial activity causing severe anoxia in the underlying sediment layers entailing decreased meiofaunal biomass and changes in the vertical distribution of macrofauna. While productivity in terms of bacterial biomass and C turnover are enhanced on the short term, mortality of nematodes and resulting shifts in benthic community composition might induce unforeseen consequences on the longer term. While possibly less obvious in measurements of abundance, physical disturbance and changes in sediment characteristics may substantially influence infauna community composition, particularly that of meiofauna (Schratzberger, Rees and Boyd, 2000; Leduc and Pilditch, 2013). Zeppilli *et al.* (2016) identified a positive exponential relationship between nematode biodiversity and ecosystem functioning and efficiency in different deep-sea habitats. Hence, reductions in biodiversity and changes in community composition may result in decreased ecosystem functioning and a reduced resilience of the system to different additional stressors (Gessner and Hines, 2012; Steudel *et al.*, 2012; Zeppilli *et al.*, 2016).

We need to be aware of the differential response to burial with different substrates when assessing impacts of mine tailings placement on the benthic environment. This study shows that the particular characteristics of the sediment, e.g., organic matter content, porosity or grain size, strongly influence the biochemistry inside the sediments and the way the ecosystem responses to substrate burial. Therefore, more research is needed using substrate with similar characteristics of the effectively placed tailings. Furthermore, our study indicates that vast areas impacted by low tailings deposition might experience a reduced C mineralization capacity, especially over the short-term. While the thickness of mine tailings in the direct surrounding of the deposition site can reach very high values with deposition rates of several m y^{-1}, the seafloor may still be impacted by deposition rates of 1 mm y^{-1} several km off the deposition site (Olsgard and Hasle, 1993). The wider implications will depend on the scale of tailings discharge and the resilience of the targeted ecosystem. If DSTP is implemented in more regions worldwide environmental managers need to be aware that even small deposition rates might negatively impact very large areas disrupting the functioning of important benthic environments.

Acknowledgments

The authors want to acknowledge A. Rigaux for her valuable assistance during the experiment and L. Pedersen and M. Berry for assistance at sea. We thank P. van Rijswijk, P. van Breugel, and J. Peene for technical assistance during sample analysis and L. Burdorf for her assistance during O_2 microprofile interpretations and subsequent O_2 flux calculations.

Chapter 9 : Mediterranean submarine canyon food webs respond to dense shelf water cascading events

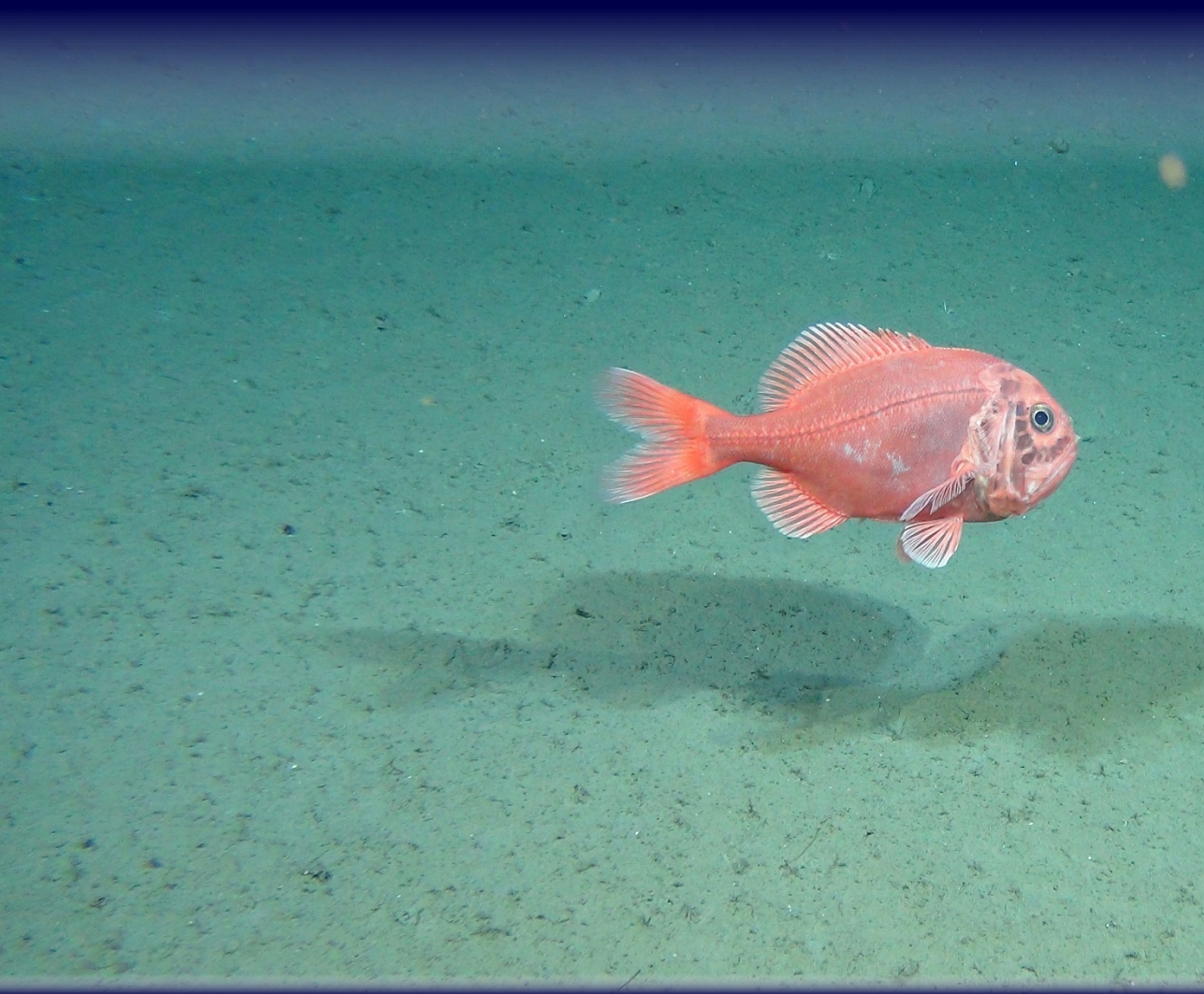

9. Mediterranean submarine canyon food webs respond to dense shelf water cascading events

Tanja Stratmann, Antonio Pusceddu, Silvia Bianchelli, Cinzia Corinaldesi, Antonio Dell'Anno, Cristina Gambi, Roberto Danovaro, Karline Soetaert, and Dick van Oevelen;
In preparation.

9.1 Abstract

Deep-sea canyons play a major role in the transport of organic matter from the continental shelf to the deep Mediterranean Sea. Especially at the Catalan margin, dense shelf water cascading is an important driver of organic matter input. Responses of the benthic food web to these inputs of organic matter, however, have been less studied. Here, we developed food-web models for the upper, middle, and lower canyon sections of the Cap de Creus canyon and the upper and middle Lacaze-Duthiers canyon to study spatial differences in carbon cycling. Based on our modeling results, carbon processing in the upper Lacaze-Duthiers canyon and in the middle section of the Cap de Creus canyon can be classified as "active faunal carbon uptake", dominated by meiofauna, whereas the upper and lower Cap de Creus canyon sections are bacteria uptake dominated.

As the periodic cascading events impact higher trophic levels, such as the deep-sea shrimp *Aristeus antennatus*, but less is known about how lower trophic levels react to these events. Therefore, we developed additional food-web models for the upper and lower Cap de Creus canyon sections for April 2005, directly after a major dense shelf water cascading event, and followed changes in food-web structure and carbon flows 0.5, 3, 3.5, 4, and 4.5 yr later. Our modeling outputs show that benthic C uptake, respiration, as well as the network indices "total system troughput", number of food-web links and Finn's cycling index were very similar to identical at the upper and lower Cap de Creus canyon section in April 2005. Half a year after the cascading event, the two sections differed again. We therefore assume that meiofauna recovered from the impacts of these cascading events within 0.5 yr and hypothesize that dense shelf water cascading might facilitate passive dispersal of meiofauna.

9.2 Introduction

The Mediterranean Sea holds 8.9% of all submarine canyons on Earth (Canals *et al.*, 2013), although it covers only 0.7% of the world ocean's surface and 0.3% of the world ocean's volume. Mediterranean canyons are on average 26.5 km long, cover a depth range of 1.61 km, and have a slope of 6.5° (Harris and Whiteway, 2011). They channel sediment and fresh organic matter from the continental shelf to the Mediterranean deep sea (Martín, Palanques and Puig, 2006; Lopez-Fernandez, Bianchelli, Pusceddu, Calafat, Danovaro, *et al.*, 2013; Lopez-Fernandez, Bianchelli, Pusceddu, Calafat, Sanchez-Vidal, *et al.*, 2013; Martín *et al.*, 2013) via offshore convection, eastern storms, and dense shelf water cascading events (DSWC) (Canals *et al.*, 2006, 2013; Lopez-Fernandez, Bianchelli, Pusceddu, Calafat, Danovaro, *et al.*, 2013).

DSWC is a particular case of a buoyancy driven current (Shapiro, Huthnance and Ivanov, 2003) that occurs in the western Mediterranean Sea when cold, dry winds from the North lead to increased evaporation and cooling of the waters at the coast of the Gulf of Lion and the Catalan margin (Canals *et al.*, 2006). The cooling causes the density of the shelf water to increase until its density is higher than the density of the surrounding water. This instability drives shelf water to cascade down the continental slope into the canyons until it reaches water masses with equivalent sea water density. Such DSWC events were detected in the Lacaze-Duthiers (LD) canyon nearly every winter since 1993 (Durrieu de Madron *et al.*, 2005) and in winter 2005 the DSWC event lasted from February to end of March (Canals *et al.*, 2006). During this period about 66% of the shelf water from the Gulf of Lion was exported, thereby transporting an estimated 15 kt of total organic carbon (C) per day (Canals *et al.*, 2006). In the Cap de Creus (CdC) canyon, the upper canyon (400–1,000 m; Lastras *et al.*, 2007) was regularly affected by DSWC (Canals *et al.*, 2006; Sanchez-Vidal *et al.*, 2008), whereas the middle canyon (1,000–1,600 m; Lastras *et al.*, 2007) was only impacted by DSWC during extreme atmospheric conditions (Canals *et al.*, 2006; Sanchez-Vidal *et al.*, 2008). Such an extreme DSWC event in late winter-early spring of 2005 eroded bioavailable C in the sediments of the CdC canyon floor at 1,800 m (Pusceddu *et al.*, 2013). Meiofauna abundance at this site was significantly lower in April 2005 compared to April 2009 (Pusceddu *et al.*, 2013). From October 2005 to April 2009, meiofauna abundances and biomasses increased and remained similar except in April 2008, when meiofauna biomass was lower (Pusceddu *et al.*, 2013). This reduction in meiofaunal biomass in April 2008 might be related to the weak DSWC event from mid-January to late March 2008 (Ribó *et al.*, 2011).

The strong DSWC event in early spring 2005 was also correlated with a temporary fishing collapse of the deep-sea shrimp *Aristeus antennatus* at the fishing harbors of Roses, Palamós, Blanes, and Arenys de Mar at the NW Mediterranean coast (Company *et al.*, 2008). The authors hypothesized that the physical disturbance of the water cascading down the shelf of the Gulf of Lions and the Catalan margin flushed *A. antennatus* specimens from the fishing grounds (500–900 m water depth) to larger depths. The shrimp population remained reduced up

to 3 yr after the event (Company *et al.*, 2008), but landings of adult shrimps increased above pre-DSWC levels in the 2 to 3 subsequent years, before the landings of small and large shrimps decreased again, probably due to overfishing (Company *et al.*, 2008). Though the exact process of the enhanced recruitment is not fully understood, Company *et al.* (2008) identified two possible scenarios: the first scenario implies that after the DSWC event the adult population increases its reproductive output because of favorable nutritive conditions. The second scenario suggests that the turbidity anomaly in the Western Mediterranean Deep Water that is created by the DSWC event reduces the visual predation pressure on *A. antennatus* larvae and juveniles. Independent of the mechanism that causes this increased recruitment after DSWC events, apparently the regularity with which these DSWC events occur protects the species from overexploitation (Company *et al.*, 2008). Hence, this inter-annual climate variation can have large impacts on higher trophic levels of the deep-sea food web, but effects on lower trophic levels are less well described.

One approach to analyze these properties in a coherent way is linear inverse modeling, a mass balancing method that combines data on C stocks with C flux constraints to calculate C flows between abiotic and biotic compartments within a pre-defined topological food web (Vézina and Platt, 1988). Linear inverse modeling has been used already to assess both temporal and spatial patterns in food web properties at Station M (NE Pacific; Dunlop *et al.*, 2016) and in the Nazaré canyon (NE Atlantic; van Oevelen *et al.*, 2011). Here, we used linear inverse modeling (1) to investigate potential spatial differences in food-web structure and C fluxes between the LD canyon and the CdC canyon in October 2005, 0.5 yr after a major DSWC occurred and (2) to assess temporal food web dynamics in the CdC canyon over a period of 4 yr following the major DSWC event in winter 2005.

9.3 Material and methods

9.3.1 Study sites

The CdC canyon is located 4 km off the N Catalan margin (Canals *et al.*, 2013) and has a length of 96.1 km. It starts at 125 m water depth going down to 2,140 m depth, where it converges with the LD canyon and ends in the Sète Canyon (Lastras *et al.*, 2007). The CdC canyon can be sectioned into the canyon head (125–400 m), the upper canyon (400–1,000 m depth), the middle canyon (1,000–1,600 m), and the lower canyon (1,600–2,100 m) (Lastras *et al.*, 2007). The canyon head is covered with shell material and coarse-grained sand (DeGeest *et al.*, 2008). The upper canyon section is characterized by a 4 to 22 cm thick muddy layer consisting of silty clay in the thalweg at 400 to 780 m water depth (DeGeest *et al.*, 2008) and coarse sand and gravel (southern flank) or silty clay (northern flank) at the flanks (DeGeest *et al.*, 2008). Surface sediment in the middle and lower canyon is composed of fine-grained silt (Contreras-Rosales *et al.*, 2012).

The LD canyon in the W Gulf of Lion is 92 km long and stretches from 120 m to 2,080 m water depth (Canals *et al.*, 2013). It can be subdivided into the three branches of the canyon head (120–400 m), the V-shaped upper canyon

(400–1,100 m), the middle canyon (1,100–1,600 m), and the lower canyon (1,600–2,100 m) (Courp and Monaco, 1990). At the canyon head, >50% of the coarse sediment has a grain size of >40µm (Courp and Monaco, 1990). The sediment of the upper canyon contains terrigenous fine-grained, muddy material, whereas the canyon walls contain coarser sediment material with shell fragments (Courp and Monaco, 1990; de Bovée, Guidi and Soyer, 1990; Vénec-Peyré, 1990). The middle canyon section is covered with a fluffy layer of brown mud and the lower canyon is covered by coarse sediment (>50% of the grain size is >40µm) (Courp and Monaco, 1990).

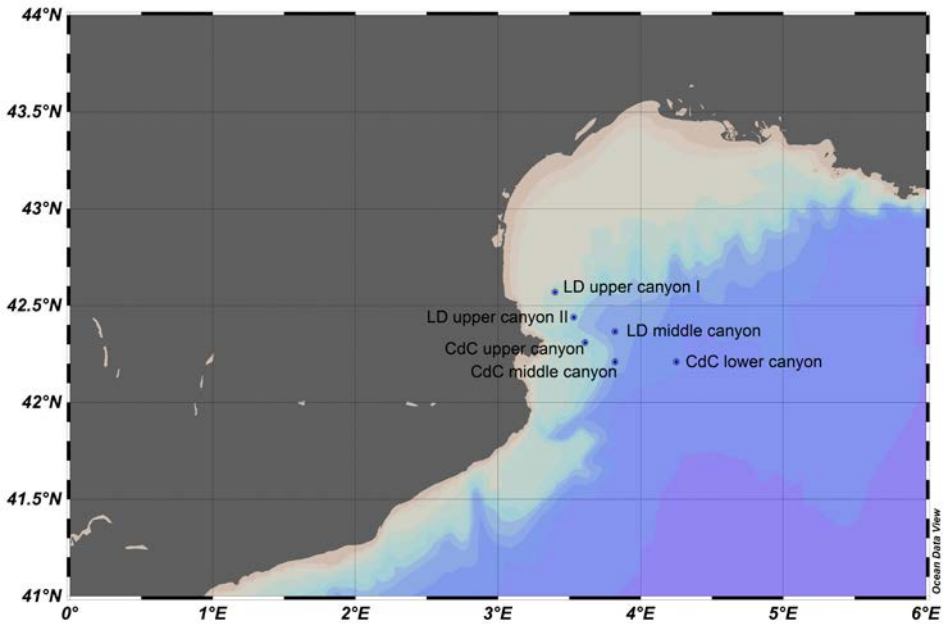

Figure 9-1. Map of the Catalan Margin (NW Mediterranean Sea) with the locations of all sampling stations for which food-web models were developed to investigate spatial differences in food-web structure among canyon sections. A list of geographical coordinates is presented in Supplementary table 9-1.

For this study, food-web models were developed for three stations in the CdC canyon (upper, middle, and lower canyon sections) and for three stations in the LD canyon (upper and middle canyon sections) that were sampled in October 2005 (Figure 9-1; Supplementary table 9-1). Additional food-web models for the CdC upper and lower canyon sections were developed for 6 points in time after a major DSWC event in winter 2005 (Figure 9-2; Supplementary table 9-1).

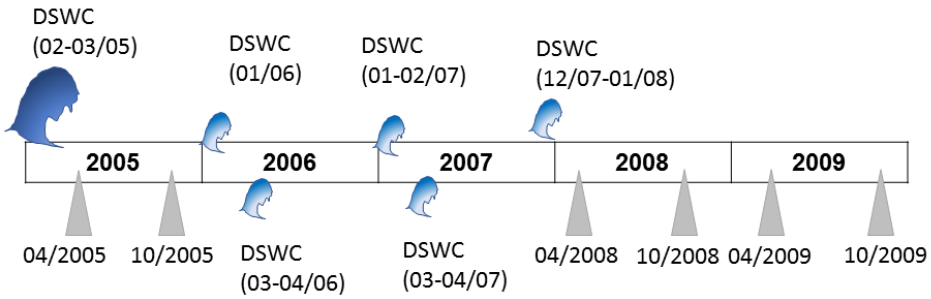

Figure 9-2. Timeline of the six sampling events (gray triangles) for which food-web models were developed for the upper and lower Cap de Creus canyon sections (Section 9.3.2.2 Temporal comparison at the Cap de Creus canyon). The dark blue wave shows the major dense shelf water cascading event (DSWC) in winter/ early spring 2005 and smaller light-blue waves represent smaller DSWC events. A table with specific sampling locations and depths is presented in Supplementary table 9-1.

9.3.2 Food-web structure and links

9.3.2.1 Spatial comparison of canyon sections

The food-web model contained the compartments detritus consisting of labile (lDet), semi-labile (sDet), and refractory detritus (rDet) (*sensu* van Oevelen, Soetaert and Heip, 2012), prokaryotes, meiofaunal nematodes, other metazoan meiofauna, macrofaunal polychaetes, and other macrofauna. Nematodes were subdivided into selective deposit feeders (NemSDF), non-selective deposit feeders (NemNSDF), epistratum feeders (NemEF), and carnivores (NemC). Metazoan meiofauna was subdivided into deposit feeders (MeiDF), filter and suspension feeders (MeiFSF), and carnivores (MeiC) based on taxon-specific feeding types (Table 9-1). Macrofauna included deposit feeders (MacDF) and filter and suspension feeders (MacFSF). Based on observed polychaete families, polychaetes were identified as deposit feeders (PolDF).

The food web received C via the external sources suspended labile, semi-labile, and refractory detritus that fed the corresponding sedimentary detritus stocks. The semi-labile detritus stock increased furthermore by feces and faunal mortality. Labile, semi-labile, and refractory detritus stocks decreased by hydrolysis to dissolved organic carbon (DOC). C was lost via respiration (dissolved inorganic carbon, DIC), burial of refractory detritus, DOC efflux to the water column, and external predation. Suspended labile and semi-labile detritus were consumed by MeiFSF and MacFS. Sedimentary labile and semi-labile detritus, and prokaryotes were consumed by deposit feeders (NemEF, NemSDF, NemNSDF, MeiDF, MacDF, and PolDF). Epistratum feeding nematodes grazed upon labile detritus and prokaryotes. Carnivorous nematodes and meiofauna preyed upon all other nematodes and meiofauna. Prokaryotes took up DOC and they contributed to the DOC stock again when they died due to viral lysis. A schematic representation of this food web structure is shown in Figure 9-2A.

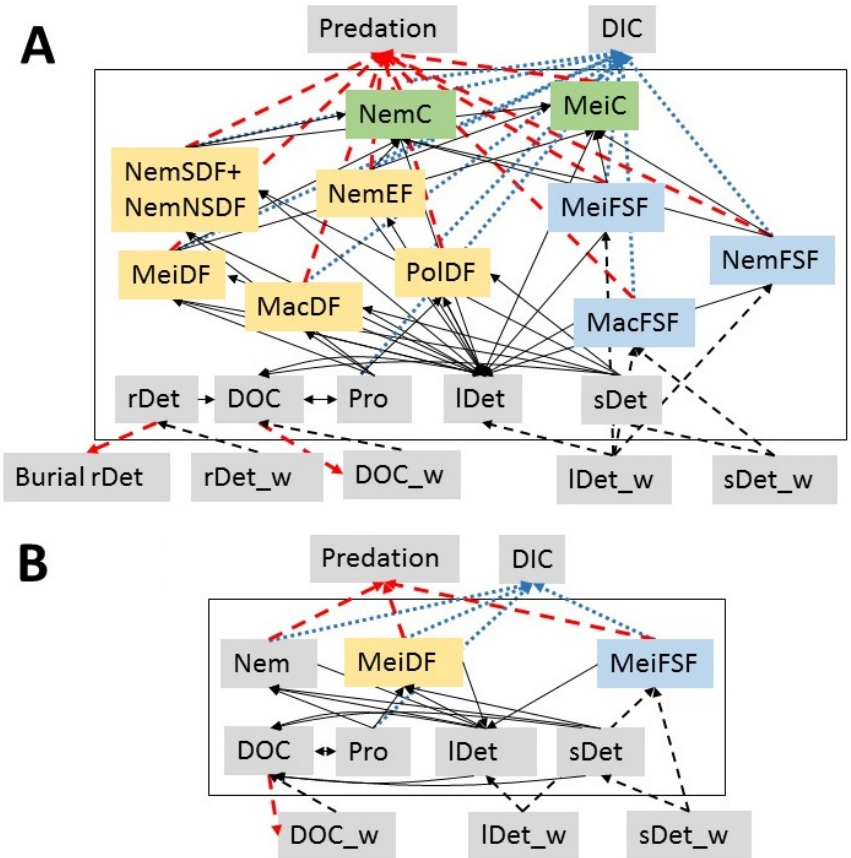

Figure 9-3. (A) Schematic representation of the food-web structure for the spatial comparison of the Cap de Creus and Lacaze-Duthiers canyon sections and (B) representation of the food-web structure for the temporal comparison at the Cap de Creus canyon.
The black frame includes all compartments that are part of the food-web model and the gray compartments outside this frame are either C input to the food web or C loss from the food web. Yellow boxes show the deposit feeder compartments, green boxes show carnivores, and blue boxes represent filter and suspension feeders. Solid black arrows show the C fluxes among food-web compartments and dashed black arrows represent the influx of C to the model. Blue dotted arrows stand for loss of C as respiration (DIC) and red dashed arrows symbolize C loss due to external predation, DOC efflux to the water column and refractory detritus burial.
The abbreviations are: DIC = dissolved inorganic carbon, DOC = dissolved organic carbon in the sediment, DOC_w = dissolved organic carbon in the water column, lDet = labile detritus, lDet_w = suspended labile detritus, MacDF = deposit feeding macrofauna, MacFSF = filter and suspension feeding macrofauna, MeiC = carnivorous meiofauna, MeiDF = deposit feeding meiofauna, MeiFSF = filter and suspension feeding meiofauna, Nem = nematodes, NemC = carnivorous nematodes, NemEF = epistratum feeding nematodes, NemNSDF = non-selective deposit feeding nematodes, NemSDF = selective deposit feeding nematodes, PolDF = deposit feeding polychaetes, Pro = prokaryotes, rDet = refractory detritus, rDet_w = suspended refractory detritus, sDet = semi-labile detritus, and sDet_w = suspended semi-labile detritus.

Table 9-1. Taxon-specific feeding types for meiofauna and macrofauna.
The abbreviations are: C = carnivore, DF = deposit feeder, EF = epistratum feeder, FSF = filter and suspension feeder, NSDF = non-selective deposit feeder, SDF = selective deposit feeder, and SF = suspension feeder.

Taxon	Feeding type	Reference
Metazoan meiofauna		
Amphipoda	DF	Cartes and Sorbe (1999a)
Bivalvia	FSF	Fox, Barnes and Ruppert (2003)
Copepoda	DF	Fox, Barnes and Ruppert (2003)
Cumacea	DF	Fox, Barnes and Ruppert (2003)
Gastrotricha	DF	Fox, Barnes and Ruppert (2003)
Isopoda	C	Fox, Barnes and Ruppert (2003)
Kinorhyncha	DF	Fox, Barnes and Ruppert (2003)
Nematodes	SDF, NSDF, EF, C	Wieser (1953)
Nemertea	C	Fox, Barnes and Ruppert (2003)
Oligochaeta	DF	Fox, Barnes and Ruppert (2003)
Ostracoda	FSF	Fox, Barnes and Ruppert (2003)
Polychaeta	DF	Mamouridis *et al.* (2011)
Tanaidacea	DF	Fox, Barnes and Ruppert (2003)
Tardigrada	DF	Fox, Barnes and Ruppert (2003)
Turbellaria	C	Fox, Barnes and Ruppert (2003)
Metazoan macrofauna		
Bivalvia (*Nucula sulcate*)	DF	Horton *et al.* (2018)
Oligochaeta	DF	Fox, Barnes and Ruppert (2003)
Polychaeta	DF	Jumars, Dorgan and Lindsay (2015)
Sipunculida	DF, SF	Fox, Barnes and Ruppert (2003)

9.3.2.2 Temporal comparison at the Cap de Creus canyon

For the temporal comparison of the CdC upper and lower canyon section food webs, we identified the compartments labile and semi-labile detritus, meiofaunal nematodes, and other meiofauna consisting of filter- and suspension feeders (MeiFSF) and deposit feeders (MeiDF).

The food webs received C as suspended labile and semi-labile detritus. C was lost from the food web as DIC, efflux of DOC to the water column and predation. Nematode and meiofaunal carcasses and feces contributed to the semi-labile sedimentary detritus stock. Labile and semi-labile detritus stocks were reduced by the hydrolysis of detritus to DOC. Nematodes and deposit-feeding meiofauna fed upon labile and semi-labile detritus, and prokaryotes, whereas filter and suspension-feeding meiofauna fed upon suspended labile and semi-labile detritus in the water column. Prokaryotes consumed DOC and contributed to this C stock again when they died because of viral lysis. The food web structure of this temporal comparison is shown in Figure 9-2B.

9.3.3 Data availability

Sediment samples for the analysis of detritus, prokaryotes, meiofauna, and macrofauna were taken at each sampling site (Figure 9-1; Supplementary table 9-1) with box cores and multicores.

Labile detritus is defined as the total phytopigment content in sediment. This phytopigment content was extracted from surface sediment (0–1 cm) as described in Lorenzen and Jeffrey (1980) and it was converted to the labile detritus stock (mmol C m^{-2}) using a C/ chl-a ratio of 40 (de Jonge, 1980), a sediment porosity of 0.70 (Danovaro, unpublished), and a sediment density of 2.55 g cm^{-3}. Semi-labile detritus corresponds to the sum of carbohydrates, lipids, and proteins, i.e., the so-called biopolymeric C (Fabiano, Danovaro and Fraschetti, 1995). Total carbohydrate, lipid, and protein contents were measured spectrophotometrically as described in Danovaro (2010c) and subsequently converted to C using a conversion factor of 0.49 for protein, 0.40 for carbohydrates, and 0.75 for lipids (Pusceddu *et al.*, 2010). Refractory detritus is defined as the total organic C stock from which the labile and semi-labile detritus stock are subtracted. This total organic C stock (mmol C m^{-2}) was calculated based on the organic C content in sediment (Table 9-2), a sediment density of 2.55 g cm^{-3}, and a porosity of 0.70 (Danovaro, unpublished).

Total prokaryotic cell numbers (TPN) in the 0–1 cm sediment layer were assessed by staining the sediment samples with acridine orange and counting the cells under an epifluorescent microscope (Danovaro, 2010e). Subsequently, TPN was converted to prokaryotic C stock by determining cell biovolume as described in Danovaro (2010f) and multiplying it with a conversion factor of 310 fg C μm^{-3} (Fry, 1990).

To assess the metazoan meiofaunal stock in the different canyon sections (section 9.3.2.1), sediment (0–1 cm layer) was sieved through a 1,000 µm mesh and subsequently through a 20 µm mesh. The fraction that was retained on the 20 µm mesh was re-suspended and extracted using density centrifugation with Ludox HS40 (Danovaro, 2010a). Meiofauna were sorted by taxa and counted under a stereomicroscope (40× magnification) after staining with Rose Bengal. Stocks of all meiofauna taxa were determined by bio-volumetric measurements as described in Danovaro (2010d) and grouped according to feeding types (Table 9-1). Meiofauna data for the temporal comparison (section 9.3.2.2) were extracted from literature. These data were only reported as total meiofaunal stock data (mmol $C_{meiofauna}$ m^{-2}) and were therefore converted to stock per taxon data using published percentages of the most abundant meiofauna taxa (Mea, 2011).

Metazoan macrofauna in the upper 20 cm of sediment included all metazoan fauna that were retained on a 300 µm mesh. The macrofaunal taxa were sorted under a stereomicroscope and identified to the lowest possible taxonomic resolution. Taxon-specific macrofaunal stocks were determined by measuring wet-weight biomasses and converting them to ash-free dry weight and organic C content using conversion factors from Rowe (1983). Subsequently, the different taxon-specific macrofaunal stocks were grouped in feeding types according to Table 9-1.

Table 9-2. Site specific data used to calculate C stocks and flux constraints that were implemented in the food-web models as inequalities [minimum, maximum] or equalities (single value). Abbreviations are: CdC = Cap de Creus, LD = Lacaze-Duthiers.
References: [1]Danovaro *et al.* (1999), [2]García *et al.* (2008), [3]Pasqual *et al.* (2010), [4](Danovaro *et al.*, 1999), [5]Accornero *et al.* (2003), [6]Rowe, Morse, *et al.* (2008), [7]Danovaro *et al.* (2008).

Parameter	LD upper canyon I	LD upper canyon II	LD middle canyon	CdC upper canyon	CdC middle canyon	CdC lower canyon	Ref.
Organic C content in sediment (%)	0.94	0.94	0.77	0.55	0.86	0.68	[1, 2]
POC flux (mmol C m^{-2} d^{-1})	<13.9	<13.9	<13.9	[3.11, 124]⁂; <13.9⁑⁑	<13.9	[0.26, 9.96] ⁂; <13.9⁑⁑	[3,4]
Burial rates (mmol C m^{-2} d^{-1})	3.15	1.82	1.11	1.88	1.18	0.76	
SCOC (mmol C m^{-2} d^{-1})	[0.84, 2.05]	[1.69, 6.02]	[0.21, 0.32]	[1.69, 6.02]*; <6.02⁑⁑	[0.21, 0.32]	[0.20, 6.02]*; <6.02⁑⁑	[5, 6]
DOC efflux (mmol C m^{-2} d^{-1})	[0.08, 0.21]	[0.17, 0.60]	[0.02, 0.03]	[0.17, 0.60]	[0.02, 0.03]	[0.02, 0.60]	
Heterotrophic prokaryotic production (mmol C m^{-2} d^{-1})	0.18	0.26	0.12	0.39	0.20	0.11	[7]

*Spatial comparison. ⁂Temporal comparison, directly after the DSWC event in April 2005 and April 2008; ⁂Temporal comparison, October 2005, October 2010, April 2009, October 2009.

9.3.4 Site-specific flux constraints

C flows between different food-web compartments were constrained by implementing site-specific flux and physiological constraints in the linear inverse models. A list with site-specific constraints is presented in Table 9-2 and details about the specific parameters are presented in the following text.

Particulate organic carbon (POC) flux to the Gulf of Lions/ Catalan margin area was measured with moorings that were equipped with sediment traps (Danovaro *et al.*, 1999; Pasqual *et al.*, 2010)

Degradation rates of sedimentary detritus in the western Mediterranean Sea were unknown and therefore they were adopted from the Iberian margin: Labile detritus was degraded with rates between 1.81×10^{-4} d^{-1} and 2.17×10^{-2} d^{-1} and refractory detritus was degraded with rates ranging from 5.48×10^{-7} d^{-1} to 8.74×10^{-4} d^{-1} (Epping *et al.*, 2002).

Burial rate of rDet b_{rDet} (mmol C m^{-2} d^{-1}) was calculated following Epping *et al.* (2002) as:

$$b_{rDet} = 4.83 \times e^{\frac{-z}{1{,}015}}, \qquad \text{[Equation 9-1]}$$

where *z* is the water depth (in m).

Sediment community oxygen consumption (SCOC; mmol C m^{-2} d^{-1}) was only recorded with a benthic lander in the LD upper canyon section (Accornero *et al.*, 2003), but not in the LD middle canyon section, nor in the CdC canyon. Therefore, a systematic literature review was conducted to identify SCOC rates in submarine canyons following the PRISMA guidelines for systematic reviews and meta-analyses (Moher *et al.*, 2009). The keywords "respiration canyon", "respiration submarine canyon", and "sediment community oxygen consumption canyon" identified 52 articles in the "Web of Science" and additional 35 articles were identified through other sources, including "Google Scholar". After removing duplicates, the abstract of 66 articles were screened for relevancy. Nine articles reported SCOC data and 5 of these 9 articles presented *in situ* measurements of SCOC data from submarine canyons (Lacaze-Duthiers Canyon, Barrow Canyon, Whittard Canyon, Cap-Ferret Canyon, Mississippi Canyon). These data were extracted and are presented in Supplementary table 9-2; SCOC data from water depths that are similar to the sampling sites in this study (Supplementary table 9-1) were implemented in the food-web models (Table 9-2)

DOC efflux of the sediment was constrained to be 10% of the C oxidation rate (Burdige *et al.*, 1999).

9.3.5 Physiological constraints

Physiological constraints were predominantly extracted from the literature (Table 9.2 and 9.3)

Prokaryotic growth efficiency *PGE* in deep-sea sediments was measured in a pulse-chase experiment for a treatment with fecal pellets and a treatment with diatoms (Mayor *et al.*, 2012). It was calculated as:

$$PGE = \frac{I_P}{(I_P + R_P)}, \qquad \text{[Equation 9-2]}$$

where I_P is the amount of C that was taken up by the prokaryotes, and R_P is the amount of C that was respired by prokaryotes (Mayor *et al.*, 2012).

Heterotrophic prokaryotic production was measured by ^{3}H-leucine incorporation (Danovaro, Dell'Anno, *et al.*, 2008) and minimum and maximum virus-induced prokaryotic mortality rates was equivalent to the $mean_{VIPM} - SD_{VIPM}$ and the $mean_{VIPM} + SD_{VIPM}$ values for sediments below 1,000 m water depth (Danovaro, Dell'Anno, *et al.*, 2008).

Assimilation efficiency *AE* was defined as:

$$AE = \frac{(I-F)}{I}, \quad \text{[Equation 9-3]}$$

where *I* was the amount of ingested food and *F* was the amount of feces (Crisp, 1971).

Net growth efficiency (*NGE*) was defined as:

$$NGE = \frac{G}{(G+R)}, \quad \text{[Equation 9-4]}$$

where *G* was the growth and *R* was the respiration (Crisp, 1971).

Production *P* (mmol C m^{-2} d^{-1}) was calculated as:

$$P = \frac{P}{B}\text{-}ratio \times C\ stock, \quad \text{[Equation 9-5]}$$

where *P/B-ratio* was the production/biomass-ratio (d^{-1}).

Respiration *R* (mmol C m^{-2} d^{-1}) was calculated as:

$$R = r \times C\ stock, \quad \text{[Equation 9-6]}$$

where *r* was the biomass-specific respiration rate (d^{-1}).

The proportionally higher uptake of labile and semi-labile detritus and prokaryotes by nematode non-selective deposit feeders, nematode selective feeders, meiofauna deposit feeders, and macrofauna deposit feeders (spatial comparison) and nematodes (temporal comparison) were constrained as feeding selectivity *sensu* van Oevelen, Soetaert and Heip (2012).

9.3.6 Linear inverse modeling and network indices

Linear inverse models were solved in R (R-Core Team, 2017) using the *LIM* package (van Oevelen *et al.*, 2010). Average and standard deviations of each C flow from a set of 15,000 model solutions were calculated using the likelihood approach (van Oevelen *et al.*, 2010).

For a quantitative food-web comparison, the network indices "Total System Throughput" *T..* (i.e., the sum of all C flows in the food web), number of links *L*, "Finn's cycling index" *FCI* (i.e., the portion of *T..* that is cycled; Finn, 1980), and the "Average Mutual Information" *AMI* (i.e., information about how much a food-web flow is constrained; Kones *et al.*, 2009) were calculated directly from the set of food web solutions (15,000 for each model) using the R-package *NetIndices* (Kones *et al.*, 2009).

Table 9-3. Process constraints (equalities = single values, inequalities = [minimum, maximum]) that were implemented in the food web models.
References: [1]Mayor *et al.* (2012), [2]Corinaldesi *et al.* (2010), [3]**Chapter 2** and references therein, [4]Clausen and Riisgård (1996), [5]Nielsen *et al.* (1995), [6]van Oevelen, Soetaert and Heip (2012).

Processes	**Size classes/ compartments**	**Value**	**Ref.**
Prokaryotic growth efficiency (-)	Prokaryotes	[0.28, 0.73]	1
Virus-induced prokaryotic mortality (-)	Prokaryotes	[0.75, 0.85]	2
Assimilation Efficiency (-)*	Meiofauna Macrofauna	[0.26, 0.41] [0.48, 0.87]	3
Net growth efficiency (-)‡	Meiofauna⁂ Macrofauna	[0, 0.69] [0.60, 0.72]	4, 5
Secondary production (mmol C m^{-2} d^{-1})	Meiofauna Macrofauna	[4.50×10^{-2}, 0.13]×C stock [1.37×10^{-2}, 2.21×10^{-2}]×C stock	3
Mortality[1] (mmol C m^{-2} d^{-1})	Meiofauna Macrofauna	[0, 0.13]×C stock [0, 2.21×10^{-2}]×C stock	3
Respiration (mmol C m^{-2} d^{-1})	Meiofauna Macrofauna	[2.03×10^{-2}, 6.96×10^{-2}]×C stock [7.12×10^{-5}, 2.28×10^{-2}]×C stock	3
Feeding selectivity (-)	MacDF, PolDF	[1, 10]	6

*As only insufficient data were found for the continental slope, data from the near-shore area were used in the model.
‡Net growth efficiency for meiofauna was calculated as described in Equation 9-4 using production and respiration rates from **Chapter 2**.
⁂The minimum constraint of meiofaunal net growth efficiency was adjusted in the linear inverse modeling step.

9.4 Results

9.4.1 Comparison of canyon sections

9.4.1.1 Food-web structure

Total C stocks including detritus, prokaryotes, meiofauna, and macrofauna were highest at LD upper canyon I section (6.07×10^3 mmol C m^{-2}) and lowest at CdC lower canyon section (3.35×10^3 mmol C m^{-2}) (Figure 9-5). Sedimentary detritus contributed between 98.8% (LD upper canyon I) and 99.7% (LD middle canyon section, CdC middle canyon section, CdC lower canyon section) to total C stocks. When only biomasses, i.e., prokaryotic and faunal C stocks,

[1] By default, in linear inverse models mortality rates range from 0 to the maximum secondary production *P*.

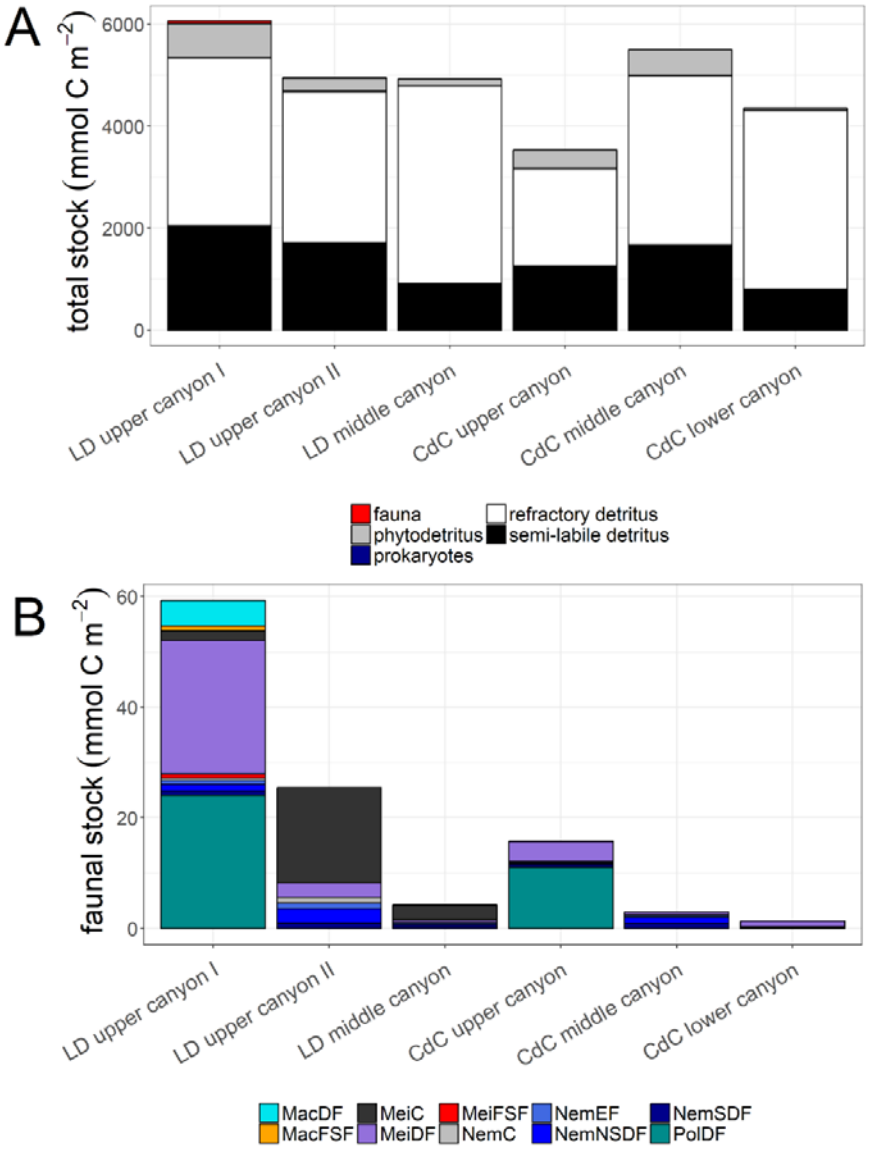

Figure 9-5. (A) Total C stocks (mmol C m^{-2}) of the food-web compartments labile, semi-labile, and refractory detritus, prokaryotes, and fauna for all 6 investigated canyon sections. (B) C stocks (mmol C m^{-2}) of all faunal food-web compartments for all 6 investigated canyon sections. For information about sampling sites see Supplementary table 9-1.

The abbreviations are: MacDF = macrofauna deposit feeder, MacFSF = macrofauna filter and suspension feeder, MeiC = meiofauna carnivore, MeiDF = meiofauna deposit feeder, MeiFSF = meiofauna filter and suspension feeder, NemC = nematode carnivore, NemEF = nematode epistratum feeder, NemNSDF = nematode non-selective deposit feeder, NemSDF = nematode selective deposit feeder, and PolDF = polychaete deposit feeding.

were considered, the contribution of prokaryotes to total biomass increased with increasing water depth. At 434 m water depth in the LD canyon (LD upper canyon I section), prokaryotes accounted for 20.0% of the total biomass, whereas at 1,497 m water depth (LD middle canyon section) they accounted for 69.9% of the total biomass. At the CdC canyon, prokaryotes contributed 57.6% to total biomass at 960 m and 90.6% at 1,874 m water depth. Macrofauna were present at the highest canyon sections (LD upper canyon I section, CdC upper canyon section) and absent at all lower canyon sections except at the LD middle canyon section where macrofauna contributed 1.13% to total biomass. Deposit feeders dominated faunal biomass in the upper canyon sections (93.6% of total faunal biomass at the LD upper canyon I section, mainly meiofaunal polychaetes; 98.6% of total faunal biomass at the CdC upper canyon section) and predators dominated the faunal biomass at the LD upper canyon II section (71.8% of total faunal biomass, mainly meiofaunal Nemertea) and the LD middle canyon section (62.0% of total faunal biomass).

9.4.1.2 Carbon flows

In the LD canyon, estimated total C input to the food web decreased with water depth, ranging from 11.8±0.14 mmol C m^{-2} d^{-1} at the LD upper canyon I (434 m) to 2.02±0.02 mmol C m^{-2} d^{-1} at the LD middle canyon (1,497 m) (Figure 9-6). In the CdC canyon, however, the estimated total C input was highest in the CdC middle canyon (6.56±0.08 mmol C m^{-2} d^{-1}) (Figure 9-6). Modelled C input consisted of 53.2% labile, 32.7% semi-labile, and 14.1% refractory detritus at the shallowest station (LD upper canyon I; 434 m) and of 25.4% labile, 28.5% semi-labile, and 46.1% refractory detritus at the deepest station (CdC lower canyon; 1,874 m) (Figure 9-6).

Estimated total respiration was lowest at the CdC middle canyon section (0.27±0.03 mmol C m^{-2} d^{-1}) and highest at the LD upper canyon II section (1.73±0.03) (Table 9-4). Bacteria dominated the respiration in the CdC canyon and in the LD middle canyon section, and they contributed between 60.3% (LD middle canyon section) and 87.5% (CdC lower canyon section) to the total benthic respiration. At the LD upper canyon I section, meiofaunal and polychaete deposit feeder contributed together 72.7% to the total benthic respiration and at the LD upper canyon II section meiofaunal carnivores had a contribution of 50.5% to the total benthic respiration.

Model results showed that between 0.43±0.01 mmol C m^{-2} d^{-1} (CdC lower canyon section) and 1.46±0.04 mmol C m^{-2} d^{-1} (LD upper canyon section I) were lost due to the burial of refractory detritus and between $7.32\times10^{-3}\pm9.50\times10^{-4}$ mmol C m^{-2} d^{-1} (LD middle canyon section) and 0.19±0.02 mmol C m^{-2} d^{-1} (LD upper canyon I section) left the system as DOC to the water column. Additionally, predation on meiofauna by external predators outside the modelled system were estimated to be maximum 7.53±0.13 mmol C m^{-2} d^{-1} (LD upper canyon I section). Maximum predation on macrofauna by external predators was modelled to be 0.69±0.03 mmol C m^{-2} d^{-1} in the LD upper canyon I section.

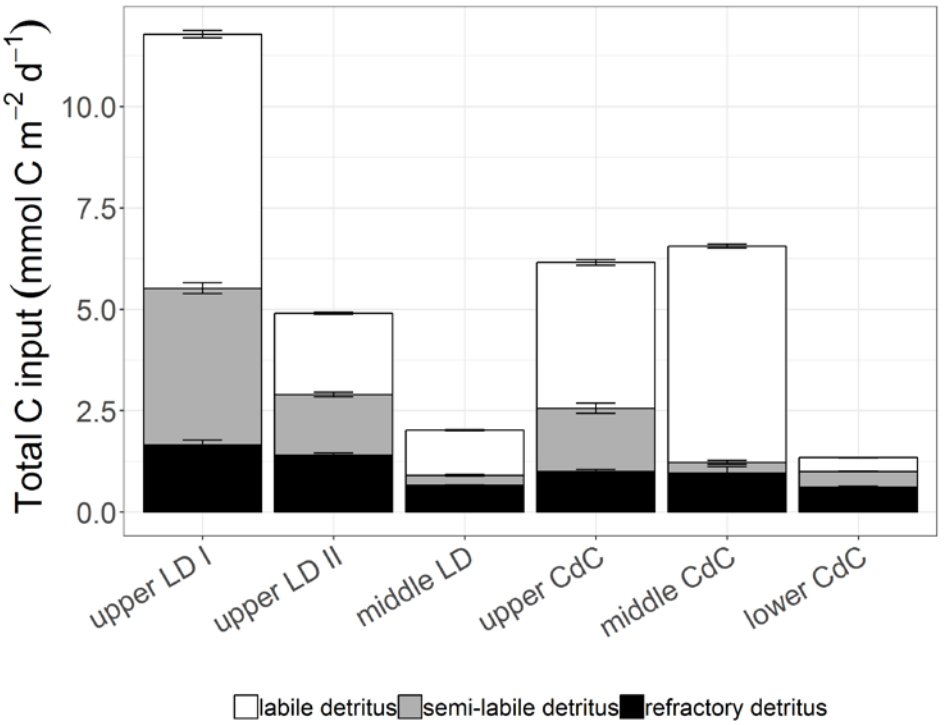

Figure 9-6. Contribution of labile, semi-labile, and refractory detritus to TOC input (mmol C m^{-2} d^{-1}) at the Lacaze-Duthiers (LD) upper canyon I section (upper LD I, 434 m), LD upper canyon II section (upper LD II, 990 m), LD middle canyon section (middle LD, 1,497 m), Cap de Creus (CdC) upper canyon section (upper CdC, 960 m), CdC middle canyon section (middle CdC, 1,434 m), and CdC lower canyon section (lower CdC, 1,874 m).

9.4.2 Time series analysis

The model estimated that the food web in the upper CdC canyon section took up between 0.69±0.16 mmol C m^{-2} d^{-1} (April 2005; DSWC event: T_0) and 2.59±0.32 mmol C m^{-2} d^{-1} (April 2009; 4 yr post-DSWC: T_4) (Figure 9-7). This organic C consisted for 36.6% ($T_{4.5}$) to 72.7% (T_0) of labile detritus. In the lower CdC canyon section, the food web was estimated to take up 0.30± 0.03 mmol C m^{-2} d^{-1} (T_0) to 0.67±0.08 mmol C m^{-2} d^{-1} ($T_{3.5}$) which contained 38.2% ($T_{4.5}$) to 64.1% (T_3) labile detritus.

Estimated 0.35±0.06 mmol C m^{-2} d^{-1} (T_0) to 0.73±0.11 mmol C m^{-2} d^{-1} (T_4) were respired in the CdC upper canyon section and estimated 0.13±0.01 mmol C m^{-2} d^{-1} (T_0) to 0.21±0.03 mmol C m^{-2} d^{-1} (T_4) were respired in the CdC lower canyon section (Figure 9-7). The model estimated that the predation from outside its boundaries ranged from 3.34×10^{-2}± 1.03×10^{-2} mmol C m^{-2} d^{-1} (T_0) to 1.35±0.26 mmol C m^{-2} d^{-1} (T_4) in the CdC upper canyon section and from 4.93×10^{-2}±1.35×10^{-2} mmol C m^{-2} d^{-1} (T_0) to 0.38±0.05 mmol C m^{-2} d^{-1} (T_4) in the CdC lower canyon section (Figure 9-7).

Table 9-4. Prokaryotic and faunal contribution (%) to total respiration (mmol C m^{-2} d^{-1}) in all canyon food webs. For information about specific station locations see Supplementary table 9-1. "n.p." signifies that the specific feeding group was not present.
The abbreviations are: MacDF = macrofauna deposit feeder, MacFSF = macrofauna filter and suspension feeder, MeiC = meiofauna carnivore, MeiDF = meiofauna deposit feeder, MeiFSF = meiofauna filter and suspension feeder, NemC = nematode carnivore, NemEF = nematode epistratum feeder, NemNSDF = nematode non-selective deposit feeder, NemSDF = nematode selective deposit feeder, PolDF = polychaete deposit feeding, and Pro = prokaryotes.

Compartment	**LD upper canyon I**	**LD upper canyon II**	**LD middle canyon**	**CdC upper canyon**	**CdC middle canyon**	**CdC lower canyon**
Total respiration	1.95±0.05	1.73±0.03	0.29±0.02	0.99±0.05	0.27±0.03	$0.31\pm3.53\times10^{-3}$
Pro	12.9	32.9	60.3	71.6	76.5	87.5
NemSDF	1.79	3.14	3.43	1.38	8.33	1.06
NemNSDF	1.51	1.02	5.00	0.85	2.76	1.04
NemEF	1.72	2.69	5.35	1.08	5.79	0.92
NemC	0.59	1.61	0.91	0.48	1.93	0.29
MeiFSF	1.41	9.80×10^{-3}	9.33×10^{2}	9.90×10^{-3}	2.01×10^{2}	n.p.
MeiDF	56.2	8.21	3.98	9.65	4.59	9.19
MeiC	3.83	50.5	20.4	0.23	4.94×10^{2}	3.96×10^{2}
MacFSF	0.51	n.p.	n.p.	n.p.	n.p.	n.p.
MacDF	3.07	n.p.	0.52	n.p.	n.p.	n.p.
PolDF	16.5	n.p.	n.p.	14.7	n.p.	n.p.

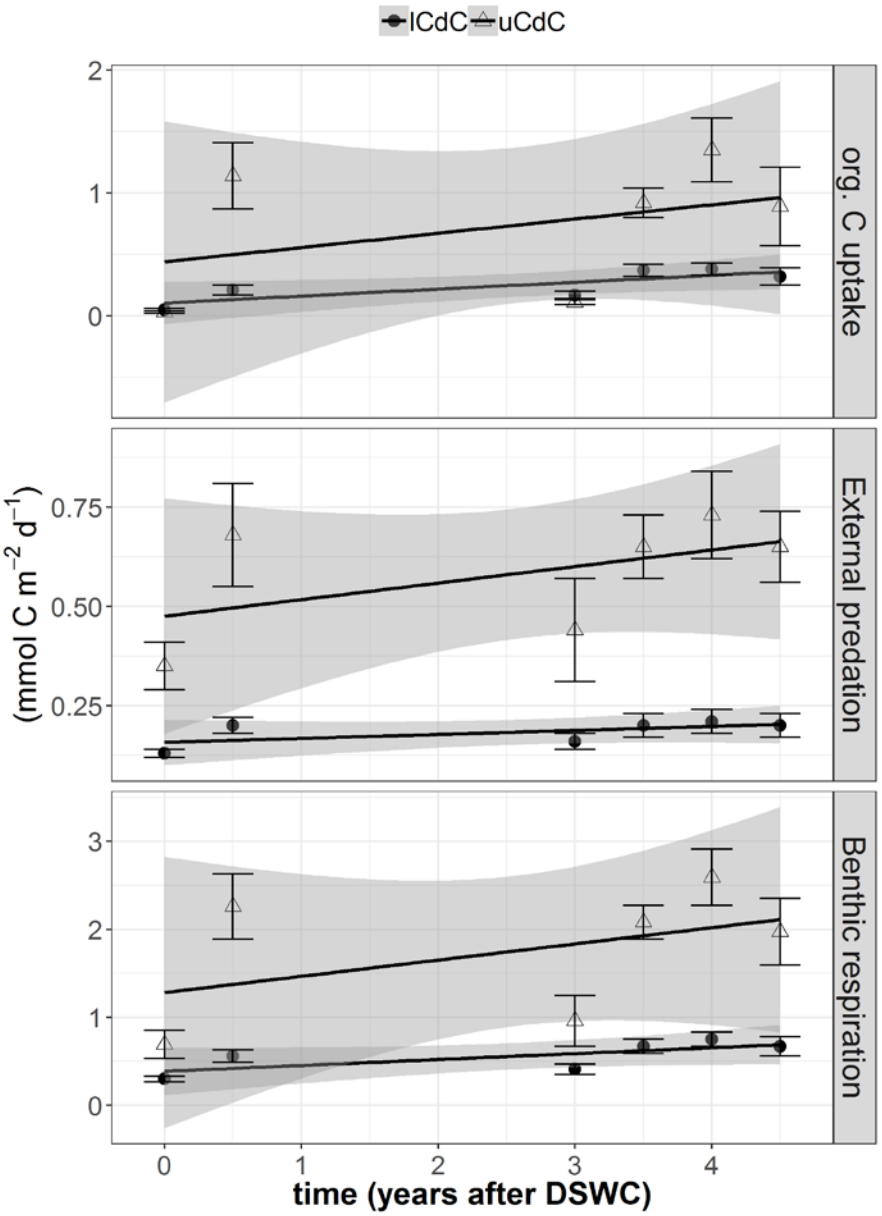

Figure 9-7. C flows (mmol C m^{-2} d^{-1}) in (organic C uptake = labile + semi-labile detritus uptake; upper panel) and out (external predation, middle panel; benthic respiration, lower panel) of the food web at the Cap de Creus upper canyon section (uCdC, 960 m; open triangles) and the CdC lower canyon section (lCdC, 1,874 m; black dots). The data are plotted over time as years after the dense shelf water cascading (DSWC) event starting with April 2005, i.e., the dense shelf water cascading event in winter 2004/ 2005. Error bars show 1 standard deviation; the lines correspond to linear regression models and the shades are the corresponding 95% confidence intervals.

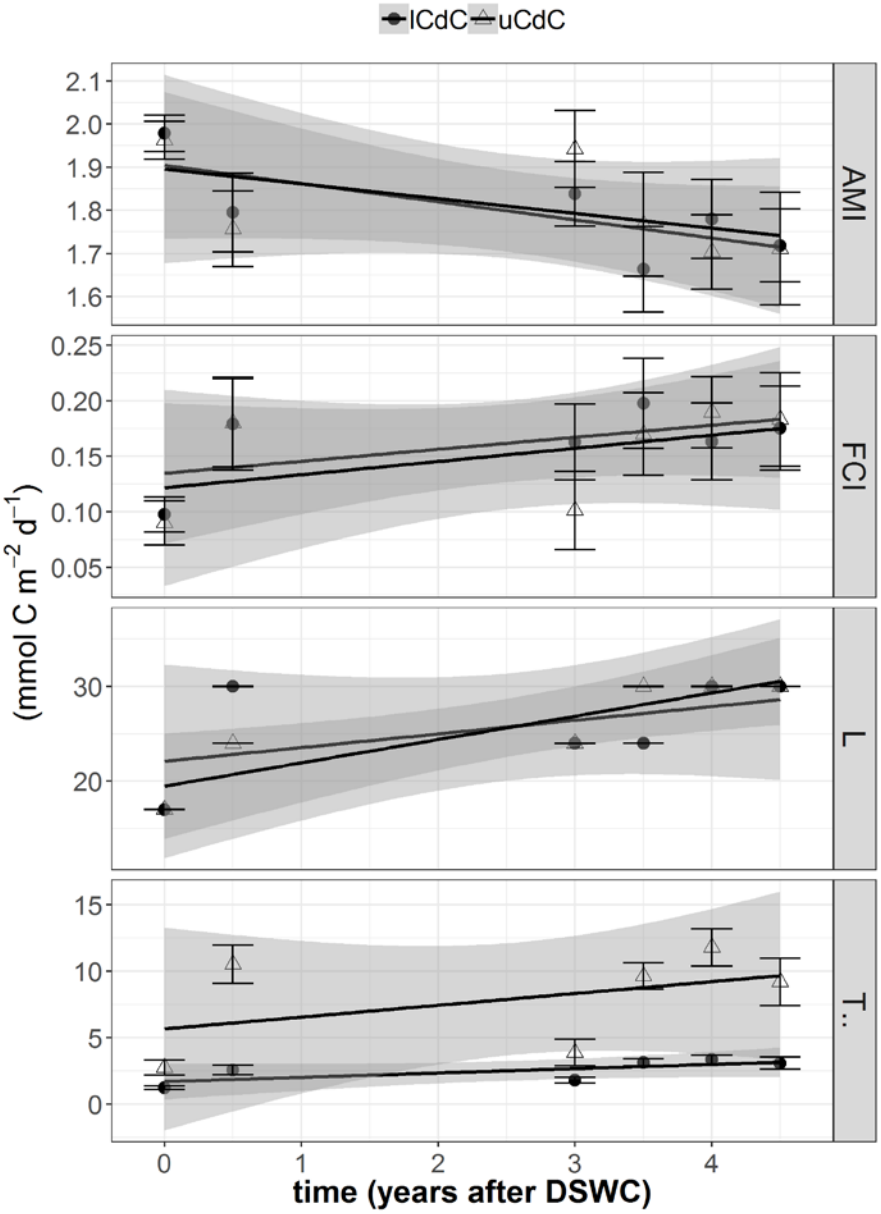

Figure 9-8. Network indices (total system throughput = *T..* in mmol C m^{-2} d^{-1}, Finn's cycling index = *FCI*, average mutual information = *AMI*, and number of links = L) calculated for the Cap de Creus upper canyon section (uCdC, 960 m; open triangles) and the CdC lower canyon section (lCdC, 1,874 m; black dots). Error bars show 1 standard deviation; the lines correspond to linear regression models and the shades are the corresponding 95% confidence intervals.

Model results implied that *AMI* in the CdC upper and lower canyon sections decreased over time after the major DSWC event, whereas *FCI*, *L*, and *T*.. (mmol C m^{-2} d^{-1}) increased over time in both canyon sections (Figure 9-9).

9.5 Discussion

This study compares food-web structure and C flows among food-web compartments for sections of the Cap de Creus (CdC) canyon and the Lacaze-Duthiers (LD) canyon in the NW Mediterranean Sea. Furthermore, the study assesses signs of microbial and meiofaunal recovery after a major dense shelf water cascading (DSWC) event by comparing food webs of the upper and lower CdC canyon directly after the cascading event in April 2005 and 0.5, 3, 3.5, 4, and 4.5 yr later.

9.5.1 Model limitations

Our models are limited by a lack of site-specific detritus degradation rates, missing megafauna and partly macrofauna data: Using degradation rates for detritus from the Nazaré canyon implied that we could not adequately investigate whether DSWC affects the degradation of organic matter in the canyons. A study by Tesi *et al.* (2010) showed that DSWC events can likely generate a shear stress that is high enough to mobilize the layer of coarse surface sediment and erode the underlying stratum that consists of aged organic C. In that case, we would have two refractory detritus pools with very different degradation rates: One pool would include younger refractory detritus and the other pool would be composed of organic matter that was deposited during the last sea-level minimum (Tesi *et al.*, 2010) and likely has a lower lability because of its terrestrial origin with a high lignin content (Arndt *et al.*, 2013).

Cold-water coral colonies (CCC) consisting of *Madrepora oculata*, *Desmophyllum pertusum* (prior name: *Lophelia pertusa*), and *Dendrophyllia cornigera* are present in the CdC and the LD canyon (Orejas *et al.*, 2009; Gori *et al.*, 2013): During video surveys with the submersible *Jago* and with remotely operated vehicles (ROV) all three cold-water coral species were observed to a depth of ~300 m in the CdC canyon (Orejas *et al.*, 2009; Gori *et al.*, 2013), which is more than 600 m shallower than upper CdC canyon section site in this study. We therefore do not expect any CCC at the sites of our food-web studies in the CdC canyon. In contrast, in the LD canyon, several *M. oculata* and *D. pertusum* colonies were observed down to 540 m depth (Gori *et al.*, 2013). Hence, it is possible that *M. oculata* was present in the sediment of the upper LD canyon section. However, if there were individual corals present, they would contribute significantly to total respiration: van Oevelen *et al.* (2009) measured the respiration of *D. pertusum* and *M. oculata* at Rockall Bank (NE Atlantic) and found a value of 1.83±1.10 mmol C m^{-2} d^{-1} for a cold-water coral stock of 1,222.0 mmol C m^{-2}. In comparison, respiration rates of *D. pertusum* and *M. oculata* in the Croisic canyon and the Guilvinec canyon (Britanny continental slope, Bay of Biscay, NE Atlantic) were 7.7 mmol C m^{-2} d^{-1} (Khripounoff *et al.*, 2014). Hence, filter-feeding

megafauna could double to quadruple the benthic respiration rates estimated in our food-web models.

Besides CCC, also deposit feeding megafauna can sometimes have an increased abundance and/ or biomass in submarine canyons: De Leo *et al.* (2010) observed very high densities of holothurians, echiurans, polychaetes, and echinoids at 900–1,100 m water depth in the Kaikoura canyon (New Zealand, SW Pacific). Furthermore, in the middle section of the Nazaré canyon (2,700–4,000 m water depth), total C stock of deposit feeding megafauna was 495±703 mmol C m^{-2} (van Oevelen, Soetaert, *et al.*, 2011). This implies that without adequate knowledge about sessile and mobile megafauna we might severely underestimate C cycling in the LD and the CdC canyon.

9.5.2 Comparison of Cap de Creus and Lacaze-Duthiers canyon food webs

The food-web models estimated that the upper CdC canyon section at 960 m and the upper LD canyon section at 990 m depth received 6.16±0.15 mmol C m^{-2} d^{-1} and 4.90±0.03 mmol C m^{-2} d^{-1}, respectively. This was approximately twice the average organic C flux to the open slope of the Catalan margin (2.8 mmol C m^{-2} d^{-1}), but less than the average organic C flux to the Blanes canyon (22.9 mmol C m^{-2} d^{-1}) (Lopez-Fernandez, Bianchelli, Pusceddu, Calafat, Sanchez-Vidal, *et al.*, 2013). However, the average organic C input to the Blanes canyon was also almost 3 times higher than the C input to the upper Nazaré canyon section (7.98±0.84 mmol C m^{-2} d^{-1}; van Oevelen, Soetaert, *et al.*, 2011) and could be related to a strong storm event during the study period (Lopez-Fernandez, Bianchelli, Pusceddu, Calafat, Danovaro, *et al.*, 2013). From November 2008 to January 2009 when organic C fluxes were measured continuously over sampling periods of 15 d each, organic C fluxes between 22.5 mmol C m^{-2} d^{-1} and 28.83 mmol C m^{-2} d^{-1} were measured, whereas from late February 2009 to late March 2009, the organic C fluxes ranged from 0.42 mmol C m^{-2} d^{-1} to 0.68 mmol C m^{-2} d^{-1} (Lopez-Fernandez, Bianchelli, Pusceddu, Calafat, Danovaro, *et al.*, 2013). Since the samples for this part of our study were collected in October 2005 – between the DSWC events in winter/ early spring 2005 and 2006 (Canals *et al.*, 2006; Palanques *et al.*, 2012) – the modelled organic C inputs to the food webs are in the expected range.

C processing in the food webs of the LD upper canyon I and II sections and the CdC middle canyon section follow the C processing of the "active faunal uptake category" (Woulds *et al.*, 2009): Meiofauna was estimated to contribute >50% to the total benthic respiration in the upper LD canyon, and in the CdC middle canyon, epistrate feeding nematodes were modelled to ingest 83% of the TOC input. Though this contribution of meiofauna to C processing seems high, studies reported previously that meiofauna can play an important role in benthic C cycling at continental margins. Using food-web models, van Oevelen, Soetaert, *et al.* (2011) estimated that meiofauna contribute 21% to total respiration in the upper Nazaré canyon section. Rowe *et al.* (2008) even calculated a meiofaunal contribution of up to 51% to total respiration in the NE Gulf of Mexico. As Leduc, Pilditch and Nodder (2016) found a positive relationship between chloroplastic

pigment equivalents in sediment and meiofauna respiration when comparing the Challenger Plateau with the Chatham Rise (waters around New Zealand, SW Pacific), the strong contribution of meiofauna to respiration and C uptake in this study was very likely the result of increased input of labile and semi-labile detritus to the upper the upper LD canyon and the middle CdC canyon (Figure 9-6).

C processing in the upper and lower CdC canyon sections can be classified as "bacteria uptake dominated" (Woulds *et al.*, 2009), because the microbial loop accounts for 42.5% (CdC upper canyon section) to 57.1% (CdC lower canyon section) of the total C input to the system. As the upper Nazaré canyon section falls under the same category (van Oevelen, Soetaert, *et al.*, 2011), further research on food webs from submarine canyons could give valuable information whether it is coincidence, that in both cases, the Nazaré and the CdC canyon, upper canyon sections are dominated by bacteria uptake. In comparison, middle canyon sections are dominated by faunal uptake, though in the CdC canyon, meiofauna is the dominating benthic size class, whereas in the Nazaré canyon megafaunal holothurians dominate the C uptake.

9.5.3 Effect of dense shelf water cascading on canyon food webs

During the study period from April 2005 to October 2009, the Gulf of Lion and the Catalan margin experienced DSCW events during winter 2005 (from late February to late March 2005; Canals *et al.*, 2006), winter 2006 (early January 2006, late January 2006, from early March to mid-April 2006; Palanques *et al.*, 2012), winter 2007 (late January 2007, mid-February 2007, late March to late April 2007; Ribó *et al.*, 2011) and winter 2008 (late December 2007, early January 2008; Ribó *et al.*, 2011). Each of these events is usually characterized by a reduction of water temperature, an increase in down-canyon current speed and increased concentrations of suspended particles (Canals *et al.*, 2006). Additionally, after the DSWC events in 1999 and in 2005/ 2006, a bottom nepheloid layer (BLN) was observed that started in the Gulf of Lion and at the Catalan margin and extended into the NW Mediterranean basin (Puig *et al.*, 2013). During the 2005/ 2006 DSWC events, this BLN stretched over the entire W Mediterranean basin (Puig *et al.*, 2013). Hence, the benthos lives in a highly unstable environment and only species that recover before the next DSWC event occurs can live here.

The intensive DSWC event in April 2005 led to a reduction in meiofauna biomass and a change in meiofauna composition compared to after the DSWC event (Pusceddu *et al.*, 2013). Nematodes were reduced by 23-fold at the CdC upper canyon section and by 5-fold at the CdC lower canyon section compared to 0.5 yr later (Mea, 2011; Pusceddu *et al.*, 2013). Filter and suspension feeding nematodes as well as deposit feeding nematodes were completely absent. Consequently, the food-web structure was altered as shown in the estimated lower total number of food-web links L for both canyon sections compared to 0.5 yr later. In fact, the models showed that L and the total amount of C that was processed within the food web, i.e., the total system throughput $T..$, were the same or very

similar for both canyon sections because the whole canyon was impacted by the very strong DSWC event: Recordings at the CdC canyon mouth at 2,141 m depth in April 2005 showed a lower potential temperature, a higher potential density, a higher chlorophyll-a fluorescence and a higher concentration of suspended sediment compared to normal conditions in July 1993, February 1995 and March 1998 (Canals *et al.*, 2006). However, within 0.5 yr, *T.*. had increased by 7.78 mmol C m^{-2} d^{-1} at the upper canyon indicating meiofauna recovery from the disturbance.

Marine meiofauna can disperse actively by emerging from the sediment and selectively reentering it, or passively, when a disturbance leads to sediment suspension and/ or erosion (Palmer, 1988). DSWC events in the Gulf of Lions can erode the canyon floor of the CdC canyon and transport 0.75 to 2.78 g suspended sediment m^{-2} s^{-1} (Puig *et al.*, 2017). Meiofauna that inhabits the canyon seafloor will likewise be resuspended and passively transported with the deep slope currents. In this way, meiofauna organisms can disperse towards the bottom nepheloid layer (BLN) which was ~600 m thick in 1999 and had sediment concentrations of 0.08 mg L^{-1} (Puig *et al.*, 2013). The BLN in 1999 extended towards the Catalan Margin and vanished within a year (Puig *et al.*, 2013), but the BLN in 2005/ 2006 covered the whole western Mediterranean basin. The suspended particles inside the BLN form large aggregates of 1 mm size (Puig *et al.*, 2013) which might be an appropriate intermediate habitat for meiofauna, but this hypothesis needs to be tested by further research. When the meiofauna in the BLN is transported passively by currents to shore, the fauna might descent in the water column and settle selectively on appropriate habitat (Lins *et al.*, 2013; Mevenkamp, Van Campenhout and Vanreusel, 2016) or deposit passively (DePatra and Levin, 1989).

Hence, whereas DSWC events have an immediate negative effect on the lower trophic levels of deep-sea canyon food webs as exemplified by estimated reduced C cycling in April 2008 compared to years without DSWC events, the cascading events might enhance the dispersal ability of benthic meiofauna. However, the frequency of DSWC events is expected to decrease due to climate change (Herrmann *et al.*, 2008). Therefore, passive meiofaunal dispersal along the continental margin of the northern Mediterranean Sea might be reduced. For higher trophic levels, a reduced frequency of DSWC events will likely lead to a collapse of the deep-sea shrimp *Aristeus antennatus* because Company *et al.* (2008) hypothesized that, in the long run, DSWC events counterbalance the high fishing pressure.

9.6 Supplement

Supplementary table 9-1. Sampling locations and depths in the Cap de Creus canyon section. The "initial disturbance" refers to the major dense shelf water cascading event from later February to late March 2005 (Canals *et al.*, 2006).

Date	Time since 'initial disturbance'	Canyon section	Depth (m)	Latitude (N)	Longitude (E)
Sampling for section 9.3.2.1 "Spatial comparison of canyon sections"					
10/2005	0.5 yr	LD upper canyon I	434	42°34'26''	3°24'03''
	0.5 yr	LD upper canyon II	990	42°26'34''	3°31'50''
	0.5 yr	LD middle canyon	1,497	42°21'58''	3°49'25''
	0.5 yr	CdC upper canyon	960	42°18'36''	3°36'36''
	0.5 yr	CdC middle canyon	1,434	42°12'39''	3°49'13''
	0.5 yr	CdC lower canyon	1,874	42°12'53''	4°15'26''
Sampling for section 9.4.2 "Time series analysis"					
04/2005	0 yr	CdC upper canyon	940	42°18'30"	3°36'00"
		CdC lower canyon	1,801	42°12'54"	4°15'18"
10/2005	0.5 yr	CdC upper canyon	960	42°18'30"	3°36'00"
		CdC lower canyon	1,874	42°12'54"	4°15'18"
04/2008	3 yr	CdC upper canyon	1,000	42°18'30"	3°36'42"
		CdC lower canyon	1,800	42°12'54"	4°15'24"
10/2008	3.5 yr	CdC upper canyon	1,000	42°18'30"	3°36'42"
		CdC lower canyon	1,800	42°12'54"	4°15'24"
04/2009	4 yr	CdC upper canyon	983	42°18'12"	3°37'00"
		CdC lower canyon	1,845	42°12'54"	4°15'24"
10/2009	4.5 yr	CdC upper canyon	983	42°18'12"	3°37'00"
		CdC lower canyon	1,845	42°12'54"	4°15'24"

Supplementary table 9-2: Sediment community oxygen consumption (SCOC; mmol C m^{-2} d^{-1}) rates in submarine canyons. Data are presented as individual measurements, as ranges or as mean±SE.
References: [1]Accornero *et al.* (2003), [2]Clough, Renaud and Ambrose Jr. (2005), [3]Duineveld *et al.* (2001), [4]Etcheber *et al.* (1999), [5]Rowe, Morse, *et al.* (2008).

Canyon	**Geographic location**	**Location**		**Water depth (m)**	**SCOC**	**Ref.**
		°N	°W			
Lacaze-Duthiers Canyon	Gulf of Lions continental margin, Mediterranean Sea	42.29	-3.30	330	0.84–2.05	1
		42.26	-3.42	785	0.72–2.41	
		42.28	-3.30	912	1.69–6.02	
Barrow Canyon	Western Arctic Ocean	72.05	-154.07	1,136	2.99	2
Whittard Canyon	Celtic continental margin, NE Atlantic	48.13	-10.44	3760	1.3	3
		47.41	-10.26	4375	0.6	
Cap-Ferret Canyon	Aquitanian margin, Bay of Biscay, NE Atlantic	44.85	-2.14	445	0.28	4
		44.61	-2.08	720	0.22	
		44.61	-2.05	555	0.31	
		44.83	-2.20	490	0.21	
		44.82	-2.19	875	0.21	
		44.75	-2.16	950	0.20	
		44.75	-2.14	515	0.26	
		44.64	-2.14	513	0.23	
		44.60	-2.22	710	0.22	
		44.80	-2.17	1,400	0.22–0.28	
		44.81	-2.17	110	0.25–0.25	
		44.67	-2.11	1,415	0.21–0.32	
		44.82	-2.17	1,050	0.30	
		44.67	-2.13	1,170	0.33	
		44.63	-2.28	1,015	0.32	
		44.65	-2.10	1,670	0.34	
		44.73	-2.21	1,750	0.21	
		44.59	-2.51	1,975	0.20	
		44.79	-2.38	1,930	0.17	
		44.74	-2.29	2,300	0.21	
		44.73	-2.29	2,300	0.21	
		44.75	-2.63	2,985	0.26	
Mississippi Canyon	Gulf of Mexico	28.1	89.9	460–500	3.58±1.48	5
		28.0	89.7	900–1,000	3.56±1.27	
		27.0	88.1	2750	2.09	

Chapter 10 : General discussion

10. General discussion

The abyss is the largest ecosystem on Earth and extends over 85% of the seafloor (Harris et al., 2014). The Clarion Clipperton Fracture Zone (CCZ) in the central Pacific (0°N, 160°W to 23.5°N, 115°W; International Seabed Authority, 2011) covers ~11,921,826 km^2 of the ocean floor which corresponds to 3.89% of the total abyss on our planet (306,595,900 km^2 area, Harris *et al.*, 2014).

Using the global biomass predictions from **Chapter 2**, I estimated that meiofauna in the CCZ has a total biomass of 6.44×10^{-5} Pg C which corresponds to 3.68×10^{-5}% of the estimated global abyssal meiofaunal biomass (Table 2-3, **Chapter 2**). Total estimated macrofaunal biomass in the CCZ amounts to 1.02×10^{-4} Pg C (7.20×10^{-5}% of the estimated global abyssal macrofauna) and the estimated megafaunal biomass in the CCZ is 2.29×10^{-5} Pg C (7.20×10^{-5}% of the global abyssal megafauna) (Table 2-3, **Chapter 2**).

Benthic prokaryotes and fauna in the CCZ (Figure 1-1) are estimated to respire 4.98×10^{-7} Pg C yr^{-1}, which corresponds to 0.21% of the estimated global benthic respiration in abyssal plains (Table 10-1). Prokaryotes form the benthic size class in the CCZ that contributes most to the size-specific global abyssal plain respiration (0.31%), whereas benthic invertebrate megafauna contributes only 5.03×10^{-12}% to the global abyssal plain megafaunal respiration (Table 10-1).

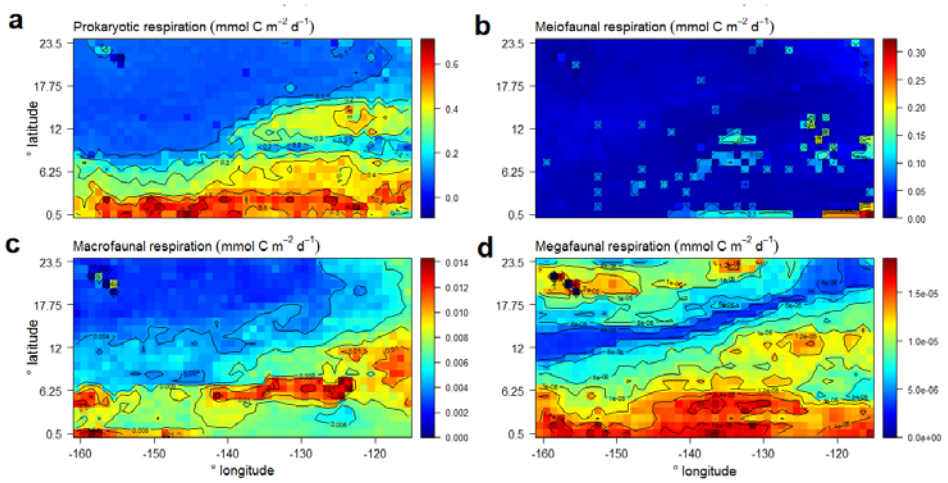

Figure 10-1. Benthic respiration (mmol C m^{-2} d^{-1}) of (a) prokaryotes, (b) meiofauna, (c) macrofauna, and (d) invertebrate megafauna in the Clarion Clipperton Fracture Zone. Note the differences in scales among panels.
Data source: This figure is based on data from section 2.4.4 and Figure 2-2 in **Chapter 2**.

Furthermore, the CCZ accounts for 1.13% of the global benthic secondary production of fauna in abyssal plains and for 1.07% of the global ingestion rate of benthic fauna in abyssal plains (Table 10-1). Whereas I estimated that benthic invertebrate megafauna in the CCZ contributes only 1.57×10^{-6}% to the global benthic invertebrate megafaunal ingestion in abyssal plains, benthic meiofauna in

the CCZ ingest 0.75% of all the C that is ingested by benthic meiofauna in abyssal plains.

Table 10-1. Estimated benthic prokaryotic and faunal respiration rates, faunal secondary production, and faunal ingestion in the CCZ (0°N, 160°W to 23.5°N, 115°W; 11,921,826 km^2) in proportion to the estimates for the global continental rise/ abyssal plains. Data are presented as mean±SE (median); area integrated C flows are calculated based on **Chapter 2**, section 2.3.5. "Prop." refers to the proportional contribution of the CCZ to the global continental rise/ abyssal plains based on area integrated estimates.

Benthos type	Continental rise/ abyssal plains* (mmol C m^{-2} d^{-1})	(Pg C)	Clarion Clipperton Fracture Zone⁂ (mmol C m^{-2} d^{-1})	(Pg C yr^{-1})	Prop. (%)
Respiration rate					
PRO	$0.51\pm3.29\times10^{-3}$ (0.34)	0.46	$0.22\pm4.98\times10^{-3}$ (0.13)	6.79×10^{-3}	0.31
MEI	$8.84\times10^{-2}\pm6.81\times10^{-4}$ (5.79×10^{-2})	7.88×10^{-2}	$2.67\times10^{-2}\pm9.87\times10^{-4}$ (1.72×10^{-2})	8.98×10^{-4}	7.08×10^{-3}
MAC	$4.79\times10^{-2}\pm4.20\times10^{-4}$ (1.34×10^{-2})	1.82×10^{-2}	$5.69\times10^{-3}\pm8.16\times10^{-5}$ (5.04×10^{-3})	2.63×10^{-4}	4.79×10^{-4}
MEG	$1.17\times10^{-7}\pm3.52\times10^{-9}$ (7.43×10^{-8})	1.01×10^{-7}	$9.67\times10^{-6}\pm1.11\times10^{-7}$ (9.53×10^{-6})	4.98×10^{-7}	5.03×10^{-12}
Total benthos		0.56		1.16×10^{-3}	0.21
Secondary production					
MEI	$0.16\pm1.24\times10^{-3}$ (0.10)	0.14	$4.63\times10^{-2}\pm1.71\times10^{-3}$ (2.98×10^{-2})	1.56×10^{-3}	2.18×10^{-2}
MAC	$1.18\times10^{-2}\pm1.71\times10^{-4}$ (3.03×10^{-3})	4.12×10^{-3}	$1.27\times10^{-3}\pm1.80\times10^{-5}$ (1.14×10^{-3})	5.95×10^{-5}	2.45×10^{-5}
MEG	$5.88\times10^{-4}\pm7.75\times10^{-6}$ (3.59×10^{-4})	4.89×10^{-4}	$2.45\times10^{-4}\pm2.82\times10^{-6}$ (2.41×10^{-4})	1.26×10^{-5}	6.15×10^{-7}
Total benthic fauna		0.14		1.63×10^{-3}	1.13

Table 10-1 continued.

Benthos type	Continental rise/ abyssal plains* (mmol C m^{-2} d^{-1})	(Pg C)	Clarion Clipperton Fracture Zone‡ (mmol C m^{-2} d^{-1})	(Pg C yr^{-1})	Prop. (%)
Ingestion rate					
MEI	0.98±9.20×10^{-3} (0.62)	0.85	0.27±0.01 (0.17)	8.88×10^{-3}	0.75
MAC	8.42×10^{-2}±9.57×10^{-4} (1.96×10^{-2})	2.67×10^{-2}	9.67×10^{-3}±1.37×10^{-4} (8.62×10^{-3})	4.50×10^{-4}	1.20×10^{-3}
MEG	8.96×10^{-4}±8.04×10^{-6} (5.74×10^{-4})	7.81×10^{-4}	3.92×10^{-4}±4.51×10^{-6} (3.86×10^{-4})	2.02×10^{-5}	1.57×10^{-6}
Total benthic fauna		0.88		9.35×10^{-3}	1.07

*Data sources: Tables 2-4 to 2-6 from **Chapter 2**. ‡Data on respiration, secondary production, and ingestion were extracted from the corresponding maps (e.g., Figure 10-1) for the specific area of the Clarion Clipperton Fracture Zone (0°N, 160°W to 23.5°N, 115°W).

This CCZ that contributes <5% to the global abyssal plain C cycle is a target area for deep-sea mining. The extraction of polymetallic nodules will lead to the removal of important hard substrate (Purser *et al.*, 2016; Vanreusel *et al.*,

2016; **Chapter 3**). Surface sediment will be removed (K. Murphy *et al.*, 2016) and the sediment in nodule collector tracks and their surroundings will be restructured and compacted (Miljutin *et al.*, 2011). Sediment plumes (Rolinski, Segschneider and Sündermann, 2001; K. Murphy *et al.*, 2016) and potentially gravity currents (L. Thomsen, Jacobs University Bremen, Germany, and J. Marsh, Environmental Tracing, UK, personal communication) will be created whose sediment particles resettle on large areas (K. Murphy *et al.*, 2016) and blanket fauna. Additionally, toxic metals might be released (Koschinsky, Borowski and Halbach, 2003).

Here, I address the environmental impacts that were investigated in the PhD thesis (Figure 10-2) and discuss how the ecosystem might respond to them. To conclude each section, I attempt to answer deep-sea mining related research questions that were presented in section 1.7 (**Chapter 1**). Subsequently, I integrate schematically all information about which food-web compartments were affected by the small-scale sediment disturbance experiment DISCOL and whether the specific compartments were able to recover (Figure 10-3). I also assess how valid the use of analogues is to predict the impact of deep-sea mining and I compare the DISCOL experiment with future industrial mining of polymetallic nodules in the CCZ. Finally, I view polymetallic nodule extraction in the global mining context and compare the environmental impacts of land-based mining with polymetallic nodule extraction in the deep sea.

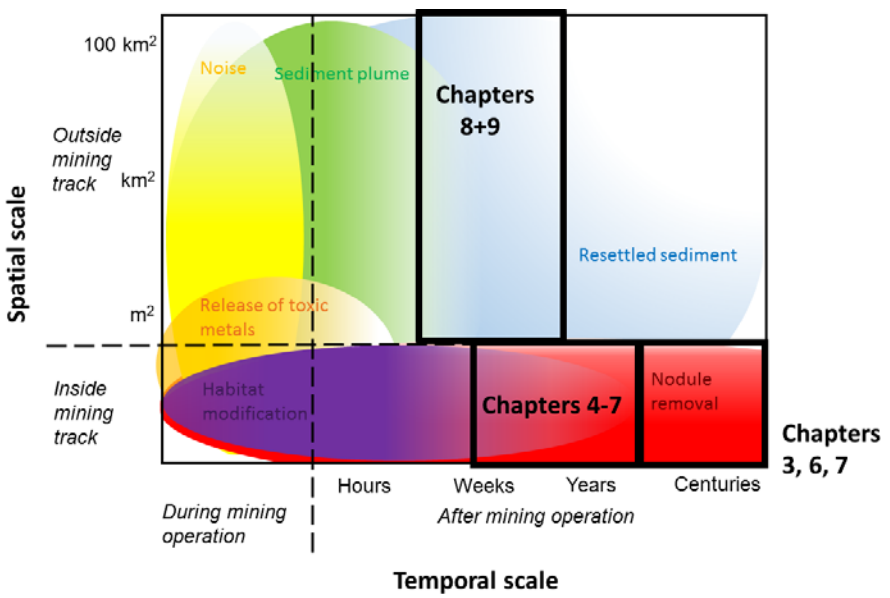

Figure 10-2. Temporal and spatial scale of environmental impacts of polymetallic nodule extraction and indication which impacts were investigated in the different chapters of this PhD thesis.

10.1 Benthic ecosystem response to the removal of polymetallic nodules

Polymetallic nodules provide an essential hard substrate in abyssal plains of the Pacific and Indian Ocean. Results in **Chapter 3** indicate that 22 sessile meiobenthic and megabenthic taxa (11% of all network compartments) in the Peru Basin and 46 sessile macrobenthic and megabenthic taxa (10% of all compartments) in the CCZ are obligatorily dependent on nodules as hard substrate. Further 21 (Peru Basin) and 43 (CCZ) taxa are facultatively dependent on nodules, but they also live in or on soft sediment. Most of the obligatory dependent taxa are filter feeders (71% in the Peru Basin, 51% in the CCZ) or detritivores and bacterivores (24% in the Peru Basin, 44% in the CCZ) and predominantly belong to the phyla Porifera, Cnidaria, and Foraminifera (including monothalamid Foraminifera). In particular stalked Porifera, such as *Caulophacus* sp., *Chondrocladia* sp., *Hyalostylus* sp., *Hyalonema* sp., *Staurocalyptus* sp., or *Bathyxiphus* sp., are so-called "structural species" (*sensu* Huston, 1994) and provide habitat for a high diversity of commensal fauna like e.g., Actiniaria, Alcyonacea, Cirripedia, Comatulida, *Freyella* sp., *Munidopsis* sp., *Ophiura* sp., or Phlebobranchia (**Chapter 3**).

Chapter 3 estimated that the absence of polymetallic nodules leads to the loss of 20% (CCZ) to 26% (Peru Basin) of all network compartments and 20 to 37% of all network links. As a result, 64% of the exclusively filter feeding, 55% of the exclusively bacterivores, and 50% exclusively scavenging fauna are expected to be lost in the Peru Basin when nodules are missing. In the CCZ, >50% of the filter feeders and >50% of the detritivores/ bacterivores are likely missing when nodules are absent.

Removal of polymetallic nodules does not only lead to reduced biodiversity, but it also results in a loss of benthic biomass. In **Chapter 6** we showed that removing polymetallic nodules from the sediment surface by ploughing them into the sediment caused a loss of 75% of the biomass 0.1 yr after the DISCOL experiment was conducted in 1989. In particular macro- and megafaunal filter and suspension feeders had a 0.64 mmol C m^{-2} lower biomass inside plough tracks compared to outside plough tracks (Stratmann, Lins, *et al.*, 2018/ **Chapter 6**). Even 26 yr later, we observed a 42% lower biomass of filter and suspension feeders inside plough tracks compared to outside the tracks (**Chapter 7**). As polymetallic nodules grow extremely slowly (1–250 mm Myr^{-1}; von Stackelberg, 2000; Petersen *et al.*, 2016), sessile filter and suspension feeders that are obligatory attached to nodules will never return to pre-mining diversities, densities, and biomasses after the nodules are removed. This has also consequences for benthic carbon cycling as **Chapter 6** models a 99% lower respiration rate of filter and suspension feeders inside plough tracks 0.1 yr after the DISCOL disturbance experiment compared to outside the tracks. Even 26 yr after the nodules were ploughed into the sediment, the respiration rate of filter and suspension feeders is 71% to 80% lower inside plough tracks compared to outside plough tracks.

What have we learned? – Nodule removal

- *Would the extraction of polymetallic nodules impact trophic and/ or non-trophic interactions among species?* Yes.
- *How would the number of network compartments, number of links, link density, and web connectance be affected?* The number of network compartments, number of links, and link density would decrease, whereas web connectance would increase.
- *Do faunal biomass […] of the food webs vary and/ or has the difference between the two sites converged over time?* The biomass of filter and suspension feeders remains depressed for at least 26 yr after nodules were ploughed into the sediment. As a result, also their respiration rates are lower inside plough tracks where the nodules are absent compared to outside the tracks where nodules are present.
- *How do the model outcomes [for nodule-dependent fauna] compare with conceptual model predictions on benthic community recovery from polymetallic nodule mining published by Jumars (1981)?* Jumars (1981) predicted that nodule-dependent fauna will not recover from nodule removal for more than 10,000 yr. Though we lack data on nodule absence for 10,000 yr, our results show that the absence of nodules impedes filter and suspension feeding fauna to recover in biomass and respiration rates within 26 yr.

10.2 Benthic ecosystem response to sediment removal

Current scenarios for future industrial deep-sea mining indicate that the extraction of polymetallic nodule by a hydraulic collector will remove the upper 15 cm of surface sediment inside the collector track (K. Murphy *et al.*, 2016). In the CCZ this surface sediment, however, has the highest total organic carbon content that decreases with depth in the upper 30 cm of sediment (Volz *et al.*, 2018). Hence, deposit feeders are likely most affected by sediment removal. In **Chapter 4**, we assessed holothurian recovery over time and found that holothurians in the DISCOL experimental area required 3 yr for a partial recolonization of the area instead of 1 year, a time span that was calculated based on holothurian movement activity alone. We related this retarded recolonization to unfavorable food conditions inside the plough tracks (Stratmann, Voorsmit, *et al.*, 2018) and in fact, even 26 yr after the disturbance experiment in the Peru Basin, results from **Chapter 7** indicate that, on average, phytodetritus (=labile detritus) and bioavailable carbon contents (= semi-labile detritus) are lower inside plough tracks compared to outside plough tracks.

The presence of holothurians has an impact on the quality of food that is available for other benthic fauna: In **Chapter 5**, a non-linear regression analysis of individual biomass vs. biomass-specific phytodetritus carbon incorporation for nematodes, macrofauna, and holothurians is highly significant implying that larger organisms in the deep sea might be more efficient in exploiting labile phytodetritus than smaller organisms (Stratmann, Mevenkamp, *et al.*, 2018/ **Chapter 5**). Smaller size classes, however, dominate in the abyss (Rex *et al.*,

2006) because 52% to 64% of the carbon input to the Peru Basin is estimated to consist of refractory detritus as modelled by the food-web models in **Chapter 7**.

Holothurians are additionally important for sediment reworking: Based on an individual gut throughput time of (mean±SD) 23.6±2.36 h for the deep-sea holothurian species *Stichopus tremulus* (Hudson, Wigham and Tyler, 2004), a mean gut content of 2.79±2.99 g DW sediment for 25 holothurian specimens collected in the Peru Basin (Table 10-2), and a mean holothurian density in the Peru Basin of 241±51 ind. ha^{-1} (reference sites, Stratmann, Voorsmit, *et al.*, 2018/ **Chapter 4**), it can be estimated that holothurians in the Peru Basin consume 249.8 kg DW sediment ha^{-1} yr^{-1}. This corresponds to 1,249,103 cm^3 wet sediment yr^{-1} (1 ml wet sediment from the Peru Basin: 0.20±0.03 g dry sediment, n =14; Stratmann, unpublished) or the 0–1 cm sediment layer on an area of 124.9 m^2 yr^{-1}. Hence, the holothurian population in the Peru Basin reworks the upper centimeter of 125 m^2 of sediment per 10,000 m^2 per year.

Table 10-2. Dry weight (in g) of gut content or feces of eleven Holothuroidea species collected during RV *Sonne* SO242-2 in the Peru Basin (Stratmann, unpublished). *n* corresponds to the number of specimens. Data are presented as mean±SE.

Species	***n***	**Gut content or feces (in g DW)**
Achlyoinice sp.	1	0.88
Amperima sp.	5	0.27±0.17
Benthodytes sp.	5	2.64±1.26
Benthodytes typica	6	2.35±1.01
Galatheathuria sp.	1	0.51
Oneirophanta sp.	1	3.90
Peniagone sp. (benthic)	1	0.11
Peniagone sp. (benthopelagic)	1	0.45
Psychropodes longicauda	1	1.08
Psychropodes semperima	1	1.78
Psychronaetes hanseni	2	9.63±2.88

This reworking of sediment might facilitate meiofauna to recolonize areas with compacted sediment, as sediment compaction and change in granulometric composition of sediment seems to be more important for meiofaunal recovery than carbon content in the sediment. Miljutin *et al.* (2011), e.g., observed that 26 yr after a dredging track was created in the French claim of the CCZ, the 0–0.5 cm sediment layer was denser inside the track than in the surrounding sediment. The authors hypothesized that this compactness might explain the significantly decreased nematode density and biomass inside the dredging track. Hence, removal of sediment triggers a downward spiral as a slow recolonization of the area by holothurians may subsequently lead to a reduced recovery of other fauna due to sediment compaction and low bioturbation inside plough tracks.

Global predictions in **Chapter 2** show that prokaryotes in abyssal plain sediments respire $0.51±3.29×10^{-3}$ mmol C m^{-2} d^{-1} and modeling results from **Chapter 7** estimate that the microbial loop contributes 62% to the total carbon throughput *T*... Hence, an impaired microbial loop inside plough tracks in the

DISCOL experimental area leads to a significantly reduced benthic respiration compared to reference sites (**Chapter 7**). Also the reduced processing of phytodetritus carbon in **Chapter 5** can be linked to decreased bacterial uptake of fresh phytodetritus carbon inside plough tracks.

This impaired microbial loop and the associated reduced processing of phytodetritus in the plough tracks (Stratmann, Mevenkamp, *et al.*, 2018/ **Chapter 4**; **Chapter 7**) might be related to compacted subsurface sediment in the plough tracks that might host a different microbial community compared to the original surface sediment community at reference sites. In fact, in the CCZ the microbial community composition changes with the sediment horizon (Shulse *et al.*, 2017) and if this change in community composition is associated with an alternation in prokaryotic heterotrophic productivity (Luna *et al.*, 2013), the microbial loop will be reduced. Additionally, increased heavy metal concentrations of deposited sediment in the plough tracks (Paul *et al.*, 2018) might impede the recolonization of the sediment by sediment surface bacteria if they have no tolerance for these metals or the metal concentrations are too high.

However, the diminished prokaryotic remineralization of organic matter will have no effect on a global scale as estimates of prokaryotic respiration at the begin of **Chapter 10** (Table 10-1) show that the total CCZ contributes only 0.31% to the global prokaryotic respiration in abyssal plains. Therefore, the deep sea will not turn into a sink for carbon if deep-sea mining starts.

What have we learned? – Sediment removal

- *Do the Holothuroidea assemblages differ inside plough tracks, outside plough tracks, and in reference areas?* The Holothuroidea assemblages did not differ among sites and the similarity in species composition was driven by *Benthodytes typica*, *Amperima* sp., and the group of unknown Holothuroidea.
- *Have Holothuroidea population densities recovered after 26 yr?* Yes.
- *Do Holothuroidea respiration rates differ between sites?* No.
- *Has ecosystem functioning in the form of carbon uptake and partitioning recovered 26 yr after a disturbance event?* The total phytodetritus uptake by bacteria, nematodes, and holothurians differs between the treatment “inside plough tracks with holothurians” and the treatment “reference sites with holothurians”.
- *Do faunal biomass and trophic composition of the food webs vary and/ or has the difference between the two sites converged over time?* Polychaete subsurface deposit feeders have a strongly reduced carbon stock directly after the DISCOL experiment, but their carbon stock recovered logarithmically over time. Twenty-six years after the disturbance experiment, deposit feeders have the least affected feeding type.
- *How do the model outcomes compare with conceptual model predictions on benthic community recovery from polymetallic nodule mining published by Jumars (1981)?* Jumars' (1981) predicted that subsurface sediment feeders inside mining tracks would have high mortalities. Our re-

sults show that the experiment had indeed a strong effect on the carbon stock.

- *Is total carbon cycling different between reference sites, outside plough tracks, and inside plough tracks?* Total carbon cycling is different between reference sites and inside plough tracks as well as between outside and inside plough tracks. In contrast, carbon cycling does not differ between reference sites and outside plough tracks.

10.3 Benthic ecosystem response to sediment suspension and settlement

Current scenarios for industrial deep-sea mining operations indicate that >450 t sediment h^{-1} could be discharged by the collector at the seafloor (K. Murphy *et al.*, 2016). This will create sediment plumes with particle concentrations between estimated 0.1 mg L^{-1} to 50 mg L^{-1}, whereupon the highest particle concentrations will likely not disperse very far and stay in the vicinity of the collector. In comparison, during dense shelf water cascading (DSWC) events in the Cap de Creus (Gulf of Lions) in Winter 2007 increased suspended particle concentrations of 6.4 mg L^{-1} to 5.7 mg L^{-1} were measured (Ribó *et al.*, 2011). The bottom nepheloid layer (BNL), which formed during DSWC events in 1999 and 2005/ 2006, had suspended particle concentrations of 0.08 mg L^{-1} (Puig *et al.*, 2013). Hence, DSWC could be used as a deep-sea mining analogue to assess how the benthic ecosystem responds to sediment suspension.

Modeling results in **Chapter 9** indicate that directly after the DSWC event the total system throughput *T*.., i.e., the total carbon that is processed in the food web, in the Cap de Creus upper canyon section was reduced (2.75±0.56 mmol C m^{-2} d^{-1}). Half a year later, *T*.. was three times higher (10.5±1.44 mmol C m^{-2} d^{-1}) indicating a recovery of the benthic ecosystem from the effect of the DSWC. Especially nematodes had a more than one order of magnitude higher C stock (4.53 mmol C m^{-2}) compared to directly after the cascading event (0.20 mmol C m^{-2}). We hypothesized in **Chapter 9** that meiofauna is suspended when the canyon seafloor and flanks are eroded during DSWC events (Puig *et al.*, 2013). This suspended meiofauna might subsequently settle on larger particle aggregates (size: 1 mm) in the BNL, before they are passively transported back to shore. There, they could colonize again the partly defaunated canyon sections. Even if meiofauna do not settle on the particles in the BNL or never reach this layer, DSWC leads to an increased passive dispersal over longer distances. In comparison, nematodes might migrate actively only a few millimeter per day: In **Chapter 8**, nematodes migrated 3 cm vertically in 16 days (3 DS treatment) (Mevenkamp, Stratmann, *et al.*, 2017). Hence, if nematodes survive being flushed by water jets, sucked into the collector and discharged again at the back of the collector, they could disperse passively with the sediment plume over larger distances. Lins *et al.* (2013) and Mevenkamp, Van Campenhout and Vanreusel (2016) investigated the selective settlement of deep-sea meiofauna onto different substrate types in *ex situ* experiments. Under no-flow conditions, nematodes and

harpacticoid copepods from white Beggiatoa mats at the Håkon Mosby mud volcano settled selectively on a sulfidic medium (Mevenkamp, Van Campenhout and Vanreusel, 2016). Also nematodes from the Whittard canyon (Bay of Biscay) settled selectively on different substrates and hereby showed genera-specific preferences (Lins *et al.*, 2013). Hence, meiofauna might selectively settle on areas with freshly re-deposited sediment: This sediment consists of the upper 15 cm of surface sediment from the collector tracks and contains higher particulate organic carbon than the subsurface sediment that is now exposed in the tracks (Paul *et al.*, 2018; Volz *et al.*, 2018). Even if the meiofauna does not settle selectively because current velocities are too high, they will still deposit passively (DePatra and Levin, 1989) like the particles in the sediment plume and again will settle on a loose layer of freshly deposited surface sediment. Compacted surface sediment, however, is not a good habitat: Miljutin *et al.* (2011) investigated the recovery of the deep-sea nematode assemblage in an experimental dredging track in the CCZ after 26 yr. They found that total nematode density and biomass were significantly lower than outside the track and related it to the higher compactness of the sediment inside the track compared to outside the track. Furthermore, the granulometry of the subsurface sediment which is the surface sediment inside the track might be different than the granulometry of the original surface sediment, but no data were available to test this hypothesis.

Though meiofauna dispersal capacities might be enhanced by the deep-sea mining induced sediment plume, blanketing of the abyssal bottom sediments by even a few millimeters of sediment will likely result in impaired ecosystem functioning: In **Chapter 8**, *ex situ* experiments with sediment cores taken at 200 m water depth in a Norwegian fjord show that the deposition of 0.1 cm of inert mine tailings caused a reduced sediment community oxygen consumption and reduced uptake rates of ^{13}C-enriched *Skeletonema costatum* by the sediment community (Mevenkamp, Stratmann, *et al.*, 2017). Within 11 d the deposition of 3 cm of dead sediment led to an increased oxygen consumption and subsequently anoxic conditions inside the natural sediment that were associated with increased nematode mortality (Mevenkamp, Stratmann, *et al.*, 2017). However, even if the seafloor is blanketed with several centimeters of sediment when the sediment plume settles, no anoxia is expected in the surface sediment as oxygen penetrates at 1 to 4.5 m into the sediment of the abyssal plains in the CCZ (Volz *et al.*, 2018).

What have we learned? – Sediment suspension and settlement

- *Does the exposure to burial with mine tailings alter the benthic community structure on the short term due to mortality and changes in vertical community distribution?* Yes.
- *Do changes in benthic community structure due to tailings disposal cause a reduced processing of organic matter as assessed from O_2 consumption, ^{13}C-labeled phytodetritus uptake and production of dissolved inorganic carbon?* Yes.

- *Is the response of benthic organisms to tailings different than to a deposition event with natural subsurface sediment?* Yes, mine tailing deposition caused food-limitation for the benthic community, whereas high microbial respiration in the dead sediment layer led to oxygen limitation in the subsurface sediment.
- *How does the food web in the Cap de Creus canyon react to the major DSWC event in winter 2005?* Food web models indicated that amount of carbon that is processed in the food web (*T.*.) was strongly reduced directly after the DSWC event compared to 0.5 yr later. This recovery within 0.5 yr was mainly the result of an increased nematode stock which could be the consequence of fast recolonization due to passive dispersal of meiofauna.

10.4 How does the food web respond to sediment disturbance in the deep sea?

In the following Figure 10.3 all chapters related to the DISCOL experiment (**Chapters 4**, **5**, **6**, **7**) were integrated to assess how the food web responds to the sediment disturbance. For this purpose, community composition data (**Chapter 4**), data on processing of fresh phytodetritus (**Chapter 5**), biomasses and modelled respiration rates (results from PD_{26} in **Chapter 6**, **Chapter 7**) were treated equally. When the assessed parameters gave different levels of recovery for the same feeding type/ size class, the min–max range of recovery is presented together with the data source (chapter number).

Even though various scientific approaches were used in this PhD thesis to assess the ecosystem response to a small-scale sediment disturbance, the individual studies reveal comparable levels of recovery of individual food-web compartments as indicated by arrows in different shades of the same color. Only bacteria show opposite trends: The *in situ* uptake rates of fresh phytodetritus (**Chapter 5**) were compared with estimates of total carbon respiration (**Chapter 7**) for the treatments “reference sites” vs. “inside plough tracks”. A large discrepancy between the two approaches therefore indicates that labile phytodetritus is less important for the overall metabolic activity of prokaryotes than semi-labile or refractory detritus. This is not uncommon for the deep sea and has been described already by van Oevelen, Soetaert and Heip (2012) for the Porcupine Abyssal Plain (NE Atlantic).

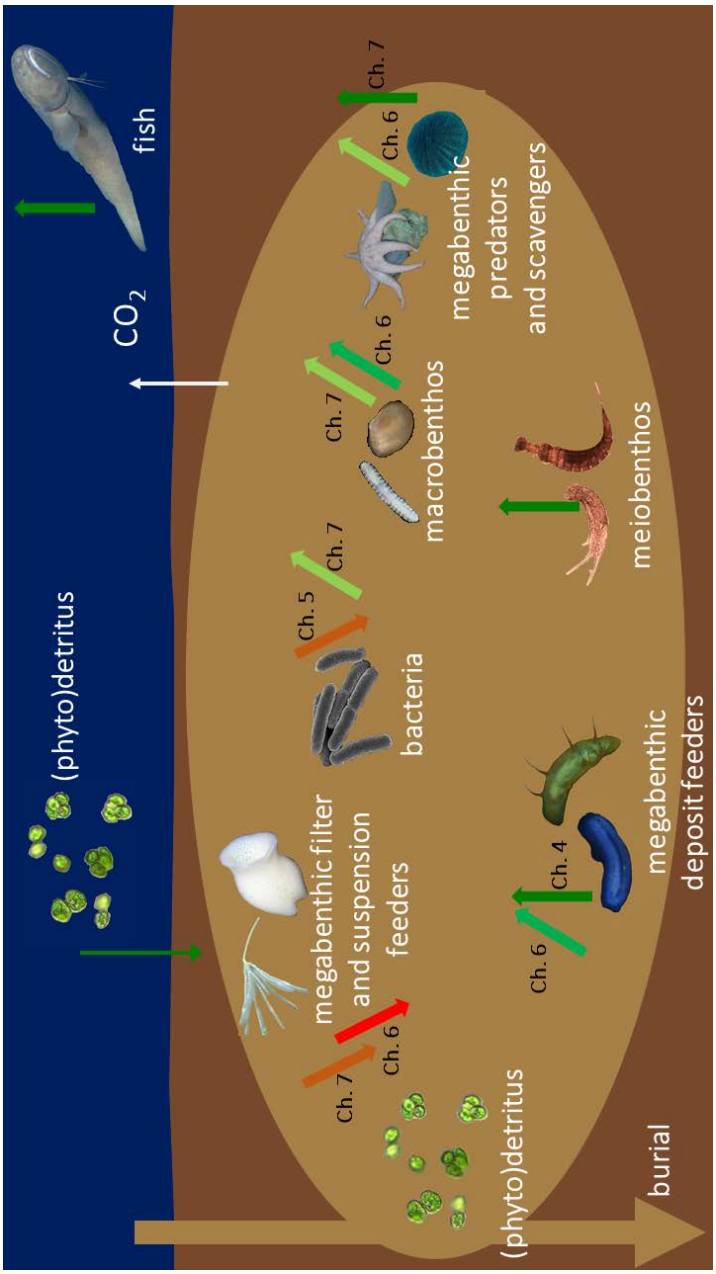

Figure 10-3. Modified schematic presentation of the deep-sea food web from **Chapter 1** to indicate if and how long food-web compartments/ size classes are affected by the sediment disturbance experiment DISCOL in the Peru Basin. When possible disturbed sites vs. reference sites were compared, when this was not possible due to a lack of data, disturbed vs. undisturbed sites were compared.
The color code and direction of arrows indicate the following: upwards directing **dark-green** arrow: complete (100%) recovery, upwards directing **green** arrow: 75–99% recovery, upwards directing **lime-green** arrow: 51–74% recovery, horizontal **yellow** arrow: 50% recovery, downwards directing **orange** arrow: 26–49% recovery, downwards directing **red** arrow: 1–25% recovery, downwards directing **purple** arrow: 0% recovery.

10.5 How valid are analogues to predict environmental impacts of deep-sea mining

Since the DISCOL experiment was conducted in February/ March 1989 (Thiel *et al.*, 1989), it has been used as an analogue for future deep-sea mining in the CCZ. The CCZ and the Peru Basin are, however, ~6,000 km apart (*Google Earth*, 2018) and belong to different trophic regimes: The CCZ belongs to the mesotrophic abyss (*sensu* Hannides and Smith, 2003) and experiences a POC input gradient from 1.3 mg C m^{-2} d^{-1} in the North to 1.8 mg C m^{-2} d^{-1} in the South (Vanreusel *et al.*, 2016) and from 1.5 mg C m^{-2} d^{-1} in the West to 2.0 mg C m^{-2} d^{-1} in the East (Volz *et al.*, 2018); sedimentation rates range from 0.2 to 1.15 cm kyr^{-1} (Volz *et al.*, 2018). The sediment consists of siliceous, silty clay (International Seabed Authority, 2010) and has an organic carbon content of 0.2 to 0.5 wt% at the sediment surface and <0.2 wt% below 30 cm (Volz *et al.*, 2018). Oxygen penetrates between 1 to 4.5 m into the sediment (Volz *et al.*, 2018). In comparison, the DISCOL experimental area (DEA) in the Peru Basin belongs to the eutrophic abyss and receives a POC flux of 2.16 to 3.96 mg C m^{-2} d^{-1} (Haeckel *et al.*, 2001); sedimentation rates are between 0.4 and 2 cm kyr^{-1} (Haeckel *et al.*, 2001). The sediment consists of a semi-liquid, dark brown surface layer (upper 5–15 cm) with an organic carbon content of 0.55±0.11 wt% and a grayish sub-surface clay layer with an organic carbon content of 0.70±0.08 wt% (Grupe, Becker and Oebius, 2001). The oxygen penetration depth ranges from 12 to >20 cm and increases from the eastern DEA to the western DEA (Paul *et al.*, 2018).

During future industrial scale mining operations in the CCZ, the hydraulic collector will extract the polymetallic nodules and remove the upper 15 cm of sediment leaving compacted subsurface sediment inside the collector track (K. Murphy *et al.*, 2016). About 90% of the extracted sediment will likely be discharged via the collector exhaust at the seafloor and create a sediment plume (K. Murphy *et al.*, 2016). Coarser sediment particles in the plume are expected to resettle within a month, whereas finer particles might remain in suspension for up to 7 yr (Rolinski, Segschneider and Sündermann, 2001). After one year of mining operation, the mined area is expected to be blanketed by more than 10 cm of sediment (K. Murphy *et al.*, 2016). Furthermore, a 10× larger area around the mined area will likely be covered by 0.1 to 1 mm of re-settled sediment (K. Murphy *et al.*, 2016). When the sediment particles have settled, more than 20 yr of sediment consolidation might be required until the sediment fabric has returned to pre-mining conditions (Becker *et al.*, 2001). Hence, within the first 20 yr after the mining operation has ceased, the nodule-free sediment inside collector tracks consists of compacted subsurface sediment with a 10 cm thick layer of re-settled coarser sediment and a layer of very fine re-settled sediment on top. Outside the collector tracks, the uncompacted sediment will be covered with a thin (0.1–1 cm) layer of loosely re-deposited sediment. In comparison, during the DISCOL experiment, nodules were not extracted, but ploughed into the sediment (Thiel *et al.*, 1989). Surface sediment inside the plough tracks was turned upside down (Figure 10-3) and more compacted subsurface sediment with a slightly lower sediment porosity (average porosity in the surface sediment at Reference South: 0.93, Reference

West: 0.94, DEA West plough track: 0.93, DEA East plow track: 0.91, DEA East white patch: 0.92; Paul *et al.*, 2018) was exposed at the sediment surface. Reduced solid phase manganese concentrations in the top 15 cm of disturbed sediment indicated that the top manganese-oxide rich layer was mixed or completely removed, like in the case of the white sediment patches (Paul *et al.*, 2018). Additionally, increased concentrations of manganese, molybdenum, nickel, cobalt, and iron, and higher porositities in the upper 2 to 4 cm sediment layer inside plough track valleys indicated that suspended sediment has loosely deposited on those tracks (Paul *et al.*, 2018).

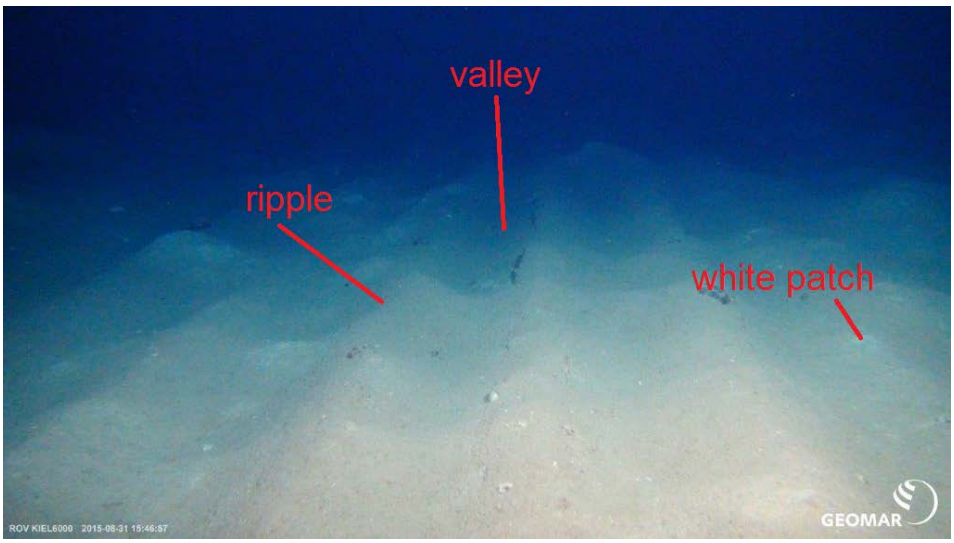

Figure 10-3: Disturbed seafloor in the DISCOL experimental area (Peru Basin, SE Pacific). Photo by ROV Kiel 6000 (GEOMAR, Kiel, Germany).

Hence, the DISCOL experiment can only be considered a valid analogue for deep-sea mining when the absence of polymetallic nodules is investigated. Furthermore, the effect of mining/ sediment disturbance should be scale-independent, as the DISCOL experimental area covers only 10.8 km (Thiel *et al.*, 1989), whereas a single mining operation is expected to mine an area between 300 km^2 to >1000 km^2 (Smith *et al.*, 2009).

10.6 Polymetallic nodule extraction in the global mining context

In the future, cobalt, nickel, and copper might be recovered from polymetallic nodules in the CCZ, but at present, these metals are extracted from land-based reserves. Cobalt is mostly recovered as by-product of nickel and copper ore mining (Hawkins, 1998) in open-pit extractions or underground extractions, or a combination of both (Hannis, Bide and Minks, 2009). During open-pit extraction, the overburden is removed, the ore is dug up or blasted with explosives and subsequently removed by trucks or conveyor belts (Hannis, Bide and Minks, 2009). Standard methods of underground extractions are “block caving” when the

deposits are large and uniform or "room-and-pillar-mining"[1] when the deposits are flat dipping (<30°) (Hannis, Bide and Minks, 2009). Cobalt can also be extracted from tailings of copper sulfide ore processing (Roberts and Gunn, 2014). For example, in the Kolwezi tailings project, the Eurasian Natural Resources Corporation (ENRC) planned to extract 70,000 t of copper and 10,000 t of cobalt per year from a tailings reserve of 1.7 Mt of copper (grade: 1.49%) and 363,000 t of cobalt (grade: 0.32%) in the Katanga Province (Democratic Republic of Congo) (Roberts and Gunn, 2014). In addition, stockpiles of slag that is produced during smelting of copper contain substantial amounts of cobalt (Roberts and Gunn, 2014). The Nkana slag dump on the Zambian Copperbelt, for example, contains 20 Mt of slag with a cobalt grade of 0.3% to 2.6% (Jones *et al.*, 2002).

Copper is recovered by open-pit extraction, underground extraction or *in situ* leaching (British Geological Survey, 2007). Open-pit extraction is the most common extraction method of copper ores (British Geological Survey, 2007) and the Bingham Canyon mine (Utah, USA) that is 4 km wide and 1 km deep is the largest anthropogenic excavation on Earth (Hibert, Ekström and Stark, 2014). Underground mining is used to extract small or deep ore bodies of higher ore grade, and when ore bodies are of low grade and lay deep in the underground, *in situ* leaching is applied (British Geological Survey, 2007). During this process, sulfuric acid leach solution is pumped via injection wells into the ore body to dissolve the copper (British Geological Survey, 2007). The copper solution is pumped up via recovery wells, the well system is cleaned with fresh-water and cemented afterwards (British Geological Survey, 2007).

Magmatic nickel sulfide deposits are mined either via underground extraction, open-pit extraction or a combination of the two extraction methods depending on the mine sizes, ore grade, and morphology (Bide *et al.*, 2008). However, when the nickel ore body lays less than 100 m underground, open-pit extraction is favored because it is more profitable than underground extraction (Bide *et al.*, 2008). In contrast, lateritic nickel ore deposits are mined in open-pit mines using strip mining, i.e., overburden is removed in the new strip, deposited in the extraction hole of the previous strip, and the nickel ore is extracted (Bide *et al.*, 2008).

[1] Room-and-pillar-mining: During "room-and-pillar-mining", the ore is extracted along roadways or "bords", while the ore between these bords act as pillars to hold the roof. Afterwards, the outer pillars are mined and as a result, the roof collapses controlled while the miners retreat to the exit. (Sherwood and Phillips, 2018).

Box 10.1: Environmental impacts of land-based cobalt and copper mining: The case of the Katanga's mines (Democratic Republic of Congo)

The former province of Katanga lays in the SE Democratic Republic of Congo (central Africa) and forms part of the 'Central African Copperbelt' (Figure 10-6). It experiences environmental damage due to copper and cobalt mining: The protected 'Basse Kando Reserve', for instance, is downsized (Edwards *et al.*, 2014) and its vegetation fragmented and altered (Dupin *et al.*, 2013).

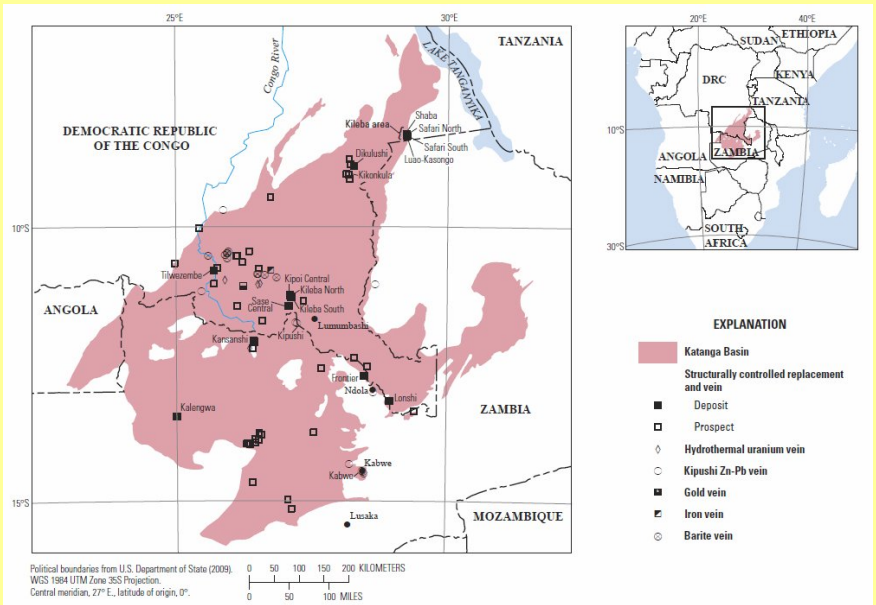

Figure 10-6. Map of the Katanga Basin in the Central African Copperbelt. Source: Taylor *et al.* (2010).

Untreated drainage water from waste tailings leachates of a hydrometallurgical plant and copper mine flow into the Lufira river system (Squadrone *et al.*, 2016). This river has been dammed and forms the artificial lake Tshangalele, whose fish population accumulates cobalt, copper, aluminum, iron, manganese, zinc and cadmium (Squadrone *et al.*, 2016). By eating only 100 g fish from the most contaminated site, the population that resides around the lake takes up more cobalt than the minimum risk dose level of 0.6 mg cobalt d^{-1} (Squadrone *et al.*, 2016).

Even in areas with abandoned copper and cobalt mines, sediments of rivers, such as the Tshamilemba Canal and the Lubumbashi River (both southern Katanga), can be "extremely severely enriched" in copper and cobalt: Narendrula, Nkongolo and Beckett (2012) showed that copper and cobalt concentrations in soils from Lubumbashi were 200 fold higher than in contaminated sites and tailings in Sudbury (Ontario, Canada) where e.g., nickel and copper have been produced. Especially NW of Gécamine's metal processing

site in Lubumbashi, atmospheric deposition of non-ferrous metal particles resulted in a higher habitat fragmentation and lower presence of vegetation (Vranken *et al.*, 2013).

Besides environmental impacts, cobalt and copper mining in Katanga has severely negative social impacts, especially for artisanal miners (see e.g., Tsurukawa, Prakash and Manhart, 2011).

Box 10.2: Environmental impacts of copper mining: The case of the El Salvador copper mine (Chile)

The Chilean copper mine El Salvador lays at 2,600 m height in the southern Andes at 26°15'33''S, 69°34'15''W (Figure 10-17; Castilla and Nealler, 1978).

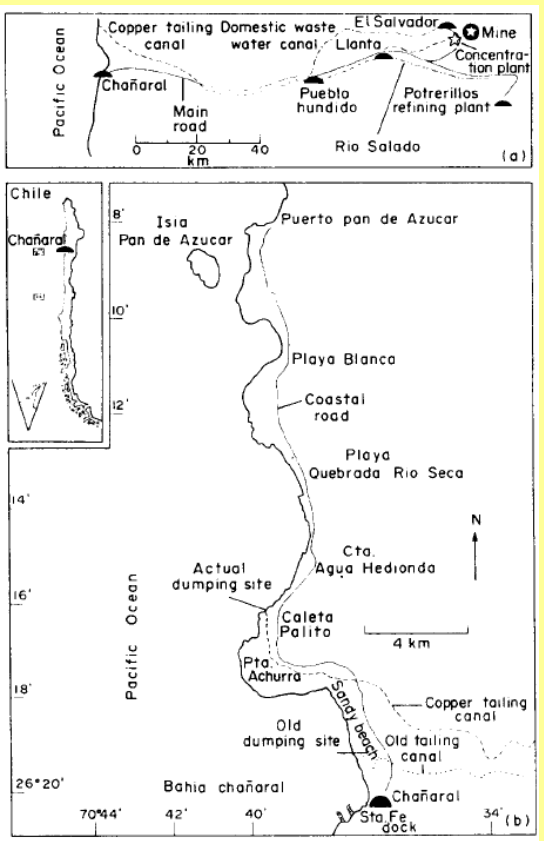

Figure 10-7. Map of the El Salvador copper mine and the location of the tailing canal in 1978. Source: Castilla and Nealler (1978).

From 1938 to 1974, 150 Mt untreated copper mining waste was discharged via a semi-artificial canal to Chañaral beach (Castilla and Nealler, 1978). In 1975, the dumping site was moved 8 km further north to Caleta Palito where from January 1975 to July 1976, alone, more than 13 Mt sedi-

ment were discharged (Castilla and Nealler, 1978). Days after the new dumping site was inaugurated (February 1975), locals observed high fish and mollusk mortalities and in July 1975 and July 1976 high mortalities of intertidal and subtidal fauna were observed (Castilla and Nealler, 1978). Furthermore, the water depth in the Caleta Palito area from the coast to 600 m offshore decreased from 10 m before the opening of the new dumping site to 5 m in July 1976 (Castilla and Nealler, 1978). From 1976 to 1989, additional 130 million t of untreated mine tailings were discharged and since 1990 tailings-free wastewater has been discharged at rates of 200 to 250 L s^{-1} (Andrade, Moffett and Correa, 2006). In 1994, the dissolved copper concentration at the mouth of the discharge canal was 2,390 to 2,410 µg L^{-1}, whereas 50 m away, the concentration was between 26.8 and 31.8 µg L^{-1} which was one order of magnitude higher than the copper concentration in seawater at the control site Caleta Zenteno, 68 km south of the dumping site (Castilla, 1996). Beach sediment was likewise highly contaminated (copper concentration in sediment of the Chañaral area: 7–1,985 µg g^{-1}, Ramirez *et al.*, 2005; copper concentration in uncontaminated sediment of the US east coast: 0–20 µg g^{-1}, Windom *et al.*, 1989).

Benthos in the Caleta Palito area, however, showed signs of recovery: Species richness increased from 6 species observed between 1976 and 1994 (Castilla, 1996), to 21 species observed between 1995 and 1999 (Correa *et al.*, 1999), and to 42 species recorded in 2003 (Medina *et al.*, 2005).

Box 10.3: Environmental impacts of nickel mining: Two cases of nickel treatment plants in New Caledonia

New Caledonia, an oversea territory of France located east of Australia in the S Pacific, hosts ~8% of the Earth's known nickel reserves (U.S. Geological Survey, 2017, 2018). During the last 20 yr two new large nickel-mining projects have been developed: the Koniambo project in the North Province (*province Nord*) and the Goro project in the South Province (*province Sud*) (Figure 10-21). The Koniambo project is owned by Xstrate (formerly: Falconbridge; 49%) and the North Province company Société Minière du Sud Pacifique (SMSP) (51%), whereas the Goro project is owned by Vale Inco (formerly Inco; 74%) Sumitomo and Mitsui (21%), and the New Caledonian provincial company Société de Participation Minière du Sud Calédonien (SPMSC; 5%) (Mudd, 2010).

The **Goro** mine contains 124.3 Mt nickel ore with an ore grade of 1.46% which is equivalent to 1,815 kt nickel (Mudd, 2010). The mine was expected to have an annual capacity of 60 kt nickel and 4.7 kt cobalt that would be processed in a metallurgical nickel processing plant using high-pressure acid leaching technology (HPAL) (Ali and Grewal, 2006; Moran, Petersone and Verones, 2016). Tailings produced during the nickel processing would be disposed in the Kwe Basin on land where a dam would be constructed to separate the tailings from the three rivers that converge in the Basin

(Ali and Grewal, 2006). In contrast, 35°C warm, potentially acidic effluent contaminated with chromium and manganese would flow directly into the Pacific Ocean (Ali and Grewal, 2006). Furthermore, atmospheric pollution from the nickel processing plant would affect the Forêt du Nord forest reserve (Ali and Grewal, 2006). The owner of the mine and processing plant promised to fight against erosion and biodiversity loss caused by nickel mining and processing by massive reforestation, but it was doubtful whether the promised efforts would be made (Ali and Grewal, 2006). Since its opening in 2010, there were five spills at the Goro processing plant until May 2014 when the processing plant was suspended after another spill with ~100 kL of effluent (Radio New Zealand, 2014). In December 2017, Vale Inco announced that it would abandon its Goro project in the second half of 2018 if the company did not find a strategic partner willing to purchase 20 to 40% of the project's stakes (Hume, 2017).

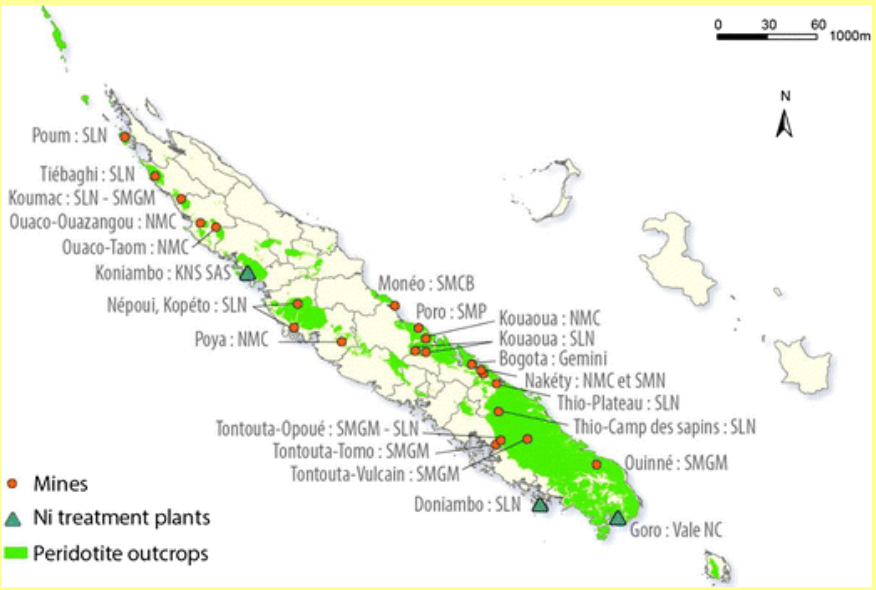

Figure 10-8. Map of nickel mines and nickel treatment plants on New Caledonia. Source: Losfeld *et al.* (2015).

The **Koniambo** Massif contained 132 to 150 Mt nickel ore with an ore grade of 2.46% resulting in up to 4 Mt nickel (Elias, 2002; Angleviel, 2003). This ore would be processed in the pyrometallurgical nickel processing plant at the coast that would have an annual processing capacity of 54 to 60 kt nickel (Angleviel, 2003; Horowitz, 2004). During nickel processing, nickel slag would be produced as waste which would be deposited on land before it would harden (Ali and Grewal, 2006). Additionally, there were plans to sell this nickel slag for the production of asphalt (Ali and Grewal, 2006). Pyrometallurgical processing would require a 180 to 250 MW coal-fueled power plant that would burn 1.5 times the amount of coal per year that the power plant at Goro consumed (Horowitz, 2004; Ali and Grewal, 2006). The emitted

sulfur dioxide emissions would be reduced by using 25.5 kt limestone per year, but nevertheless, the emissions would be likely higher than the emissions from the Goro plant (Ali and Grewal, 2006). Additionally, a dam on the Pouembout River would be built to provide 1 million L freshwater per year to cool the machines (Angleviel, 2003; Horowitz, 2004).

The coral reefs that surround New Caledonia would be impacted when a channel would be dredged to build a deep-water port and sediment input would cause increased turbidity (Angleviel, 2003; Chabanet *et al.*, 2010). The Koniambo project was also seen as an economic development project which would likely lead to demographic growth and consequently to increased fishing pressure (Chabanet *et al.*, 2010). Eventually, the project was inaugurated by the French President François Holland on November 17th 2014 (https://smsp.nc/en/historical/; accessed: June 4th 2018).

To reach a well-educated decision whether polymetallic nodules should be extracted from the deep sea in the future, the environmental impacts of deep-sea mining have to be weighted up against the environmental impacts of land-based mining. Based on Figure 10-9, the environmental impacts of land-based mining and polymetallic nodule extraction are qualitatively similar, but they might differ quantitatively in temporal and spatial scale. However, an important aspect that is often neglected in discussions about deep-sea mining is processing of polymetallic nodules. Nodules will be transported ashore where they will be processed to extract the metals, such as copper, cobalt, and nickel. The environmental impacts that are associated with these smelting and refining processes have to be taken into account when deciding about the future of deep-sea mining.

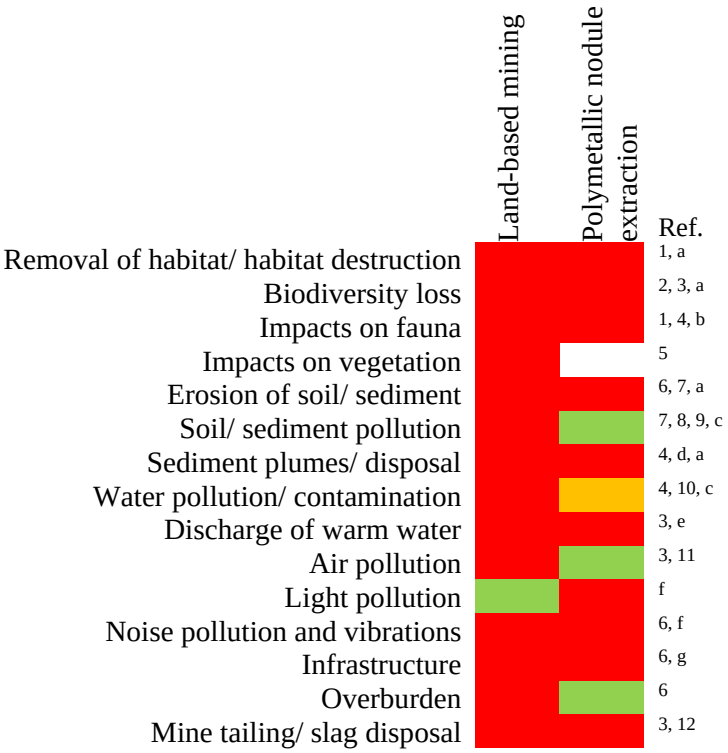

Figure 10-9. Qualitative comparison of environmental impacts of land-based mining of cobalt, copper, and nickel vs. the extraction of polymetallic nodules.
Color code: red = impact, yellow = maybe an impact, green = no impact, white = specific parameter does not exist.
References for land-based mining: [1]Cooke and Johnson (2002), [2]Edwards *et al.* (2014), [3]Ali and Grewal (2006), [4]Castilla and Nealler (1978), [5]Dudka and Adriano (1997), [6]Environmental Law Alliance Worldwide (2010), [7]Atibu *et al.* (2016), [8]Ramirez *et al.* (2005), [9]Dudka and Adriano (1997), [10]Squadrone *et al.* (2016), [11]Vranken *et al.* (2013), [12]Andrade, Moffett and Correa (2006).
References for polymetallic nodule extraction: [a]this PhD thesis, [b]Jumars (1981), [c]Koschinsky *et al.* (2001), [d]Murphy *et al.* (2016), [e]Steiner (2009), [f]Miller *et al.* (2018), [g]Hein *et al.* (2013).

10.7 Knowledge gaps about benthic ecosystem responses to polymetallic nodule extraction in the deep sea

This thesis shows that the deep-sea ecosystem in the Peru Basin has not recovered from a small-scale sediment disturbance experiment in the abyssal plains within 26 years. We still do not know how long the ecosystem recovery will actually take. We additionally lack knowledge about the potential recovery rates from future industrial-scale mining.

In all studies on deep-sea mining that were conducted within the framework of the EU-projects MIDAS (Managing Impacts of Deep-seA reSource exploitation) and MiningImpact (JPI Oceans – Ecological Aspects of Deep Sea Mining), only individual aspects, such as toxicity (Mevenkamp, Brown, *et al.*,

2017; Brown and Hauton, 2018), sediment plumes (Aleynik *et al.*, 2017), or nodule absence (**Chapter 3**) were considered. Although a wealth of new information has been gathered, we do not comprehend how the ecosystem will respond to them when they have cumulative effects. Furthermore, projections for 2091 to 2100 predict a decrease in carbon export flux of 5.2% (Jones *et al.*, 2014) and we have little knowledge on how benthos in the abyssal plains will react to deep-sea mining combined with climate change, including a decreased POC flux, increased water temperatures, and acidification.

In addition, we have not investigated the impact of sediment plumes on the deep-sea pelagic and benthic ecosystem and we lack an understanding about larval dispersal and (re-)colonization.

Cited literature

Aberle, N. and Witte, U. (2003) ‘Deep-sea macrofauna exposed to a simulated sedimentation event in the abyssal NE Atlantic: *In situ* pulse-chase experiments using ^{13}C-labelled phytodetritus’, *Marine Ecology Progress Series*, 251, pp. 37–47. doi: 10.3354/meps251037.

Accornero, A. *et al.* (2003) ‘Organic carbon budget at the sediment–water interface on the Gulf of Lions continental margin’, *Continental Shelf Research*, 23, pp. 79–92. doi: 10.1016/S0278-4343(02)00168-1.

Adiansyah, J. S. *et al.* (2015) ‘A framework for a sustainable approach to mine tailings management: Disposal strategies’, *Journal of Cleaner Production*, 108, pp. 1050–1062. doi: 10.1016/j.jclepro.2015.07.139.

Ahnert, A. and Schriever, G. (2001) ‘Response of abyssal copepoda Harpacticoida (Crustacea) and other meiobenthos to an artificial disturbance and its bearing on future mining for polymetallic nodules’, *Deep-Sea Research II*, 48, pp. 3779–3794. doi: 10.1016/S0967-0645(01)00067-4.

Albertelli, G. *et al.* (1999) ‘Differential responses of bacteria, meiofauna and macrofauna in a shelf area (Ligurian Sea , NW Mediterranean): Role of food availability’, *Journal of Sea Research*, 42, pp. 11–26.

Alexandrov, G. (2008) ‘Climate change 1: Short-term dynamics’, in Jorgensen, S. E. and Fath, B. (eds) *Encyclopedia of Ecology*. 1st edn. Amsterdam: Elsevier, pp. 588–592. doi: 10.1016/B978-008045405-4.00724-2.

Aleynik, D. *et al.* (2017) ‘Impact of remotely generated eddies on plume dispersion at abyssal mining sites in the Pacific’, *Scientific Reports*, 7, p. 16959. doi: 10.1038/s41598-017-16912-2.

Ali, M. H. and Salman, S. D. (1987) ‘Growth and production of the amphipod *Parhyale basrensis* (Talitridae) in the Shatt al-Arab region’, *Marine Ecology Progress Series*, 40, pp. 231–238. doi: 10.3354/meps040231.

Ali, S. H. and Grewal, A. S. (2006) ‘The ecology and economy of indigenous resistance: Divergent perspectives on mining in New Caledonia’, *The Contemporary Pacific*, 18, pp. 361–392.

Allaby, M. (2008a) ‘Particle size’, *Dictionary of Earth Sciences*. 3rd edn. Oxford University Press.

Allaby, M. (2008b) ‘Passive margin’, *Dictionary of Earth Sciences*. 3rd edn. Oxford University Press.

Allen, C. E., Tyler, P. A. and Varney, M. S. (2000) ‘Lipid profiles of *Nematocarcinus gracilis* a deep-sea shrimp from below the Arabian sea oxygen minimum zone’, *Hydrobiologia*, 440, pp. 273–279. doi: 10.1023/A:1004147900461.

Allen, J. . A. . and Morgan, R. E. . (1981) ‘The functional morphology of

Atlantic deep water species of the families Cuspidariidae and Poromyidae (Bivalvia): An analysis of the evolution of the septibranch condition', *Philosophical Transactions of the Royal Society of London B*, 294, pp. 413–546. doi: 10.1098/rstb.1981.0117.

Alongi, D. M. and Tenore, K. R. (1985) 'Effect of detritus supply on trophic relationships within experimental benthic food webs. I. Meiofauna-polychaete (*Capitella capitata* (Type I) Fabricius) interactions', *Journal of Experimental Marine Biology and Ecology*, 88, pp. 153–166. doi: 10.1016/0022-0981(85)90035-8.

Alt, C. H. S. *et al.* (2013) 'Trawled megafaunal invertebrate assemblages from bathyal depth of the Mid-Atlantic Ridge (48°-54°N)', *Deep-Sea Research Part II: Topical Studies in Oceanography*. Elsevier, 98, pp. 326–340. doi: 10.1016/j.dsr2.2013.02.003.

Amaro, T. *et al.* (2010) 'The trophic biology of the holothurian *Molpadia musculus*: Implications for organic matter cycling and ecosystem functioning in a deep submarine canyon', *Biogeosciences*, 7, pp. 2419–2432. doi: 10.5194/bg-7-2419-2010.

Ambrogi, R. (1990) 'Secondary production of *Prionospio caspersi* (Annelida: Polychaeta: Spionidae)', *Marine Biology*, 104, pp. 437–442.

Amon, D. J. *et al.* (2016) 'Insights into the abundance and diversity of abyssal megafauna in a polymetallic-nodule region in the eastern Clarion-Clipperton Zone', *Scientific Reports*, 6, p. 30492. doi: 10.1038/srep30492.

Amon, D. J., Ziegler, A. F., Drazen, J. C., *et al.* (2017) 'Megafauna of the UKSRL exploration contract area and eastern Clarion-Clipperton Zone in the Pacific Ocean: Annelida, Arthropoda, Bryozoa, Chordata, Ctenophora, Mollusca', *Biodiversity Data Journal*, 5, p. e14598. doi: 10.3897/BDJ.5.e14598.

Amon, D. J., Ziegler, A. F., Kremenetskaia, A., *et al.* (2017) 'Megafauna of the UKSRL exploration contract area and eastern Clarion-Clipperton Zone in the Pacific Ocean: Echinodermata', *Biodiversity Data Journal*, 5, p. e11794. doi: 10.3897/BDJ.5.e11794.

Amon, D. J., Hilário, A., *et al.* (2017) 'Observations of organic falls from the abyssal Clarion-Clipperton Zone in the tropical eastern Pacific Ocean', *Marine Biodiversity*, 47, pp. 311–321. doi: 10.1007/s12526-016-0572-4.

Anderson, M., Gorley, R. N. and Clarke, K. R. (2008) *Permanova+ for Primer: Guide to software and statistical methods*. Plymouth: PRIMER-E Ltd.

Andersson, J. H. *et al.* (2004) 'Respiration patterns in the deep ocean', *Geophysical Research Letters*, 31, p. L03304. doi: 10.1029/2003GL018756.

Andrade, S., Moffett, J. and Correa, J. A. (2006) 'Distribution of dissolved species and suspended particulate copper in an intertidal ecosystem affected by

copper mine tailings in Northern Chile', *Marine Chemistry*, 101, pp. 203–212. doi: 10.1016/j.marchem.2006.03.002.

Angleviel, F. (2003) 'Restoring the economic balance: The nickel stakes in New Caledonia', *The New Pacific Review*, 2, pp. 155–167.

Ansell, A. D. (1973) 'Oxygen consumption by the bivalve *Donax vittatus* (da Costa)', *Journal of Experimental Marine Biology and Ecology*, 11, pp. 311–328.

Arifin, Z. and Bendell-Young, L. I. (1997) 'Feeding response and carbon assimilation by the blue mussel *Mytilus trossulus* exposed to environmentally relevant seston matrices', *Marine Ecology Progress Series*, 160, pp. 241–253.

Arístegui, J. *et al.* (2009) 'Microbial oceanography of the dark ocean's pelagic realm', *Limnology and Oceanography*, 54, pp. 1501–1529. doi: 10.4319/lo.2009.54.5.1501.

Armstrong, C. W. *et al.* (2012) 'Services from the deep: Steps towards valuation of deep sea goods and services', *Ecosystem Services*, 2, pp. 2–13. doi: 10.1016/j.ecoser.2012.07.001.

Arndt, S. *et al.* (2013) 'Quantifying the degradation of organic matter in marine sediments: A review and synthesis', *Earth-Science Reviews*, 123, pp. 53–86. doi: 10.1016/j.earscirev.2013.02.008.

Arntz, W. E. *et al.* (1987) 'Changes in the structure of a shallow sandy-beach community in Peru during an El Niño event', *South African Journal of Marine Science*, 5, pp. 645–658. doi: 10.2989/025776187784522504.

Asmus, H. (1984) *Freilanduntersuchungen zur Sekundärproduktion und Respiration benthischer Gemeinschaften im Wattenmeer der Nordsee*. List/ Sylt. doi: 10.3289/IFM_BER_122.

Asmus, H. (1987) 'Secondary production of an intertidal mussel bed community related to its storage and turnover compartments', *Marine Ecology Progress Series*, 39, pp. 251–266. doi: 10.3354/meps039251.

Astall, C. M. and Jones, M. B. (1991) 'Respiration and biometry in the sea cucumber *Holothuria forskali*', *Journal of the Marine Biological Association of the UK*, 71, pp. 73–81. doi: 10.1017/S0025315400037401.

Atibu, E. K. *et al.* (2016) 'Assessment of trace metal and rare earth elements contamination in rivers around abandoned and active mine areas. The case of Lubumbashi River and Tshamilemba Canal, Katanga, Democratic Republic of the Congo', *Chemie der Erde - Geochemistry*, 76, pp. 353–362. doi: 10.1016/j.chemer.2016.08.004.

Bachelet, G. (1982) 'Quelques problèmes liés à l'estimation de la production secondaire. Cas des bivalves *Macoma balthica* et *Scrobicularia plana*',

Oceanologica Acta, 5, pp. 421–431.

Bachelet, G. and Yacine-Kassab, M. (1987) ‘Intégration de la phase post-recrutée dans la dynamique des populations du gastéropode intertidal Hydrobia ulvae (Pennant)’, *Journal of Experimental Marine Biology and Ecology*, 111, pp. 37–60.

Bailey, D. M., Ruhl, H. A. and Smith, K. L. (2006) ‘Long-term change in benthopelagic fish abundance in the abyssal Northeast Pacific Ocean’, *Ecology*, 87, pp. 549–555. doi: 10.1890/04-1832.

Baird, D. and Ulanowicz, R. E. (1989) ‘The seasonal dynamics of the Chesapeake Bay ecosystem’, *Ecological Monographs*, 59, pp. 329–364.

Baiser, B., Whitaker, N. and Ellison, A. M. (2013) ‘Modeling foundation species in food webs’, *Ecosphere*, 4, pp. 1–14. doi: 10.1890/ES13-00265.1.

Banakar, V. K. (2010) ‘Deep-sea ferromanganese deposits and their resource potential for India’, *Journal of the Indian Institute of Science*, 90, pp. 535–541.

Barnard, J. L. and Ingram, C. L. (1986) ‘The supergiant amphipod *Alicella gigantea* Chevreux from the North Pacific Gyre’, *Journal of Crustacean Biology*, 6, pp. 825–839.

Barnes, N. and Ferrero, T. J. (2009) ‘Two new species of *Manunema* (Plectida: Peresianidae) from the Arabian Gulf, with notes on the phylogeny of the genus’, *Zootaxa*, 58, pp. 43–58.

Bau, M. *et al.* (2014) ‘Discriminating between different genetic types of marine ferro-manganese crusts and nodules based on rare earth elements and yttrium’, *Chemical Geology*, 381, pp. 1–9. doi: 10.1016/j.chemgeo.2014.05.004.

Baumgarten, S. *et al.* (2014) ‘Population structure, growth and production of a recent brachiopod from the Chilean fjord region’, *Marine Ecology*, 35, pp. 401–413. doi: 10.1111/maec.12097.

Baumiller, T. K. (2008) ‘Crinoid ecological morphology’, *Annual Review of Earth and Planetary Sciences*, 36, pp. 221–249. doi: 10.1146/annurev.earth.36.031207.124116.

Baumiller, T. K. and Labarbera, M. (1989) ‘Metabolic rates of caribbean crinoids (Echinodermata), with special reference to deep-water stalked and stalkless taxa’, *Comparative Biochemistry and Physiology Part A: Physiology*, 93A, pp. 391–394. doi: 10.1016/0300-9629(89)90053-4.

Beaulieu, S. E. (2001) ‘Life on glass houses: Sponge stalk communities in the deep sea’, *Marine Biology*, 138, pp. 803–817. doi: 10.1007/s002270000500.

Becker, H. J. *et al.* (2001) ‘The behaviour of deep-sea sediments under the impact of nodule mining processes’, *Deep-Sea Research II*, 48, pp. 3609–3627. doi: 10.1016/S0967-0645(01)00059-5.

Belcher, A. *et al.* (2016) ‘The role of particle associated microbes in remineralization of fecal pellets in the upper mesopelagic of the Scotia Sea, Antarctica’, *Limnology and Oceanography*, 61, pp. 1049–1064. doi: 10.1002/lno.10269.

Beldean, C. and Filipescu, S. (2008) ‘“Flysch-type” agglutinated foraminifera from the Lower Miocene of the Transylvanian Basin (Romania)’, in Kaminiski, M. A. and Filipescu, S. (eds) *Proceedings of the Eighth International Workshop On Agglutinated Foraminifera*. Cluj-Napoca: Grzybowski Foundation Special Publication, pp. 1–18.

Belman, B. W. and Giese, A. C. (1974) ‘Oxygen consumption of an asteroid and an echinoid from the Antarctic’, *The Biological Bulletin*, 146, pp. 157–164.

Bergstad, O. A. *et al.* (2012) ‘Distribution, population biology, and trophic ecology of the deepwater demersal fish *Halosauropsis macrochir* (pisces: Halosauridae) on the Mid-Atlantic Ridge’, *PLoS ONE*, 7, p. e31493. doi: 10.1371/journal.pone.0031493.

Berry, A. J. and bin Othman, Z. (1983) ‘An annual cycle of recruitment, growth and production in a Malaysian population of the trochacean gastropod *Umbonium vestiarium* (L.)’, *Estuarine, Coastal and Shelf Science*, 17, pp. 357–363. doi: 10.1016/0272-7714(83)90027-6.

Bett, B. J. *et al.* (2001) ‘Temporal variability in phytodetritus and megabenthic activity at the seabed in the deep Northeast Atlantic’, *Progress in Oceanography*, 50, pp. 349–368. doi: 10.1016/S0079-6611(01)00066-0.

Bharatdwaj, K. (2006) ‘Reliefs of the ocean basins’, in *Physical Geography (Oceanography)*. New Delhi: Discovery Publishing House, pp. 1–53.

Bhavan, I. (2018) *Indian Minerals Yearbook 2017 (Part- II: Metals & Alloys) - Copper*. 56th edn. Nagpur, India: Government of India, Ministry of Mines, Indian Bureau of Mines.

Bian, Z. *et al.* (2012) ‘The challenges of reusing mining and mineral-processing wastes’, *Science*, 337, pp. 702–703. doi: 10.1126/science.1224757.

Bianchelli, S. *et al.* (2010) ‘Metazoan meiofauna in deep-sea canyons and adjacent open slopes: A large-scale comparison with focus on the rare taxa’, *Deep-Sea Research I*, 57, pp. 420–433. doi: 10.1016/j.dsr.2009.12.001.

Biard, T. *et al.* (2016) ‘*In situ* imaging reveals the biomass of giant protists in the global ocean’, *Nature*, 532, pp. 504–507. doi: 10.1038/nature17652.

Bide, T. *et al.* (2008) *Nickel*. Keyworth.

Billett, D. S. M. *et al.* (2001) ‘Long-term change in the megabenthos of the Porcupine Abyssal Plain (NE Atlantic)’, *Progress in Oceanography*, 50, pp. 325–348. doi: 10.1016/S0079-6611(01)00060-X.

Billett, D. S. M. *et al.* (2010) ‘Long-term change in the abyssal NE Atlantic: The “Amperima Event” revisited’, *Deep-Sea Research II*, 57, pp. 1406–1417. doi: 10.1016/j.dsr2.2009.02.001.

Billett, D. S. M., Lampitt, R. S. and Rice, A. L. (1983) ‘Seasonal sedimentation of phytoplankton to the deep-sea benthos’, *Nature*, 302, pp. 520–522.

Birklund, J. (1977) ‘Biomass, growth and production of the amphipod *Corophium insidiosum crawford*, and preliminary notes on *Corophium volutator* (Pallas)’, *Ophelia*, 16, pp. 187–203. doi: 10.1080/00785326.1977.10425470.

Bligh, E. G. and Dyer, W. J. (1959) ‘A rapid method of total lipid extraction and purification’, *Canadian Journal of Biochemistry and Physiology*, 37, pp. 911–917. doi: 10.1139/o59-099.

Bluhm, H. (1993) ‘Effects of deep-sea mining for manganese nodules on the abyssal megabenthic community’, in *Proceedings of the 25th Annual Offshore Technology Conference*, pp. 521–529.

Bluhm, H. (1994) ‘Monitoring megabenthic communities in abyssal manganese nodule sites of the East Pacific Ocean in association with commercial deep-sea mining’, *Aquatic Conservation Marine and Freshwater Ecosystems*, 4, pp. 187–201.

Bluhm, H. (2001) ‘Re-establishment of an abyssal megabenthic community after experimental physical disturbance of the seafloor’, *Deep-Sea Research II*, 48, pp. 3841–3868. doi: 10.1016/S0967-0645(01)00070-4.

Bluhm, H. and Gebruk, A. V. (1999) ‘Holothuroidea (Echinodermata) of the Peru Basin - ecological and taxonomic remarks based on underwater images’, *Marine Ecology*, 20, pp. 167–195. doi: 10.1046/j.1439-0485.1999.00072.x.

Bluhm, H., Schriever, G. and Thiel, H. (1995) ‘Megabenthic recolonization in an experimentally disturbed abyssal manganese nodule area’, *Marine Georesources and Geotechnology*, 13, pp. 393–416. doi: 10.1080/10641199509388295.

Bluhm, H. and Thiel, H. (1996) ‘Photographic and video surveys for large scale animal and seafloor surface charting aiming at ecological characterization of habitats and communities’, in *Proceedings of the International Seminar on Deep Seabed Mining Technology, COMRA*. Peking, PR China, pp. 15–23.

Boetius, A. (2015) *RV SONNE SO242/2. Cruise Report/Fahrtbericht. DISCOL revisited. Guayaquil: 28 August 2015 - Guayaquil: 1 October 2015. SO242/2: JPI Oceans Ecological Aspects of Deep-Sea Mining*. Bremen.

Bolam, S. G. (2011) ‘Burial survival of benthic macrofauna following deposition of simulated dredged material’, *Environmental Monitoring and Assessment*, 181, pp. 13–27. doi: 10.1007/s10661-010-1809-5.

Bonvicini Pagliai, A. M. *et al.* (1985) ‘Environmental impact of extensive

dredging in a coastal marine area', *Marine Pollution Bulletin*, 16, pp. 483–488. doi: 10.1016/0025-326X(85)90381-9.

Borowski, C. (1994) 'Three new deep-sea species of Sphaerodoridae (Annelida, Polychaeta) from the eastern tropical South Pacific', *Zoologica Scripta*, 23, pp. 193–203.

Borowski, C. (2001) 'Physically disturbed deep-sea macrofauna in the Peru Basin, Southeast Pacific, revisited 7 years after the experimental impact', *Deep-Sea Research II*, 48, pp. 3809–3839. doi: 10.1016/S0967-0645(01)00069-8.

Borowski, C. and Thiel, H. (1998) 'Deep-sea macrofaunal impacts of a large-scale physical disturbance experiment in the Southeast Pacific', *Deep-Sea Research II*, 45, pp. 55–81. doi: 10.1016/S0967-0645(97)00073-8.

Borsje, B. W. *et al.* (2014) 'Formation and erosion of biogeomorphological structures: A model study on the tube-building polychaete Lanice conchilega', *Limnology and Oceanography*, 59, pp. 1297–1309. doi: 10.4319/lo.2014.59.4.1297.

Boschker, H. T. S. (2008) 'Section 8 update: Linking microbial community structure and functioning: Stable isotope (^{13}C) labeling in combination with PLFA analysis', in Kowalchuk, G. A. et al. (eds) *Molecular Microbial Ecology Manual*. Dordrecht: Springer Netherlands, pp. 3575–3590. doi: 10.1007/978-1-4020-2177-0_807.

Boschker, H. T. S., de Brouwer, J. F. C. and Cappenberg, T. E. (1999) 'The contribution of macrophyte-derived organic matter to microbial biomass in salt-marsh sediments: Stable carbon isotope analysis of microbial biomarkers', *Limnology and Oceanography*, 44, pp. 309–319. doi: 10.4319/lo.1999.44.2.0309.

Boschker, H. T. S. and Middelburg, J. J. (2002) 'Stable isotopes and biomarkers in microbial ecology', *FEMS Microbiology Ecology*, 40, pp. 85–95. doi: 10.1111/j.1574-6941.2002.tb00940.x.

de Bovée, F., Guidi, L. D. and Soyer, J. (1990) 'Quantitative distribution of deep-sea meiobenthos in the northwestern Mediterranean (Gulf of Lions)', *Continental Shelf Research*, 10, pp. 1123–1145. doi: 10.1016/0278-4343(90)90077-Y.

Bradford-Grieve, J. M. (2004) 'Deep-sea benthopelagic calanoid copepods and their colonization of the near-bottom environment', *Zoological Studies*, 43, pp. 276–291.

Braeckman, U. *et al.* (2010) 'Role of macrofauna functional traits and density in biogeochemical fluxes and bioturbation', *Marine Ecology Progress Series*, 399, pp. 173–186. doi: 10.3354/meps08336.

Braeckman, U. *et al.* (2013) 'Meiofauna metabolism in suboxic sediments:

Currently overestimated', *PLoS ONE*, 8, p. e59289. doi: 10.1371/journal.pone.0059289.

Brandt, A. *et al.* (2015) 'Abyssal macrofauna of the Kuril-Kamchatka Trench area (Northwest Pacific) collected by means of a camera-epibenthic sledge', *Deep-Sea Research II*, 111, pp. 175–187. doi: 10.1016/j.dsr2.2014.11.002.

Bratton, J. F., Colman, S. M. and Seal, R. R. (2003) 'Eutrophication and carbon sources in Chesapeake Bay over the last 2700 yr: Human impacts in context', *Geochimica et Cosmochimica Acta*, 67, pp. 3385–3402. doi: 10.1016/S0016-7037(03)00131-5.

Breiman, L. (2001) 'Random forests', *Machine Learning*, 45, pp. 5–32.

Breiman, L. *et al.* (2017) 'randomForest'.

Brey, T. *et al.* (1995) 'Growth and production of *Sterechinus neumayeri* (Echinoidea: Echinodermata) in McMurdo Sound, Antartica', *Marine Biology*, 124, pp. 279–292.

Brey, T. *et al.* (1998) 'Growth and productivity of the high Antarctic bryozoan *Melicerita obliqua*', *Marine Biology*, 132, pp. 327–333. doi: 10.1007/s002270050398.

Brey, T. *et al.* (2010) 'Body composition in aquatic organisms - A global data bank of relationships between mass, elemental composition and energy content', *Journal of Sea Research*, 64, pp. 334–340. doi: 10.1016/j.seares.2010.05.002.

Brey, T. and Clarke, A. (1993) 'Population dynamics of marine benthic invertebrates in Antarctic and subantarctic environments: Are there unique adaptations?', *Antarctic Sciences*, 5, pp. 253–266.

British Geological Survey (2007) *Copper*. Keyworth. Available at: www.mineralsuk.com.

Brooke, S., Holmes, M. and Young, C. M. (2009) 'Sediment tolerance of two different morphotypes of the deep-sea coral *Lophelia pertusa* from the Gulf of Mexico', *Marine Ecology Progress Series*, 390, pp. 137–144. doi: 10.3354/meps08191.

Brown, A. *et al.* (2018) 'Metabolic rates are significantly lower in abyssal Holothuroidea than in shallow-water Holothuroidea', *Royal Society Open Science*, 5, p. 172162. doi: 10.1098/rsos.172162.

Brown, A. and Hauton, C. (2018) 'Ecotoxicological responses to chalcopyrite exposure in a proxy for deep-sea hydrothermal vent shrimp: Implications for seafloor massive sulphide mining', *Chemistry and Ecology*, 34, pp. 391–396. doi: 10.1080/02757540.2018.1427231.

Brown, W. I. and Shick, J. M. (1979) 'Bimodal gas exchange and the regulation of oxygen uptake in holothurian', *The Biological Bulletin*, 156, pp. 272–288.

Buchanan, J. B. (1984) ‘Sediment analysis’, in Holme, N. A. and McIntyre, A. D. (eds) *Methods for the Study of Marine Benthos*. 2nd edn. Oxford: Blackwell Scientific Publications, pp. 41–65.

Buchanan, J. B. and Warwick, R. M. (1974) ‘An estimate of benthic macrofaunal production in the offshore mud of the Northumberland coast’, *Journal of the Marine Biological Association of the UK*, 54, pp. 197–222. doi: 10.1017/S0025315400022165.

Buhl-Mortensen, L. *et al.* (2010) ‘Biological structures as a source of habitat heterogeneity and biodiversity on the deep ocean margins’, *Marine Ecology*, 31, pp. 21–50. doi: 10.1111/j.1439-0485.2010.00359.x.

Burd, B. J. (2002) ‘Evaluation of mine tailings effects on a benthic marine infaunal community over 29 years’, *Marine Environmental Research*, 53, pp. 481–519. doi: 10.1016/S0141-1136(02)00092-2.

Burdige, D. J. *et al.* (1999) ‘Fluxes of dissolved organic carbon from California continental margin sediments’, *Geochimica et Cosmochimica Acta*, 63, pp. 1507–1515. doi: 10.1016/S0016-7037(99)00066-6.

Burgess, R. (2001) ‘An improved protocol for separating meiofauna from sediments using colloidal silica sols’, *Marine Ecology Progress Series*, 214, pp. 161–165. doi: 10.3354/meps214161.

Burke, M. V and Mann, K. H. (2003) ‘Productivity and production: Biomass ratios of bivalve and gastropod populations in a eastern Canadian estuary’, *Journal Fisheries Research Board of Canada*, 31, pp. 167–177.

Bussau, C. (1993) *Taxonomische und ökologische Untersuchungen an Nematoden des Peru-Beckens, PhD-Thesis*. Christian-Albrechts-Universität zu Kiel.

Bussau, C., Schriever, G. and Thiel, H. (1995) ‘Evaluation of abyssal metazoan meiofauna from a manganese nodule area of the eastern South Pacific’, *Vie et Milieu*, 45, pp. 39–48.

Bussau, C. and Vopel, K. (1999) ‘New nematode species and genera (Chromadorida, Microlaimidae) from the deep sea of the eastern tropical South Pacific’, *Annalen des Naturhistorischen Museums Wien*, 101, pp. 405–421. Available at: http://aut.researchgateway.ac.nz/handle/10292/1502%5Cnhttp://aut.researchgateway.ac.nz/bitstream/10292/1502/2/Bussau and Vopel 1999.pdf.

Byrne, M. and O’Hara, T. (2017) *Australian Echinoderms: Biology, Ecology and Evolution*. Clayton: CSIRO Publishing.

Caetano, C. H. S. *et al.* (2006) ‘Population biology and secondary production of *Excirolana braziliensis* (Isopoda: Cirolanidae) in two sandy beaches of southeastern Brazil’, *Journal of Coastal Research*, 224, pp. 825–835. doi:

10.2112/04-0224.1.

Caetano, C. H. S., Veloso, V. G. and Cardoso, R. S. (2003) 'Population biology and secondary production of *Olivancillaria vesica vesica* (Gmelin , 1791) (Gastropoda: Olividae) on a sandy beach in southeastern Brazil', *Journal of Molluscan Studies*, 69, pp. 67–73. doi: 10.1093/mollus/69.1.67.

Cairns, S. D. (2016) 'New abyssal Primnoidae (Anthozoa: Octocorallia) from the Clarion-Clipperton Fracture Zone, equatorial northeastern Pacific', *Marine Biodiversity*, 46, pp. 141–150. doi: 10.1007/s12526-015-0340-x.

Calbert, A. and Landry, M. R. (2004) 'Phytoplankton growth, microzooplankton grazing, and carbon cycling in marine systems', *Limnology and Oceanography*, 49, pp. 51–57.

Canals, M. *et al.* (2006) 'Flushing submarine canyons', *Nature*, 444, pp. 354–357. doi: 10.1038/nature05271.

Canals, M. *et al.* (2013) 'Integrated study of Mediterranean deep canyons: Novel results and future challenges', *Progress in Oceanography*, 118, pp. 1–27. doi: 10.1016/j.pocean.2013.09.004.

Canty, A. and Ripley, B. (2017) 'boot: Bootstrap R (S-Plus) Functions'.

Cardoso, R. S. and Veloso, V. G. (1996) 'Population biology and secondary production of the sandhopper *Pseudorchestoidea brasiliensis* (Amphipoda: Talitridae) at Prainha Beach, Brazil', *Marine Ecology Progress Series*, 142, pp. 111–119.

Cardoso, R. S. and Veloso, V. G. (2003) 'Population dynamics and secondary production of the wedge clam *Donax hanleyanus* (Bivalvia: Donacidae) on a high-energy, subtropical beach of Brazil', *Marine Biology*, 142, pp. 153–162. doi: 10.1007/s00227-002-0926-2.

Carey, A. G. (1972) 'Food sources of sublittoral, bathyal and abyssal asteroids in the northeast Pacific Ocean', *Ophelia*, 10, pp. 35–47. doi: 10.1080/00785326.1972.10430100.

Carpentier, A. *et al.* (2014) 'Feeding ecology of *Liza* spp. in a tidal flat: Evidence of the importance of primary production (biofilm) and associated meiofauna', *Journal of Sea Research*, 92, pp. 86–91. doi: 10.1016/j.seares.2013.10.007.

Cartes, J. E. *et al.* (2009) 'Small-spatial scale changes in productivity of suprabenthic and infaunal crustaceans at the continental shelf of Ebro Delta (western Mediterranean)', *Journal of Experimental Marine Biology and Ecology*, 378, pp. 40–49. doi: 10.1016/j.jembe.2009.07.025.

Cartes, J. E., Elizalde, M. and Sorbe, J. C. (2000) 'Contrasting life histories and secondary production of populations of *Munnopsurus atlanticus* (Isopoda: Asellota) from two bathyal areas of the NE Atlantic and the NW

Mediterranean', *Marine Biology*, 136, pp. 881–890. doi: 10.1007/s002270000287.

Cartes, J. E., Elizalde, M. and Sorbe, J. C. (2001) 'Contrasting life-histories, secondary production, and trophic structure of Peracarid assemblages of the bathyal suprabenthos from the Bay of Biscay (NE Atlantic) and the Catalan Sea (NW Mediterranean)', *Deep-Sea Research I*, 48, pp. 2209–2232. doi: 10.1016/S0967-0637(01)00012-7.

Cartes, J. E., Mamouridis, V. and Fanelli, E. (2011) 'Deep-sea suprabenthos assemblages (Crustacea) off the Balearic Islands (western Mediterranean): Mesoscale variability in diversity and production', *Journal of Sea Research*, 65, pp. 340–354. doi: 10.1016/j.seares.2011.02.002.

Cartes, J. E. and Sorbe, J. C. (1999a) 'Deep-water amphipods from the Catalan Sea slope (western Mediterranean): Bathymetric distribution, assemblage composition and biological characteristics', *Journal of Natural History*, 33, pp. 1133–1158. doi: 10.1080/002229399299978.

Cartes, J. E. and Sorbe, J. C. (1999b) 'Estimating secondary production in bathyal suprabenthic peracarid crustaceans from the Catalan Sea slope (western Mediterranean; 391–1255 m)', *Journal of Experimental Marine Biology and Ecology*, 239, pp. 195–210. doi: 10.1016/S0022-0981(99)00026-X.

Castilla, J. C. (1996) 'Copper mine tailing disposal in northern Chile rocky shores: *Enteromorpha compressa* (Chlorophyta) as a sentinel species', *Environmental Monitoring and Assessment*, 40, pp. 171–184. doi: 10.1007/BF00414390.

Castilla, J. C. and Nealler, E. (1978) 'Marine environmental impact due to mining activities of El Salvador copper mine, Chile', *Marine Pollution Bulletin*, 9, pp. 67–70. doi: 10.1016/0025-326X(78)90451-4.

Cathalot, C. *et al.* (2015) 'Cold-water coral reefs and adjacent sponge grounds: Hotspots of benthic respiration and organic carbon cycling in the deep sea', *Frontiers in Marine Science*, 2, pp. 1–12. doi: 10.3389/fmars.2015.00037.

Ceccherelli, V. U. and Rossi, R. (1984) 'Settlement, growth and production of the mussel *Mytilus galloprovincialis*', *Marine Ecology Progress Series*, 16, pp. 173–184. doi: 10.3354/meps016173.

Chabanet, P. *et al.* (2010) 'Baseline study of the spatio-temporal patterns of reef fish assemblages prior to a major mining project in New Caledonia (South Pacific)', *Marine Pollution Bulletin*, 61, pp. 598–611. doi: 10.1016/j.marpolbul.2010.06.032.

Chambers, M. R. and Milne, R. (1975) 'Life cycle and production of *Nereis diversicolor* O. F. Müller in the Ythan Estuary, Scotland', *Estuarine, Coastal and Shelf Science*, 3, pp. 133–144.

Chao, A. *et al.* (2014) ‘Rarefaction and extrapolation with Hill numbers: A framework for sampling and estimation in species diversity studies’, *Ecological Monographs*, 84, pp. 45–67. doi: 10.1890/13-0133.1.

Chertoprud, E. S. *et al.* (2007) ‘Spatial variability of the structure of the Harpacticoida (Copepoda) crustacean assemblages in intertidal and shallow-water zones of European seas’, *Oceanology*, 47, pp. 51–59. doi: 10.1134/S0001437007010080.

Childress, J. J. *et al.* (1980) ‘Patterns of growth, energy utilization and reproduction in some meso- and bathypelagic fishes off Southern California’, *Marine Biology*, 61, pp. 27–40.

Childress, J. J. *et al.* (1990) ‘Metabolic rates of benthic deep-sea decapod crustaceans decline with increasing depth primarily due to the decline in temperature’, *Deep-Sea Research*, 37, pp. 929–949. doi: 10.1016/0198-0149(90)90104-4.

Chou, L. M., Yu, J. Y. and Loh, T. L. (2004) ‘Impacts of sedimentation on soft-bottom benthic communities in the southern islands of Singapore’, *Hydrobiologia*, 515, pp. 91–106. doi: 10.1023/B:HYDR.0000027321.23230.2f.

Christensen, L. B. (2006) *Marine mammal populations: Reconstructing historical abundances at the global scale, Fisheries Centre Research Reports*. Vancouver, B. C. Available at: http://nova.wh.whoi.edu/palit/Christensen_2006_Fisheries Centre Research Reports_Marine mammal populations Reconstructing historical abundances at the global scale.pdf.

Clarke, K. R. (1993) ‘Non-parametric multivariate analyses of changes in community structure’, *Australian Journal of Ecology*, 18, pp. 117–143. doi: 10.1111/j.1442-9993.1993.tb00438.x.

Clarke, K. R. and Gorley, R. N. (2006) *PRIMER v6: Manual/ Tutorial*. Plymouth: PRIMER-E Ltd.

Clasing, E. *et al.* (1994) ‘Population dynamics of *Venus antiqua* (Bivalvia: Veneracea) in the Bahia de Yaldad, Isla de Chiloe, southern Chile’, *Journal of Experimental Marine Biology and Ecology*, 177, pp. 171–186.

Clausen, I. and Riisgård, H. U. (1996) ‘Growth, filtration and respiration in the mussel *Mytilus edulis*: No evidence for physiological regulation of the filter-pump to nutritional needs’, *Marine Ecology Progress Series*, 141, pp. 37–45. doi: 10.3354/meps141037.

Clough, L. M., Renaud, P. E. and Ambrose Jr., W. G. (2005) ‘Impacts of water depth, sediment pigment concentration, and benthic macrofaunal biomass on sediment oxygen demand in the western Arctic Ocean’, *Canadian Journal of Fisheries and Aquatic Sciences*, 62, pp. 1756–1765. doi: 10.1139/f05-102.

Cohen, J. (1988) *Statistical power analysis for the behavioral sciences*. 2nd edn. Mahwah, NJ: Lawrence Erlbaum Associates, Publishers.

Cole, J. J. *et al.* (2007) 'Plumbing the global carbon cycle: Integrating inland waters into the terrestrial carbon budget', *Ecosystems*, 10, pp. 172–185. doi: 10.1007/s10021-006-9013-8.

Van Colen, C. *et al.* (2009) 'Tidal flat nematode responses to hypoxia and subsequent macrofauna-mediated alterations of sediment properties', *Marine Ecology Progress Series*, 381, pp. 189–197. doi: 10.3354/meps07914.

Collie, J. S. (1985) 'Life history and production of three amphipod species on Georges Bank', *Marine Ecology Progress Series*, 22, pp. 229–238.

Collins, M. A. *et al.* (1998) 'Acoustic tracking of the dispersal of organic matter by scavenging fishes in the deep-sea', *Hydrobiologia*, 371/372, pp. 181–186. doi: 10.1023/A:1017083107914.

Collins, M. A. *et al.* (2005) 'Trends in body size across an environmental gradient: A differential response in scavenging and non-scavenging demersal deep-sea fish', *Proceedings of the Royal Society B: Biological Sciences*, 272, pp. 2051–2057. doi: 10.1098/rspb.2005.3189.

Collins, M. A., Priede, I. G. and Bagley, P. M. (1999) '*In situ* comparison of activity in two deep-sea scavenging fishes occupying different depth zones', *Proceedings of the Royal Society B: Biological Sciences*, 266, pp. 2011–2016. doi: 10.1098/rspb.1999.0879.

Company, J. B. *et al.* (2008) 'Climate influence on deep sea populations', *PLoS ONE*, 3, p. e1431. doi: 10.1371/journal.pone.0001431.

Conover, R. J. (1966) 'Assimilation of organic matter by zooplankton', *Limnology and Oceanography*, 11, pp. 338–345. doi: 10.4319/lo.1966.11.3.0338.

Contreras-Rosales, L. A. *et al.* (2012) 'Living deep-sea benthic foraminifera from the Cap de Creus Canyon (western Mediterranean): Faunal-geochemical interactions', *Deep-Sea Research II*, 64, pp. 22–42. doi: 10.1016/j.dsr.2012.01.010.

Cooke, J. A. and Johnson, M. S. (2002) 'Ecological restoration of land with particular reference to the mining of metals and industrial minerals: A review of theory and practice', *Environmental Reviews*, 10, pp. 41–71. doi: 10.1139/a01-014.

Corinaldesi, C. *et al.* (2010) 'Viral decay and viral production rates in continental-shelf and deep-sea sediments of the Mediterranean Sea', *FEMS Microbiology Ecology*, 72, pp. 208–218. doi: 10.1111/j.1574-6941.2010.00840.x.

Cormier, M.-H. and Sloan, H. (2018) ‘Abyssal hills and abyssal plains’, in Micallef, A., Krastel, S., and Savini, A. (eds) *Submarine Geomorphology*. Cham: Springer International Publishing (Springer Geology), pp. 389–408. doi: 10.1007/978-3-319-57852-1.

Correa, J. A. *et al.* (1999) ‘Copper, copper mine tailings and their effect on marine algae in northern Chile’, *Journal of Applied Phycology*, 11, pp. 57–67.

Coull, B. C. (1999) ‘Role of meiofauna in estuarine soft-bottom habitats’, *Australian Journal of Ecology*, 24, pp. 327–343. doi: 10.1046/j.1442-9993.1999.00979.x.

Coull, B. C. and Vernberg, W. B. (1970) ‘Harpacticoid copepod respiration: *Enhydrosoma propinquum* and *Longipedia helgolandica*’, *Marine Biology*, 5, pp. 341–344.

Courp, T. and Monaco, A. (1990) ‘Sediment dispersal and accumulation on the continental margin of the Gulf of Lions: Sedimentary budget’, *Continental Shelf Research*, 10, pp. 1063–1087. doi: 10.1016/0278-4343(90)90075-W.

Courtene-Jones, W. *et al.* (2017) ‘Microplastic pollution identified in deep-sea water and ingested by benthic invertebrates in the Rockall Trough, North Atlantic Ocean’, *Environmental Pollution*, 231, pp. 271–280. doi: 10.1016/j.envpol.2017.08.026.

Crabtree, R. E., Carter, J. and Musick, J. A. (1991) ‘The comparative feeding ecology of temperate and tropical deep- sea fishes from the western North Atlantic’, *Deep-Sea Research*, 38, pp. 1277–1298.

Crisp, D. (1971) ‘Energy flow measurements’, in Holme, N. A. and McIntyre, A. D. (eds) *Methods for the Study of Marine Benthos*. 1st edn. Oxford: Blackwell Scientific Publications, pp. 284–367.

Cummings, V., Vopel, K. and Thrush, S. F. (2009) ‘Terrigenous deposits in coastal marine habitats: Influences on sediment geochemistry and behaviour of post-settlement bivalves’, *Marine Ecology Progress Series*, 383, pp. 173–185. doi: 10.3354/meps07983.

Cunha, M. R., Moreira, M. H. and Sorbe, J. C. (2000) ‘The amphipod *Corophium multisetosum* (Corophiidae) in Ria de Aveiro (NW Portugal). II. Abundance, biomass and production’, *Marine Biology*, 137, pp. 651–660. doi: 10.1007/s002270000385.

Daas, T. *et al.* (2011) ‘Reproduction, population dynamics and production of *Nereis falsa* (Nereididae: Polychaeta) on the rocky coast of El Kala National Park, Algeria’, *Helgoland Marine Research*, 65, pp. 165–173. doi: 10.1007/s10152-010-0212-5.

Dahlgren, T. G. *et al.* (2016) ‘Abyssal fauna of the UK-1 polymetallic nodule exploration area, Clarion-Clipperton Zone, central Pacific Ocean: Cnidaria’,

Biodiversity Data Journal, 4, p. e9277. doi: 10.3897/BDJ.4.e9277.

Danovaro, R. *et al.* (1995) 'Vertical distribution of meiobenthos in bathyal sediments of the eastern Mediterranean Sea: Relationship with labile organic matter and bacterial biomasses', *Marine Ecology*, 16, pp. 103–116. doi: 10.1111/j.1439-0485.1995.tb00398.x.

Danovaro, R. (1996) 'Detritus-bacteria-meiofauna interactions in a seagrass bed (*Posidonia oceanica*) of the NW Mediterranean', *Marine Biology*, 127, pp. 1–13. doi: 10.1007/BF00993638.

Danovaro, R. *et al.* (1999) 'Benthic response to particulate fluxes in different trophic environments: A comparison between the Gulf of Lions-Catalan Sea (western-Mediterranean) and the Cretan Sea (eastern-Mediterranean)', *Progress in Oceanography*, 44, pp. 287–312. doi: 10.1016/S0079-6611(99)00030-0.

Danovaro, R., Gambi, C., *et al.* (2008) 'Exponential decline of deep-sea ecosystem functioning linked to benthic biodiversity loss', *Current Biology*, 18, pp. 1–8. doi: 10.1016/j.cub.2007.11.056.

Danovaro, R., Dell'Anno, A., *et al.* (2008) 'Major viral impact on the functioning of benthic deep-sea ecosystems', *Nature*, 454, pp. 1084–1087. doi: 10.1038/nature07268.

Danovaro, R. (2010a) 'Abundance of metazoan meiofauna', in *Methods for the Study of Deep-Sea Sediments, Their Functioning and Biodiversity*. 1st edn. Boca Raton: CRC Press - Taylor & Francis Group, pp. 149–160.

Danovaro, R. (2010b) 'Benthic prokaryotic heterotrophic production using the leucin incorporation method', in *Methods for the Study of Deep-Sea Sediments, Their Functioning and Biodiversity*. 1st edn. Boca Raton: CRC Press - Taylor & Francis Group, pp. 337–342.

Danovaro, R. (2010c) 'Bioavailable organic matter: Total and enzymaticlaly hydrolyzable proteins, carbohydrates, and lipids', in *Methods for the Study of Deep-Sea Sediments, Their Functioning and Biodiversity*. 1st edn. Boca Raton: CRC Press - Taylor & Francis Group, pp. 23–44.

Danovaro, R. (2010d) 'Meiofaunal biomass and secondary production', in *Methods for the Study of Deep-Sea Sediments, Their Functioning and Biodiversity*. 1st edn. Boca Raton: CRC Press - Taylor & Francis Group, pp. 351–367.

Danovaro, R. (2010e) 'Prokaryotic abundance', in *Methods for the Study of Deep-Sea Sediments, Their Functioning and Biodiversity*. 1st edn. Boca Raton: CRC Press - Taylor & Francis Group, pp. 95–106.

Danovaro, R. (2010f) 'Prokaryotic biomass in marine sediments', in *Methods for the Study of Deep-Sea Sediments, Their Functioning and Biodiversity*. 1st edn. Boca Raton: CRC Press - Taylor & Francis Group, pp. 331–336.

Danovaro, R., Fabiano, M. and Della Croce, N. (1993) ‘Labile organic matter and microbial biomasses in deep-sea sediments (Eastern Mediterranean Sea)’, *Deep-Sea Research I*, 40, pp. 953–965. doi: 10.1016/0967-0637(93)90083-F.

Danovaro, R., Snelgrove, P. V. R. and Tyler, P. A. (2014) ‘Challenging the paradigms of deep-sea ecology’, *Trends in Ecology & Evolution*, 29, pp. 465–475. doi: 10.1016/j.tree.2014.06.002.

Darwin, C. (1859) ‘Struggle for existence’, in *On the Origin of Species by Means of Natural Selection*. London: John Murray, pp. 60–79.

Davenport, E. S., Shull, D. H. and Devol, A. H. (2012) ‘Roles of sorption and tube-dwelling benthos in the cycling of phosphorus in Bering Sea sediments’, *Deep-Sea Research II*, 65–70, pp. 163–172. doi: 10.1016/j.dsr2.2012.02.004.

Decraemer, W. (1996) ‘New information on the ultrastructure of the lip region in the genus Desmoscolex and description of Desmoscolex (Desmoscolex) parvospiculatus sp. n. (Nemata: Desmoscolecida) from Papua New Guinea’, *Nematologica*, 42, pp. 9–23.

DeGeest, A. L. *et al.* (2008) ‘Sediment accumulation in the western Gulf of Lions, France: The role of Cap de Creus canyon in linking shelf and slope sediment dispersal systems’, *Continental Shelf Research*, 28, pp. 2031–2047. doi: 10.1016/j.csr.2008.02.008.

Deming, J. W. (1985) ‘Bacterial growth in deep-sea sediment trap and boxcore samples’, *Marine Ecology Progress Series*, 25, pp. 305–312. doi: 10.3354/meps025305.

Deming, J. W. and Baross, J. A. (1993) ‘The early diagenesis of organic matter: Bacterial activity’, in Engel, M. H. and Macko, S. A. (eds) *Organic Geochemistry: Principles and Applications*. Boston, MA: Springer US, pp. 119–144. doi: 10.1007/978-1-4615-2890-6_5.

DePatra, K. D. and Levin, L. A. (1989) ‘Evidence of the passive deposition of meiofauna into fiddler crab burrows’, *Journal of Experimental Marine Biology and Ecology*, 125, pp. 173–192. doi: 10.1016/0022-0981(89)90095-6.

Dernie, K. M., Kaiser, M. J. and Warwick, R. M. (2003) ‘Recovery rates of benthic communities following physical disturbance’, *Journal of Animal Ecology*, 72, pp. 1043–1056. doi: 10.1046/j.1365-2656.2003.00775.x.

Devey, C. W. *et al.* (2018) ‘Habitat characterization of the Vema Fracture Zone and Puerto Rico Trench’, *Deep-Sea Research II*, 148, pp. 7–20. doi: 10.1016/j.dsr2.2018.02.003.

Diaz, R. J. and Rosenberg, R. (1995) ‘Marine benthic hypoxia: A review of its ecological effects and the behavioural responses of benthic macrofauna’, *Oceanography and Marine Biology: An Annual Review*, 33, pp. 245–303.

Doughty, C. L. *et al.* (2015) ‘Mangrove range expansion rapidly increases

coastal wetland carbon storage', *Estuaries and Coasts*, 39, p. 385. doi: 10.1007/s12237-015-9993-8.

Van Dover, C. L. *et al.* (2017) 'Biodiversity loss from deep-sea mining', *Nature Geoscience*, 10, pp. 464–465. doi: 10.1038/ngeo2983.

Drazen, J. C. *et al.* (2008) 'Bypassing the abyssal benthic food web: Macrourid diet in the eastern North Pacific inferred from stomach content and stable isotopes analyses', *Limnology and Oceanography*, 53, pp. 2644–2654. doi: 10.4319/lo.2008.53.6.2644.

Drazen, J. C., Baldwin, R. J. and Smith, K. L. (1998) 'Sediment community response to a temporally varying food supply at an abysal station in the NE', *Deep-Sea Research II*, 45, pp. 893–913.

Drazen, J. C., Reisenbichler, K. R. and Robison, B. H. (2007) 'A comparison of absorption and assimilation efficiencies between four species of shallow- and deep-living fishes', *Marine Biology*, 151, pp. 1551–1558. doi: 10.1007/s00227-006-0596-6.

Drazen, J. C. and Seibel, B. A. (2007) 'Depth-related trends in metabolism of benthic and benthopelagic deep-sea fishes', *Limnology and Oceanography*, 52, pp. 2306–2316. doi: 10.4319/lo.2007.52.5.2306.

Drazen, J. C. and Sutton, T. T. (2017) 'Dining in the deep: The feeding ecology of deep-sea fishes', *Annual Review of Marine Science*, 9, pp. 337–366. doi: 10.1146/annurev-marine-010816-060543.

Drazen, J. C. and Yeh, J. (2012) 'Respiration of four species of deep-sea demersal fishes measured in situ in the eastern North Pacific', *Deep-Sea Research I*, 60, pp. 1–6. doi: 10.1016/j.dsr.2011.09.007.

Duarte, C. M. (2017) 'Reviews and syntheses: Hidden forests, the role of vegetated coastal habitats in the ocean carbon budget', *Biogeosciences*, 14, pp. 301–310. doi: 10.5194/bg-14-301-2017.

Duarte, C. M. and Cebrian, J. (1996) 'The fate of marine autotrophic production', *Limnology and Oceanography*, 41, pp. 1758–1766.

Dudka, S. and Adriano, D. C. (1997) 'Environmental impacts of metal ore mining and processing: A review', *Journal of Environmental Quality*, 26, pp. 590–602. doi: 10.2134/jeq1997.00472425002600030003x.

Duineveld, G. G. C. A. *et al.* (2001) 'Activity and composition of the benthic fauna in the Whittard Canyon and the adjacent continental slope (NE Atlantic)', *Oceanologica Acta*, 24(1), pp. 69–83. doi: 10.1016/S0399-1784(00)01129-4.

Dunlop, K. M. *et al.* (2016) 'Carbon cycling in the deep eastern North Pacific benthic food web: Investigating the effect of organic carbon input', *Limnology and Oceanography*, 61, pp. 1956–1968. doi: 10.1002/lno.10345.

Dunne, J. A., Williams, R. J. and Martinez, N. D. (2002) ‘Network structure and biodiversity loss in food webs: robustness increases with connectance’, *Ecology Letters*, 5, pp. 558–567. doi: 10.1046/j.1461-0248.2002.00354.x.

Dunne, J. P., Sarmiento, J. L. and Gnanadesikan, A. (2007) ‘A synthesis of global particle export from the surface ocean and cycling through the ocean interior and on the seafloor’, *Global Biogeochemical Cycles*, 21, p. GB4006. doi: 10.1029/2006GB002907.

Dupin, L. *et al.* (2013) ‘Land cover fragmentation using multi-temporal remote sensing on major mine sites in southern Katanga (Democratic Republic of Congo)’, *Advances in Remote Sensing*, 2, pp. 127–139. doi: 10.4236/ars.2013.22017.

Durden, J. M., Bett, B. J., *et al.* (2016) ‘Improving the estimation of deep-sea megabenthos biomass: Dimension to wet weight conversions for abyssal invertebrates’, *Marine Ecology Progress Series*, 552, pp. 71–79. doi: 10.3354/meps11769.

Durden, J. M., Schoening, T., *et al.* (2016) ‘Perspectives in visual imaging for marine biology and ecology: From acquisition to understanding’, *Oceanography and Marine Biology: An Annual Review*, 54, pp. 1–72. doi: 10.1201/9781315368597.

Durden, J. M. *et al.* (2017) ‘Differences in the carbon flows in the benthic food webs of abyssal hill and plain habitats’, *Limnology and Oceanography*, 62, pp. 1771–1782. doi: 10.1002/lno.10532.

Durrieu de Madron, X. *et al.* (2005) ‘Comments on “Cascades of dense water around the world ocean”’, *Progress in Oceanography*, 60, pp. 83–90. doi: 10.1016/j.pocean.2004.08.004.

Edwards, D. P. *et al.* (2014) ‘Mining and the African environment’, *Conservation Letters*, 7, pp. 302–311. doi: 10.1111/conl.12076.

Eiler, A. *et al.* (2003) ‘Heterotrophic bacterial growth efficiency and community structure at different natural organic carbon concentrations’, *Applied and Environmental Microbiology*, 69, pp. 3701–3709. doi: 10.1128/AEM.69.7.3701-3709.2003.

Elias, M. (2002) ‘Nickel laterite deposits – geological overview, resources and exploitation’, in Cooke, D. R. and Pongratz, J. (eds) *Giant ore deposits: Characteristics, genesis and exploration*. Hobart: University of Tasmania, pp. 205–220.

Enge, A. J. *et al.* (2016) ‘Carbon and nitrogen uptake of calcareous benthic foraminifera along a depth-related oxygen gradient in the OMZ of the Arabian Sea’, *Frontiers in Microbiology*, 7, pp. 1–12. doi: 10.3389/fmicb.2016.00071.

Enríquez-García, C., Nandini, S. and Sarma, S. S. S. (2013) ‘Feeding behaviour

of *Acanthocyclops americanus* (Marsh) (Copepoda: Cyclopoida)', *Journal of Natural History*, 47, pp. 853–862. doi: 10.1080/00222933.2012.747637.

Enríquez-Ocaña, L. F. *et al.* (2012) 'Evaluation of the combined effect of temperature and salinity on the filtration, clearance rate and assimilation efficiency of the mangrove oyster *Crassostrea corteziensis* (Hertlein, 1951)', *Archives of Biological Sciences*, 64, pp. 479–488. doi: 10.2298/ABS1202479O.

Environmental Law Alliance Worldwide (2010) *Guidebook for evaluating mining projects EIAs*. 1st edn. Eugene.

Epping, E. *et al.* (2002) 'On the oxidation and burial of organic carbon in sediments of the Iberian margin and Nazaré Canyon (NE Atlantic)', *Progress in Oceanography*, 52, pp. 399–431. doi: 10.1016/S0079-6611(02)00017-4.

Epstein, S. S., Burkovsky, I. V. and Shiaris, M. P. (1992) 'Ciliate grazing on bacteria, flagellates, and microalgae in a temperate zone sandy tidal flat: Ingestion rates and food niche partitioning', *Journal of Experimental Marine Biology and Ecology*, 165, pp. 103–123. doi: 10.1016/0022-0981(92)90292-I.

Escobar-Briones, E. *et al.* (2002) 'Carbon sources and trophic position of two abyssal species of Anomura, *Munidopsis alvisca* (Galatheidae) and *Neolithodes diomedeae* (Lithodidae)', *Contributions to the Study of East Pacific Crustaceans*, 1, pp. 37–43.

Etcheber, H. *et al.* (1999) 'Distribution and quality of sedimentary organic matter on the Aquitanian margin (Bay of Biscay)', *Deep-Sea Research II*, 46, pp. 2249–2288. doi: 10.1016/S0967-0645(99)00062-4.

Evrard, V. *et al.* (2010) 'Carbon and nitrogen flows through the benthic food web of a photic subtidal sandy sediment', *Marine Ecology Progress Series*, 416, pp. 1–16. doi: 10.3354/meps08770.

Fabiano, M., Danovaro, R. and Fraschetti, S. (1995) 'A three-year time series of elemental and biochemical composition of organic matter in subtidal sandy sediments of the Ligurian Sea (northwestern Mediterranean)', *Continental Shelf Research*, 15, pp. 1453–1469. doi: 10.1016/0278-4343(94)00088-5.

Feller, R. J. (1982) 'Empirical estimates of carbon production for a meiobenthic harpacticoid copepod', *Canadian Journal of Fisheries and Aquatic Sciences*, 39, pp. 1435–1443.

Fennel, K. (2010) 'The role of continental shelves in nitrogen and carbon cycling: Northwestern North Atlantic case study', *Ocean Science*, 6, pp. 539–548. doi: 10.5194/os-6-539-2010.

Fenton, G. E. (1996) 'Production and biomass of *Tenagomysis tasmaniae* Fenton, *Anisomysis mixta australis* (Zimmer) and *Paramesopodopsis rufa* Fenton from south-eastern Tasmania (Crustacea: Mysidacea)', *Hydrobiologia*, 323, pp. 23–30.

Filer, C. and Gabriel, J. (2017) ‘How could Nautilus Minerals get a social licence to operate the world’s first deep sea mine?’, *Marine Policy*. doi: 10.1016/j.marpol.2016.12.001.

Finn, J. T. (1980) ‘Flow analysis of models of the Hubbard Brook ecosystem’, *Ecology*, 61, pp. 562–571. doi: 10.2307/1937422.

FitzGeorge-Balfour, T. *et al.* (2010) ‘Phytopigments as biomarkers of selectivity in abyssal holothurians; interspecific differences in response to a changing food supply’, *Deep-Sea Research II*, 57, pp. 1418–1428. doi: 10.1016/j.dsr2.2010.01.013.

Fleeger, J. W. and Palmer, M. A. (1982) ‘Secondary production of the estuarine, meiobenthic copepod *Microarthridion littorale*’, *Marine Ecology Progress Series*, 7, pp. 157–162. doi: 10.3354/meps007157.

Floeter, S. R. *et al.* (2005) ‘Geographical gradients of marine herbivorous fishes: Patterns and processes’, *Marine Biology*, 147, pp. 1435–1447. doi: 10.1007/s00227-005-0027-0.

Foell, E. J. and Pawson, D. L. (1986) ‘Photographs of invertebrate megafauna from abyssal depths of the north-eastern equatorial Pacific Ocean’, *The Ohio Journal of Science*, 86, pp. 61–68.

Foell, E. J., Thiel, H. and Schriever, G. (1990) ‘DISCOL: A long-term, large-scale, disturbance-recolonization experiment in the abyssal eastern tropical south Pacific Ocean’, in. Houston, Texas: Offshore Technology Conference, pp. 497–503.

Foell, E. J., Thiel, H. and Schriever, G. (1992) ‘DISCOL: A long-term, large-scale disturbance-recolonization experiment in the abyssal eastern tropical South Pacific Ocean’, *Marine Engineering*, 44, pp. 90–94.

Forbes, E. (1854) *The natural history of the European seas*. Edited by R. Godwin-Austen. London: John van Voorst.

Fourquean, J. W. *et al.* (2012) ‘Seagrass ecosystems as a globally significant carbon stock’, *Nature Geoscience*, 5, pp. 505–509. doi: 10.1038/ngeo1477.

Fox, H. M. (1936) ‘The activity and metabolism of poikilothermal animals in different latitudes’, *Proceedings of the Zoological Society of London*, pp. 945–955.

Fox, R., Barnes, R. D. and Ruppert, E. E. (2003) *Invertebrate Zoology: A functional evolutionary approach*. Belmont, California: Brooks/ Cole Thompson Learning.

Franks, D. M. *et al.* (2011) ‘Sustainable development principles for the disposal of mining and mineral processing wastes’, *Resources Policy*, 36, pp. 114–122. doi: 10.1016/j.resourpol.2010.12.001.

Franz, D. R. and Tanacredi, J. T. (1992) ‘Secondary production of the amphipod *Ampelisca abdita* Mills and its importance in the diet of juvenile Winter Flounder (*Pleuronectes americanus*) in Jamaica Bay, New York’, *Estuaries*, 15, pp. 193–203.

Fraschetti, S. *et al.* (1997) ‘Life-history of the bivalve *Spisula subtruncata* (da Costa) in the Ligurian Sea (North-Western Mediterranean): The contribution of newly settled juveniles’, *Scientia Marina*, 61, pp. 25–32.

Fratt, D. B. and Dearborn, J. H. (1984) ‘Feeding biology of the Antarctic brittle star *Ophionotus victoriae* (Echinodermata: Ophiuroidea)’, *Polar Biology*, 3, pp. 127–139. doi: 10.1007/BF00442644.

Fredette, T. J. *et al.* (1990) ‘Secondary production within a seagrass bed (*Zostera marina* and *Ruppia maritima*) in lower Chesapeake Bay’, *Estuaries*, 13, pp. 431–440.

Froese, R. and Pauly, D. (2017) *FishBase*. Available at: www.fishbase.org (Accessed: 21 February 2018).

Froese, R., Thorson, J. T. and Reyes, R. B. (2014) ‘A Bayesian approach for estimating length-weight relationships in fishes’, *Journal of Applied Ichthyology*, 30, pp. 78–85. doi: 10.1111/jai.12299.

Fry, J. C. (1990) ‘Determination of biomass’, in *Methods in Aquatic Bacteriology*. New York: John Wiley & Sons, pp. 27–72.

Fukuda, R. *et al.* (1998) ‘Direct determination of carbon and nitrogen contents of natural bacterial assemblages in marine environments’, *Applied and Environmental Microbiology*, 64, pp. 3352–3358.

Gage, J. D. and Tyler, P. A. (1991) *Deep-sea biology: A natural history of organisms at the deep-sea floor*. Cambridge, UK: Cambridge University Press.

Gale, K. S. P., Hamel, J.-F. and Mercier, A. (2013) ‘Trophic ecology of deep-sea Asteroidea (Echinodermata) from eastern Canada’, *Deep-Sea Research I*, 80, pp. 25–36. doi: 10.1016/j.dsr.2013.05.016.

Galéron, J. *et al.* (2000) ‘Variation in structure and biomass of the benthic communities at three contrasting sites in the tropical Northeast Atlantic’, *Marine Ecology Progress Series*, 197, pp. 121–137. doi: 10.3354/meps197121.

Gallucci, F., Fonseca, G. and Soltwedel, T. (2008) ‘Effects of megafauna exclusion on nematode assemblages at a deep-sea site’, *Deep-Sea Research I*, 55, pp. 332–349. doi: 10.1016/j.dsr.2007.12.001.

García, R. *et al.* (2008) ‘Deposition rates, mixing intensity and organic content in two contrasting submarine canyons’, *Progress in Oceanography*, 76(2), pp. 192–215. doi: 10.1016/j.pocean.2008.01.001.

Gardiner, L. F. (1975) ‘The systematics, postmarsupial development, and

ecology of the deep-sea family Neotanaidae (Crustacea: Tanaidacea)', *Smithsonian Contributions to Zoology*, (170), pp. 1–265. doi: 10.5479/si.00810282.170.

Geller, E. (2003) 'Calcite compensation depth', *Dictionary of Earth Sciences*. Geller, E. McGraw-Hill Companies, Inc.

George, C. L. and Warwick, R. M. (1985) 'Annual macrofauna production in a hard-bottom reef community', *Journal of the Marine Biological Association of the UK*, 65, pp. 713–735.

Gerlach, S. A. (1971) 'On the importance of marine meiofauna for benthos communities', *Oecologia*, 6, pp. 176–190. doi: 10.1007/BF00345719.

Gerlach, S. A. (1978) 'Food-chain relationships in subtidal silty sand marine sediments and the role of meiofauna in stimulating bacterial productivity', *Oecologia*, 33, pp. 55–69. doi: 10.1007/BF00376996.

Gerringer, M. E. *et al.* (2017) 'Comparative feeding ecology of abyssal and hadal fishes through stomach content and amino acid isotope analysis', *Deep-Sea Research I*, 121, pp. 110–120. doi: 10.1016/j.dsr.2017.01.003.

Geslin, E. *et al.* (2011) 'Oxygen respiration rates of benthic foraminifera as measured with oxygen microsensors', *Journal of Experimental Marine Biology and Ecology*, 396, pp. 108–114. doi: 10.1016/j.jembe.2010.10.011.

Gessner, M. O. and Hines, J. (2012) 'Stress as a modifier of biodiversity effects on ecosystem processes?', *Journal of Animal Ecology*, 81, pp. 1143–1145. doi: 10.1111/1365-2656.12011.

Giangrande, A. and Fraschetti, S. (1993) 'Life cycle, growth and secondary production in a brackish-water population of the polychaete *Notomastus latericeus* (Capitellidae) in the Mediterranean Sea', *Marine Ecology*, 14, pp. 313–327. doi: 10.1111/j.1439-0485.1993.tb00003.x.

Giere, O. (2006) 'Ecology and biology of marine Oligochaeta – an inventory rather than another review', *Hydrobiologia*, 564, pp. 103–116. doi: 10.1007/s10750-005-1712-1.

Giere, O. (2009) *Meiobenthology - The Microscopic Motile Fauna of Aquatic Sediment*. 2nd edn. Berlin: Springer-Verlag.

Gilbertson, W. W., Solan, M. and Prosser, J. I. (2012) 'Differential effects of microorganism-invertebrate interactions on benthic nitrogen cycling', *FEMS Microbiology Ecology*, 82, pp. 11–22. doi: 10.1111/j.1574-6941.2012.01400.x.

Gillet, P. and Torresani, S. (2003) 'Structure of the population and secondary production of *Hediste diversicolor* (O. F. Müller, 1776), (Polychaeta, Nereidae) in the Loire estuary, Atlantic Coast, France', *Estuarine, Coastal and Shelf Science*, 56, pp. 621–628. doi: 10.1016/S0272-7714(02)00211-1.

Gillikin, D. P. and Bouillon, S. (2007) 'Determination of $\delta^{18}O$ of water and $\delta^{13}C$ of dissolved inorganic carbon using a simple modification of an elemental analyser-isotope ratio mass spectrometer: An evaluation', *Rapid Communications in Mass Spectrometry*, 21, pp. 1475–1478. doi: 10.1002/rcm.2968.

Ginger, M. L. *et al.* (2001) 'Organic matter assimilation and selective feeding by holothurians in the deep sea: Some observations and comments', *Progress in Oceanography*, 50, pp. 407–421.

del Giorgio, P. A. and Duarte, C. M. (2002) 'Respiration in the open ocean', *Nature*, 420, pp. 379–384.

Giri, C. *et al.* (2011) 'Status and distribution of mangrove forests of the world using earth observation satellite data', *Global Ecology and Biogeography*, 20, pp. 154–159. doi: 10.1111/j.1466-8238.2010.00584.x.

Glasby, G. P. (1977) 'Historical introduction', in Glasby, G. P. (ed.) *Marine Manganese Deposits*. Amsterdam: Elsevier Scientific Publishing Company.

Glasby, G. P. *et al.* (1997) 'Environments of formation of ferromanganese concretions in the Baltic Sea: A critical review', in Nicholson, K. et al. (eds) *Manganese Mineralization: Geochemistry and Mineralogy of Terrestrial and Marine Deposits*. London: Geological Society, pp. 213–237.

Glasby, G. P. (2000) 'Lessons learned from deep-sea mining', *Science*, 289, pp. 551–553.

Glasby, G. P. (2006) 'Manganese: Predominant role of nodules and crusts', in Schulz, H. D. and Zabel, M. (eds) *Marine Geochemistry*. Berlin/Heidelberg: Springer-Verlag, pp. 371–427. doi: 10.1007/3-540-32144-6_11.

Glover, A. G. *et al.* (2016) 'Abyssal fauna of the UK-1 polymetallic nodule exploration claim, Clarion-Clipperton Zone, central Pacific Ocean: Echinodermata', *Biodiversity Data Journal*, 4, p. e7251. doi: 10.3897/BDJ.4.e7251.

Glud, R. N. (2008) 'Oxygen dynamics of marine sediments', *Marine Biology Research*, 4, pp. 243–289. doi: 10.1080/17451000801888726.

Goineau, A. and Gooday, A. J. (2015) 'Radiolarian tests as microhabitats for novel benthic foraminifera: Observations from the abyssal eastern equatorial Pacific (Clarion–Clipperton Fracture Zone)', *Deep-Sea Research I*, 103, pp. 73–85. doi: 10.1016/j.dsr.2015.04.011.

Goineau, A. and Gooday, A. J. (2017) 'Novel benthic foraminifera are abundant and diverse in an area of the abyssal equatorial Pacific licensed for polymetallic nodule exploration', *Scientific Reports*, 7, p. 45288. doi: 10.1038/srep45288.

Gollner, S. *et al.* (2017) 'Resilience of benthic deep-sea fauna to mining

activities', *Marine Environmental Research*, 129, pp. 76–101. doi: 10.1016/j.marenvres.2017.04.010.

Gooday, A. J. (1988) 'A response by benthic foraminifera to the deposition of phytodetritus in the deep sea', *Nature*, 332, pp. 70–73. doi: 10.1038/332070a0.

Gooday, A. J. (1996) 'Epifaunal and shallow infaunal foraminiferal communities at three abyssal NE Atlantic sites subject to differing phytodetritus input regimes', *Deep-Sea Research I*, 43, pp. 1395–1421. doi: 10.1016/S0967-0637(96)00072-6.

Gooday, A. J. (2002) 'Biological responses to seasonally varying fluxes of organic matter to the ocean floor: A review', *Journal of Oceanography*, 58, pp. 305–332. doi: 10.1023/A:1015865826379.

Gooday, A. J. *et al.* (2014) *Atlas of Abyssal Megafauna Morphotypes of the Clipperton-Clarion Fracture Zone*. Available at: http://ccfzatlas.com/wiki/index.php?title=Main_Page (Accessed: 25 November 2017).

Gooday, A. J. *et al.* (2017) 'Giant protists (Xenophyophores, Foraminifera) are exceptionally diverse in parts of the abyssal eastern Pacific licensed for polymetallic nodule exploration', *Biological Conservation*, 207, pp. 106–116. doi: 10.1016/j.biocon.2017.01.006.

Gooday, A. J., Goineau, A. and Voltski, I. (2015) 'Abyssal foraminifera attached to polymetallic nodules from the eastern Clarion Clipperton Fracture Zone: A preliminary description and comparison with North Atlantic dropstone assemblages', *Marine Biodiversity*, 45, pp. 391–412. doi: 10.1007/s12526-014-0301-9.

Google Earth (2018). Available at: https://www.google.com/earth/ (Accessed: 31 May 2018).

Gori, A. *et al.* (2013) 'Bathymetrical distribution and size structure of cold-water coral populations in the Cap de Creus and Lacaze-Duthiers canyons (northwestern Mediterranean)', *Biogeosciences*, 10, pp. 2049–2060. doi: 10.5194/bg-10-2049-2013.

Gorny, M. *et al.* (1993) 'Growth, development and productivity of *Chorismus antarcticus* (Pfeffer) (Crustacea: Decapoda: Natantia) in the eastern Weddell Sea, Antarctica', *Journal of the Marine Biological Association of the UK*, 174, pp. 261–275.

Gowing, M. M. and Wishner, K. F. (1986) 'Trophic relationships of deep-sea calanoid copepods from the benthic boundary layer of the Santa Catalina Basin, California', *Deep-sea Research*, 33, pp. 939–962.

Grahame, J. (1973) 'Assimilation efficiency of *Littorina littorea* (L.) (Gastropoda: Prosobranchiata)', *Journal of Animal Ecology*, 42, pp. 383–389.

De Grave, S. and Whitaker, A. (1999) ‘Benthic community re-adjustment following dredging of a muddy-maerl matrix’, *Marine Pollution Bulletin*, 38, pp. 102–108. doi: 10.1016/S0025-326X(98)00103-9.

Greinert, J. (ed.) (2015) *RV Sonne Fahrtbericht/ Cruise Report SO242-1. JPI OCEANS Ecological aspects of deep-sea mining. DISCOL revisited*. Kiel: GEOMAR Helmholtz-Zentrum für Ozeanforschung Kiel. doi: 10.3289/GEOMAR_REP_NS_26_2015.

Griffiths, J. R. *et al.* (2017) ‘The importance of benthic-pelagic coupling for marine ecosystem functioning in a changing world’, *Global Change Biology*, 23, pp. 2179–2196. doi: 10.1111/gcb.13642.

Grupe, B., Becker, H. J. and Oebius, H. U. (2001) ‘Geotechnical and sedimentological investigations of deep-sea sediments from a manganese nodule field of the Peru Basin’, *Deep-Sea Research II*, 48, pp. 3593–3608. doi: 10.1016/S0967-0645(01)00058-3.

Guichard, F., Reyss, J.-L. and Yokoyama, Y. (1978) ‘Growth rate of manganese nodule measured with ^{10}Be and ^{26}Al’, *Nature*, 272, pp. 155–156. doi: 10.1038/272155a0.

Guilini, K. *et al.* (2010) ‘Nutritional importance of benthic bacteria for deep-sea nematodes from the Arctic ice margin: Results of an isotope tracer experiment’, *Limnology and Oceanography*, 55, pp. 1977–1989. doi: 10.4319/lo.2010.55.5.1977.

Guilini, K. *et al.* (2011) ‘Deep-sea nematodes actively colonise sediments, irrespective of the presence of a pulse of organic matter: Results from an *in situ* experiment’, *PLoS ONE*, 6, p. e18912. doi: 10.1371/journal.pone.0018912.

Gwyther, D. and Wright, M. (2008) *Environmental Impact Statement - Solwara 1 Project. Executive Summary*. Brisbane.

Haeckel, M. *et al.* (2001) ‘Pore water profiles and numerical modelling of biogeochemical processes in Peru Basin deep-sea sediments’, *Deep-Sea Research I*, 48, pp. 3713–3736.

Haedrich, R. L. and Merrett, N. R. (1991) ‘Production/ biomass ratios, size frequencies, and biomass spectra in deep-sea demersal fish’, in *Deep-sea food chains and the global carbon cycle*. Dordrecht: Kluwer Academic Publisher, pp. 157–182.

Hale, R. *et al.* (2011) ‘Predicted levels of future ocean acidification and temperature rise could alter community structure and biodiversity in marine benthic communities’, *Oikos*, 120, pp. 661–674. doi: 10.1111/j.1600-0706.2010.19469.x.

Hall, S. J. and Raffaelli, D. G. (1993) ‘Food webs: Theory and reality’, *Advances in Ecological Research*, 24, pp. 187–239. doi: 10.1016/S0065-

2504(08)60043-4.

Han, K. N., Lee, S. W. and Wang, S. Y. (2008) ‘The effect of temperature on the energy budget of the Manila clam, *Ruditapes philippinarum*’, *Aquaculture International*, 16, pp. 143–152. doi: 10.1007/s10499-007-9133-y.

Hannah, F., Rogerson, A. and Laybourn-Parry, J. (1994) ‘Respiration rates and biovolumes of common benthic Foraminifera (Protozoa)’, *Journal of the Marine Biological Association of the UK*, 74, pp. 301–312. doi: 10.1017/S0025315400039345.

Hannides, A. K. and Smith, C. R. (2003) ‘The Northeast Pacific abyssal plain’, in Black, K. D. and Shimmield, G. B. (eds) *Biogeochemistry of Marine Systems*. Oxford: Blackwell Publishing, pp. 208–237.

Hannis, S., Bide, T. and Minks, A. (2009) *Cobalt*. Keyworth. Available at: www.MineralsUK.com.

Harris, P. T. *et al.* (2014) ‘Geomorphology of the oceans’, *Marine Geology*, 352, pp. 4–24. doi: 10.1016/j.margeo.2014.01.011.

Harris, P. T. and Whiteway, T. (2011) ‘Global distribution of large submarine canyons: Geomorphic differences between active and passive continental margins’, *Marine Geology*, 285, pp. 69–86. doi: 10.1016/j.margeo.2011.05.008.

Harrold, C. and Reed, D. C. (1985) ‘Food availability, sea urchin grazing, and kelp forest community structure’, *Ecology*, 66, pp. 1160–1169.

Hawkins, M. J. (1998) ‘Recovering cobalt from primary and secondary sources’, *JOM*, 50, pp. 46–50. doi: 10.1007/s11837-998-0353-z.

Hedges, L. V. and Olkin, I. (1985a) ‘Estimation of a single effect size: Parametric and nonparametric methods’, in *Statistical Methods for Meta-Analysis*. Orlando: Academic Press, Inc., pp. 75–106. doi: 10.1016/B978-0-08-057065-5.50010-5.

Hedges, L. V. and Olkin, I. (1985b) ‘Parametric estimation of effect size from a series of experiments’, in *Statistical Methods for Meta-Analysis*. Orlando: Academic Press, Inc., pp. 107–145. doi: 10.1016/B978-0-08-057065-5.50011-7.

Hein, J. R. *et al.* (2013) ‘Deep-ocean mineral deposits as a source of critical metals for high- and green-technology applications: Comparison with land-based resources’, *Ore Geology Reviews*, 51, pp. 1–14. doi: 10.1016/j.oregeorev.2012.12.001.

Hein, J. R. *et al.* (2015) ‘Critical metals in manganese nodules from the Cook Islands EEZ, abundances and distributions’, *Ore Geology Reviews*, 68, pp. 97–116. doi: 10.1016/j.oregeorev.2017.06.032.

Hein, J. R. (2016) ‘Manganese nodules’, *Encyclopedia of Marine Geosciences*. Springer Science+Business Media Dordrecht.

Hein, J. R. and Koschinsky, A. (2014) ‘Deep-ocean ferromanganese crusts and nodules’, in Holland, H. and Turekian, K. (eds) *Treatise on Geochemistry*. 2nd edn. Amsterdam: Elsevier Ltd., pp. 273–291. doi: 10.1016/B978-0-08-095975-7.01111-6.

Heiner, I., Vinther Sørensen, M. and Møbjerg Kristensen, R. (2018) ‘Loricifera (Girdle Wearers)’, *Grzimek’s Animal Life Encyclopedia*. Encyclopedia.com. Available at: http://www.encyclopedia.com/environment/encyclopedias-almanacs-transcripts-and-maps/loricifera-girdle-wearers.

Heip, C. H. R. *et al.* (2001) ‘The role of the benthic biota in sedimentary metabolism and sediment-water exchange processes in the Goban Spur area (NE Atlantic)’, *Deep-Sea Research II*, 48, pp. 3223–3243. doi: 10.1016/S0967-0645(01)00038-8.

Heip, C. H. R. and Herman, R. (1979) ‘Production of *Nereis diversicolor* O. F. Müller (Polychaeta) in a shallow brackish-water pond’, *Estuarine and Coastal Marine Science*, 8, pp. 297–305.

Heip, C. H. R., Vincx, M. and Vranken, G. (1985) ‘The ecology of marine nematodes’, *Oceanography and Marine Biology: An Annual Review*, 23, pp. 399–489.

Hendelberg, M. and Jensen, P. (1993) ‘Vertical distribution of the nematode fauna in a coastal sediment influenced by seasonal hypoxia in the bottom water’, *Ophelia*, 37, pp. 83–94. doi: 10.1080/00785326.1993.10429909.

Henschke, N. *et al.* (2013) ‘Salp-falls in the Tasman Sea: A major food input to deep-sea benthos’, *Marine Ecology Progress Series*, 491, pp. 165–175. doi: 10.3354/meps10450.

Herman, P. M. J., Heip, C. H. R. and Vranken, G. (1983) ‘The production of *Cyprideis torosa* Jones 1850 (Crustacea, Copepoda)’, *Oecologia*, 58, pp. 326–331.

Herman, P. M. J. and Vranken, G. (1988) ‘Studies of the life-history and energetics of marine and brackish-water nematodes’, *Oecologia*, 77, pp. 457–463.

Herrmann, M. *et al.* (2008) ‘Dense water formation in the Gulf of Lions shelf: Impact of atmospheric interannual variability and climate change’, *Continental Shelf Research*, 28, pp. 2092–2112. doi: 10.1016/j.csr.2008.03.003.

Hessler, R. R. and Jumars, P. A. (1974) ‘Abyssal community analysis from replicate box cores in the central North Pacific’, *Deep-Sea Research*, 21, pp. 185–209. doi: 10.1016/0011-7471(74)90058-8.

Hibert, C., Ekström, G. and Stark, C. P. (2014) ‘Dynamics of the Bingham Canyon Mine landslides from seismic signal analysis’, *Geophysical Research Letters*, 41, pp. 4535–4541. doi: 10.1002/2014GL060592.

Higgins, R. P. and Thiel, H. (1988) *Introduction to the Study of Meiofauna*. Washington, DC: Smithonian Institution Press.

Highsmith, R. C. and Coyle, K. O. (1990) 'High productivity of northern Bering Sea benthic amphipods', *Nature*, 344, pp. 862–864.

Hill, M. O. (1973) 'Diversity and evenness: A unifying notation and its consequences', *Ecology*, 54, pp. 427–432. doi: 10.2307/1934352.

Hinchey, E. K. *et al.* (2006) 'Responses of estuarine benthic invertebrates to sediment burial: The importance of mobility and adaptation', *Hydrobiologia*, 556, pp. 85–98. doi: 10.1007/s10750-005-1029-0.

Hoffmann, R. (2009) 'A new *Rhabdammina* species (Foraminifera: Textulariina) with an unusual distribution pattern from Cretaceous (Germany) and Recent (Greece: Aegina) localities René', *Berliner paläobiologische Abhandlungen*, 10, pp. 215–222.

Hofmann, E. E. *et al.* (2011) 'Modeling the dynamics of continental shelf carbon', *Annual Review of Marine Science*, 3, pp. 93–122. doi: 10.1146/annurev-marine-120709-142740.

Holovachov, O. *et al.* (2011) '*Endeolophos skeneae* sp. nov. (Chromadoridae) - A free-living marine nematode epibiotically associated with deep-sea gastropod *Skenea profunda* (Skeneidae)', *Journal of the Marine Biological Association of the United Kingdom*, 91, pp. 387–394. doi: 10.1017/S0025315410001669.

Honjo, S. *et al.* (1995) 'Export production of particles to the interior of the equatorial Pacific Ocean during the 1992 EqPac experiment', *Deep-Sea Research*, 42, pp. 831–870.

Horowitz, L. S. (2004) 'Toward a viable independence? The Koniambo Project and the political economy of mining in New Caledonia', *The Contemporary Pacific*, 16, pp. 287–319.

Horton, T. *et al.* (2018) *World Register of Marine Species (WoRMS)*. WoRMS Editorial Board. doi: 10.14284/170.

Hoving, H.-J. T. *et al.* (2017) 'Bathyal feasting: Post-spawning squid as a source of carbon for deep-sea benthic communities', *Proceedings of the Royal Society B: Biological Sciences*, 284, p. 20172096. doi: 10.1098/rspb.2017.2096.

Howe, J. A. *et al.* (2010) 'Fjord systems and archives: A review', *Geological Society, London, Special Publications*, 344, pp. 5–15. doi: 10.1144/SP344.2.

Howe, S., Maurer, D. and Leathem, W. A. (1988) 'Secondary production of benthic molluscs from the Delawere Bay and coastal area', *Estuarine, Coastal and Shelf Science*, 26, pp. 81–94.

Howell, K. L. *et al.* (2004) 'Feeding ecology of deep-sea seastars (Echinodermata: Asteroidea): A pigment biomarker approach', *Marine Ecology*

Progress Series, 266, pp. 103–110. doi: 10.3354/meps266103.

Hsieh, T. C., Ma, K. H. and Chao, A. (2016) 'iNEXT: An R package for rarefaction and extrapolation of species diversity (Hill numbers)', *Methods in Ecology and Evolution*. Edited by G. McInerny, 7, pp. 1451–1456. doi: 10.1111/2041-210X.12613.

Hudson, I. R. *et al.* (2004) 'Temporal variations in fatty acid composition of deep-sea holothurians: Evidence of bentho-pelagic coupling', *Marine Ecology Progress Series*, 281, pp. 109–120. doi: 10.3354/meps281109.

Hudson, I. R. *et al.* (2005) 'Feeding behaviour of deep-sea dwelling holothurians: Inferences from a laboratory investigation of shallow fjordic species', *Journal of Marine Systems*, 57, pp. 201–218. doi: 10.1016/j.jmarsys.2005.02.004.

Hudson, I. R., Wigham, B. D. and Tyler, P. A. (2004) 'The feeding behaviour of a deep-sea holothurian, Stichopus tremulus (Gunnerus) based on in situ observations and experiments using a remotely operated vehicle', *Journal of Experimental Marine Biology and Ecology*, 301, pp. 75–91. doi: 10.1016/j.jembe.2003.09.015.

Huffard, C. L. *et al.* (2016) 'Demographic indicators of change in a deposit-feeding abyssal holothurian community (Station M, 4000m)', *Deep-Sea Research I*, 109, pp. 27–39. doi: 10.1016/j.dsr.2016.01.002.

Hughes, S. J. M. (2010) *Towards deep-sea toxicology: Experimental approaches with echinoderms, PhD-Thesis*. University of Southampton.

Hughes, S. J. M. *et al.* (2011) 'Deep-sea echinoderm oxygen consumption rates and an interclass comparison of metabolic rates in Asteroidea, Crinoidea, Echinoidea, Holothuroidea and Ophiuroidea', *Journal of Experimental Biology*, 214, pp. 2512–2521. doi: 10.1242/jeb.055954.

Hume, N. (2017) 'Vale to mothball New Caledonia nickel mine if no stake buyers found', *Financial Times*, 8 December. Available at: https://www.ft.com/content/763d5ede-d4f6-3aca-b94e-fe35eb3337f6.

Humes, A. G. (1974) 'New cyclopoid copepods associated with an abyssal holothurian in the eastern North Atlantic', *Journal of Natural History*, 8, pp. 101–117. doi: 10.1080/00222937400770071.

Huston, M. A. (1994) 'Introduction', in *Biological Diversity. The coexistence of species on changing landscapes*. Cambridge: Cambridge University Press, pp. 1–11.

Iken, K. *et al.* (2001) 'Food web structure of the benthic community at the Porcupine Abyssal Plain (NE Atlantic): A stable isotope analysis', *Progress in Oceanography*, 50, pp. 383–405.

Ilan, M., Ben-Eliahu, M. N. and Galil, B. (1994) ‘Three deep water sponges from the eastern Mediterranean and their associated Fauna’, *Ophelia*, 39, pp. 45–54. doi: 10.1080/00785326.1994.10429901.

Ingole, B. S. *et al.* (2000) ‘Response of meiofauna to immediate benthic disturbance in the central Indian Ocean basin’, *Marine Georesources and Geotechnology*, 18, pp. 263–272. doi: 10.1080/10641190009353794.

Ingole, B. S. *et al.* (2001) ‘Response of deep-sea macrobenthos to a small-scale environmental disturbance’, *Deep-Sea Research II*, 48, pp. 3401–3410. doi: 10.1016/S0967-0645(01)00048-0.

Ingole, B. S. and Koslow, J. A. (2005) ‘Deep-sea ecosystems of the Indian Ocean’, *Indian Journal of Marine Sciences*, 34, pp. 27–34.

Ingole, B. S., Pavithran, S. and Ansari, Z. A. (2005) ‘Restoration of deep-sea macrofauna after simulated benthic disturbance in the Central Indian Basin’, *Marine Georesources and Geotechnology*, 23, pp. 267–288. doi: 10.1080/10641190500446573.

International Seabed Authority (2010) *A geological model of polymetallic nodule deposits in the Clarion Clipperton Fracture Zone. ISA technical study No. 6*. Kingston, Jamaica: International Seabed Authority.

International Seabed Authority (2011) *Draft environmental management plan for the Clarion-Clipperton Zone I*. Kingston, Jamaica: International Seabed Authority.

International Seabed Authority (2013) *Decision of the Council of the International Seabed Authority relating to amendments to the Regulations on Prospecting and Exploration for Polymetallic Nodules in the Area and related matters*. Kingston, Jamaica: International Seabed Authority. Council.

Iseki, K. (1981) ‘Particulate organic matter transport to the deep sea by salp fecal pellets’, *Marine Ecology Progress Series*, 5, pp. 55–60. doi: 10.3354/meps005055.

Ishida, H. *et al.* (2013) ‘Effects of CO_2 on benthic biota: An *in situ* benthic chamber experiment in Storfjorden (Norway)’, *Marine Pollution Bulletin*, 73, pp. 443–451. doi: 10.1016/j.marpolbul.2013.02.009.

James, G. (2013) *An Introduction to Statistical Learning with Applications in R*. 1st edn. New York: Springer Verlag.

Jamieson, A. J. *et al.* (2011) ‘Functional effects of the hadal sea cucumber *Elpidia atakama* (Echinodermata: Holothuroidea, Elasipodida) reflect small-scale patterns of resource availability’, *Marine Biology*, 158, pp. 2695–2703. doi: 10.1007/s00227-011-1767-7.

Jamieson, H. E. (2011) ‘Geochemistry and mineralogy of solid mine waste: Essential knowledge for predicting environmental impact’, *Elements*, 7, pp.

381–386. doi: 10.2113/gselements.7.6.381.

Jangoux, M. (1982) ‘Food and feeding mechanisms: Asteroidea’, in Jangoux, M. and Lawrence, J. M. (eds) *Echinoderm Nutrition*. Rotterdam: Balkema, pp. 117–159.

Jankowski, J. A. and Zielke, W. (2001) ‘The mesoscale sediment transport due to technical activities in the deep sea’, *Deep-Sea Research II*, 48, pp. 3487–3521. doi: 10.1016/S0967-0645(01)00054-6.

Janssen, A. *et al.* (2015) ‘A reverse taxonomic approach to assess macrofaunal distribution patterns in abyssal pacific polymetallic nodule fields’, *PLoS ONE*, 10, pp. 1–26. doi: 10.1371/journal.pone.0117790.

Jansson, B.-O. (1967) ‘The significance of grain size and pore water content for the interstitial fauna of sandy beaches’, *Oikos*, 18, pp. 311–322.

Jeffrey, S. W. and Humphrey, G. F. (1975) ‘New spectrophotometric equations for determining chlorophylls a, b, c_1 and c_2 in higher plants, algae and natural phytoplankton’, *Biochemie und Physiologie der Pflanzen*, 167, pp. 191–194. doi: 10.1016/S0015-3796(17)30778-3.

Jeffreys, R. M. *et al.* (2013) ‘Feeding preferences of abyssal macrofauna inferred from *in situ* pulse chase experiments’, *PLoS ONE*, 8, p. e80510. doi: 10.1371/journal.pone.0080510.

Jennings, S. *et al.* (2008) ‘Global-scale predictions of community and ecosystem properties from simple ecological theory’, *Proceedings of the Royal Society B: Biological Sciences*, 275, pp. 1375–1383. doi: 10.1098/rspb.2008.0192.

Johansen, P.-O. *et al.* (2018) ‘Temporal changes in benthic macrofauna on the west coast of Norway resulting from human activities’, *Marine Pollution Bulletin*. Elsevier, 128, pp. 483–495. doi: 10.1016/j.marpolbul.2018.01.063.

Johnson, W. S. (1973) ‘Respiration rates of some New Zealand echinoderms (note)’, *New Zealand Journal of Marine and Freshwater Research*, 7, pp. 165–169. doi: 10.1080/00288330.1973.9515463.

Johnson, W. S. (1976) ‘Population energetics of the intertidal isopod *Cirolana harfordi*’, *Marine Biology*, 36, pp. 351–357. doi: 10.1007/BF00389197.

Jones, C. G., Lawton, J. H. and Shachak, M. (1994) ‘Organisms as ecosystem engineers’, *Oikos*, 69, pp. 373–386.

Jones, D. O. B. *et al.* (2014) ‘Global reductions in seafloor biomass in response to climate change’, *Global Change Biology*, 20, pp. 1861–1872. doi: 10.1111/gcb.12480.

Jones, D. O. B. *et al.* (2017) ‘Biological responses to disturbance from simulated deep-sea polymetallic nodule mining’, *PLOS ONE*, 12, p. e0171750.

doi: 10.1371/journal.pone.0171750.

Jones, H. and Boger, D. V. (2012) ‘Sustainability and waste management in the resource industries’, *Industrial & Engineering Chemistry Research*, 51, pp. 10057–10065. doi: 10.1021/ie202963z.

Jones, M. K. (2008) ‘Swedish scientific expeditions to Spitsbergen, 1758-1908’, *TijdSchrift voor Skandinavistiek*, 29, pp. 219–235.

Jones, R. T. *et al.* (2002) ‘Recovery of cobalt from slag in a DC arc furnace at Chambishi, Zambia’, *The Journal of The South African Institute of Mining and Metallurgy*, 1, pp. 5–9.

de Jonge, V. N. (1980) ‘Fluctuations in the organic carbon to chlorophyll a ratios for estuarine benthic diatom populations’, *Marine Ecology Progress Series*, 2, pp. 345–353. doi: 10.3354/meps002345.

Jordana, E. *et al.* (2001) ‘Food sources, ingestion and absorption in the suspension-feeding polychaete, *Ditrupa arietina* (O. F. Müller)’, *Journal of Experimental Marine Biology and Ecology*, 266, pp. 219–236. doi: 10.1016/S0022-0981(01)00357-4.

Josefson, A. B. (1982) ‘Regulation of population size, growth, and production of a deposit-feeding bivalve: A long-term field study of three deep-water populations off the Swedish west coast’, *Journal of Experimental Marine Biology and Ecology*, 59, pp. 125–150.

Josefson, A. B. and Widbom, B. (1988) ‘Differential response of benthic macrofauna and meiofauna to hypoxia in the Gullmar Fjord basin’, *Marine Biology*, 100, pp. 31–40. doi: 10.1007/BF00392952.

Jumars, P. A. (1981) ‘Limits in predicting and detecting benthic community responses to manganese nodule mining’, *Marine Mining*, 3, pp. 213–229.

Jumars, P. A., Dorgan, K. M. and Lindsay, S. M. (2015) ‘Diet of worms emended: An update of polychaete feeding guilds’, *Annual Review of Marine Science*, 7, pp. 497–520. doi: 10.1146/annurev-marine-010814-020007.

Jung, H.-S. *et al.* (1998) ‘Geochemical and mineralogical characteristics in two-color core sediments from the Korea Deep Ocean Study (KODOS) area, northeast equatorial Pacific’, *Marine Geology*, 144, pp. 295–309. doi: 10.1016/S0025-3227(97)00108-4.

Junqueira De Souza Dantas, R., Laut, L. L. M. and Caetano, C. H. S. (2017) ‘Diet of the amphi-Atlantic scaphopod Fissidentalium candidum in the deep waters of Campos Basin, south-eastern Brazil’, *Journal of the Marine Biological Association of the United Kingdom*, 97(06), pp. 1259–1266. doi: 10.1017/S002531541600059X.

Kaartvedt, S. and Svendsen, H. (1990) ‘Impact of freshwater runoff on physical oceanography and plankton distribution in a Western Norwegian fjord: An

experiment with a controlled discharge from a hydroelectric power plant', *Estuarine, Coastal and Shelf Science*, 31, pp. 381–395. doi: 10.1016/0272-7714(90)90033-N.

Kalejta, B. (1992) 'Distribution, biomass and production of *Ceratonereis erythraeensis* (Fauvel) and *Ceratonereis keiskama* (Day) at the Berg River Estuary, South Africa', *South African Journal of Zoology*, 27, pp. 121–129.

Kallmeyer, J. *et al.* (2012) 'Global distribution of microbial abundance and biomass in subseafloor sediment', *Proceedings of the National Academy of Sciences*, 109, pp. 16213–16216. doi: 10.1073/pnas.1203849109.

Kamenskaya, O. (2005) '*Spiculammina delicata* gen. et sp. n., a new xenophyophore from the eastern Pacific (Psamminidae)', *Invertebrate Zoology*, 2, pp. 23–27.

Kamenskaya, O. *et al.* (2012) 'Large, enigmatic foraminiferan-like protists in the eastern part of the Clarion-Clipperton Fracture Zone (abyssal north-eastern subequatorial Pacific): Biodiversity and vertical distribution in the sediment', *Marine Biodiversity*, 42, pp. 311–327. doi: 10.1007/s12526-012-0114-7.

Kamenskaya, O. *et al.* (2015) 'Xenophyophores (Protista, Foraminifera) from the Clarion-Clipperton Fracture Zone with description of three new species', *Marine Biodiversity*, 45, pp. 581–593. doi: 10.1007/s12526-015-0330-z.

Kamenskaya, O. *et al.* (2017) 'Xenophyophores (Rhizaria, Foraminifera) from the Russian license area of the Clarion-Clipperton Zone (eastern equatorial Pacific), with the description of three new species', *Marine Biodiversity*, 47, pp. 299–306. doi: 10.1007/s12526-016-0595-x.

Kamenskaya, O., Melnik, V. F. and Gooday, A. J. (2013) 'Giant protists (xenophyophores and komokiaceans) from the Clarion-Clipperton ferromanganese nodule field (eastern Pacific)', *Biology Bulletin Reviews*, 3, pp. 388–398. doi: 10.1134/S2079086413050046.

Kapiris, K. (2012) 'Feeding habits of both deep-water red shrimps, *Aristaeomorpha foliacea* and *Aristeus antennatus* (Decapoda, Aristeidae) in the Ionian Sea (E. Mediterranean)', in Kapiris, K. (ed.) *Food Quality*. Rijeka: InTech, pp. 111–134. doi: 10.5772/33623.

Kaufmann, R. S. and Smith, K. L. (1997) 'Activity patterns of mobile epibenthic megafauna at an abyssal site in the eastern North Pacific : Results from a 17-month time-lapse photographic study', *Deep-Sea Research I*, 44, pp. 559–579.

Kędra, M. *et al.* (2015) 'Status and trends in the structure of Arctic benthic food webs', *Polar Research*, 34, p. 23775. doi: 10.3402/polar.v34.23775.

Kéfi, S. *et al.* (2012) 'More than a meal… integrating non-feeding interactions into food webs', *Ecology Letters*, 15, pp. 291–300. doi: 10.1111/j.1461-

0248.2011.01732.x.

Kersken, D., Janussen, D. and Martínez Arbizu, P. (2017a) ‘Biodiversity of deep-sea sponges (Porifera) in the Clarion-Clipperton Fracture Zone (CCFZ), NE-Pacific’.

Kersken, D., Janussen, D. and Martínez Arbizu, P. (2017b) ‘Deep-sea glass sponges (Hexactinellida) from polymetallic nodule fields in the Clarion-Clipperton Fracture Zone (CCFZ), northeastern Pacific: Part I – Amphidiscophora’, *Marine Biodiversity*, pp. 1–6. doi: 10.1007/s12526-017-0805-1.

Khripounoff, A. *et al.* (2006) ‘Geochemical and biological recovery of the disturbed seafloor in polymetallic nodule fields of the Clipperton-Clarion Fracture Zone (CCFZ) at 5,000-m depth’, *Limnology and Oceanography*, 51, pp. 2033–2041. doi: 10.4319/lo.2006.51.5.2033.

Khripounoff, A. *et al.* (2014) ‘Deep cold-water coral ecosystems in the Brittany submarine canyons (Northeast Atlantic): Hydrodynamics, particle supply, respiration, and carbon cycling’, *Limnology and Oceanography*, 59(1), pp. 87–98. doi: 10.4319/lo.2014.59.1.0087.

Khripounoff, A. and Sibuet, M. (1980) ‘La nutrition d’echinodermes abyssaux. I. Alimentation des holothuries’, *Marine Biology*, 60, pp. 17–26.

Kidd, R. B. and Huggett, J. (1981) ‘Rock debris on abyssal plains in the Northeast Atlantic: A comparison of epibenthic sledge hauls and photographic surveys’, *Oceanologica Acta*, 4, pp. 99–104.

Kirchman, D. L., Morán, X. A. G. and Ducklow, H. (2009) ‘Microbial growth in the polar oceans — role of temperature and potential impact of climate change’, *Nature Reviews Microbiology*, 7, pp. 451–459. doi: 10.1038/nrmicro2115.

Kirchman, D. L. and Rich, J. H. (1997) ‘Regulation of bacterial growth rates by dissolved organic carbon and temperature in the equatorial Pacific Ocean’, *Microbial Ecology*, 33, pp. 11–20. doi: 10.1007/s002489900003.

Klein, G., Rachor, E. and Gerlach, S. A. (1975) ‘Dynamics and productivity of two populations of the benthic tube-dwelling amphipod *Ampelisca brevicornis* (Costa) in Helgoland Bight’, *Ophelia*, 14, pp. 139–159. doi: 10.1080/00785236.1975.10421973.

Klein, H. (1993) ‘Near-bottom currents in the deep Peru Basin, DISCOL experimental area’, *Deutsche Hydrographische Zeitschrift*, 45, pp. 31–42. doi: 10.1007/BF02226550.

Klepper, O. and Van De Kamer, J. P. G. (1987) ‘The use of mass balances to test and improve the estimates of carbon fluxes in an ecosystem’, *Mathematical Biosciences*, 85, pp. 37–49. doi: 10.1016/0025-5564(87)90098-8.

Knight-Jones, E. W. (1952) ‘Feeding in *Saccoglossus* (Enteropneusta)’, *Proceedings of the Zoological Society of London*, 123, pp. 637–654.

Knol, M. J., Pestman, W. R. and Grobbee, D. E. (2011) ‘The (mis)use of overlap of confidence intervals to assess effect modification’, *European Journal of Epidemiology*, 26, pp. 253–254. doi: 10.1007/s10654-011-9563-8.

Koch, V. and Wolff, M. (2002) ‘Energy budget and ecological role of mangrove epibenthos in the Caeté estuary, North Brazil’, *Marine Ecology Progress Series*, 228, pp. 119–130. doi: 10.3354/meps228119.

Kones, J. K. *et al.* (2009) ‘Are network indices robust indicators of food web functioning? A Monte Carlo approach’, *Ecological Modelling*, 220, pp. 370–382. doi: 10.1016/j.ecolmodel.2008.10.012.

Koopmans, M., Martens, D. and Wijffels, R. H. (2010) ‘Growth efficiency and carbon balance for the sponge *Haliclona oculata*’, *Marine Biotechnology*, 12, pp. 340–349. doi: 10.1007/s10126-009-9228-8.

Koricheva, J., Gurevitch, J. and Mengersen, K. (2013) *Handbook of Meta-Analysis in Ecology and Evolution*. Princeton: Princeton University Press.

Koschinsky, A. *et al.* (2001) ‘Experiments on the influence of sediment disturbances on the biogeochemistry of the deep-sea environment’, *Deep-Sea Research II*, 48, pp. 3629–3651. doi: 10.1016/S0967-0645(01)00060-1.

Koschinsky, A., Borowski, C. and Halbach, P. (2003) ‘Reactions of the heavy metal cycle to industrial activities influence on heavy metal cycle in the deep sea’, *International Review of Hydrobiology*, 88, pp. 102–127.

Kostadinov, T. S. *et al.* (2016) ‘Carbon-based phytoplankton size classes retrieved via ocean color estimates of the particle size distribution’, *Ocean Science*, 12, pp. 561–575. doi: 10.5194/os-12-561-2016.

Kreeger, D. A., Hawkins, A. J. S. and Bayne, B. L. (1996) ‘Use of dual-labeled microcapsules to discern the physiological fates of assimilated carbohydrate, protein carbon, and protein nitrogen in suspension-feeding organisms’, *Limnology and Oceanography*, 41, pp. 208–215.

Kreeger, D. A. and Newell, R. I. E. (2001) ‘Seasonal utilization of different seston carbon sources by the ribbed mussel, *Geukensia demissa* (Dillwyn) in a mid-Atlantic salt marsh’, *Journal of Experimental Marine Biology and Ecology*, 260, pp. 71–91. doi: 10.1016/S0022-0981(01)00242-8.

Kristensen, E. (1984) ‘Life cycle, growth and production in estuarine populations of the polychaetes *Nereis virens* and *Nereis diversicolor*’, *Holarctic Ecology*, 7, pp. 249–256.

Krylova, E. M. *et al.* (2015) ‘Vesicomyinae (Bivalvia: Vesicomyidae) of the Kuril–Kamchatka Trench and adjacent abyssal regions’, *Deep-Sea Research II*,

111, pp. 198–209. doi: 10.1016/j.dsr2.2014.10.004.

Kuhn, T. *et al.* (2017) 'Composition, formation, and occurrence of polymetallic nodules', in Sharma, R. (ed.) *Deep-Sea Mining*. Cham: Springer International Publishing, pp. 23–63. doi: 10.1007/978-3-319-52557-0_2.

Kuhnt, W. and Collins, E. S. (1995) 'Fragile abyssal Foraminifera from the Northwestern Sargasso Sea: Distribution, ecology, and paleoceanographic significance', in Kaminski, M. A., Gerroch, S., and Gasiński, M. A. (eds) *Proceedings of the Fourth International Workshop on Agglutinated Foraminifera*. Kraków: Grzybowski Foundation Special Publication, pp. 159–172.

Kvassnes, A. J. S. and Iversen, E. (2013) 'Waste sites from mines in Norwegian fjords', *Mineralproduksjon*, 3, pp. A27–A38.

Kwasnitschka, T. *et al.* (2016) 'DeepSurveyCam - a deep ocean optical mapping system', *Sensors*, 16. doi: 10.3390/s16020164.

De La Rocha, C. L. and Passow, U. (2007) 'Factors influencing the sinking of POC and the efficiency of the biological carbon pump', *Deep-Sea Research II*, 54, pp. 639–658. doi: 10.1016/j.dsr2.2007.01.004.

Labarta, U., Fernández-Reiríz, M. J. and Babarro, J. M. F. (1997) 'Differences in physiological energetics between intertidal and raft cultivated mussels *Mytilus galloprovincialis*', *Marine Ecology Progress Series*, 152, pp. 167–173.

Laguionie-Marchais, C. *et al.* (2013) 'Inter-annual dynamics of abyssal polychaete communities in the North East Pacific and North East Atlantic—A family-level study', *Deep-Sea Research I*, 75, pp. 175–186. doi: 10.1016/j.dsr.2012.12.007.

Lahajnar, N. *et al.* (2005) 'Dissolved organic carbon (DOC) fluxes of deep-sea sediments from the Arabian Sea and NE Atlantic', *Deep-Sea Research II*, 52, pp. 1947–1964. doi: 10.1016/j.dsr2.2005.05.006.

Langenkämper, D. *et al.* (2017) 'BIIGLE 2.0 - Browsing and annotating large marine image collections', *Frontiers in Marine Science*, 4, pp. 1–10. doi: 10.3389/fmars.2017.00083.

Larson, R. J. (1979) 'Feeding in coronate medusae (Class Scyphozoa, Order Coronatae)', *Marine and Freshwater Behaviour and Physiology*, 6, pp. 123–129. doi: 10.1080/10236247909378559.

Lasker, R., Wells, J. B. J. and McIntyre, A. D. (1970) 'Growth, reproduction, respiration and carbon utilization of the sand-dwelling harpacticoid copepod, *Asellopsis intermedia*', *Journal of the Marine Biological Association of the UK*, 50, pp. 147–160. doi: 10.1017/S0025315400000679.

Lasserre, P. (1970) 'Action des variations de salinité sur le métabolisme respiratoire d'oligochètes euryhalins du genre Marionina Michaelsen', *Journal*

of Experimental Marine Biology and Ecology, 4, pp. 150–155.

Lastras, G. *et al.* (2007) 'A walk down the Cap de Creus canyon, northwestern Mediterranean Sea: Recent processes inferred from morphology and sediment bedforms', *Marine Geology*, 246, pp. 176–192. doi: 10.1016/j.margeo.2007.09.002.

Laubier, L. and Monniot, C. (1985) *Peuplements profonds du Golfe de Gascogne. Campagnes BIOGAS*. Paris: Ifremer.

Laudien, J., Brey, T. and Arntz, W. E. (2003) 'Population structure, growth and production of the surf clam *Donax serra* (Bivalvia, Donacidae) on two Namibian sandy beaches', *Estuarine, Coastal and Shelf Science*, 58S, pp. 105–115. doi: 10.1016/S0272-7714(03)00044-1.

Lebrato, M. and Jones, D. O. B. (2009) 'Mass deposition event of *Pyrosoma atlanticum* carcasses off Ivory Coast (West Africa)', *Limnology and Oceanography*, 54, pp. 1197–1209. doi: 10.4319/lo.2009.54.4.1197.

Leduc, D. and Pilditch, C. A. (2013) 'Effect of a physical disturbance event on deep-sea nematode community structure and ecosystem function', *Journal of Experimental Marine Biology and Ecology*, 440, pp. 35–41. doi: 10.1016/j.jembe.2012.11.015.

Leduc, D., Pilditch, C. A. and Nodder, S. D. (2016) 'Partitioning the contributions of mega-, macro- and meiofauna to benthic metabolism on the upper continental slope of New Zealand: Potential links with environmental factors and trawling intensity', *Deep-Sea Research I*, 108, pp. 1–12. doi: 10.1016/j.dsr.2015.12.003.

Lee, S. Y. (1997) 'Potential trophic importance of the faecal material of the mangrove sesarmine crab *Sesarma messa*', *Marine Ecology Progress Series*, 159, pp. 275–284. doi: 10.3354/meps159275.

Legal and Technical Commission (2008) *Report on the International Seabed Authority's workshop on polymetallic nodule mining technology: Current status and challenges ahead*. Kingston, Jamaica.

Legal and Technical Commission (2011) *Environmental management plan for the Clarion-Clipperton Zone*. Kingston, Jamaica: International Seabed Authority.

Leitner, A. B. *et al.* (2017) 'Environmental and bathymetric influences on abyssal bait-attending communities of the Clarion Clipperton Zone', *Deep-Sea Research I*, 125, pp. 65–80. doi: 10.1016/j.dsr.2017.04.017.

De Leo, F. C. *et al.* (2010) 'Submarine canyons: Hotspots of benthic biomass and productivity in the deep sea', *Proceedings of the Royal Society B: Biological Sciences*, 277, pp. 2783–2792. doi: 10.1098/rspb.2010.0462.

Leslie, A. (1879) *The Arctic voyages of Adolf Erik Nordenskiöld*. London: Macmillan & Co.

Levin, L. A. (1994) 'Paleoecology and ecology of xenophyophores', *Advances in Deepsea Paleoecology*, 9, pp. 32–41.

Levin, L. A. *et al.* (1999) 'Macrofaunal processing of phytodetritus at two sites on the Carolina margin: *In situ* experiments using ^{13}C-labeled diatoms', *Marine Ecology Progress Series*, 182, pp. 37–54. doi: 10.3354/meps182037.

Levin, L. A. *et al.* (2016) 'Defining "serious harm" to the marine environment in the context of deep-seabed mining', *Marine Policy*, 74, pp. 245–259. doi: 10.1016/j.marpol.2016.09.032.

Licker, M. D. (2008) 'Overdeepening', *Dictionary of Earth Sciences*. 2nd edn. McGraw-Hill Companies, Inc. doi: 10.1036/0071417982.

Ligas, A. *et al.* (2009) 'Effects of chronic trawling disturbance on the secondary production of suprabenthic and infaunal crustacean communities in the Adriatic Sea (NW Mediterranean)', *Ciencias Marinas*, 35, pp. 195–207.

Lim, S.-C. *et al.* (2017) 'A new genus and species of abyssal sponge commonly encrusting polymetallic nodules in the Clarion-Clipperton Zone, East Pacific Ocean', *Systematics and Biodiversity*, pp. 1–13. doi: 10.1080/14772000.2017.1358218.

Linke, P. (2011) *FS Sonne Fahrtbericht/ Cruise Report SO-210 ChiFlux. Identification and investigation of fluid flux, mass wasting and sediments in the forearc of the central Chilean subduction zone. Valparaiso 23.09.2010 - Valparaiso 01.11.2010*. Kiel.

Linley, T. D. (2014) *Atlas of Abyssal Megafauna Morphotypes of the Clipperton-Clarion Fracture Zone: Osteichthyes, Online Identification Guide*. Available at: http://ccfzatlas.com/wiki/index.php?title=Fish (Accessed: 8 May 2018).

Linley, T. D. *et al.* (2016) 'Fishes of the hadal zone including new species, *in situ* observations and depth records of Liparidae', *Deep-Sea Research I*, 114, pp. 99–110. doi: 10.1016/j.dsr.2016.05.003.

Lins, L. *et al.* (2013) 'Selective settlement of deep-sea canyon nematodes after resuspension — an experimental approach', *Journal of Experimental Marine Biology and Ecology*, 441, pp. 110–116. doi: 10.1016/j.jembe.2013.01.021.

Littler, M. M. *et al.* (1985) 'Deepest known plant life discovered on an uncharted seamount', *Science*, 227, pp. 57–59. doi: 10.1126/science.227.4682.57.

Lizarralde, Z. I. and Cazzaniga, N. J. (2009) 'Population dynamics and production of *Tellina petitiana* (Bivalvia) on a sandy beach of Patagonia, Argentina', *Thalassas*, 25, pp. 45–57.

Lodge, M. *et al.* (2014) ‘Seabed mining: International Seabed Authority environmental management plan for the Clarion-Clipperton Zone. A partnership approach’, *Marine Policy*, 49, pp. 66–72. doi: 10.1016/j.marpol.2014.04.006.

Loeblich, A. and Tappan, H. (1960) ‘*Saedeleeria*, new genus of the family Allogromiidae (Foraminifera)’, *Proceedings of the Biological Society of Washington*, 73, pp. 195–196.

Löhr, S. C. and Kennedy, M. J. (2015) ‘Micro-trace fossils reveal pervasive reworking of Pliocene sapropels by low-oxygen-adapted benthic meiofauna’, *Nature Communications*, 6, p. 6589. doi: 10.1038/ncomms7589.

Lohrer, A. M., Thrush, S. F. and Gibbs, M. M. (2004) ‘Bioturbators enhance ecosystem function through complex biogeochemical interactions’, *Nature*, 431, pp. 1092–1095. doi: 10.1038/nature03042.

Loo, L.-O. and Rosenberg, R. (1996) ‘Production and energy budget in marine suspension feeding populations: *Mytilus edulis*, *Cerastoderma edule*, *Mya arenaria* and *Amphiura filiformis*’, *Journal of Sea Research*, 35, pp. 199–207. doi: 10.1016/S1385-1101(96)90747-9.

Lopez-Fernandez, P., Bianchelli, S., Pusceddu, A., Calafat, A., Sanchez-Vidal, A., *et al.* (2013) ‘Bioavailability of sinking organic matter in the Blanes canyon and the adjacent open slope (NW Mediterranean Sea)’, *Biogeosciences*, 10, pp. 3405–3420. doi: 10.5194/bg-10-3405-2013.

Lopez-Fernandez, P., Bianchelli, S., Pusceddu, A., Calafat, A., Danovaro, R., *et al.* (2013) ‘Bioavailable compounds in sinking particulate organic matter, Blanes Canyon, NW Mediterranean Sea: Effects of a large storm and sea surface biological processes’, *Progress in Oceanography*, 118, pp. 108–121. doi: 10.1016/j.pocean.2013.07.022.

Lorenzen, C. J. and Jeffrey, S. W. (1980) *Determination of chlorophyll in seawater, Unesco Technical Papers in Marine SCience*. Paris.

Losfeld, G. *et al.* (2015) ‘Mining in New Caledonia: Environmental stakes and restoration opportunities’, *Environmental Science and Pollution Research*, 22, pp. 5592–5607. doi: 10.1007/s11356-014-3358-x.

Louis, K. S. and Siegel, A. C. (2011) ‘Cell viability analysis using Trypan blue: Manual and automated methods’, in Stoddart, M. J. (ed.) *Mammalian Cell Viability: Methods and Protocols*. Totowa, NJ: Springer Science+Business Media, LLC, pp. 7–12. doi: 10.1007/978-1-61779-108-6_2.

Luna, G. M. *et al.* (2013) ‘Patterns and drivers of bacterial α- and β-diversity across vertical profiles from surface to subsurface sediments’, *Environmental Microbiology Reports*, 5, pp. 731–739. doi: 10.1111/1758-2229.12075.

Lynn, D. (2008) *The Ciliated Protozoa*. Dordrecht: Springer Science+Business Media B. V. doi: 10.1007/978-1-4020-8239-9.

MacAvoy, S. E. *et al.* (2008) 'Stable isotope variation among the mussel *Bathymodiolus childressi* and associated heterotrophic fauna at four cold-seep communities in the Gulf of Mexico', *Journal of Shellfish Research*, 27, pp. 147–151. doi: 10.2983/0730-8000(2008)27[147:SIVATM]2.0.CO;2.

Magniez, P. and Féral, J.-P. (1988) 'The effect of somatic and gonadal size on the rate of oxygen consumption in the subantarctic echinoid *Abatus cordatus* (Echinodermata) from Kerguelen', *Comparative Biochemistry and Physiology Part A: Physiology*, 90, pp. 429–434.

Magurran, A. E. (2004) *Measuring Biological Diversity*. Oxford: Blackwell Science Ltd.

Mahatma, R. (2009) *Meiofauna communities of the Pacific nodule province: Abundance, diversity and community structure, PhD-Thesis*. Carl von Ossietzky Universität Oldenburg.

Mahatma, R., Martínez Arbizu, P. and Ivanenko, V. N. (2008) 'A new genus and species of Brychiopontiidae Humes, 1974 (Crustacea: Copepoda: Siphonostomatoida) associated with an abyssal holothurian in the Northeast Pacific nodule province', *Zootaxa*, 1866, pp. 290–302.

Mahaut, M.-L., Sibuet, M. and Shirayama, Y. (1995) 'Weight-dependent respiration rates in deep-sea organisms', *Deep-Sea Research I*, 42, pp. 1575–1582.

Mamouridis, V. *et al.* (2011) 'A temporal analysis on the dynamics of deep-sea macrofauna: Influence of environmental variability off Catalonia coasts (western Mediterranean)', *Deep-Sea Research I*, 58, pp. 323–337. doi: 10.1016/j.dsr.2011.01.005.

Manzetti, S. and Stenersen, J. H. V. (2010) 'A critical view of the environmental condition of the Sognefjord', *Marine pollution bulletin*, 60, pp. 2167–74. doi: 10.1016/j.marpolbul.2010.09.019.

Marchig, V. *et al.* (2001) 'Compositional changes of surface sediments and variability of manganese nodules in the Peru Basin', *Deep-Sea Research II*, 48, pp. 3523–3547. doi: 10.1016/S0967-0645(01)00055-8.

Marcon, Y. and Purser, A. (2017) 'PAPARA(ZZ)I : An open-source software interface for annotating photographs of the deep-sea', *SoftwareX*, 6, pp. 69–80. doi: 10.1016/j.softx.2017.02.002.

Mare, M. F. (1942) 'A study of a marine benthic community with special reference to the micro-organisms', *Journal of the Marine Biological Association of the United Kingdom*, 25, p. 517. doi: 10.1017/S0025315400055132.

Margulis, L. and Chapman, M. (2009) *Kingdoms and Domains - An Illustrated Guide to the Phyla of Life on Earth*. Burlington: Academic Press.

Markhaseva, E. L., Mohrbeck, I. and Renz, J. (2017) 'Description of

Pseudeuchaeta vulgaris n. sp. (Copepoda: Calanoida), a new aetideid species from the deep Pacific Ocean with notes on the biogeography of benthopelagic aetideid calanoids', *Marine Biodiversity*. Marine Biodiversity, 47, pp. 289–297. doi: 10.1007/s12526-016-0527-9.

Marsay, C. M. *et al.* (2015) 'Attenuation of sinking particulate organic carbon flux through the mesopelagic ocean', *Proceedings of the National Academy of Sciences*, 112, pp. 1089–1094. doi: 10.1073/pnas.1415311112.

Martín, D. and Grémare, A. (1997) 'Secondary production of Capitella sp. (Polychaeta: Capitellidae) inhabiting different organically enriched environments', *Scientia Marina*, 61, pp. 99–109.

Martín, J. *et al.* (2013) 'Sediment transport along the Cap de Creus Canyon flank during a mild, wet winter', *Biogeosciences*, 10, pp. 3221–3239. doi: 10.5194/bg-10-3221-2013.

Martín, J., Palanques, A. and Puig, P. (2006) 'Composition and variability of downward particulate matter fluxes in the Palamós submarine canyon (NW Mediterranean)', *Journal of Marine Systems*, 60, pp. 75–97. doi: 10.1016/j.jmarsys.2005.09.010.

Martínez Arbizu, P. and Haeckel, M. (2015) *RV SONNE Fahrtbericht / Cruise Report SO239. EcoResponse assessing the ecology, connectivity and resilience of polymetallic nodule field systems*. Kiel. doi: 10.3289/GEOMAR_REP_NS_7_2013.

Massin, C. (1982) 'Food and feeding mechanisms: Holothuroidea', in Jangoux, M. and Lawrence, J. M. (eds) *Echinoderm Nutrition*. Rotterdam: Balkema, pp. 43–55.

Matsumoto, G. I., Baxter, C. and Chen, E. H. (1997) 'Observations of the deep-sea trachymedusa *Benthocodon pedunculata*', *Invertebrate Biology*, 116, pp. 17–25. doi: 10.2307/3226920.

Maurer, D. *et al.* (1986) 'Vertical migration and mortality of marine benthos in dredged material: A synthesis', *Internationale Revue der gesamten Hydrobiologie und Hydrographie*, 71, pp. 49–63. doi: 10.1002/iroh.19860710106.

Maxwell, K. H., Gardner, J. P. A. and Heath, P. L. (2009) 'The effect of diet on the energy budget of the brown sea cucumber, *Stichopus mollis* (Hutton)', *Journal of the World Aquaculture Society*, 40, pp. 157–170. doi: 10.1111/j.1749-7345.2009.00239.x.

Mayor, D. J. *et al.* (2012) 'Resource quality affects carbon cycling in deep-sea sediments', *The ISME Journal*, 6, pp. 1740–1748. doi: 10.1038/ismej.2012.14.

McClain, C. R. *et al.* (2012) 'Energetics of life on the deep seafloor', *Proceedings of the National Academy of Sciences*, 109, pp. 15366–15371. doi:

10.1073/pnas.1208976109.

McClain, C. R., Johnson, N. A. and Rex, M. A. (2004) ‘Morphological disparity as a biodiversity metric in lower bathyal and abyssal gastropod assemblages’, *Evolution*, 58, pp. 338–348.

McDermott, J. J. and Roe, P. (1985) ‘Food, feeding behavior and feeding ecology of Nemerteans’, *American Zoologist*, 25, pp. 113–125.

McIntyre, A. (1969) ‘Ecoloy of marine meiobenthos’, *Biological Reviews*, 44, pp. 245–288. doi: 10.1111/j.1469-185X.1969.tb00828.x.

Mclachlan, A. (1979) ‘Growth and production of *Donax soridus* Hanley on an open sandy beach in Algoa Bay’, *South African Journal of Zoology*, 14, pp. 61–66.

Mcowen, C. *et al.* (2017) ‘A global map of saltmarshes’, *Biodiversity Data Journal*, 5, p. e11764. doi: 10.3897/BDJ.5.e11764.

Mea, M. (2011) *Temporal variability and impact of dense water cascading events on deep-sea biodiversity and ecosystem functioning in the Catalan margin (Mediterranean Sea), PhD-Thesis*. Università Politecnica delle Marche.

Meadows, P. S. and Tait, J. (1989) ‘Modification of sediment permeability and shear strength by two burrowing invertebrates’, *Marine Biology*, 101, pp. 75–82. doi: 10.1007/BF00393480.

Medina, M. *et al.* (2005) ‘Biodiversity of rocky intertidal benthic communities associated with copper mine tailing discharges in northern Chile’, *Marine Pollution Bulletin*, 50, pp. 396–409. doi: 10.1016/j.marpolbul.2004.11.022.

Mees, J., Abdulkerim, Z. and Hamerlynck, O. (1994) ‘Life history, growth and production of *Neomysis integer* in the Westerschelde estuary (SW Netherlands)’, *Marine Ecology Progress Series*, 109, pp. 43–57.

Melake, K. (1993) ‘Ecology of macrobenthos in the shallow coastal areas of Tewalit (Massawa), Ethiopia’, *Journal of Marine Systems*, 4, pp. 31–44. doi: 10.1016/0924-7963(93)90018-H.

Mengerink, K. J. *et al.* (2014) ‘A call for deep-ocean stewardship’, *Science*, 344, pp. 696–698. doi: 10.1126/science.1251458.

Menzel, D. W. and Goering, J. J. (1966) ‘The distribution of organic detritus in the ocean’, *Limnology and Oceanography*, 11, pp. 333–337. doi: 10.4319/lo.1966.11.3.0333.

Menzies, R. J. (1962) ‘On the food and feeding habits of abyssal organisms as exemplified by the isopoda’, *Internationale Revue der gesamten Hydrobiologie und Hydrographie*, 47, pp. 339–358. doi: 10.1002/iroh.19620470303.

Mermillod-Blondin, F. *et al.* (2004) ‘Influence of bioturbation by three benthic

infaunal species on microbial communities and biogeochemical processes in marine sediment', *Aquatic Microbial Ecology*, 36, pp. 271–284. doi: 10.3354/ame036271.

Mevenkamp, L., Brown, A., *et al.* (2017) 'Hydrostatic pressure and temperature affect the tolerance of the free-living marine nematode Halomonhystera disjuncta to acute copper exposure', *Aquatic Toxicology*, 192, pp. 178–183. doi: 10.1016/j.aquatox.2017.09.016.

Mevenkamp, L., Stratmann, T., *et al.* (2017) 'Impaired short-term functioning of a benthic community from a deep Norwegian fjord following deposition of mine tailings and sediments', *Frontiers in Marine Science*, 4, pp. 1–16. doi: 10.3389/fmars.2017.00169.

Mevenkamp, L., Van Campenhout, J. and Vanreusel, A. (2016) 'Experimental evidence for selective settlement ofmeiofauna from two distinct environments after sediment suspension', *Journal of Experimental Marine Biology and Ecology*, 474, pp. 195–203. doi: 10.1016/j.jembe.2015.10.005.

Meysman, F. J. R., Middelburg, J. J. and Heip, C. H. R. (2006) 'Bioturbation: A fresh look at Darwin's last idea', *Trends in Ecology & Evolution*, 21, pp. 688–695. doi: 10.1016/j.tree.2006.08.002.

Michel, L. N. *et al.* (2016) 'Trophic plasticity of Antarctic echinoids under contrasted environmental conditions', *Polar Biology*, 39(5), pp. 913–923. doi: 10.1007/s00300-015-1873-y.

Michels, J. *et al.* (2008) 'Short-term biogenic particle flux under late spring sea ice in the western Weddell Sea', *Deep-Sea Research II*, 55, pp. 1024–1039. doi: 10.1016/j.dsr2.2007.12.019.

Middelburg, J. J. *et al.* (2000) 'The fate of intertidal microphytobenthos carbon: An *in situ* ^{13}C-labeling study', *Limnology and Oceanography*, 45, pp. 1224–1234. doi: 10.4319/lo.2000.45.6.1224.

Middelburg, J. J. (2011) 'Chemoautotrophy in the ocean', *Geophysical Research Letters*, 38, p. L24604. doi: 10.1029/2011GL049725.

Middelburg, J. J. (2014) 'Stable isotopes dissect aquatic food webs from the top to the bottom', *Biogeosciences*, 11, pp. 2357–2371. doi: 10.5194/bg-11-2357-2014.

Middelburg, J. J. (2018) 'Reviews and syntheses: To the bottom of carbon processing at the seafloor', *Biogeosciences*, 15, pp. 413–427. doi: 10.5194/bg-15-413-2018.

Middelburg, J. J., Duarte, C. M. and Gattuso, J.-P. (2005) 'Respiration in coastal benthic communities', in del Giorgio, P. A. and le B. Williams, P. J. (eds) *Respiration in Aquatic Ecosystems*. Oxford: Oxford University Press, pp. 206–224. doi: 10.1093/acprof:oso/9780198527084.003.0011.

Miljutin, D. M. *et al.* (2011) 'Deep-sea nematode assemblage has not recovered 26 years after experimental mining of polymetallic nodules (Clarion-Clipperton Fracture Zone, tropical eastern Pacific)', *Deep-Sea Research I*, 58, pp. 885–897. doi: 10.1016/j.dsr.2011.06.003.

Miljutin, D. M. and Miljutina, M. A. (2009a) 'Deep-sea nematodes of the family Microlaimidae from the Clarion-Clipperton Fracture Zone (north-eastern tropic Pacific), with the descriptions of three new species', *Zootaxa*, pp. 137–172.

Miljutin, D. M. and Miljutina, M. A. (2009b) 'Description of *Bathynema nodinauti* gen. n., sp. n. and four new Trophomera species (Nematoda: Benthimermithidae) from the Clarion-Clipperton Fracture Zone (Eastern Tropic Pacific), supplemented with the keys to genera and species', *Zootaxa*, pp. 173–196.

Miljutin, D. M., Miljutina, M. A. and Messié, M. (2015) 'Changes in abundance and community structure of nematodes from the abyssal polymetallic nodule field, tropical Northeast Pacific', *Deep-Sea Research I*, 106, pp. 126–135. doi: 10.1016/j.dsr.2015.10.009.

Miljutina, M. A. *et al.* (2010) 'Deep-sea nematode assemblages of the Clarion-Clipperton Nodule Province (tropical north-eastern Pacific)', *Marine Biodiversity*, 40, pp. 1–15. doi: 10.1007/s12526-009-0029-0.

Miljutina, M. A. and Miljutin, D. M. (2012) 'Seven new and four known species of the genus Acantholaimus (Nematoda: Chromadoridae) from the abyssal manganese nodule field (Clarion-Clipperton Fracture Zone, north-eastern tropical Pacific)', *Helgoland Marine Research*, 66, pp. 413–462. doi: 10.1007/s10152-011-0282-z.

Miller-Way, T. *et al.* (1994) 'Sediment oxygen consumption and benthic nutrient fluxes on the Louisiana Continental Shelf: A methodological comparison', *Estuaries*, 17, pp. 809–815.

Miller, D. C., Muir, C. L. and Hauser, O. A. (2002) 'Detrimental effects of sedimentation on marine benthos: What can be learned from natural processes and rates?', *Ecological Engineering*, 19, pp. 211–232. doi: 10.1016/S0925-8574(02)00081-2.

Miller, J. E. and Pawson, D. L. (1990) 'Swimming sea cucumbers (Echinodermata: Holothuroidea): A survey, with analysis of swimming behavior in four bathyal species', *Smithsonian Contributions to the Marine Sciences*, pp. 1–18.

Miller, K. A. *et al.* (2018) 'An overview of seabed mining including the current state of development, environmental impacts, and knowledge gaps', *Frontiers in Marine Science*, 4. doi: 10.3389/fmars.2017.00418.

Miller, R. J. *et al.* (2000) 'Feeding selectivity and rapid particle processing by

deep-sea megafaunal deposit feeders: A ^{234}Th tracer approach', *Journal of Marine Research*, 58, pp. 653–673. doi: 10.1357/002224000321511061.

Mincks, S. L., Smith, C. R. and Demaster, D. J. (2005) 'Persistence of labile organic matter and microbial biomass in Antarctic shelf sediments: Evidence of a sediment "food bank"', *Marine Ecology Progress Series*, 300, pp. 3–19.

Mistri, M. and Ceccherelli, V. U. (1994) 'Growth and secondary production of the Mediterranean gorgonian *Paramuricea clavata*', *Marine Ecology Progress Series*, 103, pp. 291–296. doi: 10.3354/meps103291.

Moens, T., Verbeeck, L. and Vincx, M. (1999) 'Feeding biology of a predatory and a facultatively predatory nematode (*Enoploides longispiculosus* and *Adoncholaimus fuscus*)', *Marine Biology*, 134, pp. 585–593. doi: 10.1007/s002270050573.

Moens, T. and Vincx, M. (1997) 'Observations on the feeding ecology of estuarine nematodes', *Journal of the Marine Biological Association of the UK*, 77, pp. 211–227. doi: 10.1017/S0025315400033889.

Moher, D. *et al.* (2009) 'Preferred reporting items for systematic reviews and meta-analyses: The PRISMA statement', *PLoS Medicine*, 6, p. e1000097. doi: 10.1371/journal.pmed.1000097.

Möller, P. and Rosenberg, R. (1982) 'Production and abundance of the amphipod *Corophium volutator* on the west coast of Sweden', *Netherlands Journal of Sea Research*, 16, pp. 127–140.

Molodtsova, T. N. and Opresko, D. M. (2017) 'Black corals (Anthozoa: Antipatharia) of the Clarion-Clipperton Fracture Zone', *Marine Biodiversity*, 47, pp. 349–365. doi: 10.1007/s12526-017-0659-6.

Mondal, S. (2006) 'Effect of temperature and body size on food utilization in the marine pearl oyster *Pinctada fucata* (Bivalvia: Pteridae)', *Indian Journal of Marine Sciences*, 35, pp. 43–49.

Moodley, L. *et al.* (1997) 'Differential response of benthic meiofauna to anoxia with special reference to Foraminifera (Protista: Sarcodina)', *Marine Ecology Progress Series*, 158, pp. 151–163. doi: 10.3354/meps158151.

Moodley, L., Boschker, H. T. S., *et al.* (2000) 'Ecological significance of benthic foraminifera: ^{13}C labelling experiments', *Marine Ecology Progress Series*, 202, pp. 289–295. doi: 10.3354/meps202289.

Moodley, L., Chen, G., *et al.* (2000) 'Vertical distribution of meiofauna in sediments from contrasting sites in the Adriatic Sea: Clues to the role of abiotic versus biotic control', *Ophelia*, 53, pp. 203–212. doi: 10.1080/00785326.2000.10409450.

Moodley, L. *et al.* (2002) 'Bacteria and Foraminifera: Key players in a short-

term deep-sea benthic response to phytodetritus', *Marine Ecology Progress Series*, 236, pp. 23–29. doi: 10.3354/meps236023.

Moodley, L. *et al.* (2005) 'Similar rapid response to phytodetritus deposition in shallow and deep-sea sediments', *Journal of Marine Research*, 63, pp. 457–469. doi: 10.1357/0022240053693662.

Moodley, L. *et al.* (2008) 'Biomass-specific respiration rates of benthic meiofauna: Demonstrating a novel oxygen micro-respiration system', *Journal of Experimental Marine Biology and Ecology*, 357, pp. 41–47. doi: 10.1016/j.jembe.2007.12.025.

Moodley, L., Heip, C. H. R. and Middelburg, J. J. (1998) 'Benthic activity in sediments of the northwestern Adriatic Sea: Sediment oxygen consumption, macro- and meiofauna dynamics', *Journal of Sea Research*, 40, pp. 263–280. doi: 10.1016/S1385-1101(98)00026-4.

Moran, D., Petersone, M. and Verones, F. (2016) 'On the suitability of input-output analysis for calculating product-specific biodiversity footprints', *Ecological Indicators*, 60, pp. 192–201. doi: 10.1016/j.ecolind.2015.05.015.

Morgan, C. L. and Cronan, D. S. (2000) 'Resource estimates of the Clarion-Clipperton manganese nodule deposits', in Cronan, D. S. (ed.) *Handbook of Marine Mineral Deposits*. Boca Raton: CRC Press LLC, pp. 145–170.

Moriarty, R. *et al.* (2013) 'Distribution of known macrozooplankton abundance and biomass in the global ocean', *Earth System Science Data*, 5, pp. 241–257. doi: 10.5194/essd-5-241-2013.

Mudd, G. M. (2010) 'Global trends and environmental issues in nickel mining: Sulfides versus laterites', *Ore Geology Reviews*, 38, pp. 9–26. doi: 10.1016/j.oregeorev.2010.05.003.

Muller-Karger, F. E. *et al.* (2005) 'The importance of continental margins in the global carbon cycle', *Geophysical Research Letters*, 32, p. L01602. doi: 10.1029/2004GL021346.

Mullineaux, L. S. (1987) 'Organisms living on manganese nodules and crusts: Distribution and abundance at three North Pacific sites', *Deep-Sea Research*, 34, pp. 165–184.

Mullineaux, L. S. (1988) 'Taxonomic notes on large agglutinated foraminifers encrusting manganese nodules, including the description of a new genus, Chondrodapis (Komokiacea)', *Journal of Foraminiferal Research*, 18, pp. 46–53.

Murphy, E. J. *et al.* (2016) 'Understanding the structure and functioning of polar pelagic ecosystems to predict the impacts of change', *Proceedings of the Royal Society B: Biological Sciences*, 283, p. 20161646. doi: 10.1098/rspb.2016.1646.

Murphy, K. *et al.* (2016) *Register of main impacts and causative factors. MIDAS deliverable 7.3*. London.

Murray, J. and Renard, A.-F. (1891) *Report on deep-sea deposits based on the speciments collected during the voyage of H.M.S. Challenger in the years 1872 to 1876*. Edited by J. Murray. London: HM Stationery Office.

Murray, J. W. (2014) 'Ecology and Palaeoecology of Benthic Foraminifera', in Group, R.-T. & F. (ed.) *Ecology and Palaeoecology of Benthic Foraminifera*. 2nd edn. London, p. 396.

Nacken, M. and Reise, K. (2000) 'Effects of herbivorous birds on intertidal seagrass beds in the northern Wadden Sea', *Helgoland Marine Research*, 54, pp. 87–94. doi: 10.1007/s101520050006.

Nakamura, M., Chen, C. and Mitarai, S. (2015) 'Insights into life-history traits of *Munidopsis* spp. (Anomura: Munidopsidae) from hydrothermal vent fields in the Okinawa Trough, in comparison with the existing data', *Deep-Sea Research I*, 100, pp. 48–53. doi: 10.1016/j.dsr.2015.02.007.

Nanajkar, M. and Ingole, B. (2010) 'Comparison of tropical nematode communities from the three harbours, west coast of India', *Cahiers de Biologie Marine*, 51, pp. 9–18.

Naranjo-Elizondo, B. *et al.* (2016) 'Feeding habits of the Pacific bearded brotula *Brotula clarkae* Hubbs, 1944 (Ophidiidae) along the Pacific coast of Costa Rica, Central America', *Journal of Applied Ichthyology*, 32, pp. 439–447. doi: 10.1111/jai.13029.

Narendrula, R., Nkongolo, K. K. and Beckett, P. (2012) 'Comparative soil metal analyses in Sudbury (Ontario, Canada) and Lubumbashi (Katanga, DR-Congo)', *Bulletin of Environmental Contamination and Toxicology*, 88, pp. 187–192. doi: 10.1007/s00128-011-0485-7.

Navarro, E. *et al.* (1994) 'The basis for a functional response to variable food quantity and quality in cockles *Cerastoderma edule* (Bivalvia, Cardiidae)', *Physiological Zoology*, 67, pp. 468–496.

Navarro, J. . and Thompson, R. (1996) 'Physiological energetics of the horse mussel *Modiolus modiolus* in a cold ocean environment', *Marine Ecology Progress Series*, 138, pp. 135–148. doi: 10.3354/meps138135.

Nelson, E. J., MacDonald, B. A. and Robinson, S. M. C. (2012) 'The absorption efficiency of the suspension-feeding sea cucumber, *Cucumaria frondosa*, and its potential as an extractive integrated multi-trophic aquaculture (IMTA) species', *Aquaculture*, 370–371, pp. 19–25. doi: 10.1016/j.aquaculture.2012.09.029.

Neuendorf, K. K., James, P. M. and Jackson, J. A. (2005) 'Relief', *Glossary of Geology*. 5th edn. American Geological Institute.

Nielsen, A. M. *et al.* (1995) ‘Feeding, growth and respiration in the polychaetes *Nereis diversicolor* (facultative filter-feeder) and *N. virens* (omnivorous) - a comparative study’, *Marine Ecology Progress Series*, 125, pp. 149–158. doi: 10.3354/meps125149.

Nienhuis, P. H. and Groenendijk, A. M. (1986) ‘Consumption of eelgrass (*Zostera marina*) by birds and invertebrates: An annual budget’, *Marine Ecology Progress Series*, 29, pp. 29–35. doi: 10.3354/meps029029.

Nieves-Soto, M. *et al.* (2013) ‘Combined effect of temperature and food concentration on the filtration and clarification rates and assimilation efficiency of *Atrina tuberculosa* Sowerby, 1835 (Mollusca: Bivalvia) under laboratory conditions’, *Archives of Biological Sciences*, 65, pp. 99–106. doi: 10.2298/ABS1301099N.

Niner, H. J. *et al.* (2018) ‘Deep-sea mining with no net loss of biodiversity - An impossible aim’, *Frontiers in Marine Science*, 5(53). doi: 10.3389/fmars.2018.00053.

Nobes, K. and Uthicke, S. (2008) *Benthic Foraminifera of the Great Barrier Reef: A guide to species potentially useful as water quality indicators*. Chairns.

Nøhr Glud, R. *et al.* (1994) ‘Diffusive and total oxygen uptake of deep-sea sediments in the eastern South Atlantic Ocean: *In situ* and laboratory measurements’, *Deep Sea Research Part I: Oceanographic Research Papers*, 41, pp. 1767–1788. doi: 10.1016/0967-0637(94)90072-8.

Nomaki, H. *et al.* (2007) ‘Deep-sea benthic foraminiferal respiration rates measured under laboratory conditions’, *The Journal of Foraminiferal Research*, 37, pp. 281–286. doi: 10.2113/gsjfr.37.4.281.

Nordenskiöld, A. E. (1868) ‘Account of explorations by the Swedish Arctic expedition at the close of the season 1868’, *Proceedings of the Royal Society of London*, 17, pp. 128–131.

Nordenskiöld, A. E. (1881) *The voyage of the Vega round Asia and Europe*. London: Macmillan & Co.

Norderhaug, K. M. and Christie, H. (2011) ‘Secondary production in a *Laminaria hyperborea* kelp forest and variation according to wave exposure’, *Estuarine, Coastal and Shelf Science*, 95, pp. 135–144. doi: 10.1016/j.ecss.2011.08.028.

Nozawa, F. *et al.* (2006) ‘“Live” benthic foraminifera at an abyssal site in the equatorial Pacific nodule province: Abundance, diversity and taxonomic composition’, *Deep-Sea Research I*, 53, pp. 1406–1422. doi: 10.1016/j.dsr.2006.06.001.

Oebius, H. U. *et al.* (2001) ‘Parametrization and evaluation of marine environmental impacts produced by deep-sea manganese nodule mining’, *Deep-*

Sea Research II, 48, pp. 3453–3467. doi: 10.1016/S0967-0645(01)00052-2.

van Oevelen, D., Soetaert, K., *et al.* (2006) 'Carbon flows through a benthic food web: Integrating biomass, isotope and tracer data', *Journal of Marine Research*, 64, pp. 453–482. doi: 10.1357/002224006778189581.

van Oevelen, D., Middelburg, J. J., *et al.* (2006) 'The fate of bacterial carbon in an intertidal sediment: Modeling an *in situ* isotope tracer experiment', *Limnology and Oceanography*, 51, pp. 1302–1314. doi: 10.4319/lo.2006.51.3.1302.

van Oevelen, D. *et al.* (2009) 'The cold-water coral community as hotspot of carbon cycling on continental margins: A food-web analysis from Rockall Bank (northeast Atlantic)', *Limnology and Oceanography*, 54, pp. 1829–1844. doi: 10.4319/lo.2009.54.6.1829.

van Oevelen, D. *et al.* (2010) 'Quantifying food web flows using linear inverse models', *Ecosystems*, 13, pp. 32–45. doi: 10.1007/s10021-009-9297-6.

van Oevelen, D., Soetaert, K., *et al.* (2011) 'Canyon conditions impact carbon flows in food webs of three sections of the Nazaré canyon', *Deep-Sea Research II*, 58, pp. 2461–2476. doi: 10.1016/j.dsr2.2011.04.009.

van Oevelen, D., Bergmann, M., *et al.* (2011) 'Carbon flows in the benthic food web at the deep-sea observatory HAUSGARTEN (Fram Strait)', *Deep-Sea Research I*, 58, pp. 1069–1083. doi: 10.1016/j.dsr.2011.08.002.

van Oevelen, D., Soetaert, K. and Heip, C. H. R. (2012) 'Carbon flows in the benthic food web of the Porcupine Abyssal Plain: The (un)importance of labile detritus in supporting microbial and faunal carbon demands', *Limnology and Oceanography*, 57, pp. 645–664. doi: 10.4319/lo.2012.57.2.0645.

Ohgushi, T. (2008) 'Herbivore-induced indirect interaction webs on terrestrial plants: The importance of non-trophic, indirect, and facilitative interactions', *Entomologia Experimentalis et Applicata*, 128, pp. 217–229. doi: 10.1111/j.1570-7458.2008.00705.x.

Olsgard, F. and Hasle, J. R. (1993) 'Impact of waste from titanium mining on benthic fauna', *Journal of Experimental Marine Biology and Ecology*, 172, pp. 185–213. doi: 10.1016/0022-0981(93)90097-8.

Orejas, C. *et al.* (2009) 'Cold-water corals in the Cap de Creus canyon, northwestern Mediterranean: Spatial distribution, density and anthropogenic impact', *Marine Ecology Progress Series*, 397, pp. 37–51. doi: 10.3354/meps08314.

Otegui, M. B. P., Blankensteyn, A. and Pagliosa, P. R. (2012) 'Population structure, growth and production of *Thoracophelia furcifera* (Polychaeta: Opheliidae) on a sandy beach in southern Brazil', *Helgoland Marine Research*, 66, pp. 479–488. doi: 10.1007/s10152-011-0284-x.

Ott, J. A. (1972) ‘Determination of fauna boundaries of nematodes in an intertidal sand flat’, *Internationale Revue der gesamten Hydrobiologie und Hydrographie*, 57, pp. 645–663. doi: 10.1002/iroh.19720570413.

Ott, J. A. and Schiemer, F. (1973) ‘Respiration and anaerobiosis of free living nematodes from marine and limnic sediments’, *Netherlands Journal of Sea Research*, 7, pp. 233–243. doi: 10.1016/0077-7579(73)90047-1.

Oyenekan, J. A. (1986) ‘Population dynamics and secondary production in an estuarine population of *Nepthys hombergii* (Polychaeta: Nephtydiae)’, *Marine Biology*, 93, pp. 217–223.

Oyenekan, J. A. (1987) ‘Population dynamics and secondary production in an estuarine population of *Caulleriella caputesocis* (Polychaeta: Cirratulidae)’, *Marine Biology*, 95, pp. 267–273.

Oyenekan, J. A. (1988) ‘Population dynamics and secondary production in *Melinna palmata* (Polychaeta: Ampharetidae)’, *Marine Biology*, 98, pp. 247–251. doi: 10.1007/BF00391202.

Palanques, A. *et al.* (2012) ‘Sediment transport to the deep canyons and open-slope of the western Gulf of Lions during the 2006 intense cascading and open-sea convection period’, *Progress in Oceanography*, 106, pp. 1–15. doi: 10.1016/j.pocean.2012.05.002.

Palmer, M. A. (1988) ‘Dispersal of marine meiofauna: A review and conceptual model explaining passive transport and active emergence with implications for recruitment’, *Marine Ecology Progress Series*, 48, pp. 81–91.

Pape, E. *et al.* (2017) ‘Limited spatial and temporal variability in meiofauna and nematode communities at distant but environmentally similar sites in an area of interest for deep-sea mining’, *Frontiers in Marine Science*, 4, pp. 1–16. doi: 10.3389/fmars.2017.00205.

Pasqual, C. *et al.* (2010) ‘Flux and composition of settling particles across the continental margin of the Gulf of Lion: the role of dense shelf water cascading’, *Biogeosciences*, 7, pp. 217–231. doi: 10.5194/bg-7-217-2010.

Paul, S. A. L. *et al.* (2018) ‘Biogeochemical regeneration of a nodule mining disturbance site: Trace metals, DOC and amino acids in deep-sea sediments and pore waters’, *Frontiers in Marine Science*, 5, pp. 1–17. doi: 10.3389/fmars.2018.00117.

Pawlowski, J., Holzmann, M. and Tyszka, J. (2013) ‘New supraordinal classification of Foraminifera: Molecules meet morphology’, *Marine Micropaleontology*, 100, pp. 1–10. doi: 10.1016/j.marmicro.2013.04.002.

Pearson, M. and Gage, J. D. (1984) ‘Diets of some deep-sea brittle stars in the Rockall Trough’, *Marine Biology*, 82, pp. 247–258.

Peel, J. S. (2017) ‘Feeding behaviour of a new worm (Priapulida) from the

Sirius Passet Lagerstätte (Cambrian Series 2, Stage 3) of North Greenland (Laurentia)', *Palaeontology*. Edited by I. Rahman, 60, pp. 795–805. doi: 10.1111/pala.12316.

Peña-Messina, E. *et al.* (2009) 'A preliminary evaluation of physiological filtration variables for *Crassostrea corteziensis* (Hertlein, 1951) and *Anadara tuberculosa* (Sowerby, 1833) in shrimp aquaculture effluents', *Aquaculture Research*, 40, pp. 1750–1758. doi: 10.1111/j.1365-2109.2009.02280.x.

Le Pennec, G. *et al.* (2003) 'Aspects of the feeding biology of the pectinacean Bathypecten vulcani, a peri-hydrothermal vent bivalve', *Journal of the Marine Biological Association of the UK*, 83, pp. 479–482. doi: 10.1017/S0025315403007379h.

Pentreath, R. J. (1971) 'Respiratory surfaces and respiration in three New Zealand intertidal ophiuroids', *Journal of Zoology*, 163, pp. 397–412.

Pérez Camacho, A., Labarta, U. and Navarro, E. (2000) 'Energy balance of mussels *Mytilus galloprovincialis*: The effect of length and age', *Marine Ecology Progress Series*, 199, pp. 149–158.

Pérez, V., Marquiegui, M. A. and Belzunce, M. J. (2007) 'Life history and production of *Corophium urdaibaiense* (Crustacea: Amphipoda) in the Urdaibai estuary (NE Spain)', *Marine Biology*, 151, pp. 1163–1174. doi: 10.1007/s00227-006-0558-z.

Petersen, J. K., Schou, O. and Thor, P. (1995) 'Growth and energetics in the ascidian *Ciona intestinalis*', *Marine Ecology Progress Series*, 120, pp. 175–184. doi: 10.3354/meps120175.

Petersen, S. *et al.* (2016) 'News from the seabed – Geological characteristics and resource potential of deep-sea mineral resources', *Marine Policy*, 70, pp. 175–187. doi: 10.1016/j.marpol.2016.03.012.

Petracco, M. *et al.* (2012) 'Production of *Excirolana armata* (Dana, 1853) (Isopoda, Cirolanidae) on an exposed sandy beach in southeastern Brazil', *Helgoland Marine Research*, 66, pp. 265–274. doi: 10.1007/s10152-011-0268-x.

Petracco, M. *et al.* (2014) 'Population biology of the gastropod *Olivella minuta* (Gastropoda, Olividae) on two sheltered beaches in southeastern Brazil', *Estuarine, Coastal and Shelf Science*, 150, pp. 149–156. doi: 10.1016/j.ecss.2013.10.015.

Petracco, M., Veloso, V. G. and Cardoso, R. S. (2003) 'Population dynamics and secondary production of *Emerita brasiliensis* (Crustacea: Hippidae) at Prainha Beach, Brazil', *Marine Ecology*, 24, pp. 231–245. doi: 10.1046/j.0173-9565.2003.00837.x.

Pfannkuche, O. (1993) 'Benthic response to the sedimentation of particulate

organic matter at the BIOTRANS station, 47°N, 20°W', *Deep-Sea Research II*, 40, pp. 135–149. doi: 10.1016/0967-0645(93)90010-K.

Pfannkuche, O. and Lochte, K. (1993) 'Open ocean pelago-benthic coupling: Cyanobacteria as tracers of sedimenting salp faeces', *Deep-Sea Research I*, 40, pp. 727–737. doi: 10.1016/0967-0637(93)90068-E.

Pimm, S. L., Lawton, J. H. and Cohen, J. E. (1991) 'Food web patterns and their consequences', *Nature*, 350, pp. 669–674. doi: 10.1038/354056a0.

Piot, A., Nozais, C. and Archambault, P. (2014) 'Meiofauna affect the macrobenthic biodiversity-ecosystem functioning relationship', *Oikos*, 123, pp. 203–213. doi: 10.1111/j.1600-0706.2013.00631.x.

Ploug, H. (2001) 'Small-scale oxygen fluxes and remineralization in sinking aggregates', *Limnology and Oceanography*, 46, pp. 1624–1631. doi: 10.4319/lo.2001.46.7.1624.

Pozzato, L. *et al.* (2013) 'Sink or link? The bacterial role in benthic carbon cycling in the Arabian Sea's oxygen minimum zone', *Biogeosciences*, 10, pp. 6879–6891. doi: 10.5194/bg-10-6879-2013.

Price, R. and Warwick, R. M. (1980) 'Temporal variations in annual production and biomass in estuarine populations of two polychaetes, *Nephtys hombergi* and *Ampharete acutifrons*', *Journal of the Marine Biological Association of the UK*, 60, pp. 481–487.

Priede, I. G. *et al.* (1991) 'Direct measurement of active dispersal of food-falls by deep-sea demersal fishes', *Nature*, 351, pp. 647–649.

Priede, I. G. (2017) *Deep-sea fishes*. Cambridge: Cambridge University Press. doi: 10.1017/9781316018330.

Puig, P. *et al.* (2013) 'Thick bottom nepheloid layers in the western Mediterranean generated by deep dense shelf water cascading', *Progress in Oceanography*, 111, pp. 1–23. doi: 10.1016/j.pocean.2012.10.003.

Puig, P. *et al.* (2017) 'Dense shelf water cascades and sedimentary furrow formation in the Cap de Creus Canyon, northwestern Mediterranean Sea', *Continental Shelf Research*, 28, pp. 2017–2030. doi: 10.1016/j.csr.2008.05.002.

Purser, A. *et al.* (2016) 'Association of deep-sea incirrate octopods with manganese crusts and nodule fields in the Pacific Ocean', *Current Biology*, 26, pp. R1268–R1269. doi: 10.1016/j.cub.2016.10.052.

Pusceddu, A. *et al.* (2010) 'Organic matter in sediments of canyons and open slopes of the Portuguese, Catalan, Southern Adriatic and Cretan Sea margins', *Deep-Sea Research I*, 57, pp. 441–457. doi: 10.1016/j.dsr.2009.11.008.

Pusceddu, A. *et al.* (2013) 'Major consequences of an intense dense shelf water cascading event on deep-sea benthic trophic conditions and meiofaunal

biodiversity', *Biogeosciences*, 10, pp. 2659–2670. doi: 10.5194/bg-10-2659-2013.

R-Core Team (2017) 'R: A language and environment for statistical computing'. Vienna: R Foundation for Statistical Computing. Available at: https://www.r-project.org/.

Rachor, E. *et al.* (1982) 'Seasonal and long-term population fluctuations in *Diastylis rathkei* (Crustacea: Cumacea) of Kiel Bay and German Bight', *Netherlands Journal of Sea Research*, 16, pp. 141–150.

Radio New Zealand (2014) 'New Caledonia nickel plant suspended', *Radio news*, 8 May. Available at: http://www.radionz.co.nz/international/pacific-news/243692/new-caledonia-nickel-plant-suspended.

Radziejewska, T. (2002) 'Responses of deep-sea meiobenthic communities to sediment disturbance simulating effects of polymetallic nodule mining', *International Review of Hydrobiology*, 87, p. 457. doi: 10.1002/1522-2632(200207)87:4<457::AID-IROH457>3.0.CO;2-3.

Radziejewska, T. (2014) 'Characteristics of the sub-equatorial north-eastern Pacific Ocean's abyss, with a particular reference to the Clarion-Clipperton Fracture Zone', in *Meiobenthos in the Sub-Equatorial Pacific Abyss*. Berlin, Heidelberg: Springer, pp. 13–28. doi: 10.1007/978-3-642-41458-9.

Raffaelli, D. *et al.* (2003) 'The ups and downs of benthic ecology: Considerations of scale, heterogeneity and surveillance for benthic–pelagic coupling', *Journal of Experimental Marine Biology and Ecology*, 285–286, pp. 191–203. doi: 10.1016/S0022-0981(02)00527-0.

Ramirez-Llodra, E. *et al.* (2015) 'Submarine and deep-sea mine tailing placements: A review of current practices, environmental issues, natural analogs and knowledge gaps in Norway and internationally', *Marine Pollution Bulletin*, 97, pp. 13–35. doi: 10.1016/j.marpolbul.2015.05.062.

Ramírez-Llodrà, E. *et al.* (2010) 'Deep, diverse and definitely different: Unique attributes of the world's largest ecosystem', *Biogeosciences*, 7, pp. 2851–2899. doi: 10.5194/bg-7-2851-2010.

Ramírez-Llodrà, E. *et al.* (2011) 'Man and the last great wilderness: Human impact on the deep sea', *PLoS ONE*, 6, p. e22588. doi: 10.1371/journal.pone.0022588.

Ramirez, M. *et al.* (2005) 'Metal speciation and environmental impact on sandy beaches due to El Salvador copper mine, Chile', *Marine Pollution Bulletin*, 50, pp. 62–72. doi: 10.1016/j.marpolbul.2004.08.010.

Randall, R. G. (2002) 'Using allometry with fish size to estimate production to biomass (P/B) ratios of salmonid populations', *Ecology of Freshwater Fish*, 11, pp. 196–202. doi: 10.1034/j.1600-0633.2002.00012.x.

Rees, H. L. (1983) ‘Pollution investigations off the north-east coast of England: Community structure, growth and production of benthic macrofauna’, *Marine Environmental Research*, 9, pp. 61–110.

Ren, J. S., Ross, A. H. and Hayden, B. J. (2006) ‘Comparison of assimilation efficiency on diets of nine phytoplankton species of the greenshell mussel *Perna canaliculus*’, *Journal of Shellfish Research*, 25, pp. 887–892.

Renaud, P. E. *et al.* (2007) ‘Carbon cycling by seafloor communities on the eastern Beaufort Sea shelf’, *Journal of Experimental Marine Biology and Ecology*, 349, pp. 248–260. doi: 10.1016/j.jembe.2007.05.021.

Rex, M. A. *et al.* (2006) ‘Global bathymetric patterns of standing stock and body size in the deep-sea benthos’, *Marine Ecology Progress Series*, 317, pp. 1–8. doi: 10.3354/meps317001.

Rex, M. A. and Etter, R. J. (2010) *Deep-sea biodiversity*. Massachusetts: Harvard University Press.

Ribó, M. *et al.* (2011) ‘Dense shelf water cascades in the Cap de Creus and Palamós submarine canyons during winters 2007 and 2008’, *Marine Geology*, 284, pp. 175–188. doi: 10.1016/j.margeo.2011.04.001.

Roberts, C. M. *et al.* (2002) ‘Marine biodiversity hotspots and conservation priorities for tropical reefs’, *Science*, 295, pp. 1280–1284. doi: 10.1126/science.1067728.

Roberts, D. *et al.* (2000) ‘Feeding and digestive strategies in deposit-feeding holothurians’, *Oceanography and Marine Biology: An Annual Review*, 38, pp. 257–310.

Roberts, D. *et al.* (2001) ‘Sediment distribution, hydrolytic enzyme profiles and bacterial activities in the guts of Oneirophanta mutabilis, Psychropotes longicauda and Pseudostichopus villosus: What do they tell us about digestive strategies of abyssal holothurians?’, *Progress in Oceanography*, 50, pp. 443–458. doi: 10.1016/S0079-6611(01)00065-9.

Roberts, D. and Moore, H. M. (1997) ‘Tentacular diversity in deep-sea deposit-feeding holothurians: Implications for biodiversity in the deep sea’, *Biodiversity and Conservation*, 6, pp. 1487–1505. doi: 10.1023/A:1018362319053.

Roberts, J. M., Wheeler, A. J. and Freiwald, A. (2006) ‘Reefs of the deep: The biology and geology of cold-water coral ecosystems’, *Science*, 312, pp. 543–547. doi: 10.1126/science.1119861.

Roberts, S. and Gunn, G. (2014) ‘Cobalt’, in Gunn, G. (ed.) *Critical Metals Handbook*. 1st edn. Chichester: John Wiley & Sons, Ltd., pp. 122–149.

Rodrigues, N., Sharma, R. and Nagender Nath, B. (2001) ‘Impact of benthic disturbance on megafauna in Central Indian Basin’, *Deep-Sea Research II*, 48(16), pp. 3411–3426. doi: 10.1016/S0967-0645(01)00049-2.

Rogacheva, A., Gebruk, A. V. and Alt, C. H. S. (2012) ‘Swimming deep-sea holothurians (Echinodermata : Holothuroidea) on the northern Mid-Atlantic Ridge’, *Zoosymposia*, 7, pp. 213–224. doi: 10.11646/zoosymposia.7.1.19.

Rolinski, S., Segschneider, J. and Sündermann, J. (2001) ‘Long-term propagation of tailings from deep-sea mining under variable conditions by means of numerical simulations’, *Deep-Sea Research II*, 48, pp. 3469–3485. doi: 10.1016/S0967-0645(01)00053-4.

Rowe, G. T. (1983) ‘Biomass and production of the deep-sea macrobenthos’, in Rowe, G. T. (ed.) *Deep-Sea Biology*. New York: John Wiley & Sons, Inc.

Rowe, G. T., Wei, C.-L., *et al.* (2008) ‘Comparative biomass structure and estimated carbon flow in food webs in the deep Gulf of Mexico’, *Deep-Sea Research II*, 55, pp. 2699–2711. doi: 10.1016/j.dsr2.2008.07.020.

Rowe, G. T., Morse, J., *et al.* (2008) ‘Sediment community oxygen consumption in the deep Gulf of Mexico’, *Deep-Sea Research II*, 55, pp. 2686–2691. doi: 10.1016/j.dsr2.2008.07.018.

Rowe, G. T. and Deming, J. W. (1985) ‘The role of bacteria in the turnover of organic matter in the deep-sea sediments’, *Journal of Marine Research*, 43, pp. 925–950.

Ruhl, H. A. (2007) ‘Abundance and size distribution dynamics of abyssal epibenthic megafauna in the northeast Pacific’, *Ecology*, 88, pp. 1250–1262. doi: 10.1890/06-0890.

Ruhl, H. A. *et al.* (2014) ‘Links between deep-sea respiration and community dynamics’, *Ecology*, 95, pp. 1651–1662. doi: 10.1890/13-0675.1.

Ruhl, H. A., Ellena, J. A. and Smith, K. L. (2008) ‘Connections between climate, food limitation, and carbon cycling in abyssal sediment communities’, *Proceedings of the National Academy of Sciences*, 105, pp. 17006–17011. doi: 10.1073/pnas.0803898105.

Ruhl, H. A. and Smith, K. L. (2004) ‘Shifts in deep-sea community structure linked to climate and food supply’, *Science*, 305, pp. 513–515. doi: 10.1126/science.1099759.

Salomon, M. and Buchholz, F. (2000) ‘Effects of temperature on the respiration rates and the kinetics of citrate synthase in two species of Idotea (Isopoda, Crustacea).’, *Comparative biochemistry and physiology. Part B, Biochemistry & molecular biology*, 125, pp. 71–81. doi: 10.1016/S0305-0491(99)00158-3.

San Vincente, C. and Sorbe, J. C. (1995) ‘Biology of the suprabenthic mysid *Schistomysis spiritus* (Norman, 1860) in the southeastern part of the Bay of Biscay’, *Scientia Marina*, 59, pp. 71–86.

Sanchez-Vidal, A. *et al.* (2008) ‘Impact of dense shelf water cascading on the

transfer of organic matter to the deep western Mediterranean basin', *Geophysical Research Letters*, 35, p. L05605. doi: 10.1029/2007GL032825.

Sanders, D. *et al.* (2014) 'Integrating ecosystem engineering and food webs', *Oikos*, 123, pp. 513–524. doi: 10.1111/j.1600-0706.2013.01011.x.

Sarda, R., Valiela, I. and Foreman, K. (1995) 'Life cycle, demography, and production of *Marenzellaria viridis* in a salt marsh of southern New England', *Journal of the Marine Biological Association of the UK*, 75, pp. 725–738.

Sarmiento, J. L. *et al.* (1998) 'Simulated response of the ocean carbon cycle to anthropogenic climate warming', *Nature*, 393, pp. 245–249. doi: 10.1038/30455.

Sarvala, J. and Uitto, A. (1991) 'Production of the benthic amphipods *Pontoporeia affinis* and *P. femorata* in a Baltic archipelago', *Ophelia*, 34, pp. 71–90. doi: 10.1080/00785326.1991.10429697.

Sayre, R. *et al.* (2017) 'A three-dimensional mapping of the ocean based on environmental data', *Oceanography*, 30, pp. 90–103. doi: 10.5670/oceanog.2017.116.

Schade, H. *et al.* (2016) 'Simulated leakage of high pCO_2 water negatively impacts bivalve dominated infaunal communities from the western Baltic Sea', *Scientific Reports*, 6, p. 31447. doi: 10.1038/srep31447.

Schoening, T., Jones, D. O. B. and Greinert, J. (2017) 'Compact-morphology-based polymetallic nodule delineation', *Scientific Reports*, 7, p. 13338. doi: 10.1038/s41598-017-13335-x.

Schratzberger, M. and Ingels, J. (2018) 'Meiofauna matters: The roles of meiofauna in benthic ecosystems', *Journal of Experimental Marine Biology and Ecology*, 502, pp. 12–25. doi: 10.1016/j.jembe.2017.01.007.

Schratzberger, M., Rees, H. L. and Boyd, S. E. (2000) 'Effects of simulated deposition of dredged material on structure of nematode assemblages - the role of burial', *Marine Biology*, 136, pp. 519–530. doi: 10.1007/s002270050712.

Schratzberger, M. and Warwick, R. M. (1998) 'Effects of physical disturbance on nematode communities in sand and mud: A microcosm experiment', *Marine Biology*, 130, pp. 643–650. doi: 10.1007/s002270050286.

Schriever, G. (1990) *Cruise Report DISCOL 2, Sonne-Cruise 64. Callao/Peru - Valparaiso/Chile 02.09. - 02.10.1989*. Hamburg.

Schriever, G., Koschinsky, A. and Bluhm, H. (1996) *Cruise Report ATESEPP. Impacts of potential technical interventions on the deep-sea ecosystem of the southeast Pacific off Peru. Sonne Cruise 106. January 1 – March 9, 1996. Balboa/Panama - Balboa/ Panama*. Hamburg.

Schriever, G. and Thiel, H. (1992) *Cruise report DISCOL 3, Sonne-Cruise 77.*

Balboa/ Panama - Balboa/ Panama 26.01. - 27.02.1992. Hamburg.

Schückel, S. *et al.* (2013) 'Meiofauna as food source for small-sized demersal fish in the southern North Sea', *Helgoland Marine Research*, 67, pp. 203–218. doi: 10.1007/s10152-012-0316-1.

Seibel, B. A. and Drazen, J. C. (2007) 'The rate of metabolism in marine animals: Environmental constraints, ecological demands and energetic opportunities', *Philosophical Transactions of the Royal Society B: Biological Sciences*, 362, pp. 2061–2078. doi: 10.1098/rstb.2007.2101.

Seiderer, L. J. and Newell, R. C. (1999) 'Analysis of the relationship between sediment composition and benthic community structure in coastal deposits: Implications for marine aggregate dredging', *ICES Journal of Marine Science*, 56, pp. 757–765. doi: 10.1006/jmsc.1999.0495.

Sejr, M. K. *et al.* (2004) 'Effects of food concentration on clearance rate and energy budget of the Arctic bivalve *Hiatella arctica* (L) at subzero temperature', *Journal of Experimental Marine Biology and Ecology*, 311, pp. 171–183. doi: 10.1016/j.jembe.2004.05.005.

van Senus, P. and McLachlan, A. (1986) 'Growth, production, and a partial energy budget for the amphipod, *Talorchestria capensis* (Crustacea: Talitridae) in the Eastern Cape, South Africa', *Marine Ecology*, 7, pp. 165–179.

Shaikh, M. A., Meadows, A. and Meadows, P. S. (1998) 'Biological control of avalanching and slope stability in the intertidal zone', in Black, K. S., Paterson, D. M., and Cramp, A. (eds) *Sedimentary processes in the intertidal zone*. London: Geological Society, pp. 309–329. doi: 10.1144/GSL.SP.1998.139.01.25.

Shapiro, G. I., Huthnance, J. M. and Ivanov, V. V. (2003) 'Dense water cascading off the continental shelf', *Journal of Geophysical Research*, 108, p. 3390. doi: 10.1029/2002JC001610.

Sharma, R. (2017) 'Deep-sea mining: Current status and future considerations', in Sharma, R. (ed.) *Deep-Sea Mining: Resource Potential, Technical and Environmental Considerations*. Cham: Springer International Publishing, pp. 3–21. doi: 10.1007/978-3-319-52557-0.

Sheader, M. (1977) 'Production and population dynamics of *Ampelisca tenuicornis* (Amphipoda) with notes on the biology of its parasite *Sphaeronella longpipes* (Copepoda)', *Journal of the Marine Biological Association of the UK*, 57, pp. 955–968.

Sherwood, A. and Phillips, J. (2018) *Coal and coal mining - The miners' work, Te Ara - the Encyclopedia of New Zealand*. Available at: http://www.teara.govt.nz/en/diagram/7445/bord-and-pillar-mining (Accessed: 26 May 2018).

Shirayama, Y. (1992) ‘Respiration rates of bathyal meiobenthos collected using a deep- sea submersible SHINKA12000’, *Deep-Sea Research*, 39, pp. 781–788.

Short, F. *et al.* (2007) ‘Global seagrass distribution and diversity: A bioregional model’, *Journal of Experimental Marine Biology and Ecology*, 350, pp. 3–20. doi: 10.1016/j.jembe.2007.06.012.

Shulse, C. N. *et al.* (2017) ‘Polymetallic nodules, sediments, and deep waters in the equatorial North Pacific exhibit highly diverse and distinct bacterial, archaeal, and microeukaryotic communities’, *MicrobiologyOpen*, 6, p. e00428. doi: 10.1002/mbo3.428.

Singh, R. *et al.* (2016) ‘Nematode communities inhabiting the soft deep-sea sediment in polymetallic nodule fields: Do they differ from those in the nodule-free abyssal areas?’, *Marine Biology Research*, 12, pp. 345–359. doi: 10.1080/17451000.2016.1148822.

Smaal, A. C. and Vonck, A. (1997) ‘Seasonal variation in C, N and P budgets and tissue composition of the mussel *Mytilus edulis*’, *Marine Ecology Progress Series*, 153, pp. 167–179. doi: 10.3354/meps153167.

Smallwood, B. J. *et al.* (1999) ‘Megafauna can control the quality of organic matter in marine sediments’, *Naturwissenschaften*, 86, pp. 320–324. doi: 10.1007/s001140050624.

De Smet, B. *et al.* (2017) ‘The community structure of deep-sea macrofauna associated with polymetallic nodules in the eastern part of the Clarion-Clipperton Fracture Zone’, *Frontiers in Marine Science*, 4, pp. 1–14. doi: 10.3389/fmars.2017.00103.

Smit, M. G. D. *et al.* (2008) ‘Species sensitivity distribution for suspended clays, sediment burial, and grain size change in the marine environment’, *Environmental Toxicology and Chemistry*, 27, pp. 1006–1012. doi: 10.1897/07-339.1.

Smith, A. B. and Stockley, B. (2005) ‘The geological history of deep-sea colonization by echinoids: Roles of surface productivity and deep-water ventilation.’, *Proceedings of the Royal Society B: Biological Sciences*, 272, pp. 865–869. doi: 10.1098/rspb.2004.2996.

Smith, A., Matthiopoulos, J. and Priede, I. G. (1997) ‘Areal coverage of the ocean floor by the deep-sea elasipodid holothurian *Oneirophanta mutabilis*: Estimates using systematic, random and directional search strategy simulations’, *Deep-Sea Research I*, 44, pp. 477–486. doi: 10.1016/S0967-0637(96)00112-4.

Smith, C. R. *et al.* (1997) ‘Latitudinal variations in benthic processes in the abyssal equatorial Pacific: Control by biogenic particle flux’, *Deep-Sea Research II*, 44, pp. 2295–2317. doi: 10.1016/S0967-0645(97)00022-2.

Smith, C. R. *et al.* (2008) ‘Abyssal food limitation, ecosystem structure and

climate change', *Trends in Ecology & Evolution*, 23, pp. 518–528. doi: 10.1016/j.tree.2008.05.002.

Smith, C. R. *et al.* (2009) 'The near future of the deep-sea floor ecosystems', in Polunin, N. V. C. (ed.) *Aquatic Ecosystems*. Cambridge: Cambridge University Press, pp. 334–350.

Smith, C. R. and Baco, A. R. (2003) 'Ecology of whale falls at the deep-sea floor', *Oceanography and Marine Biology: An Annual Review*, 41, pp. 311–354.

Smith, C. R. and Demopoulos, A. W. J. (2003) 'The deep Pacific ocean floor', in Tyler, P. A. (ed.) *Ecosystems of the deep oceans*. Amsterdam: Elsevier Science B.V., pp. 179–218.

Smith, C. R., Mincks, S. L. and Demaster, D. J. (2006) 'A synthesis of bentho-pelagic coupling on the Antarctic shelf: Food banks, ecosystem inertia and global climate change', *Deep-Sea Research II*, 53, pp. 875–894. doi: 10.1016/j.dsr2.2006.02.001.

Smith, K. L. (1978) 'Metabolism of the abyssopelagic rattail *Coryphaenoides armatus* measured *in situ*', *Nature*, 274, pp. 362–364. doi: 10.1038/274362a0.

Smith, K. L. (1983) 'Metabolism of two dominant epibenthic echinoderms measured at bathyal depths in the Santa Catalina Basin', *Marine Biology*, 72, pp. 249–256. doi: 10.1038/470444a.

Smith, K. L. (1992) 'Benthic boundary layer communities and carbon cycling at abyssal depths in the central North Pacific', *Limnology and Oceanography*, 37, pp. 1034–1056. doi: 10.4319/lo.1992.37.5.1034.

Smith, K. L. *et al.* (2014) 'Large salp bloom export from the upper ocean and benthic community response in the abyssal northeast Pacific: Day to week resolution', *Limnology and Oceanography*, 59, pp. 745–757. doi: 10.4319/lo.2014.59.3.0745.

Smith, K. L. and Brown, N. O. (1983) 'Oxygen consumption of pelagic juveniles and demersal adults of the deep-sea fish *Sebastolobus altivelis*, measured at depth', *Marine Biology*, 76, pp. 325–332. doi: 10.1007/BF00393036.

Smith, K. L. and Hessler, R. R. (1974) 'Respiration of benthopelagic fishes: *In situ* measurements at 1230 meters', *Science*, 184, pp. 72–73.

Smith, K. L., Kaufmann, R. S. and Baldwin, R. J. (1994) 'Coupling of near-bottom pelagic and benthic processes at abyssal depths in the eastern North Pacific Ocean', *Limnology and Oceanography*, 39, pp. 1101–1118. doi: 10.4319/lo.1994.39.5.1101.

Smith, K. L., Kaufmann, R. S. and Wakefield, W. W. (1993) 'Mobile megafaunal activity monitored with a time-lapse camera in the abyssal North

Pacific', *Deep-Sea Research I*, 40, pp. 2307–2324. doi: 10.1016/0967-0637(93)90106-D.

Smith, K. L. and Laver, M. B. (1981) 'Respiration of the bathypelagic fish *Cyclothone acclinidens*', *Marine Biology*, 61, pp. 261–266. doi: 10.1007/BF00401564.

Snelgrove, P. V. R. *et al.* (2018) 'Global carbon cycling on a heterogeneous seafloor', *Trends in Ecology & Evolution*, 33, pp. 96–105. doi: 10.1016/j.tree.2017.11.004.

Snelgrove, P. V. R. and Butman, C. A. (1994) 'Animal-sediment relationships revisited: Cause versus effect', *Oceanography and Marine Biology: An Annual Review*, 32, pp. 111–177.

Soetaert, K. and Heip, C. H. R. (1995) 'Nematode assemblages of deep-sea and shelf break sites in the North Atlantic and Mediterranean Sea', *Marine Ecology Progress Series*, 125, pp. 171–183.

Soetaert, K. and van Oevelen, D. (2009) 'Modeling food web interactions in benthic deep-sea ecosystems: A practical guide', *Oceanography*, 22, pp. 128–143. doi: 10.5670/oceanog.2009.13.

Sole, R. V. and Montoya, M. (2001) 'Complexity and fragility in ecological networks', *Proceedings of the Royal Society B: Biological Sciences*, 268, pp. 2039–2045. doi: 10.1098/rspb.2001.1767.

Soltwedel, T. *et al.* (2003) 'What a lucky shot! Photographic evidence for a medium-sized natural food-fall at the deep seafloor', *Oceanologica Acta*, 26, pp. 623–628. doi: 10.1016/S0399-1784(03)00060-4.

Sommer, S. *et al.* (2010) 'Benthic respiration in a seep habitat dominated by dense beds of ampharetid polychaetes at the Hikurangi Margin (New Zealand)', *Marine Geology*, 272, pp. 223–232. doi: 10.1016/j.margeo.2009.06.003.

de Souza, J. R. B. and Borzone, C. A. (2007) 'Population dynamics and secondary production of *Euzonus furciferus* Ehlers (Polychaeta, Opheliidae) in an exposed sandy beach of southern Brazil', *Revista Brasileira de Zoologia*, 24, pp. 1139–1144.

Sprung, M. (1993) 'Estimating macrobenthic secondary production from body weight and biomass: A field test in a non-boreal intertidal habitat', *Marine Ecology Progress Series*, 100, pp. 103–109. doi: 10.3354/meps100103.

Squadrone, S. *et al.* (2016) 'Human exposure to metals due to consumption of fish from an artificial lake basin close to an active mining area in Katanga (D.R. Congo)', *Science of The Total Environment*, 568, pp. 679–684. doi: 10.1016/j.scitotenv.2016.02.167.

von Stackelberg, U. (2000) 'Manganese nodules of the Peru Basin', in Cronan, D. S. (ed.) *Handbook of Marine Mineral Deposits*. Boca Raton: CRC Press

LLC, pp. 197–238.

Ståhl, H. *et al.* (2004) ‘Recycling and burial of organic carbon in sediments of the Porcupine Abyssal Plain, NE Atlantic’, *Deep-Sea Research I*, 51, pp. 777–791. doi: 10.1016/j.dsr.2004.02.007.

Steiner, R. (2009) *Independent review of the environmental impact statement for the proposed Nautilus Minerals Solwara 1 seabed mining project , Papua New Guinea*. Madang, Papua New Guinea.

Steudel, B. *et al.* (2012) ‘Biodiversity effects on ecosystem functioning change along environmental stress gradients’, *Ecology Letters*, 15, pp. 1397–1405. doi: 10.1111/j.1461-0248.2012.01863.x.

Steyaert, M. *et al.* (2007) ‘Responses of intertidal nematodes to short-term anoxic events’, *Journal of Experimental Marine Biology and Ecology*, 345, pp. 175–184. doi: 10.1016/j.jembe.2007.03.001.

Stratmann, T., Lins, L., *et al.* (2018) ‘Abyssal plain faunal carbon flows remain depressed 26 years after a simulated deep-sea mining disturbance’, *Biogeosciences*, 15, pp. 4131–4145. doi: 10.5194/bg-15-4131-2018.

Stratmann, T., Mevenkamp, L., *et al.* (2018) ‘Has phytodetritus processing by an abyssal soft-sediment community recovered 26 years after an experimental disturbance?’, *Frontiers in Marine Science*, 5, pp. 1–13. doi: 10.3389/fmars.2018.00059.

Stratmann, T., Voorsmit, I., *et al.* (2018) ‘Recovery of Holothuroidea population density, community composition and respiration activity after a deep-sea disturbance experiment’, *Limnology and Oceanography*, 00, pp. 00–00. doi: 10.1002/lno.10929.

Subida, M. D., Cunha, M. R. and Moreira, M. H. (2005) ‘Life history, reproduction, and production of *Gammarus chevreuxi* (Amphipoda: Gammaridae) in the Ria de Aveiro, northwestern Portugal’, *Journal of the North American Benthological Society*, 24, pp. 82–100. doi: 10.1899/0887-3593(2005)024<0082:LHRAPO>2.0.CO;2.

Sudo, H. and Azeta, M. (1996) ‘Life history and production of the amphipod *Byblis japonicus* Dahl (Gammaridea: Ampeliscidae) in a warm temperate zone habitat, Shijiki Bay, Japan’, *Journal of Experimental Marine Biology and Ecology*, 198, pp. 203–222. doi: 10.1016/0022-0981(96)00012-3.

Sulak, K. J. *et al.* (1985) ‘The life history and systematics of deep-sea lizard fishes, genus Bathysaurus (Synodontidae)’, *Canadian Journal of Zoology*, 63, pp. 623–642.

Suttle, C. A. (2005) ‘Viruses in the sea’, *Nature*, 437, pp. 356–361. doi: 10.1038/nature04160.

Svavarsson, J., Gudmundsson, G. and Brattegard, T. (1993) ‘Feeding by asellote isopods (Crustacea) on foraminifers (Protozoa) in the deep sea’, *Deep-Sea Research I*, 40, pp. 1225–1239. doi: 10.1016/0967-0637(93)90135-P.

Svensson, P. A. and Wong, B. B. M. (2011) ‘Carotenoid-based signals in behavioural ecology: A review’, *Behaviour*, 148, pp. 131–189. doi: 10.1163/000579510X548673.

Sverdrup, H. U., Ragnarsdottir, K. V. and Koca, D. (2017) ‘Integrated modelling of the global cobalt extraction, supply, price and depletion of extractable resources using the WORLD6 model’, *BioPhysical Economics and Resource Quality*, 2, pp. 1–29. doi: 10.1007/s41247-017-0017-0.

Sweetman, A. K. *et al.* (2010) ‘Impacts of exotic mangrove forests and mangrove deforestation on carbon remineralization and ecosystem functioning in marine sediments’, *Biogeosciences*, 7, pp. 2129–2145. doi: 10.5194/bg-7-2129-2010.

Sweetman, A. K., Norling, K., *et al.* (2014) ‘Benthic ecosystem functioning beneath fish farms in different hydrodynamic environments’, *Limnology and Oceanography*, 59, pp. 1139–1151. doi: 10.4319/lo.2014.59.4.1139.

Sweetman, A. K., Smith, C. R., *et al.* (2014) ‘Rapid scavenging of jellyfish carcasses reveals the importance of gelatinous material to deep-sea food webs’, *Proceedings of the Royal Society B: Biological Sciences*, 281, p. 20142210. doi: 10.1098/rspb.2014.2210.

Sweetman, A. K., Smith, C. R., *et al.* (2016) ‘Bacteria, not macrofauna, are key players in the short-term degradation of phytodetritus in abyssal CCZ sediments’, in Willams, J. and Palmer, M. (eds) *Challenger Society for Marine Science*. Liverpool: Challenger Society for Marine Science.

Sweetman, A. K., Chelsky, A., *et al.* (2016) ‘Jellyfish decomposition at the seafloor rapidly alters biogeochemical cycling and carbon flow through benthic food-webs’, *Limnology and Oceanography*, 61, pp. 1449–1461. doi: 10.1002/lno.10310.

Sweetman, A. K. *et al.* (2017) ‘Major impacts of climate change on deep-sea benthic ecosystems’, *Elementa - Science of the Anthropocene*, 5. doi: 10.1525/elementa.203.

Sweetman, A. K. *et al.* (2018) ‘Key role of bacteria in the short-term cycling of carbon at the abyssal seafloor’, *Limnology and Oceanography*.

Sweetman, A. K. and Chapman, A. (2011) ‘First observations of jelly-falls at the seafloor in a deep-sea fjord’, *Deep-Sea Research I*, 58, pp. 1206–1211. doi: 10.1016/j.dsr.2011.08.006.

Sweetman, A. K. and Chapman, A. (2015) ‘First assessment of flux rates of jellyfish carcasses (jelly-falls) to the benthos reveals the importance of

gelatinous material for biological C-cycling in jellyfish-dominated ecosystems', *Frontiers in Marine Science*, 2, pp. 1–7. doi: 10.3389/fmars.2015.00047.

Sweetman, A. K. and Witte, U. (2008) 'Macrofaunal response to phytodetritus in a bathyal Norwegian fjord', *Deep-Sea Research I*, 55, pp. 1503–1514. doi: 10.1016/j.dsr.2008.06.004.

Takemae, N., Nakaya, F. and Motokawa, T. (2009) 'Low oxygen consumption and high body content of catch connective tissue contribute to low metabolic rate of sea cucumbers', *The Biological Bulletin*, 216, pp. 45–54. doi: 10.1086/BBLv216n1p45.

Tanaka, T. (2009) 'Structure and function of the mesopelagic microbial loop in the NW Mediterranean Sea', *Aquatic Microbial Ecology*, 57, pp. 351–362. doi: 10.3354/ame01370.

Taylor, C. D. *et al.* (2010) *Descriptive models, grade-tonnage relations, and databases for the assessment of sediment-hosted copper deposits - With emphasis on deposits in the Central African Copperbelt, Democratic Republic of the Congo and Zambia*. Reston.

Teal, J. M. and Wieser, W. (1966) 'The distribution and ecology of nematodes in a Georgia salt marsh', *Limnology and Oceanography*, 11, pp. 217–222.

Tesi, T. *et al.* (2010) 'Reexposure and advection of ^{14}C-depleted organic carbon from old deposits at the upper continental slope', *Global Biogeochemical Cycles*, 24, p. GB4002. doi: 10.1029/2009GB003745.

Thayer, G. W. *et al.* (1984) 'Role of larger herbivores in seagrass community', *Estuaries*, 7, pp. 351–376.

Thiel, H. (1975) 'The size structure of the deep-sea benthos', *Internationale Revue der gesamten Hydrobiologie und Hydrographie*, 60, pp. 575–606.

Thiel, H. *et al.* (1989) *Cruise Report DISCOL 1, Sonne - Cruise 61. Balboa/ Panama - Calloa/ Peru 02.02. - 05.03.1989; Callao/ Peru - Callao/ Peru 07.03. - 03.04.1989*. Hamburg.

Thiel, H. (1991) 'From MESEDA to DISCOL - A new approach to deep-sea mining risk assessments.', *Marine Mining*, 10, pp. 369–386.

Thiel, H. *et al.* (1993) 'Manganese nodule crevice fauna', *Deep-Sea Research I*, 40, pp. 419–423.

Thiel, H. and Forschungsverbund Tiefsee-Umweltschutz (2001) 'Evaluation of the environmental consequences of polymetallic nodule mining based on the results of the TUSCH Research Association', *Deep-Sea Research II*, 48, pp. 3433–3452. doi: 10.1016/S0967-0645(01)00051-0.

Thistle, D. (2003) 'The deep-sea floor: An overview', in Tyler, P. A. (ed.) *Ecosystems of the Deep Oceans*. Amsterdam: Elsevier Science B. V., pp. 5–37.

Thrush, S. F. and Dayton, P. K. (2002) ‘Disturbance to marine benthic habitats by trawling and dredging: Implications for marine biodiversity’, *Annual Review of Ecology and Systematics*, 33, pp. 449–473. doi: 10.1146/annurev.ecolsys.33.010802.150515.

Thurber, A. R. *et al.* (2014) ‘Ecosystem function and services provided by the deep sea’, *Biogeosciences*, 11, pp. 3941–3963. doi: 10.5194/bg-11-3941-2014.

Tilot, V. (1992) *La structure des assemblages mégabenthiques d’une province à nodules polymétalliques de l’océan Pacifique tropical est, PhD-Thesis*. Université de Bretagne Occidentale. Available at: http://archimer.ifremer.fr/doc/00000/3754/.

Tilot, V. (2006) *Biodiversity and distribution of the megafauna. Vol. 1: The polymetallic nodule ecosystem of the Eastern Equatorial Pacific Ocean; Vol. 2: Annotated photographic atlas of the echinoderms of the Clarion-Clipperton fracture zone*. Paris.

Trenberth, K. E. (1997) ‘The definition of El Niño’, *Bulletin of the American Meteorological Society*, 78, pp. 2771–2777. doi: 10.1175/1520-0477(1997)078<2771:TDOENO>2.0.CO;2.

Treude, T. *et al.* (2002) ‘Metabolism and decompression tolerance of scavenging lysianassoid deep-sea amphipods’, *Deep-Sea Research I*, 49, pp. 1281–1289. doi: 10.1016/S0967-0637(02)00023-7.

Tsurukawa, N., Prakash, S. and Manhart, A. (2011) *Social impacts of artisanal cobalt mining in Katanga, Democratic Republic of Congo*. Freiburg. Available at: http://resourcefever.com/publications/reports/OEKO_2011_cobalt_mining_congo.pdf.

Tsushima, M. (2007) ‘Carotenoids in sea urchins’, in Miller Lawrence, J. (ed.) *Edible Sea Urchins: Biology and Ecology*. Amsterdam: Elsevier Science B.V., pp. 159–166.

Turra, A. *et al.* (2015) ‘Population biology and secondary production of the harvested clam *Tivela mactroides* (Born, 1778) (Bivalvia, Veneridae) in southeastern Brazil’, *Marine Ecology*, 36, pp. 221–234. doi: 10.1111/maec.12137.

Tyler, P. A. *et al.* (1992) ‘Reproductive strategies and diet in deep-sea nuculanid protobranchs (Bivalvia: Nuculoidea) from the Rockall Trough’, *Marine Biology*, 114, pp. 571–580. doi: 10.1007/BF00357254.

U.S. Geological Survey (2001) *Mineral commodity summaries 2001*. Reston.

U.S. Geological Survey (2017) *Mineral commodity summaries 2017*. Reston. doi: 10.3133/70180197.

U.S. Geological Survey (2018) *Mineral commodity summaries 2018*. Reston.

doi: 10.3133/70194932.

UN General Assembly (1982) *Convention on the Law of the Sea*. New York: UN General Assembly. doi: 10.1163/15718089720491594.

UNEP/MAP (2012) *State of the marine and coastal Mediterranean*. Athens.

Vacelet, J., Kelly, M. and Schlacher-Hoenlinger, M. (2009) 'Two new species of *Chondrocladia* (Demospongiae: Cladorhizidae) with a new spicule type from the deep south Pacific, and a discussion of the genus Meliiderma', *Zootaxa*, 2073, pp. 57–68.

Valls, M., Rueda, L. and Quetglas, A. (2017) 'Feeding strategies and resource partitioning among elasmobranchs and cephalopods in Mediterranean deep-sea ecosystems', *Deep-Sea Research I*, 128, pp. 28–41. doi: 10.1016/j.dsr.2017.09.002.

Vanaverbeke, J. *et al.* (2008) 'Benthic respones to sedimentation of phytoplankton on the Belgian continental shelf', in Coursseau, V., Lancelot, C., and Cox, D. (eds) *Current Status of Eutrophication in the Belgian Coastal Zone*. Brussels: Presses Universitaires de Bruxelles, pp. 73–90.

Vanhove, S., Arntz, W. and Vincx, M. (1999) 'Comparative study of the nematode communities on the southeastern Weddell Sea shelf and slope (Antarctica)', *Marine Ecology Progress Series*, 181, pp. 237–256. doi: 10.3354/meps181237.

Vannier, J., Abe, K. and Ikuta, K. (1998) 'Feeding in myodocopid ostracods: Functional morphology and laboratory observations from videos', *Marine Biology*, 132, pp. 391–408. doi: 10.1007/s002270050406.

Vanreusel, A. *et al.* (2016) 'Threatened by mining, polymetallic nodules are required to preserve abyssal epifauna', *Scientific Reports*, 6, p. 26808. doi: 10.1038/srep26808.

Veillette, J. (2006) *Analyse de la distribution spatiale de la faune associée aux nodules polymétalliques en fonction des facteurs environnementaux en milieu océanique profond, M.Sc. Thesis*. Université du Québec à Montréal.

Velasco, L. . and Navarro, J. . (2003) 'Energetic balance of infaunal (*Mulinia edulis* King, 1831) and epifaunal (*Mytilus chilensis* Hupé, 1854) bivalves in response to wide variations in concentration and quality of seston', *Journal of Experimental Marine Biology and Ecology*, 296, pp. 79–92. doi: 10.1016/S0022-0981(03)00316-2.

Veloso, V. G., Cardoso, R. S. and Petracco, M. (2003) 'Secondary production of the intertidal macrofauna of Prainha beach, Brazil', *Journal of Coastal Research*, 35, pp. 385–391.

Vénec-Peyré, M.-T. (1990) 'Contribution of foraminifera to the study of recent

sedimentation in the Gulf of Lions (western Mediterranean Sea)', *Continental Shelf Research*, 10, pp. 869–883. doi: 10.1016/0278-4343(90)90064-S.

Verardo, D. J., Froelich, P. N. and McIntyre, A. (1990) 'Determination of organic carbon and nitrogen in marine sediments using the Carlo Erba NA-1500 analyzer', *Deep-Sea Research*, 37, pp. 157–165. doi: 10.1016/0198-0149(90)90034-S.

Verdugo, P. (2012) 'Marine microgels', *Annual Review of Marine Science*, 4, pp. 375–400. doi: 10.1146/annurev-marine-120709-142759.

Verlaan, P. A., Cronan, D. S. and Morgan, C. L. (2004) 'A comparative analysis of compositional variations in and between marine ferromanganese nodules and crusts in the South Pacific and their environmental controls', *Progress in Oceanography*, 63, pp. 125–158. doi: 10.1016/j.pocean.2004.11.001.

Vetter, E. W. (1996) 'Secondary production of a southern California Nebalia (Crustacea: Leptostraca)', *Marine Ecology Progress Series*, 137, pp. 95–101. doi: 10.3354/meps137095.

Veuger, B. *et al.* (2005) 'Analysis of ^{15}N incorporation into D-alanine: A new method for tracing nitrogen uptake by bacteria', *Limnology and Oceanography: Methods*, 3, pp. 230–240. doi: 10.4319/lom.2005.3.230.

Vézina, A. F. and Platt, T. (1988) 'Food web dynamics in the ocean. I. Best-estimates of flow networks using inverse methods', *Marine Ecology Progress Series*, 42, pp. 269–287.

Vincx, M. *et al.* (1994) 'Meiobenthos of the deep Northeast Atlantic', *Advances in Marine Biology*, 30, pp. 1–88. doi: 10.1016/S0065-2881(08)60061-9.

Vogt, C. (2013) *International assessment of marine and riverine disposal of mine tailings. Final report adopted by the International Maritime Organization (London Convention/Protocol)*. IMO.

Volz, J. *et al.* (2018) 'Natural spatial variability of depositional conditions, biogeochemical processes and element fluxes in sediments of the eastern Clarion-Clipperton Zone, Pacific Ocean', *Deep-Sea Research I*, pp. 0–1. doi: 10.1016/j.dsr.2018.08.006.

Vonnahme, T. R. (2016) *Microbial diversity and function of deep-sea manganese nodule ecosystems, M.Sc. Thesis*. Alfred-Wegener-Institute.

Vopel, K. and Thiel, H. (2001) 'Abyssal nematode assemblages in physically disturbed and adjacent sites of the eastern equatorial Pacific', *Deep-Sea Research II*, 48, pp. 3795–3808. doi: 10.1016/S0967-0645(01)00068-6.

Vranken, G. and Heip, C. H. R. (1986) 'The productivity of marine nematodes', *Ophelia*, 26, pp. 429–442. doi: 10.1080/00785326.1986.10422004.

Vranken, I. *et al.* (2013) 'The spatial footprint of the non-ferrous mining

industry in Lubumbashi', *Tropicultura*, 31, pp. 22–29.

Walsh, J. J. (1991) 'Importance of continental margins in the marine biogeochemical cycling of carbon and nitrogen', *Nature*, 350, pp. 53–55.

Wang, X. and Müller, W. E. G. (2009) 'Marine biominerals: Perspectives and challenges for polymetallic nodules and crusts', *Trends in Biotechnology*, 27, pp. 375–383. doi: 10.1016/j.tibtech.2009.03.004.

Warner, G. (1982) 'Food and feeding mechanisms: Ophiuroidea', in Jangoux, M. and Lawrence, J. (eds) *Echinoderm Nutrition*. Rotterdam: Balkema, pp. 161–184.

Warnock, R. E. and Liddell, W. D. (1985) 'Oxygen consumption in two shallow-water comatulid crinoids', *Journal of Experimental Marine Biology and Ecology*, 91, pp. 169–182. doi: 10.1016/0022-0981(85)90228-X.

Warren, P. H. (1989) 'Spatial and temporal variation in the structure of a freshwater food web', *Oikos*, 55, pp. 299–311.

Warwick, R. M., George, C. L. and Davies, J. R. (1978) 'Annual macrofauna production in a Venus community', *Estuarine and Coastal Marine Science*, 7, pp. 215–241.

Warwick, R. M. and Price, R. (1975) 'Macrofauna production in an estuarine mud-flat', *Journal of Experimental Marine Biology and Ecology*, 55, pp. 1–18.

Warwick, R. M. and Price, R. (1979) 'Ecological and metabolic studies on free-living nematodes from an estuarine mud-flat', *Estuarine and Coastal Marine Science*, 9, pp. 257–271. doi: 10.1016/0302-3524(79)90039-2.

Watling, L. (ed.) (1990) 'VIIth International Colloquium on Amphipoda', in *Proceedings of the VIIth International Colloquium on Amphipoda*. Maine, USA: Springer-Science+Business Media, B.V. doi: 10.1007/978-94-011-3542-9.

Watson, J. R., Stock, C. A. and Sarmiento, J. L. (2015) 'Exploring the role of movement in determining the global distribution of marine biomass using a coupled hydrodynamic – Size-based ecosystem model', *Progress in Oceanography*, 138, pp. 521–532. doi: 10.1016/j.pocean.2014.09.001.

Weber, T. *et al.* (2016) 'Deep ocean nutrients imply large latitudinal variation in particle transfer efficiency', *Proceedings of the National Academy of Sciences*, 113, pp. 8606–8611. doi: 10.1073/pnas.1604414113.

Webster, S. K. (1975) 'Oxygen consumption in echinoderms from several geographical locations, with particular reference to the Echinoidea', *The Biological Bulletin*, 148, pp. 157–164.

Wedding, L. M. *et al.* (2013) 'From principles to practice: A spatial approach to systematic conservation planning in the deep sea', *Proceedings of the Royal Society B: Biological Sciences*, 280, p. 20131684. doi: 10.1098/rspb.2013.1684.

Wegorzewski, A. V. and Kuhn, T. (2014) ‘The influence of suboxic diagenesis on the formation of manganese nodules in the Clarion Clipperton nodule belt of the Pacific Ocean’, *Marine Geology*, 357, pp. 123–138. doi: 10.1016/j.margeo.2014.07.004.

Wei, C.-L. *et al.* (2010) ‘Global patterns and predictions of seafloor biomass using random forests’, *PLoS ONE*, 5, p. e15323. doi: 10.1371/journal.pone.0015323.

Weigelt, M. and Rumohr, H. (1986) ‘Effects of wide-range oxygen depletion on benthic fauna and demersal fish in Kiel Bay 1981-1983’, *Meeresforschung*, 31, pp. 124–136.

Wentworth, C. K. (1922) ‘A scale of grade and class terms for clastic sediments’, *The Journal of Geology*, 30, pp. 377–392.

Wernberg, T., Smale, D. A. and Thomsen, M. S. (2012) ‘A decade of climate change experiments on marine organisms: Procedures, patterns and problems’, *Global Change Biology*, 18, pp. 1491–1498. doi: 10.1111/j.1365-2486.2012.02656.x.

Wetzel, M. A., Fleeger, J. W. and Powers, S. P. (2001) ‘Effects of hypoxia and anoxia on meiofauna: A review with new data from the Gulf of Mexico’, in Rabalais, N. N. and Turner, R. E. (eds) *Coastal Hypoxia: Consequences for Living Resources and Ecosystems*. Washington, DC: American Geophysical Union, pp. 165–184. doi: 10.1029/CE058p0165.

Whitman, W. B., Coleman, D. C. and Wiebe, W. J. (1998) ‘Prokaryotes: The unseen majority’, *Proceedings of the National Academy of Sciences*, 95, pp. 6578–6583. doi: 10.1073/pnas.95.12.6578.

Whittaker, J. M. *et al.* (2013) ‘Global sediment thickness data set updated for the Australian-Antarctic Southern Ocean’, *Geochemistry, Geophysics, Geosystems*, 14, pp. 3297–3305. doi: 10.1002/ggge.20181.

Wicksten, M. *et al.* (2017) ‘Presumed filter-feeding in a deep-sea benthic shrimp (Decapoda, Caridea, Stylodactylidae), with records of the deepest occurrence of carideans’, *ZooKeys*, 2017(646), pp. 17–23. doi: 10.3897/zookeys.646.10969.

Wicksten, M. K. and Packard, J. M. (2005) ‘A qualitative zoogeographic analysis of decapod crustaceans of the continental slopes and abyssal plain of the Gulf of Mexico’, *Deep-Sea Research I*, 52, pp. 1745–1765. doi: 10.1016/j.dsr.2005.04.006.

Widdicombe, S. *et al.* (2009) ‘Effects of CO_2 induced seawater acidification on infaunal diversity and sediment nutrient fluxes’, *Marine Ecology Progress Series*, 379, pp. 59–75. doi: 10.3354/meps07894.

Wiedicke, M. H. and Weber, M. E. (1996) ‘Small-scale variability of seafloor

features in the northern Peru Basin: Results from acoustic survey methods', *Marine Geophysical Researches*, 18, pp. 507–526.

Wieser, W. (1953) 'Die Beziehung zwischen Mundhöhlengestalt, Ernährungsweise und Vorkommen bei freilebenden marinen Nematoden', *Arkiv für Zoologie*, 4, pp. 439–484.

Wieser, W. (1960) 'Benthic studies in Buzzard Bay. II. The meiofauna', *Limnology and Oceanography*, 5, pp. 121–137.

Wieser, W. *et al.* (1974) 'An ecophysiological study of some meiofauna species inhabiting a sandy beach at Bermuda', *Marine Biology*, 26, pp. 235–248. doi: 10.1007/BF00389254.

Wieser, W. and Kanwisher, J. (1960) 'Growth and metabolism in a marine nematode, *Enoplus communis Bastian*', *Zeitschrift für vergleichende Physiologie*, 43, pp. 29–36.

Wieser, W. and Kanwisher, J. (1961) 'Ecological and physiological studies on marine nematodes from a small salt marsh near Woods Hole, Massachusetts', *Limnology and Oceanography*, 6, pp. 262–270.

Wigham, B. D. *et al.* (2003) 'Is long-term change in the abyssal northeast Atlantic driven by qualitative changes in export flux? Evidence from selective feeding in deep-sea holothurians', *Progress in Oceanography*, 59, pp. 409–441. doi: 10.1016/j.pocean.2003.11.003.

Wiklund, H. *et al.* (2017) 'Abyssal fauna of the UK-1 polymetallic nodule exploration area, Clarion-Clipperton Zone, central Pacific Ocean: Mollusca', *ZooKeys*, pp. 1–46. doi: 10.3897/zookeys.707.13042.

Wildish, D. J. (1984) 'Secondary production of four sublittoral, soft-sediment amphipod populations in the Bay of Fundy', *Canadian Journal of Zoology*, 62, pp. 1027–1033. doi: 10.1139/z84-146.

Wildish, D. J. and Peer, D. (1981) 'Methods for estimating secondary production in marine Amphipoda', *Canadian Journal of Fisheries and Aquatic Sciences*, 38, pp. 1019–1026.

Wilson, E. E. and Wolkovich, E. M. (2011) 'Scavenging: How carnivores and carrion structure communities', *Trends in Ecology & Evolution*, 26, pp. 129–135. doi: 10.1016/j.tree.2010.12.011.

Wilson, G. D. F. (1987) *Crustacean communities of the manganese nodule province (Domes Site A compared with Domes site C)*. La Jolla.

Wilson, G. D. F. (2017) 'Macrofauna abundance, species diversity and turnover at three sites in the Clipperton-Clarion Fracture Zone', *Marine Biodiversity*, 47, pp. 323–347. doi: 10.1007/s12526-016-0609-8.

Wilson, S. *et al.* (2013) 'Metabolism of shallow and deep-sea benthic

crustaceans and echinoderms in Hawaii', *Marine Biology*, 160, pp. 2363–2373. doi: 10.1007/s00227-013-2230-8.

Windom, H. L. *et al.* (1989) 'Natural trace metal concentrations in estuarine and coastal marine sediments of the southeastern United States', *Environmental Science and Pollution Research*, 23, pp. 314–320. doi: 10.1021/es00180a008.

Witbaard, R. *et al.* (2001) 'The response of *Oneirophanta mutabilis* (Holothuroidea) to the seasonal deposition of phytopigments at the Porcupine Abyssal Plain in the Northeast Atlantic', *Progress in Oceanography*, 50, pp. 423–441. doi: 10.1016/S0079-6611(01)00064-7.

Witte, U., Wenzhöfer, F., *et al.* (2003) '*In situ* experimental evidence of the fate of a phytodetritus pulse at the abyssal sea floor', *Nature*, 424, pp. 763–766. doi: 10.1038/nature01799.

Witte, U., Aberle, N., *et al.* (2003) 'Rapid response of a deep-sea benthic community to POM enrichment: An *in situ* experimental study', *Marine Ecology Progress Series*, 251, pp. 27–36. doi: 10.3354/meps251027.

Wolff, T. (1962) *The systematics and biology of bathyal and abyssal isopoda asellota*. Edited by R. Spärck, S. Greve, and F. Jensenius Madsen. Copenhagen: Danish Science Press, Ltd.

Wolff, W. J. and de Wolf, L. (1977) 'Biomass and production of zoobenthos in the Grevelingen estuary, the Netherlands', *Estuarine and Coastal Marine Science*, 5, pp. 1–24.

Womersley, C. and Ching, C. (1989) 'Natural dehydration regimes as a prerequisite for the successful induction of anhydrobiosis in the nematode *Rotylenchulus reniformis*', *Journal of Experimental Biology*, 143, pp. 359–372.

Woodward, F. I. (2007) 'Global primary production', *Current Biology*, 17, pp. R269–R273. doi: 10.1016/j.cub.2007.01.054.

Woodwell, G. M. *et al.* (1978) 'The biota and the world carbon budget', *Science*, 199, pp. 141–146. doi: 10.1126/science.199.4325.141.

Woolley, S. N. C. *et al.* (2016) 'Deep-sea diversity patterns are shaped by energy availability', *Nature*, 533, pp. 393–396. doi: 10.1038/nature17937.

Woulds, C. *et al.* (2009) 'The short-term fate of organic carbon in marine sediments: Comparing the Pakistan margin to other regions', *Deep-Sea Research II*, 56, pp. 393–402. doi: 10.1016/j.dsr2.2008.10.008.

Wyville Thomson, C. (1873) 'Notes from the "Challenger" II.', *Nature*, 8, pp. 51–53.

Wyville Thomson, C. (1880) *Report on the scientific results of the voyage of H.M.S. Challenger during the years 1873-76. Zoology - Vol. 1*. London: HM Stationery Office. Available at:

http://www.vliz.be/imisdocs/publications/215308.pdf.

Yamamoto, J. *et al.* (2007) 'Transportation of organic matter to the sea floor by carrion falls of the giant jellyfish Nemopilema nomurai in the Sea of Japan', *Marine Biology*, 153, pp. 311–317. doi: 10.1007/s00227-007-0807-9.

Yamamoto, J. *et al.* (2009) 'Observations of food falls off the Shiretoko Peninsula, Japan, using a remotely operated vehicle', *Fisheries Science*, 75, pp. 513–515. doi: 10.1007/s12562-008-0055-z.

Yool, A. *et al.* (2017) 'Big in the benthos: Future change of seafloor community biomass in a global, body size-resolved model', *Global Change Biology*, 23, pp. 3554–3566. doi: 10.1111/gcb.13680.

Youmans, E. L. (1875) 'Notes', *The Popular Science Monthly*. New York City: D. Appleton & Company, p. 511.

Young, C. M. (2003) 'Reproduction, development and life-history traits', in Tyler, P. A. (ed.) *Ecosystems of the deep oceans*. 1st edn. Amsterdam: Elsevier Science B.V., pp. 381–426.

Yu, O. H. and Suh, H.-L. (2002) 'Secondary production of *Synchelidium lenorostralum* (Amphipoda, Oedicerotidae) on a temperate sandy shore, Southern Korea', *Journal of Crustacean Biology*, 22, pp. 467–473. doi: 10.1163/20021975-99990364.

Yu, Z., Qi, Z., *et al.* (2013) 'Effects of salinity on ingestion, oxygen consumption and ammonium excretion rates of the sea cucumber *Holothuria leucospilota*', *Aquaculture Research*, 44, pp. 1760–1767. doi: 10.1111/j.1365-2109.2012.03182.x.

Yu, Z., Hu, C., *et al.* (2013) 'Survival and growth of the sea cucumber *Holothuria leucospilota* Brandt: A comparison between suspended and bottom cultures in a subtropical fish farm during summer', *Aquaculture Research*, 44, pp. 114–124. doi: 10.1111/j.1365-2109.2011.03016.x.

Yukihira, H., Lucas, J. S. and Klumpp, D. W. (2000) 'Comparative effects of temperature on suspension feeding and energy budgets of the pearl oysters *Pinctada margaritifera* and *P. maxima*', *Marine Ecology Progress Series*, 195, pp. 179–188.

van der Zee, E. M. *et al.* (2016) 'How habitat-modifying organisms structure the food web of two coastal ecosystems', *Proceedings of the Royal Society B: Biological Sciences*, 283, p. 20152326. doi: 10.1098/rspb.2015.2326.

Zeng, Q. *et al.* (2018) 'Deep-sea metazoan meiofauna from a polymetallic nodule area in the Central Indian Ocean Basin', *Marine Biodiversity*, 48, pp. 395–405. doi: 10.1007/s12526-017-0778-0.

Zeppilli, D. *et al.* (2016) 'Seafloor heterogeneity influences the biodiversity–

ecosystem functioning relationships in the deep sea', *Scientific Reports*, 6, p. 26352. doi: 10.1038/srep26352.

Zezina, O. N. (1997) 'Biogeography of the bathyal zone', *Advances in Marine Biology*, 32, pp. 389–426. doi: 10.1016/S0065-2881(08)60020-6.

Zhinan, Z. (1983) 'Three new species of the free-living marine nematodes from a sub-littoral station in Firemore Bay, Scotland', *Cahiers de Biologie Marine*, 24, pp. 219–229.

Zhou, Y. *et al.* (2006) 'Feeding and growth on bivalve biodeposits by the deposit feeder *Stichopus japonicus* Selenka (Echinodermata: Holothuroidea) co-cultured in lantern nets', *Aquaculture*, 256, pp. 510–520. doi: 10.1016/j.aquaculture.2006.02.005.

Zograf, J. K. *et al.* (2017) 'Revision of the genus *Parasphaerolaimus* (Nematoda: Sphaerolaimidae) with description of new species', *Zootaxa*, 4232, pp. 58–70. doi: 10.11646/zootaxa.4232.1.4.

Publications

A1 Publications

Stratmann, T., Lins, L., Purser, A., Marcon, Y., Rodrigues, C. F., Ravara, A., Cunha, M. R., Simon-Lledó, E., Jones, D. O. B., Sweetman, A. K., Köser, K. and van Oevelen, D. (2018) 'Abyssal plain faunal carbon flows remain depressed 26 years after a simulated deep-sea mining disturbance', *Biogeosciences*, 15, pp. 4131–4145. doi: 10.5194/bg-15-4131-2018.

Stratmann, T., Voorsmit, I., Gebruk, A. V., Brown, A., Purser, A., Marcon, Y., Sweetman, A. K., Jones, D. O. B. and van Oevelen, D. (2018) 'Recovery of Holothuroidea population density, community composition and respiration activity after a deep-sea disturbance experiment', *Limnology and Oceanography*, 00, pp. 00–00. doi: 10.1002/lno.10929.

Brown, A., Hauton, C., **Stratmann, T.**, Sweetman, A. K., van Oevelen, D. and Jones, D. O. B. (2018) 'Metabolic rates are significantly lower in abyssal Holothuroidea than in shallow-water Holothuroidea', *Royal Society Open Science*, 5, p. 172162. doi: 10.1098/rsos.172162.

Stratmann, T., Mevenkamp, L., Sweetman, A. K., Vanreusel, A. and van Oevelen, D. (2018) 'Has phytodetritus processing by an abyssal soft-sediment community recovered 26 years after an experimental disturbance?', *Frontiers in Marine Science*, 5, pp. 1–13, doi:10.3389/fmars.2018.00059.

Stratmann, T., Lund-Hansen, L. C., Sorrell, B. K. and Markager, S. (2017) 'Concentrations of organic and inorganic bound nutrients and chlorophyll a in the Eurasian Basin, Arctic Ocean, early autumn 2012', *Regional Studies in Marine Science*, 9, pp. 69-75, doi:10.1016/j.rsma.2016.11.008.

Mevenkamp, L., **Stratmann, T.**, Guilini, K., Moodley, L., van Oevelen, D., Vanreusel, A., Westerlund, S. and Sweetman, A. K. (2017) 'Impaired short-term functioning of a benthic community from a deep Norwegian fjord following deposition of mine tailings and sediments', *Frontiers in Marine Science*, 4, pp. 1–16. doi:10.3389/fmars.2017.00169.

Jones, D. O. B., Kaiser, S., Sweetman, A. K., Smith, C. R., Menot, L., Vink, A., Trueblood, D., Greinert, J., Billett, D. S. M., Martínez Arbizu, P., Radziejewska, T., Singh, R., Ingole, B., **Stratmann, T.**, Simon-Lledó, E., Durden, J. M. and Clark, M. R. (2017) 'Biological responses to disturbance from simulated deep-sea polymetallic nodule mining', *PLoS One*, 12, pp. e0171750. doi:10.1371/journal.pone.0171750.

Lund-Hansen, L. C., Markager, S., Hancke, K., **Stratmann, T.**, Rysgaard, S., Ramløv, H. and Sorrell, B. K. (2015) 'Effects of sea-ice light attenuation and CDOM absorption in the water below the Eurasian sector of central Arctic Ocean (>88°N)', *Polar Research*, 34, pp. 23978. doi:10.3402/polar.v34.23978.

C1 Conference Proceedings

Seibt, M., **Stratmann, T.** and Stumm, M. (2013) 'Dissolved Organic Matter (DOM) - small in size but large in impact: Basis of life in the world's ocean', in Einsporn, M. H., Wiedling, J., and Beilfuss, S. (eds) *Recent Impulses to Marine Science and Engineering - From coast to deep sea: Multiscale approaches to marine sciences*. 1st edn. Hamburg: Deutsche Gesellschaft für Meeresforschung (DGM) e.V., pp. 18–28.

C2 Publications (Dissertations, conference abstracts and internal reports)

Dissertations

Stratmann, T. (2014) *Degradation of dissolved organic matter in the Arctic deep-sea, M.Sc. Thesis.* Aarhus Universitet.

Stratmann, T. (2011) *Diversität dehalogenierender Bakterien in marinen Sedimenten, B.Sc. Thesis*. Universität Bremen.

Conference contributions

Stratmann T., Voorsmit I., Sweetman A., Mevenkamp L., Vanreusel A., Gebruk A., Brown A., Purser A., Marcon Y., Jones D., Soetaert K., Wei C.-L. and van Oevelen D. (2017) 'Assessing deep-sea nodule mining impacts on the benthic ecosystem: From large to small scale', in Goldschmidt Paris 2017, Program Book. Paris, France, p. 277. (oral presentation)

Schupp, P. J., Rohde, S., Mills, S., Cahn, J., Busch, K., **Stratmann, T.**, Versluis, D., Petersen, L.-E., Kelly, M., Clemes, T. and Wörheide, G. (2017) 'Sponges don't like pumice, they like hard rock!' in *Book of Abstracts, 10th World Sponge Conference, NUI Galway, 25-30 June 2017*. Galway, Ireland, p. 242. (poster presentation)

Stratmann, T., Sweetman, A., Moodley, L., Mevenkamp, L., Vanreusel, A. and van Oevelen, D. (2015) 'Impact of mine tailing deposition on the ecology and biogeochemistry of marine sediments', in *2015 Aquatic Sciences Meeting, Aquatic Sciences: Global and regional perspectives – North meets S*outh, Program Book. Granada, Spain, p. 69. (oral presentation)

Internal reports

Stratmann T., Husson B., Menot L., Sarrazin J., Lins L., Purser A., Marcon Y., Vonnahme T. R., Wenzhöfer F., Rodrigues C., Ravara A., Cunha M. R., Dell'Anno A., Gambi C., Danovaro R., Sweetman A. K. and van Oevelen D (2016) 'Assessing food-web recovery in the deep sea through ecosystem modeling', MIDAS Deliverable 5.4. 56 pp.

Sweetman A .K., **Stratmann T.**, Vorsmit I., Gebruk A., Brown A., Purser A., Marcon Y., Jones D. O. B, Simon-Llédo E., van Oevelen, D., Dell'Anno A., Corinaldesi C., Gambi C., Tangherlini M., Manea E., Fioretti A., Danovaro R.,

Mevenkamp L. and Vanreusel (2016) ‘Report on impacts of deep-sea sediment disturbance on abyssal sea-floor ecosystem processes and ecosystem recovery’, MIDAS Deliverable 5.2. 35 pp.